(18)

Synthesis and Application of Carbohydrate-Templated Amino Acids and Use as Peptidomimetics

by

Kai-Dong Zhang

A thesis submitted to the Faculty of Graduate Studies of

University of Manitoba

in partial fulfillment of the requirement for the degree of

Doctor of Philosophy

DEPARTMENT OF CHEMISTRY

Winnipeg, Manitoba

THE UNIVERSITY OF MANITOBA

FACULTY OF GRADUATE STUDIES

*****

COPYRIGHT PERMISSION

Synthesis and Application of Carbohydrate - templated Amino Acids and Use as Peptidomimetics

BY

Kai-Dong Zhang

A Thesis/Practicum submitted to the Faculty of Graduate Studies of The University of Manitoba in partial fulfillment of the requirement of the degree

Of

Doctor of Philosophy

Abstract

Carbohydrate-templated amino acids (CTAAs) have found their wide application in the synthesis of peptidomimetics and glycomimetics. Herein, we describe the design, synthesis and conformational properties of three new types of CTAAs: spirocyclic glucose-templated 3(*S*)-hydroxy-*L*-proline analogues (Glc(3*S*)-Hyp), glucose-templated *D*- and *L*-lysine analogues (GlcTk, GlcTK) and glucose-templated *L*-proline lysine hybrids (GlcTProLysHs). In order to explore the use of these building blocks in peptide chemistry all three CTAAs were incorporated into peptides or peptide mimics and the thermodynamic, kinetic and β-turn-inducing properties were studied. These studies have resulted in the following observations and conclusions:

1. The studies of peptide mimics Ac-Glc(3*S*)-Hyp-OMe, Ac-Glc(3*S*)-Hyp-NHMe and tetrapeptides Ac-Leu-D-Phe-Glc(3*S*)-Hyp-Val-NMe_2 demonstrate that (5′*R*)-Glc(3*S*)-Hyp increases the prolyl amide *cis* rotamer population with accelerated *cis/trans* isomerization kinetics in water and induces a type VIa *β*-turn in the tetrapeptide when compared to unmodified reference peptides Ac-Pro-OMe, Ac-Pro-NHMe, Ac-(3*S*)-Hyp-OMe and Ac--(3*S*)-Hyp-NHMe. Whereas the diastereomer (5′*S*)-GlcTPro prefers the prolyl amide *trans* rotamer with a retarded *cis/trans* isomerization rate in water. ROESY and temperature coefficient experiments indicate that replacement of Pro with (5′*S*)-Glc(3*S*)-Hyp doesn't disturb the original conformation of the tetrapeptide.

2. Antibacterial *in vitro* tests of the dipeptides H_2N-GlcTk-Tyr-OBn and H_2N-GlcTk-Tyr-NHBn show that substitution of D-lysine by carbohydrate-templated-D-lysine analog GlcTk results in decreased antibacterial activity against Gram-positive and Gram-negative organisms. In addition, we discovered that the nature of the *C*-terminal substituent and the presence of hydrophobic moieties are crucial for antibacterial activity.

3. The conformational analysis of peptide mimics Ac-GlcTProLysHs-OMe (NHMe) demonstrate that unnatural, high lysyl *cis* amide rotamer populations can be achieved. This enables peptide chemists now to explore the biological implications of the lysyl *cis* amide population in lysine-rich antimicrobial peptides and other peptides.

Acknowledgements

The work for this PhD thesis has been carried out in Dr. Frank Schweizer's research group last five years.

Firstly, I would like to thank my supervisor, Dr. Frank Schweizer, for his excellent guidance, continued support and encouragement throughout my studies. I showed my gratefulness to him for his cultivation of my professional growth as a scientist. I very much enjoyed the great scientific freedom, the inspiring and amicable atmosphere at his group.

I would like to thank the other members of my examining committee: Dr. Athar Ata, Dr. Xiaochen Gu, Dr. Ulf Nilsson and Dr. Jörg Stetefeld for taking the time to review the thesis and participating in the defense.

I would like to thank my all colleagues in the department of chemistry. Especially: Dr. Kirk Marat for his great help in NMR analysis; People from our laboratory: Neil Owens, Dr. Dhananjoy Mandal, Dr. Smritilekha Bera, Andrian Lee, Zhizhi Sui, Jialiang Wang for the excellent working atmosphere.

I would like to thank my friends: Yingli Chen, Linjun Liu, Tong Li, Jian Yao. I had a great time with you guys in Winnipeg.

I also would like to thank my family: my grandparents, my parents: Aizhen and Hongtao; my sisters: Xinling and Ruiling; my brother: Kaiming; my nephews: Niuniu, Yangyang and Aohan.This degree would not have been possible without my family's support.

Dedicated to my parents, Aizhen Wang and Hongtao Zhang, who provided the motivation.

List of Abbreviations

Ac	acetyl
AIBN	azobisisobutyronitrile
Ala	*L*-alanine
AMPs	antimicrobial peptides
BAIB	bis(acetoxy)iodobenzene
BGAAs	bicyclic glycosyl amino acids
Bn	benzyl
Boc	*tert*-butoxycarbonyl
Cbz	benzyloxycarbonyl
CD	circular dichroism
CF	5(6)-carboxyfluorescein
Cys	*D*-cysteine
DFT	density functional theory
DIPEA	diisopropylethylamine
DMF	*N*,*N*-dimethylformamide
DMPU	1,3-dimethyl-3,4,5,6-tetrahydro-2(1*H*)-pyrimidinone
DMSO	dimethyl sulfoxide
Fmoc	9-fluorenylmethoxycarbonyl
k	*D*-lysine

K	*L*-lysine
$k_{c/t}$	rate constant from *cis* to *trans*
$k_{t/c}$	rate constant from *trans* to *cis*
$K_{c/t}$	equilibrium constant from *trans* to *cis*
$K_{t/c}$	equilibrium constant from *cis* to *trans*
Leu	*L*-leucine
LHMDS	lithium hexamethyldisilazide
Lys	*L*-lysine
MOM	methoxymethyl
MTBE	*tert*-butyl methyl ether
NMO	*N*-methylmorpholine *N*-oxide
Pfp	pentafluorophenyl
Phe	*L*-phenylalanine
PhF (PhFl)	9-phenylfluorenyl
PhTRAP	bis(diphenylphosphinoethyl)biferrocenes
PMP	*p*-methoxyphenyl
pNA	4-nitroanilide
Pro	*L*-proline
PyBOP	benzotriazol-1-yl oxytripyrrolidino-phosphonium hexafluorophosphate
Pyr	pyridine

Ser	*L*-serine
TBAF	tetrabutylammonium fluoride
TBS	*tert*-butyldimethylsilyl
TBTU	O-(1H-benzotriazole-1-yl)-N,N,N',N'-tetramethyluronium tetrafluoroborate
TEA	triethylamine
TEMPO	2,2,6,6-tetramethylpiperidine-1-oxyl
Tf	trifluoromethanesulfonyl
TFA	trifluoroacetic acid
TFAA	trifluoroacetic anhydride
Th	thiazole
THF	tetrahydrofuran
Thr	*L*-threonine
TMSOTf	trimethylsilyl trifluoromethane-sulfonate
Ts	tolunesulfonyl
Val	*L*-valine

Table of Contents

Chapter 1

Introduction

1.1. Background: peptidomimetics in drug design

Peptides are essential to virtually every biochemical process such as metabolism, immune defense and reproduction. They are involved in receptor recognition and signal transduction as hormones, neurotransmitters and neuromodulators in plants and animals. Besides this, peptides are also related with various diseases such as the plaques associated with Alzheimer's disease.[1]

This broad spectrum of activity has prompted great interest in the area of organic, medicinal and peptide chemistry. However, the poor pharmacological properties of most peptides limit their use as drugs through the following aspects:[2] (a) their low metabolic stability towards proteolysis in the gastrointestinal tract and in serum; (b) their poor absorption after oral ingestion, in particular due to their relatively high molecular mass or the lack of specific transport systems or both; (c) their rapid excretion through liver and kidneys; and (d) their undesired effects caused by interaction of the conformationally flexible peptides with various receptors.

1.1.1. Peptidomimetics

As what Gante described,[3] "a peptidomimetic is defined as a substance having it

secondary structure as well as other structural features analogous to that of the original peptide, which allows it to displace the original peptide from receptors or enzymes. As a result the effects of the original peptide are inhibited (antagonist, inhibitor) or duplicated (agonist)."

The aim of peptide modification is to determine the structure-activity relationships (SAR) of endogenous peptides and to produce analogues that can overcome the problems described above, while retaining selected activity (i.e. specific receptor agonists). Conversely, receptor antagonists and enzyme inhibitors are also desirable targets attainable through peptide modification.[2-4]

During the last 25 years, a plethora of concepts of peptidomimetics have been developed.[2,3,5] These include:

- Partially modified retro-inverso peptides (PMRI)
- Modification of the peptide backbone
- Modification of the amino acid side chain
- Induction and stabilization of secondary structures (β turns, γ turns, α helices)
- Development of conformationally constrained amino acids

Among them modifications of the amino acid side chain resulting in a reduction of the conformational flexibility has gained considerable attention. Herein, the progress in this area with emphasis on proline- and lysine-mimetics is summarized.

1.2. Proline analogues

Proline (Pro) is the only cyclic amino acid of the twenty DNA-encoded amino acids, which is characterized by limited rotation of the φ dihedral angle (C′-N-C$^{\alpha}$-C′, ~ -75 °) as its side chain is fused to the peptide backbone. Consequently, there is a reduction in the energy difference between the prolyl amide *trans*- and *cis*-isomers (Figure 1.1) making them nearly isoenergetic, which leads to a higher *cis N*-terminal amide content relative to

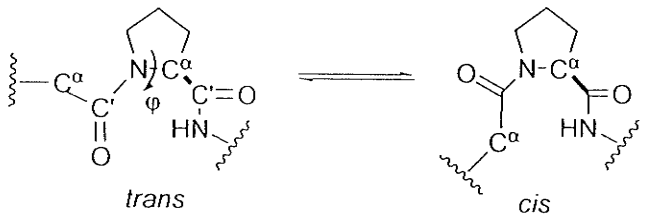

Figure 1.1 *Trans/cis* isomerization in *N*-terminal prolyl amide

the other amino acids. The prolyl *cis/trans* isomerization is found to be the rate-determining step in the folding pathways of many peptides and proteins.[6-10] Moreover, proline induces β-turns and extended helical structures (polyproline helix) in peptides that are crucial in protein/protein and protein/peptide interactions.[11,12] Besides the occurrence of proline in β-turns, proline-rich sequences also exist in antimicrobial peptides.[13] In nature, proline undergoes post-translational modifications such as hydroxylation to 4(*R*)-hydroxyproline (4-Hyp) and 3(*S*)-hydroxyproline (3-Hyp), which are critical to the stability of the triple helix in collagens and contributes to the stability of the poly-Hyp helix in plant-derived Hyp-rich glycopeptides.[14] In addition, hydroxylated proline residues were also found in virotoxin cyclic heptapeptides[15] and other

peptides.[16,17]

Over the years a plethora of proline analogues have been developed to study the structural and biological properties of proline surrogates in peptides. These analogues are approximately classified into two categories: introduction of alkyl or aryl groups into C^{α}-, C^{β}-, C^{γ}- or C^{δ}- positions of the proline ring; and replacement of one carbon of pyrrolidine ring with nitrogen, sulfur, oxygen or silicon which are referred to the azaproline, pseudoproline and silaproline, respectively. In addition, as a special case of the first category the rigid bicyclic proline analogues are also covered in this part.

1.2.1. Proline analogues with alkylation or arylation at C^{α}-, C^{β}-, C^{γ}- or C^{δ} position

1.2.1.1. C^{α}-proline analogues

C^{α}-proline analogues are compounds in which the α proton is replaced by an alkyl group such as methyl group[18] or by an aryl group like a phenyl group[19]. These α-tetrasubstituted proline derivatives show some interesting properties. For example, studies of model peptides have demonstrated the Ac-*L*-αMePro-NHMe **1** (Figure 1.2)

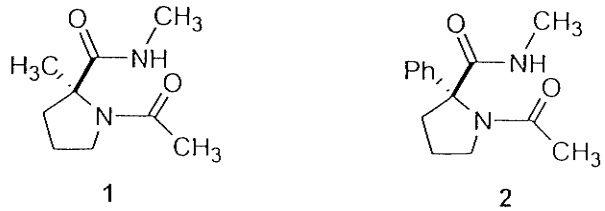

1 **2**

Figure 1.2 Peptide mimics **1** and **2** containing α-tetrasubstituted prolines

derivative had a preference for a γ-turn conformation in solution.[20,21] Whereas crystallographic analysis indicates the existence of an α-helical structure in its solid state.[22]

Recently, Flores-Ortega *et al* have investigated the intrinsic conformational preferences of Ac-*L*-αMePro-NHMe **1** and Ac-*L*-αPhPro-NHMe **2** using a Density Functional Theory (DFT) based computational method.[23] In comparison with Ac-*L*-Pro-NHMe, both compounds **1** and **2** (Figure 1.2) destabilize the *cis* configuration of the amide bond involving the pyrrolidine nitrogen resulting in an enhanced *trans* rotamer population.

In proteins, polyproline I (PPI) and II (PPII) conformations are important for many protein-protein interactions. PPI is a rare, compact, right-handed helix in which the prolyl *cis* isomer conformation is required. Whereas the common, extended, left-handed PPII helix structures adopt the Prolyl amide *trans* geometry. Interestingly, DFT calculation demonstrated that C^{α}–tetrasubstitution seemed to stabilize the semi-extended polyproline II conformation in water, which was not observed in the proteinogenic amino acids. In addition, the conformation of polyproline is also affected by the particular nature of the substituent incorporated at C^{α}. For example, the α-helical conformation with *trans* amide bonds have been found to be accessible for αMePro derivative but not for the αPhPro-containing peptide.

1.2.1.2 C^{β}-proline analogues

C^{β}-proline analogues are often called proline-amino acid chimeras which combine

amino acid side-chain functionality with proline conformational rigidity. These analogues provide a way to explore the geometric relationship of the side-chain group to peptide backbone. Therefore, replacement of the natural amino acids in peptides by proline-amino acid chimeras has led to better understanding of the bioactive conformations of cholecystokinin,[24] angiotensin II,[25] bradykinin,[26] and opioid peptides.[27] Furthermore, C^{β}-proline analogues have been used in the development of enzyme inhibitors,[28] as well as peptidomimetics exhibiting improved bioactivity and greater metabolic stability.[25-28]

Lubell *et al* have developed an effective way in which the 4-hydroxyproline was regioselectively enolized and alkylated to prepare the β,β-dimethylprolines **6a**, **6b** (Scheme 1.1) and **8** (Scheme 2).[29] The precursor **4** is prepared from amino ketone **3**, which is made from the commercially available (2*S*,4*R*)-hydroxyproline,[29] via regioselective enolization and alkylation using potassium bis(trimethylsilyl) amide base and iodomethane. 3,3-Dimethyl-4-hydroxy-*N*-(PhFl)proline **5** is obtained from reduction of compound **4** with sodium borohydride or lithium aluminium hydride, albeit with low diastereoselectivity. Reduction with $NaBH_4$ in MeOH at 0 °C provides a 3:2 mixture of 4*R*:4*S* diastereomers **5** in a quantitative yield. On the other hand, $LiAlH_4$ in THF gives a 1:2 mixture of (4*R*)-**5a**:(4*S*)-**5b**. **5a** and **5b** are readily separated by flash chromatography. Finally, hydroxyproline-valine chimeras, (4*R*)- and (4*S*)-3,3-dimethyl-4-hydroxy-*N*-(BOC)prolines **6a** and **6b**, are produced, respectively, in excellent yield by catalytic hydrogenolysis of (4*R*)- and (4*S*)-3,3-dimethyl-4-hydroxy-*N*-(PhFl)proline benzyl esters

5a and **5b**.

Scheme 1.1 Synthesis of hydroxyproline-valine chimeras **6**

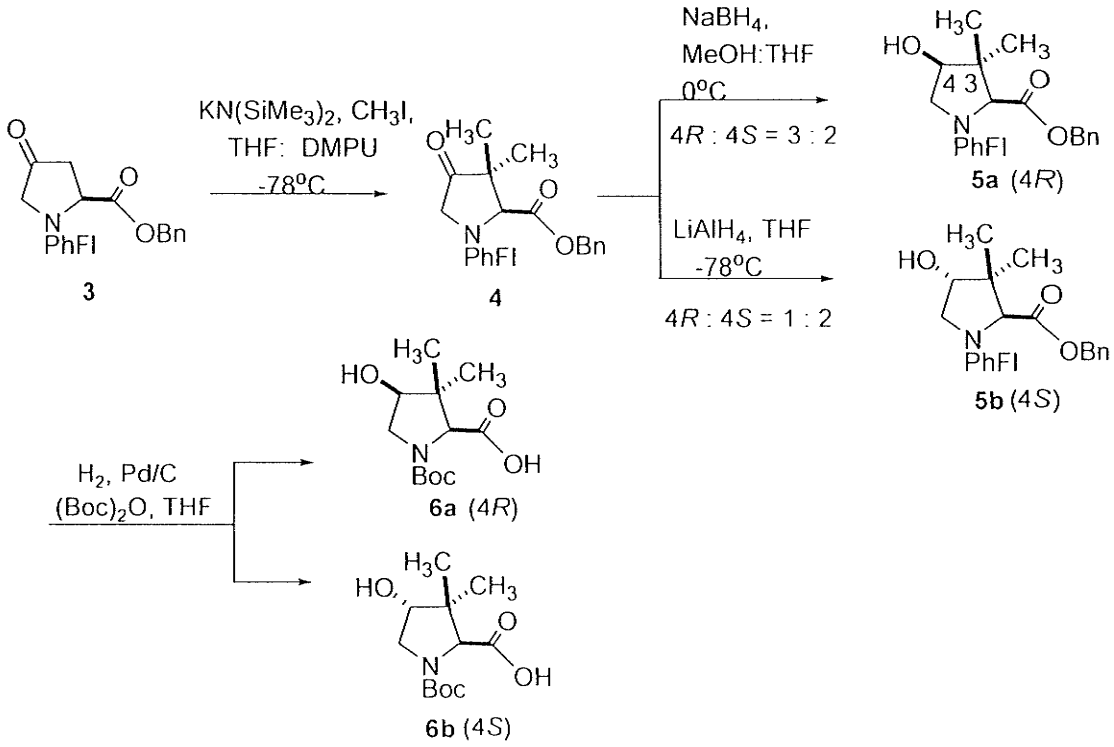

Synthesis of β,β-dimethyl-*N*-(BOC)prolines **8** (Scheme 1.2) is prepared from alcohol **5** through a three-step procedure: Initially, alcohol **5** is converted into xanthate **7** by

Scheme 1.2 Synthesis of β,β-dimethyl-*N*-(BOC)proline **8**

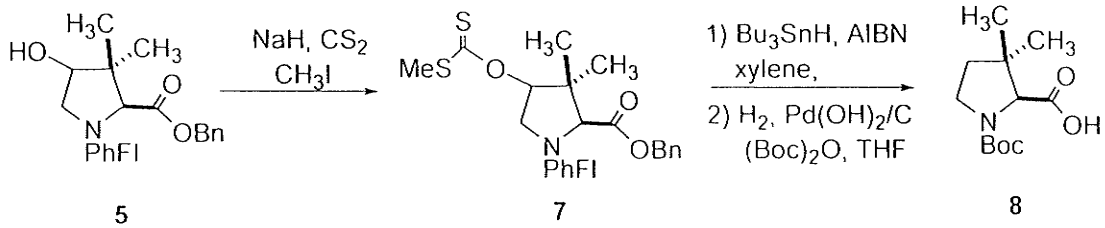

acylation of the sodium alkoxide with carbon disulfide in THF and subsequent alkylation with iodomethane. Secondly, the xanthate 7 is reduced with tributylstannane and AIBN as radical initiator in refluxing xylene before subjected to catalytic hydrogenolysis in the presence of di-*tert*-butyl dicarbonate to provide proline-valine chimera **8**.

In order to investigate the influence of these proline analogues on proline amide *cis/trans* isomerization, the same group has prepared a series of *N*-(acetyl)proline-*N'*-methylamide derivatives **9-14** (Figure 1.3).[30] Compared with model

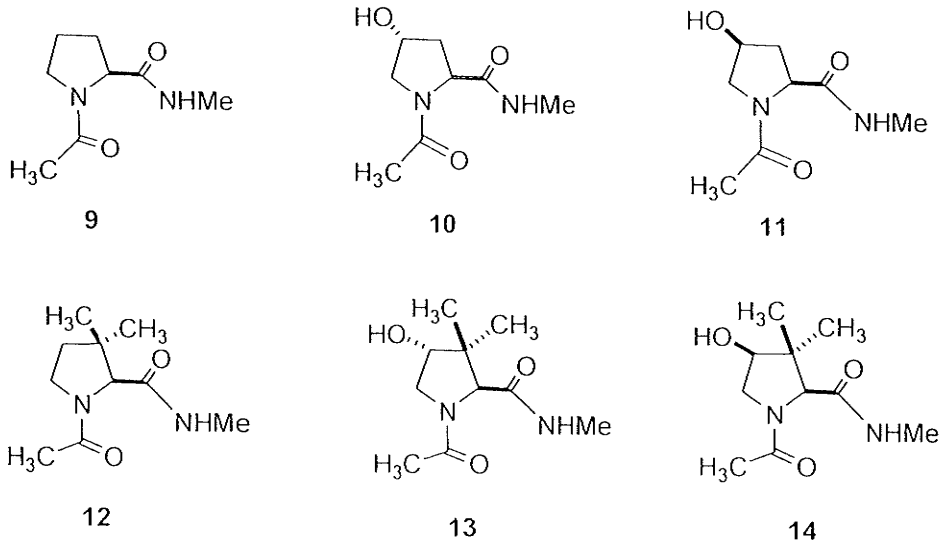

Figure 1.3 *N*-(acetyl)proline-*N'*-methylamides **9-14**

peptide mimic **9**, 4-hydroxyl group and 3 (or β)-alkyl substitutes have little effect on the equilibrium constant of isomerization and C^{γ}-endo conformation (Figure 1.4),in which the γ-carbon is out of plane defined by C^{β}-C^{α}-*N*-C^{δ} and located at the same side of the plane as *C*-terminal ester or amide, of the pyrrolidine ring in **10-14**.

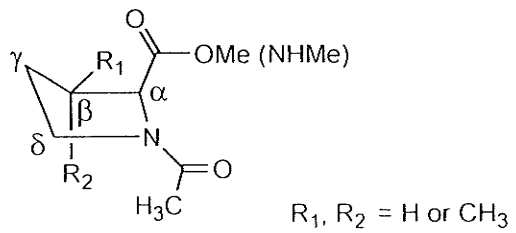

Figure 1.4 C^{γ}-endo conformation of the pyrrolidine ring

However, a decreasing order of *cis-to-trans* amide isomerization in water, **9** ≈ **11** > **10** > **14** > **13** > **12**, is observed. The steric effect caused by methyl substituents at C^{β}, which may place the *C*-terminal carbonyl oxygen in position to repel the developing lone pair of the pyramidalized nitrogen by Coulomb interactions resulting in a high energy barrier for isomerization.[31] This may be responsible for the relative low rate constants of amides **12-14**. Whereas the hydrogen bond between (4*S*)-hydroxyl group and *C*-terminal carbonyl oxygen may reduce the effects of Coulomb repulsion. As a result, an increased rate constant of amide **14** (or **11**) is observed relative to amide **13** (or **10**).

1.2.1.3. C^{γ}- proline analogues

Proline analogues functionalized with an appropriate pharmacophore at the γ-position have found wide applications in medicinal chemistry and feature therapeutic agents such as inhibitors of angiotensin-converting enzyme (ACE)[32] and potential inhibitors of proline dehydrogenase.[33]

From a synthetic point of view, C^{γ}-substituted proline analogues are also of great interest because of their accessibility from naturally abundant *trans*-4-hydroxyproline **15**.

Goodman *et al* have developed a versatile approach to the preparation of γ-alkylprolines from exocyclic olefin intermediates (Scheme 1.3).[34] The synthesis of the target compounds **20a-e** and **22b-e** begins with the preparation of the desired pyrrolidinone intermediate **16** starting from *trans*-4-hydroxyproline **15** through a few routine steps. Reaction of pyrrolidinone **16** with various triphenylphosphoranes provides the desired olefins **17a-f** in good yield. To obtain *trans*-substituted 4-alkylprolinols, silyl ether deprotection of compounds **17a-f** was first carried out to unmask the hydroxyl directing groups. Treatment of the resulting olefins **18** with the Crabtree catalyst, under H_2 atmosphere, gave excellent selectivities (dr > 40:1) for the *trans*-substituted prolinols **19a-f**. This result indicated that reduction with the Crabtree catalyst was an effective

Scheme 1.3 Synthesis of γ-alkylprolines **20** and **22**

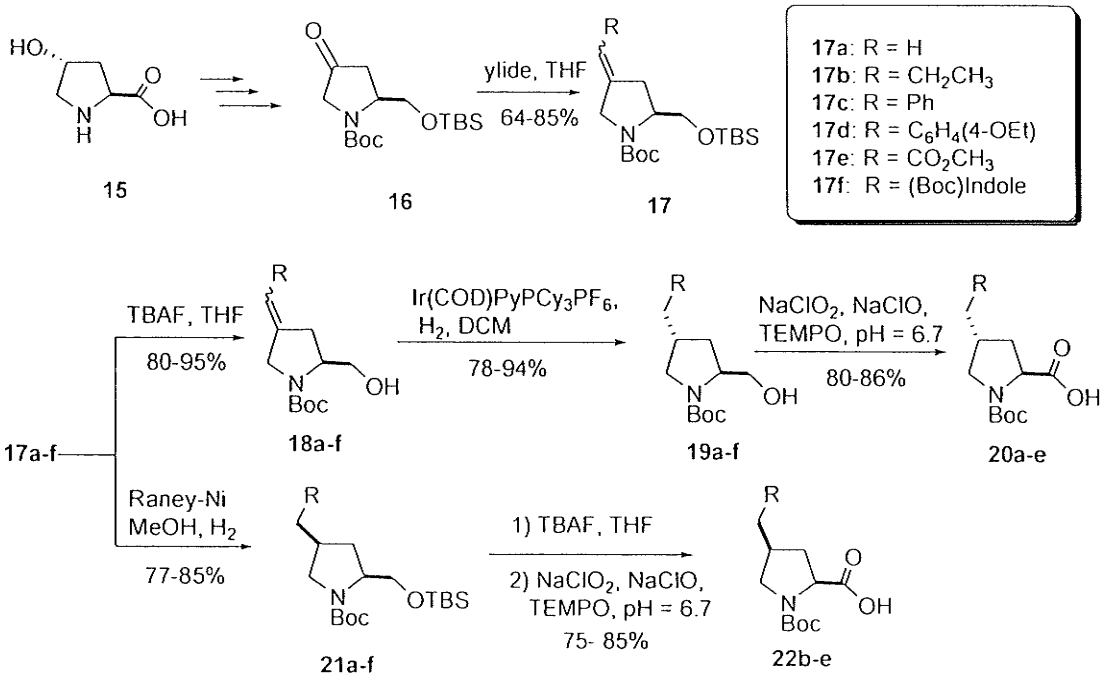

method to control the C-4 stereochemistry. Finally, the oxidation of **19a-e** with TEMPO, 5% sodium hypochlorite solution, and sodium chlorite afforded the desired proline analogues **20a-e**. In the sterically directed synthesis of the *cis*-substituted pyrrolidines, Raney-nickel, as the hydrogenation catalyst, showed an increased selectivity (13:1 < dr < 22:1) over Pd/C (dr ≈ 3:1) for the reduction of **21a-f**. Desilylation and oxidation of **21b-e** afforded *cis*-substituted proline analogues **22b-e**. Unfortunately, the oxidation of indolylprolinols **19f**, **21a** and **21f** using various conditions failed to give the desired product **20f**, **22a** and **22f**. This strategy provides to control the stereochemistry at theC^{γ}-position, but fails to introduce more hindered groups into this position.

Recently, Rissanen *et al* have reported a synthesis of γ-*tert*-butyl proline analogues **28** and **29** (Scheme 1.4).[35] It has been shown that the bulky *tert*-butyl group is commonly

Scheme 1.4 Synthesis of *N*-Boc-protected γ-*tert*-butylprolines

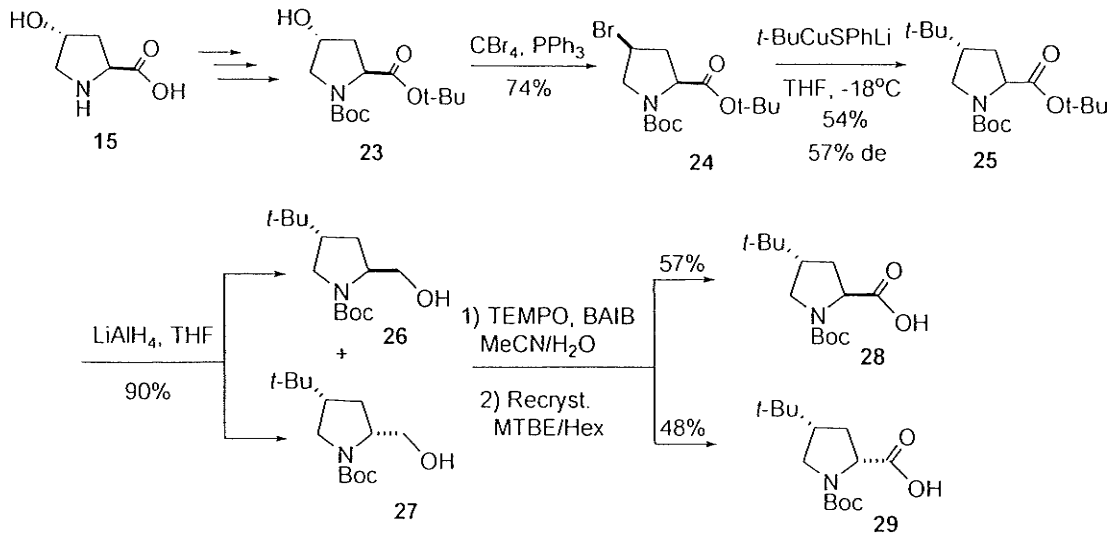

used to lock ring conformations due to its tendency to orient equatorially for spatial and entropic reasons. For proline, this approach has previously been applied to C^{β}- and C^{δ}-positions,[36,37] in which *tert*-butyl substituents sterically interfere with the peptide backbone. Whereas introduction of this bulky group at C^{γ} is expected not to interfere with the peptide backbone and solely lock the ring conformation.

The synthesis begins with the preparation of ester **23** from *trans*-4-hydroxyproline using routine chemistry. The hydroxyprolinate **23** is then submitted to a Mitsunobu-type bromination to afford the bromo prolinate **24**. The bromo-substitutent is substituted with a *tert*-butyl group in a Corey-House reaction using *tert*-butylthiophenolcuprate as the nucleophile to give an inseparable mixture of γ-*tert*-butylprolinates **25**. For the sake of separation, compound **25** is reduced to the separable diastereomers **26** and **27.** Finally, TEMPO-catalyzed oxidation of **26** or **27** followed by recrystallization provided the *trans* isomer **28** and *cis* isomer **29** with high enantiopurity.

The spectral simulation and DFT modeling indicates that both *cis*- and *trans*-γ-*tert*-butyl groups in the model peptides *N*-Ac-*trans*-γ-^{t}BuPro-*N'*-OMe **30** and *N*-Ac-*cis*--γ-^{t}BuPro-*N'*-OMe **31** (Figure 1.5) strongly favor a pseudoequatorial orientation, thereby causing opposite puckering effects for the pyrrolidine ring: C^{γ}-endo for *trans*-γ-*tert*-butyl-*L*-proline and C^{γ}-exo for *cis* -4-*tert*-butyl-*D*-proline.

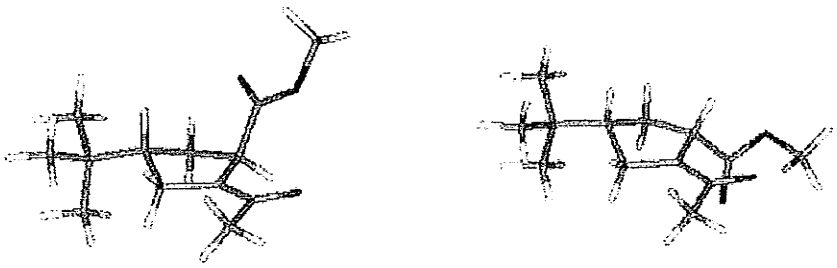

trans-L-endo **30** *cis-D*-exo **31**

Figure 1.5 DFT B3LYP 6-31G* geometry optimized conformation in model peptides **30** and **31**.[35]

1.2.1.4. C^{δ}-proline analogues

One representative example for this class of compounds is the δ-*tert*-butylproline analogue,[38] which dramatically enhances the *cis* population and induces a type VI β-turn conformation. The type VI β-turn is a relatively rare secondary structure that features an amide *cis* isomer *N*-terminal to a proline residue situated at $i + 2$ position of the peptide bend.[39,40] This conformation plays important roles in protein folding. They have been shown to be recognition sites for peptidyl prolyl isomerases (PPIases) which can accelerate protein folding by catalyzing the conversion of the *cis* isomer to its more thermodynamically stable *trans* isomer.[41,42] Type VI β-turns have also been implicated in other important recognition events of bioactive proteins. For example, a type VI β-turn conformation has been proposed for thrombin catalyzed cleavage of the V3 loop of HIV gp120, a prerequisite to viral infection.[43] In addition, in the X-ray structure of the ribonuclease S protein, a type VIa β-turn is located at the central position of a hairpin conformation.[40] Type VI β-turns are classified into two sub-types based on the dihedral

angle values of their central i + 1 and i + 2 residues (Table 1.1).[40] In the type VIa β-turn, the proline ψ-dihedral angle is equal to 0 °, and a 10-membered intramolecular hydrogen

Table 1.1 Main chain torsion values for ideal type VI β-turns

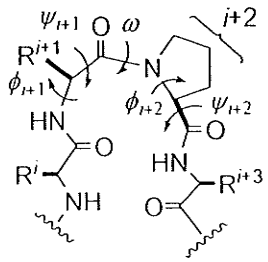

Conformation	ϕ_{i+1}	ψ_{i+1}	ω	ϕ_{i+2}	ψ_{i+2}
β VIa turn	-60	120	0	-90	0
β VIb turn	-120	120	0	60	150

bond exists between the carbonyl oxygen of the i residue and the amide hydrogen of the i + 3 residue. This intramolecular hydrogen bond is not present in the type VIb β -turn in which the proline ψ-dihedral angle value is equal to 150 °.

Because of the biological importance of prolyl amide *cis* conformer[44] stabilization of this geometry is of great interest in medicinal chemistry and biology. Lubell and co-workers have reported the synthesis of δ-*tert*-butylprolines (Scheme 1.5).[38] Their synthesis begins with the intermediate **34**, which is prepared from glutamate **32** by a two-step procedure: Initially, treatment of **32** with lithium bis(trimethylsilyl)amide and pivaloyl chloride provides β-ketoester **33**; Secondly, the hydrolysis and decarboxylation of **33** under basic condition give the acid **34**. For the preparation of

(2*S*,5*R*)-5-*tert*-butylproline **37**, esterification of acid **34** is accomplished with standard conditions to give methyl ester **35**. A one-pot reductive amination/nitrogen protection process is applied to prepare the desired proline analogues **36**: cleavage of PhF with

Scheme 1.5 Synthesis of (2*S*,5*R*)-5-*tert*-butylproline **37** and (2*S*,5*S*)-5-*tert*-butylproline **39**

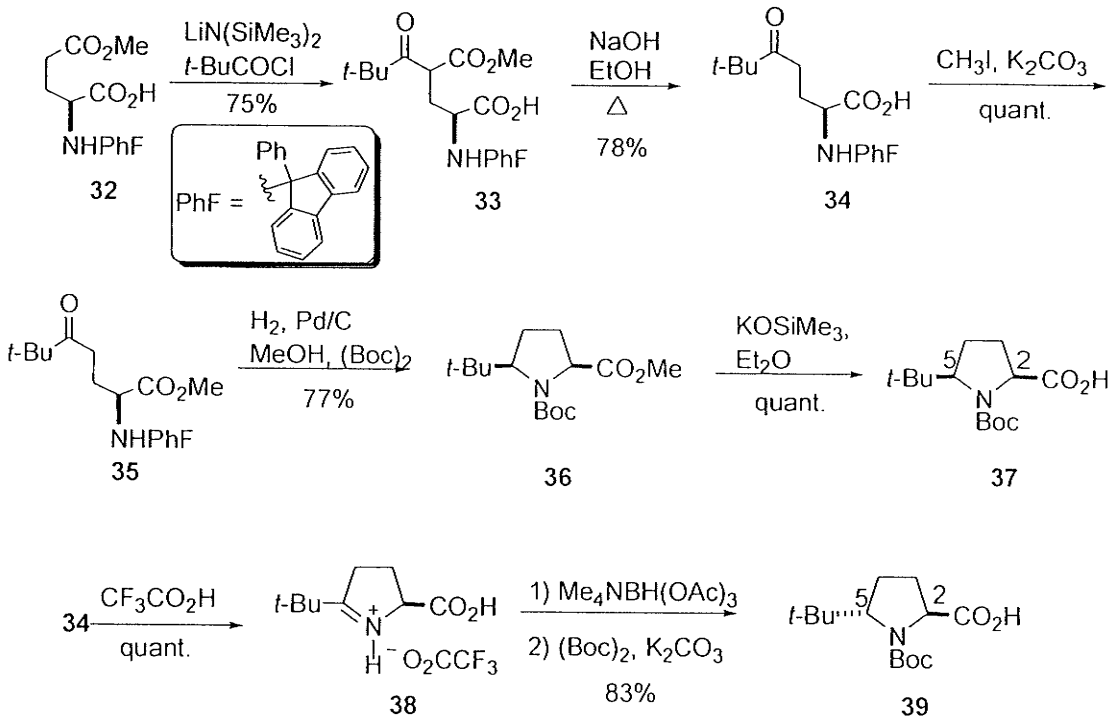

hydrogenation, cyclization with intramolecular reductive amination and Boc-protection of nitrogen. Finally, the hydrolysis of methyl ester **36** with potassium trimethylsilanolate furnishes (2*S*,5*R*)-5-*tert*-butylproline **37**. But for the synthesis of (2*S*,5*S*)-5-*tert*-butylproline **39**, a different procedure is used. Treatment of acid **34** with trifluoroacetic acid provided the imino acid **38**, which is reduced with

tetramethylammonium triacetoxyborohydride to give the desired *trans* diastereomer **39**.

Table 1.2 Amide isomer equilibrium of prolyl *N*-aceyl *N'*-methyl amides in D_2O

trans *cis*

Compd.	R_1	R_2	*cis* (±3%)	$\triangle G^{\neq}$ (kcal/mol)	$\triangle G$ (kcal/mol)
9	H	H	27	20.4	0.57
40	*t*-Bu	H	49	16.5	0.03
41	H	*t*-Bu	66	20.2	-0.38

As shown in Table 1.2, δ-*tert*-butylproline analogues **40** and **41** increase the *cis* population relative to **9** (27%) in water.[45] The augmented *cis* population is also reflected in the thermodynamic parameters: a smaller $\triangle G$ value demonstrates a smaller energy between two rotamers in (5*R*)-^{t}BuPro derivatives. Alternatively, a negative value of $\triangle G$ indicates a predominant population of *cis*-rotamer. The lower barrier for isomerization of compound **40** may be due in part to the steric effect on the ψ dihedral angle, because the *C*-terminal NH group at $\psi \approx 0^{\circ}$ may stabilize the pyramidalized amide transition states by interacting with either the nitrogen lone pair or the carbonyl oxygen. In diastereomer **41**, the dihedral angle $\psi \approx 125^{\circ}$ results in the absence of this stabilizing effect in the transition state.

Incorporation of (5*R*)-^{t}BuPro into dipeptides Ac-Xaa-5-^{t}BuPro-NHMe or tetrapeptides

Ac-Xaa-Yaa-5-^{t}BuPro-Zaa-NHMe (or OMe) was carried out by the same group.[36a] NMR studies indicated a high *cis* population (65-95%) in water. The circular dichroism (CD) spectrum (190 ± 5 nm (negative, strong), 230 ± 10 nm (negative, weak), 205 ± 6 nm (positive, strong)) demonstrated the existence of type VIa β-turn conformation in dipeptides. In tetrapeptides Ac-Ala-Phe-5-^{t}BuPro-Zaa-OMe (Zaa = Ala, Lys) the amide proton at i + 3 residue is involved in hydrogen bonding in DMSO. As an effective VIa-β-turn inducer, 5-*tert*-butylproline promises to find use in structure activity relationships (SAR) of VIa-β-turn mimetics.

The compound 5,5-dimethylproline (dmP)[46] is another proline analogue used to stabilize the *cis* conformer through the steric interaction. Tyr-Pro-Asn (YPN) and Asn-Pro-Tyr (NPY) are the fragments of bovine pancreatic ribonuclease (RNase A), in which the X-Pro peptide bond in the *cis* conformation. Replacement of Pro with dmP results in the tripeptides Ac-Tyr-dmP-Asn (YdmPN) and Ac-Asn-dmP-Tyr (NdmPY).[47] YdmPN is found to exist solely in the *cis* conformation, whereas NdmPY is found to have 90% *cis* conformer. Both YdmPN and *cis*-NdmPY adopt a type VI reverse turn.

1.2.1.5. Fused bicyclic proline analogues

Bicyclic proline analogues[48] have been studied as angiotensin,[49] bradykinin,[49] thyroliberin,[50] and glutamic acid[51] analogues and have served as building blocks for the synthesis of peptidomimetics.[48,52] Besides these applications, conformationally

constrained proline analogs and its derivatives have gained considerable importance in asymmetric synthesis. [53,54]

The fused arylprolines are challenging synthetic targets that have potential to serve phenylalanine-proline and phenylglycine-proline chimeras in structure-activity studies of biologically relevant compounds. For example, indoline-2-carboxylate has been used to develop ACE inhibitors related to the drugs captopril[55,56] and enalapril.[57] Kuwano *et al*[58] have developed a straightforward synthetic method (Scheme 1.6), in which the catalytic asymmetric hydrogenation of indoles **42** is accomplished by use of the $[Rh(nbd)_2]SbF_6$-PhTRAP-base catalyst, providing a variety of optically active indolines **43** with up to 95% ee in high yield (83-98%).

Scheme 1.6 Asymmetric synthesis of indole-prolines

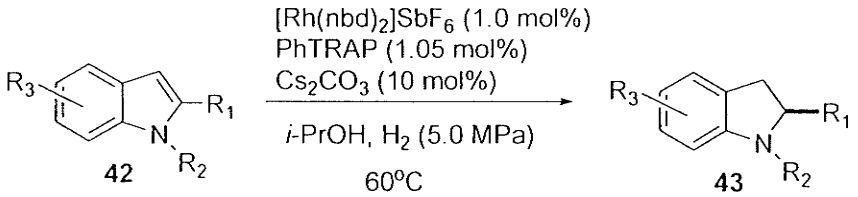

R_1 = CO_2Me, Ph, Bu, ^{t}Bu
R_2 = Ac, Boc
R_3 = H, *p*-Me, *p*-CF_3, *m*-OMe

Recently, Jeannnotte *et al* [59] have reported the synthesis of other arylproline analogs termed pyrrole-prolines. The method involves the aldol condensation of ketone **44** with *N*-(Boc)-α-amino aldehydes **45**, followed by acid-induced cyclization of the

β-hydroxyketone intermediate **46** to yield the pyrrole **47** (Scheme 1.7). This approach may be amenable to diversity oriented synthesis. In particular, *N*-alkylation allows synthesis

Scheme 1.7 Synthesis of protected pyrrole-proline **47**.

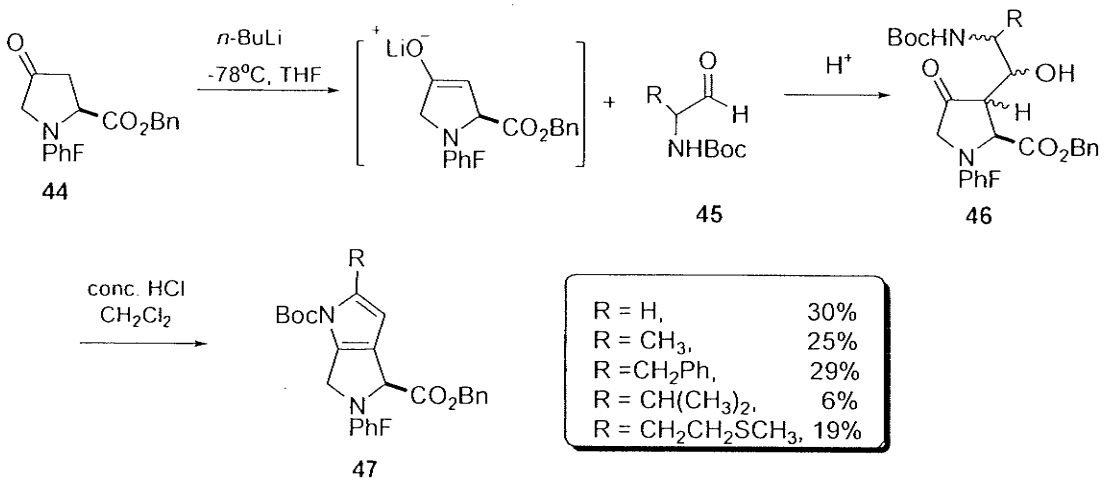

of a variety of fused arylproline analogues from a common intermediate. The directionality of the pyrrole could prevent racemization and oxidation of the neighboring pyrrolidine ring.

1.2.2. Replacement of one carbon of the pyrrolidine ring with other elements

1.2.2.1. Pseudoproline (ΨPro)

Pseudoprolines are a class of compounds in which a carbon atom of the pyrrolidine ring is replaced by a sulfur or oxygen atom. Pseudoprolines are readily accessible by cyclization of Ser, Thr, or Cys with aldehydes or ketones (Figure 1.6).[60]

Variation of the *C*-2 substituents within the heterocyclic system results in different physicochemical and conformational properties. NMR studies of a series of pseudo-proline (ψPro)-containing peptides reveal a pronounced effect of the *C*-2

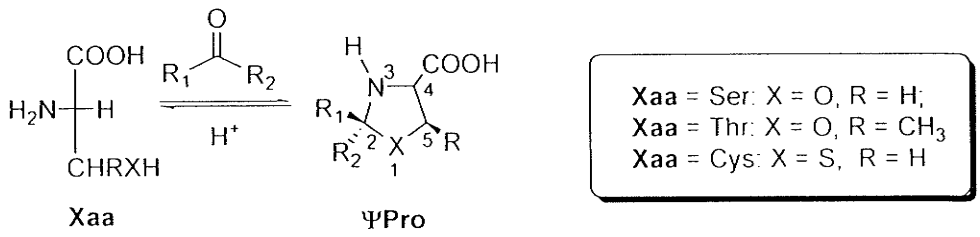

Figure 1.6 ΨPro are obtained by condensation reaction of aldehyde or ketone with Xaa = Ser, Thr and Cys.

substituents upon the *cis* to *trans* ratio of the adjacent amide bond in solution (Table 1.3).[61] *C*-2 unsubstituted systems show a preference similar to that of the proline residue for the *trans* form, whereas 2, 2-dimethylated derivatives exhibit a strong preference for the *cis* amide conformation. For 2-monosubstituted ψPro, the *cis/trans* distribution depends on the *C*-2 chirality. For the 2-(*S*)-diastereoisomer, both forms are rather equally populated in solution, whereas the 2-(*R*)-epimer adopts preferentially the *trans* form. The results suggest that, by tailoring the degree of substitution, pseudo-prolines may serve as a temporary proline mimetic or as a hinge in peptide backbones.

Table 1.3 *Cis* to *trans* ratio of peptides Ac-Ala-Xaa[Ψ^{R_1, R_2}pro]-NHMe and succinyl -Val-Xaa [Ψ^{R_1, R_2}pro]-Phe- NH-pNA in DMSO

ΨPro	R_1	R_2	R	Xaa	X	cis (%)
1	Me	Me	H	Ser	O	~100
2	Me	Me	Me	Thr	O	~100
3	Me	Me	H	Cys	S	~100
4	H	H	H	Ser	O	~33
5	H	H	H	Pro	CH_2	~18
6	biphenyl	H	H	Ser	O	~63
7	H	H	H	Ser	O	~15
8	Me	Me	H	Ser	O	>95
9	H	PMP	H	Ser	O	~10
10	PMP	H	H	Ser	O	~50

1.2.2.2. Silaproline (Sip)

Silaproline (Sip) is a proline analog in which the γ-methylene carbon is substituted by the dimethylsilyl group. Replacement of Sip for Pro in peptides should increase lipophilicity because the octanol-water partition coefficient of Sip was experimentally determined to be 14 times greater than that of Pro.[62] Increased lipophilicity may therefore facilitate membrane permeability. Reduced sensitivity to enzymatic degradation may also arise from substitution of Sip for Pro in peptides. Moreover, the similarity of the Sip and Pro rings should result in similar conformational properties for analogous Sip- and Pro-containing peptides. The synthesis begins with the Schöllkopf's bis-lactim ether **48** (Scheme 1.8).[63] Treatment of ether **48** with butyl lithium and (iodomethyl)dimethylsilane provides the diastereomer **49**. The hydrolysis of bis-lactim ether **49** under acidic condition gives the iodide **50** which is treated with DIEA and Boc_2O to afford

Boc-protected cyclized product **51**. Finally, saponification of Boc-Sip-OMe with standard condition leads to the silaproline **52**.

In model di- and tripeptides, silaproline exhibits similar conformational properties as

Scheme 1.8 Synthesis of Silaproline from Schöllkopf's bis-lactim ether

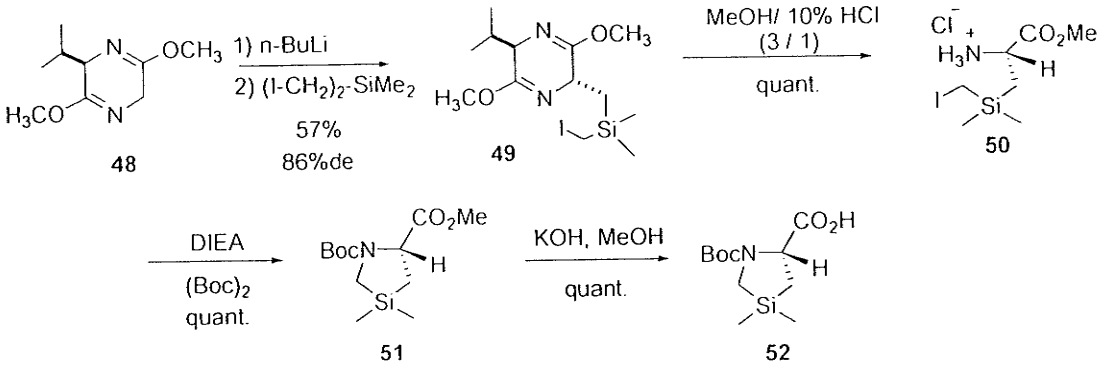

proline.[62] Moreover, the presence of the dimethylsilyl group confers on silaproline a high lipophilicity and improved resistance to biodegradation. For example, an analogue of the *C*-terminal segment NT(8-13) of neurotensin require injection with a cocktail of protease inhibitors to be active, whereas [Sip10]NT(8-13), in which Pro10 is replaced by Sip10, is active without the addition of any ptotease inhibitors.

Recently, Giralt *et al*[64] have incorporated Sip into a Pro-rich cell-penetrating peptide, [CF-VRLPPSip(VRLPPP)$_2$], in which Sip is used to replace Pro-6, which is located in the hydrophobic face of the amphipathic PP II helix. This peptidomimetic causes a 20-fold increase in cellular uptake of the peptide without perturbing secondary structure.

1.2.2.3. Azaproline (azPro)

Azaproline (azPro) contains a nitrogen atom in place of the C^{α} of proline.[65] The azPro can be used to stabilize the *N*-terminal amide *cis* conformer because of the lone pair/lone pair repulsion between the α-nitrogen and *N*-terminal carbonyl oxygen in *trans*

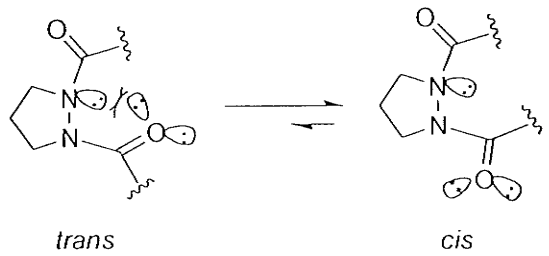

Figure 1.7 Preferred *cis* geometry of azPro *N*-terminal amide

conformer (Figure 1.7).

Recently, Che *et al* have investigated the influence of azPro on the peptide conformation using DFT calculation methods.[66] Compared with *N*-Ac-Pro-*N'*-NHMe, *N*-Ac-azPro-*N'*-NHMe favors a *cis* amide by 3.15 kcal/mol (MP2/6-31+G**). As compared to most types of type VI β-turn mimetics such as δ-^{t}BuPro and δ,δ-dimethylPro, azPro strongly stabilizes the *cis*-amide conformation. In addition, azPro is a fairly conservative replacement of Pro and induces only small changes to the overall steric/geometric structure of Pro, thereby avoiding introduction of steric bulk that could compromise receptor interactions.

1.3. Constrained lysine analogues

The synthesis of conformationally constrained amino acids is of considerable current interest.[3,5,66] In addition to their use as ligands for a wide variety of biological receptors, incorporation of these structural elements into peptide chains can be used to generate novel structures of relevance to biological chemistry and materials science.[67] Lysine, a positively charged basic amino acid, occurs frequently in many cationic antimicrobial peptides (AMPs). Although the mode of action of AMPs is not fully understood, most AMPs appear to manifest their biological action by enhancing the permeability of lipid membranes of bacterial cells. This typically involves initial electrostatic interactions between the positively charged basic side chains of amino acids such as lysine, arginine and ornithine to the negatively charged lipid membrane of pathogens, followed by adoption of an amphipathic α-helical or β-sheet structure.[68,69] However, *in vivo* efficacy studies of several cationic peptide antibiotics have been disappointing most likely due to the fact that many AMPs exhibit poor bioavailability, susceptibility to proteolytic cleavage and low *in vivo* antimicrobial activity.[70] As mentioned early, constrained lysine analogues could be used to increase the stability and specificity of AMPs. A summary of previously synthesized constrained lysine analogues, in which the side chain is partially (**53-55**, **58-60**) or completely (**56**, **57**) restricted, is given in Table 1.4.

Table 1.4 Constrained lysine analogues

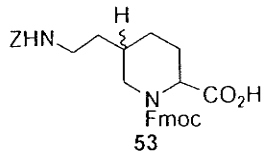 **53** Murray *et al* [71]	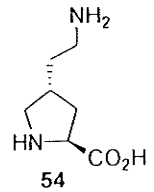 **54** Barkallah *et al* [72]	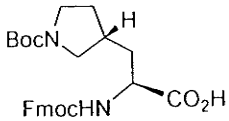 **55** Murray *et al* [73]	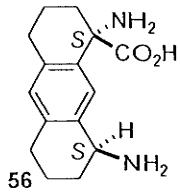 **56** Stalker *et al* [74]
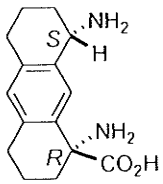 **57** Stalker *et al* [74]	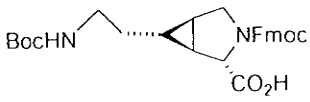 **58** Ganorkar *et al* [75]	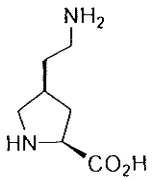 **59** Ganorkar *et al* [75]	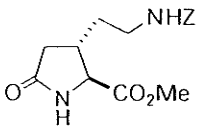 **60** Goswami *et al* [76]

1.4. Glycosamino acids in drug design

As highly functionalized building blocks, glycosamino acids (GAAs) have attracted attention in the field of peptidomimetics, glycomimetics, biopolymers and combinatorial chemistry in the last 15 years.[77] GAAs are molecules that combine the structural features of simple amino acids (amino and carboxylic acid functions) with those of simple carbohydrates (cyclic polyols, which may contain additional acetamido or amino functions).

1.4.1. The concept of GAAs in drug design

Among the major classes of biomolecules, carbohydrates can be infinitely derivatized due to their chiral diversity and high density of functional groups amenable to derivatization. The molecular diversity of carbohydrates offers a valuable tool for drug

discovery in the areas of biologically important peptidomimetics, oligosaccharides, glycoconjugates and molecular scaffolds by investigating their structural and functional impact. For instance, the engineering of an amino acid moiety into the sugar template enables the GAA to be incorporated into short bioactive peptide sequences providing novel peptidomimetics. Additional hydroxyl derivatization of the polyol could increase the lipophilicity of the GAAs and render them likely to permeate cell memberanes. In addition, monosaccarides also provide a rigid molecular scaffold that can be used to reduce the conformational flexibility of peptides. On the other hand, GAAs can be derivatized and oligomerized into compound libraries through well-established automated peptide protocols. This approach is particularly attractive for the preparation of glycomimetic libraries, since oligosaccharide library synthesis has not yet reached the same level of automation as peptide synthesis. Finally, the rich stereochemistry and the high degree of functionalization of GAAs can be used to display pharmacophoric groups in well defined spatial orientations.

1.4.2. Natural occurrence of GAAs

GAAs can be widely found in nature. The most prominent and abundant example is sialic acid, which is found in all living organisms, with the exception of certain bacteria. Many inter- and intracellular molecular recognition events depend on sialic acid residues. In the course of an infection, bacteria and viruses recognize sialic acid-containing structures on the cell surface as adhesion receptors. This family of natural GAAs consists

of *N*- and *O*-substituted derivatives (*O*-methyl, -sulfate, -acetyl, -phosphate, *N*-glycolyl, or free amine) of neuraminic acid **61** (Figure 1.8). Glycosaminuronic acids, **62-65**, are usually found in form of derivatives, such as 2-acetamido-2-deoxy-glucuronic acid, found in bacterial cell walls[78] and 2-acetamido-2-deoxygalacturonic acid as one component of bacterial Vi antigen of *Escherchia coli*.[79] The GAA-based peptidyl nucleoside antibiotic polyoxin (**66**) mimics UDP-N-acetylglucosamine, a substrate of chitin synthase, which catalyzes the final step in the biosynthesis of chitin, an essential component of fungal cell walls.[80] Two different 3-amino-3-deoxy uronic acids, derivatives of 3-amino-3-deoxy-D-

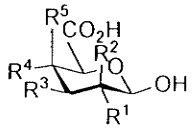

Glycosaminuronic acids		R^1	R^2	R^3	R^4	R^5
Glycosaminuronic acid	**62**	NH_2	H	OH	OH	H
Galactosaminuronic acid	**63**	NH_2	H	OH	H	OH
mannosaminuronic acid	**64**	H	NH_2	OH	OH	H
4-amino-4-deoxy-glucuronic acid	**65**	OH	H	OH	NH_2	H

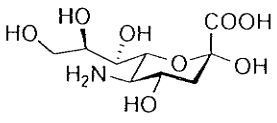

61

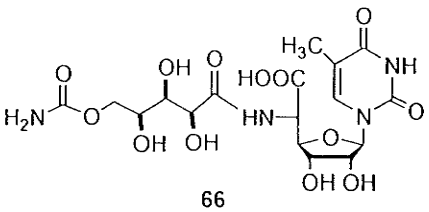

66

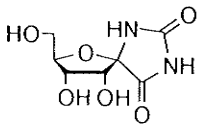

68

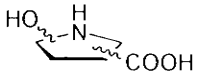

69

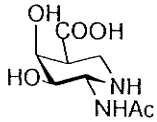

70

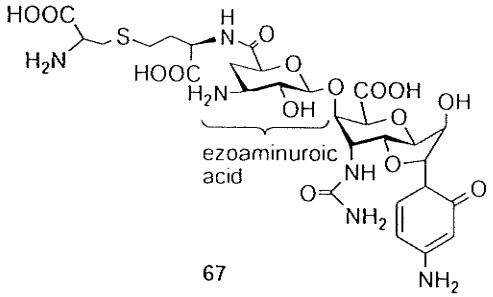

67

Figure 1.8 Naturally occurring GAAs

gulopyranuronic acid and 3-amino-3,4-dideoxy-D-xylohexopyranuronic acid, were found in ezomycine A (**67**).[81,82] The α,α-disubstituted hydantoin derivative **68**, which represents a spirocyclic structure, exhibits potent and selective antiherbal activity with no toxicity to microorganisms and animals.[82] Replacement of endocyclic oxygen atom in the pyranose with a nitrogen atom leads to azasugar-based GAAs found in hydroxylated proline **69**[84] and Siastatin B **70**.[85] Hydroxylated prolines have been shown to significantly influence secondary structures in peptides.[84]

1.4.3. Classification of GAAs

In the last 15 years many types of GAAs have been developed. Schweizer[77] classified 6 types GAAs according to the position of the amino acid moiety on the cyclic polyol. Herein we will focus on A_0 and A_1 GAAs which are relatively well studied (Figure 1.9). A_0 GAAs have also been termed sugar amino acids (SAAs), which are compounds with two immediate linkages of the amino and carboxy functionalities to the carbohydrate frame. Kessler's group and Fleet's groups have developed various synthetic routes to prepare A_0-type GAAs (SAAs).[86,87] Whereas A_1 GAAs are formed by linking the amino acid moiety adjacent to the endocyclic oxygen such as the anomeric position. Several approaches to this class of compounds have been developed by Dondoni and co-workers.[88]

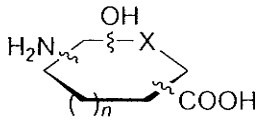

A_0

(sugar amino acids (SAAs))

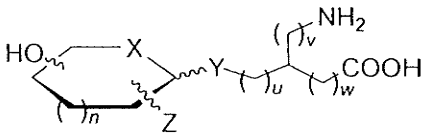

A_1

Figure 1.9 A_0-A_1 types of GAAs. n = 0, 1, 2,...; X = O, S, P...;Y = CH, CH_2, S, O, NHCO, NR; u = 0, 1, 2, ...; v = 0, 1, 2...; w = 0, 1, 2...; Z = NHAc, OH, H.

In the following section, some of the current approaches to the synthesis of pyranose-templated A_1 GAAs (X = O, n = 1, Y = CH, CH_2, Z = NHAc, OH, H) is summarized. In addition, incorporation of A_0- or A_1-type GAAs into peptidic structures and their potential use in medicinal chemistry are discussed.

1.4.4. Synthesis of pyranose-templated A_1 GAAs

In this class of compounds the entire α-amino acid group $(CH)_v(NH_2)CO_2H$ (v = 1) is connected either directly or through an all carbon tether to the anomeric carbon of the pyranose. The tether can be a saturated or an unsaturated carbon chain or part of an aromatic ring.

1.4.4.1. Pyranose-based *C*-glycosyl glycine

These compounds exhibit a single carbon-carbon bond holding the glycinyl group to the anomeric carbon atom of the pyranoid ring. Dondoni *et al* provided an elegant approach to overcome the problem of controlling the stereochemistry at the anomeric center of the sugar moiety.[89] The key step consists of the construction of the glycinyl

moiety via addition of a suitable *C*-nucleophile (2-lithiothiazole **71** or 2-lithiofuran **72**) to the nitrone group linked in a stereochemically well-defined manner to anomeric carbon of the sugar moiety. Specifically, the nitrone group serves as the precursor of the amino group and the thiazole or furan ring as the precursor of carboxylate function (Figure 1.10). The above procedure is employed to prepare the epimers **77** and **78** starting from the

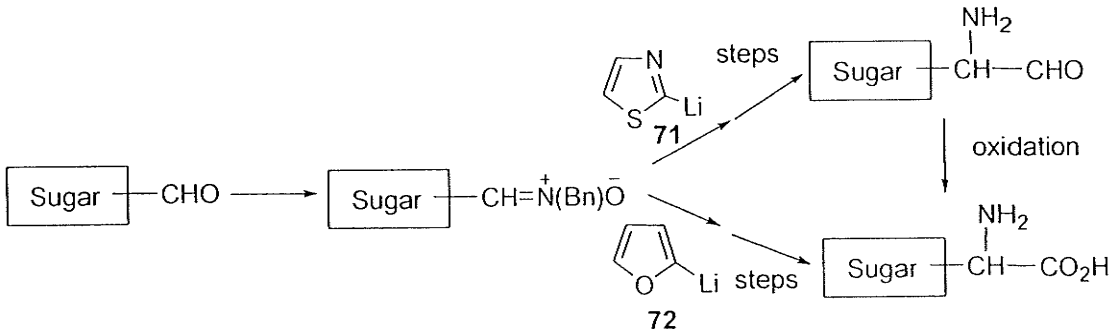

Figure 1.1 Nitrone approach to *C*-glycosyl glycine

galactoside nitrone **74** (Scheme 1.9). However, the addition of 2-lithiothiazole **71** to **74** affords mixtures of *N*-benzylhydroxylamine **75** and **76** in a 3 to 1 ratio. The assignment of the structure of these compounds is based on a CD study of the corresponding *N*-Boc amines. According to earlier observations on similar compounds, the *R*- and *S*-isomers are characterized by the positive and negative Cotton effect, respectively. The lack of stereo-control as observed in the addition of 2-lithiothiazole **71** to **74** may be a limitation on the use of this nitrone-based approach to *C*-glycosyl glycine.

Scheme 1.9 Synthesis of epimers **77** and **78** through Dondoni's nitrone approach

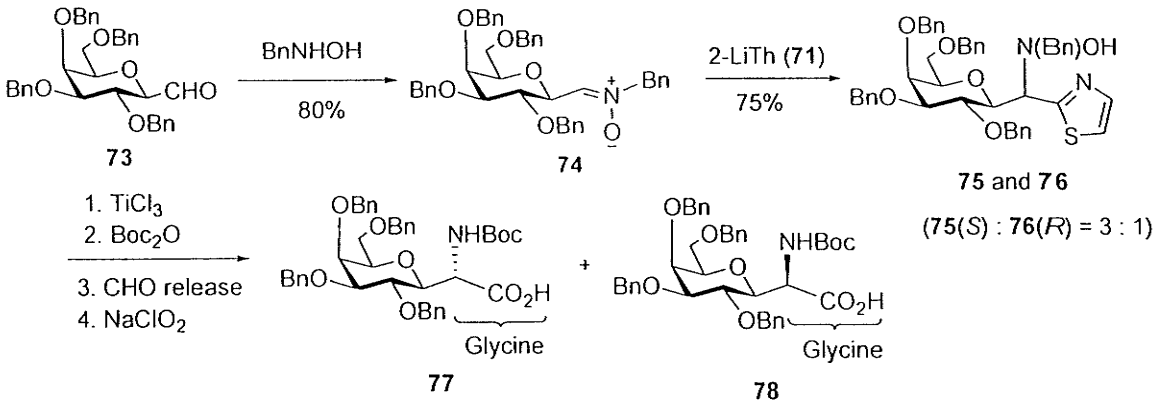

73 74 75 and 76 (75(*S*) : 76(*R*) = 3 : 1) 77 78

1.4.4.2. *C*-glycosyl alanine

Axon and Beckwith have reported an efficient route to synthesize a *C*-glycosyl alanine, in which sugar unit is connected to methyl group of alanine (Scheme 1.10).[90] The *L*-alanine precursor is converted into a chiral methyleneoxazolidinone, such as the *R*-enantiomer **81**. The $Bu_3SnH/NaCNBH_3$-promoted radical addition of the peracetylated iodosugars **79** (D-*galacto*) and **80** (D-*gluco*) to **81** affords the corresponding α-linked

Scheme 1.10 Synthesis of *R*-configured *C*-glycosyl alanine

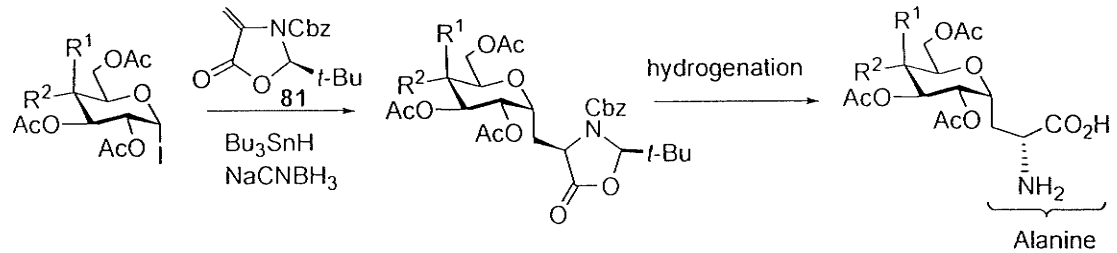

79 R^1 = OAc, R^2 = H
80 R^1 = H, R^2 = OAc

82 R^1 = OAc, R^2 = H (73%)
83 R^1 = H, R^2 = OAc (88%)

84 R^1 = OAc, R^2 = H (92%)
85 R^1 = H, R^2 = OAc (100%)

C-glycosides **82** and **83** as single diastereomers, respectively. Subsequent hydrogenolysis

of these compounds proceeds almost quantitatively to afford the α-D-galactosyl D-alanine **84** and the α-D-glucosyl isomer **85**. Evidently, in both cases the addition of **81** occurs exclusively on the α-face of the glycosyl radical. In a similar fashion, the hydrogen-atom transfer to the intermediate oxazolidinoyl radical occurs with high stereoselectivity in an *anti* manner to the *tert*-butyl group. Hence, the original configuration of the *L*-alanine appears to have been inverted in the resulting *C*-glycosyl amino acids.

1.4.4.3. Preparation of *C*-glycosyl serines and asparagines from the chiral amino aldehyde 87

The *C*-glycosyl serines can be considered formally derived from *O*-glycosyl serines (Figure 1.11, left) by replacement of the anomeric *O*-glycosidic linkage with a carbon

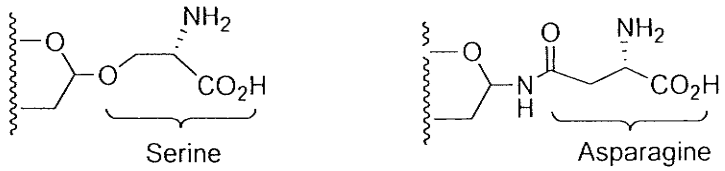

Figure 1.11 Natural glycosyl serines (left) and asparagines (right)

-carbon bond. Similarily, *C*-glycosyl asparagines are the analogues of *N*-glycosyl asparagines (Figure 1.11, right) wherein the anomeric amidic bond has been substituted by a carbon-carbon bond.

The synthesis of these *C*-glycosyl amino acids started with readily accessible

N–Boc–*N,O*–isopropylidine-D-serinal **87**.[91] For example, D-galactosylmethyl phosphonium salt **86** is coupled with the amino aldehyde **87** through a Wittig-type reaction to afford the olefin **88** as a mixture of *Z*- and *E*-isomer (7:1 ratio) in 62% isolated yield (Scheme 1.11).[92] This mixture is reduced with diimide, and the resulting *C*-galactoside **89** is transformed into *C*-galactosyl *N*-Boc L-serine **90** using Jones reagent. The hydrolysis-oxidation of the oxazolidine ring to carboxylic acid is accomplished in a single step.

Scheme 1.11 Synthesis of *C*-β-D-galactosyl serine.

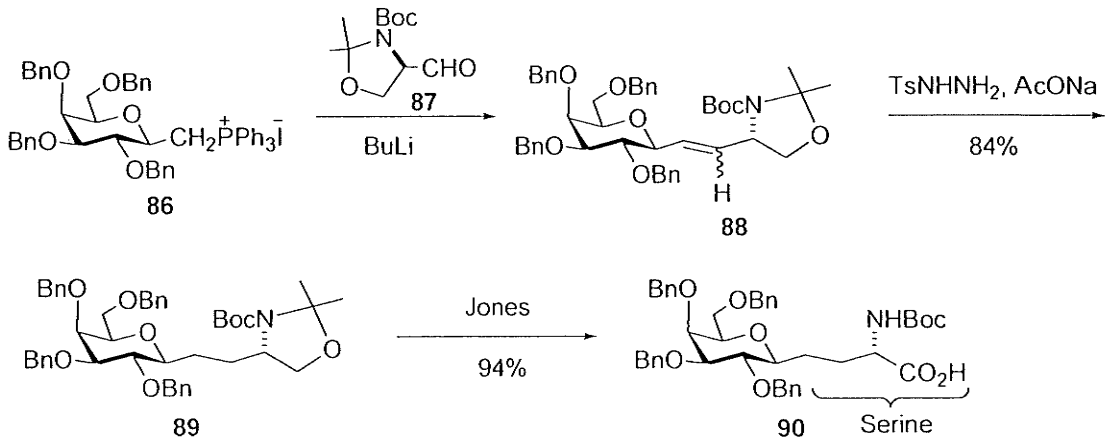

On the basis of this work, Dondoni and coworkers have developed a versatile approach that allowed an entry to the α- and β-anomers of various *C*-glycosyl asparagines.[93] The coupling of configurationally stable anomeric sugar acetylenes with the chiral amino aldehyde **87** constitutes the key carbon-carbon bond-forming reaction for the construction of the five carbon atom linkage to the anomeric center of the selected sugar. This method

is illustrated in Schemes 1.12 and 1.13 with the synthesis of the *C*-analogues of α-D- and β-D-linked GalNAc *L*-asparagines. Identical reaction conditions are used in both cases.

Initially, the sugar acetylene (**91** or **94**) is metalated with LHMDS and then reacts with the amino aldehyde **87**. The resulting propargylic alcohol (**92**, 52%, or **94**, 75%) is reduced by the diimide and deoxygenated using Barton-McCombie conditions, and the oxazolidine ring is oxidatively cleaved with Jones reagent to the glycinyl moiety to give the target α-amino acid (**93** or **96**).

Scheme 1.12 Synthesis of α-D-GalNAc *L*-asparagine

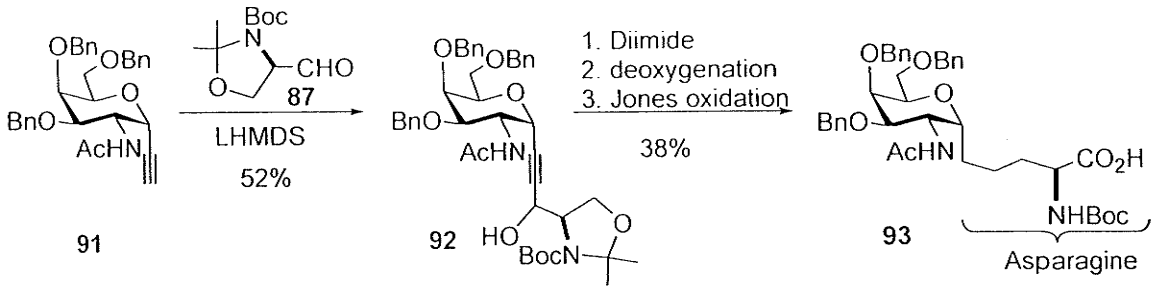

Scheme 1.13 Synthesis of β-D-GalNAc *L*-asparagine

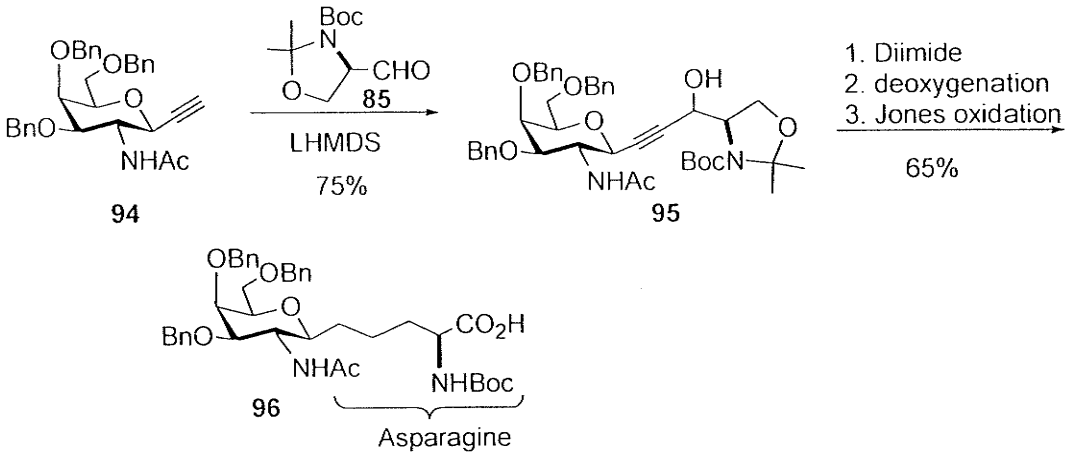

Based on the above method, other ethylene isosteres of *C*-glycosyl asparagines have been prepared and their structures are shown in Table 1.5.

Table 1.5 Ethylene isosteres of *C*-glycosyl asparagines

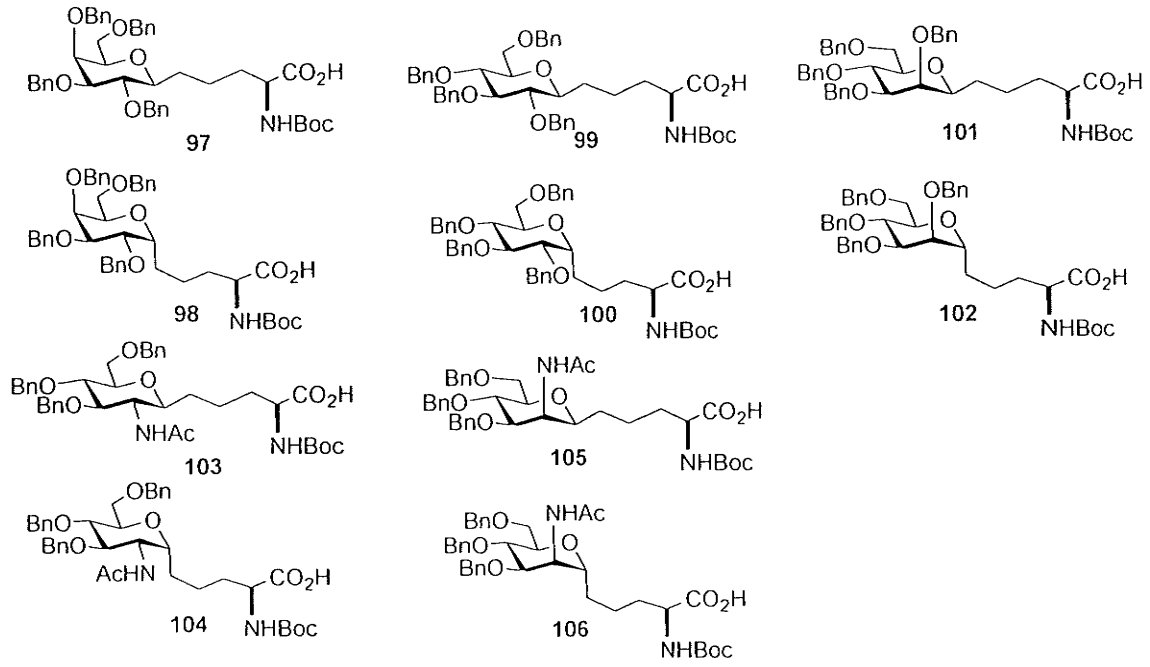

In addition, other types of *C*-glycosyl asparagine isostere are represented by **109** and **110** shown in Scheme 1.14.[94] These compounds feature only the substitution of the NH of the amide group by a CH_2. The key step for the assembly of the carbohydrate and amino acid moieties involves a Horner-Emmons-Wadsworth olefination and Michael addition between the protected *N*-acetylglucosamine **107** and the aspartic acid-derived *β*-ketophosphonate **108**. The coupling product is obtained in satisfactory yield (53%) under suitable conditions (CsOH in MeOH, room temperature). Nonetheless, the reaction

Scheme 14. Synthesis of *C*-glycosyl asparagine isosteres **109** and **110**

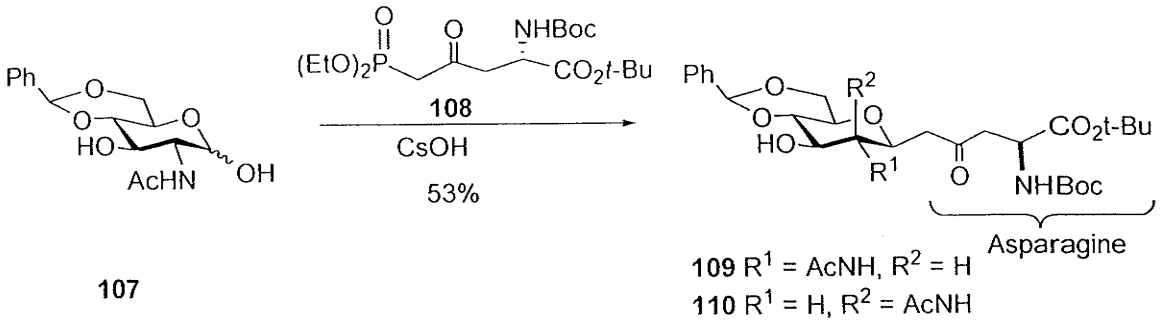

affords a 1:1 mixture of *C*-glycoside isomers that after separation by chromatography is characterized as the GlcNAc derivative **109** and the ManNAc isomer **110**.

1.4.4.4. *C*-glycosyl tyrosine

The synthesis of a unique *C*-glycosyl tyrosine, featuring a methylene group instead of phenolic oxygen of tyrosine (Figure 1.12), is reported by Gallagher and co-workers[95] The method relies on two coupling reactions with organozinc reagents (Scheme 1.15),

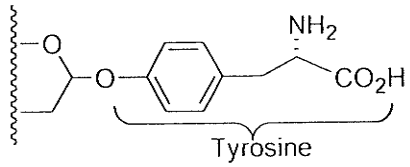

Figure 1.12 Natural *O*-linked glycosyl tyrosine

wherein the *C*-glycosidic linkage is formed by the boron trifluoride etherate-promoted addition reaction of the 4-iodobenzyl bromide derived zinc reagent **112** with the D-glucal **111**. The introduction of the glycinyl moiety on compound **115** is carried out using the

iodoalanine-derived zinc reagent **114** and Pd(0)-mediated catalysis.

Scheme 1.15 Synthesis of α-D-mannopyranose *L*-tyrosine.

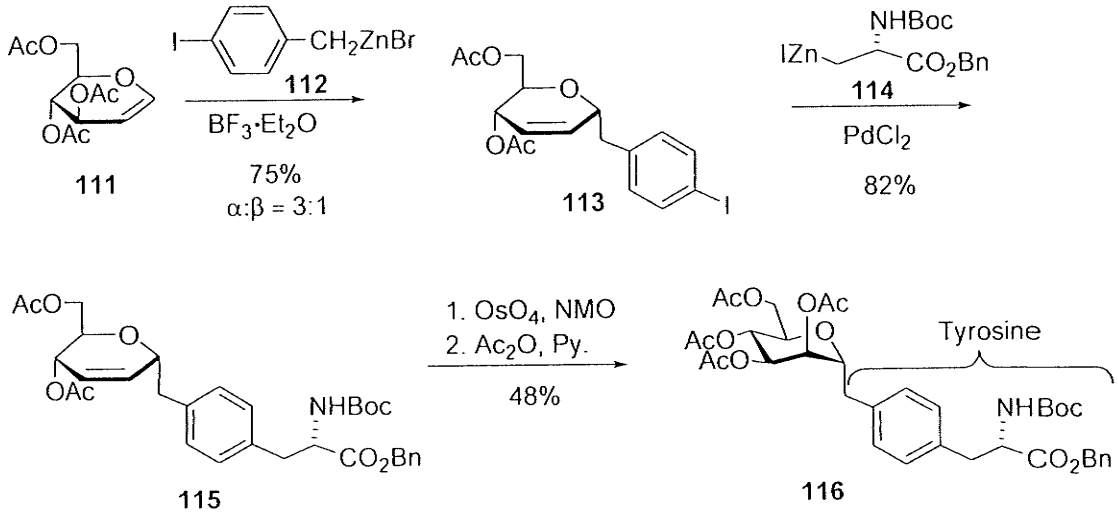

The osmium-mediated *cis*-dihydroxylation of the glycal **115** affords the final sugar amino acid **116** in 23% overall yield from **111**.

1.4.4.5. *C*-glycosyl tryptophan

The stereoselective synthesis of a naturally occurring *C*-glycosyl tryptophan **117** (Figure 1.13) and incorporation into a peptide has been described by Manabe and Ito.[96] Taking advantage of parallel studies on *C*-glycosylation of *N*-protected indoles via metalation at the C-2 position and coupling with 1,2-anhydro-D-mannose **118**, a convergent synthetic approach was developed starting from the indole derivative **119**

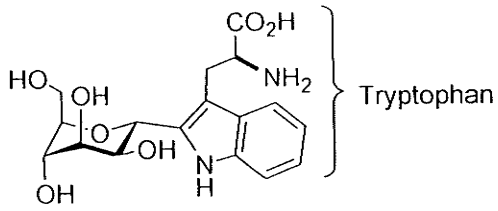

117

Figure 1.13 Naturally occurring *C*-glycosyl tryptophan **117**

(Scheme 1.16). The latter reagent served as a precursor of the tryptophan moiety that is readily prepared from commercially available *L*-tryptophanol. The coupling reaction of

Scheme 1.16 Synthesis of *C*-glycosyl tryptophan **117**

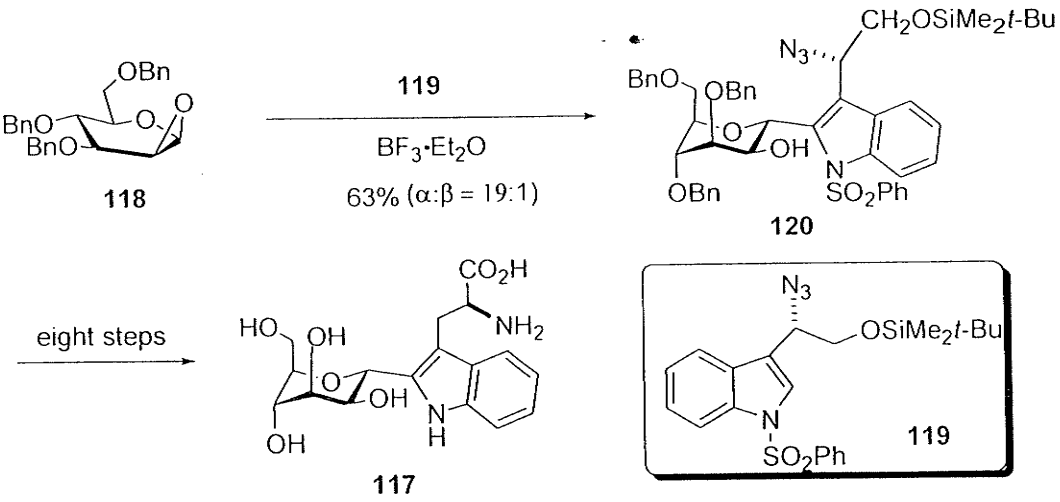

118 and **119** affords the α-linked *C*-glycoside **120** in satisfactory chemical yield (63%). The subsequent transformation of **120** to D-mannopyranosyl-*L*-tryptophan **117** was achieved using standard synthetic methodology involving two functional group conversions (oxidation of alcohol function to a carboxylic acid and reduction of the azido

group to an amino group) and deblocking.

1.4.4.6. Other pyranoid-based GAA_1 (Table 1.6)

A list of other pyranose-based GAA_1 structure is provided in Table 1.6.

Table 1.6 Other pyranoid-based GAA_1

C-glycosyl glycine

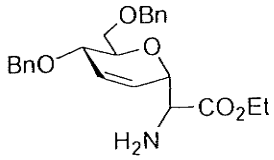

121

(*R*) and (*S*)
Wernicke *et al* [97]

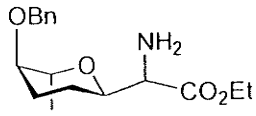

122

(*R*) and (*S*)
Frappa *et al* [98]

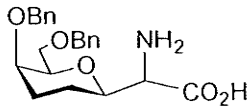

123

(*R*) and (*S*)
Brakta *et al* [99]

C-glycosyl alanine

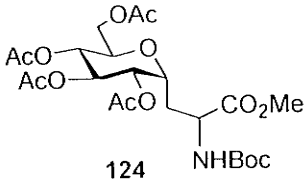

124

(*R*) and (*S*)
Gurjar *et al* [100]

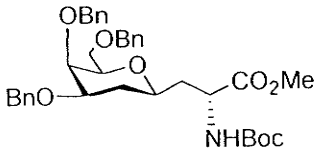

125

Liberknecht *et al* [101]

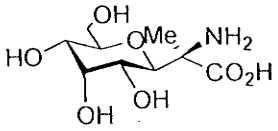

126

Colombo *et al* [102]

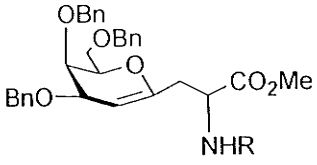

127

Vidal *et al* [103]

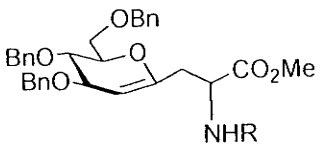

128

Vidal *et al* [103]

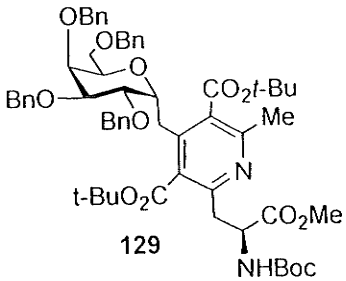

129

Dondoni *et al* [104]

continued on next page

Table 1.6 (*continued*)

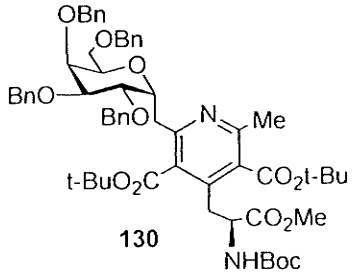

130

Dondoni *et al* [104]

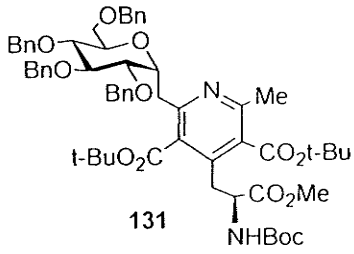

131

Dondoni *et al* [104]

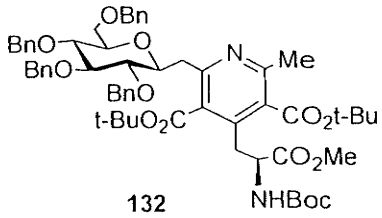

132

Dondoni *et al* [104]

C-glycosyl serine

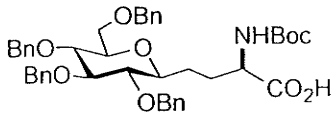

133

Campbell *et al* [105]

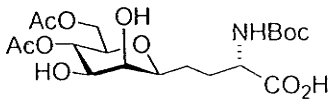

134

Dorgan *et al* [106]

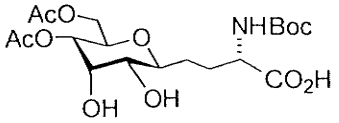

135

Dorgan *et al* [106]

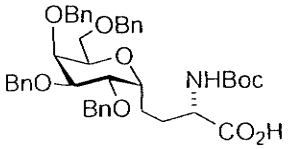

136

Dondoni *et al* [107]

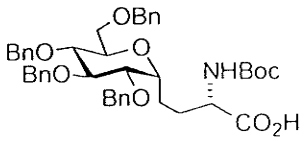

137

Dondoni *et al* [107]

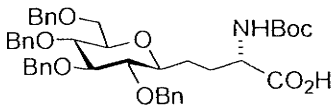

138

Dondoni *et al* [107]

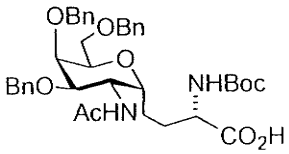

139

Urban *et al* [108]

C-glycosyl hydroxylysine

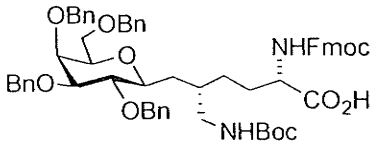

140

Gustafsson *et al* [109]

C-glycosyl tyrosine

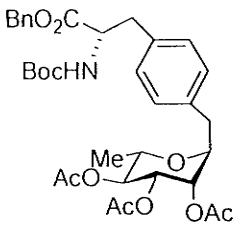

141

Pearce *et al* [95]

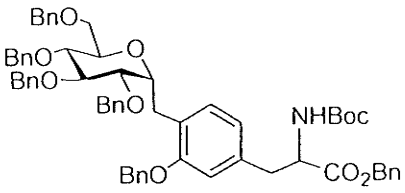

142

Brenna *et al* [110]

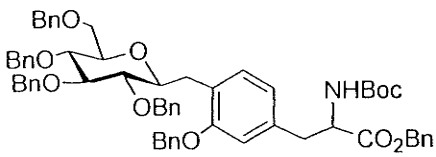

143

Brenna *et al* [110]

1.4.5. Bicyclic glycosyl amino acids (BGAAs)

With their rigid and well-defined conformations, BGAAs have been used as reverse turn mimics, and spiro BGAAs have been used in particular to constrain peptides. A series of GBAAs are shown in Table 1.7.

Table 1.7 Glycosyl bicyclic amino acids

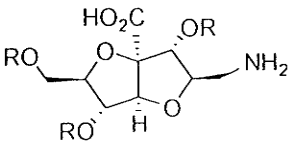

144

Cipolla et al.[111]

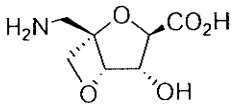

145

Van Well et al[112]

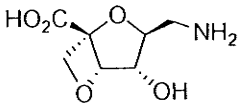

146

Van Well et al[112]

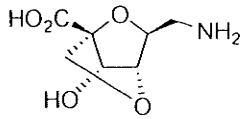

147

Van Well et al[113]

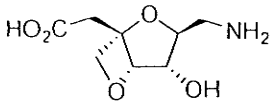

148

Van Well et al[113]

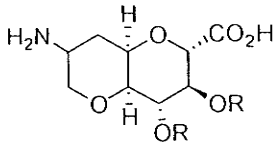

149

(*R*) and (*S*); Grotenbreg et al[114]

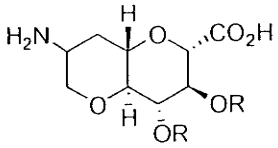

150

(*R*) and (*S*); Risseeuw et al[115]

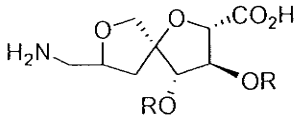

151

(*R*) and (*S*); Peri et al[116]

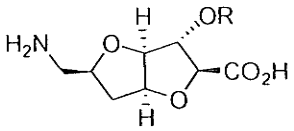

152

Peri et al[116]

1.4.6. Carbohydrate-based peptidomimetics.

1.4.6.1. A_0 GAAs-based peptidomimetics

1.4.6.1.1. Types of turn structure

Protein secondary structures are believed to be important structural domains involved in molecular recognition processes and protein folding. In this respect, tight turns are being studied in detail. Depending on the number of residues forming the turn, the tight

turns are classified as δ-turns, γ-turns, β-turns, α-turns and π-turns.[117] Among these tight turns, β- and γ-turns have been studied in detail and precisely classified because of their higher occurrence in protein and peptides.

1.4.6.1.1.1. β-turn and classification

A β-turn is a region of the protein involving four consecutive residues where the polypeptide chain folds back on itself by nearly 180 degrees.[118] The turn region may or may not be stabilized by an intra-turn hydrogen bond between the backbone CO (i) and the backbone NH(i+3). Although there are many definitions for classification of β-turns, the Richardson classification is the system most widely used at present.[119] He has suggested there are only 7 distinct types (I, I', II, II', VIa, VIb and VIII) based on ϕ, ψ

Table 1.8 Main chain torsion values for other ideal types of β-turns

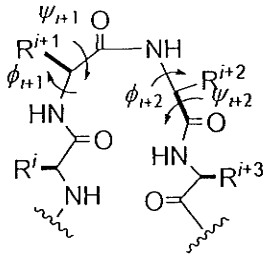

Conformation	ϕ_{i+1}	ψ_{i+1}	ϕ_{i+2}	ψ_{i+2}
I	-60	-30	-90	0
I'	60	30	90	0
II	-60	120	80	0
II'	60	-120	-80	0
VIII	-60	-30	-120	120
IV	-	-	-	-

ranges (Table 1.8), along with a miscellaneous category IV. Since type VI β-turns have been introduced earlier (Table 1.1), other types of β-turns are here summarized in Table 8.[120]

1.4.6.1.1.2. γ-turn and classification

A γ-turn involves three amino acid residues and the intra-turn hydrogen bond between the backbone CO(i) and the backbone NH(i+2). Two types of γ-turn, classical and reverse (Table 1.9), have been defined based on ϕ, ψ angles.

Table 1.9 Main chain torsion values for the types of γ-turns

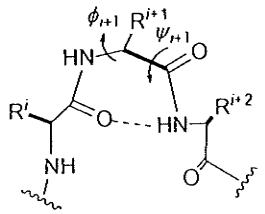

Conformation	ϕ_{i+1}	ψ_{i+1}
Classic	75	-64
Reverse	-79	69

1.4.6.1.2.Turn mimetics

Since proteins tend to exert their biological activity through only small regions of their folded surfaces, their functions could in principle be reproduced in much smaller designer molecules that retain these crucial surfaces. There are many options for modifications, such as introduction of constraints, cyclization, and/or replacement of the peptidic

backbone or part of it to stabilize the bioactive conformation and fine tune pharmacokinetics. Some of these modifications can be achieved via incorporation of carbohydrate moieties into the side chain of amino acids that results in the formation of sugar amino acids (SAAs).

SAAs can adopt robust secondary turn or helical structures and thus have the potential to mimic helices or sheets. They can be used as substitutes for single amino acids or as

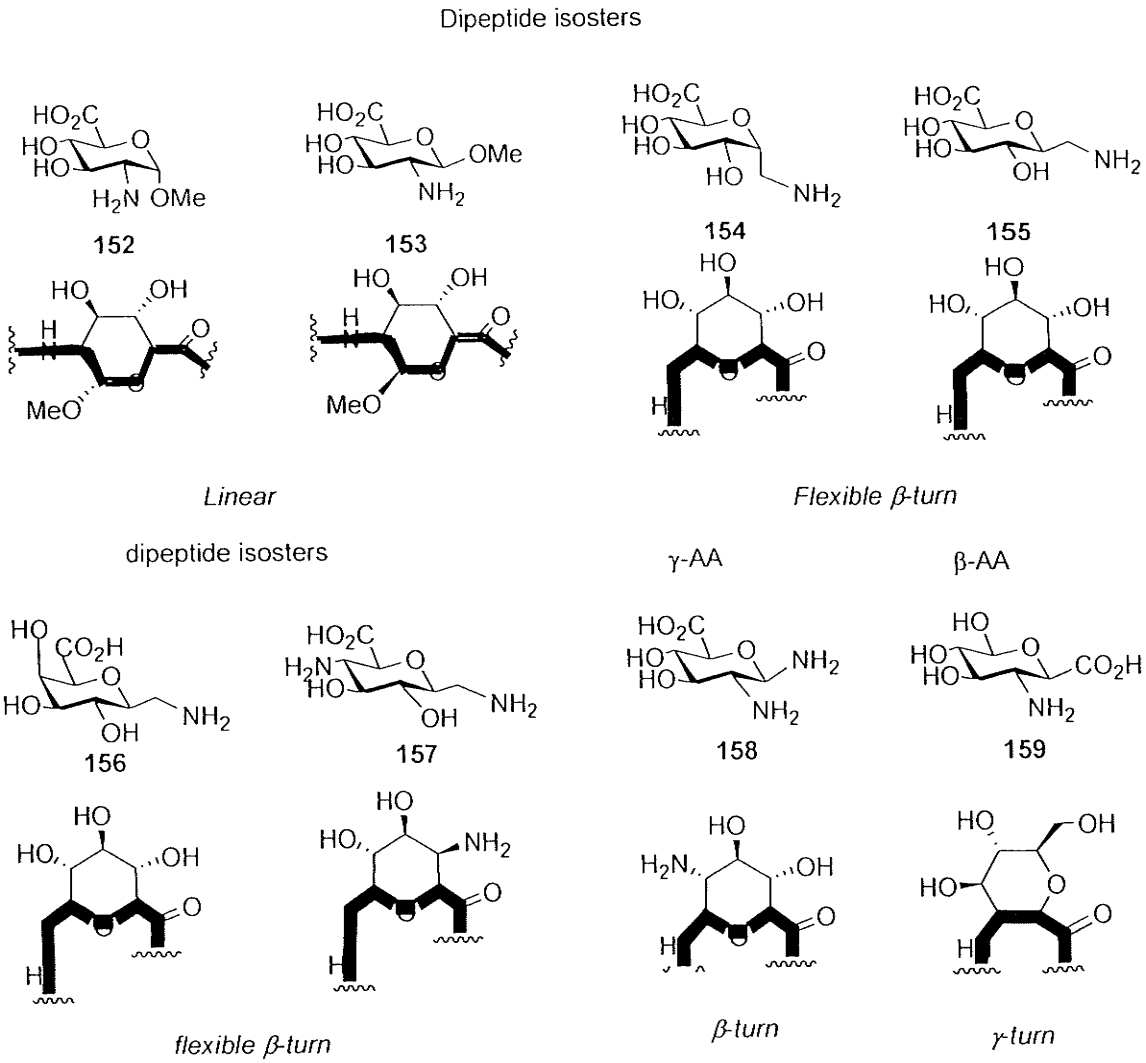

Figure 1.14 Extended SAA construction kit

dipeptide isosters. If used as replacement of hydrophobic residues, the sugar can also be functionalized with hydrophobic side chains (e.g., they may be benzylated), however, if hydrophilic residues are replaced, or if solubility should be improved, the sugar hydroxyl groups can be unprotected or functionalized with hydrophilic residues.

Kessler's group has explored the conformational influence of SAAs **152-159** on the peptide backbone conformations.[121,122] The results show SAA can be used to produce the secondary structure of synthetic peptides as effective turn-inducers (Figure 1.14),[121] SAAs **154-158** induce β-turns independent of the substitution pattern of the sugar ring while SAA **159** mimics a γ-turn.

1.4.6.1.3. Bioactive peptides containing A_0 GAAs

1.4.6.1.3.1. Somatostatin Analogues

Somatostatin is a 14-residue cyclic peptide hormone formed in the hypothalamus. It plays an important role in a large number of physiological actions. For instance it inhibits the release of growth hormone (GH),[123,124] and plays a role in the inhibition of insulin secretion.[125,126] Interestingly, of all bioactive peptides, it was a somatostatin analogue that first incorporated a SAA. The SAA used is glucosyluronic acid methylamine (GUM) **155**.[127] Starting from the cyclic somatostatin analog *cyclo*(-Phe-Pro-Phe-D-Trp-Lys-Thr-) **160**,[125] the SAA **155** is used as a dipeptide isostere to replace the amino acids phenylalanine and proline, forming *cyclo*[SAA **155**-Phe-D-Trp-Lys-Thr-] **161** (Figure

1.15), in which SAA **155** induces a β-turn.[121]

Biological tests show that **161** has an inhibition constant (IC_{50}) of 0.15 μM in displacing the receptor-bound radioligand [^{125}I]Try^{11} somatostatin-14 in AtT20 cell membranes obtained from mice hypophysis. In fact, compound **161** is only 75 times less active than **160**. This is particularly remarkable, since **161** does not contain the lipophilic residues on both sides of the active tetrapeptide sequence that are considered to be important for high somatostatin activity.[128,129]

More recently, it has been demonstrated that the furanoid-based SAA **162**-containing cyclic somatostatin analogues **163** and **164** exhibit strong antiproliferative and apoptotic activity against multidrug-resistant hepatoma carcinoma (Figure 1.16).[130] This is of

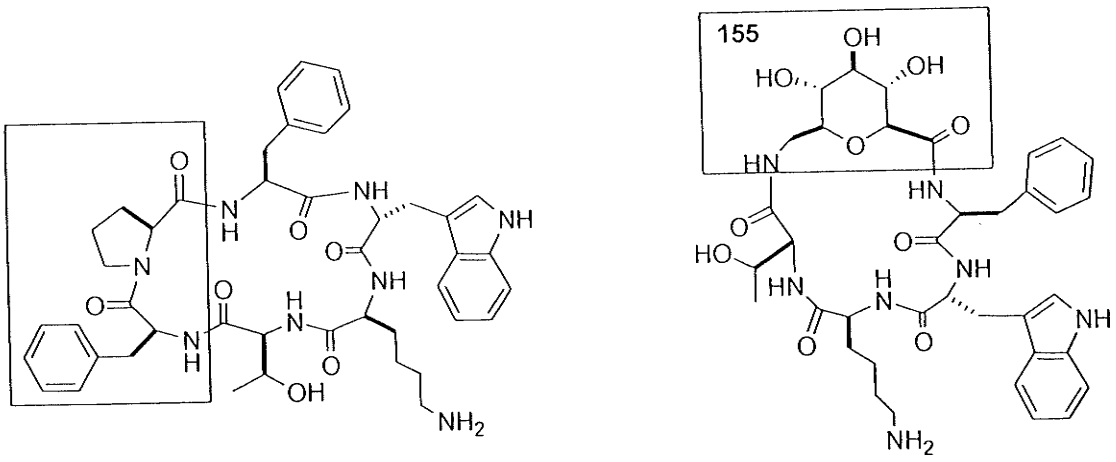

160 161

Figure 1.15 Somatostatin analogs **160** and **161**.

special interest, since resistance to chemotherapy has become a major problem in cancer therapy. The biological tests indicate an aromatic residue in the Thr^{10} position is required

for high antiproliferative and apoptotic activity. The IC_{50} values are 75 and 47 μM for compound **163** and 31 and 25 μM for compound **164** for drug sensitive and multidrug-resistant hepatoma cancer cell lines, respectively. This makes them promising lead compounds for potential chemotherapeutic drugs against multidrug-resistant hepatoma carcinoma. Preliminary results have shown that activity can be enhanced by replacement of the D-Trp with *L*-benzothienylalanine (Bta) resulting in compound **165** or

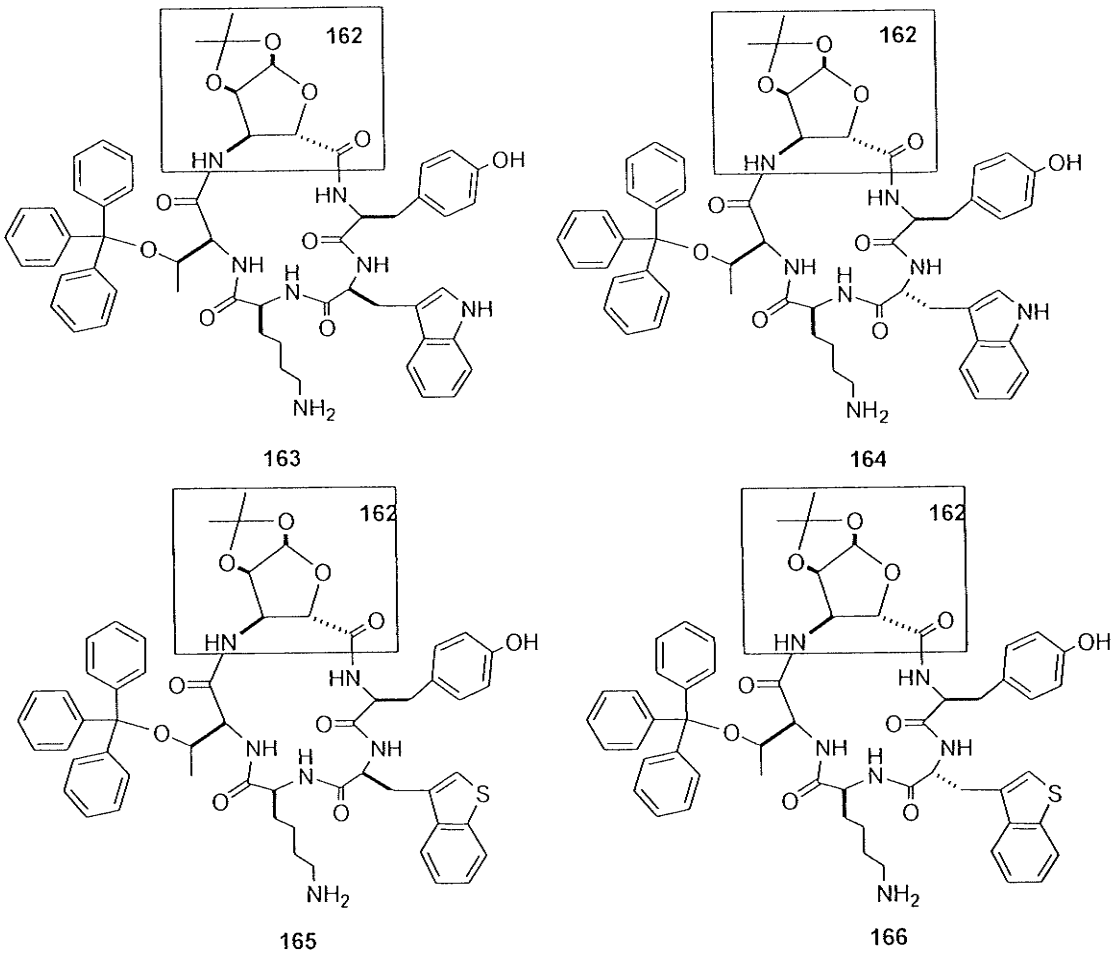

Figure 1.16 Somatostatin analogs **163-166** containing furanoid-based SAA **162**.

D-Bta compound **166**. These compounds are more active than TT232

(*cyclo*[2,6]-D-Phe-Cys-Tyr-D-Trp -Lys-Cys-Thr-NH_2);[131] the only other compound known that shows apoptotic and antiproliferative activity against multidrug-resistant carcinoma cell lines. Thus, by introducing SAA **162** into the peptide backbone, pharmacokinetic properties can easily be improved, and enzymatic stability of the compounds will most likely be enhanced.

1.4.6.1.3.2. Gramicidine S (GS)

Gramicidin S (GS, Figure 1.17) is an amphiphilic cyclic decapeptide having the C_2-symmetrical sequence *cyclo*(Pro-Val-Orn-Leu-DPhe)$_2$ that acts as an antibiotic by targeting the membrane lipid bilayer.[132,133] Upon accumulation into the lipid bilayer, GS induces lysis, with bacterial cell death as the ultimate result. The ability of GS to interact with the bacterial membrane is attributed to its amphiphilic nature, with the two basic Orn residues occupying one side of the cyclic peptide and the aliphatic Leu and Val residues located at the opposite side.

Peptide antibiotics such as GS that target the lipid bilayer as a whole, and not a specific subcellular target, are of great interest in the search for new antibiotics.[134] In general, bacterial strains can readily become resistant against compounds that interfere with a specific metabolic process, or block a specific enzyme or receptor, by genetically altering the target such that it defies recognition.[135] Gaining resistance against GS would require a strategy that specifically destroys it or blocks its accumulation in the lipid bilayer. Arguably, such alterations are less easily attained through genetic mutations. However,

GS appears rather indiscriminate toward the nature of the lipid bilayer and kills mammalian cells with equal efficiency. For instance, GS displays potent hemolytic activity, and it is for this reason that the use of GS in human medicine is restricted to topical applications.[132,136]

In order to understand the mode of action with which GS disrupts lipid bilayers, Grotenbreg and co-workers have synthesized GS-based analogues **167a-d** (Figure 1.17) in which one of the two type II' β-turns was replaced with SAAs.[137] NMR studies demonstrated that **167a-d** had a distorted β-hairpin structure in which one of two

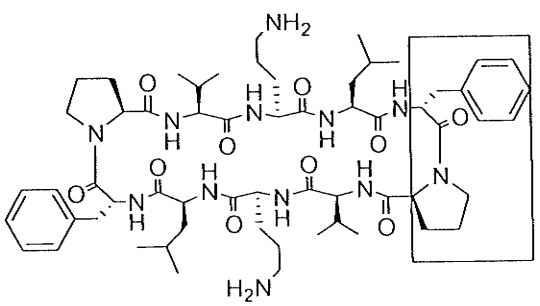

GS

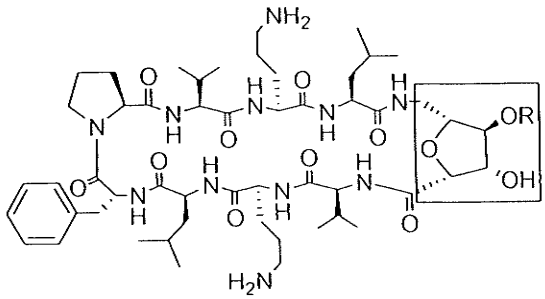

167a: R = H
167b: R = benzyl
167c: R = biphenyl
167d: R = naphthyl

Figure 1.17 GS and GS-based analogues **167a-d**

hydroxyl functionalities of the SAA moiety is involved in an intra-residue hydrogen bond, as compared to GS. Examination of the biological activity revealed aromatic SAA-containing GS analogues **167b-d** exhibit similar antimicrobial activity as GS, with a concomitant increase in hemolytic activity. Whereas **167a** shows a dramatically reduced

antibacterial activity. This finding suggests that hydroxyl derivatization of the polyol provides a tool to improve the bioactivity of peptides.

1.4.6.2. A_1 GAAs-based peptidomimetics

As mentioned earlier, the sensitivity of the glycosidic linkage towards both enzymatic and chemical degradation is problematic. Therefore, it is of great interest to exchange the less stable *O*-glycosidic linkage between amino acid and the carbohydrate to a more stable *C*-linked analogue.

1.4.6.2.1. Mouse hemoglobin (Hb) segment (67-76)

Previous studies have demonstrated that glycoconjugation of mouse Hb VITAFNEGLK can convert the non-immunogenic peptide into strong glycan specific immunogens.[138] In order to develop metabolically stable T-cell glycopeptide antigen

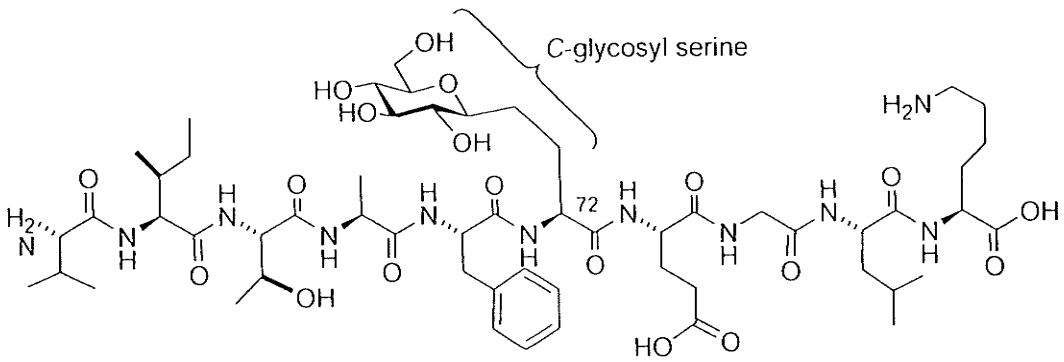

168

Figure 1.18 A decapeptide **168** containing *C*-glycosyl serine.

Meldal *et al* [139] introduced an unprotected *C*-β-D–gluco-pyranosyl serine into the mouse Hb (67-76) to provide *C*-glycosyl decapeptide **168** by the solid phase peptide synthesis (Figure 1.18). However, no information on the biological activity was reported.

1.4.6.2.2. Type II collagen peptide epitope (259-273) from rat

In rheumatoid arthritis (RA), which is regarded as an autoimmune disease, native collagen is attacked and degraded by the immune system, eventually resulting in bone erosion in peripheral joints.[140] In collagen-induced arthritis (CIA), which is a widely used model for RA, immunization of mice with type II collagen (CII) from rat leads to symptoms similar to RA (e.g., erythema and swelling of peripheral joints).[141,142] The CII (259-273) **169** has a galactosylated hydroxylysine in position 264 (Figure 1.19). Previous studies have shown that the fine structure of position 264 is important for the recognition by the T cell receptor.[143]

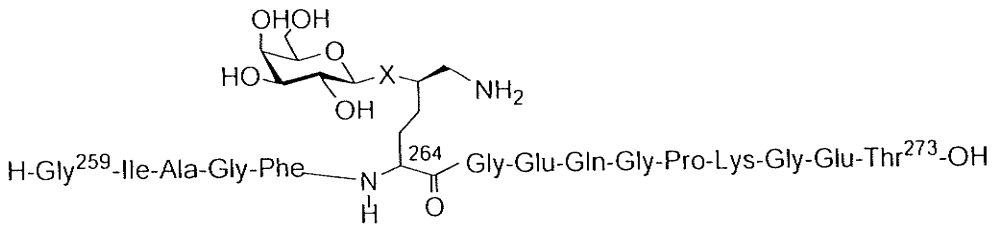

169 X = O
170 X = CH_2

Figure 1.19 Structure of glycopeptides **169** and **170**

Recently, Gustafsson *et al* [109] have synthesized a *C*-glycosyl hydroxylysine **140** (Table

1.6), which is incorporated into position 264 of peptide **169** to replace the labile *O*-glycosidic linkage through the solid phase peptide synthesis. The resulted *C*-glycosyl peptide **170** is evaluated by a preliminary immunological study and found to retain the ability of the corresponding, native *O*-linked glycopeptide **169** to stimulate T cell hybridomas obtained from mice having CIA. The above results indicate *C*-glycosyl amino acid can be used to improve the metabolic stability of native *O*-glycopeptides without affecting their bioactivity.

1.4.6.2.3. SB-219383: a potent, selective inhibitor of bacterial tyrosyl tRNA synthetases

Aminoacyl tRNA synthetases perform a crucial role in protein biosynthesis, catalyzing the attachment of an amino acid onto its cognate *t*RNA.[144] The development of inhibitors of bacterial *t*RNA synthetase (YRS) may give rise to new antibacterial drugs. The natural product, SB-219383, shows strong, selective inhibitory properties to this enzyme.[145] However, it has only weak antibacterial activity, probably attributable to their high polarity preventing penetration into the bacterial cell.

Brown *et al* have found that the bicyclic scaffold is not essential feature for enzyme inhibition.[146] For instance, compound **171** also show equal potency to SB-219383 (Table 1.10). The same group uses the pyranose template to mimic the hydroxylamine-containing ring.[147] As seen in Table 1.10, the *L*-arabinose-derived analogues **172b** is a potent inhibitor of bacterial YRS with an IC_{50} value of 100 nM. The

epimer **172a** is less potent, with an IC_{50} value of 260 nM. In contrast, no inhibition is

Table 1.10 Inhibition of *S. aureus* YRS

Compound	stereochemistry at $C^{1'}$	sugar ring	IC_{50} (nM)
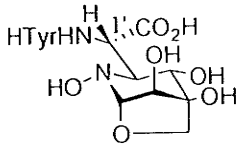 **SB-219383**	*S*		2.0
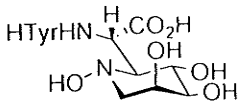 **171**	*S*		1.2
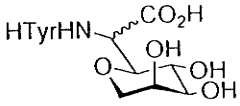 **172**	**172a**: *R* **172b**: *S*	α-L-Arabinose α-L-Arabinose	260 100
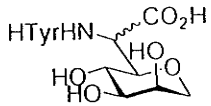 **173**	**173a**: *R* **173b**: *S*	β-D-Arabinose β-D-Arabinose	NI* NI

* NI = no inhibition at 3μM

observed for either of diastereoisomer **173a** or **173b** derived from D-arabinose. By comparison to **171**, the diastereomer **172b** is inferred to have the "*S*" configuration at $C^{1'}$. Compound **172b** was also tested against mammalian YRS and showed no inhibition up to 3 μM indicating that the bacterioselectivity seen in the hydroxylamine series has been retained.

The above results demonstrate that subtle changes in the stereochemistry of the carbohydrate moiety influence the bioactivity of the glycopeptide. As a result, it appears that the rich stereochemistry provided by the carbohydrate scaffold provides a promising tool for drug discovery.

1.5. References:

1. Halverson, K.; Fraser, P. E.; Kirschner, D. A.; Lansbury, P. T., Jr. *Biochemistry* **1990**, *29*, 2639.
2. Giannis, A.; Kolter, T. *Angew. Chem. Int. Ed. Engl.* **1993**, *32*, 1244.
3. Gante, J. *Angew. Chem. Int. Ed. Engl.* **1994**, *33*, 1699.
4. Grant, S. K.; Meek, T. D.; Metcalf, B. W.; Petteway, S. R. Jr. *Biomed. Appl. Biotechnol.* **1993**, *1*, 325.
5. Fletcher, M. D., Campbell, M. M. *Chem. Rev.* **1998**, *98*, 763.
6. Brandits, J. F.; Halvorson, H. R.; Brennan, M. *Biochemistry* **1975**, *14*, 4953.
7. Schmid, F.X.; Baldwin, R. L. *Proc. Nat. Acad. Sci. U.S.A.* **1978**, *75*, 4764.
8. Nall, B. T. In *Protein Refolding*; Gierasch, L. M., King, J., Eds.; AAAS Press: Washington, DC, 1990; pp 198-207.
9. Hurle, M. R.; Marks, C. B.; Kosen, P.A.; Anderson, S.; Kuntz, I. D. *Biochemistry* **1990**, *29*, 4410.
10. Jackson, S. E.; Fersht, A. R. *Biochemistry* **1991**, *30*, 10436.
11. Stryer, L. *Biochemistry*, 4th ed.; W. H. Freeman and Company: New York, 1999.
12. Kakinoki, S.; Hirano, Y.; Oka, M. *Polym. Bull.* (Berlin) **2005**, *53*,109.
13. Reddy, K.V. R.; Yedery, R. D.; Aranha, C. *Int. J. Antimicrobial Agents* **2004**, *24*, 536.
14. (a) Vitagliano, L.; Berisio, R.; Mazzarella, L.; Zagari, A. *Biopolymers* **2001**, *58*, 459. And references therein. (b) Pearce, G.; and Ryan, C. A. *J. Biol. Chem.* **2003**, *278*, 30044. And references therein.
15. Buku, A.; Faulstich, H.; Wieland, T.; Dabrowski, J. *Proc. Natl. Acad. Sci. USA*. **1980**, *77*, 2370.
16. Nakajima, T.; Volcani, B. E. *Science* **1969**, *164*, 1400.
17. Taylor, S. W.; Waite, J. H.; Ross, M. M.; Shabanowitz, J.; Hunt, D. F. *J. Am. Chem. Soc.* **1994**, *116*, 10803.
18. Ellington, J. J.; Honigberg, I. L. *J. Org. Chem.* **1974**, *39*, 104.
19. Smissman, E. E.; Chien, P. L.; Robinson, R. A. *J. Org. Chem.* **1970**, *35*, 104.
20. Madison, V.; Delaney, N. G. *Biopolymers* **1983**, *22*, 869.
21. Delaney, N. G.; Madison, V. *J. Am. Chem. Soc.* **1982**. *104*, 6635.
22. Flippen-Anderson, J. L.; Gilardi, R.; Karle, I. L.;Frey, M. H.; Opella, S. J.; Gierasch, L. M.; Goodman, M.; Madison, V.; Delaney, N. G. *J. Am. Chem. Soc.* **1983**. *105*, 6609.
23. Flores-Ortega, A.; Jimenez, A. I.; Cativiela, C.; Nussinov, R.; Aleman C.; Casanovas, J. *J. Org. Chem.* **2008**, *73*, 3418.
24. (a) Holladay, M. W.; Lin, C. W.; May, C. S.; Garvey, D. S.; Witte, D. G.; Miller, T. R.; Wolfram, C. A. W.; Nadzan, A. M. *J. Med. Chem.* **1991**, *34*, 457. (b) Tilley, J. W.; Danho, W.; Madison, V.; Fry, D.; Swistok, J.; Makofske, R.; Michalewsky, J.; Schwartz, A.; Weatherford, S.; Triscari, J.; Nelson, D. *J. Med. Chem.* **1992**, *35*, 4249. (c) Kolodziej, S. A.; Nikiforovich, G. V.; Skeean, R.; Lignon, M.-F.; Martinez, J.; Marshall, G. R. *J. Med. Chem.* **1995**, *38*, 137.
25. (a) Marshall, G. R. *Tetrahedron* **1993**, *49*, 3547. (b) Plucinska, K.; Kataoka, T.; Yodo, M.; Cody, W. L.; He, J. X.; Humblet, C.; Lu, G. H.; Lunney, E.; Major, T. C.; Panek, R. L.; Schelkun, P.; Skeean, R.; Marshall, G. R. *J. Med. Chem.* **1993**, *36*, 1902.
26. Kaczmarek, K.; Li, K.-M.; Skeean, R.; Dooley, D.; Humblet, C.; Lunney, E.; Marshall, G. R. In

Peptides: Chemistry, Structure and Biology; Hodges, R. S., Smith, J. A., Eds.; ESCOM Science Publishers B.V.: Leiden, Netherlands, 1994; p 687.

27. (a) Mosberg, H. I.; Kroona, H. B. *J. Med. Chem.* **1992**, *35*, 4498. (b) Mosberg, H. I.; Lomize, A. L.; Wang, C.; Kroona, H.; Heyl, D. L.; Sobczyk-Kojiro, K.; Ma, W.; Mousigian, C.; Porreca, F. *J. Med. Chem.* **1994**, *37*, 4371. (c) Nelson, R. D.; Gottlieb, D. I.; Balasubramanian, T. M.; Marshall, G. R. In *Opioid Peptides: Medicinal Chemistry*, NIDA Research Monograph 69; Rapaka, R. S. R. S.; Barnett, G.; Hawks, R. L., Eds.; 1986, p 204.
28. The use of β-alkylprolines in collagenase inhibitors is reported in: (a) Ghose, A. K.; Logan, M. E.; Treasurywala, A. M.; Wang, H.; Wahl, R. C.; Tomczuk, B. E.; Gowravaram, M. R.; Jaeger, E. P.; Wendoloski, J. J. *J. Am. Chem. Soc.* **1995**, *117*, 4671. The use of β-alkylprolines in collagen proline hydroxylase inhibitors is reported in: (b) Hutton, J. J., Jr.; Marglin, A.; Witkop, B.; Kurtz, J.; Berger, A.; Udenfriend, S. *Arch. Biochem. Biophys.* **1968**, *125*, 779.
29. Sharma, R.; Lubell, W. D.; *J. Org. Chem.* **1996**, *61*, 202.
30. Beausoleil, E.; Sharma, R.; Michnick, S. W.; Lubell, W. D. *J. Org. Chem.* **1998**, *63*, 6572.
31. Fisher, s.; Dunbrack, R. L., Jr.; Karplus, M. *J. Am. Chem. Soc.* **1994**, *116*, 11931.
32. (a) Ondetti, M. A.; Cushman, D. W. *Science* **1977**, *196*, 441. (b) Krapcho, J.; Turk, C.; Cushmen, D. W.; Powell,J. R.; Deforrest, J. M.; Spitzmiller, E. R.; Karanewski, D. S.; Duggan, M.; Rovnyak, G.; Schwartz, J.; Natarajan, S.; Godfrey, J. D.; Ryono, D. E.; Neubeck, R.; Atwal, K. S.; Petrillo, E. W. *J. Med. Chem.* **1988**. *31*. 1148.
33. Manfre, F.; Kern, J.-M.; Biellmann, J.-F. *J. Org. Chem.* **1992**, *57*, 2060.
34. Del Valle, J. R.; Goodman, M. *J. Org. Chem.* **2003**, *68*, 3923.
35. Koskinen, A. M. P.; Helaja, J.; Kumpulainen, E. T. T.; Koivisto, J.; Mansikkamaki, H.; Rissanen, K. *J. Org. Chem.* **2005**, *70*, 6447.
36. (a) Halab, L.; Lubell, W. D. *J. Am. Chem. Soc.* **2002**, *124*, 2474. (b) Wallén, E. A. A.; Christiaans, J. A. M.; Saarinen, T. J.; Jarho, E. M.; Forsberg, M. M.; Venäläinen, J. I.; Männistö, P. T.; Gynther, J. *Bioorg. Med. Chem.* **2003**, *11*, 3611.
37. Perni, R. B.; Farmer, L. J.; Cottrell, K. M.; Court, J. J.; Courtney, L. F.; Deininger, D. D.; Gates, C. A.; Harbeson, S. L.; Kim, J. L.; Lin, C.; Lin, K.; Luong, Y.-P.; Maxwell, J. P.; Murcko, M. A.; Pitlik, J.; Rao, B. G.; Schairer, W. C.; Tung, R. D.; Van Drie, J. H.; Wilson, K.; Thomson, J. A. *Bioorg. Med. Chem. Lett.* **2004**, *14*, 1939.
38. Beausoleil, E.; L'Archeveque, B.; Belec, L.; Atfani, M.; Lubell, W. D. *J. Org. Chem.* **1996**, *61*, 9447.
39. (a) Wilmot, C. M.; Thornton, J. M. *J. Mol. Biol.* **1988**, *203*, 221. (b) Rose, G. D.; Gierasch, L. M.; Smith, J. A. *Adv. Protein Chem.* **1985**, *37*, 1.
40. Müller, G.; Gurrath, M.; Kurz, M.; Kessler, H. *Proteins: Struct., Funct. Genet.* **1993**, *15*, 235.
41. Reviewed in: (a) Fischer, G. *Angew. Chem., Int. Ed. Engl.* **1994**, *33*, 1415. (b) Liu, J.; Chen, C.-M.; Walsh, C. T. *Biochemistry* **1991**, *30*, 2306.
42. (a) Fischer, S.; Michnick, S.; Karplus, M. *Biochemistry* **1993**, *32*, 13830. (b) Kallen, J.; Walkinshaw, M. D. *FEBS Lett.* **1992**, *300*, 286.
43. Johnson, M. E.; Lin, Z.; Padmanabhan, K.; Tulinsky, A.; Kahn, M. *FEBS Lett.* **1994**, *337*, 4.
44. (a) Yaron, A.; Naider, F. *CRC Biochem. Mol. Biol.* **1993**, *28*, 31. (b) Williams, K. A.; Deber, C. M. *Biochemistry* **1991**, *30*, 8919. (c) Brandl, C. J.; Deber, C. M. *Proc. Natl. Acad. Sci. U.S.A.* **1986**, *83*,

917. (d) Markley, J. L.; Hinck, A. P.; Loh, S. N.; Prehoda, K.; Truckses, D.; Walkenhorst, W. F.; Wang, J. *Pure Appl. Chem.* **1994**, *66*, 65. (e) Richards, N. G.; Hinds, M. G.; Brennand, D. M.; Glennie, M. J.; Welsh, J. M.; Robinson, J. A.; *Biochem. Pharmacol.* **1990**, *40*, 119. (f) Lin, L.-N.; Brandts, J. F. *Biochemistry* **1979**, *18*, 43.

45. Beausoleil, E.; Lubell, W. D. *J. Am. Chem. Soc.* **1996**, *118*, 12902.
46. Magaard, V. W.; Sanchez, R. M.; Bean, J. W.; Moore, M. L. *Tetrahedron Lett.* **1993**, *34*, 381.
47. An, S. S. A.; Lester C. C.; Peng, J.-L.; Li, Y.-J.; Rothwarf, D. M.; Welker, E.; Thannhauser, T. W.; Zhang, L. S.; Tam, J. P.; Scheraga, H. A. *J. Am. Chem. Soc.* **1999**, *121*, 11558.
48. (a) Esch, P. M.; Hiemstra, H.; de Boer, R. F.; Speckamp, W. N. *Tetrahedron* **1992**, *48*, 4659. (b) Hamper, B. C.; Dukesherer, D. R.; South, M. S. *Tetrahedron Lett.* **1996**, *37*, 3671. (c) Witulski, B.; Go¨ámann M. *Chem. Commun.* **1999**, 1879. (d) Bergmeier, S. C.; Fundy, S. L.; Seth, P. P. *Tetrahedron* **1999**, *55*, 8025. (e) Valls, N.; Lo´pez-Canet, M.; Vallribera, M.; Bonjoch, J. *Chem. Eur. J.* **2001**, *7*, 3446. (f) Tanimori, S.; Fukubayashi, K.; Kirihata, M. *Tetrahedron Lett.* **2001**, *42*, 4013. (g) Millet, R.; Domarkas, J.; Rombaux, P.; Rigo, B.; Houssin, R.; He´nichart, J.-P. *Tetrahedron Lett.* **2002**, *43*, 5087. (h) Zhang, J.; Xiong, C.; Wang, W.; Ying, J.; Hruby, V. *J. Org. Lett.* **2002**, *4*, 4029. (i) Maison, W.; Adiwidjaja, G. *Tetrahedron Lett.* **2002**, *43*, 5957. (j) Valls, N.; Vallribera, M.; Carmeli, S.; Bonjoch, J. *Org. Lett.* **2003**, *5*, 447. (k) Jiang, B.; Xu, M. *Org. Lett.* **2002**, *4*, 4077.
49. (a) Blankley, C. J.; Kaltenbronn, J. S.; DeJohn, D. E.; Werner, A.; Bennett, L. R.; Bobowski, G.; Krolls, U.; Johnson, D. R.; Pearlman, W. M.; Hoefle, M. L. *J. Med. Chem.* **1987**, *30*, 992. (b) Juvvadi, P.; Dooley, D. J.; Humblet, C. C.; Lu, G. H.; Lunney, E. A.; Panek, R. L.; Skeean, R.; Marshall, G. R. *Int. J. Peptide Protein Res.* **1992**, *40*, 163. (c) Blanco, M.-J.; Penide, M. R.; Sardina, F. J. *J. Org. Chem.* **1999**, *64*, 8786.
50. Li, W.; Moeller, K. D. *J. Am. Chem. Soc.* **1996**, *118*, 10 106.
51. Conti, P.; Dallanoce, C.; De Amici, M.; De Micheli, C.; Fruttero, R. *Tetrahedron* **1999**, *55*, 5623.
52. (a) Toniolo, C. *Int. J. Peptide Protein Res.* **1990**, *35*, 287. (b) Giannis, A.; Kolter, T. *Angew. Chem.* **1993**, *105*, 1303; *Angew. Chem., Int. Ed. Engl.* **1993**, *32*, 1244. (c) Adang, A. E. P.; Hermkens, P. H. H.; Linders, J. T. M.; Ottenheijm, H. C. J.; van Staveren, C. J. *Recl. TraV. Chim. Pays-Bas* **1994**, *113*, 63. (d) Gante, J. *Angew. Chem.* **1994**, *106*, 1780; *Angew. Chem., Int. Ed. Engl.* **1994**, *33*, 1699. (e) Hruby, V. J.; Li, G.; Haskell-Luevano, C.; Shenderovich, M. *Biopolymers* **1997**, *43*, 219. (f) Hänessian, S.; Mcnaughton-Smith, G.; Lombart, H. G.; Lubell, W. D. *Tetrahedron* **1997**, *53*, 12789. (g) Conti, P.; Dallanonce, C.; De Amici, M.; De Micheli, C.; Fruttero, R. *Tetrahedron* **1999**, *55*, 5623. (h) Gibson, S. E.; Guillo, N.; Tozer, M. *Tetrahedron* **1999**, *55*, 585.
53. For reviews, see: (a) Itsuno, M. *Org. React.* **1998**, *52*, 395. (b) Corey, E. J.; Helal, C. J. *Angew. Chem.* **1998**, *110*, 2092; *Angew. Chem., Int. Ed. Engl.* **1998**, *37*, 1986. (c) Job, A.; Janeck, C. F.; Bettray, W.; Peters, R.; Enders, D. *Tetrahedron* **2002**, *58*, 2253. (d) List, B. *Tetrahedron* **2002**, *58*, 5573.
54. For selected recent examples, see: (a) Laabs, S.; Munch, W.; Bats, J. W.; Nubbemeyer, U. *Tetrahedron* **2002**, *58*, 1317. (b) Amedijkouh, M.; Ahlberg, P. *Tetrahedron: Asymmetry* **2002**, *13*, 2229. (c) Bogevig, A.; Juhl, K.; Kumaragurubaran, N.; Zhuang, W.; Jørgensen, K. A. *Angew. Chem.* **2002**, *114*, 1868; *Angew. Chem., Int. Ed. Engl.* **2002**, *41*, 1790. (d) Corey, E. J.; Shibata, T.; Lee, T. W.; *J. Am. Chem. Soc.* **2002**, *124*, 3808. (e) List, B.; Pojarliev, P.; Biller, W. T.; Martin, H. J. *J. Am. Chem. Soc.* **2002**, *124*, 827.

55. Kim, D. H.; Guinosso, C. J.; Buzby, G. C. J.; Herbst, D. R.; McCaully, R. J.; Wicks, T. C.; Wendt, R. L. *J. Med. Chem.* **1983**, *26*, 394.
56. Stanton, J. L.; Gruenfeld, N.; Babiarz, J. E.; Ackerman, M. H.; Friedmann, R. C.; Yuan, A. M.; Macchia, W. *J. Med. Chem.* **1983**, *26*, 1267.
57. Gruenfeld, N.; Stanton, J. L.; Yuan, A. M.; Ebetino, F. H.; Browne, L. J.; Gude, C.; Huebner, C. F. *J. Med. Chem.* **1983**, *26*, 1277.
58. Kuwano, R.; Sato, K.; Kurokawa, T.; Karube, D.; Ito, Y. *J. Am. Chem. Soc.* **2000**, *122*, 7614.
59. Jeannotte, G.; Lubell, W. D. J. *Org. Chem.* **2004**, *69*, 4656.
60. (a) Haack, T.; Mutter, M. *Tetrahedron Lett.* **1992**, *33*, 1589. (b) Wöhr, T.; Mutter, M. *Tetrahedron Lett.* **1995**, *36*, 3847. (c) Mutter, M.; Nefzi, A.; Sato, T.; Sun, X.; Wahl, F.; Wöhr, T. *Peptide Res.* **1995**, *8*, 145.
61. Dumy, P.; Keller, M.; Ryan, D. E.; Rohwedder, B.; Wöhr, T.; Mutter, M. *J. Am. Chem. Soc.* **1997**, *119*, 918.
62. Cavelier, F.; Vivet, B.; Martinez, J.; Aubry, A.; Didierjean, C.; Vicherat, A.; Marraud, M. *J. Am. Chem. Soc.* **2002**, *124*, 2917.
63. Vivet, B.; Cavelier, F.; Martinez, J. *Eur. J. Org. Chem.* **2000**, 807.
64. Pujals, S.; Fernandez-Carneado, J.; Kogan, M. J.; Martinez, J.; Cavelier, F.; Giralt, E. *J. Am. Chem. Soc.* **2006**, *128*, 8479.
65. (a) Gante, J. *Synthesis*, **1989**, 405. (b) Lecoq, A.; Marraud, M.; Boussard, G. *Tetrahedron Lett.* **1992**, *33*, 5209.
66. Che, Y.; Marshall, G. R. *J. Org. Chem.* **2004**, *69*. 9030.
67. (a)S. Hanessian, G. McNaughton-Smith, H.-G. Lombart and W. D. Lubell, *Tetrahedron*, **1997**, *53*, 12789. (b) S. H. Gellman, *Acc. Chem. Res.*, **1998**, *31*, 173.
68. Hancock, R. E. W.; Scott, M. G. *Proc. Natl. Acad. Sci.* USA. **2000**, *97*, 8856.
69. Hancock, R. E. W; Lehrer, R. *Trends Biotech.* **1998**, *16*, 82.
70. Latham, P. W. *Nat. Biotechnol.* **1999**, *17*, 755.
71. Murray, P. J.; Starkey, I. D. Tetrahedron Lett. 1996, 37, 1875.
72. Barkallah, S.; Schneider, S. L.; Tetrahedron Lett. 2005, 46, 4985.
73. Murray, P. J.; Starkey, I. D.; Davies, J. E. Tetrahedron Lett. 1998, 39, 6721.
74. Stalker, R. A.; Munsch, T. E.; Tran, J. D.; Nie, X.; Warmuth, R.; Beatty, A.; Aakeroy, C. B. Tetrahedron 2002, 58, 4837.
75. Ganokar. R.; Natarajan, A.; Mamai, A.; Madalengoitia, J. S. *J. Org. Chem.* 2006, 71, 5004.
76. Goswami, R.; Moloney, M. G. *Chem.Commun.* 1999, 2333.
77. Schweizer, F. *Angew. Chem., Int. Ed. Engl.* **2002**, *341*, 230.
78. Williamson, A. R.; Zamenhof, S. *J. Biol. Chem.* **1963**, *238*, 2255.
79. Heyns, K.; Kiessling, G.; Lindenberg, W.; Paulsen, H.; Webster, M. E. *Chem. Ber.* **1959**, *92*, 2435.
80. K. Isono, J. *Antibiot.* **1988**, *41*, 1711. And references cited therein.
81. Knapp, S. *Chem. Rev.* **1995**, *95*, 1859.
82. Knapp, S.; Jaramillo, C.; Freeman, B. *J. Org. Chem.* **1994**, *59*, 4800.
83. Nakajima, M.; Itoi, K.; Takamatsu, Y.; Kinoshita, T.; Okazaki,T.; Kawakubo, K.; Shindo, M.; Honma, T.; Tohjigamori, M.; Haneishi, T. *J. Antibiot.* **1991**, *44*, 293.

84. a) Takeuchi, Y., Marshall, G. R., *J. Am. Chem. Soc.* **1998**, *120*, 5363. b) Bellier, B. DaNascimento, S., Meudal, H., Gincel, E., Roques, B. P., Garbay, C. *Bioorg. Med. Chem. Lett.* **1998**, *8*, 1419.

85. Umezawa, H.; Aoyagi, T.; Komiyama, T.; Morishima, H.; Hamada, M.; Takeuchi, T. *J. Antibiot.* **1974**, *27*, 963.

86. Gruner S. A. W., Locardi, E., Lohof, E., Kessler H. *Chem. Rev.* **2002**, *102*, 491.

87. Risseeuw, M. D. P.; Overhand, M.; Fleet, G. W. J.; Simone, M. I. *Tetrahedron: Asymmetry.* **2007**, *18*, 2001.

88. Dondoni, A.; Marra, A. *Chem. Rev.* **2000**, *100*, 4395.

89. Dondoni, A.; Junquera, F.; Mercha´n, F. L.; Merino, P.; Scherrmann,M.-C.; Tejero, T. *J. Org. Chem.* **1997**, *62*, 5484.

90. Axon, J. R.; Beckwith, A. L. J. *J. Chem. Soc., Chem. Commun.* **1995**, 549.

91. Dondoui, A.; Perrone, D. *Synthesis* **1997**, 527.

92. Dondoni, A.; Marra, A.; Massi, A. *Tetrahedron* **1998**, *54*, 2827.

93. (a). Dondoni, A.; Mariotti, G.; Marra, A. *Tetrahedron Lett.* **2000**, *41*, 3483; (b) Dondoni, A.; Mariotti, G.; Marra, A. *J. Org. Chem.* **2002**, *67*, 4475.

94. Werner, R. M.; Williams, L. M.; Davis, J. T. *Tetrahedron Lett.* **1998**, *39*, 9135.

95. Pearce, A. J.; Ramaya, S.; Thorn, S. N.; Bloomberg, G. B.; Walter, D. S.; Gallagher, T. *J. Org. Chem.* **1999**, *64*, 5453.

96. Manabe, S.; Ito, Y. *J. Am. Chem. Soc.* **1999**, *121*, 9754.

97. Wernicke, A and Sinou, D. *J. Carbohy. Chem.* **2001**, *20*, 181.

98. Frappa, I.; Sinou, D. *Synthetic Commun.* **1995**, *25* (9), 2941.

99. Brakta, M.; Lhoste, P.; Sinou, D. *J. Org. Chem.* **1989**, *54* (8), 1890.

100. Gurjar, M. K.; Mainkar, A. S.; Syamala, M. *Tetrahedron: Asymmetry* **1993**, *4*, 2343.

101. Lieberknecht, A.; Griesser, H.; Kra¨mer, B.; Bravo, R. D.; Colinas, P. A.; Grigera, R. J. *Tetrahedron* **1999**, *55*, 6475.

102. Colombo, L.; Casiraghi, G.; Pittalis, A. *J. Org. Chem.* **1991**, *56*, 3897.

103. Vidal, T.; Haudrechy, A.; Langlois, Y. *Tetrahedron Lett.* **1999**, *40*, 5677.

104. Dondoni, A.; Mariotti, G.; Aldhoun, M. *J. Org. Chem.* **2007**, *72*, 7677.

105. Campbell, A. D.; Paterson, D. E.; Raynham, T. M.; Taylor, R. J. K. *Chem. Commun.* **1999**, 1599.

106. Dorgan, B. J.; Jackson, R. F. W. *Synlett* **1996**, 859.

107. (a) Dondoni, A.; Marra, A.; Massi, A. *Chem. Commun.* **1998**, 1741. (b) Dondoni, A.; Marra, A.; Massi, A. *J. Org. Chem.* **1999**, *64*, 933.

108. Urban, D.; Skrydstrup, T.; Beau, J.-M. Chem. Commun. **1998**, 955.

109. Gustafsson, T.; Hedenström; M.; Kihlberg, J. *J. Org. Chem.* **2006**, *71*, 1911.

110. Brenna, E.; Grasselli, P.; Serra, S.; Zambotti, S. *Chem. Eur. J.* **2002**. *8*, 1872.

111. Cipolla, L.; Forni, E.; Jimenez, J.; Nicotra, F. *Chem. Eur. J.* **2002**, *8*, 3976.

112. van Well, R. M.; Meijer, M. E. A.; Overkleeft, H. S.; Boom, J. H. v.; van de Marel, G. A.; Overhand, M. *Tetrahedron* **2003**, *59*, 2423.

113. Verhagen, C.; Bryld, T.; Raunkjaer, M.; Vogel, S.; Buchalova, K.; Wengel, J. *Eur. J. Org. Chem.* **2006**, *11*, 2538.

114. Grotenbreg, G. M.; Tuin, A. W.; Witte, M. D.; Leeuwenburgh, M. A.; van Boom, J. H.; van

der Marel, G. A.; Overkleeft, H. S.; Overhand, M. *Synlett* **2004**, *5*, 904.

115. Risseeuw, M. D. P.; Grotenbreg, G. M.; Witte, M. D.; Tuin, A. W.; Leeuwenburgh, M. A.; van der Marel, G. A.; Overkleeft, H. S.; Overhand, M. *Eur. J. Org. Chem.* **2006**, 3877.
116. Peri, F.; Cipolla, L.; La Ferla, B.; Nicotra, F. *Chem. Commun.* **2000**, 2303.
117. Chou, K. C. *Analytical Biochem.* **2000**, *286*, 1.
118. Lewis, P. N.; Momany, F. A.; Scheraga, H. A. *Proc. Nat. Acad. Sci., U.S.A.* **1971**, *68*, 2293.
119. Richardson, J. S. *Adv. Protein Chem.* **1981**, *34*, 167.
120. Wilmot, C. M.; Thornton, J. M. *J. Mol. Biol.* **1988**, *203*, 221.
121. Graf von Roedern, E.; Lohof, E.; Hessler, G.; Hoffmann, M.; Kessler, H. *J. Am. Chem. Soc.* **1996**, *118*, 10156.
122. Lohof, E.; Planker, E.; Mang, C.; Burkart, F.; Dechantsreiter, M. A.; Haubner, R.; Wester, H.-J.; Schwaiger, M.; Hölzemann, G.; Goodman, S. L.; Kessler, H.. *Angew. Chem., Int. Ed. Engl.* **2000**, *39*, 2761.
123. Brazeau, P.; Vale, W.; Burgus, R.; Guillemin, R. *Can. J. Biochem.* **1974**, *52*, 1067.
124. Brazeau, P.; Vale, W.; Burgus, R.; Ling, N.; Butcher, M.; Rivier, J.; Guillemin, R. *Science* **1973**, *179*, 77.
125. Tamarit, J.; Tamarit-Rodriguez, J.; Goberan, R.; Lucas, M. *Rev. Esp. Fisiol.* **1974**, *30*, 299.
126. Christensen, S. E.; Hansen, A. P.; Iversen, J.; Lundbaek, K.; Orskov, H.; Seyer-Hansen, K. *J. Clin. Lab. Invest.* **1974**, *34*, 321.
127. Graf von Roedern, E.; Kessler, H. *Angew. Chem., Int. Ed. Engl.* **1994**, *33*, 667.
128. Veber, D. F.; Freidinger, R. M.; Perlow, D. S.; Paleveda, W. J.; Holly, F. W.; Strachan, R. G.; Nutt, R. F.; Arison, B. H.; Homnick, C.; Randall, W. C.; Glitzer, M. S.; Saperstein, R.; Hirschmann, R. *Nature* **1981**, *292*, 55.
129. Veber, D. F. In *Peptides, Chemistry and Biology, Proceedings of the Twelfth American Peptide Symposium*; Smith, J. A.; Rivier, J. E., Eds.; Escom: Leiden, 1992; pp 3-14.
130. Gruner, S.; Kri, G.; Schwab, R.; Venetianer, A.; Kessler, H. *Org. Lett.* **2001**, *3*, 3723. And reference therein.
131. Kéri, G.; Erchegyi, J.; Horváth, A.; Mezo, I.; Idei, M.; Vántus, T.; Balogh, A.; Vadásu, Z.; Bökönyi, G.; Seprodi, J.; Teplán, I.; Csuka, O.; Tejeda, M.; Gaál, D.; Szegedi, S.; Szende, B.; Roze, C.; Kalthoff, H.; Ullrich, A. *Proc. Natl. Acad. Sci. U.S.A.* **1996**, *93*, 12513.
132. Gause, G. F.; Brazhnikova, M. G. *Nature* **1944**, *154*, 703.
133. (a) Izumiya, N.; Kato, T.; Aoyagi, H.; Waki, M.; Kondo, M. *Synthetic aspects of biologically active cyclic peptides - gramicidin S and tyrocidines*; Halstead (Wiley): New York, 1979. (b) Waki, M.; Izumiya, N. *Biochemistry of Peptide Antibiotics*; Kleinhaug, H., van Doren, H., Eds.; Walter de Gruyter Company: Berlin, 1990. (c) Kondejewski, L. H.; Farmer, S. W.; Wishart, D. S.; Hancock, R. E. W.; Hodges, R. S. *Int. J. Peptide Protein Res.* **1996**, *47*, 460.
134. (a) Matsuzaki, K. *Biochim. Biophys. Acta* **1999**, *1462*, 1. (b) Epand, R. M.; Vogel, H. J. *Biochim. Biophys. Acta* **1999**, *1462*, 11. (c) Sitaram, N.; Nagaraj, R. *Biochim. Biophys. Acta* **1999**, *1462*, 29. (d) Shai, Y. *Biochim. Biophys. Acta* **1999**, *1462*, 55. (d) Dathe M.; Wieprecht, T. *Biochim. Biophys. Acta* **1999**, *1462*, 71. (e) Blondelle, S. E.; Lohner, K.; Aguilar, M.-I. *Biochim. Biophys. Acta* **1999**, *1462*, 89. (f) Maget-Dana, R. *Biochim. Biophys. Acta* **1999**, *1462*, 109. (g) Lohner, K.; Prenner, E. J. *Biochim.*

Biophys. Acta **1999**, *1462*, 141. (h) Bechinger, B. *Biochim. Biophys. Acta* **1999**, *1462*, 157. (i) La Rocca, P.; Biggin, P. C.; Tieleman D. P.; Sansom, M. S. P. *Biochim. Biophys. Acta* **1999**, *1462*, 185. (j) Prenner, E. J.; Lewis, R. N. A. H.; McElhaney, R. N. *Biochim. Biophys. Acta* **1999**, *1462*, 201.

135. Walsh, C. T. *Antibiotics: Actions, Origins, Resistance*; ASM: Washington, DC, 2003.
136. Kondejewski, L. H.; Farmer, S. W.; Wishart, D. S.; Hancock, R. E. W.; Hodges, R. S. *Int. J. Peptide Protein Res.* **1996**, *47*, 460.
137. Grotenbreg, G. M.; Buizert, A. E. M.; Llamas-Saiz, A. L.; Spalburg, E.; van Hooft, P. A. V.; de Neeling, A. J.; Noort, D.; van Raaij, M. J.; van der Marel, G. A.; Overkleeft, H. S.; Overhand, M.; *J. Am. Chem. Soc.* **2006**, *128*, 7559.
138. Galli-Stampino, L.; Meinjohanns, E.; Frische, K.; Meldal, M.; Jensen, T.; Werdelin, O.; Mouritsen, S. *J. Cancer. Res.***1997**, *57*, 3214.
139. Tedebark U.; Meldal M.; Panza L.; Bock K. *Tetrahedron Lett.* **1998**, *39*. 1815.
140. Arnett, F. C.; Edworthy, S. M.; Bloch, D. A.; McShane, D. J.; Fries, J. F.; Cooper, N. S.; Healey, L. A.; Kaplan, S. R.; Liang, M. H.; Luthra, H. S.; Medsger, T. A.; Mitchell, D. M.; Neustadt, D. H.; Pinals, R. S.; Schaller, J. G.; Sharp, J. T.; Wilder, R. L.; Hunder, G. G. *Arthritis Rheum.* **1988**, *31*, 315.
141. Holmdahl, R.; Andersson, M.; Goldschmidt, T. J.; Gustafsson, K.; Jansson, L.; Mo, J. A. *Immunol. Rev.* **1990**, *118*, 193.
142. Trentham, D. E.; Townes, A. S.; Kang, A. H. *J. Exp. Med.* **1977**, *146*, 857.
143. (a) Michaelsson, E.; Broddefalk, J.; Engström, A.; Kihlberg, J.; Holmdahl, R. *Eur. J. Immunol.* **1996**, *26*, 1906. (b) Holm, B.; Bäcklund, J.; Recio, M. A. F.; Holmdahl, R.; Kihlberg, J. *ChemBioChem* **2002**, *3*, 1209. (c) Holm, B.; Baquer, S. M.; Holm, L.; Holmdahl, R.; Kihlberg, J. *Bioorg. Med. Chem.* **2003**, *11*, 3981. (d) Broddefalk, J.; Bergquist, K. E.; Kihlberg, J. *Tetrahedron* **1998**, *54*, 12047. (e) Wellner, E.; Gustafsson, T.; Ba¨cklund, J.; Holmdahl, R.; Kihlberg, J. *ChemBioChem* **2000**, *1*, 272.
144. Stefanska, A. L.; Coates, N. J.; Mensah, L. M.; Pope, A. J.; Ready, S. J.; Warr, S. R. *J. Antibiot.* **2000**, *53*, 345.
145. Houge-Frydrych, C. S. V.; Readshaw, S. A.; Bell, D. J. Antibiot. *2000*, *53*. 351.
146. Berge, J. M.; Copely, R. C. B.; Eggleston, D. S.; Hamprecht, D. W.; Jarvest, R. L.; Mensah, L. M.; O'Hanlon, P. J.; Pope, A. J. *Bioorg. Med. Chem. Lett.* **2000**, *10*, 1811.
147. Brown, P.; Eggleston, D. S.; Haltiwanger, R. C.; Jarvest, R. L.; Mensah, L. M.; O'Hanlon, P. J.; Pope, A. J. *Bioorg. Med. Chem. Lett.* **2001**, *11*, 711.

Chapter 2

Research Motivation

The use of peptides as drugs is limited by their low metabolic stability towards proteolysis (degradation of proteins) in the gastrointestinal tract and in serum. In addition, peptide-based drugs are usually similar to the receptor-bound segment of any biologically active peptides and proteins. However, once being truncated from the native peptide/protein, it will lose its original conformation. Due to their intrinsic flexibility, short linear peptides usually cause undesired effects by interacting with various receptors.

In order to solve these problems, newer concepts are emerging where the fundamental building blocks used by Nature, like amino acids and sugars, are amalgamated to produce nature-like, and yet unnatural, de novo structural entities with multifunctional groups anchored on a single ensemble. One such hybrid design is represented by a class of compounds called *C*-glycosyl amino acids (C-GAAs), which are defined by an α-amino acid group [$CH(NH_2)CO_2H$] either directly attached or carbon-linked to the anomeric carbon of a carbohydrate scaffold. This approach not only increases the enzyme stability but reduces the flexibility of peptidomimetics by the introduction of relative rigidity of 5- or 6-membered rings.

The aim of this work is to develop new *C*-GAA building blocks suitable for the synthesis of novel peptidomimetics or glycomimetics. To reach these demands the

C-GAAs should meet the following requirements:

1. The synthetic routes should be cheap, fast and high yielding.

2. Being suitable for peptide synthesis (solution phase or solid phase peptide synthesis).

3. Reduction in conformational flexibility of the resulting peptidomimetics.

4. Induction of secondary structures such as β- and γ-turns.

5. Induction of chiral diversity and enhanced enzymatic stability.

The basic structural properties of novel *C*-GAAs as well as the induced secondary structures were to be investigated by synthesis and structural analysis of several model peptides containing these building blocks. The ultimate goal of this project was to provide new insight into the structure and activity relationships (SAR) of novel conformationally constrained glycoconjugates that will find future use in the design of novel peptidomimetics with improved pharmacodynamics and pharmacokinetics.

Chapter 3

Synthesis of Spirocyclic Glucose–Proline Hybrids (GlcProHs)

Abstract: *A short synthetic route to polyhydroxylated spirocyclic glucose-based L-proline hybrids (GLcProHs) is described from easily prepared 2,3,4,6 tetra-O-benzyl-D-glucono-lactone. The synthesis involves C-glycosylation of an exocyclic glucose-based epoxide with allyltributylstannane that affords functionalized C-ketosides containing an α-hydroxy ester moiety. Oxidation of the alcohol function, followed by stereoselective reductive amination provides an amine that undergoes iodine-induced aminocyclization to provide spirocyclic glucose-proline hybrids bearing an iodomethylene sidechain. The iodo function of the side-chain can be converted into other functional groups such as ester and hydroxyl groups, thereby allowing additional modifications to the pyrrolidine ring.*

3.1. Introduction

Proline plays an important role in the formation of secondary structures in peptides and proteins because it induces a reversal in backbone conformation resulting in the formation of reverse turns and disruption of helices and sheets in proteins. Besides the occurrence of proline in β-turns, proline-rich sequences also exist as extended helices[1] (polyproline-I and polyproline-II) and antimicrobial peptides[2]. Hydroxylated proline residues occur in nature in the form of collagenous peptides, virotoxin cyclic heptapeptides[3] and other peptides[4,5] and the role of hydroxylated proline residues on the conformational stability of the collagen triple helix have been extensively investigated[6]. Over the years a plethora of proline analogs such as C^{β}-, C^{γ}- and C^{δ}-substituted prolines[7-10], azaprolines[11], pseudoprolines[12], silaproline[13], proline-amino acid chimera[14]

and fused bicyclic proline[15-17] analogues have been developed to study the structural and biological properties of proline surrogates in peptides[18] (Figure 3.1).

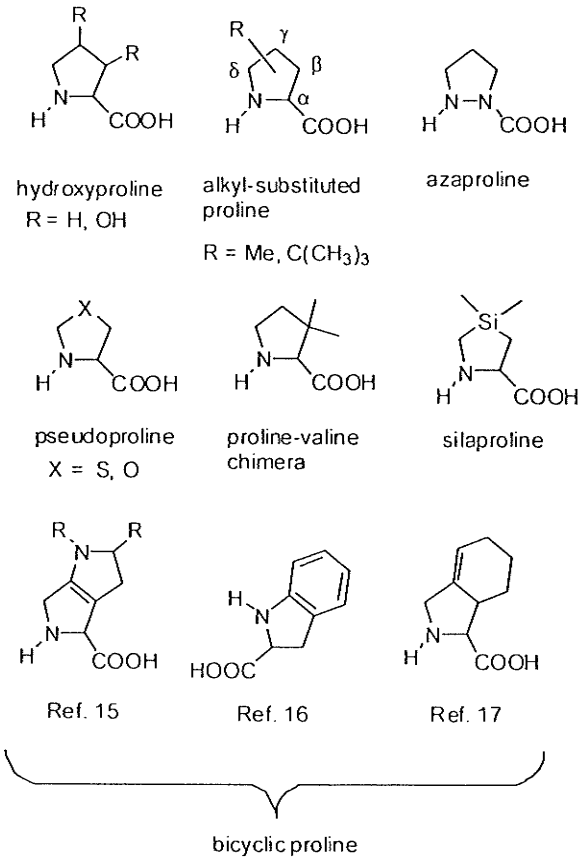

Figure 3.1 Previously synthesized proline analogues that have been proposed to mimic the properties of proline when incorporated into peptides.

To extend the molecular repertoire of bicyclic proline analogues, we became interested in the design and synthesis of spirocyclic sugar–proline hybrids[19] (SProHs, Figure 3.2). Spirocyclic sugar–proline analogues combine the molecular features of carbohydrates (furan- or pyran-based polyol) with the unique features of proline. The resulting hybrid is a polyfunctional building block, which may find use as glycomimetic, prolinemimetic, peptidomimetic[19c] and scaffold for combinatorial synthesis. In particular, the proline

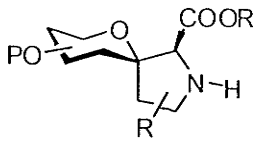

Figure 3.2 Design of sugar-proline hybrids (SProHs). The bicyclic and polyfunctional nature of SProHs may induce novel secondary structures when incorporated into peptides. In addition, decoration of the polyhydroxylated scaffold may be used to tailor the physical, chemical and biological properties of proline.

mimetic properties of spirocyclic SProHs have attracted our interest, because polyhydroxylated amino acids may induce novel secondary structures in small peptides. For instance, incorporation of unprotected sugar amino acids into small peptides such as gramicidin S[20] and opioid peptides[21] prohibited the formation of the targeted secondary structural motif. Instead, unusual turn structures stabilized by intramolecular hydrogen bonds between sugar hydroxyl groups and the peptidic amide backbone were observed.[22] Similar effects may also be observed with spirocyclic SProHs. In addition, derivatization or decoration of the polyol scaffold may be used as a tool to tailor the chemical, physical, biological and conformational properties of the proline analogue in peptides. To explore the proline mimetic properties of spirocyclic SProHs we describe here the synthesis of a spirocyclic glucose-based proline hybrids (GlcProHs). To the best of our knowledge glucose-based spirocyclic proline analogues have previously not been reported.[23]

3.2. Results and discussion

The synthesis started with the readily available D-gluco-based lactone **1**[24] (Scheme 3.1)

which reacts with the enolate of methyl bromoacetate generated from lithium bis-(trimethylsilyl)amide ($LiN(SiMe_3)_2$) in tetrahydrofuran (THF) at -78 °C, to produce the exocyclic epoxide **2** in 80% yield as a single stereoisomer.[25] Trimethylsilyl trifluoromethanesulfonate (TMSOTf)-promoted *C*-glycosylation of epoxide **2** with allyltributylstannane in dichloromethane followed by hydrolysis of the TMS-ether with trifluoroacetic acid (TFA)-containing wet THF produced a mixture containing alcohols **3** and **4** (ratio **3**:**4** = 9:1) in a combined yield of 89%. Regioselective opening of epoxide **2**

Scheme 3.1 Synthesis of the α-allylic intermediate **3**

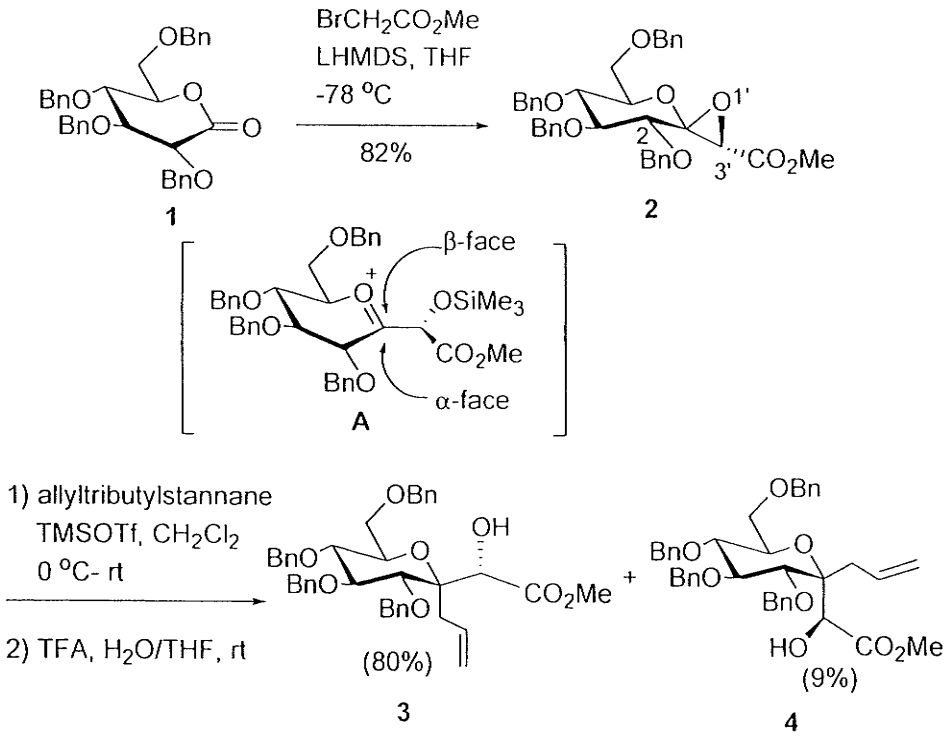

proceeded via formation of oxonium ion (intermediate **A**) that subsequently undergoes

α-selective *C*-glycosylation favored by stereoelectronic factors as observed for similar *C*-glycosylation reactions.[26] It is noteworthy that slow addition of epoxide **2** to allyltributylstannane is crucial for optimal yield of target compound **3**. The configuration at the anomeric position in compound **4** was deduced on the basis of observed/unobserved nOe[27] contacts (Figure 3.3).

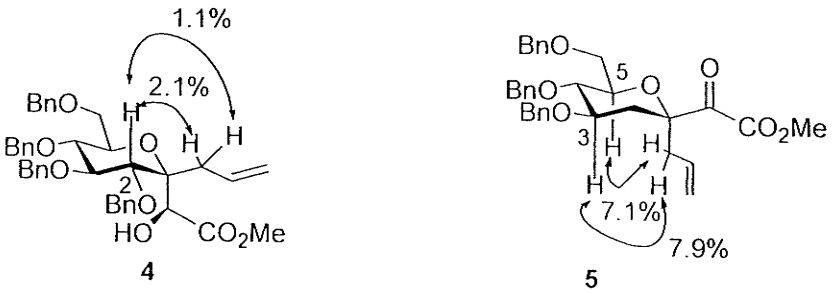

Figure 3.3 Assignment of stereochemistry at anomeric carbon in compounds **4** and **5** through 1D nOe experiments (recorded in $CDCl_3$).

Compound **3** served as starting material for the installation of the amino function at *C*-2 (Scheme 3.2). Initially, we attempted to convert the hydroxyl group at *C*-2 into an amino function. However, nucleophilic substitution of *C*-2 activated sulphonate ester (triflate) with a variety of nucleophiles including benzylamine, *p*-methoxybenzylamine, lithium and sodium azide at low and elevated temperatures resulted only in trace amounts of the desired amine. In these cases, unreacted starting material was recovered (>90%). To avoid these complications we decided to explore a reductive amination approach. Alcohol **3** was oxidized to ketone **5** at -78 °C using a mixture containing trifluoroacetic anhydride, triethylamine and dimethylsulfoxide in dichloromethane to produce ketone **5**

Scheme 3.2 Preparation of spirocyclic glucose-based proline analogues using a reductive amination route

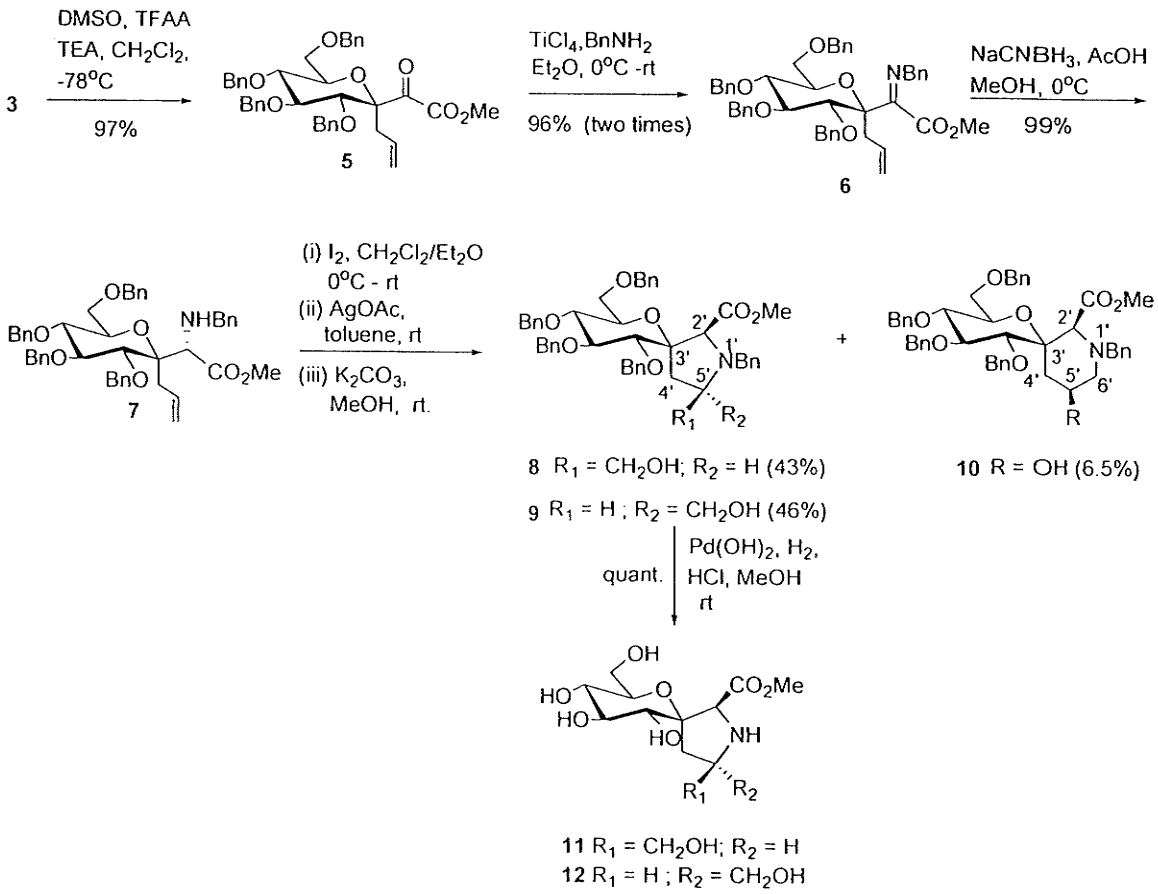

in 95% isolated yield.[28] In order to confirm the configuration of the product, we performed nOe experiments (Figure 3.3). For instance, subjection of one of the allylic protons to a one-dimensional GOESY experiment showed interproton effects to H-3 (7.9% nOe[27]) and H-5 (7.1%). This is consistent with the structure **5** bearing an allylic group at the axial position. Subsequently, the ketone **5** was converted into the amino ester **7** in a two-step procedure. At first, compound **5** was exposed to titanium tetrachloride-promoted imination using benzylamine in ether to afford the imine **6** in 96% after chromatographic purification.[29] The imine 6 was stereoselectively reduced to amino

ester **7** in quantitative yield using sodium cyanoborohydride in acidified methanol at 0 °C. The high diastereoselectivity can be explained using the Felkin model (Figure 3.4),[30] in

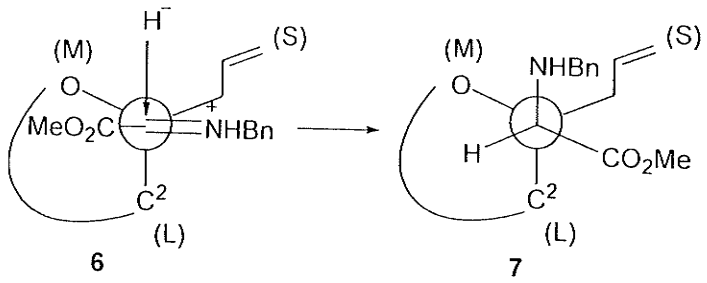

Figure 3.4 A rational explanation for stereoselective reductive amination using Felkin model

which the nucleophile approaches the immmonium ion from the less hindered side (*Re* face) resulting in the formation of C-2(*S*) configured product **7**, which was confirmed by nOe experiments (Figure 3.5). With amino ester **7** in hand we installed the pyrrolidine ring by iodocyclization in dichloromethane to produce an inseparable isomeric mixture containing various iodo-compounds. To separate the compounds from each other we converted the mixture into the alcohols **8**, **9** and **10** via a two-step process. At first, the mixture was exposed to silver acetate in toluene[31] to produce an inseparable mixture of esters **13**, **14** and **15** (Scheme 3.3) that, by treatment with potassium carbonate in methanol, afforded the alcohols **8**, **9** and **10** in 44%, 45% and 6% isolated yield, respectively. Subsequently, exposure of compounds **8** and **9** to catalytic hydrogenolysis condition using Pearlman's catalyst provided the unprotected proline analogues **11** and **12** in quantitative yield, respectively.

To assign the stereochemistry at *C*-2′ the alcohols **8**, **9** and **10** were converted into the acetates **13**, **14** and **15** using acetic anhydride and pyridine (Scheme 3). We selected the

Scheme 3.3 Acylation of compounds **8-10**

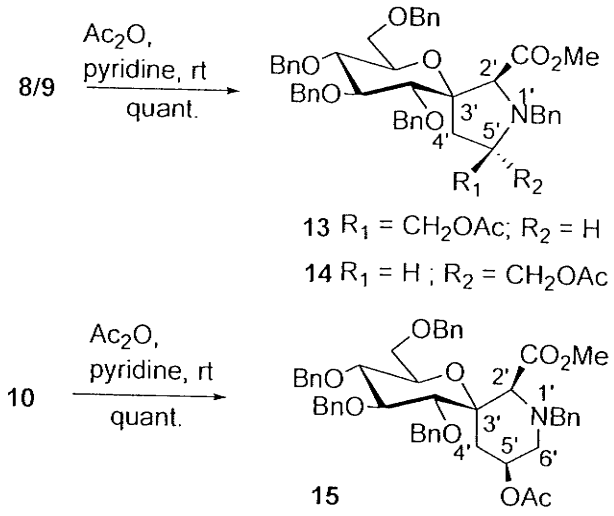

pipecolic acid analogue **15** to assign the stereochemistry at *C*-2′ (Figure 3.5). The spirocyclic compound **15** consists of both a pyranose and a piperidine ring. The large

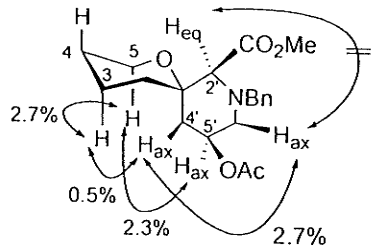

Figure 3.5 Assignment of stereochemistry at *C*-2′ position in compound **15** through 1D nOe experiment (recorded in C_6D_6). Some of the substituents in the glucose ring are omitted for clarity

coupling constants for $J_{2,3}$, $J_{3,4}$ and $J_{4,5}$ (> 9.0 Hz) in conjunction with interproton nOe

effects between H-3 and H-5, establishes the $^4C_1$ chair conformation of the sugar ring. The chair conformation of the piperidine ring is deduced from the observed vicinal diaxial and long-range coupling constants. For instance, the axial position of protons H-4′$_{ax}$, H-5′$_{ax}$ and H-6′$_{ax}$ can be deduced by their large vicinal diaxial coupling constants ($J_{4'ax,5'ax}$, $J_{5'ax,6'ax}$ > 10.5 Hz), while the observed long-range coupling constants between $J_{4'eq,6'eq}$ is equal to $J_{2'eq,4'eq}$ (~1.0 Hz); confirming the equatorial position of H-2′$_{eq}$, H-4′$_{eq}$ and H-6′$_{eq}$ in the piperidine ring. In addition, the observed interproton effects (nOe) between H-5/H-5′$_{ax}$, H-5/H-3, and H-3/H-4′$_{ax}$, together with the unobserved effect between H-6′$_{ax}$/H-2′$_{eq}$ using a one-dimensional GOESY experiment, determines the *C*-2′ (*S*) configuration (Figure 3.5).[27]

Once we had established the configuration at *C*-2′ in compound **15**, we turned our interest to the stereochemistry at *C*-5′ of the spirocyclic proline analogues **13** and **14**. Since the iodocyclization was performed on a single stereoisomer **7**, we assume that the stereochemistry at *C*-2′ of the proline analogues **13** and **14** remained "*S*" based on the previous assignment with piperidine analogue **15**. To discriminate between compounds **13** and **14** we again used nOe[27] experiments (Figure 3.6). As an example, the observed interproton effects between H-2′/H-5′ and H-5′/H-5 for compound **13** are consistent with the *C*-5′ (*R*) stereochemistry. By comparison, proline analogue **14** did not show any interproton effect between H-2′/H-5′, which is consistent with a *C*-5′ (*S*) configuration.

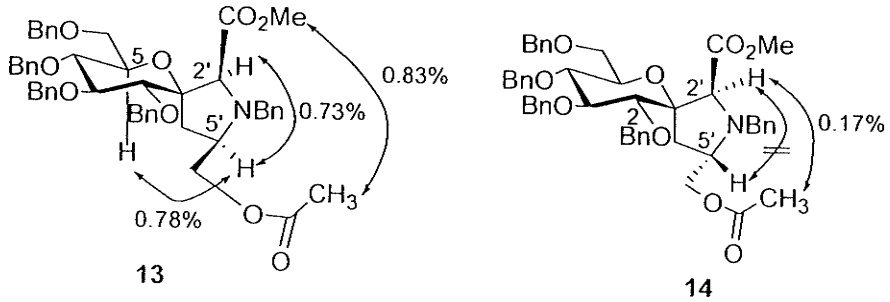

Figure 3.6 Assignment of stereochemistry at *C*-5′-position in compounds **13** and **14** through 1D nOe experiment (recorded in C_6D_6).

3.3. Conclusions

We have developed a novel and short synthetic pathway into spirocyclic polyhydroxylated glucose based *L*-proline analogues. It can be envisaged that decoration of the carbohydrate scaffold provides a tool to adjust the physical, biological and pharmacological properties of the proline analogues. We are currently investigating the prolinemimetic and glycomimetic properties of the synthesized GlcProHs and glucose–pipecolic acid hybrid.

3.4. Experimental

General procedures: ^1H and ^{13}C NMR spectra were taken in $CDCl_3$, C_6D_6, CD_3OD, D_2O at 300 MHz (or 500 MHz) and 75 MHz respectively. 1D and 2D NOE experiments were performed on Bruker AMX500 MHz. CH_2Cl_2, Et_2O, Toluene, MeOH, and THF were obtained from a dry solvent system (alumina) and used without further drying. DMF (anhydrous 99.8%), DMSO (anhydrous 99.8%), and $CHCl_3$ (ACS grade) were purchased directly from Aldrich and used without further purification. $TiCl_4$ (1.0 M in CH_2Cl_2),

Trimethylsilyltrifluoromethanesulfonate (TMSOTf), trifluoroacetic acid (TFA), triethylamine, pyridine and lithium bis(trimethylsilyl)amide (LHMDS) were directly purchased from Aldrich. All other reagents were used as supplied. Analytical thin layer chromatography was performed on 0.20 mm silica gel 60 Å plates. Flash chromatography was performed on 40-63 μm 60 Å silica gel.

(1*R*)-2,3,4,6-Tetra-*O*-benzyl-3′(*S*)-carboxy methyl-spiro[1,5-anhydro-D-glucitol-1,2′-oxirane] (2). Under nitrogen atmosphere, methyl bromoacetate (4.1 mmol) was dissolved in dry THF (20 mL) and cooled to -78 °C before lithium bis(trimethylsilyl)-amide (4 mL of a 1 M solution in THF) was slowly added. The reaction mixture was kept at -78 °C for an additional 30 minutes. Subsequently, a THF solution (5 mL) containing the lactone **1** (1 mmol) was added over a period of 10 minutes and kept at -78 °C for 1 more hour. The temperature was raised to room temperature and stirred for 15 minutes before a saturated aq. NH_4Cl solution was added. The reaction mixture was evaporated under reduced pressure and the residue was dissolved in dichloromethane and portioned with water (3 × 20 mL). The organic layer was dried over anhydrous Na_2SO_4, concentrated and purified by flash column chromatography (hexanes/ethyl acetate: 5/1) to get **2** as a colorless oil (500 mg, 82%). $[\alpha]_D$ = 99.6 (*c* 1.0, $CHCl_3$); ^{1}H NMR (500 MHz, $CDCl_3$): δ = 3.53 (m, H-7), 3.63 (dd, H-8a, *J* = 11.2 Hz, *J* = 2.1 Hz), 3.68 (dd, H-8b, *J* = 11.2 Hz, *J* = 4.4 Hz), 3.72 (s, 3H), 3.75-3.83 (m, H-5, H-6), 3.90 (s, H-2), 3.95 (d, H-4, *J* = 9.1 Hz), 4.48 (d, 1H, *J* = 12.2 Hz), 4.55 (d, 1H, *J* = 10.7

Hz), 4.58 (d, 1H, J = 12.2 Hz), 4.62 (d, 1 H, J = 11.0 Hz), 4.73 (d, 1H, J = 11.0 Hz), 4.82 (d, 1H, J= 11.2 Hz), 4.84 (d, 1H, J = 10.7 Hz), 4.94 (d, 1H, J = 11.2 Hz), 7.13-7.36 (m, 20H); ^{13}C NMR (75 MHz, $CDCl_3$): δ = 52.5, 54.5, 68.3, 73.5, 74.9, 75.2, 75.7, 76.8, 77.0, 77.3, 84.7, 86.29, 127.6-128.5 (aromatic carbons), 137.4, 137.8, 137.9, 138.3, 166.7; Anal. calcd for $C_{37}H_{38}O_8$: C, 72.77; H, 6.27. Found: C, 72.48; H, 6.54. MS (ES, $[M + Na]^+$) calcd for $C_{37}H_{38}NaO_8$ 633.25, found 633.71

Methyl (2*S*)-hydroxy-2-(1-allyl-2,3,4,6-tetra-*O*-benzyl-*β*-D-glucopyranosyl) -ethanoate (3) Under a nitrogen atmosphere, to a solution of allyltributylstannane (0.99 mL, 3.15 mmol) in dichloromethane (5 mL) was added dropwise the solution of trimethylsilyltrifluoromethanesulfonate (TMSOTf, 0.427 mL, 2.36 mmol) in dichloromethane (5 mL) at 0 °C followed by the syringe pump-controlled (50 μL/min) addition of the solution of epoxide **2** (480 mg, 0.79 mmol) in dichloromethane (10 mL). And then the mixture was stirred for 1 more hour at room temperature, the saturated sodium bicarbonate solution (10 mL) was added to quench the reaction, followed by the extraction with dichloromethane (3 × 15 mL). The organic layer was dried (Na_2SO_4), concentrated and treated with trifluoroacetic acid (0.20 mL, 5 equiv.) in aqueous tetrahydrofuran (THF/H_2O: 5/1) overnight. The mixture was concentrated and purified by flash column chromatography (hexanes/dichloromethane/ethyl acetate: from 2/1/0.2 to 2/1/0.4) to get **3** (410 mg, 80%) and **4** (46 mg, 9%). **(3)** $[\alpha]_D$ = 77.3 (*c* 1.0, $CHCl_3$); ^{1}H NMR (300 MHz, $CDCl_3$): δ = 2.77 (dd, 1H, J = 16.1 Hz, J = 6.8 Hz), 2.89 (dd, 1H, J =

16.1 Hz, J = 7.2 Hz), 3.48 (br, OH), 3.85-3.65 (m, 7H), 4.04 (dd, 1H, J = 9.8 Hz, J = 8.0 Hz), 4.13(d, 1H, J = 9.8 Hz), 4.33 (s, 1H), 4.63 (d, 1H, J = 12.5 Hz), 4.68-4.75 (m, 2H), 4.85-4.98 (m, 3H), 5.02 (d, 1H, J = 10.9 Hz), 5.08 (d, 1H, J = 11.4 Hz), 5.28-5.16 (m, 2H), 5.89 (m, 1H), 7.25-7.49 (m, 20H); ^{13}C NMR (75 MHz, $CDCl_3$): δ = 32.0, 52.2, 68.9, 73.5 (2 carbons), 73.6, 75.3, 75.3, 75.6, 78.7, 79.2, 80.6, 84.1, 118.7, 127.7-128.5 (aromatic carbons), 131.7, 138.1, 138.4, 138.4, 138.6, 173.1; Anal. calcd for $C_{40}H_{44}O_8$: C, 73.60; H, 6.79. Found: C, 73.29; H, 7.04. MS (ES, $[M + Na]^+$) calcd for $C_{40}H_{44}NaO_8$ 675.29, found 675.40.

Methyl (2*S*)-hydroxy-2-(1-allyl-2,3,4,6-tetra-*O*-benzyl-α-D-glucopyranosyl)-ethanoate (4) $[\alpha]_D$ = 84.5 (*c* 1.0, $CHCl_3$); ^{1}H NMR (300 MHz, $CDCl_3$): δ = 2.62-2.73 (m, 1H), 2.78-2.90 (dd, 1H, J = 15.3 Hz, J = 9.4 Hz), 3.59-3.73 (m, 6H), 3.74-3.81 (dd, 1H, J = 11.0 Hz, J = 3.7 Hz), 3.85 (d, 1H, J = 9.6 Hz), 3.99 (d, 1H, J = 1.6 Hz), 4.05-4.19 (m, 2H), 4.53 (d, 1H, J = 12.3 Hz), 4.62-4.71 (m, 2H), 4.82-4.95 (m, 4H), 5.00 (d, 1H, J = 11.0 Hz), 5.10-5.24(m, 2H), 5.88-6.05(m, 1H), 7.20-7.40 (m, 20H); ^{13}C NMR (75 MHz, $CDCl_3$): δ = 36.6, 52.1, 69.1, 73.0, 73.4, 74.2, 75.1, 75.7, 76.2, 78.4, 78.6, 82.3, 84.0, 119.2, 127.5-128.7 (aromatic carbons), 133.4, 137.3, 138.1, 138.3, 138.5, 170.7; Anal. calcd for $C_{40}H_{44}O_8$: C, 73.60; H, 6.79. Found: C, 73.41; H, 6.92. MS (ES, $[M + Na]^+$); calcd for $C_{40}H_{44}NaO_8$ 675.29, found 675.40.

Methyl 2-oxo-2-(1-allyl-2,3,4,6-tetra-*O*-benzyl-*β*-D-glucopyranosyl)-ethanoate (5)

Under a nitrogen atmosphere, to a solution of dry dimethyl sulfoxide (133 μL, 1.88 mmol)) in anhydrous dichloromethane (12 mL) cooled below -65 °C with a dry ice-acetone bath, trifluoroacetic anhydride (TFAA, 200 μL, 1.41 mmol) was slowly added with efficient stirring in ca. 10 min. After 10 min below -65 °C, a solution of compound **3** (307 mg, 0.47 mmol) in dichloromethane (8 mL) was added to the mixture in ca. 15min. The rate of addition of TFAA or alcohol **3** was controlled to keep the temperature below -65 °C. The mixture was stirred below -65 °C for 40min, followed by addition of triethylamine (394 μL, 2.82 mmol) dropwise in ca. 15min. The reaction was kept below -65 °C for 2 more hours. The cooling bath was then removed and the reaction was allowed to warm up to room temperature, then quenched with H_2O (10ml) and the aqueous layer was backwashed with dichloromethane (2 × 15 mL). The combined organic solution was dried with anhydrous Na_2SO_4, concentrated and purified by flash column chromatography (hexanes/ethyl acetate: 6/1) to get **5** (296 mg, 97%). $[\alpha]_D$ = 59.9 (*c* 1.0, $CHCl_3$); ^{1}H NMR (300 MHz, $CDCl_3$): δ = 2.66 (dd, 1H, *J* = 15.6 Hz, *J* = 8.0 Hz), 3.21 (dd, 1H, *J* = 15.6 Hz, *J* = 5.9 Hz), 3.74 (s, 3H), 3.73-3.66 (m, 2H), 3.91-3.76 (m, 3H), 4.24 (d, 1H, *J* = 9.6 Hz), 4.51 (d, 1H, *J* = 11.9 Hz), 4.57 (d, 1H, *J* = 10.3 Hz), 4.61 (d, 1H, *J* = 12.2 Hz), 4.66 (d, 1H, *J* = 10.7 Hz), 4.73 (d, 1H, *J* = 10.3 Hz), 4.83-4.89 (m, 3H), 5.09-5.21 (m, 2H), 5.64 (m, 1H), 7.21-7.40 (m, 20H); ^{13}C NMR (75 MHz, $CDCl_3$): δ = 31.2, 52.3, 68.7, 73.4, 73.5, 75.3, 75.6, 75.7, 77.8, 80.3, 83.4, 84.5, 119.2, 127.4-128.5 (aromatic carbons), 130.9, 137.7, 138.0, 138.3, 138.5, 164.9, 195.8; Anal. calcd for

$C_{40}H_{42}O_8$: C, 73.83; H, 6.51. Found: C, 73.43; H, 6.39. MS (ES, $[M + Na]^+$); calcd for $C_{40}H_{42}NaO_8$ 673.28, found 673.39.

Methyl 2-benzyl imino-2-(1-allyl-2,3,4,6-tetra-*O*-benzyl-*β*-D-glucopyranosyl)-ethanoate (6) Under a nitrogen atmosphere, to an ice-cooled solution of **5** (296 mg, 0.45 mmol) and benzylamine (148 μL, 1.36 mmol) in anhydrous diethyl ether (15 mL) was added dropwise $TiCl_4$ (0.23 mL of a 1 M solution in CH_2Cl_2, 0.23 mmol). After complete addition, the ice bath was removed and the reaction mixture stirred for 4 h at room temperature. After this period, the resulting suspension was cooled at 0 °C and poured into 1 M sodium hydroxide solution. The organic layer was separated and the water layer extracted two times with dichloromethane (2 × 15 mL). The combined organic layer was dried (Na_2SO_4), concentrated and purified by flash column chromatography (hexanes/ethyl acetate: 6/1) to get the mixture of **5** and **6**, which was exposed to the same procedure again, and get **6** (323 mg, 96%). $[\alpha]_D$ = 30.5 (*c* 1.0, $CHCl_3$); ^1H NMR (300 MHz, $CDCl_3$): δ = 2.67 (dd, 1H, *J* = 15.6 Hz, *J* = 8.6 Hz), 3.48 (dd, 1H, *J* = 15.6 Hz, *J* = 5.3 Hz), 3.86-3.66 (m, 7H), 3.91 (dd, 1H, *J* = 9.2 Hz, *J* = 8.9 Hz), 4.16 (d, 1H, *J* = 9.2 Hz), 4.43-4.56 (m, 3H), 4.59-5.72 (m, 4H), 4.86-4.93 (m, 3H), 5.03-5.16 (m, 2H), 5.77 (m, 1H), 7.15-7.42 (m, 25H); ^{13}C NMR (75 MHz, $CDCl_3$): δ = 32.2, 51.6, 58.7, 69.0, 72.9, 73.4, 75.3, 75.5, 75.8, 78.2, 81.5, 82.4, 84.1, 117.9, 127.7-128.5 (aromatic carbons), 132.5, 138.1, 138.2, 138.4, 138.6, 138.7, 163.7, 165.5; Anal. calcd for $C_{47}H_{49}NO_7$: C, 76.30; H, 6.68; N, 1.89. Found: C, 75.77; H, 7.05; N, 1.86. MS (ES, $[M + Na]^+$) calcd for

$C_{47}H_{49}NNaO_7$ 762.34, found 762.38.

Methyl (2*S*)-benzylamino-2-(1-allyl-(2,3,4,6-tetra-*O*-benzyl-*β*-D-glucopyranosyl)-ethanoate (7) To an ice-cooled solution of **6** (240 mg, 0.32 mmol) in methanol (9 mL) was added $NaCNBH_3$ (128 mg, 1.95 mmol), followed by 98% AcOH (39 μL, 0.65 mmol). The reaction mixture was stirred for 3 hours at 0 °C and then quenched with water (5 mL) and extracted with CH_2Cl_2 (3 × 15 mL). The combined organic extracts were dried (Na_2SO_4), concentrated and purified by flash column chromatography (hexanes/ethyl acetate: 5/1) to afford **7** (239 mg, quant.). $[\alpha]_D$ = 32.3 (*c* 1.0, $CHCl_3$); ^1H (300 MHz, $CDCl_3$): δ = 2.71 (dd, 1H, *J* = 16.3 Hz, *J* = 6.0 Hz), 2.84 (dd, 1H, *J* = 16.3 Hz, *J* = 7.4 Hz), 3.39 (d, 1H, *J* = 12.8 Hz), 3.47 (s, 1H), 3.59-3.79 (m, 8H), 3.93 (dd, 1H, *J* = 9.5 Hz, *J* = 8.9 Hz), 4.28 (d, 1H, *J* = 9.5 Hz), 4.50 (d, 1H, *J* = 11.6 Hz), 4.58 (d, 1H, *J* = 12.0 Hz), 4.65 (d, 1H, *J* = 10.8 Hz), 4.67 (d, 1H, *J* = 12.0 Hz), 4.80-4.95 (m, 4H), 5.17-5.04 (m, 2H), 5.77 (m, 1H), 7.45-7.10 (m, 26H); ^{13}C NMR (75 MHz, $CDCl_3$): δ = 32.4, 51.5, 51.8, 64.8, 69.1, 73.4, 73.5, 74.9, 75.1, 75.7, 78.8, 79.7, 80.2, 84.7, 118.1, 127.7-128.5 (aromatic carbons), 132.0, 138.2, 138.5, 138.7, 138.8, 139.7, 174.0; Anal. calcd for $C_{47}H_{51}NO_7$: C, 76.09; H, 6.93; N, 1.89. Found: C, 75.84; H, 7.36; N, 2.37. MS (ES, $[M + Na]^+$) calcd for $C_{47}H_{51}NNaO_7$ 764.37, found 764.32.

(1*S*)-2,3,4,6-Tetra-*O*-benzyl-1′-*N*-benzyl-5′(*R*)-hydroxymethylene-spiro[1,5-anhydro-D-glucitol-1,3′-*L*-proline methyl ester] (8) To a solution of **7** (340 mg, 0.46 mmol) in dichloromethane and diethyl ether(12 mL, 1:1) was added iodine (175 mg, 0.69 mmol) at 0 °C. The mixture was quenched with saturated sodium thiosulfate solution (5 mL) after overnight. The organic layer was separated and the aqueous layer was backwashed with dichloromethane (2 × 10 mL), the combined organic solution was dried with anhydrous Na_2SO_4 and concentrated followed by dissolvation in toluene (15 mL) and treated with silver acetate (1.146 g, 6.88 mmol) for overnight at room temperature to get an inseparable mixture of **13**, **14** and **15** (323 mg, 93%), which was hydrolyzed with K_2CO_3 (73 mg, 1.3 equiv) in methanol (8 mL) for 1 h at room temperature, and then quenched with saturated ammonium chloride (10 mL) and extracted with CH_2Cl_2 (3 × 15 mL). The combined organic solution was dried with anhydrous Na_2SO_4, concentrated and purified by flash column chromatography (hexanes/ethyl acetate: from 4/1 to 2/1) to get **8** (132 mg, 43%), **9** (141 mg, 46%) and **10** (20 mg, 6.5%). **(8)** $[\alpha]_D = 47.7$ (*c* 1.0, $CHCl_3$); ^{1}H NMR (300 MHz, $CDCl_3$): δ = 2.13 (dd, 1H, *J* = 13.9 Hz, *J* = 5.4 Hz), 2.60 (dd, 1H, *J* = 13.9 Hz, *J* = 11.0 Hz), 3.09 (s, 3H), 3.30 (m, 1H), 3.45-3.85 (m, 11H), 4.02 (d, 1H, *J* = 13.5 Hz), 4.38 (d, 1H, *J* = 12.9 Hz), 4.57-4.71 (m, 4H), 4.83 (d, 1H, *J* = 11.0 Hz), 4.86 (d, 1H, *J* = 11.0 Hz), 5.10 (d, 1H, *J* = 12.7 Hz), 7.10-7.45 (m, 25H); ^{13}C NMR (75 MHz, $CDCl_3$): δ = 27.2, 51.8, 59.0, 60.0, 63.0, 69.5, 72.4, 72.7, 73.5, 74.8, 75.1, 75.5, 76.7, 78.8, 86.1, 88.2, 125.8-128.9 (aromatic carbons), 138.0, 138.0, 138.3, 138.8, 138.9, 172.6; HRMS (ES) calcd for $C_{47}H_{52}NO_8$ $[M + H]^+$ 758.3693, found 758.3687.

(1*S*)-2,3,4,6-Tetra-*O*-benzyl-1′-*N*-benzyl-5′(*S*)-hydroxymethylene-spiro[1,5-anhydro-D-glucitol-1,3′-*L*-proline methyl ester] (9) $[\alpha]_D$ = -3.6 (*c* 1.70, $CHCl_3$); ^1H NMR (300 MHz, $CDCl_3$): δ = 2.24 (d, 1H, *J* = 14.6 Hz), 2.83 (dd, 1H, *J* = 13.9 Hz, *J* = 10.5 Hz), 3.05-3.23 (br, OH), 3.31 (s, 3H), 3.43 (d, 1H, *J* = 11.1 Hz), 3.62-3.9 (m, 10H), 4.00(d, 1H, *J* = 14.6 Hz), 4.47 (d, 1H, *J* = 12.5 Hz), 4.54-4.77 (m, 4H), 4.82-4.94 (m, 2H), 5.24 (d, 1H, *J* = 11.8 Hz), 7.12-7.44 (m, 25H); ^{13}C NMR (75 MHz, $CDCl_3$): δ = 27.9, 51.1, 51.7, 61.3, 62.6, 69.1, 72.5, 72.9, 73.0, 73.7, 74.9, 75.7, 77.0, 78.5, 85.7, 86.2, 126.0-128.6 (aromatic carbons), 138.0, 138.2, 138.4, 138.8, 138.9, 170.5; HRMS (ES) calcd for $C_{47}H_{52}NO_8$ $[M + H]^+$ 758.3693, found 758.3696.

(1*S*)-2,3,4,6-Tetra-*O*-benzyl-1′-*N*-benzyl-5′(*S*)-hydroxy-spiro[1,5-anhydro-D-glucitol-1,3′-*L*-pipecolic methyl ester] (10) $[\alpha]_D$ = 34.7 (*c* 1.0, $CHCl_3$); ^1H NMR (300 MHz, $CDCl_3$): δ = 2.25-2.36 (m, 2H), 2.76 (dd, 1H, *J* = 11.0 Hz, *J* = 5.2 Hz), 3.04 (dd, 1H, *J* = 10.6 Hz, *J* = 9.6 Hz), 3.32 (s, 3H), 3.42 (s, 1H), 3.53-3.82 (m, 7H), 3.90-4.07 (m, 2H), 4.58-4.73 (m, 5H), 4.82 (d, 1H, *J* = 11.2 Hz), 4.87 (d, 1H, *J* = 10.9 Hz), 5.10 (d, 1H, *J* = 11.7 Hz), 7.12-7.39 (m, 25H); ^{13}C NMR (75 MHz, $CDCl_3$) δ = 29.7, 30.7, 51.0, 54.5, 59.0, 63.5, 69.5, 69.9, 72.4, 73.3, 73.9, 74.9, 75.4, 78.1, 79.1, 80.4, 84.6, 126.3-128.6 (aromatic carbons), 138.1, 138.2, 138.3, 138.6, 138.7, 170.7; HRMS (ES) calcd for $C_{47}H_{52}NO_8$ $[M + H]^+$ 758.3693, found 758.3686.

(1*S*)-5′(*R*)-hydroxymethylene-spiro[1,5-anhydro-D-glucitol-1,3′-*L*-proline methyl ester] (11) Under the nitrogen atmosphere, to the solution of compound **8** (200 mg, 0.25 mmol) in methanol (10 mL) was added the 1 M hydrochloride acid solution (0.38 mL, 0.38 mmol) and the palladium hydroxide (20 wt % Pd on carbon, 50 mg). The mixture was exposed to hydrogen condition (H_2, 10 psi) and stirred for 6 hours. The solution was filtrated and evaporated in vacuum to get the product **11** (75 mg, quant.) $[\alpha]_D = 64.1$ (*c* 1.0, MeOH); ^{1}H NMR (300 MHz, CD_3OD): δ = 2.13 (dd, 1H, J = 15.0 Hz, J = 2.8 Hz), 2.41 (dd, 1H, J = 15.0 Hz, J = 10.8 Hz), 3.23-3.21 (m, 5H), 3.49 (m, 1H), 3.6-3.71 (m, 2H), 3.85-4.00 (m, 4H), 4.22 (s, 1H); ^{13}C NMR (75 MHz, CD_3OD): δ = 27.3, 54.3, 61.5, 61.9, 63.0, 68.7, 70.8, 71.6, 76.6, 77.0, 88.3, 168.5; HRMS (ES) calcd for $C_{12}H_{22}NO_8$ [M + H]$^+$ 308.1340, found 308.1343.

(1*S*)-5′(*S*)-hydroxymethylene-spiro[1,5-anhydro-D-glucitol-1,3′-*L*-proline methyl ester] (12) (The same synthetic procedure as described for compound **11** was used); $[\alpha]_D$ = 75.7 (*c* 1.10, MeOH); ^{1}H NMR (300 MHz, CD_3OD) δ = 2.09 (m, 1H), 2.56 (dd, 1H, J = 10.3 Hz, J = 13.6 Hz), 3.24 (m, 1H), 3.30-3.40 (m, br, 1H, overlapping with solvent peak), 3.47 (m, 1H), 3.57-3.68 (m, 2H), 3.72-3.95 (m, 6H), 4.18-4.33 (m, 2H); ^{13}C NMR (75 MHz, CD_3OD): δ = 27.8, 54.2, 62.6, 63.1, 63.2, 69.1, 71.2, 71.7, 76.7, 76.9, 88.2, 167.9; HRMS (ES) calcd for $C_{12}H_{22}NO_8$ [M + H]$^+$ 308.1340, found 308.1348.

(1*S*)-2,3,4,6-Tetra-*O*-benzyl-1′-*N*-benzyl-5′(*R*)-methylenehydroxy acetate-spiro[1,5-anhydro-D-glucitol-1,3′-*L*-proline methyl ester] (13) To a solution of **8** (60 mg, 0.079 mmol) in pyridine (1 mL) was added acetic anhydride (37 μL, 0.395 mmol) and stirred for 5 hours. The pyridine was removed with high vacuum. The crude product was purified by flash column chromatography (hexanes/ethyl acetate: 4/1) to get **13** (62 mg, quant.). $[\alpha]_D = 50.3$ (*c* 1.0, $CHCl_3$); ^1H NMR (300 MHz, $CDCl_3$): δ = 2.05 (s, 3H), 2.18 (dd, 1H, *J* = 13.0 Hz, *J* = 10.8 Hz), 2.33 (dd, 1H, *J* = 13.6 Hz, *J* = 5.7 Hz), 3.13 (s, 3H), 3.32 (m, 1H), 3.53 (s, 1H), 3.63-3.78 (m, 6H), 3.83 (d, 1H, *J* = 14.4 Hz), 4.08 (d, 1H, *J* = 13.7 Hz), 4.24 (d, 2H, *J* = 6.0 Hz), 4.42 (d, 1H, *J* = 12.3 Hz), 4.58-4.70 (m, 4H), 4.83 (d, 1H, *J* = 9.9 Hz), 4.86 (d, 1H, *J* = 9.9 Hz), 5.06 (d, 1H, *J* = 12.3 Hz), 7.13-7.43 (m, 25H); ^{13}C NMR (75 MHz, $CDCl_3$): δ = 20.9, 30.0, 51.5, 60.4, 60.8, 67.2, 69.4, 72.5, 72.8, 73.5, 75.1, 75.5, 76.0, 76.7, 78.7, 86.1, 87.5, 126.0-128.8 (aromatic carbons),138.03, 138.04, 138.4, 138.9, 139.3, 171.0, 172.0; HRMS (ES) calcd for $C_{49}H_{54}NO_9$ $[M + H]^+$ 800.3793, found 800.3794.

(1*S*)-2,3,4,6-Tetra-*O*-benzyl-1′-*N*-benzyl-5′(*S*)-methylenehydroxy acetate-spiro[1,5-anhydro-D-glucitol-1,3′-*L*-proline methyl ester] (14) (The same synthetic procedure as described for compound **13** was used); $[\alpha]_D = 6.2$ (*c* 1.0, $CHCl_3$); ^1H NMR (300 MHz, $CDCl_3$): δ = 2.01 (s, 3H), 2.14 (dd, 1H, *J* = 15.4 Hz, *J* = 1.1 Hz), 2.82 (dd, 1H, *J* = 13.9 Hz, *J* = 10.0 Hz), 3.26 (s, 3H), 3.58-3.82 (m, 9H), 3.59-3.82 (m, 2H), 4.21 (dd, 1H, *J* = 10.7 Hz, *J* = 5.0 Hz), 4.43 (d, 1H, *J* = 12.6 Hz), 4.57-4.75 (m, 4H), 4.82 (d, 1H, *J* = 11.2

Hz), 4.86 (d, 1H, J = 11.2 Hz), 5.15 (d, 1H, J = 12.3 Hz), 7.10-7.40 (m, 25H); ^{13}C NMR (75 MHz, $CDCl_3$): δ = 21.0, 27.7, 51.1, 53.0, 60.0, 67.2, 69.0, 72.9, 73.0, 73.2, 73.7, 75.1, 75.6 (2 carbons), 78.7, 85.9, 86.9, 126.0-128.5 (aromatic carbons), 137.0 (2 carbons), 138.5, 138.9, 139.5, 170.9, 170.9; HRMS (ES) calcd for $C_{49}H_{54}NO_9$ $[M + H]^+$ 800.3793, found 800.3793.

(1*S*)-2,3,4,6-Tetra-*O*-benzyl-1′-*N*-benzyl-5′(*S*)-*O*-acetyl-spiro[1,5-anhydro-D-glucitol-1,3′-*L*-pipecolic methyl ester] (15) (The same synthetic procedure as described for compound **13** was used); $[\alpha]_D$ = 44.0 (*c* 1.0, $CHCl_3$); ^{1}H NMR (300 MHz, $CDCl_3$): δ = 2.05 (s, 3H), 2.32 (dd, 1H, J = 13.6 Hz, J = 11.9 Hz), 2.52 (dd, 1H, J = 13.7 Hz, J = 4.0 Hz), 2.90 (dd, 1H, J = 10.4 Hz, J = 5.6 Hz), 3.24(dd, 1H, J = 10.4 Hz, J = 10.8 Hz), 3.29 (s, 3H), 3.46-3.99 (m, 9H), 4.45 (d, 1H, J = 12.9 Hz), 4.59-4.93(m, 6H), 5.09(m, 1H), 5.15 (d, 1H, J = 12.4 Hz), 7.10-7.44 (m, 25H); ^{13}C NMR (75 MHz, $CDCl_3$): δ = 21.6, 26.4, 50.2, 50.4, 59.5, 69.7, 72.8, 73.4, 74.4 (2 carbons), 75.4 (2 carbons), 75.8, 78.7, 79.4, 80.9, 85.3, 126.50-128.90 (aromatic carbons), 138.8 (3 carbons), 139.2, 139.4, 170.7 (2 carbons); HRMS (ES) calcd for $C_{49}H_{54}NO_9$ $[M + H]^+$ 800.3793, found 800.3788.

3.5. References:

1. Kakinoki, S.; Hirano, Y.; Oka. M. *Polym. Bull. (Berlin)* **2005**, *53*, 109.
2. Reddy, K. V. R.; Yedery, R. D.; Aranha, C. *Int. J. Antimicrobial Agents* **2004**, *24*, 536.
3. Buku, A.; Faulstich, H.; Wieland, T.; Dabrowski, J. *Proc. Natl. Acad. Sci. USA*. **1980**, *77*, 2370.
4. Nakajima, T.; Volcani, B. E. *Science* **1969**, *164*, 1400.
5. Taylor, S. W.; Waite, J. H.; Ross, M. M.; Shabanowitz, J.; Hunt, D. F. *J. Am. Chem. Soc.* **1994**, *116*, 10803..
6. Vitagliano, L.; Berisio, R.; Mazzarella, L.; Zagari, A. *Biopolymers* **2001**, *58*, 459. And references therein.
7. Beausoleil, E.; Lubell, W. D. *J. Am. Chem. Soc.* **1996**, *118*, 12902. And references therein.
8. Delaney, N. G.; Madison, V. J. *J. Am. Chem. Soc.* **1982**, *104*, 6635.
9. Samanen, J.; Zuber, G.; Bean, J.; Eggleston, D.; Romoff, T.; Kopple, K.; Saunders, M.; Regoli, D. *Int. J. Pept. Protein. Res.* **1990**, *35*, 501.
10. Quancard, J.; Labonne, A.; Jacquot, Y.; Chassaing, G.; Lavielle, S.; Karoyan, P. *J. Org. Chem.* **2004**, *69*, 7940.
11. Che, Y.; Marshall, G. R. *J. Org. Chem.* **2004**, *69*, 9030. And references therein.
12. Tam, J. P.; Miao, Z. *J. Am. Chem. Soc.* **1999**, *121*, 9013. And references therein.
13. Cavelier, F.; Vivet, B.; Martinez. J.; Aubry, A.; Didierjean, C.; Vicherat, A.; Marraud, M. *J. Am. Chem. Soc.* **2002**, *124*, 2917. And references therein.
14. Sharma, R.; Lubell, W. D. *J. Org. Chem.* **1996**, *61*, 202. And references therein.
15. Jeannotte, G.; Lubell, W. D. *J. Org. Chem.* **2004**, *69*, 4656.
16. (a) Wagaw, S.; Rennels, R. A.; Buchwald, S. L. *J. Am. Chem. Soc.* **1997**, *119*, 8451. (b) Kuwano, R.; Sato, K.; Kurokawa, T.; Karube, D.; Ito, Y. *J. Am. Chem. Soc.* **2000**, *122*, 7614. (c) Viswanathan, R.; Prabhakaran, E. N.; Plotkin, M. A.; Johnston, J. N. *J. Am. Chem. Soc.* **2003**, *125*, 163.
17. Koep, S.; Gais, H-J.; Raabe, R. *J. Am. Chem. Soc.* **2003**, *125*, 13243. And references therein.
18. For selected examples of bicyclic proline analogues incorporated into bioactive peptides see: (a) Cluzeau, J.; Lubell, W. D. *Biopolym., Pept. Sci.* **2005**, *80*, 98. (b) Blankley, C. J.; Kaltenbronn, J. S.; DeJohn, D. E.; Wener, A.; Bennett, L. R.; Bobowski, G.; Krolls, U.; Johnson, D. R.; Pearlman, W. M.; Hoefle, M. L. *J. Med. Chem.* **1987**, *30*, 992. (c) Dumy, P.; Keller, M; Ryan, D. E.; Rohwedder, B.; Wöhr, T.; Mutter, M. *J. Am. Chem. Soc.* **1997**, *119*, 918. (d) Li. W.; Moeller, K. D. *J. Am. Chem. Soc.* **1996**, *118*, 10106.
19. For recent reviews on the synthesis and applications of sugar amino acid hybrids and related materials see: (a) Dondoni, A.; Marra, A. *Chem. Rev.* **2000**, *100*, 4395; (b) Schweizer, F. *Angew. Chem. Intl. Ed.* **2002**, *41*, 230. For recent reviews on the use of sugar amino acids as peptidomimetics see: (c) Gruner, S.W.; Locardi, E.; Lohof, E.; Kessler, H. *Chem. Rev.* **2002**, *102*, 491. (d) Chakraborty, T. K.; Ghosh, S.; Jayaprakash, J. *Curr. Med. Chem.* **2002**, *9*, 421.
20. Grotenbreg, G. M.; Timmer, M. S. M.; Llamas-Saiz, A. L.; Verdoes, M.; Van der Marel, G. A.; van Raaij, M. J.; Overkleeft, H. S.; Overhand, M. *J. Am. Chem. Soc.* **2004**, *126*, 3444.
21. Chakraborty, T. K.; Jayaprakash, S.; Diwan, P. V.; Nagaraj, R.; Jampani, S. R. B.; Kunwar, A. C. *J. Am. Chem. Soc.* **1998**, *120*, 12962.

22. It has been reported that substitution of D-proline by *cis*-3-hydroxy-D-proline (HypC3-OH) in the sequence Boc-Leu-Pro-Gly-Leu-NHMe resulted in novel pseudo β-turn-like nine-membered ring structure involving an intramolecular LeuNH →HypC3-OH hydrogen bond. Chakraborty, T. K.; Srinivasu, P.; Vengal Rao, R.; Kiran Kumar, S.; Kunwar, A. C. *J. Org. Chem.* **2004**, *69*, 7399.
23. Prior to this publication a report on a 5-membered spirocyclic fructose-based proline analogue appeared: Cipolla, L.; Redaelli, C.; Nicotra, F. *Lett. Drug Des. Discov.* **2005**, *2*. 291.
24. Gueyrard, D.; Haddoub, R.; Salem, A.; Bacar, N. S.; Goekjian, P. G. *Synlett* **2005**, 520.
25. (a) Schweizer, F.; Inazu, T. *Org. Lett.* **2001**, *3*, 4115. (b) Zhang, K.; Wang, J.; Sun, Z.; Huang, H-D; Schweizer, F. *Synlett* **2007**, 239.
26. Dillon, M. P.; Maag, H.; Muszyski, D. M. *Tetrahedron Lett.* **1995**, *36*, 5469.
27. A 40 ms Gaussian pulse with a 560 ms mixing time was used.
28. Huang, S. K.; Omura, K.; Swern, D. *J. Org. Chem.* **1976**, *41*, 3329.
29. Boeykens, M.; Kimpe, N. D.; Tehrani, K. A. *J. Org. Chem.* **1994**, *59*, 6973.
30. Chérest, M.; Felkin, H.; Prudent, N. *Tetrahedron Lett.* **1968**, *9*, 2199.
31. Davies, S. G.; Nicholson, R. L.; Price, P. D.; Roberts, P. M.; Smith, A. D. *Synlett* **2004**, *5*, 901.

Chapter 4

Intramolecular Hydrogen Bond-controlled Prolyl Amide Isomerization in Glucosyl 3(*S*)-hydroxyproline Hybrids – The Influence of a C^{δ}-hydroxymethyl Substituent on the Thermodynamics and Kinetics of Prolyl Amide Cis/Trans Isomerization

Abstract: *Peptide mimics containing spirocyclic glucosyl-(3-hydroxy)proline hybrids (Glc3(S)HypHs) with a polar hydroxymethyl substituent at the C-5' position, such as peptide esters Ac-Glc3(S)Hyp-OMe and diamides Ac-Glc3(S)Hyp-N'-CH_3, were synthesized. Peptide esters exhibit increased cis population (23-53%) relative to 3(S)-hydroxyproline (17%) or proline (14%) in D_2O. The prolyl amide cis population is further increased to 38-74% in the diamide form in D_2O. Our study shows that the stereochemistry of the hydroxymethyl substituent at the C-5' position of proline permits tuning of the prolyl amide cis/trans isomer ratio. Inversion-magnetization transfer NMR experiments indicate that the stereochemistry of the hydroxymethyl substituent has a dramatic effect on the kinetics of prolyl amide cis/trans isomerization. A 200-fold difference in the trans-to-cis (k_{tc}) isomerization and a 90-fold rate difference in the cis-to-trans (k_{ct}) isomerization is observed between epimeric C-5' peptide esters. When compared to reference peptide mimics Ac-Pro-OMe and Ac-3(S)Hyp-OMe, our study demonstrates that a (13-16)-fold decrease in k_{tc} and k_{ct} is observed for the C-5'(S), while a (5-24)-fold acceleration is observed for the C-5'(R) epimer. DFT-calculations indicate that the pyrrolidine ring prefers a C^{β} exo pucker in both Ac-Glc3(S)Hyp-OMe diastereoisomers. Computational calculations and chemical shift temperature coefficient ($\Delta\delta/\Delta T$) experiments indicate that the hydroxymethyl group at C-5' in Ac-Glc3(S)Hyp-OMe forms a stabilizing intramolecular hydrogen bond to the carbonyl of the N-acetyl group in both epimeric cis isomers. However, a competing intramolecular hydrogen bond between the hydroxymethyl groups in the pyrrolidine ring and pyran ring stabilizes the trans isomer in the C-5'(S) diastereoisomer. The dramatic differences in the kinetic properties of the diastereoisomeric peptide mimics are rationalized by the presence or absence of an intramolecular hydrogen bond between the hydroxymethyl substituent located at C-5' and the developing lone pair on the nitrogen atom of the N-acetyl group in the transition state.*

4.1. Introduction

Proline (Pro) is the only cyclic amino acid of the twenty DNA-encoded amino acids, which is characterized by limited rotation of the ϕ dihedral angle (fixed at ~ -75°) as its side chain is fused to the peptide backbone. As a result there is a reduction in the energy difference between the prolyl amide *cis*- and *trans*-isomers making them nearly isoenergetic; this leads to a higher *cis* *N*-terminal amide content relative to the other amino acids. The kinetics of the prolyl *cis/trans* isomerization reaction is the rate-determining step in the folding pathways of many peptides and proteins.[1] Moreover, proline induces β-turns and extended helical structures (polyproline helix) in peptides that are crucial in protein/protein and protein/peptide interactions.[2] In nature, proline undergoes post-translational modifications such as hydroxylation to 4(*R*)-hydroxyproline (4-Hyp) and 3(*S*)-hydroxyproline (3-Hyp).[3,4,5,6] Hydroxylation of proline is critical to the thermal stability and modulation of the local stability of the triple helix in collagens[7] and contributes to the stability of the poly-Hyp helix in plant-derived Hyp-rich glycopeptides.[8]

Over the years a plethora of proline analogs such as C^{β}-, C^{γ}- and C^{δ}-substituted prolines,[9-12] azaprolines,[13] pseudoprolines,[14] silaproline,[15] proline-amino acid chimera,[16] fused bicyclic proline[17-19] and fused glucose-proline analogs[20] have been developed to study the structural and biological properties of proline surrogates in peptides.[21] In particular, pseudoprolines bearing two substituents adjacent to the endocyclic nitrogen of proline and C^{δ}-substituted prolines containing bulky substitutents have been shown to increase the prolyl amide *cis* conformer ratio in peptides and peptide mimics.[9,21c,22] Incorporation of pseudoprolines into peptides has been shown to induce a "kink"

conformation in the peptide backbone, originating in the preference for *cis* amide bond formation. This prevents peptide aggregation, self association and β-structure formation thus improving the solvation and coupling kinetics of the growing peptide chain considerably.[23]

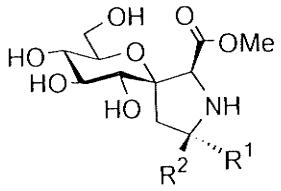

1: $R^1 = CH_2OH$; $R^2 = H$
2: $R^1 = H$; $R^2 = CH_2OH$

Figure 4.1 Structure of spirocyclic glucose-3(*S*)-hydroxyproline hybrids (Glc3(*S*)HypHs)

Recently, we have reported on the synthesis of spirocyclic glucose-3(*S*)-hydroxyproline hybrids Glc3(*S*)HypHs **1** and **2** (Figure 4.1).[24] Compounds **1** and **2** exhibit several intriguing features. The spirocyclic nature of the *gluco*-derived scaffold constrains the pyrrolidine ring of proline and introduces artificial post-translational modifications (hydroxylation + glycosylation). Chemical manipulations and derivatizations of the glucose-derived polyol scaffold provide an opportunity to tailor the chemical, physical and pharmacodynamic properties of Glc3(*S*)Hyp-containing peptides.[25] Moreover, compounds **1** and **2** contain a hydroxymethyl substituent adjacent to the imino function of proline which may permit control of prolyl amide *cis/trans* isomerization via hydrogen bonding, electrostatic or steric interactions. It is noteworthy that the influence of C^{δ}-substituted proline analogs capable of forming polar interactions on the thermodynamics and kinetics of prolyl amide *cis/trans* isomerization has not yet been investigated.

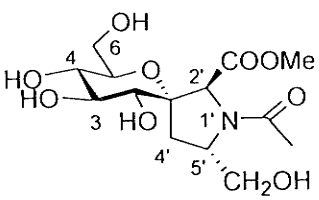

Ac-Glc3(*S*)-HypH-OMe (**3**)

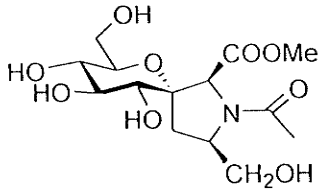

Ac-Glc3(*S*)-HypH-OMe (**4**)

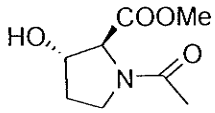

Ac-3(*S*)-Hyp-OMe (**5**)

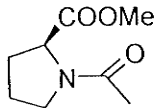

Ac-Pro-OMe (**6**)

Figure 4.2 Peptide mimics **3-6**. Esters 3 and 4 are glucose-3(*S*)-hydroxyproline analogs while esters **5** and **6** serve as reference compounds.

4.2. Results

Herein, we describe the thermodynamics and kinetics of prolyl *N*-terminal amide isomerization of peptide mimics **3** and **4** (Figure 4.2). Compounds **5** and **6**[26] serve as reference compounds and were selected to study how 3(*S*)-hydroxylation of proline influences the kinetics and thermodynamics of prolyl amide *cis*/*trans* isomerization. We initially selected *C*-terminal methyl esters to avoid complications arising from competing intramolecular hydrogen bonding of *C*-terminal amides.[27] Furthermore, the amide bond order of **3-6** can be assessed by FT-IR without interference with *C*-terminal amide. Subsequently, we extended our study to *C*-terminal methylamides.

Synthesis of peptide mimics 3-6. Peptide mimics **3** and **4** were synthesized by acetylation of proline analogs **1** and **2** in pyridine and acetic anhydride followed by *O*-deacetylation using a solution of sodium methoxide in methanol (Scheme 1.1). Peptide mimic **5**, was synthesized according to a modified procedure[26] while peptide mimic **6** was purchased.

Scheme 1.1 Synthesis of peptide mimetics **3-4**

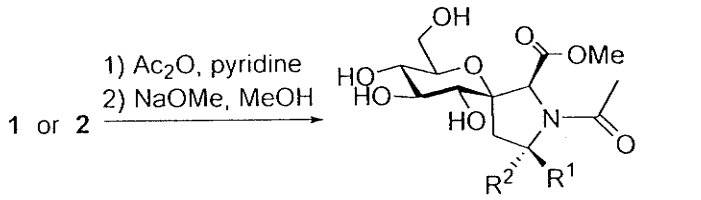

3 R^1 = H, R^2 = CH_2OH (90%)
4 R^1 = CH_2OH, R^2 = H (92%)

Assignments of *N*-terminal geometry for both major and minor isomers of 3 and 4 and determination of $K_{t/c}$. Identification of prolyl amide *trans* and *cis* isomers were based on multiple one-dimensional GOESY[28] experiments in CD_3OD in which the optimized resolution was obtained (Figure 4.3). For instance, subjection of H-2′ signal in prolyl amide *cis* isomer **3a** to a one-dimensional GOESY experiment showed interproton effect to the *N*-terminal methyl group (5.2% nOe relative to the H-2′ signal). By comparison, no interproton effect was observed between H-5′ and the *N*-terminal methyl group. The same diagnostic tools were used to assign the prolyl amide isomers in compounds **3b**, **4a** and **4b** and the observed interproton effects are summarized in Figure 3.

We also observed that the ^{13}C NMR chemical shifts of the C^{α} atoms of the *trans* rotamers in compounds **3** and **4** are high-field shifted (0.8-1.6 ppm) relative to the *cis* isomers irrespective of the solvent used (Table 4.1). For instance, in methanol, we observed C^{α} for *cis* isomer **3a** at 72.80 ppm while the *trans* isomer **3b** appeared at 71.74 ppm in the ^{13}C-NMR. This result is consistent with previous findings by Lubell[9] and may serve as an empirical rule to assign the prolyl amide *cis* and *trans* isomers in cases where GOESY experiments cannot be performed.

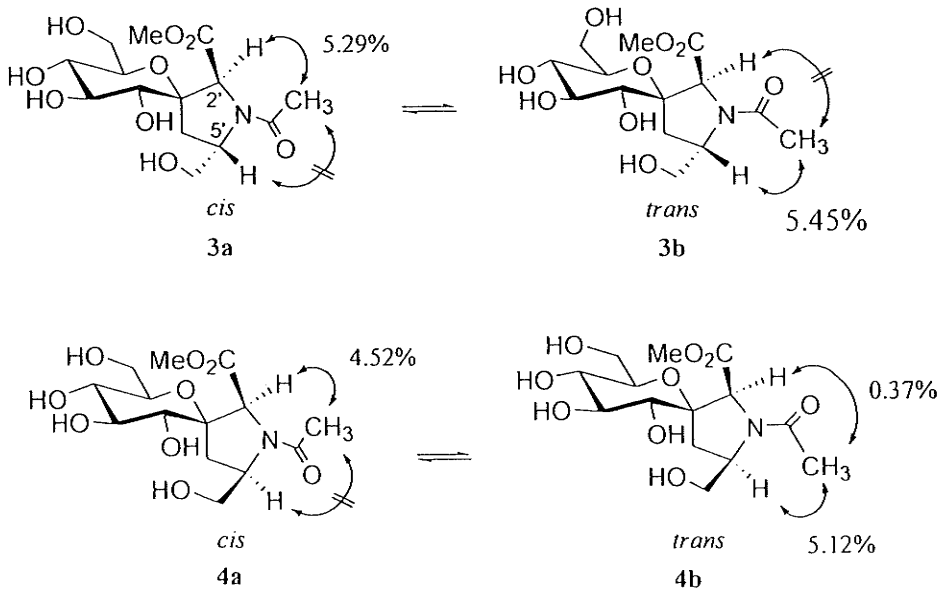

3a 3b 4a 4b

Figure 4.3 Assignment of *cis* and *trans* isomers in compounds **3** and **4** in CD_3OD through 1D nOe

Table 4.1 Chemical shift of *C*-2′ in *cis* and *trans* isomers of **3** and **4**

Compds		**3**[a]	**4**[a]	**3**[b]	**4**[b]
C^{α}	*cis*	73.63	73.55	72.80	72.67
(ppm)	*trans*	72.66	72.30	71.74	71.08

[a] Measured in D_2O; [b] measured in CD_3OD.

For each compound **3**-**6**, the ratio of *trans*/*cis* isomers was calculated by integrating and averaging as many well-resolved proton signals as possible in the ^{1}H-NMR spectra (Table 4.2).[29] We found that the hydroxymethyl substitutent at *C*-5′ enables tuning of the prolyl amide *cis*/*trans* ratio. For instance, compound **4** shows a slight preference for the *cis* rotamer (53%) while its *C*-5′ epimer exists predominantly as the *trans* rotamer (77%). In comparison, reference compounds **5** and **6** exhibit nearly identical *cis*/*trans* ratios confirming that the presence of an electron withdrawing hydroxyl group in **5** has no measurable effect on the prolyl amide *cis*/*trans* rotamer population.[26]

Table 4.2 *Trans/cis* ratio[a] $K_{t/c}$ (± 0.04) and (*cis*% ± 3%) isomer of **3–6** in water

Compd.	3	4	5	6
$K_{t/c}$ (*cis*)	3.35 (23%)	0.88 (53%)	4.88 (17%)	6.14 (14%)

[a]Determined by 500 MHz NMR at 25°C

In order to compare our results with other reported proline analogues, we converted peptide esters **3** and **4** into *N'*-methylamides **7** and **8** by nucleophilic displacement. Peptide mimics **7** and **8** show a significantly increased *cis* rotamer population when compared to esters **3** and **4**. Similar observations have been made by others and these results have been explained by enhanced n→π* interactions[30] of the oxygen lone pair of the (*i* – 1) *trans* amide residue to the antibonding orbital of the C=O bond belonging to the Pro (*i*) residue (Figure 4.4).[29] The fact that an amide carbon is less electron deficient[30b] than an ester carbon has been used to explain higher *trans* ratios in prolyl amide esters when compared to prolyl amide amides.[29]

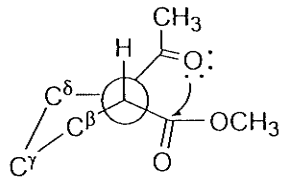

Figure 4.4 n→π* interaction (looking down C^{α}-N bond)

The *cis* population of peptide mimics **7** and **8** are presented in Table 3 together with previously published data for proline analog **9**,[9] 5-methylproline analogs **10** and **11**[31] and 5-*tert*-butylproline analogs **12** and **13** (Figure 4.5).[9] These results show that **8** induces a high *cis* rotamer population (74 ± 3%) while **7** exhibits a reduced *cis* rotamer population (38 ± 3%). Interestingly, the stereochemistry at *C*-5′ of **7** and **8** seems to have a reverse

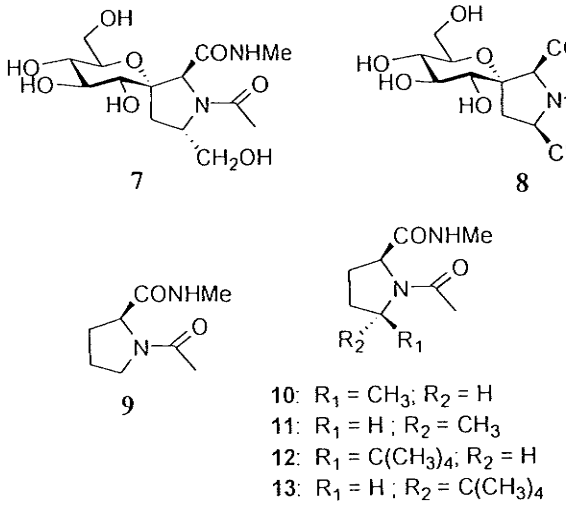

Figure 4.5 Various *N*-Acetyl *N'*-methylamides. Compounds **9-13** have been previously synthesized[9,31]

effect on the equilibrium constant of isomerization by comparison with *tert*-butyl proline analogues **12** and **13** (Table 4.3).

Table 4.3 *Cis* population of prolyl *N*-acetyl *N'*-methylamides in D_2O

Compd.	**7**	**8**	**9**[a]	**10**[b]	**11**[b]	**12**[a]	**13**[a]
Cis(±3%)	38	74	27	25	30	49	66

[a] Ref. 9; [b] Ref. 31.

Kinetics of *cis-trans* prolyl amide bond isomerization in peptide mimics 3-6. The kinetics of *cis/trans* isomerization for compounds **3-6** were determined by ^{1}H-NMR spectroscopy inversion-magnetization transfer experiments[32] in D_2O (Table 4.4). Because the rates for *cis/trans* isomerization are extremely slow in protic solvents, we performed these experiments at elevated temperatues.[33] At 83 °C, the *trans*-to-*cis* rate constants of isomerizations (k_{tc}) follows the order **4** < **5** ≈ **6** < **3**. A 200-fold rate difference is oberved for diastereomeric amides **3** and **4**. In comparison, hydroxyprolyl amide **5** and prolyl

amide **6** exhibit nearly identical rate constants indicating that the 3(*S*)-hydroxy group has little effect on the kinetics of isomerization.

Table 4.4 Rate constants of prolyl amide isomerization for **3-6**

Amide	k_{ct}[a] (s^{-1})	k_{tc}[b] (s^{-1})
3	0.18 ± 0.01	0.08 ± 0.004
4	16.19 ± 1.19	19.82 ± 1.45
5	2.63 ± 0.28	1.02 ± 0.09
6	2.95 ± 0.12	0.82 ± 0.04

[a]Carried out in D_2O at 83 °C; [b]calculated from k_{ct} and $K_{t/c}$;

The effects of temperature on k_{ct} and k_{tc} were analyzed by *Eyring* plots (Figure 4.6).[34]

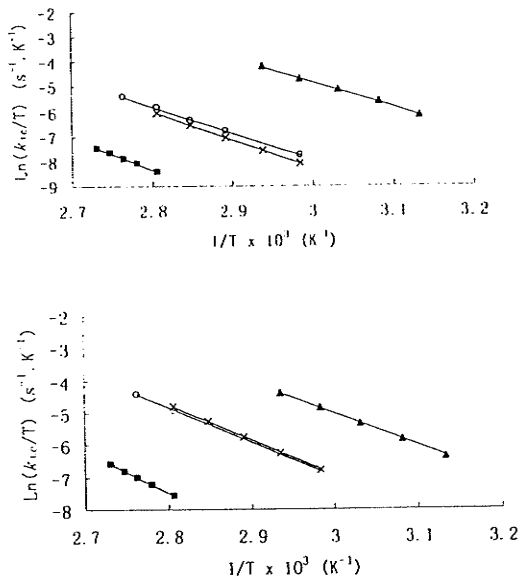

Figure 4.6 *Eyring* plots: *trans*-to-*cis* (up); *cis*-to-*trans* (down); compounds **3** (■), **4** (▲), **5** (○) and **6** (×).

The values for $\Delta H^{\ddagger}$ and $\Delta S^{\ddagger}$ (Table 4.5) were calculated from linear least squares fits of the data in these plots.[34] The activation parameters demonstrate that the free energy barriers to isomerization of compounds **3-6** are enthalpic in origin. Interestingly, amide **3**

exhibits a significantly increased activation enthalpy (3.9-6.8 kcal/mol) when compared to compounds **4-6**. However, the activation enthalpy is partially compensated by a higher activation entropy.

Table 4.5 Activation enthalpies ($\Delta H^{\ddagger}$) and entropies ($\Delta S^{\ddagger}$) as derived from Eyring plots in D_2O for **3-6**. Additionally the free energies of activation at 298K ($\Delta G^{\ddagger}$) are given.

	cis to *trans*[a]			*trans* to *cis*[a]		
	$\Delta H^{\ddagger}$[b]	$\Delta S^{\ddagger}$[c]	$\Delta G^{\ddagger}$[d]	$\Delta H^{\ddagger}$[b]	$\Delta S^{\ddagger}$[c]	$\Delta G^{\ddagger}$[d]
3	26.1	11.1	22.8	26.4	10.2	23.4
4	19.8	2.2	19.1	19.6	1.9	19.0
5	21.6	3.6	20.5	21.5	1.6	21.1
6	21.9	4.8	20.5	22.5	3.9	21.4

[a]Error limits obtained from the residuals of the linear least squares fitting of the data to equation, $\ln(k/T) = (-\Delta H^{\ddagger}/R)(1/T) + \Delta S^{\ddagger}/R + \ln(k_B/h)$, were 1-3% for $\Delta H^{\ddagger}$ in compounds **3-6**, and 3-7% for $\Delta S^{\ddagger}$ in **3** and **6**, and 16-26% for $\Delta S^{\ddagger}$ in **4** and 19-48% for $\Delta S^{\ddagger}$ in **5**; [b]unit: kcal/mol. [c]unit:cal/mol.K. [d]unit: kcal/mol.

Thermodynamics The effects of temperature on the values $K_{t/c} = (k_{ct}/k_{tc})$ for each compound were measured directly by NMR spectroscopy over the temperature range 25-93 °C. The resulting data were analyzed by *Van't Hoff* plots (Figure 4.7). Amides **3**, **5** and **6** have a positive slope indicating that the major *trans* isomer becomes increasingly

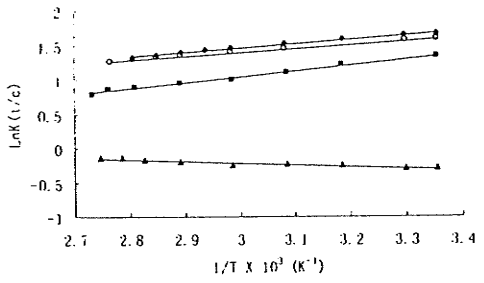

Figure 4.7 *Van't Hoff* plots for compounds **3** (■), **4** (▲), **5** (○) and **6** (◆) in D_2O

favored as the temperature decreases. However, compound **4** displays a negative slope and shows a reduction in the magnitude of $K_{t/c}$. In this case the major *cis* isomer becomes increasingly favored as the temperature decreases. Values for ΔH° and ΔS° were calculated from linear least-squares fits of these plots (Table 4.6).

Table 4.6 Thermodynamic parameters for isomerization **3-6**

Amide	ΔH° [a] (kcal/mol)	ΔS° [a] (cal/mol·K)	ΔG° [b] (298K)
3	-1.67 ± 0.06	-2.93 ± 0.20	-0.80 ±0.13
4	0.50 ± 0.06	1.05 ± 0.16	0.19 ± 0.11
5	-1.09 ± 0.03	-0.48 ± 0.08	-0.95 ±0.05
6	-1.21 ± 0.04	-0.71 ± 0.12	-1.01 ±0.08

[a]Error limits obtained by linear least-squares fitting the data of the *Van't Hoff* plots to equation $\ln K_{t/c} = (-\Delta H^{\circ}/R)(1/T) + \Delta S^{\circ}/R$;[b]Carried out in D_2O; ± SE determined by integration of two or more sets of *trans/cis* isomers.

FT-IR analysis of amide-I band (C=O stretching) for 3-6 in D_2O. We also measured the frequency of the amide I vibrational mode, which results primarily from the C=O stretching vibration.[35] The traditional picture of the amide resonance predicts that an increase in C=O bond order is accompanied by a decrease in C-N bond order. Such a decrease in C-N bond order would facilitate *cis/trans* isomerization of the amide bond. In D_2O, amide I vibrational modes of **6**, **3**, **5** and **4** are at 1608, 1609, 1612 and 1613 cm^{-1}, respectively, and follow the order **6** ~ **3** < **5** ~ **4**. It has been shown that changes in the free energy of activation ($\Delta G^{\ddagger}$) for prolyl peptide bond isomerization are proportional to changes in the frequency (ν) of the amide I vibrational mode.[36] Our results demonstrate that 3-Hyp-based amide **5** is blue shifted ($\Delta\nu$= 4 cm^{-1}) when compared to prolyl amide **6**. However, these subtle differences are not detectable by our kinetic assay. A similar trend is observed for spirocyclic amides **3** and **4**. Obviously, the blue shift ($\Delta\nu$= 4 cm^{-1})

observed for **4** is too small to account for the significant changes in $\Delta G^{\ddagger}$ between **3** and **4** and this suggests that other factors unrelated to inductive effect and C=O bond order are the cause for this dramatic rate difference. [36]

Temperature coefficient ($\Delta\delta/\Delta T$) measurement of OH resonances for 3 and 4 in DMSO-d_6. We next considered the effect of hydrogen bonding on prolyl amide *cis/trans* isomerization. The temperature coefficients ($\Delta\delta/\Delta T$) provide information about intramolecular hydrogen bonding.[37] Previous studies have shown that ($\Delta\delta/\Delta T$) > -3.0 ppb/deg are a diagnostic tool for the detection of intramolecular H-bonding.[37] The 1D spectra of compounds **3** and **4** recorded between 20 to 45 °C in 5-deg steps in DMSO-d_6 were analyzed and the temperature coefficients were determined (Table 4.7). Our data show that the temperature coefficients for HO-6′ exhibits the highest value of all hydroxyl groups. The temperature coefficients follow the general order OH-2 < OH-3 < OH-4 < OH-6 < OH-6′. In particular, the low ($\Delta\delta/\Delta T$) value for the *cis* isomers in **3** (-3.94 ppb/K) and **4** (-3.75 ppb/K), respectively, suggests the presence of intramolecular H-bonding

Table 4.7 Temperature coefficient ($\Delta\delta/\Delta T$, ppb/K) for compounds **3** and **4** in DMSO-d_6

		HO-2*	HO-3	HO-4	HO-6	HO-6′
3	*cis*	-6.87	-6.49	-5.85	-5.29	-3.94
	trans	-6.98	-6.94	-5.67	-5.14	-4.13
4	*cis*	-7.58	-6.94	-5.85	-5.48	-3.75
	trans	-6.94	-6.57	-5.55	-4.92	-4.50

* For numbering of hydroxyl groups refer to Figure 4.9.

involving OH-6′. In the *trans* isomers of **3** and **4**, the $\Delta\delta/\Delta T$ of HO-6′ were reduced to -

4.13 and -4.50 ppb/K, respectively. The relatively small value of HO-6′ in both *trans* isomers of **3** and **4** indicates that it also could be involved in hydrogen bonding.

Conformational analysis of the pyrrolidine ring in 3 and 4 using Density Functional Theory (DFT).[38] In order to gain insight into the conformational properties of peptide mimics **3** and **4** in solution and to study how intramolecular hydrogen-bonding influences the kinetics and thermodynamics of prolyl amide isomerization in compounds **3** and **4** we performed DFT calculations. These calculation were performed in collaboration with Dr. Schreckenbach's group in the Department of Chemistry at the University of Manitoba. On the basis of previous experience and literature reviews[38,39] we selected the B3LYP level of theory[40-42], as it was good enough to provide an accurate prediction of the molecular structure, and the 6-31+G(d, p) basis set,[43] which is a relatively large basis set augmented by diffuse and polarization functions to account for the correlation effect. Additionally, solvent effects were also taken into account by means of Tomasi's Polarized Continuum Model (PCM).[44] In this model, the solvent is represented as a polarizable medium characterized by its dielectric constant (i.e. water has a dielectric constant of 78.4 at 25 °C and 1atm), and the solute molecules were placed in a cavity within the solvent (see supporting information). The results of these calculations are summarized in Tables 4.8 and 4.9.

In performing the calculations, great care was taken to ensure that they cover the entire conformational space. This was achieved by a multi-step procedure: The conformational space was covered using force fields (molecular mechanics, MM) and a Monte-Carlo search procedure, augmented by systematic variations of the initial starting structure

(build and search procedure). The resulting conformers where superimposed to remove duplicate structures, resulting at the MM level in 443 and 457 unique structures, respectively, for compounds **3** and **4**. These conformers were used as input for the gas-phase DFT calculations that were then followed by solvation optimizations as described above. More details on the computational protocol can be found in the supporting information.

Table 4.8 The calculated distribution (%) of *cis* and *trans* conformers for **3** and **4** in D_2O

Compd.	calculated	experimental
3 (*cis*)	29.15	23 ±3%
3 (*trans*)	70.85	77 ± 3%
4 (*cis*)	57.75	53 ± 3%
4 (*trans*)	42.25	47 ± 3%

The computational data show that the pyranose ring in **3** and **4** exists in a $^4C_1$ chair conformation consistent with the diaxial coupling constants $J_{2,3}$, $J_{3,4}$, $J_{4,5} \geq 8.8$ Hz. The calculated distribution of prolyl amide *cis/trans* isomers in compounds **3** and **4** is in good agreement with the experimental data determined by ^{1}H-NMR integration (Table 4.8). For compound **4** the *cis* isomer population was calculated to be 57.7% while the experimentally determined value was 53 ± 3%. A slightly weaker agreement was observed for **3**. In this case the calculated *cis* ratio was 29% while the experimental value was 23 ± 3%. Next, we calculated the peptide backbone (ω', ϕ, ψ and ω) and endocyclic torsion angles (χ^0, χ^1, χ^2, χ^3 and χ^4) for peptide mimics **3** and **4** (Table 4.9). With the exception of the ψ torsion angle that exists in two families at $\psi \sim 153°$ and $\psi = -28°$ all other torsion angles show preference for only one narrowly defined range. Values close

Table 4.9 Range of backbone and endocyclic torsion angles[45] (°) for the most stable conformers of **3** and **4** accounting for 99.5% of the total conformer population determined by DFT calculations[46]. For clarity the substituents on the pyran ring are omitted.

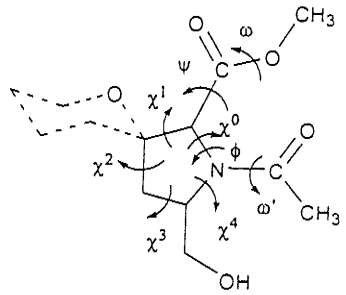

		ω'	ϕ	ψ	ω	χ^0	χ^1	χ^2	χ^3	χ^4
3	*cis*	-11,-1°	-71,-62°	153,154° -28,-27°	177±1° -177±1°	-15,-22°	30, 34°	-35,-33°	21, 25°	-5, 0°
	trans	165,178°	-67,-53°	132,154° -30,-27°	178±1° -179±1°	-16, -6°	25, 30°	-36,-34°	24, 30°	-14,-7°
4	*cis*	3,12°	-91,-77°	152,154° -28,-27°	177±1° -177±1°	-21,-15°	31, 33°	-37,-32°	20, 27°	-8, 0°
	trans	-172,-169°	-86,-79°	152,154° -28,-26°	178±1° -179±1°	-21,-19°	30, 33°	-33,-30°	18, 21°	-1, 2°

to 0° for the ω' torsion angels define the *cis* prolyl amide isomer while values close to ± 180° describe the *trans* isomer. The observed small χ^4 torsion angle (-14° ≤ χ^4 ≤ 0°) for the conformers of compounds **3** and **4** indicate a preferred C^{β}-exo pucker in which the basal plane is defined by C^{γ}, C^{δ}, N and C^{α} (Figure 4.8). Similar puckerings of the pyrrolidine ring have been observed in the crystal structure of 3-Hyp-containing peptide mimics and have also been proposed in 3-Hyp-containing collagenous peptide sequences.[26] The relative close value for χ^4 and χ^0 in the *trans* rotamer of **3** indicate a twisted conformation between a C^{β}-exo and a C^{γ}-endo pucker. The C^{β}-exo conformation places the endocyclic oxygen substituent in an axial position as observed for *trans* 3(*S*)-hydroxyproline-containing dipeptides.[47] In this conformation the pyrrolidine ring will be stabilized by gauche interaction and a stabilizing $\sigma(C^{\gamma}\text{-H})\rightarrow\sigma^*(C^{\beta}\text{-O})$ interaction. This conformation is further supported by characteristic long range "W" coupling constants (J ~ 1.0 Hz) between H-2′ and H-4′$_{eq}$ in both isomers of **3** and **4.**

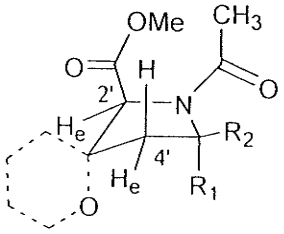

3: $R_1 = CH_2OH$; $R_2 = H$
4: $R_1 = H$; $R_2 = CH_2OH$;

Figure 4.8 C^{β}-exo conformations of compounds **3** and **4**. For clarity the substituents on the glucose ring are omitted

Next we analyzed the most stable conformers accounting for 99.5% of the total conformer population in compounds **3** and **4** for the presence and absence of characteristic hydrogen bonds. We used a ≤ 2.5Å bond length cutoff between the

hydrogen atom of the donor atom and the acceptor atom to ensure that only strong hydrogen bonds are selected.[48] We found three types of hydrogen bonds in the dominant rotamer population of **3** and two types of hydrogen bonds in the rotamer population of **4** (Figure 4.9). For compound **3**, the first type of hydrogen bond exists between OH-6′ and OH-6 (6′-OH---OH-6) with an average bond distance of around 1.9 Å. This hydrogen bond is only observed in the *trans* rotamers of **3**. The second type of hydrogen bond exists between OH-6′ and the *N*-terminal carbonyl (6′-OH---O=C-N). This hydrogen bond has an average bond length of 1.8 Å and is only found in the *cis* rotamers. A third type of hydrogen bond (not shown in Figure 9) is found between OH-2 and the *C*-terminal carbonyl (2-OH---O=C′-C^{α}) with a bond distance of 1.9Å. This H-bond was found in only one out of the 43 most stable *trans* conformers. For compound **4**, the first type of hydrogen bond exists between 6′-OH and the *N*- terminal carbonyl

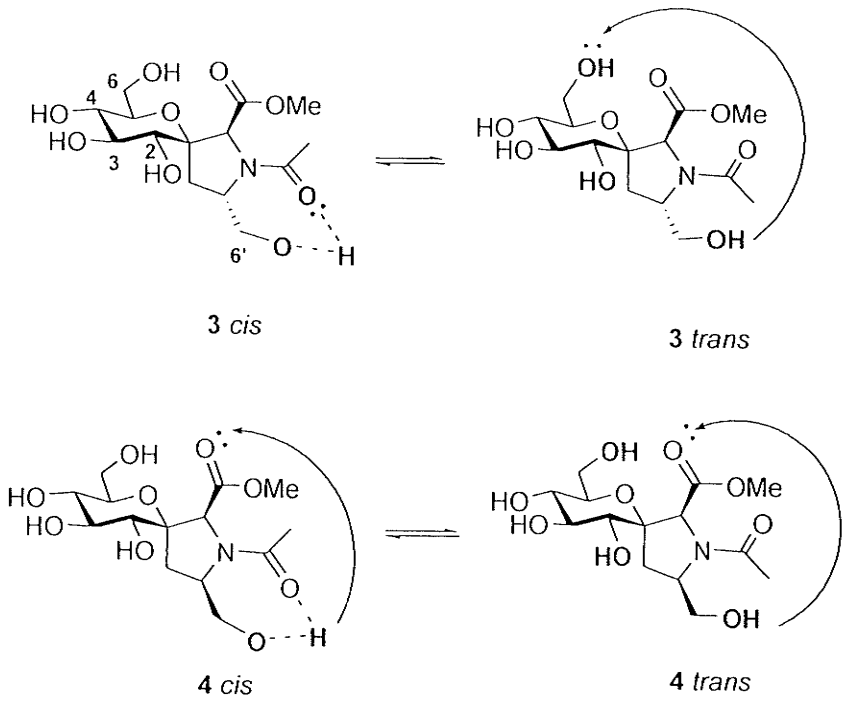

Figure 4.9 Intramolecular hydrogen bonds for the most stable conformers for the *cis*- and *trans*-isomers of compounds **3** and **4** determined by DFT calculations.

(6′-OH---O=C′-N). This H-bond has an average distance of 1.8 Å and is found only in the *cis* isomer. A second type of H-bond with a bond length of 1.9 Å exists between 6′-OH and the *C*-terminal carbonyl (C^{δ}-CH_2-OH---O=C′- C^{α}) that is found in both *cis* and *trans* conformers (Figure 4.9).

4.3. Discussion

The pyrrolidine ring in proline exhibits two predominant pucker modes: *C*-4 (C^{γ}) *exo* and *endo* envelope conformers. In the case of unsubstituted proline, the *endo* puckering mode is favored over the *exo* mode.[49] The puckering propensity can be controlled by proper choice of ring substituents.[49] Previous studies have shown that introduction of electronegative substituents like 4(*R*)-hydroxy- or 4(*R*)fluoro-substituents results in the stabilization of the C^{γ}–exo conformation and the *trans* prolyl amide isomer.[50] Our results confirm that naturally occurring 3(*S*)-hydroxyproline does not lead to a measurable increase in the *trans* prolyl amide isomer population[26] when compared to unsubstituted proline. For the first time we studied the effect of 3(*S*) hydroxylation on the kinetics of prolyl amide *cis/trans* isomerization. The nearly identical rate constants observed for peptide mimics **5** and **6** at elevated temperature demonstrate that 3(*S*)-hydroxylation has little effect on the kinetics of prolyl amide *cis/trans* isomerization. A similar effect was observed for 4(*R*)-OH proline.[50] Raines et al. have studied the crystal structure of Ac-3(*S*)-Hyp-OMe **5** and concluded it to be intermediate between a ^1E envelope and $^1E_2$ twisted conformation.[26] In the envelope conformation the flap atom is C^{β}. In the twisted conformation, atoms N, C^{β} and C^{δ} form the basal plane. Atom C^{β} resides 0.456 ± 0.004 Å above that plane, and C^{δ} resides 0.153 ± 0.005 Å below that plane.[26] Taken together these

results suggest that the hydroxyl group at the β- or γ-position in proline affects the puckering of the pyrrolidine ring in the model peptides without influencing the kinetics and thermodynamics of prolyl amide *cis/trans* isomerization.

These findings are in contrast to our results obtained with Glc3(*S*)HypH-containing peptide mimics **3** and **4**. Compounds **3** and **4** demonstrate that kinetics and thermodynamics of *cis/trans* isomerization are greatly affected by the presence of polar groups either by hybridization with D-glucose or incorporation of a hydroxymethylene substituent into the C-5′ (δ-)-position of proline. The stereochemistry of the hydroxymethylene substituent at the 5′-position influences both the rate of *cis/trans* isomerization and the stability of the *cis/trans* isomers. Compared to proline and 3(*S*)Hyp-containing peptide mimics **5** and **6**, both Glc3(*S*)HypH-modified peptide mimics **3** and **4** display a higher *cis* isomer population. The *cis* isomer population is greatly enhanced in mimic **4**. Substitution of the *C*-terminal methyl ester in compounds **3** and **4** by a methylamide group increases the *cis* isomer ratio further as expected by enhanced $n \rightarrow \pi^*$ donation. Methylamides **7** and **8** exhibit 38% and 74% *cis* isomer, respectively. Comparison of the temperature coefficients for all hydroxyl groups indicates that the increased *cis* prolyl amide isomer ratio in peptide mimics **3**, **4**, **7** and **8** is hydrogen bond-mediated and involves the hydroxymethylene group located at the δ-position of proline. Additional evidence for the involvement of intramolecular hydrogen bonds in the stabilization of the prolyl amide *cis* isomer is provided by DFT calculations. Analysis of the most stable prolyl amide *cis* conformers in **3** and **4** indicate the presence of a strong hydrogen bond between 6′-OH and the carbonyl group of NAc (6′-OH --- O=C-N). The higher *cis* isomer ratio in **4** is due to the formation of a second hydrogen bond involving

6′-OH and the carbonyl of the carboxymethyl group. Alternatively, the *trans* prolyl amide bond in **3** may be stabilized by the formation of a hydrogen bond between 6′-OH and 6-OH. In addition, the calculations support the notion that the H-bond between 6′-OH --- O=C-N is stronger in compound **4** when compared to **3**. For instance, for compound **4** ten out of the twenty most stable conformers possess this type of H-bond while the same H-bond was not present in the most stable 20 conformers of compound **3**. Conformational analysis of the pyrrolidine ring in the highly populated conformers in peptide mimics **3** and **4** indicates that the pucker ressembles a C^{β}-exo conformation in both compounds very similar to the conformation previously observed in the crystal structure of **5**. This conformation places the endocyclic oxygen substituent in an axial position as observed for *trans* 3(*S*)-hydroxyproline-containing dipeptides.[47] In this conformation the pyrrolidine ring will be stabilized by gauche interaction between endocyclic nitrogen and endocyclic oxygen and a stabilizing $\sigma(C^{\gamma}\text{-H})\rightarrow\sigma^{*}(C^{\beta}\text{-O})$ interaction. A similar C^{β}-exo conformation was also observed in the more lipophilic silaproline (Sip) analogue.[15] However, in this case no increase of the *cis* isomer population was noted. It is noteworthy that the calculated C^{β}-exo conformation is closely related to the C^{γ}-endo pucker that is found in most proline-containing peptides, the polyproline helix and the collagen triple helix.

Quite unexpected are the results for the kinetics of prolyl amide *cis/trans* isomerization in compounds **3** and **4**. Peptide mimic **3** exhibits an unusally high activation barier when compared to epimer **4**. For instance, an approximately 200-fold difference in k_{tc} and a 90-fold rate difference in k_{ct} are observed between compounds **3** and **4**. In contrast nearly identical rate constants are observed for parent compounds **5** and **6**. Interestingly, while

cis/trans isomerization is kinetically inhibited in compound **3**, compound **4** accelerates isomerization relative to parent compounds **5** and **6**. For instance, compound **4** exhibits approximately a 6-fold rate acceleration for k_{ct} and a 20-fold acceleration for k_{tc} when compared to the parent compounds. Comparison of the activation enthalpies and activation entropies of compounds **3-6** indicate that enthalpic changes are responsible for these rate differences. Enthalpic changes could be the result of ground- and transition state stabilization or destabilization.[51]

Previous studies by Lubell have shown that introduction of methyl substituents at the β-position in proline and 4-hydroxyproline induced ψ dihedral angle values around 150°. This places the *C*-terminal carbonyl oxygen in a position which disfavors amide pyramidalization by Coulomb interactions in the transition state.[52] DFT calculations on both compounds **3** and **4** indicate a ψ dihedral angle around 153° and ~-28° in their most stable conformers demonstrating that a similar destabilization may exist in peptide mimics **3** and **4**. However, compounds **3** and **4** exhibit dramatic rate differences. We suggest that the presence or absence of intramolecular H-bonds involving 6′-OH, the endocyclic nitrogen and the carboxymethyl group are responsible to explain the rate differences. Computational models on the most stable conformers of **4** suggest that the hydrogen bond 6′-OH --- O=C-OMe which is observed in the ground states of compound **4** places the 6′-OH in an orientation to interact with the lone pair of the pyrimidalized nitrogen in the transition state. By comparison, the absence of this hydrogen bond in **3** prevents stabilization of the transition state. Moreover, the H-bond 6′-OH --- HO-6 observed in the *trans* isomer of **3** places the 6′-OH in a geometry that prevents H-bonding to the endocyclic nitrogen in the transition state thereby leading to a higher activation

energy in **3**.[51] Comparison of the activation enthalpies ($\Delta H^{\ddagger}$) for *cis*-to-*trans* isomerization and *trans*-to-*cis* isomerization of compounds **3-6** indicate that the kinetics of *cis/trans* isomerization is enthalpically driven. The lower ($\Delta H^{\ddagger}$) observed for compound **4** when compared to **5** and **6** could be the result of a developing hydrogen bond between the hydroxymethylene substituent at C-5′ and the lone pair of the pyramidalized nitrogen in the transition state. In contrast the higher activation enthalpy observed for peptide mimic **3** when compared to reference compounds **5** and **6** could be the result of increased Coulomb repulsion induced by the ψ dihedral angle around 153°.[52,53]

Previously, accelerated *cis/trans* isomerizations have been observed in model peptides containing δ-*tert*-butyl-proline[53] or pseudo-proline(ΨPro).[22] In these cases a twisted amide bond caused by the steric strain of the bulky substituents adjacent to the endocyclic imide results in a destabilized ground state.[22,53] In addition, the increased distance between δ-C and the hetero atom such as sulfur or oxygen leads to a shortened δ-C-N bond in pseudo-prolines.[22] As a consequence, dimethyl groups at the δ-position come closer to the isomerizing bond and may stabilize the transition state by the presence of the hydrophobic alkyl group.[54] Our results indicate that positioning of a polar group(s) at the δ-position of proline or in the form of sugar-proline hybrids provides an alternative route to control the kinetics of prolyl amide *cis/trans* isomerization.

4.4. Conclusions

We have studied the thermodynamic and kinetic properties of a series of polyhydroxylated glucose-3(*S*)hydroxyproline-containing peptide mimics. Our study

shows that the insertion of polar substituents capable of forming hydrogen bonds in the δ-position of proline greatly impacts the kinetics and thermodynamics of prolyl amide *cis/trans* isomerization. DFT calculations and chemical shift temperature coefficient measurements indicate that these changes are not due to conformational changes in the pucker of the pyrrolidine ring but are the result of intramolecular hydrogen bonding in water. Computational modelling of the pyrroldine ring indicates that the pyrrolidine ring preferes a C^{β}-exo pucker. However, close insepection of the C^{β}-exo pucker suggests that it is closely related to the C^{γ}-endo pucker that occurs frequently in proline-containing peptides and proteins. The preferable adoption of the prolyl amide *cis* conformation in Glc3(*S*)HypH **3** allows its use as selective *cis*-XAA-GlcProH bond inducer to chemically introduce constraint into peptides and proteins and to test the *cis*-imide bond as a structural requirement for the bioactive conformation. Moreover, the presence of the unprotected glucose moiety in GlcProH provides opportunities to explore the effect of glycosylation in unusual glycopeptides while decoration of the gluco-based polyol scaffold provides rich opportunities to tailor the physical, chemical, hydrophobic, lipophilic nucleophilic, and pharmacodynamic properties of proline mimetics and proline-containing peptidomimetics.

4.5. Experimental

General ^{1}H and ^{13}C NMR spectra were taken in CD_3OD, D_2O at 500 MHz and 75 MHz, respectively. 1D NOE experiments (40ms gaussian pulse with a 560ms mixing time) and HSQC experiments were performed at AMX500 Bruker. The elemental analysis was performed by Guelph Chemical Laboratories LTD. The data from Inversion-Magnetization Transfer experiment were processed by Mathematica 5.0. DMSO,

Methanol, pyridine, acetic anhydride, trifluoroacetic acid, sodium methoxide and amberlite IRC-50S ion-exchange resin were used as supplied. Analytical thin layer chromatography was performed on 0.20 mm silica gel 60 Å plates. Flash chromatography was performed on 40-63 μm 60 Å silica gel.

(1*S*)-2,3,4,6-Tetrahydroxy-1′-*N*-acetyl-5′(*S*)-hydroxymethylene-spiro[1,5-anhydro-D-glucitol-1,3′-*L*-proline methyl ester] (3) The compound **1** (30 mg, 0.10 mmol) was dissolved in a mixture of pyridine and acetic anhydride (1 mL, 1:1) and stirred for 12 hours at room temperature. After that, the pyridine and acetic anhydride were removed in *vacuo*. The crude product was dissolved in methanol (1 mL) followed by addition of sodium methoxide (22 mg, 0.39 mmol) and stirred for 3 hours. The solution was stirred with Amberlite IRC-50S ion-exchange resin (H^+) for 15 mintues. The mixture was filtered and filtrate was concentrated and purified by the flash column chromatography (ethyl acetate/ methanol: 4/1) to get compound **3** as a colorless oil (30 mg, 90%) $[\alpha]_D$ = 31.4 (*c* 1.00, MeOH); ^{1}H NMR (500 MHz, D_2O): δ = 1.81 (s, *cis*, 0.53H), 2.09 (s, *trans*, 2.47H), 2.11-2.34 (m, both rotamers, 2H), 3.27-3.35 (m, 2H), 3.39-3.46 (m, both rotamers, 1H), 3.50-3.66 (m, 6H), 3.67-3.72 (dd, 1H, *J* = 12.6 Hz, *J* = 2.5 Hz), 3.74-3.79 (dd, *trans*, 0.83H, *J* = 11.1 Hz, *J* = 5.3 Hz), 3.82-3.86 (dd, *cis*, 0.17H, *J* = 11.11 Hz, *J* = 5.3 Hz), 4.17-4.24 (m, both rotamers, 1H), 4.26 (s, *trans*, 0.81 H), 4.43 (s, *cis*, 0.19H); ^{13}C NMR (75 MHz, D_2O): *trans*-rotamer, δ = 25.1, 25.7, 53.4, 60.2, 61.0, 63.2, 69.6, 69.9, 70.5, 74.1, 75.0, 86.0, 171.4, 174.8; *cis*-rotamer, 22.0, 24.6, 53.9, 59.7, 62.2, 63.2, 69.6, 69.9, 71.3, 74.1, 75.0, 87.5, 171.9, 174.6; HRMS calcd for $C_{14}H_{24}NO_9$ $[M + H]^+$ 350.1451, found 350.1462.

(1*S*)-2,3,4,6-Tetrahydroxy-1′-*N*-acetyl-5′(*R*)-hydroxymethylene-spiro[1,5-anhydro-D-glucitol-1,3′-*L*-proline methyl ester] (4) The compound **2** (35 mg, 0.11 mmol) was dissolved in a mixture of pyridine and acetic anhydride (1 mL, 1:1) and stirred for 12 hours at room temperature. After that, the pyridine and acetic anhydride were removed in *vacuo*. The crude product was dissolved in methanol (1 mL) followed by addition of sodium methoxide (25 mg, 0.46 mmol) and stirred for 3 hours. The solution was stirred with Amberlite IRC-50S ion-exchange resin (H^+) for 15 mintues. The mixture was filtered and filtrate was concentrated and purified by the flash column chromatography (ethyl acetate/ methanol: 4/ 1) to get compound **4** as a colorless oil (37 mg, 92%) $[\alpha]_D$ = 63.9 (*c* 1.00, MeOH); ^{1}H NMR (500 MHz, D_2O): δ = 1.86 (s, *cis*, 1.56H), 1.94 (dd, *cis*, 0.52H, *J* = 14.3 Hz, *J* = 10.3 Hz), 1.99-2.08 (m, 1.92H), 2.37 (dd, *cis*, 0.52H, *J* = 14.3 Hz, *J* = 7.2 Hz), 2.48 (dd, *trans*, 0.48H, *J* = 14.3 Hz, *J* = 7.2 Hz), 3.25-3.35 (m, 2H), 3.38-3.45 (m, 1H), 3.53-3.75 (m, 7H), 3.80-3.88 (m, 1H), 4.04 (m, *cis*, 0.52H), 4.14 (m, *trans*, 0.48H), 4.37 (s, *cis*, 0.52H), 4.40 (s, *trans*, 0.48H); ^{13}C NMR (75 MHz, D_2O): *trans*-rotamer, 21.3, 29.1, 53.6, 58.8, 61.1, 63.9, 69.7, 69.9, 70.2, 74.1, 75.3, 85.0, 172.0, 174.9; *cis*-rotamer, 21.6, 27.0, 53.7, 59.0, 61.1, 62.9, 69.8, 70.0, 71.2, 74.2, 75.4, 86.1, 172.0, 174.9; HRMS calcd for $C_{14}H_{24}NO_9$ $[M + H]^+$, 350.1451, found 350.1456.

***N*-acetyl-3(*S*)-hydroxy-*L*-proline methyl ester (5)**. To a solution of Boc-3(*S*)-OH-Pro-OH (100 mg, 0.43mmol), which was purchased from ACS Synthesis Company in U.S.A. and methyl iodide (0.08 mL, 1.29 mmol) in *N,N*-dimethylformamide was added cesium carbonate (154 mg, 0.47 mmol) and stirred for a hour at 0 °C. The reaction was quenched with water (3 mL) and extracted with ethyl acetate (3 × 10 mL). The combined organic

layers were concentrated to afford the methyl ester, which was treated with a mixture of trifluoroacetic acid and dichloromethane (v/v, 1 mL/1 mL) and stirred for 2 hours at room temperature. The mixture was concentrated at *vacuo* to afford the intermediate NH_2·TFA-3(*S*)-OH-Pro-OMe. This salt was dissolved in methanol (2 mL) and treated with triethylamine (0.12 mL, 0.86 mmol) and acetic anhydride (0.12 mL, 1.29 mmol) for 12 hours at room temperature. The mixture was concentrated and purified by flash chromatography (ethyl acetate / methanol: 20 / 1) to get the compound **5** (78 mg, yield 96%). ^{1}H NMR (500 MHz, D_2O): δ = 1.82-2.10 (both isomers, m, 5H, *N*-amide methyl group and γ-protons), 3.50 (*cis*, dd, 0.43H, δ-protons, J = 5.78 Hz, J = 9.40 Hz), 3.60-3.66 (*trans*, m, 3.95H, methyl group of ester and *δ*-protons), 3.68 (*cis*, methyl group of ester, 0.63H), 4.24 (s, *trans*, 0.79H, *α*-proton), 4.41 (m, *trans*, 0.78H, *β*-proton), 4.47 (s, *cis*, 0.21H, *α*-proton), 4.55(m, *cis*, 0.22H, *β*-proton); ^{13}C NMR (75 MHz, D_2O): *trans*-rotamer, δ = 21.4, 32.4, 46.5, 53.6, 67.4, 73.4, 172.6, 174.0; *cis*-rotamer, δ = 21.7, 30.7, 44.9, 53.9, 69.2, 74.8, 172.0, 174.2; MS (ES, $[M + Na]^+$); m/z calcd for $C_8H_{13}NNaO_4$ 210.07, found 210.13.

***N*-acetyl-*L*-proline methyl ester (6)**. This compound is purchased from Bachem and used without further purification. ^{1}H NMR (500 MHz, D_2O): δ = 1.65-2.27 (both isomers, m, 7H, *N*-amide methyl group, *β* and *γ*-protons), 3.37 (*cis*, m, 0.26H, *δ*-protons), 3.52 (*trans*, m, 1.74H, , *δ*-protons), 3.58-3.70 (both isomers, partially overlapping, methyl group of ester, 3H), 4.31 (m, *trans*, 0.87H, α-proton), 4.57 (m, *cis*, 0.13H, *α*-proton); ^{13}C NMR (75 MHz, D_2O): *trans*-rotamer, δ = 21.6, 24.6, 29.6, 48.8, 53.3, 59.4, 173.3, 175.4; *cis*-rotamer, δ = 22.8, 24.6, 31.0, 47.0, 53.6, 61.1, 173.7, 175.0; MS (ES, $[M + Na]^+$); m/z

calcd for $C_8H_{13}NNaO_3$ 194.08, found 194.18.

(1*S*)-2,3,4,6-Tetrahydroxy-1′-*N*-acetyl-5′(*S*)-hydroxymethylene-spiro[1,5-anhydro-D-glucitol-1,3′-*L*-proline methylamide] (7). (referring to the supporting information); $[\alpha]_D$ = 46 (*c* 0.8, MeOH); ^{1}H NMR (500 MHz, D_2O): δ = 1.79 (s, *cis*, 1.15H), 2.06 (s, *trans*, 1.85H), 2.11-2.30 (m, both rotamers, 2H), 2.56 (s, *trans*, 1.83H), 2.61 (s, *cis*, 1.17H), 3.25-3.50 (m, 4.4H), 3.54-3.70 (m, 2.6H), 3.74 (dd, *trans*, 0.64H, *J* = 5.1 Hz, *J* = 11.2 Hz), 3.74 (dd, *cis*, 0.36H, *J* = 4.7 Hz, *J* = 10.7 Hz), 4.12-4.25 (m, 2H); ^{13}C NMR (75 MHz, CD_3OD): *cis* rotamer, δ = 22.6, 26.7, 26.8, 61.6, 62.9, 64.7, 71.4 (2 carbons), 74.3, 75.6, 77.3, 88.5, 171.7, 173.6; *trans* rotamer, δ = 22.3, 25.7, 26.7, 61.5, 62.7, 63.9, 71.4 (2 carbons), 73.4, 75.5, 77.2, 87.2, 171.5, 173.2; HRMS calcd for $C_{14}H_{25}N_2O_8$ $[M + H]^+$ 349.1611, found 349.1626.

(1*S*)-2,3,4,6-tetrahydroxy-1′-*N*-acetyl-5′(*R*)-hydroxymethylene-spiro[1,5-anhydro-D-glucitol-1,3′-*L*-proline methylamide] (8). (referring to the supporting information); $[\alpha]_D$ = 62.3 (*c* 0.6, MeOH); ^{1}H NMR (500 MHz, D_2O): δ = 1.86 (s, *cis*, 2.22H), 2.05 (s, *trans*, 0.78H), 2.11 (m, *cis*, 0.74H), 2.25 (m, 1.26H), 2.56 (s, *trans*, 0.78H), 2.61 (s, *cis*, 2.22H), 3.25-3.35 (m, 2H), 3.37-3.43 (m, 1H), 3.53-3.61 (m, 2.79H), 3.64-3.70 (m, 1.21H), 3.96-4.04 (m, 1H), 4.07 (s, *cis*, 0.74H), 4.09-4.18 (m, 1H), 4.19 (s, *trans*, 0.26H); ^{13}C NMR (75 MHz, CD_3OD): *cis* rotamer, δ = 23.1, 26.0, 26.4, 59.6, 60.7, 62.7, 71.1, 71.3, 74.5, 75.6, 77.4, 87.0, 172.9, 173.8; *trans* rotamer, δ = 21.9, 28.4, 26.3, 59.3, 62.3, 63.1, 71.1, 71.6, 73.3, 75.9, 77.4, 85.5, 173.2, 173.8; HRMS calcd for $C_{14}H_{25}N_2O_8$ $[M + H]^+$ 349.1611, found 349.1618.

Thermodynamics. The equilibrium constants for the interconversion of the *cis* and *trans* isomers of **3-6** were determined by measuring the peak area of the 1H resonance for the two isomers. Peak areas were measured with the program Spinworks 2.5. Experiments were conducted at 298-360 K. Equilibrium constants ($K_{t/c}$ = *trans*/*cis* ratios) were calculated directly from the peak areas.

Inversion-magnetization transfer NMR experiments were performed on Bruker AMX500 spectrometer equipped with selective excitation units, and ^{1}H and broadband heteronuclear probes. Samples of **3-6** were prepared at a concentration of 0.01 M in D_2O. The rate of prolyl peptide bond isomerization can not be detected by this method at room temperature. Experiments were therefore conducted at elevated temperature at 356 K. Temperature settings of the spectrometer were calibrated to within 1 °C by reference to a glycol standard.

FT-IR spectroscopy. Samples of **3-6** were prepared at concentration of 0.10 M in D_2O. FTIR spectra were recorded on a Nicolet 5PC spectrometer. Experiments were performed at 25 °C using CaF_2 in a Spectra Tech circle cell. The frequency of amide I vibrational modes was determined to within 2 cm^{-1}.

Temperature coefficient ($\Delta\delta/\Delta T$) experiments: ^{1}H-NMR spectroscopy of 17mM solutions of **19** and **20** in 100.0% Me_2SO-d_6 were recorded on a Bruker AMX500 at 20 °C, and from 20 to 45 °C with increments of 5 °C. Chemical shift (δ) are expressed in ppm and calibrated with respect to the residual DMSO signal (^{1}H: 2.49 ppm).

4.6. References:

1. (a) Brandits, J. F.; Halvorson, H. R.; Brennan, M. *Biochemistry* **1975**, *14*, 4953. (b) Schmid, F. X.; Baldwin, R. L. *Proc. Nat. Acad. Sci. U.S.A.* **1978**, *75*, 4764. (c) Hurle, M. R.; Marks, C. B.; Kosen, P. A.; Anderson, S.; Kuntz, I. D. *Biochemistry* **1990**, *29*, 4410. (d) Jackson, S. E.; Fersht, A. R. *Biochemistry* **1991**, *30*, 10436.
2. (a) Stryer, L. *Biochemistry*, 4th ed.; W. H. Freeman and Company: New York, 1999. (b) Kakinoki, S.; Hirano, Y.; Oka, M. *Polym. Bull.* (Berlin) **2005**, *53*, 109.
3. Reddy, K.V. R.; Yedery, R. D.; Aranha, C. *Int. J. Antimicrobial Agents* **2004**, *24*, 536.
4. Buku, A.; Faulstich, H.; Wieland, T.; Dabrowski, J. *Proc. Natl. Acad. Sci. USA*. **1980**, *77*, 2370.
5. Nakajima, T.; Volcani, B. E. *Science* **1969**, *164*, 1400.
6. Taylor, S. W.; Waite, J. H.; Ross, M.M.; Shabanowitz, J.; Hunt, D. F. *J. Am. Chem. Soc.* **1994**, *116*, 10803.
7. (a) Berg, R. A.; Prockop, D. J. *Biochem. Biophys. Res. Commun.* **1973**, *52*, 115. (b) Vitagliano, L.; Berisio, R.; Mazzarella, L.; Zagari, A. *Biopolymers* **2001**, *58*, 459; And references therein. (c) Holmgren, S. K.; Taylor, K.M.; Bretscher, L. E.; Raines, R. T. *Nature* **1998**, *392*, 666. (d) Bretscher, L. E.; Jenkins, C. L.; Taylor, K. M.; deRider, M. L.; Raines, R. T. *J. Am. Chem. Soc.* **2001**, *123*, 777. (e) Jenkins, C. L.; Raines, R. T. *Nat. Prod. Rep.* **2002**, *19*, 49.
8. Pearce, G.; Ryan, C. A. *J. Biol. Chem.* **2003**, *278*, 30044; And references therein.
9. Beausoleil, E.; Lubell, W. D. *J. Am. Chem. Soc.* **1996**, *118*, 12902. And references therein.
10. Delaney, N. G.; Madison, V. J. *J. Am. Chem. Soc.* **1982**, *104*, 6635.
11. Samanen, J.; Zuber, G.; Bean, J.; Eggleston, D.; Romoff, T.; Kopple, K.; Saunders, M.; Regoli, D. *Int. J. Pept. Protein. Res.* **1990**, *35*, 501.
12. Quancard, J.; Labonne, A.; Jacquot, Y.; Chassaing, G.; Lavielle, S.; Karoyan, P. *J. Org. Chem.* **2004**, *69*, 7940.
13. Che, Y.; Marshall, G. R. *J. Org. Chem.* **2004**, *69*, 9030. And references therein.
14. Tam, J. P.; Miao, Z. *J. Am. Chem. Soc.* **1999**, *121*, 9013. And references therein.
15. Cavelier, F.; Vivet, B.; Martinez. J.; Aubry, A.; Didierjean, C.; Vicherat, A.; Marraud, M. *J. Am. Chem. Soc.* **2002**, *124*, 2917. And references therein.
16. Sharma, R.; Lubell, W. D. *J. Org. Chem.* **1996**, *61*, 202. And references therein.
17. Jeannotte, G.; Lubell, W. D. *J. Org. Chem.* **2004**, *69*, 4656.
18. (a) Wagaw, S.; Rennels, R. A.; Buchwald, S. L. *J. Am. Chem. Soc.* **1997**, *119*, 8451; (b) Kuwano, R.; Sato, K.; Kurokawa, T.; Karube, D.; Ito, Y. *J. Am. Chem. Soc.* **2000**, *122*, 7614; (c) Viswanathan, R.; Prabhakaran, E. N.; Plotkin, M. A.; Johnston, J. N. *J. Am. Chem. Soc.* **2003**, *125*, 163.
19. Koep, S.; Gais, H-J.; Raabe, R. *J. Am. Chem. Soc.* **2003**, *125*, 13243. And references therein.
20. Owens, N.; Braun, C.; Schweizer, F. *J. Org. Chem.*, **2007**, *72*, 4635.
21. For selected examples of bicyclic proline analogues incorporated into bioactive peptides see: (a) Cluzeau, J.; Lubell, W. D. *Biopolymers, Peptide Science* **2005**, *80*, 98. (b) Blankley, C. J.; Kaltenbronn, J. S.; DeJohn, D. E.; Wener, A.; Bennett, L. R.; Bobowski, G.; Krolls, U.; Johnson, D. R.; Pearlman, W. M.; Hoefle, M. L. *J. Med. Chem.* **1987**, *30*, 992. (c) Dumy, P.; Keller, M; Ryan, D. E.; Rohwedder, B.; Wöhr, T.; Mutter, M. *J. Am. Chem. Soc.* **1997**, *119*, 918. (d) Li. W.; Moeller, K. D. *J. Am. Chem. Soc.* **1996**, *118*, 10106.
22. Keller, M.; Sager, C.; Dumy, P.; Schutkowski, M.; Fisher, G. S.; Mutter, M. *J. Am. Chem. Soc.* **1998**, *120*, 2714. And references therein.
23. Wöhr, T.; Wahl, F.; Nefzi, A.; Rohwedder, B.; Sato, T.; Sun, X.; Mutter, M. *J. Am. Chem. Soc.* **1996**, *118*, 9218.
24. Zhang, K.; Schweizer, F. *Synlett* **2005**, 3111.
25. Gruner, S. W.; Locardi, E.; Lohof, E.; Kessler, H. *Chem. Rev.* **2002**, *102*, 491.
26. Jenkins, C. L.; Bretscher, L. E.; Guzei, I. A.; Raines, R. T. *J. Am. Chem. Soc.* **2003**, *125*, 6422.
27. (a) Cox, C.; Lectka, T. *J. Am. Chem. Soc.* **1998**, *120*, 10660. (b) Mizushima, S.; Shimanouchi, T.; Tsuboi, M.; Sugita, T.; Kurosaki, K.; Mataga, N.; Souda, R. *J. Am. Chem. Soc.* **1952**, *74*, 4639. (c) Liang, G. B.; Rito, C. J.; Gellman, S. H. *Biopolymers* **1992**, *32*, 507.
28. A 40 ms Gaussian pulse with a 560 ms mixing time was used.
29. Taylor, C. M.; Hardre, R.; Edwards, P. J. B.; Park, J. H. *Org. Lett.* **2003**, *23*, 4413. And references

therein.
30. (a) DeRider, M. L.; Wilkens, S. J.; Waddell, M. J.; Bretscher, L. E.; Weinhold, F.; Raines, R.T.; Markley, J. L. *J. Am. Chem.. Soc.* **2002**, *124*, 2497. (b) Hinderaker, M. P.; Raines, R. T. *Protein Sci.* **2003**, *12*, 1188.
31. Delaney, N. G.; Madison, V. *Int. J. Peptide Protein Res.* **1982**, *19*, 543.
32. (a) Perrin, C. L.; Dwyer, T. J. *Chem. Rev.* **1990**, *90*, 935. (b) Reimer, U; Scherer, G; Drewello, M; Kruber, S; Schutkowski, M; Fischer, G. *J. Mol. Biol.* **1998**, *279*, 449.
33. Stein, R. L. *Adv. Protein Chem.* **1993**, *44*, 1.
34. Eyring, H. *J. Chem. Phys.* **1935**, *3*, 107.
35. Jackson, M.; Mantsch, H. H. *Crit. Rev. Biochem. Molec. Biol.* **1995**, *30*, 95.
36. Eberhardt, E. S.; Panasik, Jr. N.; Raines, R. T. *J. Am. Chem. Soc.* **1996**, *118*, 12261.
37. (a) Leeflang, B. R.; Vliegenthart, J. F. G.; Kroon-Batenburg, L. M. J.; Eijck, B. P.; Kroon, J. *Carbohydr. Res.* **1992**, *230*, 41. (b) St.-Jacques, M.; Sundarajan, P. R.; Taylor, K. J.; Marchessault, R. H. *J. Am. Chem. Soc.* **1976**, *98*, 4386.
38. Koch, W.; Holthausen, M. C. *A Chemist's Guide to Density Functional Theory*. 2nd ed., Willey, Weinheim, 2000.
39. Cramer, C. J. *Essentials of Computational Chemistry: Theories and Models*, 2nd ed.; Wiley, New York, 2004.
40. Becke, A. D., *J. Chem. Phys.* **1993**, *98*, 5684.
41. Lee, C.; Yang, W.; Parr, R. G. *Phys. Rev. B: Codens. Matter* **1988**, *37*, 785.
42. Stephens, P. J.; Devlin, F. J.; Chabalowski, C. F.; Frisch, M. J. *J. Phys. Chem.* **1994**, *98*, 11623.
43. Hehre, W. J. *A Guide to Molecular Mechanics and Quantum Chemical Calculations*, Wavefunction Inc.: Irvine, CA, 2003, pp.393.
44. Tomasi, J.; Mennucci, B.; Cammi, R. *Chem. Rev.*, **2005**.*105*, 2999.
45. Backbone torsion angles: $\omega' = C\text{-}C'\text{-}N\text{-}C^{\alpha}$, $\phi = C'\text{-}N\text{-}C^{\alpha}\text{-}C'$, $\psi = N\text{-}C^{\alpha}\text{-}C'\text{-}O$, $\omega = C^{\alpha}\text{-}C'\text{-}O\text{-}C$. Endocyclic torsion angles: $\chi^0 = C^{\delta}\text{-}N\text{-}C^{\alpha}\text{-}C^{\beta}$, $\chi^1 = N\text{-}C^{\alpha}\text{-}C^{\beta}\text{-}C^{\gamma}$, $\chi^2 = C^{\alpha}\text{-}C^{\beta}\text{-}C^{\gamma}\text{-}C^{\delta}$, $\chi^3 = C^{\beta}\text{-}C^{\gamma}\text{-}C^{\delta}\text{-}N$, $\chi^4 = C^{\gamma}\text{-}C^{\delta}\text{-}N\text{-}C^{\alpha}$.
46. Song, H. K.; Kang, Y. K. *J. Phys. Chem. B*, **2005**, *109*, 16982.
47. Taylor, C. M.; Hardre, R.; Edwards, P. J. B. *J. Org. Chem.* **2005**, *70*, 1306.
48. Morozov, A.; Kortemme, T.; Tsemekhman, K.; Baker, D. *Proc. Natl. Acad. Sci. USA* **2004**. *101*, 6946.
49. Koskinen, A. M. P.; Helaja, J.; Kumpulainen, E. T. T.; Koivisto, J.; Mansikkamäki, H.; Rissanen, K. *J. Org. Chem.* **2005**. *70*, 6447.
50. Eberhardt, E. S.; Panasik, Jr. N.; Raines, R. T. *J. Am. Chem. Soc.* **1996**, *118*, 12261.
51. Fisher, S.; Dunbrack, Jr. R. L.; Karplus, M. *J. Am. Chem. Soc.* **1994**, *116*, 11931.
52. Beausoleil, E.; Sharma, R.; Michnick, S. W.; Lubell, W. D. *J. Org. Chem.* **1998**, *63*, 6572.
53. Halab, L.; Lubell, W. D. *J. Org. Chem.* **1999**, *64*, 3312.
Albers, M. W.; Walsh, C. T.; Schreiber, S. L. *J. Org. Chem.* **1990**, *55*. 4984.

Chapter 5

Influence of Glucose-templated Proline Hybrids on the β-turn Conformation of the Peptide Fragment Ac-Leu-D-Phe-Pro-Val-NMe_2 of Gramicidine S

Abstract: *The synthesis of tetrapeptide-based β-turn mimetics containing spirocyclic glucose-3(S)-hydroxyproline hybrids (5'R)-Glc3(S)HypHs 1 and (5'S)-Glc3(S)HypHs 2 as proline mimetics is presented. NMR-based conformational analysis of Ac-Leu-D-Phe-(5'R)-Glc3(S)HypHs-Val -NMe_2 and Ac-Leu-D-Phe-(5'S)-Glc3(S)HypHs-Val-NMe_2 demonstrates the presence of β-turn conformations. Different turn structures were observed by changing the stereochemistry at 5'-position of Glc3(S)HypHs. The major prolyl amide cis isomer of tetrapeptides Ac-Leu-D-Phe-(5'R)-Glc3(S)-Val-NMe_2 11 and 13 form a type VI β-turn conformation. Whereas the major prolyl amide trans rotamer of tetrapeptide Ac-Leu-D-Phe-(5'S)-Glc3(S)HypHs-Val-NMe_2 12 conserves a similar β-turn conformation as the Gramicidin S-based peptide fragment Ac-Leu-D-Phe-Pro-Val-NMe_2 16.*

5.1. Introduction

β-turns play an important role in the folding process of proteins and peptides[1] and are often involved in molecular recognition processes.[2] β-turns consist of four consecutive residues in a non-helical region in which the polypeptide chain folds back on itself by nearly 180 degrees.[3] β-turns are often stabilized by an intramolecular hydrogen-bond between the carbonyl oxygen of the first residue (*i*) and the amide proton of the fourth one (*i*+3) (Figure 5.1). Many β-turn mimetics have been developed to study the structural and biological properties of peptides. In particular, the use of proline analogues is an attractive strategy in this respect. Due to its conformational restrictions imposed by the pyrrolidine ring, the proteinogenic amino acid proline has an exceptional tendency to act as a turn inducer to generate reverse turn structures like β-turns and β-hairpins in peptides

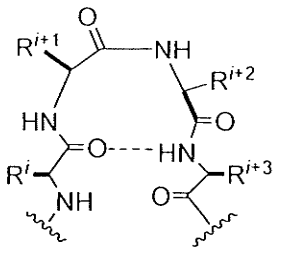

Figure 5.1 β-turn

and proteins.[4] In particular, the *cis* geometry of the proline *N*-terminal amide bond induces the type VI β-turn in which proline residue situates at the $i + 2$ position of the peptide bend. Although type VI β-turn is a relatively rare secondary structure, it plays important roles in protein folding.[5] In addition, type VI β-turn have been found in some important recognition events of bioactive proteins. For example, a type VI β-turn conformation has been proposed for thrombin-catalyzed cleavage of the V_3 loop of HIV gp120, a prerequisite to viral infection.[6] Over the years many proline analogues have been synthesized and used for tuning the peptidyl-prolyl *cis-trans* isomerization in peptides and proteins.[7] For instance, (2*S*,5*R*)-5-*tert*-butylproline favors predominantly a *cis*-conformation due to steric hindrance in short peptide models that adopt a VI β-turn.[8] Another sterically hindered residue, the δ,δ-dimethylproline, has been developed as a substitute to lock proline in the *cis* conformation in tripeptides.[9] Azaprolines (AzPro) in which the α-carbon is replaced by a nitrogen favor the *cis* isomer conformation of the azaproline-preceding amide bond by electronic effects.[10] Pseudoproline ΨPro, containing an oxozolidine or thiazolidine ring, exhibit very high prolyl amide *cis* ratios.[11]

Recently, the synthesis of spirocyclic glucose-3-hydroxyproline hybrids Glc3(*S*)HypHs **1** and **2** (Figure 5.2) was reported by our group.[12] These proline analogues exhibit several

features. The spirocyclic nature of the *gluco*-derived scaffold constrains the pyrrolidine ring of proline and introduces artificial post-translational modifications (hydroxylation +

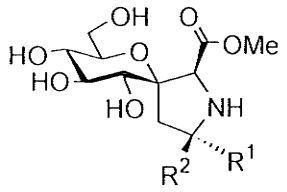

1: $R^1 = CH_2OH$; $R^2 = H$
2: $R^1 = H$; $R^2 = CH_2OH$

Figure 5.2 Structure of spirocyclic glucose-3(*S*)-hydroxyproline hybrids (Glc3(*S*)HypHs)

glycosylation). Chemical manipulations and derivatizations of the glucose-derived polyol scaffold provide an opportunity to tailor the chemical, physical and pharmacodynamic properties of Glc3(*S*)HypHs-containing peptides as previously shown by us.[13] The peptide mimics, Ac-Glc(3*S*)-Hyp-OMe and Ac-Glc(3*S*)-Hyp-NHMe display interesting conformational properties. For example, when compared to Ac-Pro-OMe or Ac-(3*S*)-Hyp-OMe, (5'*R*)-Glc(3*S*)-Hyp favored the prolyl amide *cis* rotamer (53~75%) with an accelerated *cis/trans* isomerization in water. Whereas the diastereomer (5'*S*)-Glc(3*S*)-Hyp favors the *trans* rotamer (62~77%) with a retarded *cis/trans* isomerization in water.[14] Based on the previous results, we were interested in exploring the conformational role of these proline analogues in model peptides. We selected the tetrapeptide Ac-Leu-D-Phe-Pro-Val-NMe_2 that forms the β-turn portion of Gramicidine S (GS) as a model.[15] In this peptide proline occupies the i+2 position of a β-turn. Our goal was to study how substitution of the proline residue by Glc3(*S*)HypHs influences the conformational and β-turn inducing properties.

5.2. Results and discussion

Synthesis of MOM-protected Glc3(*S*)HypHs. The use of unprotected polyhydroxylated amino acids in peptide chemistry often results in low coupling yields and difficult purification due to their nucleophilic hydroxyl groups. To avoid this potential complication we decided to use methoxymethyl (MOM) groups as temporary hydroxy protection.[16a] The MOM protecting group is relatively small, does not deactivate adjacent nucleophiles and can easily removed under acidic conditions.[16] The building block **5** was prepared from **1** through a three-step procedure (Scheme 5.1).

Scheme 5.1 Synthesis of MOM-protected Glc3(*S*)HypHs

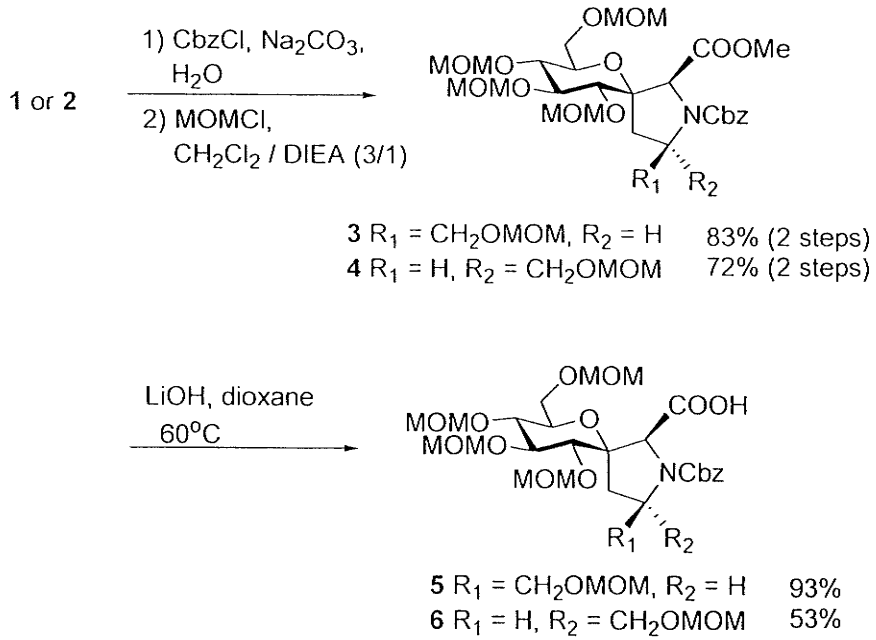

Initially, the free imine **1** was treated with benzyl chloroformate (Cbz-Cl) and sodium carbonate to provide the Cbz-protected carbamate followed by the indroduction of MOM groups using *N,N*-diisopropylethylamine and chloromethyl methyl ether to provide

MOM-protected intermediate **3** in good yield.[16a] Subsequently, lithium hydroxide-based hydrolysis of the methylester in dioxane produced the desired acid **5** in 88% yield. Surprisingly, only a small portion of methyl ester (~10%) was epimerized at the α position. The stereochemistry at the α-position of acid **5** was confirmed by converting it into the corresponding methyl ester **3**.[17] Applying the same procedure to its diastereomer **2** resulted in extended epimerization (~1:1) at the α-position. Fortunately, the mixture of the two acids was separated by column chromatography. The assignment of α-stereochemistry of compound **6** was based on the same chemical method as previously described for compound **5**.

Synthesis of tetrapeptides 11-13. With MOM-protected building block at hand, the synthesis of the tetrapeptide was carried out using solution-phase peptide chemistry (Scheme 5.2). Dipeptide **7** was prepared via coupling of NH_2-Val-NMe_2 to compound **5** (DIEA, TBTU, DMF, 80%). The *N*-terminal Cbz group was then removed by catalytic hydrogenolysis in quantitative yield using [$Pd(OH)_2$, H_2, MeOH] to provide the free imine **7** in high yield. Synthesis of tripeptide **9** proceeded from the dipeptide **7**. Coupling with Fmoc-D-Phe-OH (DIEA, PyBOP, DMF, 82%) provided Fmoc-protected tripeptide, which was treated with a mixture of piperidine and *N*, *N*-dimethylformamide to produce the tripeptide **9** with an unprotected *N*-terminus in quantitative yield. Because of the steric hindrance of the *N*-terminus, the coupling reagent PyBOP was used to improve the yield.[18] The coupling of tripeptide **9** and Fmoc-Leu-OH was carried out by using TBTU as coupling reagent in DMF followed by a deprotection-acylation procedure to provided MOM-protected tetrapeptide **11** in 92% yield. The same synthetic procedure was applied

Scheme 5.2 Synthesis of tetrapeptides **11** and **12**

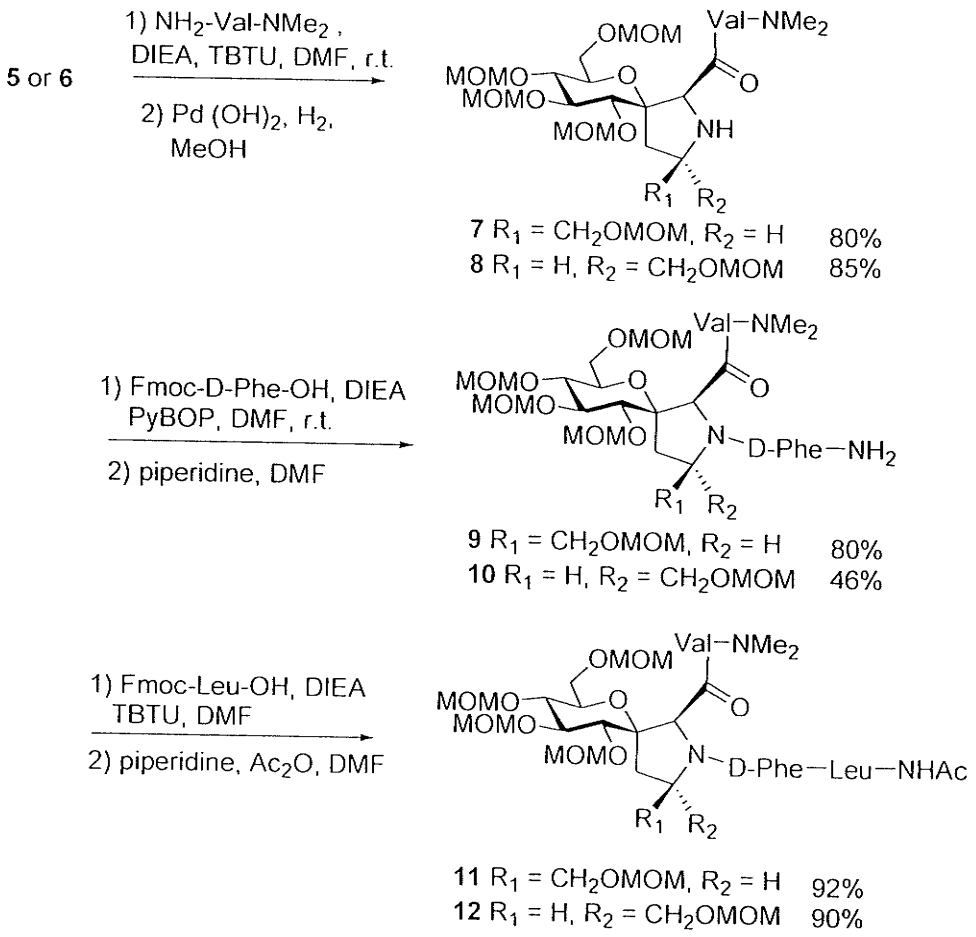

to the synthesis of tetrapeptide **12**. Similar yields were obtained in each step except for the coupling reaction between dipeptide **8** and Fmoc-D-Phe-OH. In this case, a low yield for tripeptide **10** was obtained and the dipeptide **8** was recovered in 45% yield. Modifying the reaction conditions like increasing reaction time, amount of amino acid and coupling reagent did not improve the yield. Finally, exposure of compound **11** to acidic conditions (0.3 *N* HCl in MeOH) resulted in complete deblocking of the MOM protecting groups and afforded unprotected tetrapeptide **13** (Scheme 5.3) in excellent yield (90%). Unfortunately, applying the same acidic conditions to tetrapeptide **12**

resulted in an inseparable mixture of the dipeptides **14** and **15**. Very likely the hydrolysis

Scheme 5.3 Cleavage of MOM groups of **11** and **12**

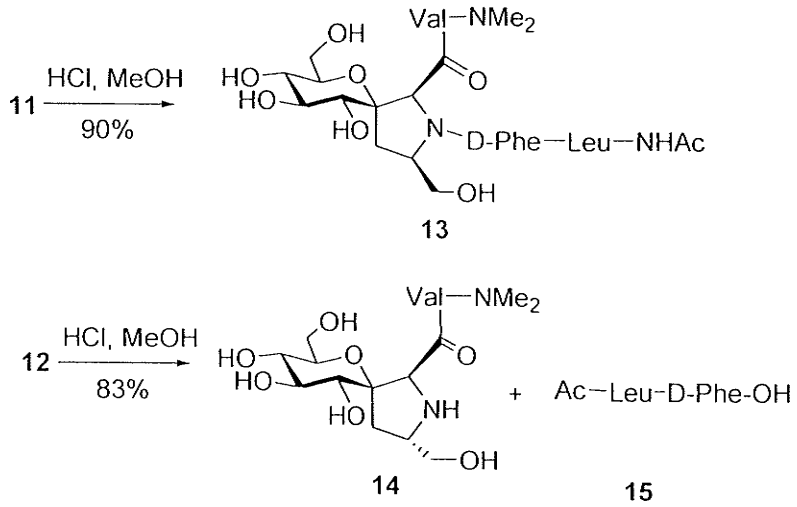

proceeds via anchimeric assistance of the hydroxymethyl substituent at the 5′-position of proline (Figure 5.3). The major isomer of prolyl amide in **A** is *cis* conformation

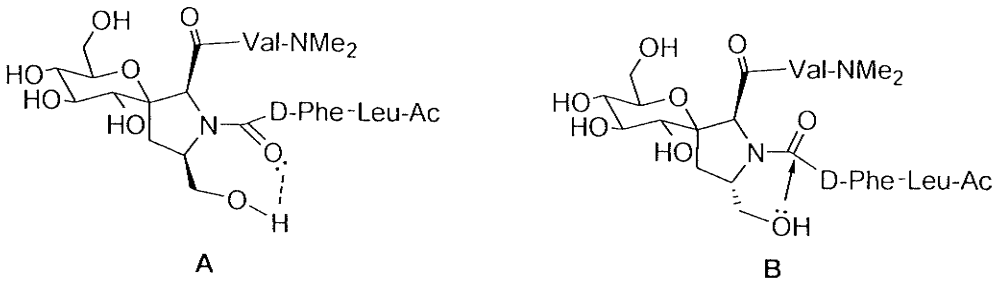

Figure 5.3 Rational explanation for the hydrolysis of prolyl amide bond in **B**. (---- H-bonding)

(see the conformational analysis) in which the 5'-hydroxymethyl group may form a hydrogen bonding to the carbonyl oxygen of the prolyl amide (see chapter 4).[14] This restricts the 5'-hydroxymethyl group into a geometry in which the carbonyl carbon of the

prolyl amide can not be nucleophilically attacked by the 5'-hydroxymethyl group using a Bürgi-Dunitz trajectory.[19] Whereas the major *trans* isomer of the prolyl amide in **B** not only makes the prolyl amide carbon more accessible to the hydroxymethyl substituent at C-5' but also facilitate nucleophilic attack on the electrophilic amide carbon, due to the absence of an intramolecular hydrogen bond between the prolyl amide oxygen and 5'-hydroxymethyl group.

The successful synthesis of unprotected tetrapeptide **13** demonstrates that MOM protecting groups are compatible with solution phase peptide synthesis for (*5'R*)-Glc3(*S*)HypHs **1**. Whereas the high acid lability of diastereoisomer (*5'S*)-Glc3(*S*)HypHs **2** does currently not permit use in peptide synthesis. For reference purposes the parent peptide **16** was also prepared by standard solution phase peptide chemistry.[15]

Conformational analysis of tetrapeptides 11-13 and 16 using NMR. Although the reference peptide **16** aggregated in CD_2Cl_2 at $\geq$ 10 mM, [15] no aggregation was observed for tetrapeptides **11-13** at concentrations $\leq$ 50 mM in CD_2Cl_2 or water. The lower tendency of aggregation of glycosylated peptides has previously been reported.[20]

The NMR spectra of all tetrapeptides were measured at the same concentration (8 mM). Intramolecular hydrogen bonding was evaluated by temperature coefficient experiments in DMSO-d_6 or H_2O/D_2O (9/1). Because exchangeable protons engaged in intramolecular hydrogen bonds are typically not influenced by strong hydrogen-bonding solvents.[21] The prolyl *N*-terminal geometry and turn structure were investigated by ROESY experiments.[22]

The chemical shifts and coupling constants of the amide protons in tetrapeptides **11-13** and **16** are provided in Table 5.1.

Table 5.1 Chemical shift (δ) for amide protons of tetrapeptides **11, 12, 13, 16** and Gramicidin S in CD_2Cl_2, DMSO-d_6 and H_2O/D_2O (9/1)

peptides	Solvent	Leu-NH δ ($^3J_{\alpha H,NH}$)	Phe-NH δ ($^3J_{\alpha H,NH}$)	Val-NH δ ($^3J_{\alpha H,NH}$)
11 (*cis*)[a]	CD_2Cl_2	6.23(8.5)	6.40(8.3)	8.20(8.3)
	DMSO-d_6	7.65(9.0)	8.18(9.7)	8.12(7.5)
11 (*trans*)[a]	CD_2Cl_2	6.18(8.6)	6.61(7.7)	7.03(ND)
	DMSO-d_6	7.78(8.9)	8.37(8.6)	7.69(8.2)
12 (*cis*)	CD_2Cl_2	ND[c]	ND[c]	ND[c]
	DMSO-d_6	7.65(9.0)	8.34(8.7)	7.45(7.0)
12 (*trans*)	CD_2Cl_2	6.88(7.7)	7.31(7.2)	6.78(8.2)
	DMSO-d_6	7.79(8.5)	8.27(8.9)	7.51(8.1)
13 (*cis*)	H_2O/D_2O	7.98(6.6)	8.25(7.7)	9.17(8.1)
	DMSO-d_6	7.75(8.8)	8.04(8.8)	8.72(7.3)
13 (*trans*)	H_2O/D_2O	ND[c]	ND[c]	ND[c]
	DMSO-d_6	7.80(9.5)	8.33(8.1)	8.39(5.9)
16 (*cis*)	CD_2Cl_2	ND[c]	ND[c]	ND[c]
	DMSO-d_6	7.74(8.3)	8.43(8.3)	8.12(8.1)
16 (*trans*)	CD_2Cl_2	7.76(7.5)	7.12(5.5)	6.85(7.0)
	DMSO-d_6	7.79(8.2)	8.37(7.8)	7.78(8.2)
Gramicidin S (*trans*)[b]	DMSO-d_6	8.32(9.2)	9.05(2.6)	7.21(9.7)

[a] *Cis* and *trans* are referred to as prolyl amide rotamers; [b] referred to lit. 15 and its supporting information ; [c] ND = not determined

The tetrapeptide 11 containing MOM-protected (*5'R*)-Glc3(*S*)HypHs. The proline mimetic in tetrapeptide **11** coexists as prolyl amide *cis* (72%) and *trans* (28%) in CD_2Cl_2, The major prolyl amide *cis* isomer is confirmed by a long range ROESY correlation between $C^{\alpha}H_{D\text{-}Phe}$ and $C^{\alpha}H_{(5'R)\text{-}Glc3(S)HypHs}$. The presence of a turn conformation in **11** is supported by long range ROESY correlations between the Leu-NH or the *N*-terminal acetyl group and the *C*-terminal dimethyl amide singlets (Figure 5.4). In addition,

sequential ROESY correlations were observed between the neighboring $C^{\alpha}H_{Leu}$ and NH_{Phe} as well as the $C^{\alpha}H_{(5'R)\text{-}Glc3(S)HypHs}$ and NH_{Val} indicating their proximity in the major

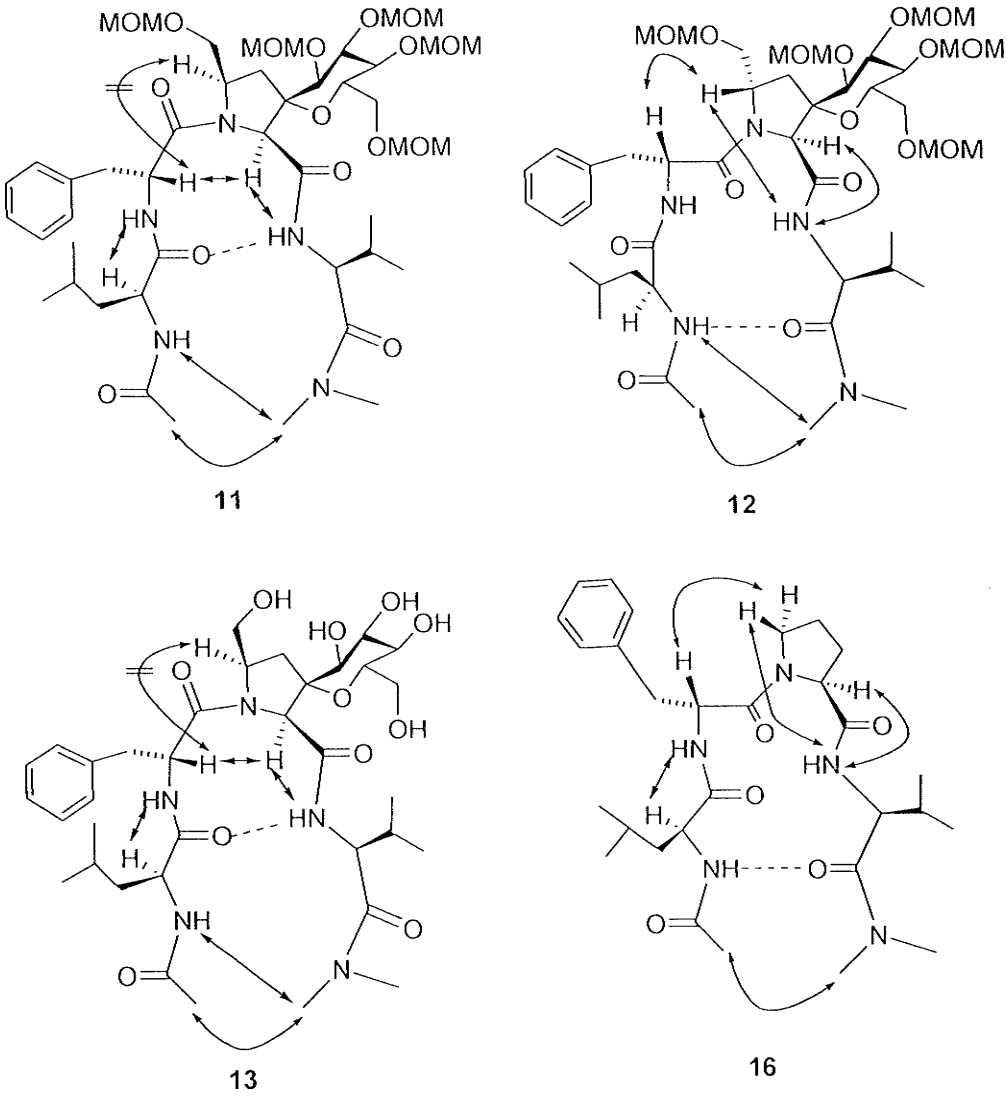

Figure 5.4 Selected ^{1}H-^{1}H ROESY cross-peaks in CD_2Cl_2 (**11**, **12** and **16**) or H_2O (**13**) as well as potential hydrogen bonds from temperature coefficient experiments in DMSO-d_6 for major isomer in peptides **11, 12** and **16** and in H_2O/ D_2O (9/1) for major isomer in **13**.

conformer. The chemical shifts and coupling constants of the amide protons in **11** (Table 1) indicate that the *cis* conformer has a different folding structure when compared to

reference peptide **16** in CD_2Cl_2. The downfield chemical shift (δ = 8.20 ppm) and large temperature coefficient value for Val-NH (Table 5.2) support that the Val-NH is involved in an intramolecular hydrogen bonding. Therefore, a type VI β-turn conformation is

Table 5.2 Temperature coefficient values ($\Delta\delta/\Delta T$, ppb/K) for peptides **11** in DMSO-d_6

	Leu-NH	Phe-NH	Val-NH
cis	-6.00	-8.13	-3.75
trans	-4.37	-11.47	-9.40

suggested for the prolyl amide *cis* conformer of **11** in which the type VI β-turn is stabilized by a 10-membered ring hydrogen bond between $(C{=}O)_{Leu}$ at *i* position and NH_{Val} at *i* +3 position.[5] This hydrogen bond is further supported by the observation that the amide proton of Val undergoes little chemical shift changes ($\Delta\delta$ = 0.08 ppm) when dissolved in DMSO and CD_2Cl_2. Due to the low concentration of *trans* conformer of **11** in CD_2Cl_2 (72% *cis*), a full conformational analysis of the minor prolyl amide *trans* isomer was not possible. However, the similar chemical shifts of the amide protons between the *trans* isomer of **11** and the *trans* isomer of **16** supports these amide protons have a similar chemical enviroment in CD_2Cl_2. Furthermore, the temperature coefficient experiments (Table 5.2 and 5.3) support that the NH_{Leu} of both *trans* conformers of **11** and **16** were involved in a hydrogen bonding to $(C{=}O)_{Val}$.

The tetrapeptide 12 containing MOM-protected (*5'S*)-Glc3(*S*)HypHs. The NMR spectrum showed one major isomer (93%) in CD_2Cl_2. The ROESY correlation (Figure 4) between $C^{\alpha}H_{D\text{-}Phe}$ and $C^{\delta}H_{(5'R)\text{-}Glc3(S)HypHs}$ confirmed its *trans* geometry. The presence of

a turn conformation in **12** is supported by long range ROESY correlations between the Leu-NH or the *N*-terminal acetyl group and the *C*-terminal dimethyl amide singlets (Figure 5.4). Temperature coefficient experiments in DMSO-d_6 (Table 5.3) indicate that NH_{Leu} is involved in hydrogen bonding to the carbonyl group of valine. In addition, the similar chemical shifts observed for the amide protons among compounds **12**, **16** and **GS** (Table 5.1) suggests that the β-turn conformation of **12** resembles the β-turn conformation that occurs in GS.

Table 5.3 Temperature coefficient values ($\Delta\delta/\Delta T$, ppb/K) for peptides **12** and **16** in DMSO-d_6

		Leu-NH	Phe-NH	Val-NH
12	*cis*	-5.20	-4.80	-4.15
	trans	-3.90	-7.40	-8.00
16	*cis*	-4.00	-8.00	-8.00
	trans	-3.92	-7.60	-6.20

Interestingly, the prolyl amide *cis* conformer of **12** may form a type VI β-turn structure on the basis of chemical shift analysis and hydrogen bond pattern of amide protons relative to the *cis* conformer of **11**(Table 5.1). That is, the stereochemistry at 5′-position (δ position) of Glc3(*S*)HypHs can be used to control the equilibrium constants of *cis*/*trans* isomerization (72% *cis* for **11**, 93% *trans* for **12**) without disturbing the β-turn conformation of each isomer (a type VI β-turn for *cis* conformer; original β-turn for *trans* conformer).

The tetrapeptide 13 containing (*5′R*)-Glc3(*S*)HypHs. The increased polarity of unprotected tetrapeptide **13** made it possible to investigate its conformation by NMR in

water. ROESY experiments on compound **13** demonstrate that the major isomer exhibits a prolyl amide *cis* conformation (91%) in H_2O/D_2O (9/1). This assignment is supported by a ROESY correlation between $C^{\alpha}H_{D\text{-Phe}}$ and $C^{\alpha}H_{(5'R)\text{-Glc3}(S)\text{HypHs}}$ (Figure 5.4). In comparison with MOM-protected peptide **11** the increased *cis* population in **13** may be due to the hydrogen bonding between $(C{=}O)_{D\text{-Phe}}$ and $5'\text{-}CH_2OH_{(5'R)\text{-Glc3}(S)\text{HypHs}}$.[14] The long range ROESY correlations between the Leu-NH or the *N*-terminal acetyl group and the *C*-terminal dimethyl amide singlets indicated the presence of a turn conformation in **13** (Figure 4). Temperature coefficient experiments (Table 5.4) indicate that compound **13** exists in a type VI β-turn conformation that is stabilized by an intramolecular hydrogen bond between the NH_{Val} and $(C{=}O)_{Leu}$ in its prolyl amide *cis* conformer.

Table 5.4 Temperature coefficient values ($\Delta\delta/\Delta T$, ppb/K) for peptides **13** in H_2O/D_2O (9/1)

	Leu-NH	Phe-NH	Val-NH
cis	-7.23	-8.45	-4.02
trans	-7.91	-7.72	-7.45

According to amide temperature coefficient experiments ($\Delta\delta/\Delta T < -7.45$ ppb/K, Table 5.4) it appears that the minor prolyl amide *trans* isomer of tetrapeptide **13** is not involved in hydrogen bonding. Due to the low concentration of the prolyl amide *trans* isomer it was not possible to observe ROESY correlations between the Leu-NH or the *N*-terminal acetyl group and the *C*-terminal dimethyl amide singlets.

Attempts to investigate the influence of the hydroxyl groups of the carbohydrate scaffold on the peptide backbone conformation failed due to poor resolution of the hydroxy protons in DMSO-d_6.[23, 24]

As indicated above, (*5'R*)-Glc3(*S*)HypHs can efficiently increase the *cis* population of

prolyl *N*-terminus that induces the type VI β-turn. Derivatization of the hydroxyl groups as MOM does not affect prolyl amide *cis/trans* isomerization as well as type VI β-turn conformation in tetrapeptide **11.** In comparison, the MOM-protected diastereoisomer (*5'S*)-Glc3(*S*)HypHs stabilizes the prolyl amide *trans* conformer resulting in a conserved β-turn structure as observed in reference peptide **16**. In conclusion, proline analogues **11-14** can be used to tune the hydrophilic or hydrophobic properties of peptides without disturbing their major bioactive conformation.

Solvent effects. In addition, the influence of different solvents on the geometry of prolyl *N*-terminus was studied (Table 5.5). The results show that equilibrium constant of MOM-protected **11** is not affected by the solvent polarity and ability of the solvent to

Table 5.5 The equilibrium constant ($K_{t/c}$) of **11**, **12**, **13** and **16** in various solvents

Compd.	Solvent			
	CD_2Cl_2	CD_3OD	DMSO-d_6	D_2O
11	0.39	0.33	0.30	-[b]
12	13.28	3.00	1.44	-[b]
13	-[b]	0.14	0.67	0.10
16	> 19.00	3.17	1.32	-[b]

[a]Determined by 500 MHz NMR at 25 °C, error is ±0.05%;
[b]not soluble.

donate a hydrogen bond. The unprotected tetrapeptide **13** also showed the absence of a strong solvent effect. However, an increased *trans* population was observed in aprotic DMSO when compared to CD_3OD and D_2O. In contrast, peptide **12** and reference peptide **16** display a solvent effect. In this case the prolyl amide *trans* rotamer population is greatly enhanced in nonpolar aprotic solvents and decreases with an increase in solvent

polarity.

5.3. Conclusions

MOM-protected Glc3(*S*)HypHs-based proline mimics have been successfully incorporated into target tetrapeptides using solution phase peptide chemistry. In particular, (*5'R*)-Glc3(*S*)HypH demonstrated its potential as a building block in peptide synthesis. Whereas the use of its diastereoisomer (*5'S*)-Glc3(*S*)HypH is limited due to accelerated hydrolysis of its *N*-terminal amide under acidic conditions.

As what we expected, (*5'R*)-Glc3(*S*)HypH dramatically increases the *cis* population (91%) of prolyl amide in water. It is an efficient type VI β-turn inducer and can be used to explore structure activity relationships (SAR) of bioactive peptides in which the *cis* geometry of prolyl amide is required for their bioactivity. In addition, as observed in tetrapeptides **11** and **13**, the derivatization of hydroxy groups can improve the solubility of tetrapeptides without affecting peptide folding (type VI β-turn). This suggests that Glc3(*S*)HypHs will find use in tuning the chemical, physical and pharmacodynamic properties of bioactive peptides without affecting their bioactive conformation.

In contrast, tetrapeptide **12** containing (*5'S*)-Glc3(*S*)HypH conserved a similar β-turn conformation to the Gramicidin S-based peptide fragment Ac-Leu-D-Phe-Pro-Val-NMe_2 **16**. Incorporation of **12** in GS may improve the antibacterial activity of GS.

Moreover, replacement of Pro with Glc3(*S*)HypHs was found to reduce the aggregation of tetrapeptides **11-13** relative to reference tetrapeptide **16**. That is, incorporation of CTAA into peptides provides a strategy to improve the physical and chemical properties of peptides.

5.4. Experimental

General ^{1}H and ^{13}C NMR spectra were taken in CD_2Cl_2, $CDCl_3$, CD_3OD, D_2O at 500 MHz and 75 MHz, respectively. HRMS data were provided by the mass spectrometry laboratory in the department of chemistry at University of Alberta. The elemental analysis was performed by Guelph Chemical Laboratories LTD. Analytical thin layer chromatography was performed on 0.20 mm silica gel 60 Å plates. Flash chromatography was performed on 40-63 μm 60 Å silica gel.

(1*S*)-2,3,4,6-Tetra-*O*-methoxymethyl-1′-*N*-benzyloxycarbonyl-5′(*R*)-methyl methoxymethyl ether-spiro[1,5-anhydro-D-glucitol-1,3′-*L*-proline methyl ester] (3)

To a mixture of compound **1** (80 mg, 0.26 mmol) and benzyl chloroformate (0.19 mL, 1.30 mmol) in water (2 mL) was added sodium carbonate (83 mg, 0.78 mmol). The reaction was stirred for 12 hours at room temperature and extracted with ethyl acetate (5 × 10 mL). The organic layers were collected, concentrated and purified by the flash column chromatography (ethyl acetate/ methanol: 4/1) to get Cbz-propected intermediate (103 mg, 90%). Which was treated with 3 mL dichloromethane and cooled in an ice bath under nitrogen atmosphere, diisopropylethylamine (1 mL) was added dropwise, followed by a careful addition of chloromethyl methyl ether (0.71 mL, 9.36 mmol). A significant amount of white smoke formed in the reaction vessel. The reaction mixture was stirred in the dark for 48 hours during which the solution gradually turned red. After cooling to 0 °C, saturated aqueous ammonium chloride (5 mL) was added. The contents diluted with water and extracted with dichloromethane (3 × 10 mL). The combined organic layers were dried ($NaSO_4$), filtered, and concentrated. The crude product was chromatographed

on silical gel (from ethyl acetate /hexanes (1:1) to ethyl acetate) to afford the product **3** (128 mg, 83%). $[\alpha]_D$ = 38.4 (*c* 1.4, $CHCl_3$); ^1H NMR (300 MHz, $CDCl_3$, two isomers): δ = 2.08-2.21 (m, 1H), 2.44-2.56 (m, 1H), 3.22-3.44 (m, 15H), 3.48-3.77 (m, 10H), 4.00-4.15 (m, 1.36H), 4.27 (dd, 0.64H, *J* = 8.9 Hz, *J* = 3.9 Hz), 4.42 (s, 0.64H), 4.50-4.82 (m, 10.36H), 5.00 (d, 0.64H, *J* = 13.0 Hz), 5.07-5.18 (m, 1.36H), 7.21-7.36 (m, 5H); ^{13}C NMR (75 MHz, $CDCl_3$, two isomers): δ = 31.5/32.9, 52.2/52.3, 55.0-56.5 (12 carbons), 66.7/66.8, 66.8/67.4, 69.4/70.2, 70.0/70.1, 72.1 (2 carbons), 74.8 (2 carbons), 76.4/76.6, 79.7/80.4, 84.8/85.4, 96.5-98.1 (10 carbons), 127.3-128.5 (10 aromatic carbons), 136.2/136.5 (aromatic carbons), 154.4/155.2, 169.9/170.1; HRMS (ES) calcd for $C_{30}H_{48}NO_{15}$ $[M + H]^+$: 662.3024, found: 662.3036.

(1*S*)-2,3,4,6-Tetra-*O*-methoxymethyl-1′-*N*-benzyloxycarbonyl-5′(*S*)-methyl methoxymethyl ether-spiro[1,5-anhydro-D-glucitol-1,3′-*L*-proline methyl ester] (4)

The synthetic procedure is described in SI. $[\alpha]_D$ = 12.3 (*c* 1.1, $CHCl_3$); ^1H NMR (300 MHz, $CDCl_3$, two isomers): δ = 2.23-2.46 (m, 2H), 3.28-3.82 (m, 25H), 3.90 (dd, 0.38H, *J* = 9.1 Hz, *J* = 4.3 Hz), 4.04 (dd, 0.62H, *J* = 8.9 Hz, *J* = 4.4 Hz), 4.16-4.31 (m, 1.62H), 4.36 (s, 0.38H), 4.46-4.84 (m, 10H), 4.91 (d, 0.62H, *J* = 12.6 Hz), 5.14 (brs, 0.76H), 5.22 (d, 0.62H, *J* = 12.6 Hz), 7.23-7.38 (m, 5H); ^{13}C NMR (75 MHz, $CDCl_3$, two isomers): δ = 26.8/27.9, 52.0/52.2, 55.2-56.9 (12 carbons), 66.8/67.0, 67.0/67.3, 68.1/68.7, 70.2/70.6, 71.9/72.0, 74.8/74.9, 76.7/76.8, 80.5/80.8, 86.0/87.0, 96.6-98.5 (10 carbons), 127.4-128.4 (10 aromatic carbons), 136.2/136.4 (aromatic carbons), 154.6/155.1, 169.7 (2 carbons); HRMS (ES) calcd for $C_{30}H_{48}NO_{15}$ $[M + H]^+$: 662.3024, found: 662.3034.

(1*S*)-2,3,4,6-Tetra-*O*-methoxymethyl-1′-*N*-benzyloxycarbonyl-5′(*R*)-methyl methoxymethyl ether-spiro[1,5-anhydro-D-glucitol-1,3′-*L*-proline] (5) To a solution of compound **3** (50 mg, 0.076 mmol) in dioxane (3 mL) was added 2M lithium hydroxide aqueous solution (0.38 mL, 0.76 mmol). The reaction mixture was stirred at 60 °C for 48 hours. Afterwards the solution was cooled to room temperature and neutralized with Amberlite IRC-50S H^+ ion-exchange resin. The mixture was filtered and concentrated to afford the crude product, which was purified by flash charomatography (ethyl acetate/ methanol: 20/ 1) to get pure product **5** (45 mg, 93%). $[\alpha]_D$ = 53.9 (*c* 1.0, CH_3OH); ^1H NMR (300 MHz, CD_3OD, two isomers): δ = 2.15-2.27 (m, 1H, *J* = 13.9 Hz, *J* = 9.7 Hz), 2.50-2.62 (m, 1H, *J* = 13.9 Hz, *J* = 6.6 Hz), 3.25-3.47 (m, 15H, partially overlapping with solvent), 3.48-3.92 (m, 7H), 4.00-4.40 (m, 3H), 4.59-4.84 (m, 10H), 5.07-5.18 (brs, 2H), 7.27-7.43 (m, 5H); ^{13}C NMR (75 MHz, CD_3OD, two isomers): δ = 32.9/40.0, 55.5-57.2 (12 carbons), 67.9/68.4, 68.3 (2 carbons), 70.6/71.4, 72.8/73.3, 73.3 (2 carbons), 76.7/76.9, 77.9 (2 carbons), 81.0/81.4, 86.3/86.8, 97.6-99.8 (10 carbons), 128.4-129.6 (10 aromatic carbons), 138.2/137.8 (aromatic carbons), 156.8 (2 carbons), 174.0 (2 carbons); HRMS (ES) calcd for $C_{29}H_{44}NO_{15}$ $[M - H]^-$: 646.2711, found: 646.2723.

(1*S*)-2,3,4,6-Tetra-*O*-methoxymethyl-1′-*N*-benzyloxycarbonyl-5′(*S*)-methyl methoxymethyl ether-spiro[1,5-anhydro-D-glucitol-1,3′-*L*-proline] (6) The synthetic procedure is described in SI. $[\alpha]_D$ = 30.3 (*c* 1.2, CH_3OH); ^1H NMR (300 MHz, CD_3OD, two isomers): δ = 2.35-2.46 (brs, 2H), 3.28-3.82 (m, 23H, partially overlapping with solvent), 4.13-4.31 (m, 2H), 4.56-4.86 (m, 10H), 5.01-5.23 (m, 2H), 7.28-7.43 (m, 5H); ^{13}C NMR (75 MHz, CD_3OD, two isomers): δ = 28.1/29.1, 55.5-57.4 (10 carbons),

57.7/58.2, 68.0/68.4, 68.4/68.6, 69.3/69.8, 73.1 (4 carbons), 77.5 (2 carbons), 78.2 (2 carbons), 81.9/82.0, 87.3/88.2, 97.6-100.0 (10 carbons), 128.6-129.6 (10 aromatic carbons), 137.8/138.0 (aromatic carbons), 156.8/157.0, 175.3 (2 carbons); HRMS (ES) calcd for $C_{29}H_{44}NO_{15}$ $[M - H]^-$: 646.2711, found: 646.2718.

Dipeptide H-5′(*R*)-(MOM)GlcTSPro-Val-NMe$_2$ (7) The amino acid TFA·NH_2-Val-NMe_2 (44 mg, 0.16 mmol) was dissolved in DMF (1 mL) and then added to a solution of acid **5** (35 mg, 0.05 mmol) and *N, N*-diisopropylethylamine (70 μL, 0.32 mmol) in DMF (3 mL). The reaction mixture was stirred for 10 minutes at room temperature followed by the addition of TBTU (41 mg, 0.11 mmol) and stirred for another 8 hours. After that the reaction is quenched with water (8 mL) and extracted with ethyl acetate (4 × 10 mL). The combined organic layer was dried with sodium sulfate and concentrated. The residue was purified by flash chromatography (ethyl acetate/methanol: 30/1) to afford the Cbz-protected intermediate, which was dissolved in ethyl acetate (5 mL) and treated with $Pd(OH)_2$ (20 mg, 20% wt on charcoal) under hydrogenation condition (H_2, 10 psi). The mixture was stirred for one and half hours at room temperature and filtered, concentrated. The resulted crude product was purified by flash chromatography (ethyl acetate/ methanol: 20/ 1) to afford the dipeptide **7** (27 mg, 80%). $[\alpha]_D$ = 27.4 (*c* 1.2, CH_3OH); ^{1}H NMR (500 MHz, CD_3OD): δ = 0.97 (d, 3H, *J* = 6.9 Hz), 1.01 (d, 3H, *J* = 6.8 Hz), 1.91 (m, 1H), 2.00-2.13 (m, 2H), 2.94 (s, 3H), 3.20 (s, 3H), 3.30-3.42 (m, 15H, partially overlapping with solvent), 3.46-3.69 (m, 9H), 3.85 (d, 1H, *J* = 12.0 Hz), 4.55 (d, 1H, *J* = 5.3 Hz), 4.62-4.82 (m, 10H); ^{13}C NMR (75 MHz, CD_3OD): δ = 18.8, 19.5, 31.7, 31.9, 36.1, 38.1, 55.5, 55.6, 55.7, 56.6, 56.7, 57.0, 57.2, 68.5, 70.7,

71.1, 74.3, 77.5, 78.5, 83.7, 89.2, 97.7, 97.9, 99.6, 99.8, 100.1, 172.8, 174.0 ; HRMS (ES) calcd for $C_{28}H_{54}N_3O_{13}$ $[M + H]^+$: 640.3657, found: 640.3646.

Dipeptide H-5′(*S*)-(MOM)GlcTSPro-Val-NMe$_2$ (8) The synthetic procedure is described in SI. $[\alpha]_D$ = 54.0 (*c* 1.0, CH_3OH); ^1H NMR (500 MHz, CD_3OD): δ = 0.95-0.97 (m, 6H), 1.78 (dd, 1H, *J* = 13.2 Hz, *J* = 6.8 Hz), 2.00-2.07 (m, 1H), 2.48 (dd, 1H, *J* = 13.2 Hz, *J* = 8.2 Hz), 2.97 (s, 3H), 3.20 (s, 3H), 3.30-3.42 (m, 14H, partially overlapping with solvent), 3.46-3.72 (m, 9H), 3.80 (s, 1H), 3.89 (d, 1H, *J* = 11.4 Hz), 4.57 (d, 1H, *J* = 4.6 Hz), 4.63-4.84 (m, 10H, partially overlapping with solvent); ^{13}C NMR (75 MHz, CD_3OD): δ = 18.4, 19.6, 31.9, 36.1, 36.2, 38.0, 55.4, 55.7, 55.8, 56.8, 57.0, 57.3, 58.0, 68.7, 70.2, 73.0, 76.1, 78.4, 79.3, 83.4, 88.0, 97.9 (2 carbons), 99.7, 99.9, 100.2, 171.4, 173.6 ; HRMS (ES) calcd for $C_{28}H_{54}N_3O_{13}$ $[M + H]^+$: 640.3657, found: 640.3649.

Tripeptide H-D-Phe-5′(*R*)-(MOM)GlcTSPro-Val-NMe$_2$ (9) To a solution of dipeptide 7 (30 mg, 0.05 mmol) and *N, N*-diisopropylethylamine (43 μL, 0.23 mmol) in DMF (3 mL) was added the D- Fmoc-Phe-OH (56 mg, 0.14 mmol) and PyBOP (73 mg, 0.14 mmol). The mixture was stirred for 18 hours at room temperature before addition of sodium bicarbonate (16 mg, 0.18 mmol). The resulted mixture was dilutated with water (5 mL) and extracted with ethyl acetate (5 × 10 mL). The combined organic layers were dried (Na_2SO_4) and concentrated. The crude product was purified by flash chromatography (ethyl acetate/methanol: 20/1) to provide the Fmoc-protected intermediate, which was dissolved in a mixture of piperidine and DMF (0.2 mL + 0.8 mL) and stirred for 1 hour at room temperature. The solution was concentrated and purified by

flash chromatography (ethyl acetate/methanol: 10/1 to 6/1; TLC was charred with the iodine) to get tripeptide **9** (29 mg, 80%). $[\alpha]_D$ = 2.0 (*c* 0.4, CH_3OH); ^1H NMR (500 MHz, CD_3OD, two isomers): δ = 0.92 (d, 3H, *J* = 6.6 Hz), 1.04 (d, 3H, *J* = 7.0 Hz), 1.98-2.06 (m, 1H), 2.19 (dd, 0.30H, *J* = 14.3 Hz, *J* = 7.8 Hz), 2.32 (dd, 0.70H, *J* = 14.0 Hz, *J* = 11.7 Hz), 2.40-2.47 (m, 2.80H), 2.51-2.60 (m, 1H), 2.67 (dd, 0.30H, *J* = 13.7 Hz, *J* = 7.3 Hz), 2.90-2.94 (m, 1.60H), 3.04 (dd, 0.30H, *J* = 14.0 Hz, *J* = 4.9 Hz), 3.13-3.44 (m, 18H, partially overlapping with solvent), 3.49 (m, 0.30H), 3.55-3.98 (m, 6.70H), 4.22-4.91 (m, 15H), 7.12-7.30 (m, 5H); ^{13}C NMR (75 MHz, CD_3OD, two isomers): δ = 19.4 (2 carbons), 19.7/19.8, 31.4/35.7, 32.5/32.6, 35.7/36.0, 38.0/38.2, 41.7/42.3, 55.4-56.9 (14 carbons), 57.1/57.8, 66.7 (2 carbons), 68.5/69.5, 72.3/73.3, 72.8/73.5, 75.9/76.2, 76.8/77.3, 78.3/78.9, 85.9/86.8, 97.6-99.4 (10 carbons), 127.7-130.8 (10 aromatic carbons), 138.6/139.1 (aromatic carbon), 170.3/170.6, 173.2/173.3, 178.0/179.0; HRMS (ES) calcd for $C_{37}H_{63}N_4O_{14}$ $[M + H]^+$: 787.4341, found: 787.4345.

Tripeptide H-D-Phe-5′(*S*)-(MOM)GlcTSPro-Val-NMe_2 (10) The synthetic procedure is described in SI. $[\alpha]_D$ = -13.2 (*c* 0.9, CH_3OH); ^1H NMR (500 MHz, CD_3OD, two isomers): δ = 0.87-1.03 (m, 6H), 1.90-2.11 (m, 1.14H), 2.27-2.44 (m, 1.86H), 2.67 (dd, 0.14H, *J* = 14.9 Hz, *J* = 7.4 Hz), 2.78 (dd, 0.86H, *J* = 12.9 Hz, *J* = 6.1 Hz), 2.91 (s, 0.42H), 2.93 (s, 2.58H), 2.97-3.11 (m, 2H), 3.28-3.48 (m, 15H, partially overlapping with solvent), 3.49-4.01 (m, 9H), 4.14-4.97 (m, 15H), 7.17-7.27 (m, 5H); ^{13}C NMR (75 MHz, CD_3OD, trans isomer): δ = 18.7, 19.7, 32.5, 32.9, 36.0, 38.1, 41.2, 55.4-56.7 (7 carbons), 57.8, 68.9, 71.7, 72.7, 72.9, 76.2, 76.5, 79.3, 86.6, 97.6-99.4 (5 carbons), 127.7-136.6 (5 aromatic carbons), 139.1 (aromatic carbon), 170.5, 173.4, 176.8; HRMS (ES) calcd for

$C_{37}H_{63}N_4O_{14}$ $[M + H]^+$: 787.4341, found: 787.4352.

Tetrapeptide Ac-Leu-D-Phe-5′(*R*)-(MOM)GlcTSPro-Val-NMe_2 (11) To a solution of tripeptide **9** (25 mg, 0.03 mmol) and *N, N*-diisopropylethylamine (29 μL, 0.16 mmol) in DMF (3 mL) was added the Fmoc-Leu-OH (34 mg, 0.10 mmol) and TBTU (31 mg, 0.10 mmol). The mixture was stirred for 18 hours at room temperature before addition of sodium bicarbonate (11 mg, 0.13 mmol). The resulted mixture was dilutated with water (5 mL) and extracted with ethyl acetate (5 × 10 mL). The combined organic layers were dried (Na_2SO_4) and concentrated. The crude product was purified by flash chromatography (dichloromethane/methanol: 20/1) to provide the Fmoc-protected intermediate, which was dissolved in a mixture of piperidine and DMF (0.2 mL + 0.8 mL) and stirred for 1 hour at room temperature. The solution was concentrated in vacuum. The resulted mixture was dissolved in methanol (2 mL) followed by the addition of pyridine (13 μL, 0.16 mmol) and acetic anhydride (9 μL, 0.10 mmol). The mixture was stirred for 2 hours at room temperature. The solution was concentrated and purified by flash chromatography (methlene chloride/methanol: 25/ 1 to 15/ 1; TLC was charred with the iodine) to get tetrapeptide **11** (25 mg, 92%). $[\alpha]_D$ = -19.8 (*c* 1.15, CH_3OH); ^1H NMR (500 MHz, CD_3OD, two isomers): δ = 0.72-1.46 (m, 15H), 1.89-1.92 (m, 3H), 2.03 (m, 1H), 2.26 (dd, 0.29H, *J* = 14.4 Hz, *J* = 8.2 Hz), 2.35 (dd, 0.71H, *J* = 14.2 Hz, *J* = 11.9 Hz), 2.47 (s, 2.13H), 2.51 (dd, 0.71H, *J* = 14.2 Hz, *J* = 6.9 Hz), 2.68 (m, 1H), 2.83 (dd, 0.29H, *J* = 14.5 Hz, *J* = 8.9 Hz), 2.92 (s, 0.87H), 3.04-3.45 (m, 19H, partially overlapping with solvent), 3.46-3.76 (m, 4.71H), 3.84-3.89 (m, 1.71H), 3.95-3.97 (m, 0.29H), 4.05 (d, 0.29H, *J* = 5.2 Hz), 4.09 (dd, 0.29H, *J* = 10.4 Hz, *J* = 5.2 Hz), 4.19-4.45 (m, 2.71H),

4.54-4.84 (m, 12.71H, partially overlapping with solvent), 5.41-5.45 (m, 0.29H), 7.08-7.25 (m, 5H); ^{13}C NMR (75 MHz, CD_3OD, two isomers): δ = 18.5/19.3, 19.7/19.8, 21.9/22.2, 22.5/22.6, 23.2/23.4, 25.7/25.8, 40.0 (2 carbons), 32.3/32.6, 38.0/38.2, 38.8 (2 carbons), 42.2/42.6, 52.6/53.4, 53.1/53.9, 55.4-56.9 (14 carbons), 57.3/57.6, 66.7 (2 carbons), 68.5/69.6, 72.1/73.4, 72.7/73.6, 75.6/76.5, 76.7/77.6, 80.1 (2 carbons), 85.9/86.5, 97.5-99.7 (10 carbons), 127.7-130.9 (10 aromatic carbons), 137.8/138.4 (aromatic carbon), 170.4/170.6, 172.6/172.9, 173.2/173.3, 173.8/173.9, 174.1/174.9; HRMS (ES) calcd for $C_{45}H_{76}N_5O_{16}$ $[M + H]^+$: 942.5287, found: 942.5293.

Tetrapeptide Ac-Leu-D-Phe-5′(*S*)-(MOM)GlcTSPro-Val-NMe$_2$ (12) The synthetic procedure is described in SI. $[\alpha]_D$ = 29.2 (*c* 0.8, CH_3OH); ^{1}H NMR (500 MHz, CD_3OD, two isomers): δ = 0.81-1.01 (m, 12H), 1.20-1.49 (m, 3H), 1.94-2.06 (m, 4H), 2.11 (dd, 0.23H, *J* = 14.1 Hz, *J* = 8.8 Hz), 2.29-2.46 (m, 1.77H), 2.85-3.19 (m, 8H), 3.30-3.54 (m, 16H, partially overlapping with solvent), 3.66-3.85 (m, 6.31H), 3.94 (d, 0.23H, *J* = 4.5 Hz), 4.0 (d, 0.23H, *J* = 4.6 Hz), 4.08 (dd, 0.23H, *J* = 8.2 Hz, *J* = 4.1 Hz), 4.26-4.88 (m, 14H, partially overlapping with solvent), 4.97 (d, 0.23H, *J* = 6.3 Hz), 5.35 (dd, 0.77H, *J* = 8.5 Hz, *J* = 6.3 Hz), 7.12-7.26 (m, 5H); ^{13}C NMR (75 MHz, CD_3OD, two isomers): δ = 19.3/19.5, 19.6 (2 carbons), 21.8/22.5, 22.6/22.7, 23.1/23.7, 25.8/25.9, 32.1/32.2, 33.0 (2 carbons), 36.0/36.1, 37.9/38.2, 38.3/38.6, 42.0/42.5, 52.8-57.5 (18 carbons), 69.0/69.3, 71.6/71.7, 72.8 (2 carbons), 73.7 (2 carbons), 75.7/76.5, 76.0/76.7, 77.2/78.9, 86.6/88.3, 97.0-99.1 (10 carbons), 127.6-130.6 (10 carbons), 138.6 (2 carbons), 170.3/171.3, 172.3/172.6, 173.2 (2 carbons), 173.7 (2 carbons), 174.2/174.4 ; HRMS (ES) calcd for $C_{45}H_{76}N_5O_{16}$ $[M + H]^+$: 942.5287, found: 942.5281.

Tetrapeptide Ac-Leu-D-Phe-5′(*R*)-GlcTSPro-Val-NMe$_2$ (13) To a solution of compound **11** (30 mg, 0.03 mmol) in methanol (1 mL) was added a 6 M HCl solution (100 μL). The mixture was stirred for 18 hours at room temperature and then concentrated. The crude product was purified by flash chromatography (methylene chloride/methanol: 5/1) to afford unprotected tetrapeptide **13** (20 mg, 90%). ^{1}H NMR (500 MHz, D_2O, *cis* isomer): δ = 0.63-1.32 (m, 15H), 1.90 (s, 3H), 1.94-1.99 (m, 1H), 2.30-2.46 (br, 5H), 2.74-2.79 (dd, 1H, *J* = 12.6 Hz, *J* = 12.9 Hz), 2.94-3.00 (dd, 1H, *J* = 17.5 Hz, *J* = 14.5 Hz), 3.17 (s, 3H), 3.44-3.53 (br, 3H), 3.64-3.87 (m, 5H), 4.04-4.11 (m, 1H), 4.17-4.25 (m, 1H), 4.34-4.40 (m, 1H), 4.59 (m, 1H), 4.77 (1H, overlapping with solvent), 7.10-7.38 (m, 5H); ^{13}C NMR (75 MHz, CD_3OD, *cis* isomer): δ = 19.4, 19.7, 22.1, 22.3, 23.2, 25.7, 25.9, 31.8, 35.9, 38.2, 38.5, 42.0, 53.0, 54.2, 56.6, 59.9, 60.8, 62.6, 71.0, 71.2, 73.2, 75.3, 77.3, 87.3, 127.7-130.4 (5 carbons), 138.5, 171.7, 173.1, 174.1, 174.5, 174.8; HRMS (ES) calcd for $C_{35}H_{56}N_5O_{11}$ $[M + H]^+$: 722.3976, found: 722.3985.

ROESY experiments. ROESY spectra of tetrapeptides **11-13** and **16** were recorded on AMX 500 with 256 points in *t*1, 2048 points in *t*2 and 64 scans per *t*2 increment.

Temperature coefficient experiments. 1 D ^{1}H-NMR spectroscopy of 8 mM solutions of **11, 12** and **16** in 100.0% Me_2SO-d_6 and **13** in H_2O/D_2O (9/1) were recorded on a Bruker AMX500 at 20 °C, and from 20 to 45 °C with increments of 5 °C, using routine techniques. Chemical shift (δ) are expressed in ppm and calibrated with respect to the residual DMSO signal (^{1}H: 2.49 ppm) or the TSP (^{1}H: 0.00 ppm) in water.

5.5. References:

1. (a) Richardson, J. S. *Adv. Protein Chem.* **1981**, *34*, 167. (b) Wilmot, C. M.; Thornton, J. M. *J. Mol. Biol.* **1988**, *203*, 221. (c) Rose, G. D.; Gierasch, L. M.; Smith, J. A. *Adv. Protein Chem.* **1985**, *37*, 1.
2. (a) Creighton, T. E. *Proteins: Structure and Molecular Properties.* Freeman: New York, 1983. (b) Rizo, J.; Gierasch, L. *Annu. Rev. Biochem.* **1992**, *61*, 387. Lewis, P. N.; Momany, F. A.; Scheraga, H. A. *Proc. Nat. Acad. Sci., U.S.A.* **1971**, *68*, 2293.
3. Lewis, P. N.; Momany, F. A.; Scheraga, H. A. *Proc. Nat. Acad. Sci., U.S.A.* **1971**, *68*, 2293.
4. (a) Branden, C.; Tooze, J. *Introduction to Protein Structure*; Garland Publishing: New York, 1991. (b) Stryer, L. *Biochemistry*, 4th ed.; W. H. Freeman and Company: New York, 1999.
5. Reviewed in: (a) Fisher, G. *Angew. Chem. Int. Ed. Engl.* **1994**, *33*, 1415. (b) Liu, J.; Chen. C.-M.; Walsh, C. T. *Biochemistry* **1991**, *30*, 2306.
6. Johnson, M. E.; Lin, Z.; Padmanabhan, K.; Tulinsky, A.; Kahn, M. *FEBS Lett.* **1994**, *337*, 4.
7. Dugave, C.; Demange, L. *Chem. Rev.* **2003**, *103*, 2475.
8. Halab, L.; Lubell, W. D. *J. Am. Chem. Soc.* **2002**, *124*, 2474. And references therein.
9. An, S. S. A.; Lester C. C.; Peng, J.-L.; Li, Y.-J.; Rothwarf, D. M.; Welker, E.; Thannhauser, T. W.; Zhang, L. S.; Tam, J. P.; Scheraga, H. A. *J. Am. Chem. Soc.* **1999**, *121*, 11558.
10. (a) Didierjean, C.; Del Duca, V.; Benedetti, E.; Aubry, A.; Zouikri, M.; Marraud, M.; Boussard, G. *J. Peptide Res.* **1997**, *50*, 451. (b) Zouikri, M.; Vicherat, A.; Aubry, A.; Marraud, M.; Boussard, G. *J. Peptide Res.* **1998**, *52*, 19.
11. (a) Dumy, P.; Keller, M.; Ryan, D. E.; Rohwedder, B.; Wöhr, T.; Mutter, M. *J. Am. Chem. Soc.* **1997**, *119*, 918. (b)Kern, D.; Schutkowski, M.; Drakenberg, T. *J. Am. Chem. Soc.* **1997**, *119*, 8403. (c) Keller, L.; Sager, C.; Dumy, P.; Schutkowski, M.; Fischer, G. S.; Mutter, M. *J. Am. Chem. Soc.* **1998**, *120*, 2714.
12. Zhang, K.; Schweizer, F. *Synlett* **2005**, 3111.
13. Owens, N.; Braun, C.; Schweizer, F. *J. Org. Chem.*, **2007**, *72*, 4635.
14. This work will be published in another paper.
15. Jeannotte, G.; Lubell, W. D. *J. Am. Chem. Soc.* **2004**, *126*, 14334.
16. (a) Walker, J. R.; Alshafie, G.; Nieves, N.; Ahrens, J.; Clagett-Dame, M.; Abou-Issa, H.; Curley, R. W. *Bioorg. Med. Chem.* **2006**, *14*, 3038. (b) Sicheral, F.; Wittmann, V. *Angew. Chem. Int. Ed.* **2005**, *44*, 2096.
17. The acid was treated with 2 equiv. iodomethane and 1.2 equiv. cesium carbonate in methanol and stirred for 1 hour to provide the corresponding methyl ester.
18. Frerot, E.; Coste, J.; Pantaloni, A.; Dufour, M. N.; Jouin, P. *Tetrahedron,* **1991**, *47*, 259.
19. Bürgi, H. B.; Dunitz, J. D.; Lehn, J. M.; Wipff, G. **1974**, *Tetrahedron 30*, 1563.
20. Runkel, L.; Neier, W.; Repinsky, R. B.; Karpusas, M.; Whitty, A.; Kimball, K.; Brickelmaier, M.; Muldowney, C.; Jones, W.; Goelz, S. E. *Pharm. Res.* **1998**, *15*, 641.
21. Koppel, K. D.; Ohnishi, M.; Go, A. *J. Am. Chem. Soc.* **1969**, *91*, 4264.
22. Misicka, A.; Verheyden, P. M. F.; Van Binst, G. *Lett. Pept. Sci.* **1998**, *5*, 375.
23. Chakraborty, T. K.; Srinivasu, P.; Vengal Rao, R.; Kiran Kumar, S.; Kunwar, A. C. *J. Org. Chem.* **2004**, *69*, 7399.
24. Leeflang, B. R.; Vliegenthart, J. F. G.; Kroon-Batenburg, L. M. J.; Eijck, B. P.; Kroon, J. *Carbohydr. Res.*1992, *230*, 41.

Chapter 6

Synthesis of Glucose-templated Lysine Analogs and Incorporation into the Antimicrobial Dipeptide Sequence kW-OBn

Abstract: *The synthesis of two glucose-templated (GlcT) lysine analogs GlcTK and GlcTk in which the side chain of D- and L-lysine (k and K) is conformationally constrained via incorporation into a D-glucose scaffold is described. Key-step in the synthesis is a high yielding, reductive ring opening of an exocyclic glucose-derived epoxide to form a α-hydroxy methyl ester that can be converted into GlcTK and GlcTk. To demonstrate the use of these building blocks in peptide synthesis we replaced D-lysine in the antimicrobial dipeptide sequence kW-OBn (W = L-tryptophan) and determined the antibacterial activity against various gram-positive and gram-negative organisms. Our results show that replacement of D-lysine by unprotected GlcTk in dipeptide kW-OBn results in reduced antibacterial activity.*

6.1. Introduction

The explosive growth of multi-drug resistant (MDR) bacteria in hospitals and the community have led to an emerging crisis where an increasing number of antimicrobial classes cease to be of clinical usefulness.[1] Despite this growing concern, only one new class of antibiotics, the oxazolidinones, has entered the clinic during the past two decades.[2] Cationic antimicrobial peptides (AMPs) with their ability to combat MDR bacteria have been proposed as new antibacterial agents.[3–5] AMPs are defined as peptides containing a net excess of positively charged residues, approximately 50% hydrophobic residues and a size ranging from 12 to 50 residues.[6] Although the mode of action of AMPs is not fully understood, most AMPs appear to manifest their biological action by

enhancing the permeability of lipid membranes of bacterial cells. This typically involves initial electrostatic interactions between the positively charged basic side chains of lysine, arginine, and ornithine to the negatively charged lipid membrane of pathogens, followed by adoption of an amphipathic helical or β-sheet structure.[6,7] The ability to kill target bacteria rapidly, the unusually broad spectrum of activity against some of the more serious antibiotic resistant pathogens, and the relative difficulty with which mutants develop resistance in vitro make AMPs attractive targets for drug development.[6,7] However, in vivo efficacy studies of several cationic peptide antibiotics have been disappointing most likely due to the fact that many AMPs exhibit poor bioavailability, susceptibility to proteolytic cleavage, and low in vivo antimicrobial activity.[8] Moreover, the size of most AMPs is so large that production costs represent additional concern. To overcome some of these drawbacks, ultrashort cationic antimicrobial peptides (UAMPs) and lipopeptides in the form of di-, tri-, and tetrapeptides have recently emerged as a novel class of potential antimicrobial drug candidates.[9–11] In particular, the small size and facile preparation reduce production costs while the presence of only a few amide bonds and the low molecular weight may improve the pharmacokinetic and pharmacodynamic properties of UAMPs.

In this respect, the potent antimicrobial activity of the dipeptide D-lysine-L-tryptophan-OBn (kW-OBn) against *Staphylococcus aureus* (*S. aureus*), methicillin-resistant *S. aureus* (MRSA), and methicillin-resistant *Staphylococcus* epidermidis (MRSE) strains attracted our attention.[9] In particular, we were interested in exploring structure

activity relationships of this dipeptide via replacement of D-lysine (k) by carbohydrate-templated D-lysine analogs CTLys (Figure 6.1).[18] CTLys are a novel class of polyfunctional lysine analogs in which the carbohydrate scaffold constrains the side chain while at the same time introducing molecular diversity such as poly(hydroxylation) and artificial glycosylation. It is noteworthy that post-translational hydroxylation of lysine[12] and arginine[12] and other amino acids[13-15] has been shown to enhance the biological activity of AMPs.[12] Furthermore, CTLys contain the 1,3-hydroxyamine binding motifs[16] of aminoglycoside antibiotics that have been proposed to interact as bidentate RNA hydrogen bond acceptor to the phosphodiester backbone or Hoogsteen face of guanosine.[16] Moreover, additional modification and derivatization of the carbohydrate scaffold may be used to tailor the physical, chemical, biological, and pharmacodynamic properties of CTLys-containing peptides.

We report the synthesis of two glucose-templated lysines, GlcTks and GlcTKs

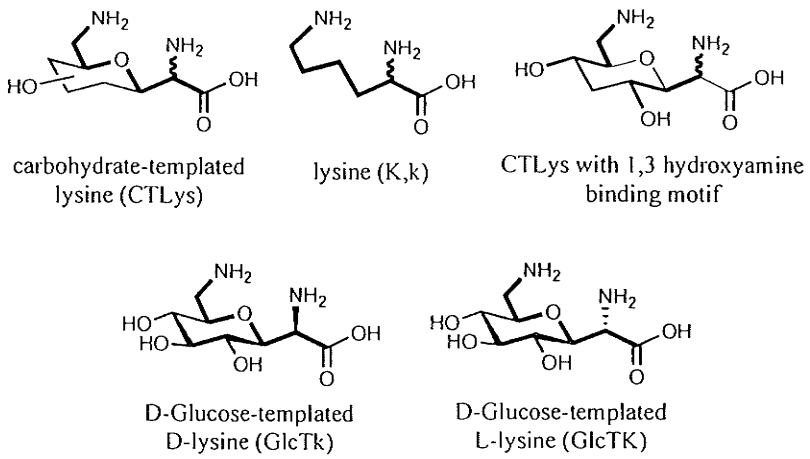

Figure 6.1 Examples of carbohydrate-templated lysine analogs (CTLys) and glucose-templated lysine analogs GlcTk and GlcTK.

(Figure 6.1), and describe the use of these building blocks in peptide synthesis. Moreover, we replaced D-lysine (k) by GlcTk in the antimicrobial dipeptide kW-OBn and determined the antibacterial activities against various gram-positive and gram-negative bacteria. A preliminary report on the synthesis of glucose-templated lysine analogs without experimental details and biological evaluation appeared recently.[17]

6.2. Results and discussion

The synthesis started with the readily available D-glucoconfigured lactone **1**[19] (Scheme 6.1), which reacts with the enolate of methyl bromoacetate generated from lithium bis-(trimethylsilyl)amide ($LiN(SiMe_3)_2$) in tetrahydrofuran (THF) at -78 °C, to produce the exocyclic epoxide **2** in 80% yield as a single stereoisomer.[17,20] Trimethylsilyl trifluoromethanesulfonate (TMSOTf)-promoted reductive ring opening of epoxide **2** with tributyltin hydride in dichloromethane at 0 °C afforded silylether **3** and alcohol **5** (ratio: **3**:**5** = 3.5:1) in a combined yield of 92%. Compounds **3** and **5** were obtained as a single diastereoisomer. Silyl ether **3** was hydrolyzed quantitatively into alcohol **5** by exposure to trifluoroacetic acid containing wet THF. The stereochemistry at C-2 of alcohol **5** was determined by conversion of **5** into the known benzyl ester **4**.[21] This was achieved in a two-step procedure. First, methyl ester **5** was hydrolyzed to the corresponding acid with lithium hydroxide in wet THF. Subsequently, esterfication of the acid using cesium carbonate and benzyl bromide in DMF afforded benzyl ester **4** as a single product in 89% yield. Hydroxy ester **5** served as the starting material to install an amino function at C-2.

In situ activation of the hydroxyl group as a trifluoromethanesulfonate ester using trifluoromethanesulfonic anhydride in pyridine followed by nucleophilic displacement with sodium azide–15-crown-5 provided azide **6** in 82% isolated yield. Catalytic hydrogenation of **6** using Pearlman's catalyst followed by protection of the amino function as *t*-butoxycarbamate provided the protected amino ester **7** in 90% yield.

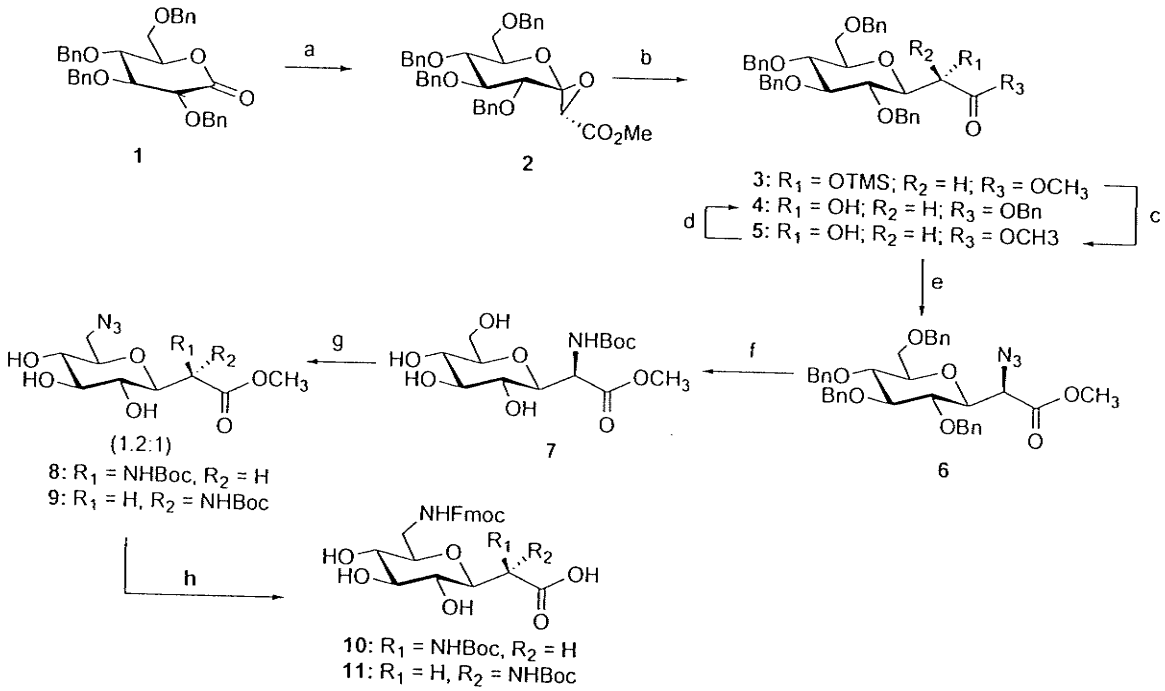

Scheme 6.1 Reagents and conditions: (a) LiHMDS, $BrCH_2COOMe$, THF, -78 °C, 80%; (b) TMSOTf, Bu_3SnH, CH_2Cl_2, 0 °C, 72%; (c) CF_3COOH, THF/H_2O (5:1), rt, quant.; (d) i) LiOH, THF/H_2O (1:1); ii) Cs_2CO_3, BnBr, DMF, rt, 89% (over 2 steps); (e) i) Tf_2O, dry pyridine, CH_2Cl_2, rt; ii) NaN_3, 15-crown-5, CH_2Cl_2, rt, 81% (over 2 steps); (f) i) $Pd(OH)_2/C$, H_2 (10 psi), MeOH, rt; ii) $(Boc)_2O$, TEA, MeOH, 90% (over 2 steps); (g) i) TsCl, pyridine, 0 °C-rt, 64%; ii) NaN_3, DMF, 100 °C, 52% (**8**) and 43% (**9**); (h) i) LiOH, THF/H_2O (1:1); ii) $Pd(OH)_2/C$, H_2 (10 psi), MeOH, rt; iii) Fmoc-OPfp, $NaHCO_3$, acetone/H_2O (1:1), rt, 63% (**10**, over 3 steps) or 65% (**11**, over 3 steps).

Compound **7** served as precursor for introducing the second amino functionality into the carbohydrate scaffold. This was achieved by selective tosylation[16] of the primary hydroxy

group using *p*-toluenesulfonyl chloride in pyridine followed by nucleophilic displacement of the tosylate with sodium azide at elevated temperature in DMF. It is noteworthy that the displacement of the primary tosylate by sodium azide does not result in epimerization at C-2 and provides only azide **8**, if the reaction is performed below 80 °C. However, we observed substantial epimerization at 100 °C affording diastereomeric azides **8** and **9** in 53% and 42% yields, respectively. Both diastereomers can be separated by flash chromatography. Exposure of esters **8** and **9** to basic conditions (LiOH, THF–H_2O) followed by catalytic hydrogenation using Pearlman's catalyst [$Pd(OH)_2$–C, H_2, MeOH] and protection of the primary amino function as 9*H*-fluorenylmethoxycarbamate using 9-fluorenylmethyl pentafluorophenyl carbonate provided the glucose-templated D-lysine analogs GlucTk **10** and glucose-templated L-lysine analogs GlucTK **11** in 63% and 65% isolated yields, respectively. Building blocks **10** and **11** are suitably protected to be used as novel lysine mimetics in solution phase peptide synthesis.

To demonstrate the use of chimeric glucose-lysine analogs in peptide synthesis, we decided to convert azide **8** into the di-N-Boc-protected acid **13** (Scheme 6.2). This was achieved via a three-step procedure. Reduction of azide **8** by catalytic hydrogenation followed by protection using di-*t*-butyl dicarbonate and triethylamine in methanol afforded the di-t-butylcarbamate-protected ester **12** in 90% yield. Saponification of ester 12 using lithium hydroxide in aqueous THF provided acid **13** in 90% yield. To study the influence of the constrained sugar moiety and the presence of the 1,3-hydroxyamine motifs on the bioactivity of small antibacterial peptides, we decided to incorporate acid**13**

into the amphiphilic antimicrobial dipeptide sequences kW-OBn **14** and kWNHBn. The

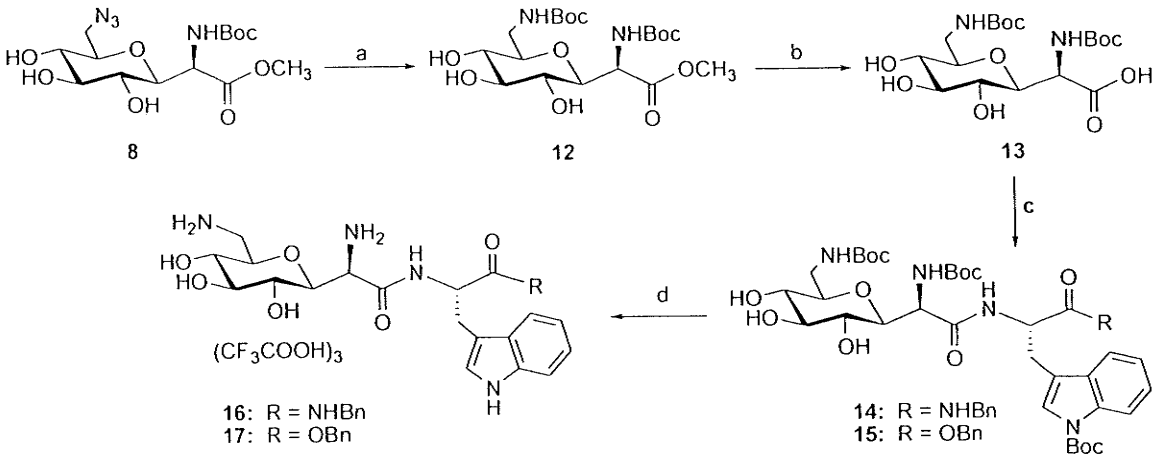

Scheme 6.2 Reagents and conditions: (a) i) $Pd(OH)_2/C$, H_2 (10 psi), MeOH, rt; ii) Boc_2O, Et_3N, MeOH, rt (90%, over 2 steps); (b) LiOH, THF/H_2O (1:1), 0 °C, 90%; (c) TBTU, H-Trp(Boc)-NHBn, DIPEA, DMF, rt, 77% (**14**) and TBTU, H-Trp(Boc)-OBn, DIPEA, DMF, rt, 83% (**15**); (d) TFA, CH_2Cl_2, rt, quant.

latter was selected to study how the nature of the C-terminus influences the antimicrobial activity. Amidation of **13** was achieved by the coupling of **13** to H-Trp(Boc)-NHBn and H-Trp(Boc)-OBn using 2-(1H-benzotriazol- e-lyl)-1,1,3,3-tetra-methyluronium tetrafluoroborate (TBTU) as coupling reagent in DMF to produce protected dipeptides **14** and **15** in 77% and 83% isolated yields, respectively. We did not observe ester formation involving the unprotected hydroxyl groups during peptide coupling demonstrating no need for protection of the secondary hydroxyl groups of **13** in peptide synthesis. Exposure of dipeptides **14** and **15** to a 50% mixture of trifluoroacetic acid in dichloromethane afforded unprotected dipeptides **16** and **17** in quantitative yields (Scheme 6.2).

With peptides **16** and **17** in hand, we investigated the antibacterial activity of these

peptides against various bacterial strains and compared them to the known antimicrobial dipeptide kW-OBn **18**[9] as well as kW-NHBn **19** (Table 6.1). *in vitro* antibacterial tests were performed in collaboration with Dr. Zhanel's laboratory at the Health Science Center at the University of Manitoba. Our results show that replacement of lysine by GlcTk reduces the antibacterial activity of kW-OBn by 4–32-fold against Gram-positive cocci and 2–16-fold versus Gram-negative bacilli. It is possible that the low antibacterial activity of dipeptide **17** is the result of decreased amphiphilicity and hydrophobicity. For instance, substitution of D-lysine by GlcTk introduces three hydroxyl groups. This results in significantly increased hydrophilicity of GlcTk-W-OBn when compared to kW-OBn. Amphiphilicity and hydrophobicity are crucial for the antibacterial activity of AMPs.[5–7]

Table 6.1 Representative minimal inhibitory concentrations (MIC) in μg/mL for various bacterial strains.

peptide	*S. aureus*[a]	MRSA[b]	MRSE[c]	*E. coli*[d]	*P. aeruginosa*[e]
16	256	>512	128	512	>512
17	256	256	128	512	>512
18	16	64	4	32	512
19	512	512	256	512	<512

[a] ATCC 29213;[b] methicillin-resistant *S. aureus* (ATCC 33592);[c] methicillin-resistant *S. epidermidis* (ATCC 14990);[d] ATCC 25922;[e] ATCC 27853.

However, other factors such as the bulkiness of the sugar fragment or the restricted rotation of the lysine motif may also contribute to the reduced activity. Interestingly, we observed that the nature of the C-terminus contributes substantially to the antimicrobial

activity of kW-OBn. For instance, dipeptide kW-OBn exhibits strong S. aureus activity while this activity is abolished in peptide kW-NHBn. The reasons for this peculiar behavior are currently not understood.

6.3. Conclusions

We have developed a synthetic pathway into suitably protected glucose-templated C-glycosidic lysine analogs with natural and unnatural C(α) configuration. The carbohydrate scaffold induces a conformational constraint into the side chain of lysine while, at the same time, introducing artificial post-translational modifications such as hydroxylation and glycosylation. To demonstrate the use of carbohydrate-templated lysine analogs in peptide synthesis and to explore the biological properties, we replaced lysine in the antibacterial dipeptide kW-OBn by GlcTk. Peptide synthesis was achieved without the need for hydroxyl group protection. Determination of the biological activity against various bacterial strains demonstrated that the replacement of lysine by GlcTk in the dipeptide kw-OBn reduces strongly the antibacterial activity. Studies of the lysinemimetic and glycomimetic properties of GlcTk and GlcTK in other peptides are in progress.

6.4. Experimental

General CH_2Cl_2 was distilled from calcium hydride. Organic solutions were concentrated under diminished pressure at <40 °C (bath temperature). NMR spectra were

recorded at 300 or 500 MHz for ^{1}H and at 75 MHz for ^{13}C. Chemical shifts are reported relative to $CHCl_3$ (δ_H 7.26, δ_c (center of triplet) 77.0 ppm) or to CH_3OH (δ_H 3.35, δ_C (center of septet) 49.0 ppm) or to acetone as internal standard (D_2O). TLC was performed on E. Merck Silica Gel 60 F254 with detection by charring with 8% H_2SO_4 acid. Silica gel (0.040–0.063 mm) was used for column chromatography. Lactone **1** was purchased from Toronto Research Chemicals. Reference peptides **18** and **19** were prepared according to the literature procedure[9] and obtained as TFA salts.

(2*S*)-Methyl 2-trimethylsilyloxy-2-(2,3,4,6-tetra-*O*-benzyl-*β*-D-glucopyranosyl)-Ethanoate (3) and (2S)-Methyl 2-hydroxy-2-(2,3,4,6-tetra-*O*-benzyl-*β*-D-glucopyranosyl)-ethanoate (5) To a mixture of epoxide **2**[21] (480 mg, 0.79 mmol) and tributyltin hydride (0.84 mL, 3.15 mmol) in dichloromethane (15 mL) was added drop wise trimethylsilyl trifluoromethanesulfonate (TMSOTf, 0.42 mL, 2.36 mmol) at 0 °C. The mixture was stirred for 30 min. at that temperature and quenched with saturated sodium bicarbonate solution (15 mL). The organic layer was separated and the aqueous phase was extracted with dichloromethane (3 x 10 mL). The combined organic layers were dried (Na_2SO_4), concentrated and purified by flash column chromatography (hexanes/ethyl acetate, 2:1) to afford **3** (388 mg, 72%) and **5** (96 mg, 20%) as a colorless syrup. The trimethylsilyl ether **3** was converted to **5** (337 mg, quant.) by treatment with trifluoroacetic acid (0.19 mL, 5 equiv.) in aq. tetrahydrofuran (THF/H_2O 5:1) for overnight. **3:** ^{1}H NMR (300 MHz, $CDCl_3$): δ 0.20 (s, 9 H), 3.46-3.54 (m, 1 H), 3.64 (dd,

1 H, J = 9.2, 9.6 Hz), 3.68-3.85 (m, 8 H), 4.55 (d, 1 H, J = 12.2 Hz), 4.62 (d, 1 H, J = 12.2 Hz), 4.63-4.74 (m, 3 H), 4.86 (d, 1 H, J = 10.9 Hz), 4.88 (d, 1 H, J = 10.9 Hz), 4.96 (d, 1 H, J = 11.4 Hz), 5.00 (d, 1 H, J = 11.4 Hz), 7.22-7.41 (m, 20 H); ^{13}C NMR (75 MHz, $CDCl_3$): δ 0.9, 52.0, 68.8, 71.7, 73.2, 74.6, 75.0, 75.6, 77.7, 78.7, 79.9, 80.2, 87.4, 127.3-128.5 (aromatic carbons), 138.2, 138.5, 138.5, 138.6, 172.4; MS (ES+): *m/z* 707.42 $[M+Na]^+$; Anal. Calcd for $C_{40}H_{48}O_8Si$: C, 70.15; H, 7.06. Found: C, 70.25; H, 7.14; **5:** $[\alpha]^{25}_D$ = +27.0 (*c* 1.15, $CHCl_3$); ^{1}H NMR (300 MHz, $CDCl_3$): δ 2.85 (br s, 1 H), 3.46-3.54 (m, 1 H), 3.59 (dd, 1 H, J = 8.4, 8.6 Hz), 3.63-3.72 (m, 3 H), 3.73-3.87 (m, 5 H), 4.47-4.59 (m, 3 H), 4.61 (d, 1 H, J = 11.0 Hz), 4.77 (d, 1 H, J = 11.0 Hz), 4.85 (d, 1 H, J = 10.8 Hz), 4.89-4.98 (m, 3 H), 7.19-7.39 (m, 20 H); ^{13}C NMR (75 MHz, $CDCl_3$): δ 52.7, 69.0, 69.6, 73.3, 75.1, 75.2, 75.6, 77.8, 78.3, 79.5, 79.5, 86.9, 127.5-128.6 (aromatic carbons), 138.1, 138.2, 138.3, 138.6, 173.3; MS (ES+): *m/z* 635.13 $[M+Na]^+$; Anal. Calcd for $C_{37}H_{40}O_8$: C, 72.53; H, 6.58. Found: C, 72.61; H, 6.46.

(2*S*)-Benzyl 2-hydroxy-2-(2,3,4,6-tetra-*O*-benzyl-*β*-D-glucopyranosyl)-ethanoate (4) LiOH (24 mg, 1.02 mmol) was added to a mixture of compound **5** (104 mg, 0.17 mmol) in THF/H_2O (3.0 mL, 1:1). The mixture was stirred at room temperature for 12 h and formic acid in water was added to quench the reaction until acidic. After extraction with ethyl acetate (5 x 20 mL), the organic layer was evaporated and the crude residue was dissolved in DMF (3.0 mL). Cs_2CO_3 (72 mg, 0.22 mmol) was added 30 minutes prior to addition of BnBr (40 μL, 0.34 mmol). The mixture was stirred at room

temperature for 2 h and water was added. The aqueous layer was extracted with ethyl acetate (3 x 20 mL) and the combined organic layers were dried (Na_2SO_4) and concentrated. Flash column chromatography (hexanes/ethyl acetate, 4:1) yielded **4** (104 mg, 89%) as a clear oil. ^{1}H NMR (300 MHz, $CDCl_3$): δ 3.30-3.36 (m, 2 H), 3.48 (dd, 1 H, J = 1.7, 11.1 Hz), 3.59-3.64 (m, 2 H), 3.67 (dd, 1 H, J = 1.9, 8.6 Hz), 3.74 (dd, 1 H, J = 8.8, 9.1 Hz), 3.83 (dd, 1 H, J = 9.1, 8.6 Hz), 4.52-4.58 (m, 3 H), 4.61 (d, 1 H, J = 10.7 Hz), 4.78 (d, 1 H, J = 10.9 Hz), 4.84 (d, 1 H, J = 10.9 Hz), 4.90-4.97 (m, 3 H), 5.10 (d, 1 H, J = 12.0 Hz), 5.33 (d, 1 H, J = 12.0 Hz), 7.19-7.38 (m, 25 H); ^{13}C NMR (75 MHz, $CDCl_3$): δ 67.3, 68.6, 69.6, 73.3, 75.1, 75.2, 75.6, 77.7, 78.1, 79.5, 79.6, 86.8, 127.6-128.6 (aromatic carbons), 135.3, 138.1, 138.2, 138.3, 138.6, 172.7; MS (ES+): *m/z* 689.44 $[M+H]^+$; Anal. Calcd for $C_{43}H_{44}O_8$: C, 74.98; H, 6.44. Found: C, 74.93; H, 6.52.

(2*R*)-Methyl 2-azido-2-(2,3,4,6-tetra-*O*-benzyl-*β*-D-glucopyranosyl)-ethanoate (6)

Compound **5** (50 mg, 0.08 mmol) was dissolved in dry CH_2Cl_2 (2.0 mL) and cooled to 0 °C. Pyridine (66 μL, 0.8 mmol) was added. The reaction mixture was stirred for 5 minutes, and then trifluoromethanesulfonic anhydride (55 μL, 0.32 mmol) was slowly added. The reaction mixture was stirred under 0 °C for 1 h. Water (5.0 mL) was added followed by extraction with CH_2Cl_2 (3 x 5 mL). The organic layer was dried (over Na_2SO_4), concentrated and re-dissolved in anhydrous CH_2Cl_2 (2.0 mL). NaN_3 (16 mg, 0.24 mmol) and 15-crown-5 (4 μL, 0.2 mmol) were added. The reaction mixture was stirred at room temperature for 24 h and then water was added. The aqueous phase was

extracted with CH_2Cl_2 (3 x 20 mL) and the combined organic layers were dried (Na_2SO_4) and concentrated. Flash column chromatography (hexanes/ethyl acetate, 4:1) yielded azide **6** (42 mg, 81%) as a pale-yellow oil. $[\alpha]^{25}_D$ = +6.0 (*c* 0.5, $CHCl_3$); ^{1}H NMR (300 MHz, $CDCl_3$) δ 3.52-3.56 (m, 4 H), 3.64 (dd, 1 H, *J* = 9.6, 8.6 Hz), 3.71-3.77 (m, 3 H), 3.80 (dd, 1 H, *J* = 9.4, 8.6 Hz), 3.92 (dd, 1 H, *J* = 1.9, 9.4 Hz), 4.37 (d, 1 H, *J* = 1.9 Hz), 4.55 (d, 1 H, *J* = 12.1 Hz), 4.57-4.65 (m, 2 H), 4.69 (d, 1 H, *J* = 10.6 Hz), 4.83 (d, 1 H, *J* = 10.9 Hz), 4.88 (d, 1 H, *J* = 10.9 Hz), 4.93-4.97 (m, 2 H), 7.23-7.36 (m, 20 H); ^{13}C NMR (75 MHz, $CDCl_3$): δ 52.6, 62.8, 68.9, 73.5, 74.7, 75.1, 75.6, 77.3, 78.2, 79.6, 79.7, 87.1, 127.6-128.5 (aromatic carbons), 137.9, 138.0, 138.2, 138.3, 167.8; MS (ES+): *m/z* 660.03 $[M+Na]^+$; Anal. Calcd for $C_{37}H_{39}N_3O_7$: C, 69.68; H, 6.16; N, 6.59. Found: C, 69.72; H, 6.21; N, 6.63.

(2*R*)-Methyl 2-(*tert*-butoxycarbonylamino)-2-(β-D-glucopyranosyl)-ethanoate (7)

Compound **6** (223 mg, 0.32 mmol) was dissolved in MeOH (6.0 mL) and aq. hydrochloric acid (0.5 mmol). Pearlman's catalyst (160 mg) was added and the mixture was hydrogenated for 6 h at atmospheric pressure. The mixture was filtered, concentrated, and re-dissolved in MeOH (2.0 mL). Triethylamine (0.5 mL) and Boc_2O (550 mg, 2.5 mmol) were added and the mixture was stirred at room temperature for 12 h. The crude residue was concentrated and purified with silica gel column chromatography (methanol/ethyl acetate, 1:6) to afford **10** (100 mg, 90%) as a syrup. $[\alpha]^{25}_D$ = -29.0 (*c* 1.45, CH_3OH); ^{1}H NMR (300 MHz, CD_3OD): δ 1.46 (s, 9 H), 3.07 (dd, 1 H, *J* = 9.3, 9.2

Hz), 3.23-3.36 (m, 2 H), 3.43-3.59 (m, 3 H), 3.74 (s, 3 H), 3.89 (dd, 1 H, J = 1.9, 11.8 Hz), 4.66 (d, 1 H, J = <1Hz); ^{13}C NMR (75 MHz, CD_3OD): δ 28.7, 52.6, 55.4, 63.6, 71.6, 72.0, 79.7, 80.8, 82.2, 82.6, 158.2, 173.0; MS (ES+): *m/z* 352.29 $[M+H]^+$; HRMS (ES+) Calcd for $C_{14}H_{26}NO_9$ $[M+H]^+$ 352.1608. Found 352.1607.

(2*R*)-Methyl 2-(*tert*-butoxycarbonylamino)-2-(6-azido-6-deoxy-β-D-glucopyranosyl)-ethanoate (8) and (2*S*)-Methyl 2-(*tert*-butoxycarbonylamino)-2-(6-azido-β-D-glucopyranosyl)-ethanoate (9) To a solution of compound 7 (100 mg, 0.29 mmol) in dry pyridine (8.0 mL) was added toluenesulfonyl chloride (128 mg, 0.68 mmol) and the reaction was stirred for 2 h at 0 °C, then raised to room temperature for 6 h. The solvent was removed in *vacuo* and then purified by gradient flash column chromatography (ethyl acetate to ethyl acetate/methanol, 20:1) to afford a crude mixture containing the 6-*O*-tosyl-β-D-glucopyranoside derivative (92 mg, 64%). Sodium azide (118 mg, 1.82 mmol) was added to the solution of tosylate in dry DMF (3.0 mL) and the mixture was heated to 100 °C for overnight. The solvent was removed in *vacuo* and the residue was purified by gradient flash column chromatography (ethyl acetate to ethyl acetate/methanol, 20:1) to afford compound **8** (36 mg, 52%) and **9** (30 mg, 43%) as a pale-yellow oil into a ratio 1.2:1 respectively. **8:** $[\alpha]^{25}_D$ = -15.0 (*c* 0.25, CH_3OH); ^{1}H NMR (300 MHz, $CDCl_3$): δ 1.44 (s, 9 H), 3.32 (dd, 1 H, J = 5.9, 13.4 Hz), 3.45 (dd, 1 H, J = 3.2, 9.2 Hz), 3.49-3.58 (m, 4 H), 3.70 (dd, 1 H, J = 3.2, 9.2), 3.75 (s, 3 H), 4.00-4.16 (br s, 1 H), 4.72-4.78 (m, 2 H) , 4.88 (br s, 1 H), 5.63 (d, 1 H, J = 8.4 Hz); ^{13}C NMR (75 MHz,

$CDCl_3$): δ 28.3, 51.3, 52.6, 53.9, 70.4, 70.6, 77.9, 79.5, 80.6, 80.8, 155.7, 169.6; HRMS (ES+) Calcd for $C_{14}H_{24}N_4NaO_8$ $[M+Na]^+$ 399.1492. Found 399.1489; **9:** $[\alpha]^{25}_D = +74.0$ (*c* 0.1, CH_3OH); ^1H NMR (300 MHz, $CDCl_3$): δ 1.46 (s, 9 H), 3.25 (t, 1 H, *J* = 9.3 Hz), 3.33 (dd, 2 H, *J* = 6.2, 13.2 Hz), 3.42 (m, 2 H), 3.47 (br s, 1 H), 3.50 (m, 1 H), 3.60 (t, 1 H, *J* = 8.9 Hz), 3.76 (dd, 1 H, *J* = 2.3, 9.5 Hz), 3.80 (s, 3 H), 4.67 (dd, 1 H, *J* = 2.3, 8.0 Hz), 4.70 (br s, 1 H), 5.57 (d, 1 H, *J* = 8.0 Hz); ^{13}C NMR (75 MHz, $CDCl_3$): δ 28.2, 51.4, 53.0, 53.8, 69.9, 70.8, 77.2, 79.4, 80.0, 81.4, 157.4, 169.9; HRMS (ES+) Calcd for $C_{14}H_{24}N_4NaO_8$ $[M+Na]^+$ 399.1492. Found 399.1490.

(2*R*)-2-(*tert*-butoxycarbonylamino)-2-[6-deoxy-6-(9*H*-fluoren-9-ylmethoxycarbonylamino)-β-D-glucopyranosyl]-ethanoic acid (10) Ester **8** (60 mg, 0.16 mmol) was treated with lithium hydroxide (21 mg, 0.96 mmol) for 1 h at 0 °C in aqueous THF (4.0 mL, 1:1), and then acidified with formic acid (99%, 100 μL). The solution was extracted with ethyl acetate (6 x 10 mL) and the combined organic layers were dried (Na_2SO_4) and concentrated to afford crude acid (58 mg, quant.), which was dissolved in MeOH (4.0 mL) and hydrogenated for 20 min. using 20% wt $Pd(OH)_2/C$. The solution was filtered and the solvent was evaporated in *vacuo*. The solid residue was dissolved in aqueous acetone (3.0 mL, 1:1) and treated with 9-fluorenylmethyl pentafluorophenyl carbonate (91 mg, 0.24 mmol) and sodium bicarbonate (31 mg, 0.37 mmol) for 4 h at room temperature. Water (10.0 mL) was added and the aqueous layer was extracted with ethyl acetate (6 x 10 mL). Finally, the solvent was dried (Na_2SO_4) and

concentrated. The crude product was purified by flash column chromatography (methanol/ethyl acetate, 1:1) to afford compound **10** (45 mg, 63%) as a colorless thick liquid. ^{1}H NMR (300 MHz, CD_3OD): δ 1.43 (s, 9 H), 2.98-3.13 (m, 2 H), 3.18 (m, 1 H), 3.22-3.44 (m, 2 H), 3.62-3.80 (m, 2 H), 4.23 (t, 1 H, J = 6.8 Hz), 4.32-4.48 (m, 3 H), 7.28-7.87 (m, 8 H); ^{13}C NMR (75 MHz, $CDCl_3$): δ 28.9, 43.4, 48.5, 56.4, 67.8, 72.0, 73.1, 79.0, 80.4, 80.8, 83.0, 120.9-128.8 (aromatic carbons), 142.6-145.4 (aromatic carbons), 157.7, 159.1, 169.5; MS (ES-): *m/z* 557.09 $[M-H]^-$.

(2*S*)-2-(*tert*-butoxycarbonylamino)-2-[6-deoxy-6-(9*H*-fluoren-9-ylmethoxycarbonylamino)-β-D-glucopyranosyl]-ethanoic acid (11) Ester **9** (40 mg, 0.11 mmol) was treated with lithium hydroxide (15 mg, 0.66 mmol) for 1 h at 0 °C in aqueous THF (4.0 mL, 1:1), and then acidified with 99% formic acid (5 drops). The solution was extracted with ethyl acetate (6 x 10 mL) and the combined organic layers were dried (Na_2SO_4) and concentrated to afford crude acid (35 mg) which was dissolved in MeOH (4.0 mL) and hydrogenated for 20 min. using 20% wt $Pd(OH)_2/C$. The solution was filtered and the solvent was evaporated in *vacuo*. The solid residue was dissolved in aqueous acetone (3.0 mL, 2:1) and treated with 9-fluorenylmethyl pentafluorophenyl carbonate (75 mg, 0.18 mmol) and sodium bicarbonate (30 mg, 0.36 mmol) for 4 h at room temperature. Water (10.0 mL) was added and the aqueous layer was extracted with ethyl acetate (6 x 10 mL). Finally, the solvent was dried (Na_2SO_4) and concentrated. The crude product was purified by flash column chromatography

(methanol/ethyl acetate, 1:1) to afford compound **11** (39 mg, 65%) as a thick colorless liquid. $[\alpha]^{25}_{D}$ +5.0 (*c* 0.7, CH_3OH); ^1H NMR (300 MHz, CD_3OD): δ 1.45 (s, 9 H), 3.13 (ABq, 1 H, *J* = 9.3 Hz), 3.17 -3.29 (m, 2 H), 3.35 (m, 2 H), 3.38 -3.45 (m, 2 H), 3.55-3.70 (m, 1 H), 3.75 (d, 1 H, *J* = 9.4 Hz), 4.20 (t, 1 H, *J* = 6.9 Hz), 4.28 -4.44 (m, 3 H), 7.28-7.42 (m, 4 H), 7.65 (dd, 2 H, *J* = 1.6, 6.8 Hz), 7.78 (d, 2 H, *J* = 7.4 Hz); ^{13}C NMR (75 MHz, CD_3OD): δ 28.8, 42.7, 48.6, 56.2, 67.9, 71.2, 71.7, 78.7, 80.2, 80.8, 81.5, 120.9-128.8 (aromatic carbons) 142.6-145.4 (aromatic carbons), 158.9, 159.3, 169.2; MS (ES-): *m/z* 556.90 $[M-H]^-$; Anal. Calcd for $C_{28}H_{34}N_2O_{10}$: C, 60.21; H, 6.14; N, 5.02. Found: C, 60.32; H, 6.19; N, 4.98.

(2*R*)-Methyl 2-(*tert*-butoxycarbonylamino)-2-[6-deoxy-6-(*tert*-butoxycarbonylamino)-β-D-glucopyranosyl]-ethanoate (12) A solution of azide **8** (170 mg, 0.50 mmol) in methanol (20.0 mL) was treated with $Pd(OH)_2/C$ under an atmosphere of hydrogen for 1 hour at room temperature. The reaction mixture was filtered through Celite, and rinsed with methanol. The filtrate was evaporated under reduced pressure to give colorless foam (155 mg, 0.44 mmol), which was treated with di-*tert*-butyl dicarbonate (193 mg, 0.88 mmol) and triethylamine (0.3 mL, 2.2 mmol) in MeOH for 4 h at room temperature. Finally, the solvent was evaporated under reduced pressure to give colorless liquid. The crude product was then purified by flash column chromatography (methanol/ethyl acetate, 1:1) to afford compound **12** (183 mg, 90%) as a colorless liquid. $[\alpha]^{25}_{D}$ = +4.0 (*c* 0.75, CH_3OH); ^1H NMR (300 MHz, CD_3OD): δ 1.50 (br s, 18 H), 3.02

(br t, 1 H, J = 7.2 Hz), 3.08 (br t, 1 H, J = 9.3 Hz), 3.24 (m, 1 H), 3.36 (m, 1 H), 3.50 (dd, 1 H, J = 1.6, 10.0 Hz), 3.56 (br d, 1 H, J = 9.0 Hz), 3.64 (m, 1 H), 3.78 (s, 3 H), 4.69 (br s, 1 H); ^{13}C NMR (75 MHz, CD_3OD): δ 28.8, 28.9, 43.0, 52.8, 55.5, 71.7, 72.9, 79.3, 80.3, 80.9, 81.0, 82.1, 158.1, 158.7, 172.0; MS (ES+): *m/z* 473.24 $[M+Na]^+$; Anal. Calcd for $C_{19}H_{34}N_2O_{10}$: C, 50.66; H, 7.61; N, 6.22. Found: C, 50.54; H, 7.59; N, 6.28.

(2*R*)-2-(*tert*-butoxycarbonylamino)-2-[6-deoxy-6-(*tert*-butoxycarbonylamino)-β-D-glucopyranosyl]-ethanoic acid (13) The ester **12** (80 mg, 0.18 mmol) was dissolved in aq. THF (4.0 mL, 1:1) and treated with LiOH (26 mg, 1.07 mmol) at 0 °C. The reaction mixture was stirred at that temperature for 1 h. After which, the mixture was acidified to pH 3 with 99% formic acid, and extracted with ethyl acetate (5 x 10 mL). The combined organic layers were dried (over anh. Na_2SO_4) and concentrated under reduced pressure to give colorless foam which was dissolved in ethyl acetate (3.0 mL). Crystallization commenced within an hour. After completion of crystallization, the precipitates were collected by filtration and rinsed with ethyl acetate (2 x 2 mL) to afford **13** (70 mg, 90%) as white crystal. Mp 205–207 °C; $[\alpha]^{25}_D$ = -7.0 (*c* 0.85, CH_3OH); ^{1}H NMR (300 MHz, CD_3OD): δ 1.45 (s, 9 H), 1.46 (s, 9 H), 2.98 (m, 1 H), 3.04 (t, 1 H, J = 9.2 Hz), 3.15-3.22 (m, 1 H), 3.33 (m, 1 H), 3.44 (dd, 1 H, J = 1.6, 10.0 Hz), 3.63 (br ABq, 2 H, J = 9.6 Hz), 4.61 (br s, 1 H); ^{13}C NMR (75 MHz, CD_3OD): δ 28.7, 28.8, 43.0, 55.2, 71.8, 72.9, 79.3, 80.3, 80.8, 80.9, 82.3, 158.1, 158.7, 173.2; MS (ES+): *m/z* 459.23 $[M+Na]^+$; Anal. Calcd for $C_{18}H_{32}N_2O_{10}$: C, 49.53; H, 7.39; N, 6.42. Found: C, 49.49; H, 7.27; N, 6.58.

***N*-[(2*R*)-2-(*tert*-butoxycarbonylamino)-2-[6-deoxy-6-(*tert*-butoxycarbonylamino)-β-D-glucopyranosyl]-acetyl]-Trp(Boc)-NHBn (14)** To the mixture of Fmoc-Trp(Boc)-OH (205 mg, 0.39 mmol) and TBTU (451 mg, 1.4 mmol) in DMF (5.0 mL) were added benzylamine (165 mL, 1.51 mmol) and *N,N*-diisopropylethylamine (334 μL, 1.87 mmol) and stirred for 2 h at room temperature. The solvent was removed in *vacuo* and the residue was purified by flash column chromatography (hexanes/ethyl acetate, 2:1) to yield the Fmoc-Trp(Boc)-NHBn (211 mg, 88%). The solution of Fmoc-Trp(Boc)-NHBn (151 mg, 0.25 mmol) and piperidine (0.5 mL) in DMF (2.0 mL) was stirred for 1 h at room temperature. The solvent was removed in *vacuo* and the crude product was purified by flash column chromatography (methanol/ethyl acetate, 1:20) to afford the H-Trp(Boc)-NHBn (129 mg, 96%). To the solution of **13** (23 mg, 0.05 mmol) in DMF (2.0 mL) were added H-Trp(Boc)-NHBn (26 mg, 0.09 mmol), TBTU (58 mg, 0.18 mmol), and *N,N*-diisopropylethylamine (43 mL, 0.24 mmol). The mixture was stirred for 4 h at room temperature before removing the solvent under reduced pressure. The crude product was purified by flash column chromatography using ethyl acetate as eluent to afford **14** (29 mg, 77%) as a thick colorless liquid. $[\alpha]^{25}_{D} = -5.0$ (*c* 1.0, $CHCl_3$); ^{1}H NMR (300 MHz, CD_3OD): δ 1.38 (s, 9 H), 1.42 (s, 9 H), 1.69 (s, 9 H), 2.88-3.09 (m, 2 H), 3.18 (dd, 2 H, *J* = 7.6, 14.2 Hz), 3.25-3.33 (m, 2 H), 3.33-3.35 (m, 4 H), 3.36-3.48 (m, 3 H), 4.29-4.40 (m, 2 H), 4.44 (br s, 1 H), 4.84 (m, 1 H), 7.08 (br d, 2 H, *J* = 7.0 Hz), 7.20-7.37 (m, 5 H), 7.52 (s, 1 H), 7.66 (br d, 1 H, *J* = 7.6 Hz), 8.13 (br d, 1 H, *J* = 8.1 Hz); ^{13}C NMR (75 MHz, CD_3OD): δ 28.5, 28.6, 28.8, 43.0, 44.1, 54.8, 72.0, 72.5, 79.0, 80.3,

81.0, 81.1, 84.9, 116.2, 117.2, 120.2, 123.7, 125.6, 128.2, 128.3, 129.5, 131.9, 136.9, 139.3, 151.0, 158.9, 160.6, 172.2, 173.3; MS (ES+): *m/z* 834.17 $[M+Na]^+$; Anal. Calcd for $C_{41}H_{57}N_5O_{12}$: C, 60.65; H, 7.08; N, 8.63. Found: C, 60.59; H, 7.07; N, 8.77.

***N*-[(2*R*)-2-(*tert*-butoxycarbonylamino)-2-[6-deoxy-6-(*tert*-butoxycarbonylamino)-*β*-D-glucopyranosyl]-acetyl]-Trp(Boc)-OBn (15)** To a solution of Fmoc-Trp(Boc) -OH (100 mg, 0.19 mmol) in DMF (5.0 mL) was added Cs_2CO_3 (249 mg, 0.77 mmol) followed by addition of benzyl bromide (90 μL, 0.76 mmol) and then stirred for 4 h at room temperature. The solvent was removed in *vacuo* and the residue was purified by flash column chromatography (hexane/ethyl acetate, 2:1) to yield the Fmoc-Trp(Boc)-OBn (107 mg, 92%). The solution of Fmoc-Trp(Boc)-OBn (107 mg, 0.17 mmol) and piperidine (0.5 mL) in DMF (2.0 mL) was stirred for 1 h at room temperature. The solvent was removed in *vacuo* and the crude product was purified by flash column chromatography (methanol/ethyl acetate, 1:20) to afford the H-Trp(Boc)-OBn (65 mg, 95%). Compound **13** (30 mg, 0.07 mmol) was dissolved in DMF (2.0 mL) and H-Trp(Boc)-OBn (36 mg, 0.09 mmol), TBTU (81 mg, 0.25 mmol), and *N*,*N*-diisopropylethylamine (60 μL, 0.34 mmol) were added and then stirred for 4 h at room temperature. The solvent was removed under reduced pressure and the crude product was purified by flash column chromatography using ethyl acetate as eluent to afford **15** (46 mg, 83%) as a thick liquid. $[\alpha]^{25}_D$ = -32.0 (*c* 1.45, CH_3OH); ^1H NMR (300 MHz, CD_3OD): δ 1.38 (br s, 18 H), 1.63 (s, 9 H), 3.00-3.15 (m, 2 H), 3.18 (d, 2 H, *J* =

7.0 Hz), 3.24 (br s, 1 H), 3.33-3.40 (m, 5 H), 4.89 (m, 1 H), 5.03 (s, 2 H), 7.06-7.12 (m, 2 H), 7.15-7.31 (m, 5 H), 7.40 (br s, 1 H), 7.50 (m, 1 H), 8.05 (d, 1 H, J = 8.2 Hz); ^{13}C NMR (75 MHz, CD_3OD): δ 26.9, 27.3, 27.4, 27.6, 40.8, 54.6, 54.9, 66.7, 69.8, 70.1, 76.8, 77.3, 78.8, 79.0, 79.7, 83.4, 114.7, 114.8, 118.2, 122.2, 123.4, 124.0, 127.4, 127.8, 127.9, 134.5, 134.9, 149.3, 155.4, 157.1, 170.0, 171.3; MS (ES+): *m/z* 835.33 $[M+Na]^+$; Anal. Calcd for $C_{41}H_{56}N_4O_{13}$: C, 60.58; H, 6.94; N, 6.89. Found: C, 60.57; H, 6.88; N, 6.93.

***N*-[(2*R*)-2-(amino)-2-[6-deoxy-6-amino)-β-D-glucopyranosyl]-acetyl]-Trp-NHBn· $(CF_3CO_2H)_3$ (16)** A solution of TFA/CH_2Cl_2 (1:1, 4.0 mL) was added to the compound **14** (80 mg, 0.10 mmol) at room temperature. After 3 h, the solution was diluted with toluene (2 x 5 mL), concentrated in *vacuo*, provided **16** (73 mg, quant.) as a salt. $[\alpha]^{25}_D$ = -8.0 (*c* 0.45, CH_3OH); ^{1}H NMR (300 MHz, D_2O): δ 2.52-2.74 (m, 2 H), 2.88-3.04 (m, 2 H), 3.28-3.40 (m, 2 H), 3.42-3.56 (m, 2 H), 3.70-3.77 (m, 1 H), 4.32-4.41 (m, 1 H), 4.45-4.54 (m, 2 H), 5.00-5.11 (m, 1 H), 7.16-7.49 (m, 8 H), 7.60-7.68 (m, 1 H), 7.78 (dd, 1 H, J = 7.8, 17.8 Hz); ^{13}C NMR (75 MHz, D_2O): δ 27.9, 40.9, 43.4, 53.4, 54.8, 69.4, 70.8, 76.0, 76.6, 77.4, 109.0, 112.6, 118.9, 119.7, 122.3, 125.1, 126.8, 127.4, 127.8, 129.1, 136.8, 137.8, 166.1, 173.3; MS (ES+): *m/z* 511.99 $[M+H]^+$.

***N*-[(2*R*)-2-(amino)-2-[6-deoxy-6-amino)-β-D-glucopyranosyl]-acetyl]-Trp-OBn· $(CF_3CO_2H)_3$ (17)** Compound **15** (100 mg, 0.12 mmol) was treated with a solution of TFA/CH_2Cl_2 (1:1, 4.0 mL) at room temperature for 3 h. The volatiles were removed with

toluene (2 x 5 mL) in *vacuo* and then the residue was rinsed with dry ether to afford **17** (91 mg, quant.) as a TFA-salt. $[\alpha]^{25}_{D}$ = -16.0 (*c* 0.3, CH_3OH); ^1H NMR (300 MHz, D_2O): δ 2.32-2.42 (m, 2 H), 2.70-2.78 (t, 1 H, *J* =9.6 Hz), 3.18 (br d, 1 H, *J* = 14.0 Hz), 3.22-3.42 (m, 3 H), 3.48-3.60 (m, 2 H), 4.30 (br s, 1 H), 5.14 (dd, 1 H, *J* = 5.7, 10.3 Hz), 5.24 (br s, 2 H), 7.17 (t, 1 H, *J* = 7.6 Hz), 7.22 (br s, 1 H), 7.28 (t, 1 H, *J* = 7.6 Hz), 7.36 (dd, 2 H, *J* = 3.8, 7.6 Hz), 7.42-7.49 (m, 3 H), 7.53 (d, 1 H *J* = 8.2 Hz), 7.70 (d, 1 H, *J* = 8.2 Hz); ^{13}C NMR (75 MHz, D_2O): δ 27.2, 40.9, 53.3, 53.6, 68.4, 69.3, 70.7, 76.0, 76.5, 77.5, 109.1, 112.6, 118.9, 119.7, 122.4, 125.0, 126.7, 128.7, 129.1, 129.2, 135.4, 136.8, 166.2, 173.3; MS (ES, $[M+Na]^+$); MS (ES+): *m/z* 513.23 $[M+H]^+$.

Determination of the MIC values for peptides 16-19. Bacterial isolates were obtained from the American Type Culture Collection (ATCC). Isolates were kept frozen in skim milk at -80°C until minimum inhibitory concentration (MIC) testing was carried out. Following two subcultures from frozen stock, the *in vitro* activities of peptides were determined by macrobroth dilution in accordance with the Clinical and Laboratory Standards Institute (CLSI) 2006 guidelines.[22] Stock solutions of peptides were prepared and dilutions made as described by CLSI. Test tubes contained doubling antimicrobial dilutions of cation adjusted Mueller-Hinton broth and inoculated to achieve a final concentration of approximately 5 x 10^5 CFU/ml then incubated in ambient air for 24 hours prior to reading. Colony counts were performed periodically to confirm inocula. Quality control was performed using ATCC QC organisms.

6.5. References:

1. Neu, H. C. *Science* **1992**, *257*, 1064.
2. Walsh, C. *Nature* **2000**, *406*, 144.
3. Diamond, G. *Biologist* **2001**, *48*, 209.
4. Hancock, R. E. W. *Drugs* **1999**, *57*, 469.
5. Zasloff, M. *Nature* **2002**, *415*, 389.
6. Hancock, R. E. W.; Scott, M. G. *Proc. Natl. Acad. Sci.* USA. **2000**, *97*, 8856.
7. Hancock, R. E. W; Lehrer, R. *Trends Biotech.* **1998**, *16*, 82.
8. Latham, P. W. *Nat. Biotechnol.* **1999**, *17*, 755.
9. Strom, M. B.; Haug B. E.; Skar M. L.; Stensen W.; Stiberg T.; Svendsen J. S. *J. Med. Chem.* **2003**, *46*, 1567.
10. Haugt, E. B.; Stensen, W.; Stiberg, T.; Svendsen, J. S. *J. Med. Chem.* **2004**, *47*, 4159.
11. Makovitzki, A.; Avrahami, D.; Shai, Y. *Proc. Natl. Acad. Sci.* USA. **2006**, *103*, 15997.
12. Taylor, S. W.; Craig, A. G.; Fischer, W. H.; Park, M.; Lehrer, R. I. *J. Biol. Chem.* **2000**, *275*, 38417.
13. Reddy, M. V. R.; Harper, M. K.; Faulkner, D. J. *Tetrahedron* **1998**, *54*, 10649.
14. Baldwin, J. E.; Claridge, T. D. W.; Goh, K. C.; Keeping, J. W.; Schofield, C. J. *Tetrahedron Lett.* **1993**, *34*, 5645.
15. Postels, H. T.; Koenig, W. A. *Tetrahedron Lett.* **1994**, *35*, 535.
16. Wong, C-H.; Hendrix, M.; Manning, D. M.; Rosenbohm, C.; Greenberg, W. A. *J. Am. Chem. Soc.* **1998**, *120*, 8319.
17. Zhang, K.; Wang, J.; Sun, Z.; Huang, H-D; Schweizer, F. *Synlett* **2007**, 239.
18. It is noteworthy that AMPs that contain unnaturally configured lysine retain biological activity[10] while enhancing proteolytic stability see: Oh, J. E.; Lee, K. H. *Bioorg. Med. Chem.* **1999**, *7*, 2985.
19. Gueyrard, D.; Haddoub, R.; Salem, A.; Bacar, N. S.; Goekjian, P. G. *Synlett*, **2005**, 520.
20. Zhang, K.; Schweizer, F. *Synlett*, **2005**, 3111.
21. Schweizer, F.; Inazu, T. *Org. Lett.* **2001**, *3*, 4115.
22. Clinical and Laboratory Standards Institute. **2006**. M100-S16. CLSI/NCCLS M100-S15.

Chapter 7

Design and Synthesis of Glucose-templated Proline-Lysine Chimera: Polyfunctional Amino Acid Chimera with High Prolyl *cis* Amide Rotamer Population

Abstract: *We describe the synthesis of two glucose-templated proline-lysine chimeras (GlcTProLysCs) that differ in the stereochemistry of the hydroxymethylene substituent at the C-5' (C-δ) position of the pyrrolidine ring. The key synthetic step involve regioselective installation of the azide group at C-6 on the glucose scaffold. Incorporation of these chimeras into the model peptides Ac-GlcTProLysC-NHMe and Ac-GlcTProLysC-OMe demonstrates that the stereochemistry of the hydroxymethyl substituent at the C-5' position has a profound effect on the equilibrium constant of prolyl amide cis/trans isomerization. The equilibrium constant $K_{c/t}$ for the peptide mimic Ac-GlcTProLysC-NHMe with C-5'(R) stereochemistry was determined to be 3.03 ± 0.04 while the $K_{t/c}$ for the C-5'(S) diastereomer was 0.56 ± 0.04 in D_2O. Temperature coefficient experiments indicate the origin of these effects are derived from two critical hydrogen bonds involving the C- δ hydroxymethyl substituent; one to the N-terminal amide carbonyl group, and a second to the primary amino group in the glucose moiety.*

7.1. Introduction

Conformationally constrained amino acids have found wide applications as building blocks to study and probe the bioactive conformation of peptides when binding to receptors.[1-3] Among all naturally occurring amino acids, proline is the only amino acid with a side chain fused onto the peptide backbone. Its cyclic structure restricts the rotation about its ϕ dihedral angle, thereby reducing the energy difference between the

prolyl amide *cis* and *trans* isomers. Thus, while most peptide amide bonds exist almost exclusively in the *trans* form, proline has a much greater propensity to form *cis* amide bonds. A variety of factors influence *cis/trans* isomerization of proline; these include electron withdrawing groups attached to the pyrrolidine ring,[4] $n \rightarrow \pi^*$ interaction,[5] Ar-Pro interactions[6] and steric effects[7] and pucker conformation.[5] In particular, incorporation of bulky substituents into the δ-position of proline has been shown to enhance the prolyl amide *cis* population significantly. *Cis/trans* isomerization of proline plays an important role in the formation of secondary structures in peptides and proteins because proline induces a reversal in backbone conformation resulting in the formation of reverse turns and disruption of helices and sheets in proteins. Besides the occurrence of proline in β-turns, proline-rich sequences also exist as extended helices[8] (polyproline-I and polyproline-II) and antimicrobial peptides.[9] Furthermore, proline undergoes post-translational modifications to form 4-(*R*)-hydroxyprolines, which are known to contribute to the enhanced stability of the polyproline-II conformation in both collagenous proteins and peptides,[4] and plant cell wall glycoproteins.[10]

Proline analogues displaying the characteristics of other amino acids are referred to as proline-amino acid chimera, and have been used to study the spatial requirements for receptor affinity and biological activity of both natural amino acids[11,12] and peptides.[13-15] For example, β-substituted-prolines such as 3-carboxyproline,[11a] 3-phenylproline[16] and 3-di-methylproline[17] combine amino acid side-chain functionality with proline conformational rigidity. In these cases, replacement of the natural amino acids in peptides

by proline-amino acid chimeras provided better understanding of the bioactive conformations of peptides binding to receptors.[13-15] While these analogues have proved useful for inducing specific constraints into amino acids and peptides, their structures do not permit additional derivatization; a trait that is often required in drug discovery and lead optimization. Polyfunctional proline-amino acid chimera may overcome these drawbacks.

Our concept for developing such polyfunctional proline-amino acid chimera was derived from glycosyl amino acids (GAAs) which are defined by an α-amino acid group [$CH(NH_2)CO_2H$] either directly attached or carbon-linked to the anomeric carbon of a carbohydrate scaffold.[18] The relative rigidity of the pyran ring combined with the polyfunctional nature of the carbohydrate scaffold has inspired the design of unusual and conformationally constrained amino acids and novel peptidomimetics.[18] While there are many examples of *C*-glycosylglycine, -alanine, -serine, and -asparagine,[18a] few proline-based GAAs exist.[19]

We report here on the design, synthesis of spirocyclic glucose-templated proline-lysine chimeras (GlcTProLysCs) and describe their properties in peptide mimics. Bicyclic GlcTProLysCs combine the molecular features of glucose (pyran-based polyol) with the unique characteristics of proline or 3-hydroxyproline and L-lysine (Figure 7.1). The characteristics of the lysine side chain including relative length and presence of amino function are presented on the pyrrolidine ring and are further constrained by incorporation into the 6-amino-6-deoxy-D-glucose scaffold. In order to control the prolyl

amide *cis/trans* isomerization we were interested in developing GlcTProLysC analogs that contain substituents at the δ-position of proline. Previous studies have shown that bulky substituents at the δ-position (including δ-*tert*-butyl proline[7] and δ,δ-dimethyl proline[3]) enhance the prolyl amide *cis* isomer population. In addition, chemical manipulations and derivatization of the polyol scaffold provides an opportunity to adjust the chemical, physical and pharmacodynamic properties of proline-containing peptides.[20] This may provide a novel tool to functionalize extended helical structures including PP1 and PP2.[21] Moreover, incorporation of polyhydroxylated amino acids have been shown to induce novel secondary structures in small peptides. For instance, incorporation of unprotected sugar amino acids into small peptides such as gramicidin S[22] and opioid peptides[23] have prohibited the formation of the targeted secondary structural motif. Instead, unusual turn structures were stabilized by intramolecular hydrogen bonds between sugar hydroxyl groups and the peptidic amide backbone.[24] Similar effects may also be observed with GlcTProLysC.

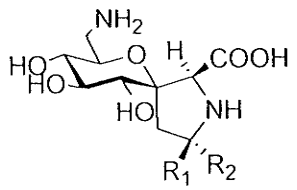

Figure 7.1 Glucose-templated proline-lysine chimera (GlcTProLysC)

7.2. Results and discussion

The synthesis (Scheme 7.1). started with the known compounds **1** and **2** which were previously prepared by our group (see chapter 3).[19b] Initially, compounds **1** and **2** were exposed to catalytic hydrogenolysis condition using Pearlman's catalyst. The resulting *N*-debenzylated imine was protected using di-*tert*-butyl dicarbonate and triethylamine in methanol to afford the carbamates **3** and **4** in 90% and 62% yield respectively without acyl migration. The azido group in compounds **3** and **4** was installed by a standard two-step procedure: first, selective activation of the primary hydroxyl group as sulfonate ester, followed by nucleophilic substitution with sodium azide in DMF at 80 °C, produced azides **5** and **6** in excellent yields.

Scheme 7.1 Installation of the azide function at the *C*-6 position.

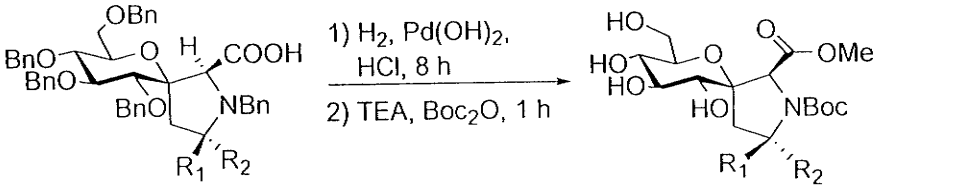

1: $R_1 = CH_2OAc$, $R_2 = H$
2: $R_1 = H$, $R_2 = CH_2OAc$

3: $R_1 = CH_2OAc$, $R_2 = H$ (90%)
4: $R_1 = H$, $R_2 = CH_2OAc$ (62%)

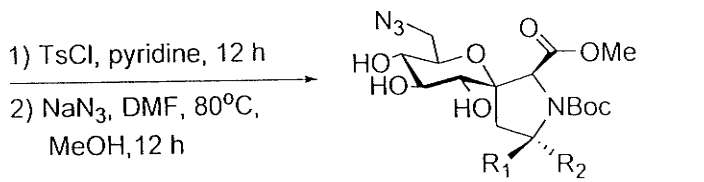

5: $R_1 = CH_2OAc$, $R_2 = H$ (92%)
6: $R_1 = H$, $R_2 = CH_2OAc$ (94%)

Azides **5** and **6** served as starting materials for incorporation into the peptide mimics **9-12,** which were used to study the thermodynamic properties of *cis/trans* isomerization of the glucose-templated proline-lysine chimera. In addition, we selected peptide esters **9** and **10** bearing a *C*-terminal methyl ester as well as methyl amides **11** and **12** as peptide mimics to study how the nature of the *C*-terminal group affects *N*-terminal prolyl amide isomerization.

Peptide esters **9** and **10** were prepared from azides **5** and **6** using the synthetic route outlined in Scheme 7.2. Deprotection of the *N*-Boc group in **5** and **6** with trifluoroacetic

Scheme 7.2 Synthesis of peptide mimics **9-12**.

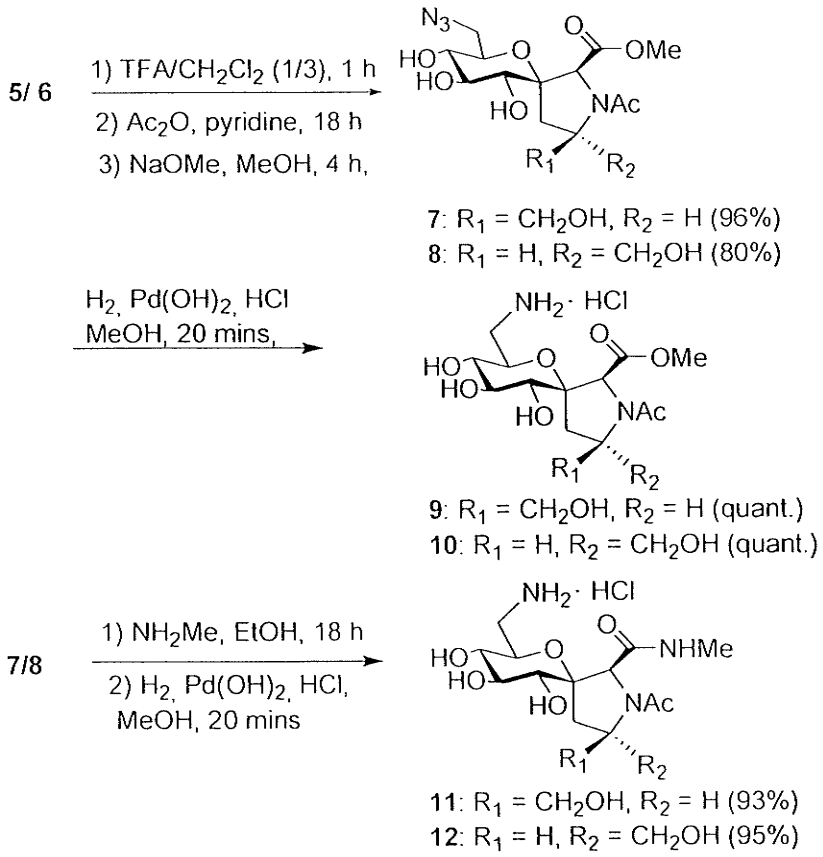

acid followed by acetylation using pyridine and acetic anhydride and *O*-deacetylation using sodium methoxide in methanol produced azides **7** and **8** in 96% and 80% yield, respectively. Attempts to perform selective *N*-acylation failed and produced complex reaction mixtures. Catalytic hydrogenation of azide **7** and **8** using Pearlman's catalyst produced peptide esters **9** and **10** in quantitative yield. The *N'*-methylamides **11** and **12** were prepared from azides **7** and **8** through a two-step procedure: first, methyl esters **7** or **8** were treated with a concentrated methylamine solution in ethanol to afford *N'*-methylamide intermediates. Subsequently, the azido function was reduced by catalytic hydrogenation to produce peptide mimics **11** and **12** in 93% and 95% yield, respectively.

The assignments of *N*-terminal geometry for model peptides **9-12** were made on the basis of nOe experiments in D_2O (Figure 7.2). For example, selective inversion of the *N*-terminal methyl group in the prolyl amide *cis* isomer **10a** showed an interproton effect to H-2' (5.63% nOe). By comparison, no interproton effect was observed between H-2' and methyl group of *N*-terminus in *trans* isomer **10b**. Moreover, selective inversion of the methyl group of *N*-terminus in **10b** showed interproton effects to H-5' (4.54% nOe) and H-6' (3.80% nOe). Similar experiments were performed to assign the *cis/trans* isomers in compounds **9**, **11** and **12**.

In addition, we observed that the ^{13}C NMR chemical shifts of the C^{α} atom of the *trans* rotamer in compounds **9-12** were high field shifted (0.75-1.02 ppm) relative to the *cis* isomer in water. This is consistent with previous observations made by Lubell and co-workers[7] on other proline-containing peptide mimics and may serve as a diagnostic

tool to assign the *trans* isomer in cases where nOe-experiments do not allow assignment

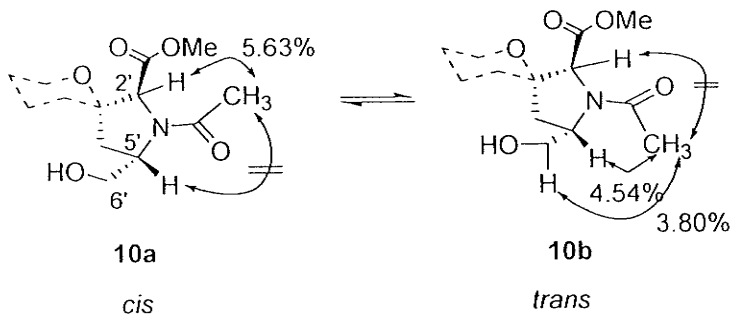

Figure 7.2 Assignment of *cis* and *trans* isomers in compound **10** in D_2O using 1D nOe experiments. The same experiments were used to assign the *cis/trans* isomers in compounds **9**, **11** and **12**.

due to spectral overlap.

The equilibrium constants $K_{c/t}$ for compounds **9-12** are shown in Table 7.1. Our results indicate that compounds **9** and **11** display a higher *cis* isomer population relative to their *C*-5′ diastereoisomers **10** and **12**, respectively. It appears that the stereochemistry at *C*-δ

Table 7.1 *Cis* population (%) and equilibrium constant $K_{c/t}$ of compounds **9-12** in D_2O

Compds	**9**	**10**	**11**	**12**
cis(±3%)	55	19	75	36
$K_{c/t}$(±0.04)	1.22	0.23	3.03	0.56

has a profound effect on the equilibrium of isomerization. Also, the *cis* prolyl amide population in esters **9** and **10**, was generally lower than *N*′-methylamides **11** and **12**. Taylor and co-workers have proposed that the *trans* conformation of esters is stabilized

relative to amides as a result of increased electron donation from the oxygen lone pair of the *N*-terminal amide carbonyl group to the antibonding orbital of the prolyl *C*-terminal carbonyl group (Figure 7.3).[25]

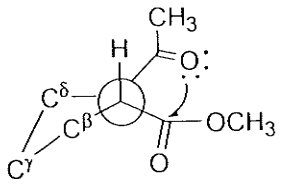

Figure 7.3 n→π* interaction (looking down C^{α}-N bond)

Effect of pH Since compound **9-12** have an ionizable amino group, we were interested to study the influence of the ionization state on $K_{t/c}$. Previous studies have indicated that ionizable groups in proximity to the imide backbone can influence thermodynamics of prolyl amide *cis/trans* isomerization.[26] We selected three buffer ranges: pH = 2.6, 7.4 and 12.4, to examine the pH effect on the isomerization of **11** and **12** (Table 7.2). Our study shows that the prolyl *N*-terminal amide *cis/trans* ratio is not affected by pH and the

Table 7.2 pH Effect on $K_{c/t}$ for Compounds **11** and **12** in D_2O

Compds	pD		
	2.6	7.4	12.4
11 (±0.04)	3.03	3.03	2.70
12 (±0.04)	0.61	0.56	0.61

observed changes are within the experimental error. Molecular modeling suggests that the large distance of the ionizable amino function from the imide function is responsible for the absence of a pH effect.

Conformational analysis of compounds 11 and 12. The relatively large coupling constants for $J_{2,3}$, $J_{3,4}$ and $J_{4,5}$ ($\geq$ 9.2 Hz) indicate a $^4C_1$ conformation of the pyranose ring in **11** and **12**. The conformation of the piperidine ring is expected to be C^{β}-exo based on previous studies using 3(*S*)-hydroxyproline-containing peptide mimics.[27] This conformation places the endocyclic oxygen substituent in an axial position.[27b] In this conformation the pyrrolidine ring will be stabilized by gauche interaction and a stabilizing $\sigma(C^{\gamma}\text{-H})\rightarrow\sigma^*(C^{\beta}\text{-O})$ interaction. This conformation is further supported by characteristic long range "W" coupling constants ($J \sim 1.0$ Hz) between H-2′$_{eq}$ and H-4′$_{eq}$ in both compounds of **11** and **12** (Figure 7.4).

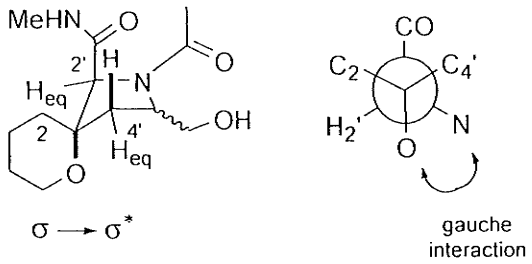

Figure 7.4 Pyrrolidine conformation in compounds **11** and **12**.

In order to explain the different *cis*/*trans* ratio in compounds **11** and **12** we considered intramolecular hydrogen bonding, which can be studied by calculating the temperature

coefficients ($\Delta\delta/\Delta T$) of key exchangeable protons.[28] Previous studies have shown that ($\Delta\delta/\Delta T$) > -3.0 ppb/deg are a diagnostic tool for the detection of intramolecular H-bonding.[28] The 1D spectra of compounds **11** and **12** were analyzed between 25 to 45 °C in 5-deg steps in DMSO-d_6 to determine the temperature coefficients (Table 7.3). Our results indicate that the protons associated with NH_2-6, OH-6′ and NHMe exhibit the

Table 7.3 Temperature coefficients ($\Delta\delta/\Delta T$, ppb/K) for compounds **11** and **12** in DMSO-d_6

		HO-2	HO-3	HO-4	NH_2-6	HO-6′	NHMe
	cis	-9.07	[a]	[a]	-2.44[b]	-3.80	-2.44[b]
11	*trans*	-8.93	[a]	[a]	-2.44[b]	-4.28	-3.02
	cis	-8.09	-6.90	-4.10	-0.92	-3.29	-2.68
12	*trans*	-7.76	-6.80	-4.20	-0.92	-2.76	-3.26

[a] not determined; [b] overlapped with NHMe.

highest temperature coefficient values suggesting that these protons are involved in intramolecular H-bonding in compounds **11** and **12**. The low ($\Delta\delta/\Delta T$) values observed for OH-2 and OH-3 reflect high solvent exposure of these hydroxyl groups while the relative high value for OH-4 in **12** may indicate some H-bond interaction with one of the nitrogen lone pairs on NH_2-6. The relative high and nearly identical ($\Delta\delta/\Delta T$) values observed for the methyl amide proton in structures **11a**, **11b**, **12a** and **12b** supports the notion that this proton is engaged in hydrogen bonding to *N*-terminal carbonyl group in *cis/trans* isomers of both compounds **11** and **12**. Moreover, the higher ($\Delta\delta/\Delta T$) value for the NH_2-6 in

compound **12** when compared to diastereomer **11** suggests that the amino group in **12** is involved in stabilization of the *trans* isomer **12b** and the destabilization of the *cis* isomer **12a** relative to **11a** and **11b**. A similar trend is observed for the OH-6′ position. Isomers **12a** and **12b** exhibit higher ($\Delta\delta/\Delta T$) values when compared to isomers **11a** and **11b** suggesting that OH-6′ is involved in stabilization of the *trans* isomer **12b** relative to **11b**. Taken together these results support the notion that compound **12** is stabilized by an intramolecular hydrogen bond (6′-OH---NH_2-6) that is absent in **11**. The hydrogen bond (OH-6′---NH_2-6) competes with the H-bond (6′-OH --- O=C(N)CH_3) of the *cis* isomer **12a** resulting in a lower *cis* population of **12a** relative to **11a** (Figure 7.5).

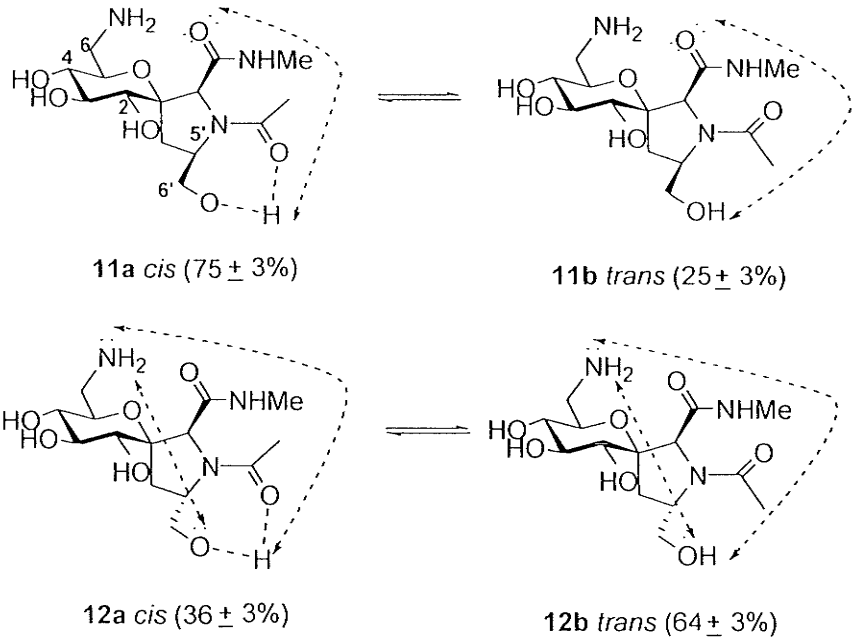

Figure 7.5 Suggested intramolecular H-bonds based on temperature coefficient experiments for compounds **11** and **12**

7.3. Conclusions

We have developed a synthetic route to two spirocyclic GlcTProLysCs that differ in the stereochemistry of the hydroxymethyl substituent at the *C*-5′ position of the pyrrolidine ring. In order to study the thermodynamic properties of prolyl amide *cis/trans* isomerization the two GlcTProLysC analogs were incorporated in peptide mimics Ac-GlcTProLysC-OMe and Ac-GlcTProLysC-NHMe. Our study indicates that the stereochemistry at the *C*-5′ position in both peptide mimics has a profound effect on the equilibrium constant. For example, incorporation of GlcTProLysC with "*R*" configuration at *C*-5′ dramatically increased the *cis* population (75%) of Ac-GlcTProLysC-NHMe in water, whereas a smaller augment *cis* population (34%) was observed in GlcTProLysC with "*S*" configuration at *C*-5′. Temperature coefficient experiments indicate that the hydroxymethyl group at *C*-5′ (*S*) is involved in H-bonding with the 6-NH_2 and vice versa. In contrast, the same hydrogen bond is absent in the diastereomer with *C*-5′ (*R*) stereochemistry. Taken together our results suggest that the *cis* isomer ratio in peptide mimic Ac-GlcTProLysC-NHMe having a *C*-5′ (*S*) hydroxymethyl substituent is decreased by competing H-bonding effects between 6′-OH---O=C(N)CH_3 and 6′-OH---6-NH_2.

Our work shows for the first time that polar groups capable of H-bonding in polyhydroxylated spirocyclic proline analogs can play important roles to control the thermodynamics of prolyl amide *cis/trans* isomerization. In particular, polar groups such as a hydroxymethyl group introduced at the δ-positon of proline are expected to increase the prolyl *N*-terminal amide *cis* isomer in peptides via H-bonding to the *N*-terminal amide

carbonyl group. Previous studies have shown that amino acid residues possessing side chains with hydrogen-bond acceptor and donor moieties are able to stabilize turn conformations when adjacent to proline.[29,30] As a result we expect that incorporation of GlcTProLysC in bioactive peptides may induce similar effects. We are currently studying the lysine- and proline- mimetic effects of GlcTProLysC in β-turn-forming peptides.

7.4. Experimental

(1*S*)-1′-*N*-*tert*-butoxycarbonyl-5′(*R*)-methylenehydroxy acetate–spiro[1,5–anhydro -D-glucitol-1,3′-*L*-proline methyl ester] (3) To a mixture of **1** (100 mg, 0.13 mmol) and $Pd(OH)_2$ (40mg, 20 % wt on charcoal) in methanol (10 mL) was added the solution of hydrochloride (250 μL of 1M HCl solution, 0.25 mmol) and stirred under H_2 (15 psi) for 8 hours at room temperature. The catalyst was removed by filtration and the solvent was removed under the vacuum. The unprotected product was treated with triethylamine (53 μL, 0.38 mmol) and di-*tert*-butyl dicarbonate (56 mg, 0.25 mmol) in methanol (2 mL) for 1 hour at room temperature. The solvent was removed under vacuum. The crude product was purified by flash column chromatography (CH_2Cl_2 / MeOH: 7/ 1) to get **3** (51 mg, 90%). $[\alpha]_D$ = 68.4 (*c* 1.3, MeOH); ^{1}H NMR (300 MHz, CD_3OD, two isomers): δ = 1.45 (s, 9H), 2.09 (s, 3H), 2.13-2.44 (m, 2H), 3.27-3.46 (m, 3H, partially overlapping with methanol peaks), 3.57-3.86 (m, 6H), 4.06 (m, 1H), 4.23 (s, 1H), 4.31-4.45 (m, 1H), 4.53-4.67 (m, 1H); ^{13}C NMR (75 MHz, CD_3OD, two isomers): δ = 20.9 (2 carbons), 28.56/28.63 (6 carbons), 29.2/29.7, 52.9 (2 carbons), 56.2/56.3, 62.8 (2 carbons),

66.0/66.4, 71.2 (2 carbons), 71.4/71.8, 71.5 (2 carbons), 75.9/76.0, 77.3 (2 carbons), 81.8/82.3, 86.2/86.7, 155.6/156.2, 172.0/171.8, 172.7/172.8; HRMS (ES) calcd for $C_{19}H_{31}NNaO_{11}$ $[M + Na]^+$ 472.1795, found 472.1783.

(1*S*)-1′-*N*-*tert*-butoxycarbonyl-5′(*S*)-methylenehydroxy acetate-spiro[1,5–anhydro -D-glucitol-1,3′-*L*-proline methyl ester] (4) (The detailed procedure was described in supporting information). $[\alpha]_D$ = 15.7 (*c* 1.35, MeOH); ^{1}H NMR (300 MHz, CD_3OD, two isomers): δ = 1.43 (s, 9H), 2.09 (s, 3H), 2.14-2.42 (m, 2H), 3.24-3.50 (m, 3H, partially overlapping with methanol peaks), 3.50-3.87 (m, 6H), 4.04-4.63 (m, 4H); ^{13}C NMR (75 MHz, CD_3OD, two isomers): δ = 20.8 (2 carbons), 25.5/ 26.1, 28.5/28.7 (6 carbons), 53.0 (2 carbons), 57.2/57.3, 62.6/62.8, 65.8/65.9, 71.2 (2 carbons), 71.35 (2 carbons), 71.8/71.4, 75.8/75.9, 77.0/77.1, 81.9/82.3, 88.4/87.4, 155.8/ 156.1, 172.1/171.6, 172.6/172.4; HRMS (ES) calcd for $C_{19}H_{31}NNaO_{11}$ $[M + Na]^+$ 472.1795, found 472.1788.

(1*S*)-6-Azido-6-deoxy-1′-*N*-*tert*-butoxycarbonyl-5′(*R*)-methylenehydroxy acetate -spiro[1,5-anhydro-D-glucitol-1,3′-*L*-proline methyl ester] (5) To a solution of compound **3** (40 mg, 0.09 mmol) in pyridine (1 mL) was added *p*-tolunesulfonyl chloride (42 mg, 0.22 mmol) and stirred for 12 hours at room temperature. The mixture was concentrated and purified by flash column chromatography (CH_2Cl_2 / MeOH: 10/ 1) to provide tosyl ester, which was treated with sodium azide (116 mg, 1.8 mmol) in DMF (1.5 mL) and stirred at 80 °C for 12 hours. The mixture was filtered, concentrated and

purified by flash column chromatography (CH_2Cl_2 / MeOH: 15/ 1) to get **5** (38 mg, 92%). $[\alpha]_D$ = 31.5 (*c* 1.35, MeOH); ^{1}H NMR (300 MHz, CD_3OD, two isomers): δ = 1.44 (s, 9H), 2.10 (s, 3H), 2.14-2.48 (m, 2H), 3.18-3.49 (m, 4H, partially overlapping with methanol peaks), 3.58-3.77 (m, 5H), 4.01-4.17 (m, 1H), 4.21 (s, 1H), 4.32-4.48 (m, 1H), 4.52-4.64 (m, 1H); ^{13}C NMR (75 MHz, CD_3OD, two isomers): δ = 20.9 (2 carbons), 28.6 (6 carbons,), 29.0/29.6, 52.6/52.8, 53.0 (2 carbons), 56.2/56.4, 66.2/66.4, 71.1 (2 carbons), 71.4/71.9, 72.4/72.8, 75.2/75.4, 77.0/77.1, 81.8/82.3, 86.4/87.0, 155.8/156.3, 171.6/171.7, 172.7/172.8; HRMS (ES) calcd for $C_{19}H_{30}N_4\ NaO_{10}$ $[M + Na]^+$ 497.1860, found 497.1849.

(1*S*)-6-Azido-6-deoxy-3′-*N*-*tert*-butoxycarbonyl-5′(*S*)-methylenehydroxy acetate –spiro[1,5-anhydro-D-glucitol-1,3′-*L*-proline methyl ester] (6) (The detailed procedure was described in supporting information). $[\alpha]_D$ = 29.1 (*c* 0.7, MeOH); ^{1}H NMR (300 MHz, CD_3OD, two isomers): δ = 1.45 (s, 9H), 2.09 (s, 3H), 2.14-2.48 (m, 2H), 3.23-3.44 (m, 3H, partially overlapping with methanol peaks), 3.50-3.78 (m, 6H), 4.06-4.34 (m, 3H), 4.39-4.63 (m, 1H); ^{13}C NMR (75 MHz, CD_3OD, two isomers): δ = 20.8 (2 carbons), 25.6/26.2, 28.5/28.6 (6 carbons,), 53.0 (2 carbons), 53.0/53.1, 57.2 (2 carbons), 65.7/65.9, 71.1 (2 carbons), 71.9/71.5, 72.2/72.3, 74.7/74.8, 76.7/76.8, 82.0/82.4, 88.8/87.8, 155.8/156.1, 171.9/171.4, 172.6/172.4; HRMS (ES) calcd for $C_{19}H_{30}N_4\ NaO_{10}$ $[M + Na]^+$ 497.1860, found 497.1852.

(1*S*)-6-Azido-6-deoxy-1′-*N*-acetyl-5′(*R*)-hydroxymethylene-spiro[1,5-anhydro-D -glucitol-1,3′-*L*-proline methyl ester] (7) The compound **5** (30 mg, 0.063 mmol) was dissolved in a mixture of dichloromethane and trifluoroacetic acid (1.5 mL / 0.5 mL) and stirred for 1 hour at room temperature. The solution was concentrated at vacuum and then treated with a mixture of pyridine and acetic acid (1 mL / 1 mL) and stirred for 12 hours at room temperature and then concentrated at vacuum. After that, it was dissolved in a solution of sodium methoxide in methanol (0.1 M, 2 mL) and stirred for 4 hours at room temperature followed by the neutralization with Amberlite IRC-50S ion-exchange resin (H^+). The mixture was filtered and filtrate was concentrated and purified by the flash column chromatography (ethyl acetate / methanol: 6 / 1) to get compound **7** (22 mg, 96%). $[\alpha]_D$ = 19.2 (*c* 0.75, MeOH); ^{1}H NMR (300 MHz, CD_3OD, two isomers): δ = 1.82 (s, 1.74H), 2.04 (s, 1.26H), 2.05-2.49 (m, 2H), 3.06-3.34 (m, 4H, partially overlapping with methanol peaks), 3.49-3.94(m, 7H), 4.04-4.16 (m, 1H), 4.20 (s, 0.58H), 4.42 (s, 0.42H); ^{13}C NMR (75 MHz, CD_3OD, two isomers): δ = 22.8/21.6, 27.7/29.7, 52.8/52.7, 53.6/53.2, 60.6/60.1, 64.9/65.6, 71.1 (2 carbons), 72.6/71.1, 72.6/72.8, 75.4/75.7, 76.9/77.0, 87.5/86.4, 171.6/171.9, 173.6 (2 carbons); HRMS (ES) calcd for $C_{14}H_{22}N_4NaO_8$ $[M + Na]^+$ 397.1335, found 397.1351.

(1*S*)-6-Azido-6-deoxy-1′-*N*-acetyl-5′(*S*)-hydroxymethylene-spiro[1,5-anhydro-D -glucitol-1,3′-*L*-proline methyl ester] (8) (The detailed procedure was described in supporting information). $[\alpha]_D$ = 46.5 (*c* 0.55, MeOH); ^{1}H NMR (300 MHz, CD_3OD, two

isomers): δ = 1.77 (s, 1.09H), 2.08 (s, 1.91 H), 2.15-2.41 (m, 2H), 3.23-3.68 (m, 10H, partially overlapping with methanol peaks), 3.79(dd, 0.64 H, J = 5.28 Hz, J = 10.95 Hz), 3.96-4.23 (m, 2.36H); ^{13}C NMR (75 MHz, CD_3OD, two isomers): δ = 22.04 (22.48), 26.54 (25.35), 52.97 (53.14), 53.13 (53.46), 61.52 (61.38), 64.76 (63.61), 71.14 (71.19), 72.03 (72.44), 72.27 (73.01), 74.68 (74.73), 76.71 (76.62), 87.40 (88.99), 170.78 (171.20), 173.56 (173.50); HRMS (ES) calcd for $C_{14}H_{22}N_4NaO_8$ $[M + Na]^+$ 397.1335, found 397.1348.

(1*S*)-6-Amino-6-deoxy-1′-*N*-acetyl-5′(*R*)-hydroxymethylene-spiro[1,5-anhydro-D-glucitol-1,3′-*L*-proline methyl ester] HCl salt (9) To a solution of **7** (20 mg, 0.053 mmol) and $Pd(OH)_2$ (20 mg, 20 % wt on charcoal) in methanol (5 mL) was added the solution of hydrochloride (800 μL of 1M HCl solution, 0.08 mmol) and stirred under H_2 (15 psi) for 20 minutes at room temperature. The catalyst was removed by the regular filtration and the solvent was removed under the vacuum to afford pure product **9** (20 mg, quant.). $[\alpha]_D$ = 65.2 (*c* 0.5, MeOH); ^{1}H NMR (500 MHz, D_2O, two isomers): δ = 1.86 (s, *cis*, 1.68H), 1.98 (dd, *cis*, 0.56H, J = 10.39 Hz, J = 14.57 Hz), 2.04-2.09 (m, *trans*, 0.44H + 1.32H), 2.36 (dd, *cis*, 0.56H, J = 6.76 Hz, J = 14.56 Hz), 2.47 (dd, *trans*, 0.44H, J = 7.42 Hz, J = 14.62 Hz), 2.98 (m, 1H), 3.19-3.37 (m, 3H), 3.59-3.67 (m, 5H), 3.68-3.74 (m, 1H), 3.81-3.88 (m, 1H), 4.00-4.07 (m, *cis*, 0.56H), 4.11-4.18 (m, *trans*, 0.44H). 4.42 (s, *cis*, 0.56H), 4.44 (s, *trans*, 0.44H); ^{13}C NMR (75 MHz, D_2O): *cis*, δ = 22.2, 26.7, 40.5, 53.5, 58.5, 62.4, 69.2, 69.7, 70.7, 71.2, 74.4, 86.2, 171.4, 174.4; *trans*, δ = 20.9, 28.8,

40.4, 53.2, 58.4, 63.5, 69.2, 69.7, 69.8, 70.9, 74.4, 85.1, 171.4, 174.5; HRMS (ES) calcd for $C_{14}H_{25}N_2O_8$ $[M + H]^+$ 349.1611, found 349.1623.

(1*S*)-6-Amino-6-deoxy-1′-*N*-acetyl-5′(*S*)-hydroxymethylene-spiro[1,5-anhydro-D-glucitol-1,3′-*L*-proline methyl ester] HCl salt (10) (The detailed procedure was described in supporting information). $[\alpha]_D$ = 24.3 (*c* 0.55, MeOH); ^{1}H NMR (500 MHz, D_2O, two isomers): δ = 1.93 (s, *cis*, 0.60H), 2.21 (s, *trans*, 2.40H), 2.29-2.46 (m, 2H), 3.20-3.59 (m, 5H), 3.63-3.82 (m, 5H), 3.85-3.94 (m, 1H), 4.33-4.41 (m, 1H), 4.43 (s, *trans*, 0.8H), 4.62 (s, 0.2H); ^{13}C NMR (75 MHz, D_2O): *cis*, δ = 21.8, 25.0, 40.2, 53.6, 59.5, 62.3, 69.3, 69.6, 70.5, 71.2, 74.2, 87.6, 171.4, 174.4; *trans*, δ = 21.3, 25.9, 39.9, 53.2, 59.7, 63.2, 69.3, 69.5, 70.3 (2 carbons), 74.2, 86.3, 170.8, 174.5; HRMS (ES) calcd for $C_{14}H_{25}N_2O_8$ $[M + H]^+$ 349.1611, found 349.1618.

(1*S*)-6-Amino-6-deoxy-1′-*N*-acetyl-5′(*R*)-hydroxymethylene-spiro[1,5-anhydro-D-glucitol-1,3′-*L*-proline methyl amide] HCl salt (11) To a solution of methylamine in ethanol (37% wt, 1 mL) was added compound 7 (15 mg, 0.04 mmol) and stirred for 18 hours at room temperature. The mixture was concentrated and purified by flash column chromatography (dichloromethane/methanol: 2/1) to quantitatively afford *C*-terminal methyl amide intermediate, which was dissolved in a solution of $Pd(OH)_2$ (15 mg, 20 % wt on charcoal) and 1 M hydrochloride acid solution (80 μL, 0.08 mmole). The mixture was stirred under H_2 (15 psi) for 20 minutes at room temperature The catalyst was removed by the regular filtration and the solvent was removed under the vacuum to

afford pure product **11** (14 mg, 93%). $[\alpha]_D$ = 54.8 (*c* 0.35, MeOH); ^{1}H NMR (500 MHz, D_2O, two isomers): δ = 2.02 (s, *cis*, 2.24H), 2.21 (s, *trans*, 0.76H), 2.27 (dd, *cis*, 0.75H, *J* = 11.31 Hz, *J* = 14.27 Hz), 2.35-2.44 (m, 1H), 2.53 (dd, *trans*, 0.25H, *J* = 6.17 Hz, *J* = 14.11 Hz), 2.67-2.83 (m, 3.75H) 2.98-3.05 (m, 0.75H), 3.25 (dd, 0.25H, *J* = 11.31 Hz, *J* = 14.27 Hz), 3.30-3.39 (m, 1.25H), 3.41-3.56 (m, 2H), 3.68-3.77 (m, 1.75H). 3.83 (dd, *trans*, 0.25H, *J* = 1.81 Hz, *J* = 12.43 Hz), 4.09-4.36 (m, 3H); ^{13}C NMR (75 MHz, D_2O): *cis*, δ = 27.2, 30.1, 30.8, 46.5, 62.9 (2 carbons), 64.5, 74.6, 76.0, 77.4, 80.1, 90.3, 176.5, 179.6; *trans*, 25.9, 30.8, 32.1, 46.4, 62.8, 63.0, 66.0, 74.5, 75.9, 76.5, 78.4, 89.0, 176.6, 179.6; HRMS (ES) calcd for $C_{14}H_{26}N_3O_7$ $[M + H]^+$ 348.1771, found 348.1759.

(1*S*)-6-Amino-6-deoxy-1′-*N*-acetyl-5′(*S*)-hydroxymethylene–spiro[1,5-anhydro-D-glucitol-1,3′-*L*-proline methyl amide] HCl salt (12) (The detailed procedure was described in supporting information). $[\alpha]_D$ = 19.2 (*c* 0.40, MeOH); ^{1}H NMR (500 MHz, D_2O, two isomers): δ = 1.80 (s, *cis*, 1.08H), 2.08 (s, *trans*, 1.92H), 2.16-2.32 (m, 2H), 2.56 (s, *trans*, 1.92H), 2.62 (s, *cis*, 1.08H), 3.09-3.54 (m, 6H), 3.62-3.68 (m, 1H), 3.76 (dd, *trans*, 0.64H, *J* = 5.26 Hz, *J* = 11.50 Hz), 3.83 (dd, *cis*, 0.36 H, *J* = 4.60 Hz, *J* = 11.04 Hz), 4.19 (s, *trans*, 0.64H), 4.21-4.30 (m, 1.36H); ^{13}C NMR (75 MHz, D_2O): *cis*, δ = 26.7, 30.1, 31.2, 45.1, 64.6, 67.3, 74.3, 74.6, 75.5, 77.4, 79.4, 92.6, 175.5, 179.2; *trans*, δ = 26.5, 31.0 (2 carbons), 44.9, 64.7, 68.2, 74.3, 74.5, 75.2, 76.6, 79.4, 91.4, 175.0, 179.1; HRMS (ES) calcd for $C_{14}H_{26}N_3O_7$ $[M + H]^+$ 348.1771, found 348.1766.

Measurement of equilibrium constant: The calculation was based on the integration of well-resovled peaks of the γ-protons, *N*-terminal methyl group and α-proton in ^{1}H NMR.

Temperature coefficient ($\Delta\delta/\Delta T$) experiment: 1 D ^{1}H-NMR spectroscopy of 16mM solutions of **24** and **25** in 100.0% Me_2SO-d_6 were recorded on Bruker AMX500 at 25 °C, and from 25 to 44 °C with increments of 5 °C, using routine techniques. Chemical shift (δ) of hydroxyl and amino groups are expressed in ppm and calibrated with respect to the residual DMSO signal (^{1}H: 2.49 ppm). The chemical shift change ($\Delta\delta$) at different temperature was calculated with respect to the chemical shift of hydroxyl and amino groups at 25 °C.

7.5. References:

1. Gellman, S. H. *Acc. Chem. Res.* **1998**, *31*, 173-180.
2. Belec, L.; Slaninova, J.; Lubell, W. D. *J. Med. Chem.* **2000**, *43*, 1448-1455.
3. An, S. S. A.; Lester, C. C.; Peng, J.; Li, Y.; Rothwarf, D. M.; Welker, E.; Thannhauser, T. W.; Zhang, L. S.; Tam, J. S.; Scheraga, H. A. *J. Am. Chem. Soc.* **1999**, *121*, 11558-11566.
4. (a) Eberhardt, E. S.; Panasik, Jr. N.; Raines, R. T. *J. Am. Chem. Soc.* **1996**, *118*, 12261-12266. (b) Improta, R.; Benzi C.; Barone, V. *J. Am. Chem. Soc.* **2001**, *123*, 12568-12577. (c) Song, Il K.; Kang, Y. K. *J. Phys. Chem. B* 2005, 109, 16982-16987.
5. Hinderaker, M. P.; Raines, R. T. *Protein Sci.* **2003**, 12, 1188-1194.
6. (a) Wu, W. J.; Raleigh, D. P. *Biopolymers*, **1998**, *45*, 381-394. (b) Thomas, K. M.; Naduthambi, D.; Zondlo, N. J. *J. Am. Chem. Soc.* **2006**, *128*, 2216-2217. (c) Halab, L.; Lubell, W. D. *J. Am. Chem. Soc.* **2002**, *124*, 2474-2484.
7. Beausoleil, E.; Lubell, W. D. *J. Am. Chem. Soc.* **1996**, *118*, 12902-12908. And references therein.
8. Kakinoki, S.; Hirano, Y.; Oka, M. *Polym. Bull. (Berlin)* **2005**, *53*, 109-115.
9. Reddy, K. V. R.; Yedery, R. D.; Aranha, C. *Int. J. Antimicrobial Agents* **2004**, *24*, 536-547.
10. Cooper, J. B.; Chen, J. A.; Van Holst, G. J.; Varner, J. E. *TIBS*, **1987**, *12*, 24-27. And references therein.
11. (a) Baldwin, J. E.; Adlington, R. M.; Gollins, D. W.; Godfrey, C. R. A. *Tetrahedron* **1995**, *51*, 5169-5180; (b) Hashimoto, K.; Yamamoto, O.; Horikawa, M.; Ohfune, Y.; Shirahama, H. *Bioorg. Med. Chem. Lett.* **1994**, *4*, 1851-1854.
12. (a) Bridges, R. J.; Stanley, M. S.; Anderson, M. W.; Cotman, C. W.; Chamberlin, A. R. *J. Med. Chem.* **1991**, *34*, 717-725. (b) Tsai, C.; Schneider, J. A.; Lehmann, J. *Neurosci. Lett.* **1988**, *92*, 298-302.
13. (a) Kolodziej, S. A.; Nikiforovich, G. V.; Skeean, R.; Lignon, M.-F.; Martinez, J.; Marshall, G. R. *J. Med. Chem.* **1995**, *38*, 137-149. (b) Holladay, M. W.; Lin, C. W.; May, C. S.; Garvey, D. S.; Witte, D. G.; Miller, T. R.; Wolfram, C. A. W.; Nadzan, A. M. *J. Med. Chem.* **1991**, *34*, 455-457. (c) Plucinska, K.; Kataoka, T.; Yodo, M.; Cody, W. L.; He, J. X.; Humblet, C.; Lu, G. H.; Lunney, E.; Major, T. C.; Panek, R. L.; Schelkun, P.; Skeean, R.; Marshall, G. R. *J. Med. Chem.* **1993**, *36*, 1902-1913.
14. Ghose, A. K.; Logan, M. E.; Treasurywala, A. M.; Wang, H.; Wahl, R. C; Tomczuk, B. E.; Gowravaram, M. R.; Jaeger, E. P.; Wendoloski, J. J. *J. Am. Chem. Soc.* **1995**, *117*, 4671-4682.
15. (a) Mosberg, H. I.; Kroona, H. B. *J. Med. Chem.* **1992**, *35*, 4498-4500. (b) Mosberg, H. I.; Lomize, A. L.; Wang, C.; Kroona, H.; Heyl, D. L.; Sobczyk-Kojiro, K.; Ma, W.;

Mousigian, C.; Porreca, F. *J. Med. Chem.* **1994**, *37*, 4371-4383.

16. Chung, J. Y. L.; Wasicak, J. T.; Arnold, W. A.; May, C. S.; Nadzan, A. M.; Holladay, M. W. *J. Org. Chem.* **1990**, *55*, 270-275.
17. Sharma, R.; Lubell, W. D. *J. Org. Chem.* **1996**, *61*, 202-209.
18. Reviews: (a) Dondoni A.; Marra, A. *Chem. Rev.* **2000**, *100*, 4395-4421. (b) Schweizer, F. *Angew. Chem. Int. Ed.* **2002**. *41*, 230-253. (c) Gruner, S. W.; Locardi, E.; Lohof, E.; Kessler, H. *Chem. Rev.* **2002**, *102*, 491-514.
19. (a) Owens, N.; Braun, C.; Schweizer, F. *J. Org. Chem.*, **2007**, *72*, 4635. (b) Zhang, K.; Schweizer, F. *Synlett.* **2005**, 3111. (c) Cipolla, L.; Redaelli, C.; Nicotra, F. *Lett.Drug Des. Discov.* **2005**, *2*, 291.
20. Haubner, R.; Wester, H-J.; Burkhart, F.; Senekowitsch-Schmidtke, R.; Weber, W.; Goodman, S. L.; Kessler, H.; Schwaiger, M. *J. Nuclear. Med.* **2001**, *42*, 326-336.
21. (a) Kuemin, M.; Sonntag, L. -S.; Wennemers, H. *J. Am. Chem. Soc.* **2007**, *129*, 466-467. (b) Shi, Z.; Chen, K.; Liu, Z.; Kallenbach, N. R. *Chem. Rev.* **2006**, *106*, 1877-1897.
22. Grotenbreg, G. M.; Timmer, M. S. M.; Llamas-Saiz, A. L.; Verdoes, M.; Van der Marel, G. A.; Van Raaij, M. J.; Overkleeft, H. S.; Overhand, M. *J. Am. Chem. Soc.* **2004**, *126*, 3444-3446.
23. Chakraborty, T. K.; Jayaprakash, S.; Diwan, P. V.; Nagaraj, R.; Jampani, S. R. B.; Kunwar, A. C. *J. Am. Chem. Soc.* **1998**, *120*, 12962-12963.
24. It has been reported that substitution of D-proline by *cis*-3-hydroxy-D-proline (HypC3-OH) in the sequence Boc-Leu-Pro-Gly-Leu-NHMe resulted in novel pseudo β-turn-like nine-membered ring structure involving an intramolecular LeuNH→HypC3-OH hydrogen bond. Chakraborty, T. K.; Srinivasu, P.; Vengal Rao, R.; Kiran Kumar, S.; Kunwar, A. C. *J. Org. Chem.* **2004**, *69*, 7399-7402.
25. Taylor, C. M.; Hardré, R.; Edwards, P. J. B.; Park, J. H. *Org. Lett.* **2003**, *5*, 4413-4416. And references therein.
26. Dugave, C.; Demange, L. *Chem. Rev.* **2003**, *103*, 2475-2532.
27. (a) Jenkins, C. L.; Bretscher, L. E.; Guzei, I. A.; Raines, R. T. *J. Am. Chem. Soc.* **2003**, *125*, 6422-6427. (b) Taylor, C. M.; Hardré, R.; Edwards, P. J. B. *J. Org. Chem.* **2005**, *70*, 1306-1315.
28. Leeflang, B. R.; Vliegenthart, J. F. G.; Kroon-Batenburg, L. M. J.; Eijck, B. P.; Kroon, J. *Carbohydr. Res.***1992**, *230*, 41-61.
29. Wilmot, C. M.; Thornton, J. M. *J. Mol. Biol.* **1988**, *203*, 221-232.
30. Marraud, M.; Aubry, A. *Int. J. Peptide Protein Res.* **1984**, *23*, 123-133.

Chapter 8

Conclusions and Future Prospects

8.1. General Conclusions

We have successfully synthesized three types of carbohydrate-templated amino acid building blocks: Glc(3*S*)-Hyp, GlcTK (or GlcTk) and GlcTProLysC (Figure 8.1). These

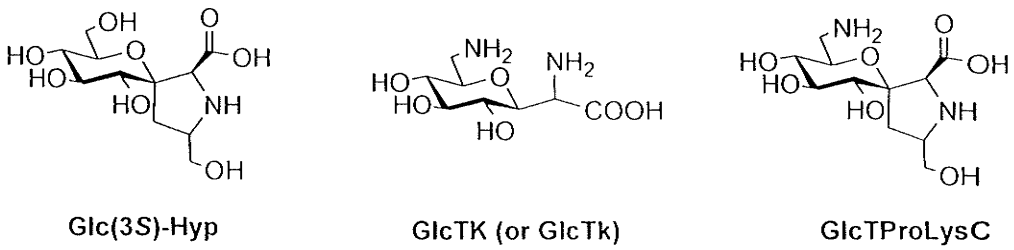

Figure 8.1 Carbohydrate-templated amino acids

novel *C*-glycosyl amino acids exhibit unique structural and conformational properties including induction of conformational constraint, artificial post-translational modifications, control of the kinetics and thermodynamics of prolyl amide *cis/trans* isomerization and generation of amino acid side chain diversity. Of particular note is the discovery that the stereochemistry of the hydroxymethyl substituent at C-δ of proline greatly effects prolyl amide *cis/trans* isomerization. For instance, (5′*R*)-Glc(3*S*)-Hyp increases the *cis* rotamer population (74 ± 3%) of model peptide Ac-Glc3(*S*)Hyp-*N*′-CH_3 in water. In addition, when compared to reference peptide mimics Ac-Pro-OMe and

Ac-3(*S*)Hyp-OMe the study shows a (5-24)-fold acceleration in k_{tc} and k_{ct}. By comparison, a (13-16)-fold decrease is observed for its epimer (5′*S*)-Glc(3*S*)-Hyp in water. NMR studies and DFT calculation support the notion that hydrogen bonds between the polar hydroxymethylene group and prolyl *N*-terminal carbonyl group or OH-6 of the glucose scaffold are in part responsible for these interesting properties.

MOM-protected proline mimetics Glc3(*S*)-Hyp differing in the stereochemistry of the hydroxymethyl substituent at C-δ(Pro) were incorporated into the β-turn inducing peptide sequence [Leu-D-Phe-Pro-Val] of gramicidine S to produce tetrapeptide Ac-Leu-D-Phe-[Glc3(*S*)-Hyp]–Val-NMe_2. NMR-studies on the MOM-protected as well as the unprotected tetrapeptides indicate that the tetrapeptides form *β*-turn conformation in dichloromethane (MOM-protected) and water (unprotected), respectively. Incorporation of (5′*R*)-Glc3(*S*)-Hyp increases the *cis* rotamer population (MOM-protected: 75% *cis* in dichloromethane; unprotected: 91% cis in water) and induces a type VIa *β*-turn. In comparison, tetrapeptide containing MOM-protected (5′*S*)-Glc3(*S*)-Hyp shows a higher prolyl amide *trans* rotamer population (93%) in dichloromethane and retains the β-turn conformation of the unmodified reference peptide. Attempts to prepare unprotected tetrapeptide Ac-Leu-D-Phe-[(5'S)Glc3(*S*)-Hyp]-Val-NMe_2 failed due to decomposition under acidic conditions.

In a different project carbohydrate-templated lysine analogs (GlcTK and GlcTk) were synthesized. Both amino acids conformationally constrain L- (K) or D-lysine (k). The goal of this project was to prepare analogs of the ultrashort, antibacterial dipeptide

kW-OBn. Biological evaluation of these dipeptide analogs demonstrates that replacement of lysine by GlcTk in the dipeptide kw-OBn reduces antibacterial activity. It is possible that the low antibacterial activity of dipeptide GlcTkW-OBn is the result of decreased amphiphilicity and hydrophobicity which are crucial for the antibacterial activity of antimicrobial peptides. In addition, I observed that the nature of the *C*-terminus contributes substantially to the antimicrobial activity of kW-OBn. For instance, dipeptide kW-OBn exhibits strong *S. aureus* activity while this activity is abolished in peptide kW-NHBn.

Finally, we have developed a synthetic route to two glucose-templated proline lysine chimeras (GlcTProLysC) and explored their conformational properties by incorporation into peptide mimics. Conformational analysis of peptide mimics Ac-GlcTProLysC-OMe (NHMe) demonstrate that both exhibit nearly identical prolyl amide *cis/trans* rotamer populations when compared to Ac-Glc3(*S*)-Hyp-OMe (NHMe) in water. Apparently, replacement of hydroxyl group by an amino function at *C*-6 of glucose does not affect thermodynamics of prolyl amide *cis/trans* isomerization.

8.2. Future Prospects

8.2.1. Glc(3*S*)-Hyp

Although the Glc(3*S*)-Hyp-based proline mimics display interesting conformational properties that will find use to explore the bioactive conformation of peptides, broad applications of this peptidomimetic is currently limited by a lengthy 9-step synthetic

procedure. Future applications of these building blocks will depend on the development of faster and more efficient synthetic routes to these building blocks.

In order to better understand the roles of the carbohydrate moiety and the C-δ hydroxymethyl group on prolyl amide *cis/trans* isomerization the present study should be extended. The following reference compounds including glucose-templated proline analogue **1** and proline analogues **2** and **3** would enable to differentiate between the sugar- and hydroxymethyl-effect (Figure 8.2).

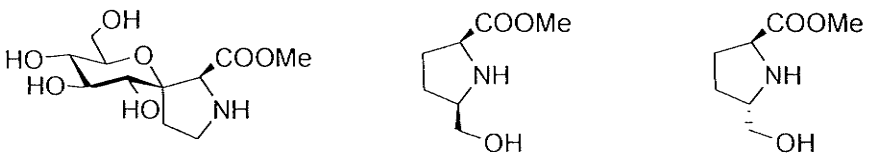

1 2 3

Figure 8.2 Proline mimics **1-3**

To further demonstrate the use of carbohydrate-templated proline analogs as peptidomimetics incorporation of (5′*R*)-Glc3(*S*)-Hyp into the opoid peptides endomorphine-1, Tyr-Pro-Trp-PheNH_2 and endomorphine-2, Tyr-Pro-Phe-PheNH_2, [1]could be attempted. These tetrapeptides play an important role in analgesia. However, the possibility of using native opioid peptides as analgesics is generally invalidated by their limited resistance towards enzymatic hydrolysis *in vivo*. For instance, endomorphine-1 is easily degraded by peptidases, such as dipeptidyl peptidase IV (DPP IV), which appears to be a major physiological regulator for some neuropeptides,

regulatory peptides and circulating hormones. Recent studies indicate that the *cis*-isomer amide of proline is essential for bioactivity.[2] Moreover, replacement of proline by proline mimics play a crucial role in *in vivo* peptide stability, due to the fact that the activity of DPP IV is particularly directed towards the degradation of proline-containing peptides.[3]

8.2.2. Hydrophobic GlcTK and GlcTk

As mentioned above, the reduced antimicrobial activity of dipeptide GlcTk-W-OBn may be due to the presence of the unprotected hydrophilic glucose moiety. Attachment or decoration of hydrophobic groups on the glucose scaffold in GlcTk or GlcTK could be a way to enhance its biological activity. Selective debenzylation[4] could be used to prepare the benzyl-protected GlcTk **5** or GlcTK **6** (Figure 8.3).

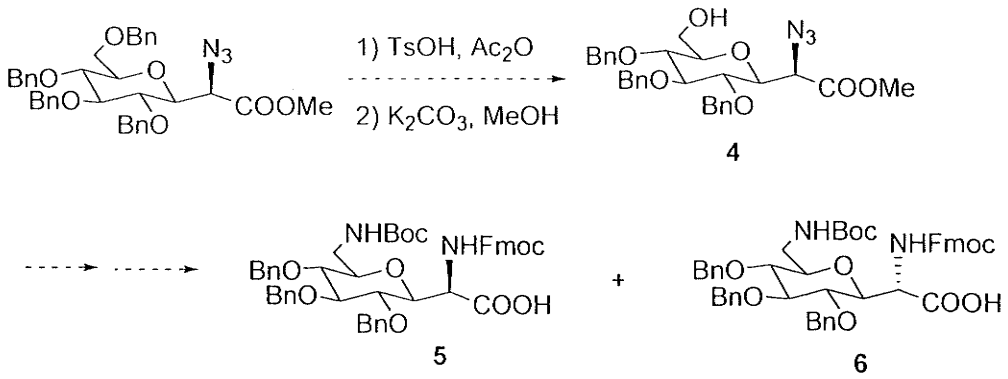

Figure 8.3 Modified Synthetic plan to prepare hydrophobic lysine analogues **5** and **6**

8.2.3. Stabilization of PPI Helix Using (5′*R*)-GlcTProLysC

The left-handed polyproline II (PPII) helix is recognized as an important peptide

conformation in biological systems.[5] However, the related right handed polyproline I (PPI) helix, in which prolyl amide has a *cis* geometry is less studied due to the low propensity of proline and hydroxyproline to populate this conformation. As an efficient prolyl amide *cis* inducer, (5′*R*)-GlcTProLysC-containing homooligomers could be used to populate the PPI conformation. Subsequently, derivatization of the glucose scaffold could be used to prepare functionalized oligoproline analogs with conformational PPI preference. In addition, (5′*S*)-GlcTProLysC-containing homooligomers could be used to functionalize the PPII conformation. Similar studies could be initiated with the corresponding Glc3(*S*)-Hyp building blocks.

8.3. References:

1. For a review see: G. Horvath, *Pharmacol. Ther.* **2000**, *88*, 437.
2. Fiori, S.; Renner, C.; Cramer, J.; Pegoraro, S.; Moroder, L. *J. Mol. Biol.* **1999**, *291*, 163.
3. Yaron, A.; Naider, F. *Crit. Rev. Biochem. Mol. Bio.* **1993**, *28*, 31.
4. Cao, Y.; Okada, Y.; Yamada, H. *Carbohydr. Res.* **2006**, 2219.
5. (a) Dalgarno, D. C.; Botfield, M. C.; Rickles, R. J. *Biopolymers* **1998**, *43*, 383. (b) Shi, Z.; Chen, K.; Liu, Z.; Kallenbach, N. R. *Chem. Rev.* **2006**, *106*, 1877. (c) Silifardi, G.; Drake, A. F. *Biopolymers* **1995**, *37*, 281.

Chapter 9

Supporting Information

9.1. SI for Chapter 3

9.1.1. ^{1}H NMR and ^{13}C NMR spectrum

Compound **2**:

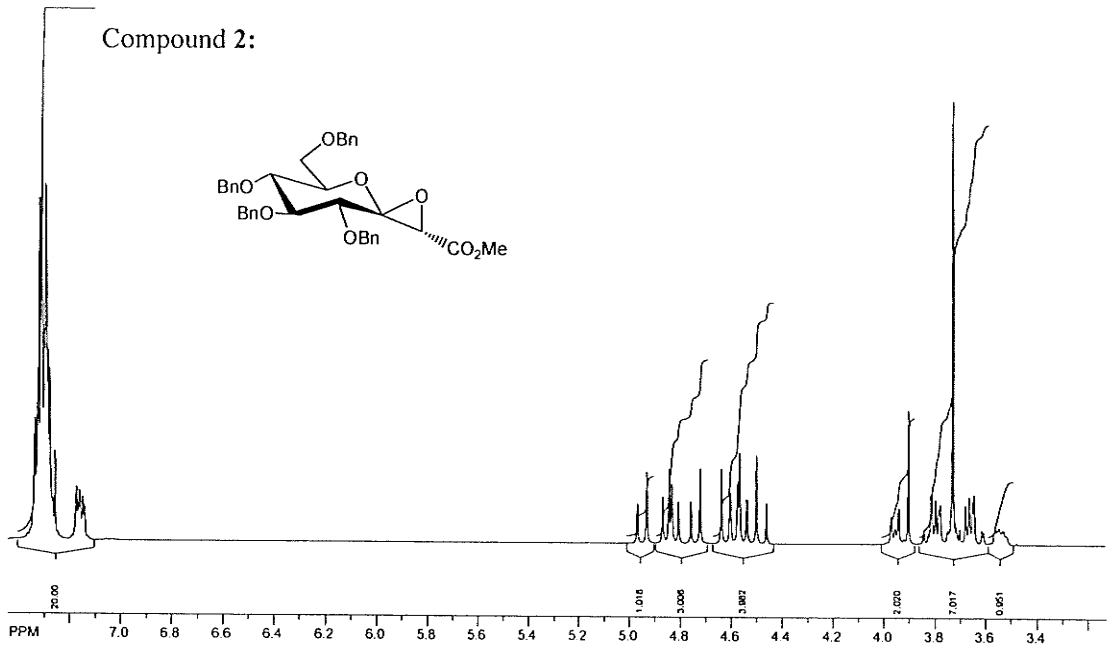

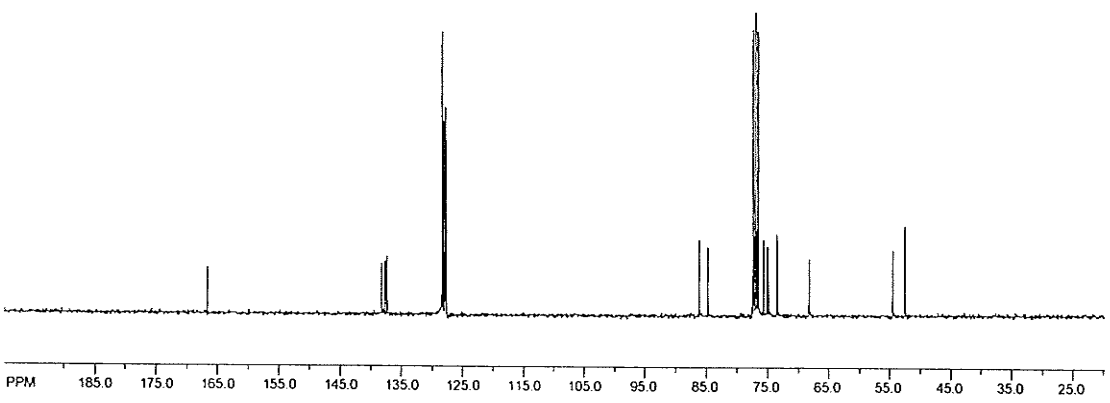

Compound **3**:

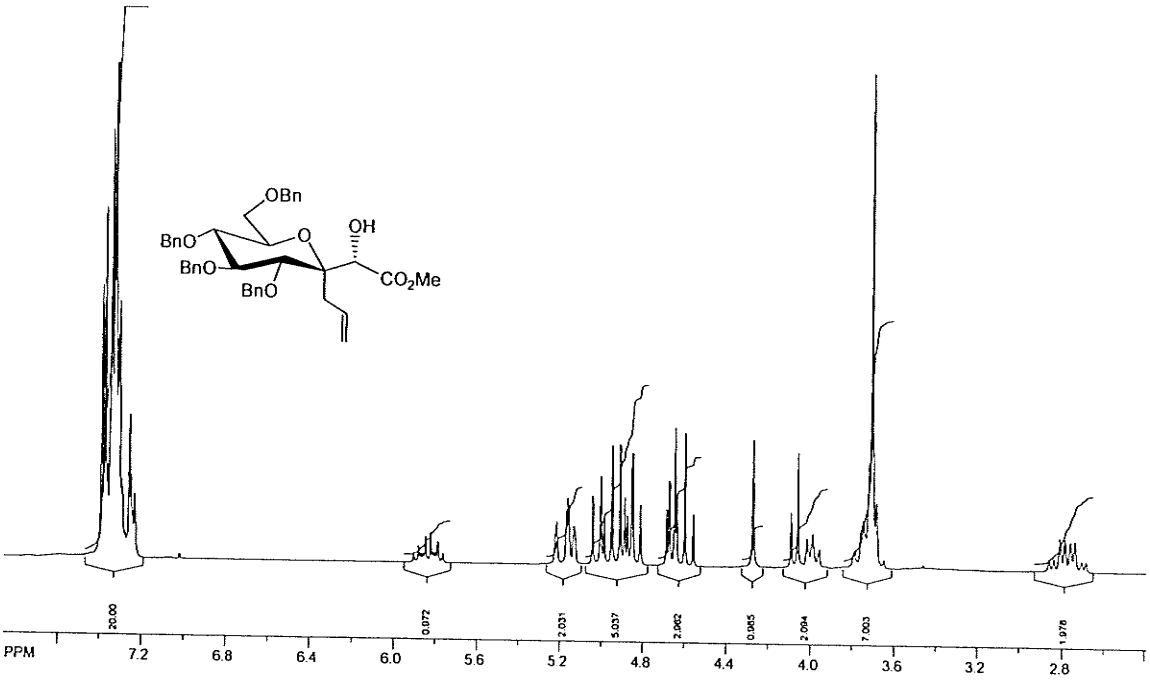
OBn
BnO
BnO
BnO
O
OH
CO2Me
PPM
7.2
6.8
6.4
6.0
5.6
5.2
4.8
4.4
4.0
3.6
3.2
2.8

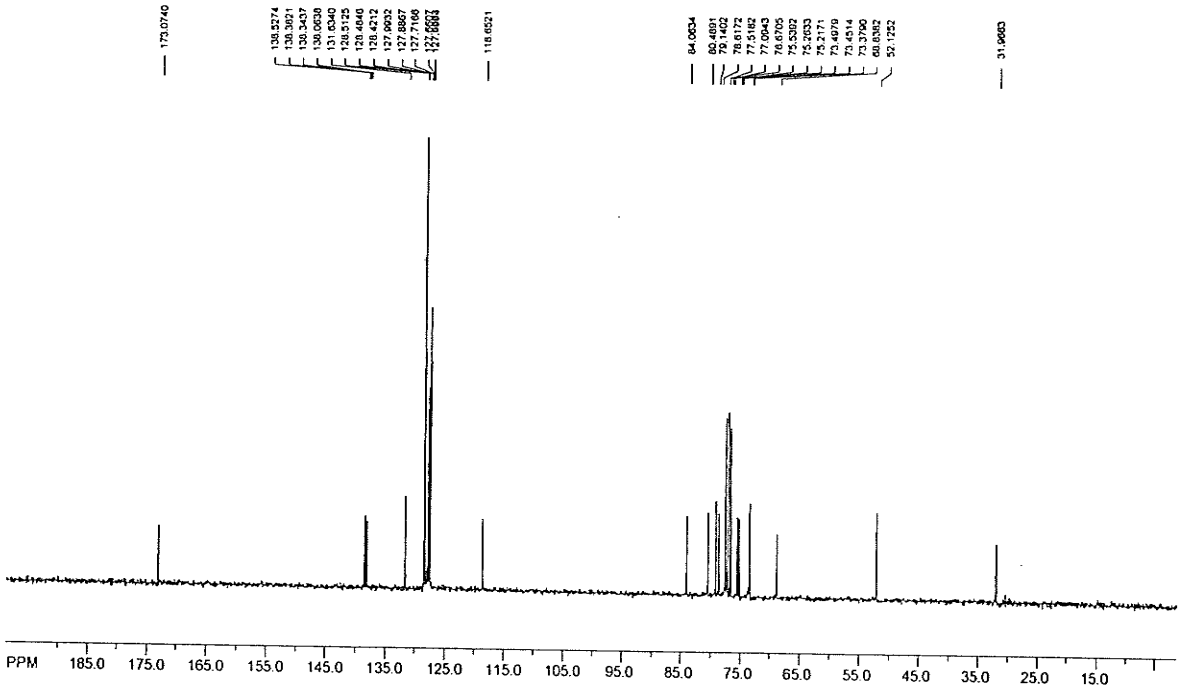
PPM
185.0
175.0
165.0
155.0
145.0
135.0
125.0
115.0
105.0
95.0
85.0
75.0
65.0
55.0
45.0
35.0
25.0
15.0

Compound **4**:

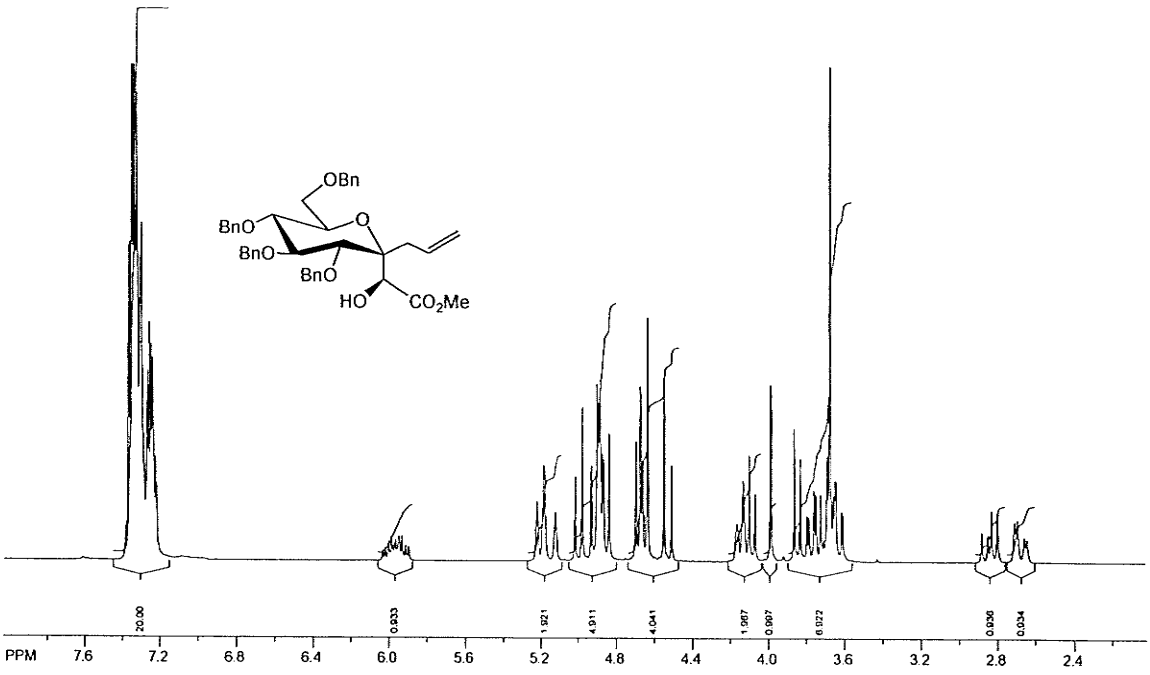
OBn
BnO
BnO
BnO
O
HO
CO2Me
20.00
0.933
1.921
4.911
4.041
1.967
0.997
6.022
0.936
0.934
PPM
7.6
7.2
6.8
6.4
6.0
5.6
5.2
4.8
4.4
4.0
3.6
3.2
2.8
2.4


170.7023
138.5315
138.3170
138.1197
137.2046
133.3001
128.7266
128.5473
128.4041
128.3456
128.2733
127.9879
119.2177
63.0778
62.3132
77.6102
77.3068
77.0832
76.6600
76.2279
75.6657
75.0905
74.1459
73.7513
73.0134
69.0714
52.0710
36.5889

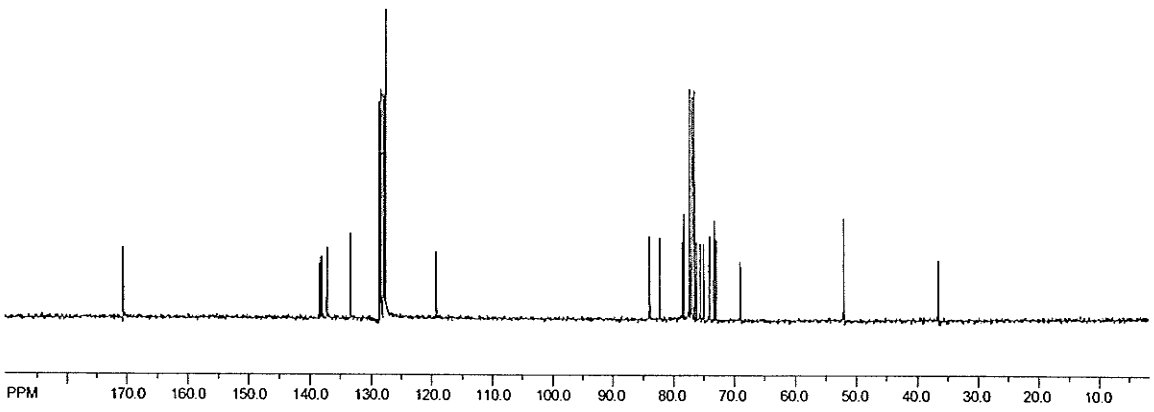
PPM
170.0
160.0
150.0
140.0
130.0
120.0
110.0
100.0
90.0
80.0
70.0
60.0
50.0
40.0
30.0
20.0
10.0

Compound **5**:

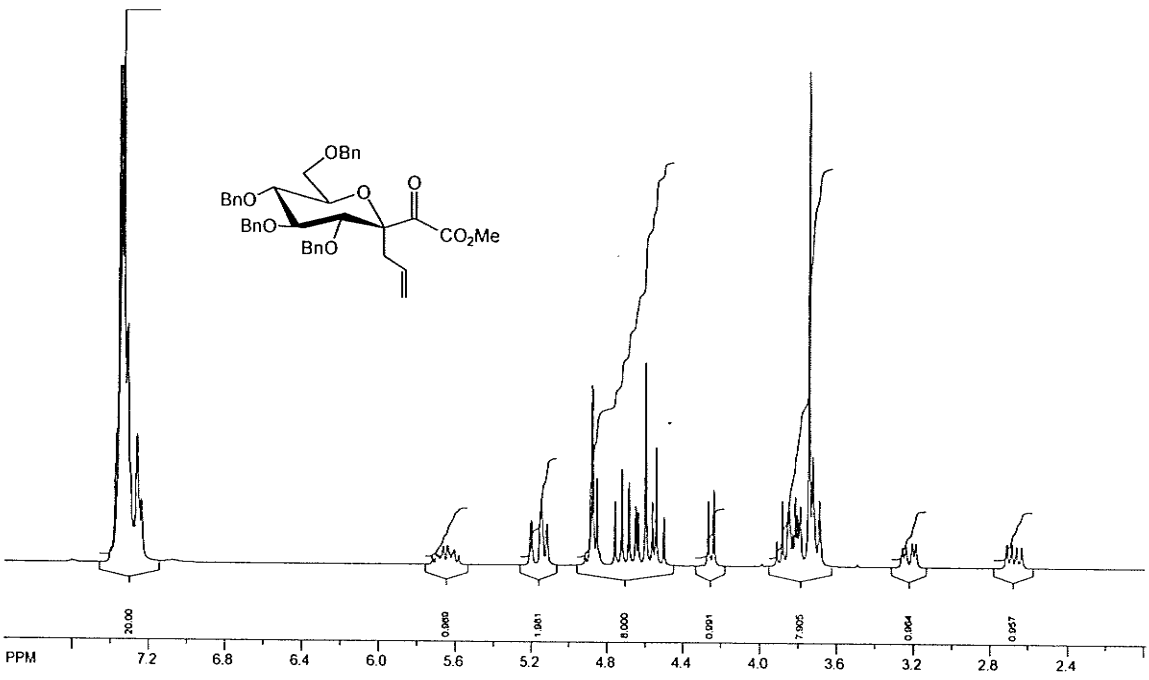
OBn
BnO
BnO
BnO
O
O
CO2Me
20.00
0.869
1.981
8.000
0.991
7.905
0.964
0.957
PPM
7.2
6.8
6.4
6.0
5.6
5.2
4.8
4.4
4.0
3.6
3.2
2.8
2.4

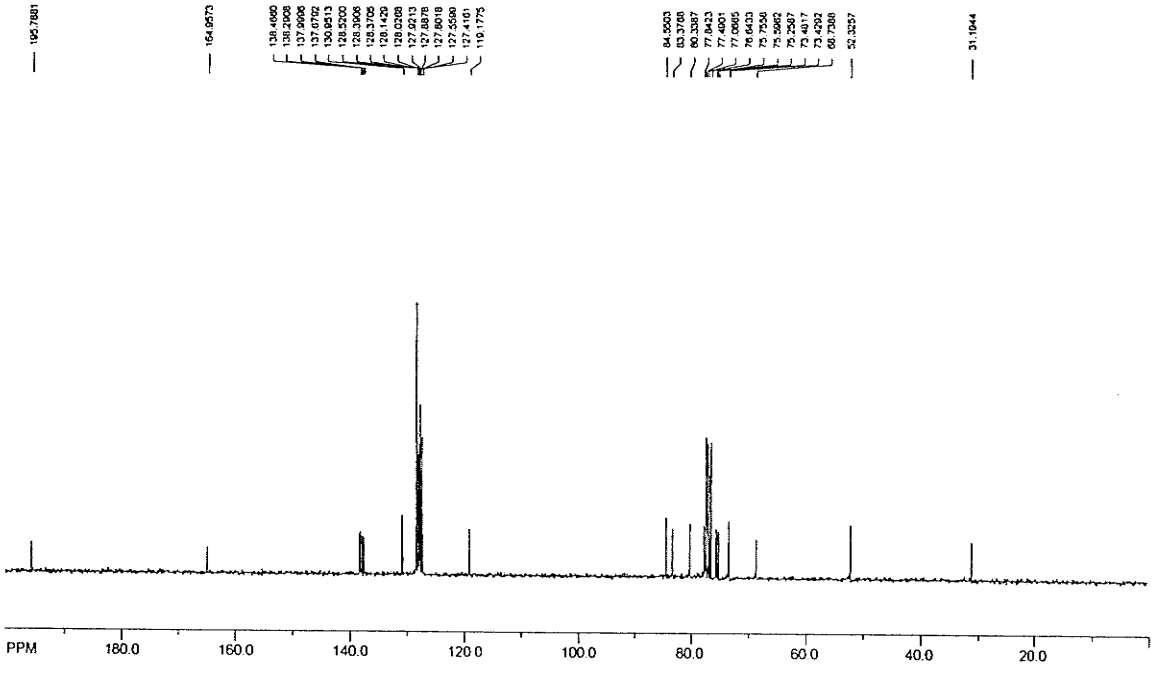
195.7881
164.9573
138.4660
138.2908
137.9995
137.6792
130.8513
128.5200
128.3906
128.3705
128.1429
128.0288
127.9213
127.8878
127.8018
127.5569
127.4161
119.1775
84.5503
83.3788
80.3387
77.8423
77.4001
77.0685
76.6433
75.7536
75.5962
75.2587
73.4017
73.4292
68.7388
52.3257
31.1944
PPM
180.0
160.0
140.0
120.0
100.0
80.0
60.0
40.0
20.0

Compound 6:

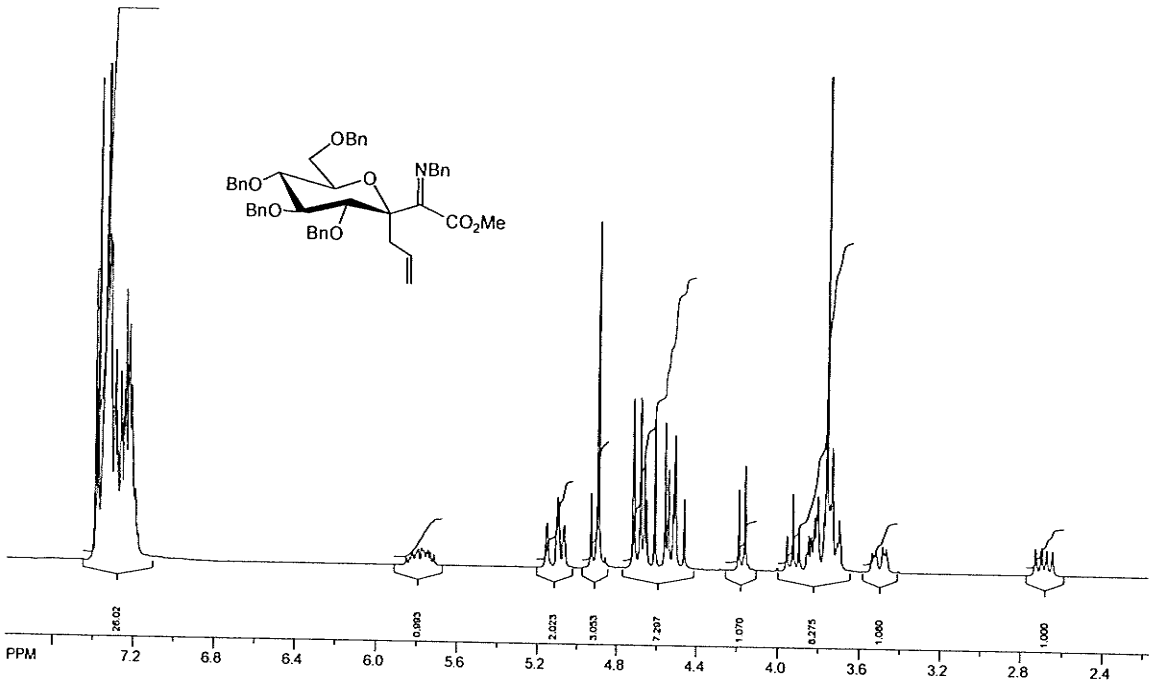
OBn
NBn
BnO
O
BnO
BnO
CO2Me
26.02
0.993
2.023
3.053
7.297
1.070
0.275
1.080
1.000
PPM
7.2
6.8
6.4
6.0
5.6
5.2
4.8
4.4
4.0
3.6
3.2
2.8
2.4

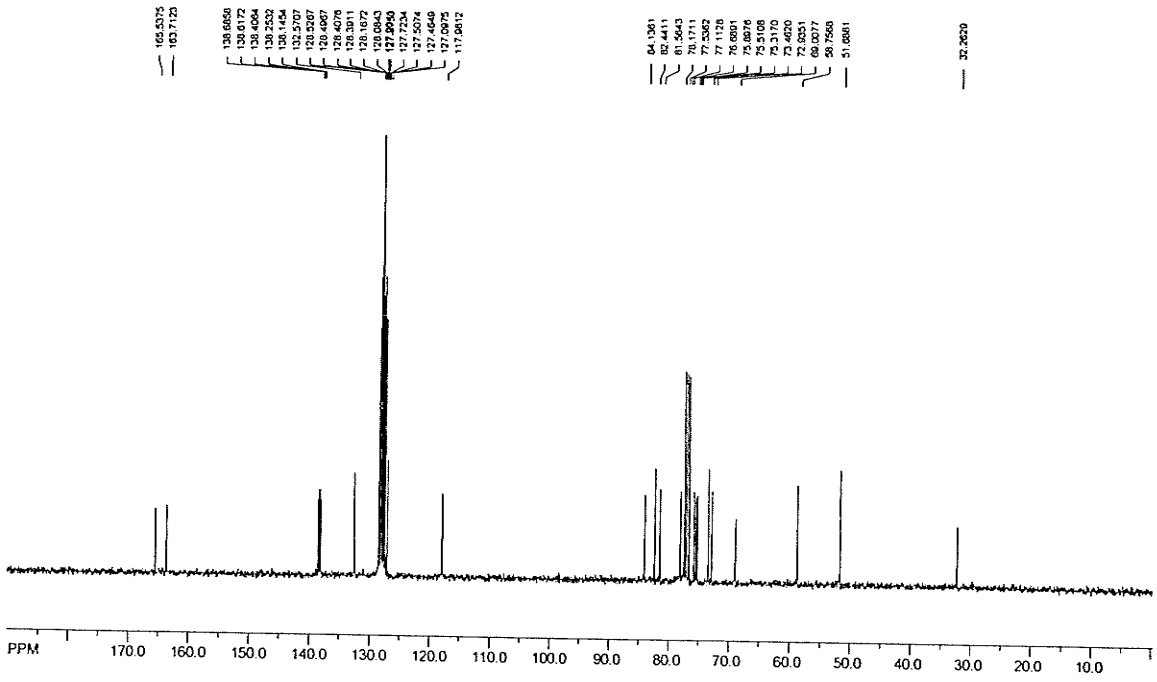
165.5375
163.7125
138.6650
138.6172
138.4064
138.2532
138.1454
132.5707
128.5267
128.4667
128.4076
128.3011
128.1672
128.0943
127.8953
127.7234
127.5074
127.4549
127.0975
117.0812
84.1361
82.4411
81.5643
70.1711
77.5362
77.1128
76.6991
75.8876
75.5108
73.3170
73.4020
72.9351
60.0077
58.7568
51.0881
32.2620
PPM
170.0
160.0
150.0
140.0
130.0
120.0
110.0
100.0
90.0
80.0
70.0
60.0
50.0
40.0
30.0
20.0
10.0

Compound 7:

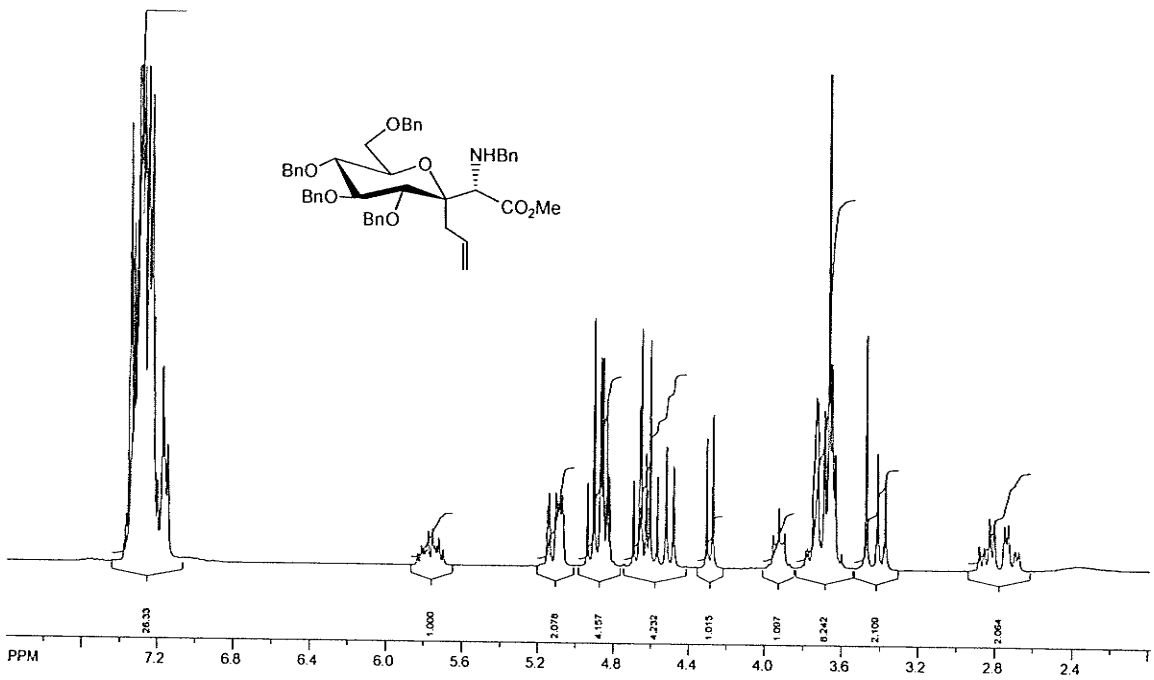
OBn
NHBn
BnO
O
BnO
CO2Me
BnO
26.33
1.000
2.078
4.157
4.232
1.015
1.007
6.242
2.109
2.064
PPM
7.2
6.8
6.4
6.0
5.6
5.2
4.8
4.4
4.0
3.6
3.2
2.8
2.4

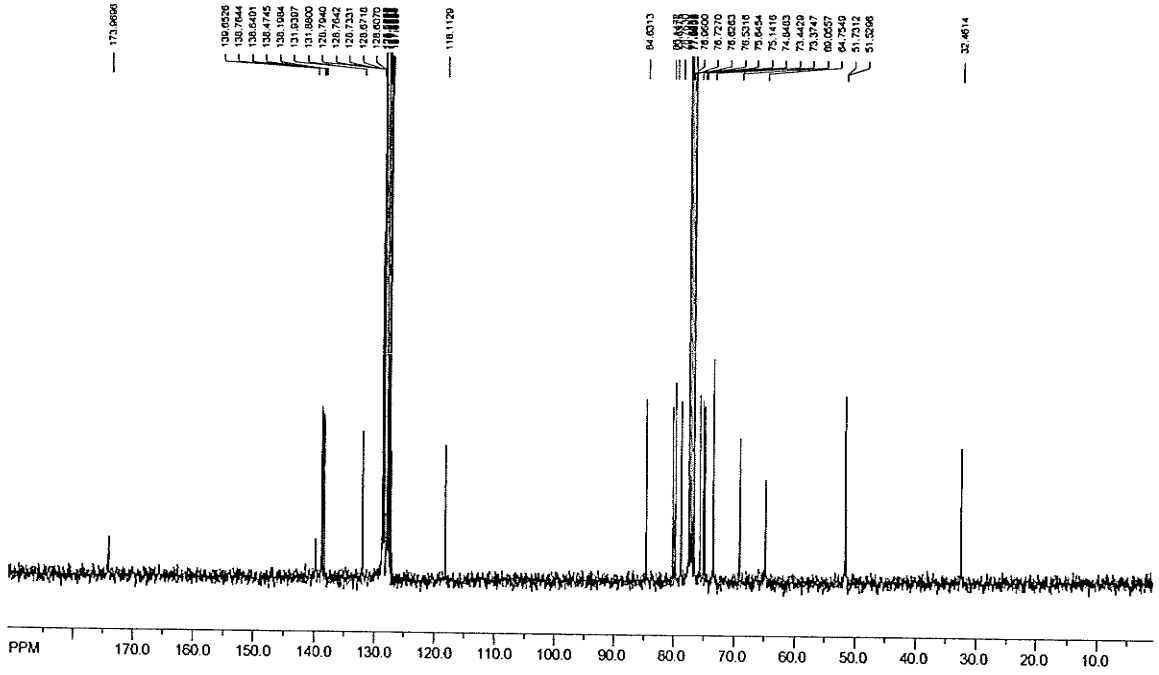
170.0696
130.0526
130.7644
130.6401
130.4745
130.1984
131.6397
131.8800
120.7940
120.7642
120.7331
128.6716
128.6070
118.1129
84.6313
78.7270
78.6263
78.5316
75.5454
75.1416
74.8483
73.4429
73.3747
69.0557
64.7549
51.7312
51.5296
32.4614
PPM
170.0
160.0
150.0
140.0
130.0
120.0
110.0
100.0
90.0
80.0
70.0
60.0
50.0
40.0
30.0
20.0
10.0

Compound **8**

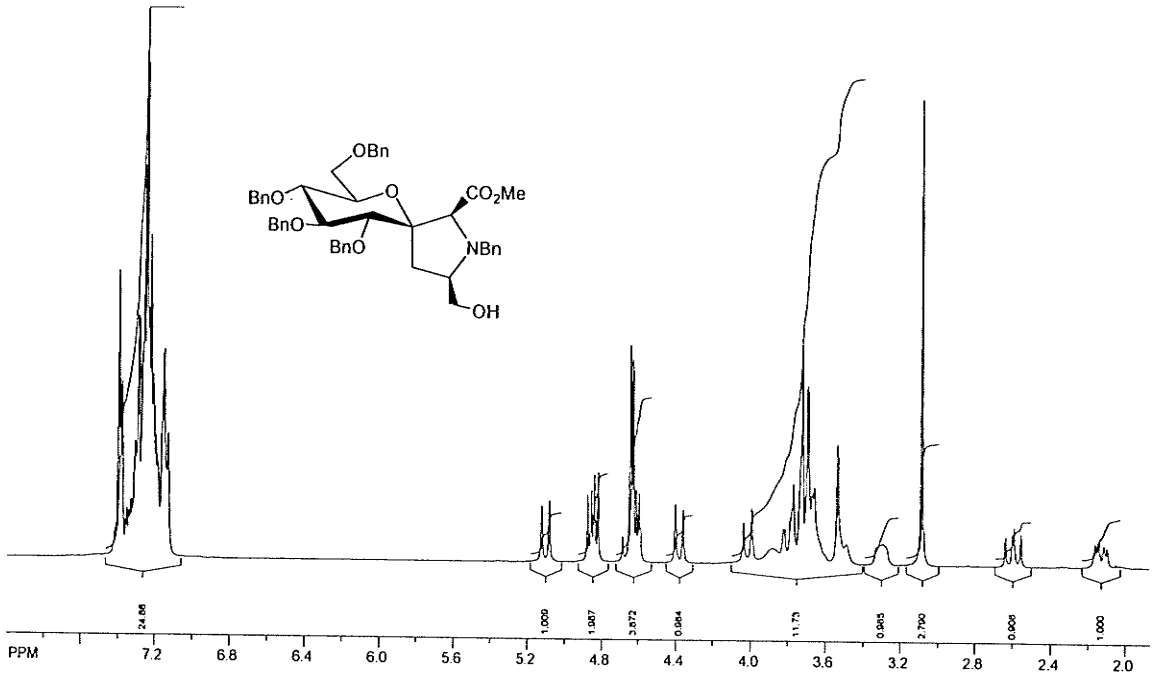
OBn
BnO
BnO
BnO
O
CO2Me
NBn
OH
PPM
7.2
6.8
6.4
6.0
5.6
5.2
4.8
4.4
4.0
3.6
3.2
2.8
2.4
2.0

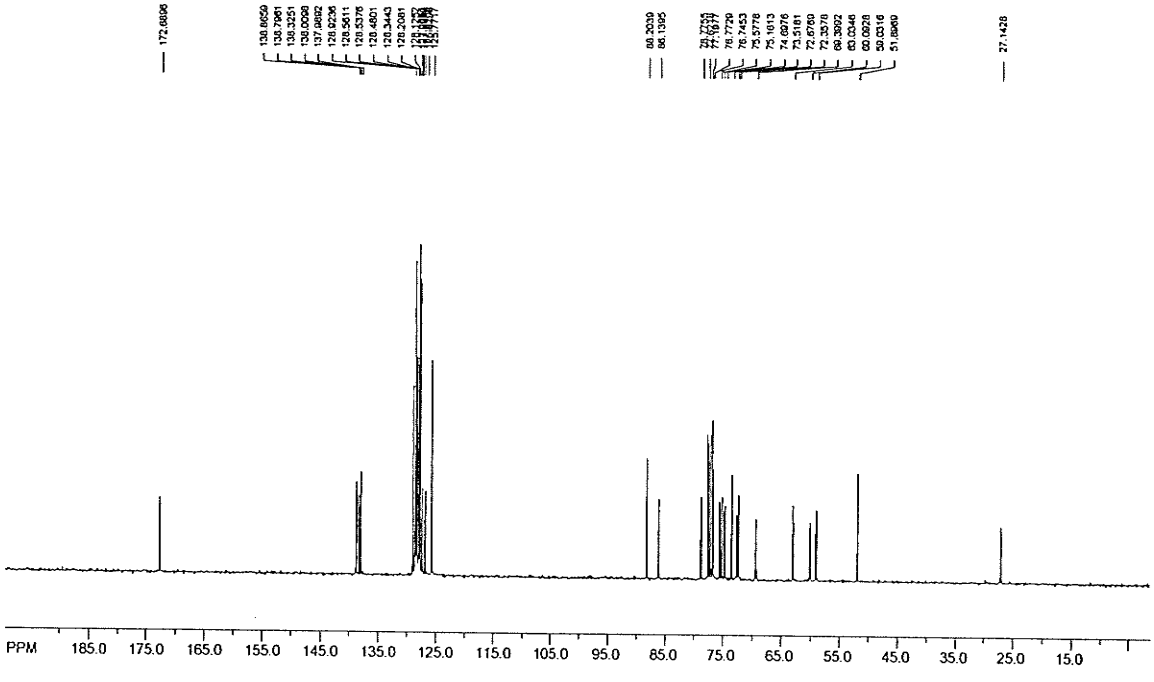
PPM
185.0
175.0
165.0
155.0
145.0
135.0
125.0
115.0
105.0
95.0
85.0
75.0
65.0
55.0
45.0
35.0
25.0
15.0

Compound **13**

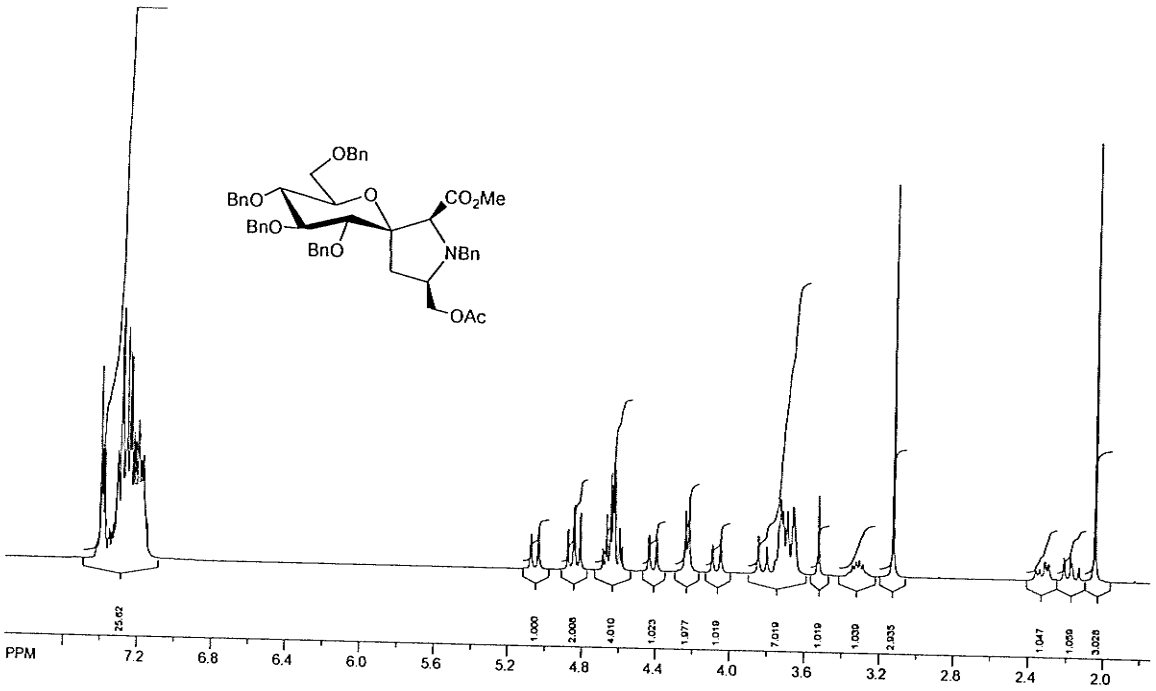
OBn
BnO
BnO
BnO
O
CO2Me
NBn
OAc
PPM
7.2
6.8
6.4
6.0
5.6
5.2
4.8
4.4
4.0
3.6
3.2
2.8
2.4
2.0

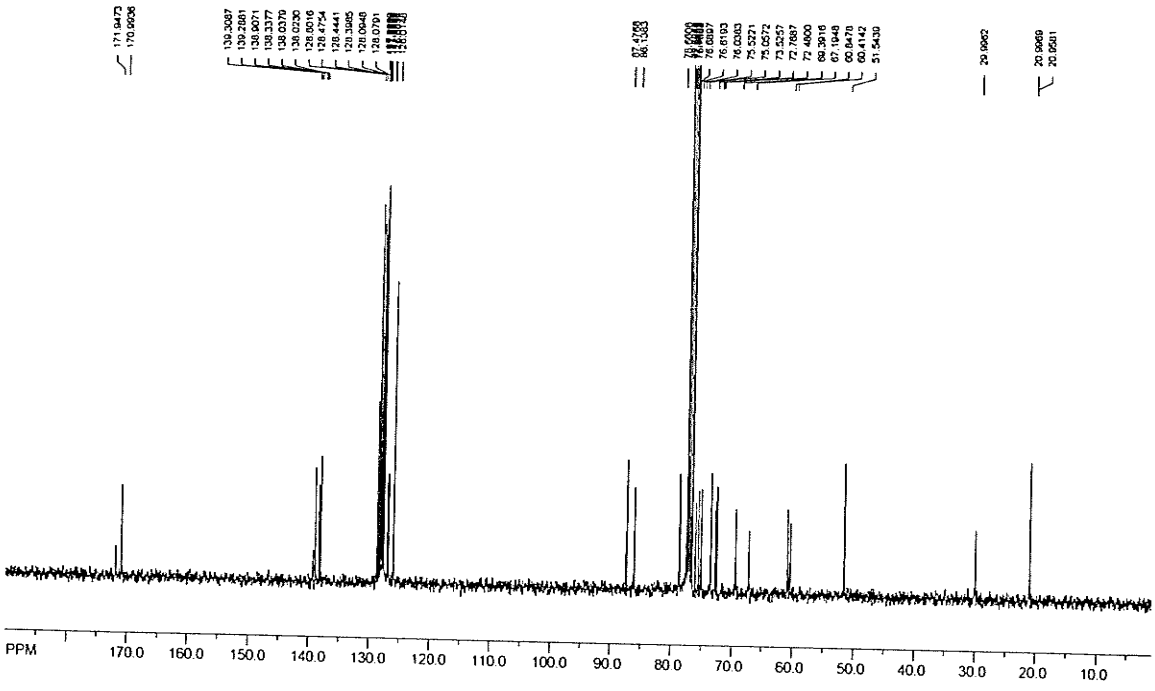
PPM
170.0
160.0
150.0
140.0
130.0
120.0
110.0
100.0
90.0
80.0
70.0
60.0
50.0
40.0
30.0
20.0
10.0

Compound 9

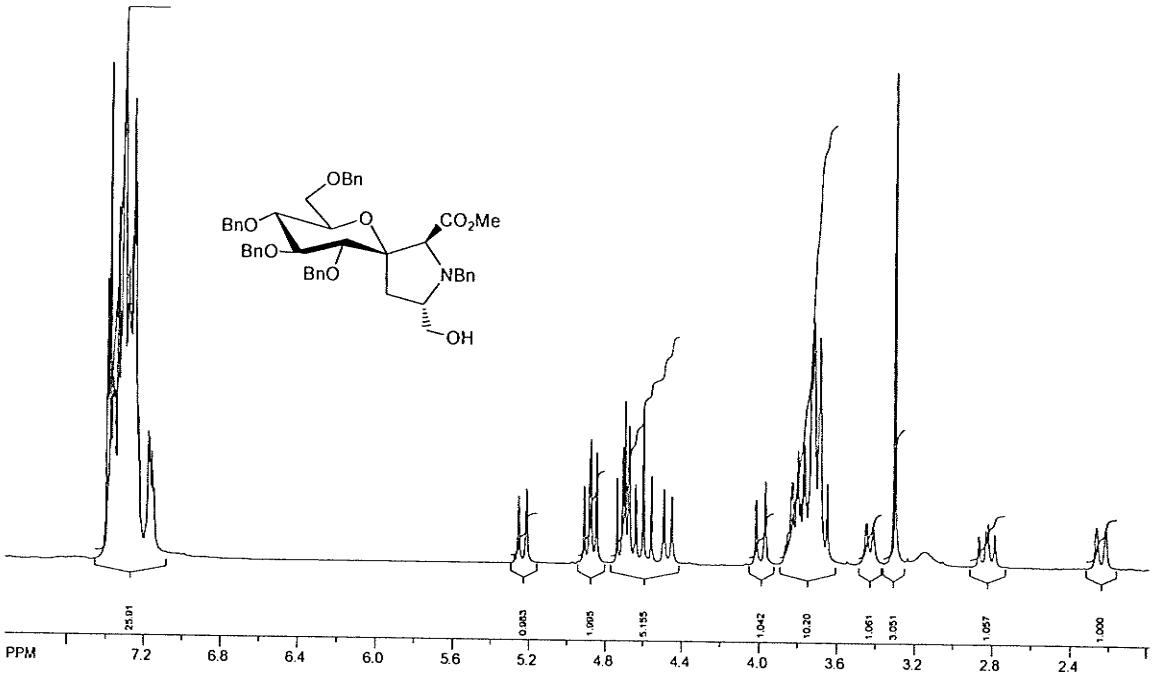
OBn
BnO
BnO
BnO
O
CO2Me
NBn
OH
25.01
0.953
1.005
5.155
1.042
10.20
1.061
3.051
1.057
1.000
PPM
7.2
6.8
6.4
6.0
5.6
5.2
4.8
4.4
4.0
3.6
3.2
2.8
2.4

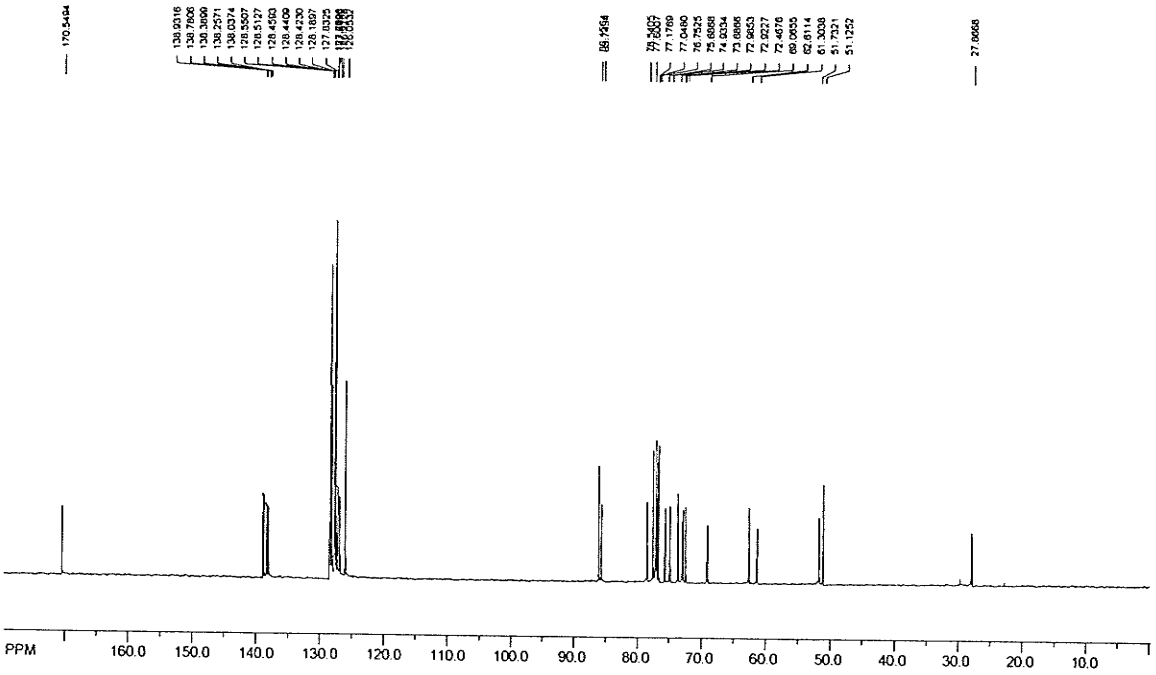
170.5494
130.9316
130.7606
130.3990
130.2571
130.0374
128.5507
128.5127
128.4503
128.4400
128.4230
128.1897
127.0325
88.1954
27.0668
PPM
160.0
150.0
140.0
130.0
120.0
110.0
100.0
90.0
80.0
70.0
60.0
50.0
40.0
30.0
20.0
10.0

Compound **14**

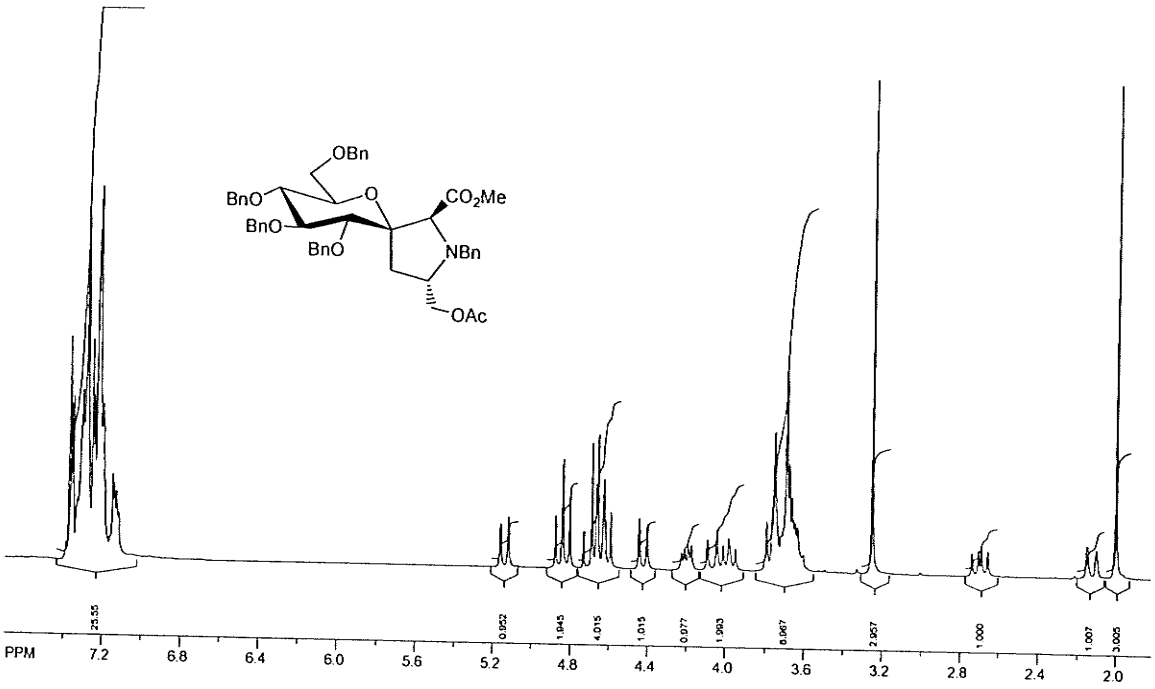
OBn
BnO
BnO
BnO
O
CO2Me
NBn
OAc
PPM
7.2
6.8
6.4
6.0
5.6
5.2
4.8
4.4
4.0
3.6
3.2
2.8
2.4
2.0

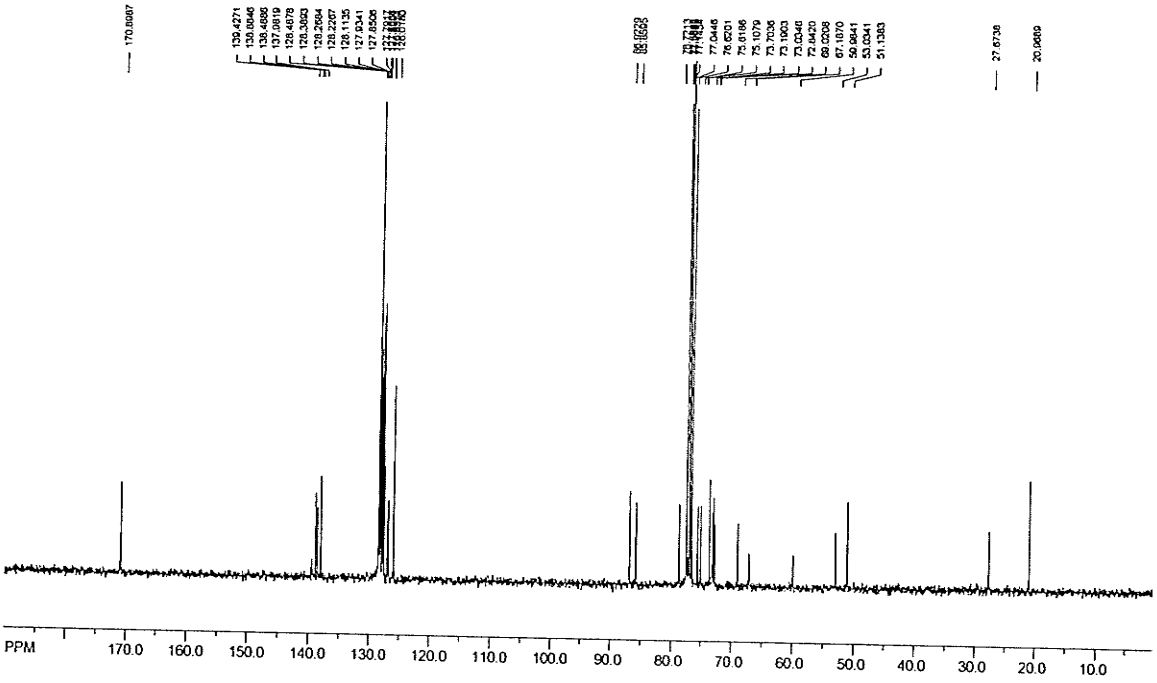
PPM
170.0
160.0
150.0
140.0
130.0
120.0
110.0
100.0
90.0
80.0
70.0
60.0
50.0
40.0
30.0
20.0
10.0

Compound **10**

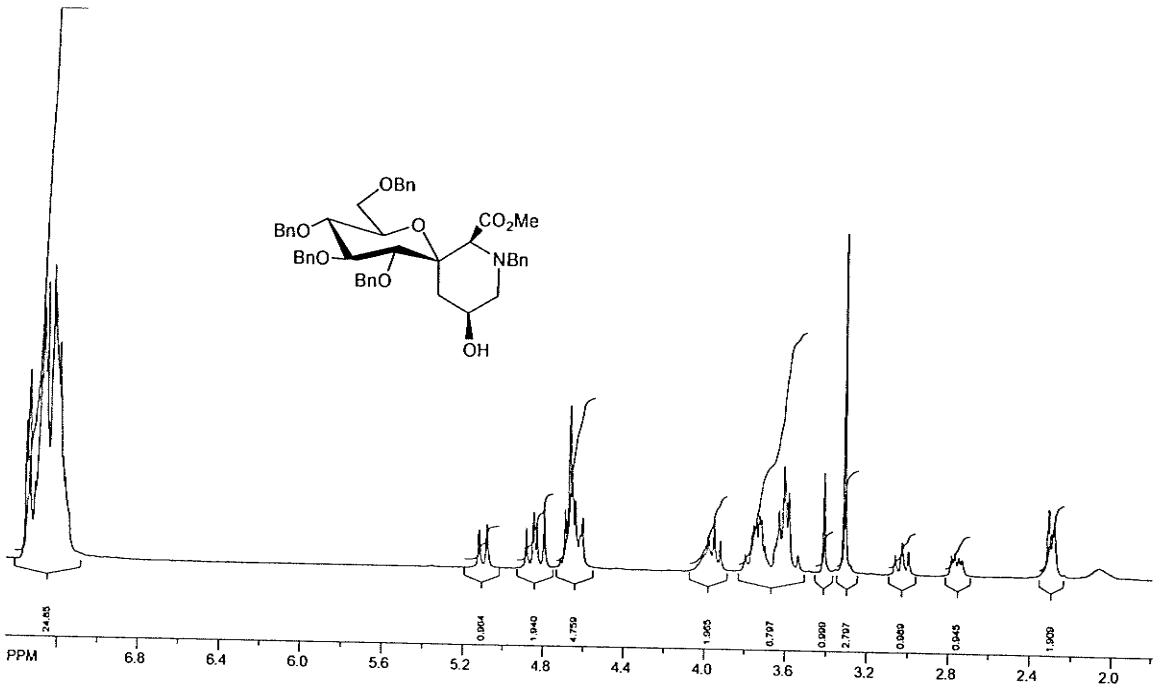
OBn
BnO
BnO
BnO
O
CO2Me
NBn
OH
24.85
0.864
1.940
4.759
1.965
0.797
0.990
2.797
0.869
0.945
1.909
PPM
6.8
6.4
6.0
5.6
5.2
4.8
4.4
4.0
3.6
3.2
2.8
2.4
2.0

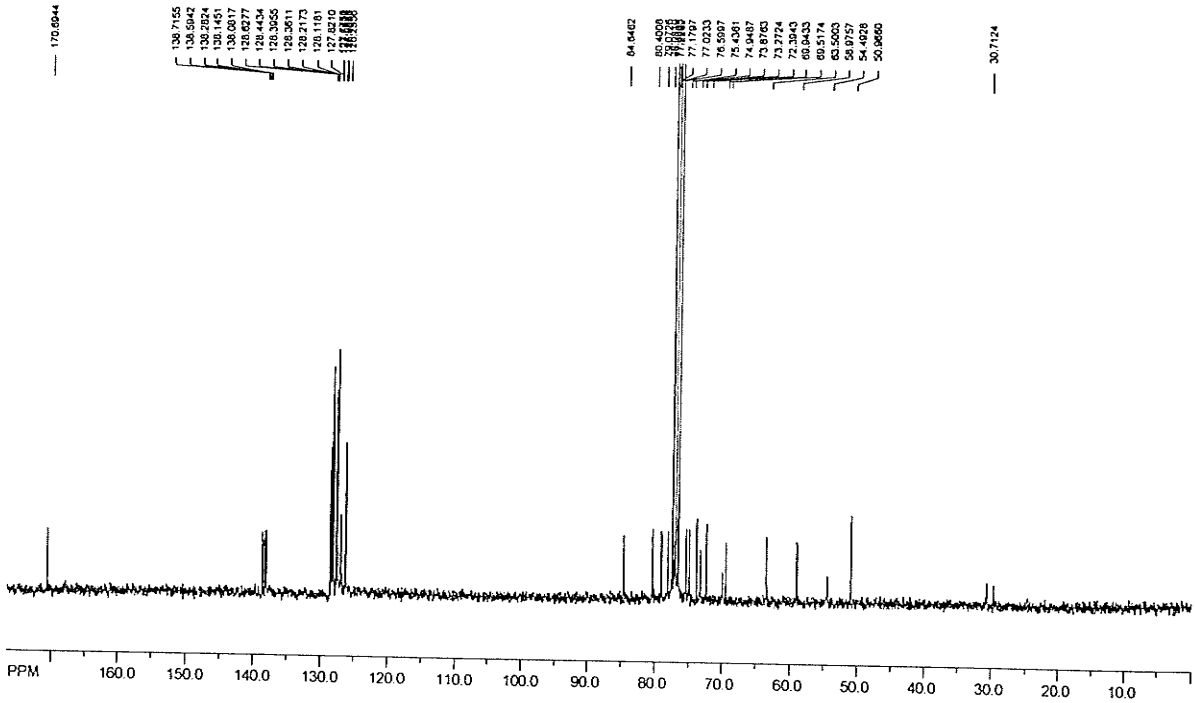
170.6944
138.7155
138.5942
138.2824
138.1451
138.0017
128.6277
128.4434
128.3955
128.3611
128.2173
128.1181
127.8210
84.5462
80.4008
79.0758
77.3203
77.1797
77.0233
76.5997
75.4361
74.9487
73.8763
73.2724
72.3943
69.8433
69.5174
63.5003
58.9757
54.4928
50.9660
30.7124
PPM
160.0
150.0
140.0
130.0
120.0
110.0
100.0
90.0
80.0
70.0
60.0
50.0
40.0
30.0
20.0
10.0

Compound **15**

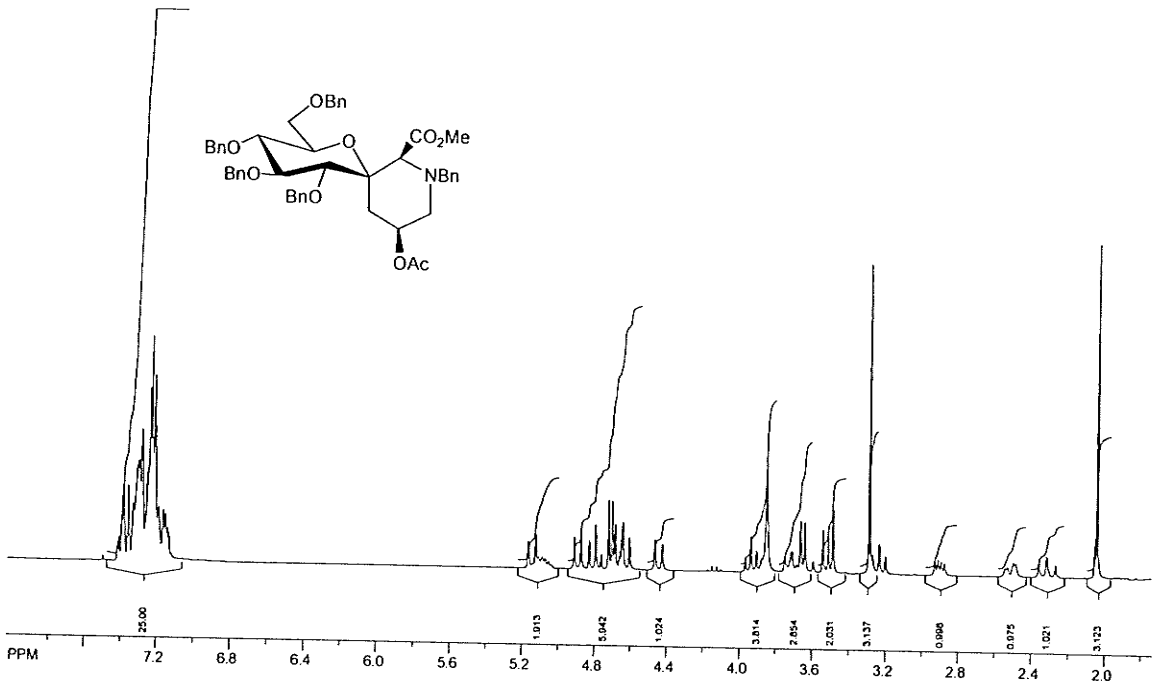
OBn
BnO
BnO
BnO
O
CO2Me
NBn
OAc
25.00
1.913
5.042
1.024
3.814
2.854
2.031
3.137
0.998
0.975
1.021
3.123
PPM
7.2
6.8
6.4
6.0
5.6
5.2
4.8
4.4
4.0
3.6
3.2
2.8
2.4
2.0

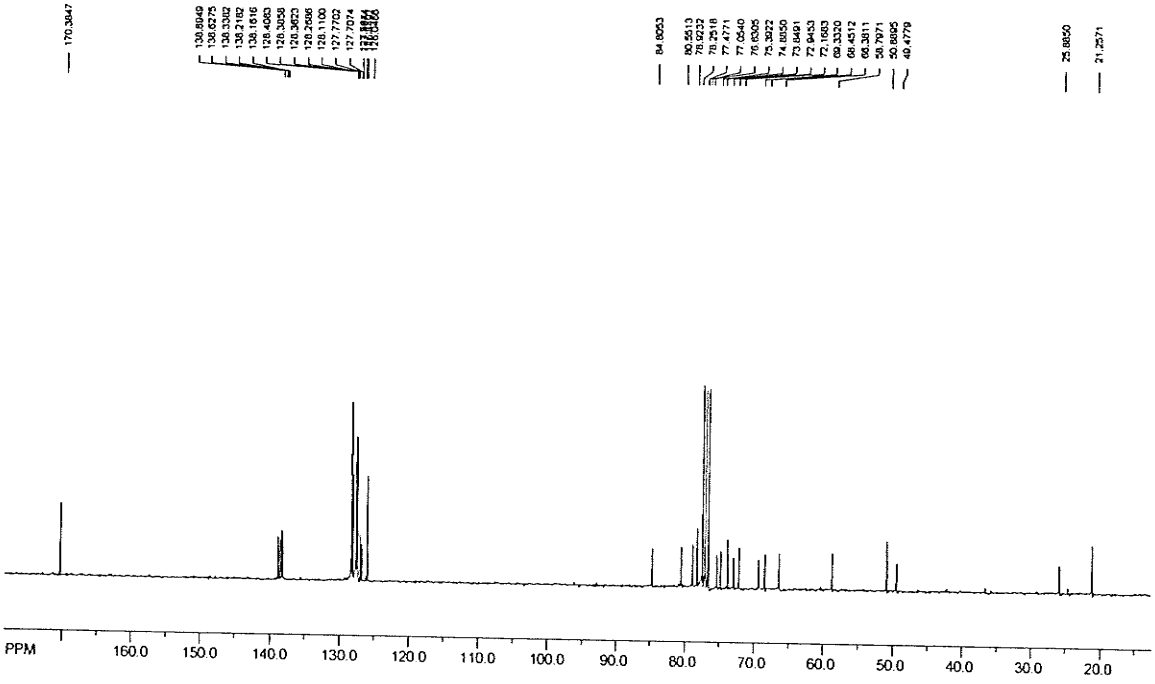
170.3847
130.8049
130.6275
130.3302
130.2182
128.1816
128.4083
128.3058
128.3623
128.2986
128.1100
127.7702
127.7074
84.8553
80.5513
78.9232
78.2518
77.4771
77.0540
76.6305
75.3922
74.6850
73.6491
72.9453
72.1503
69.3320
68.4512
68.3811
50.7971
50.8895
40.4779
25.8850
21.2571
PPM
160.0
150.0
140.0
130.0
120.0
110.0
100.0
90.0
80.0
70.0
60.0
50.0
40.0
30.0
20.0

Compound **11**

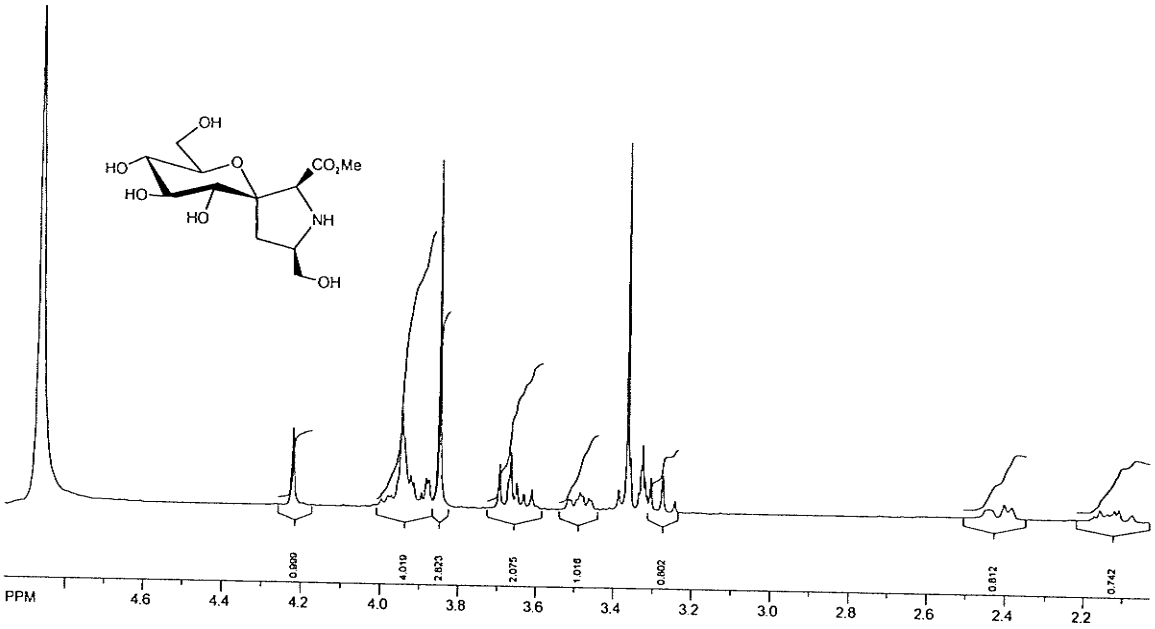
OH
HO
HO
HO
O
CO2Me
NH
OH
0.999
4.019
2.823
2.075
1.016
0.802
0.812
0.742
PPM
4.6
4.4
4.2
4.0
3.8
3.6
3.4
3.2
3.0
2.8
2.6
2.4
2.2

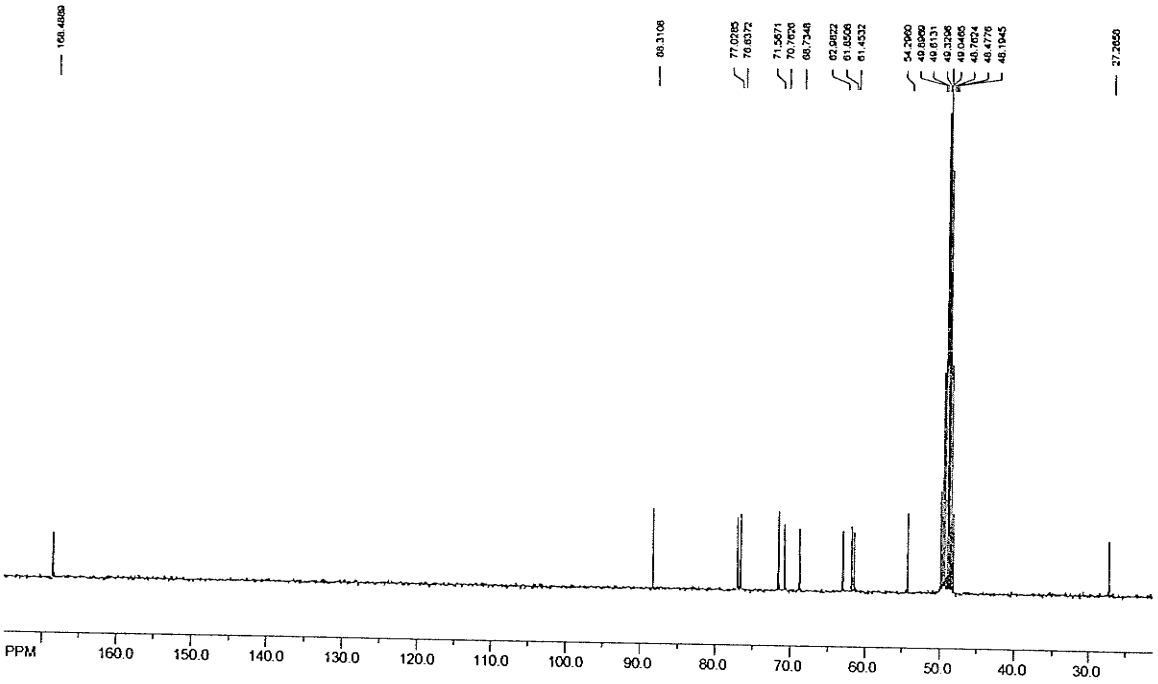
160.4889
69.3106
77.0285
70.6372
71.5671
70.7670
68.7348
62.9822
61.8506
61.4532
54.7960
49.6611
49.3298
49.0465
48.7624
48.4778
48.1945
27.2650
PPM
160.0
150.0
140.0
130.0
120.0
110.0
100.0
90.0
80.0
70.0
60.0
50.0
40.0
30.0

Compound **12**

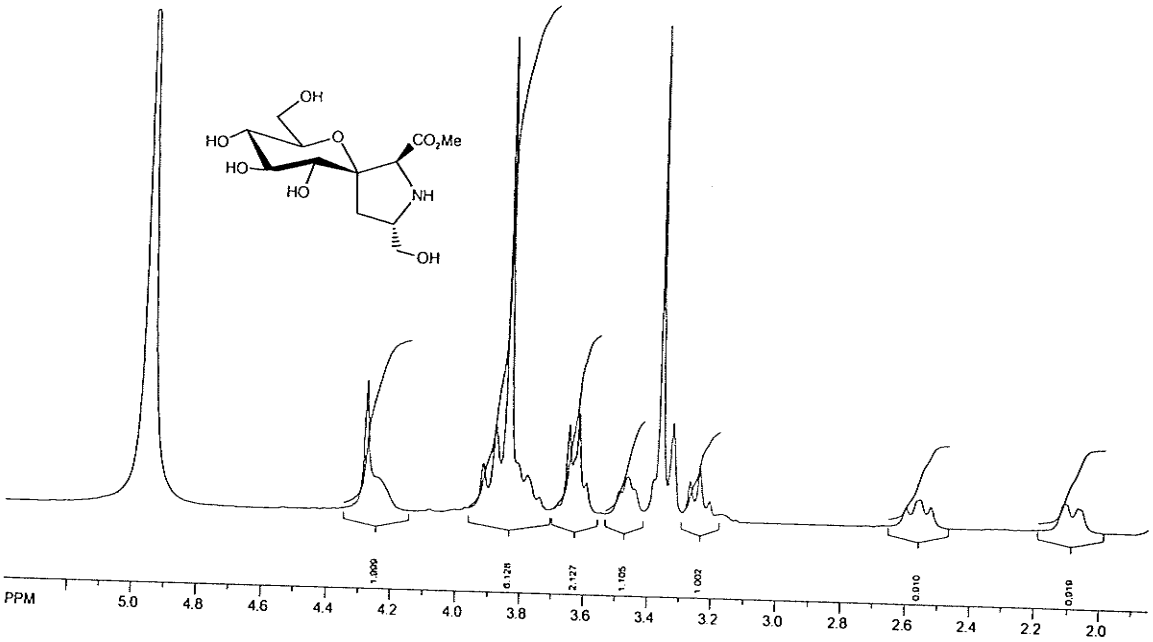
OH
HO
HO
HO
O
CO2Me
NH
OH
1.000
0.128
2.127
1.105
1.002
0.010
0.019
PPM
5.0
4.8
4.6
4.4
4.2
4.0
3.8
3.6
3.4
3.2
3.0
2.8
2.6
2.4
2.2
2.0

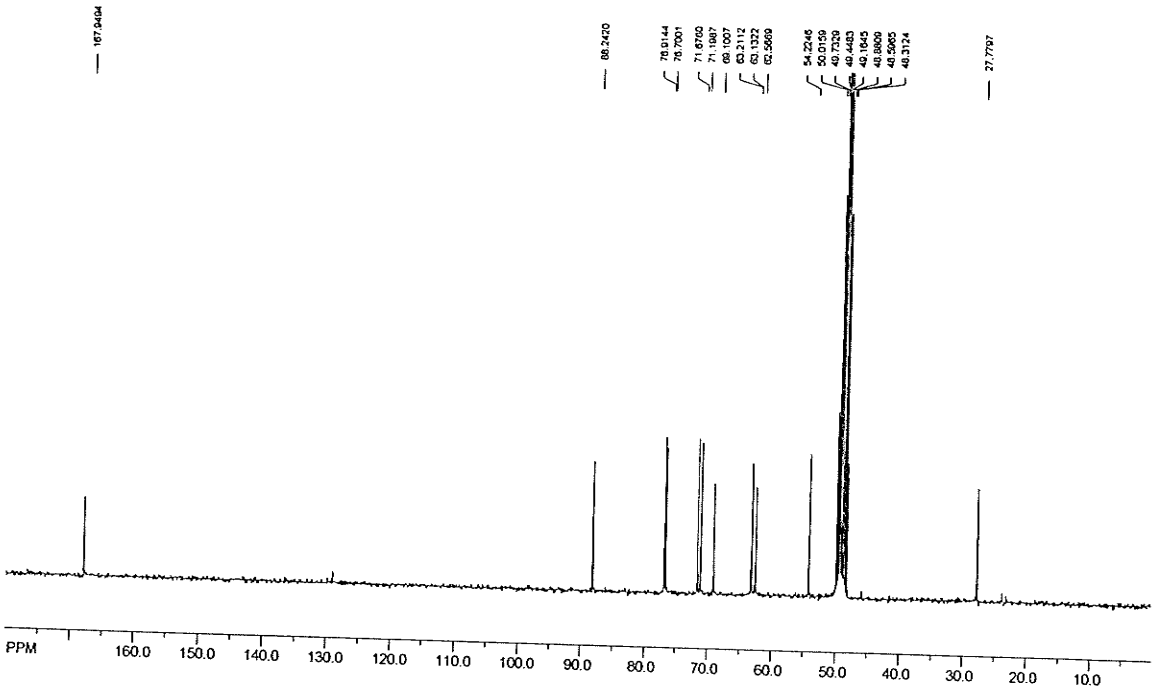
167.0494
88.2420
78.9144
78.7001
71.6700
71.1987
69.1007
63.2112
63.1322
62.3669
54.2246
50.0159
49.7739
49.4833
49.1645
48.8909
48.5965
48.3124
27.7797
PPM
160.0
150.0
140.0
130.0
120.0
110.0
100.0
90.0
80.0
70.0
60.0
50.0
40.0
30.0
20.0
10.0

9.1.2. 1D nOe spectrum for compound 4

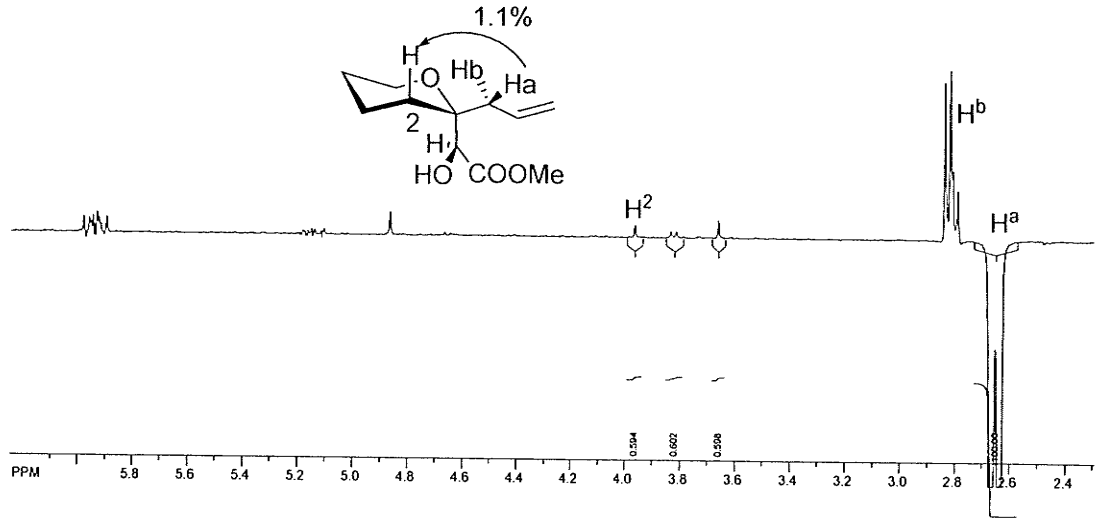

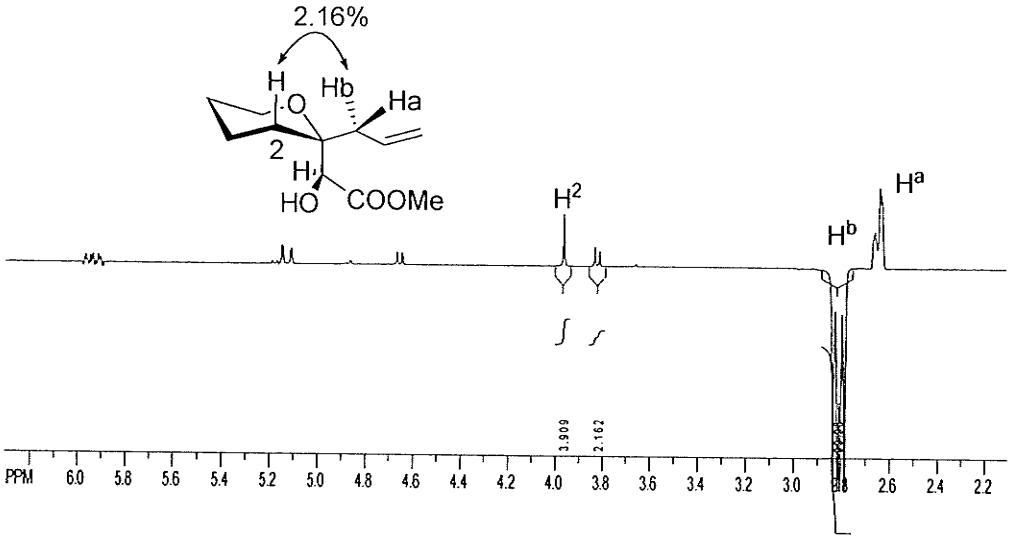

1D nOe spectrum for compound 5

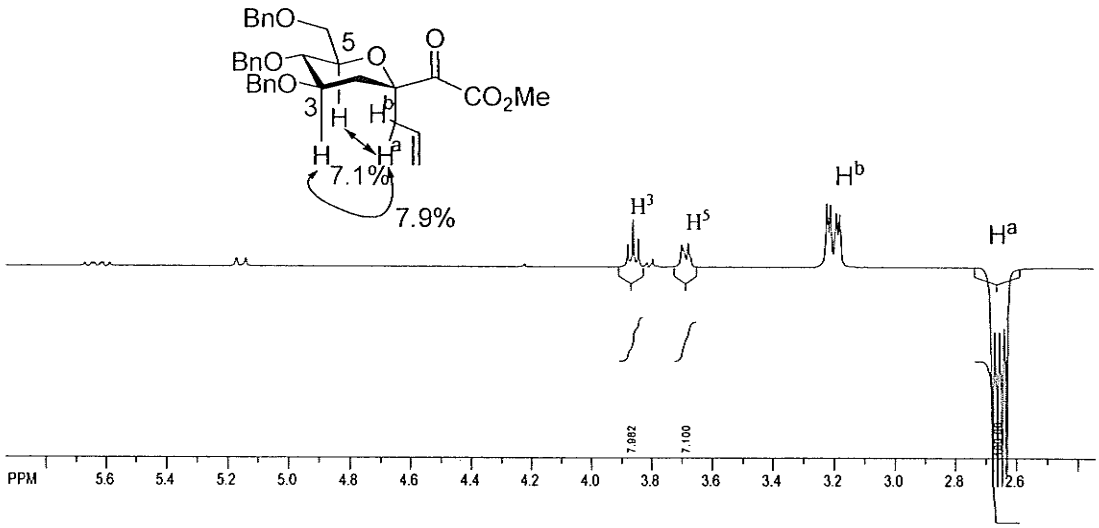

Confirmation of stereochemistry at C-2′ and C-5′ positions in compound 15

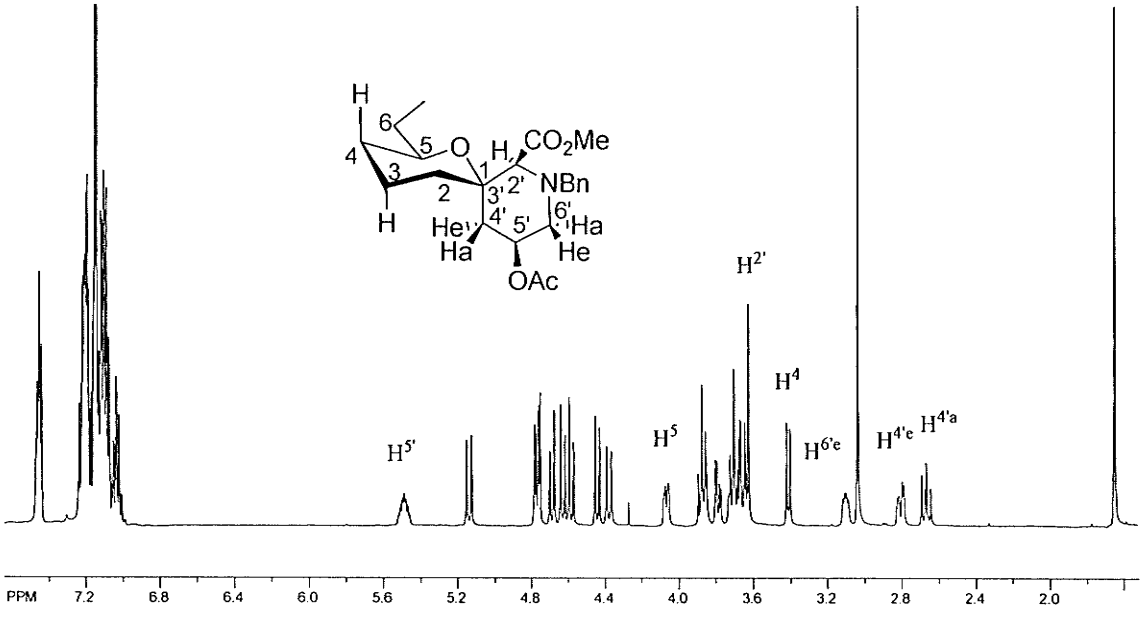

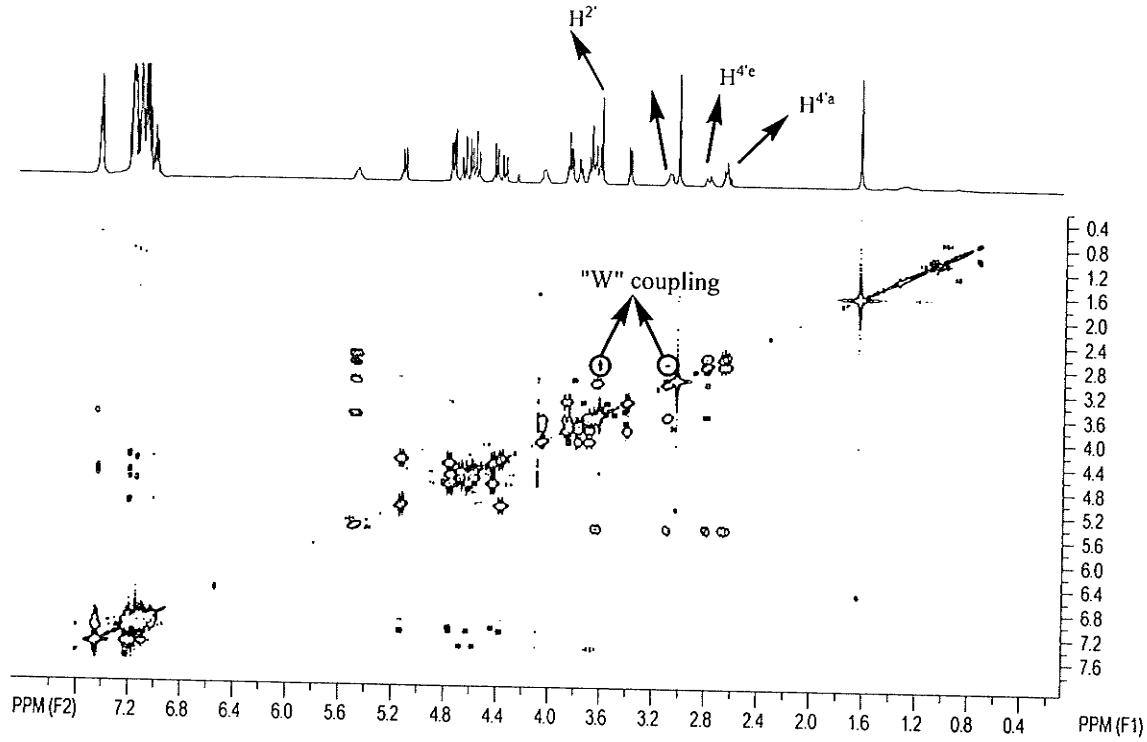
H2'
H4'e
H4'a
"W" coupling
PPM (F2)
PPM (F1)

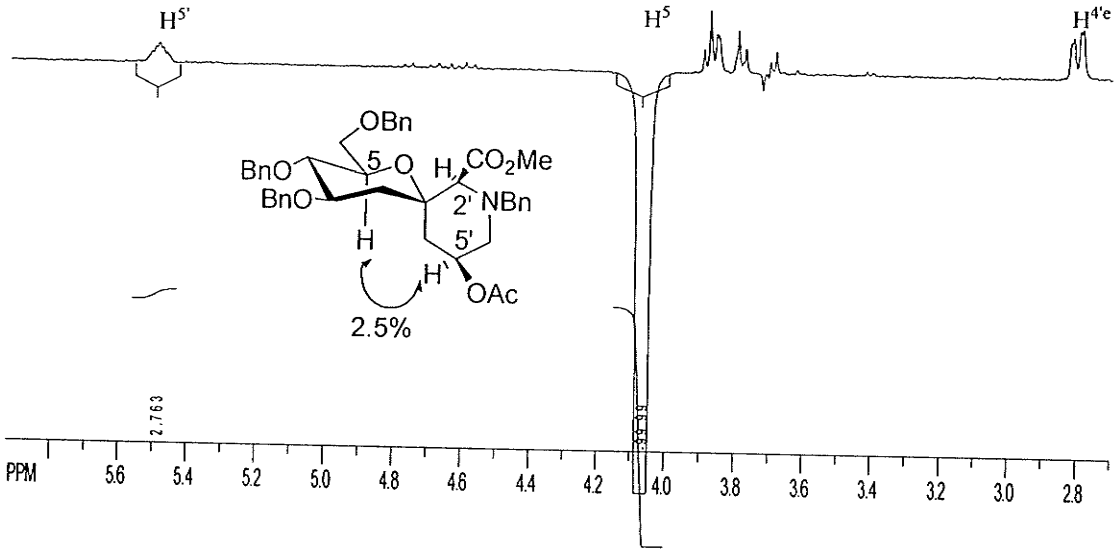
H5'
H5
H4'e
OBn
BnO
BnO
5
O
H
CO2Me
2'
NBn
5'
H
H`
OAc
2.5%
PPM

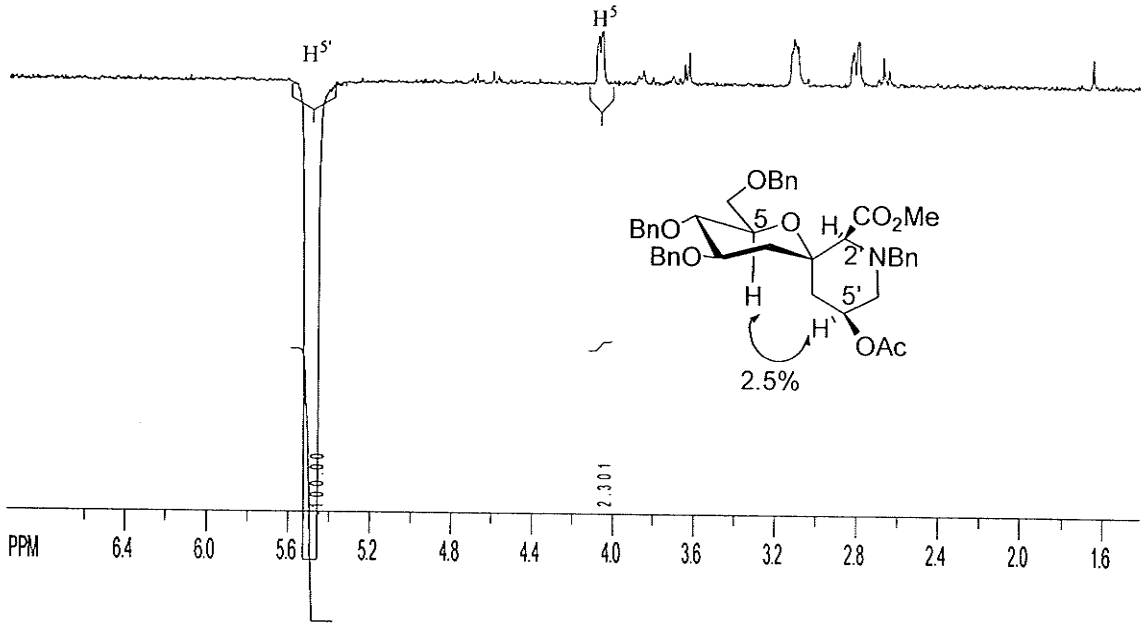

Stereochemistry at C-4′ position in compound 13

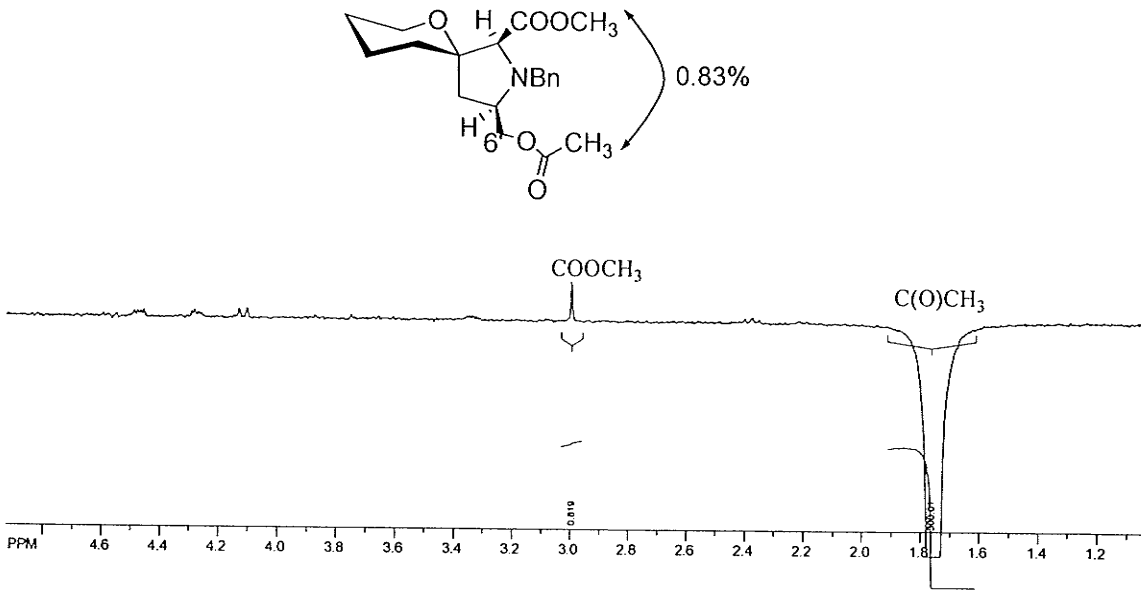

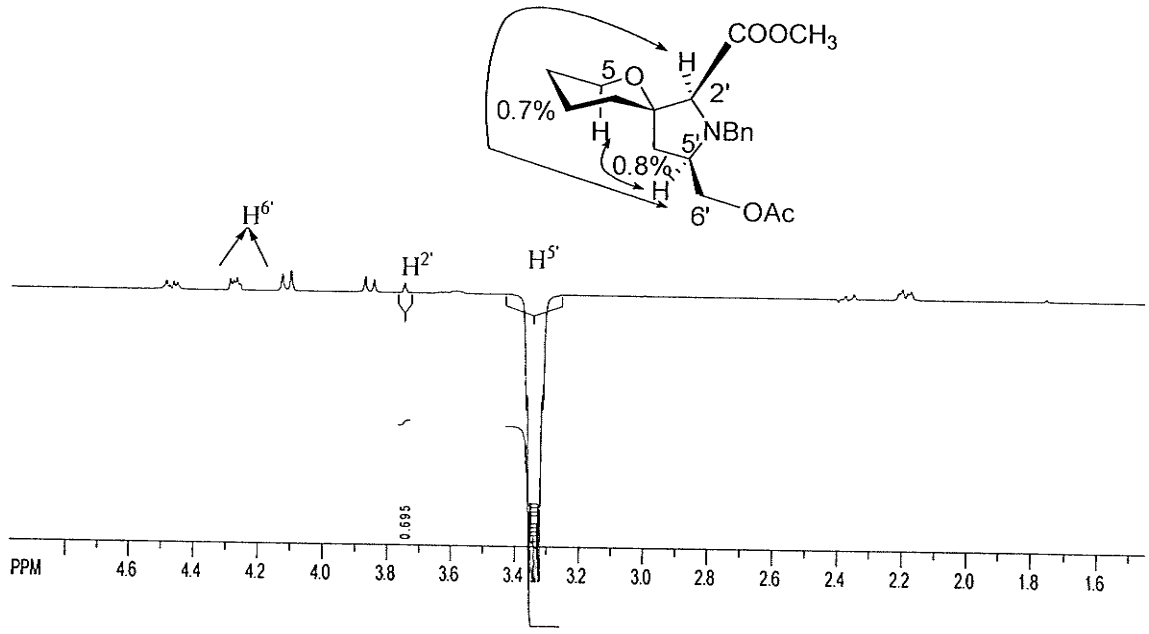

Stereochemistry at C-4′ position in compound 14

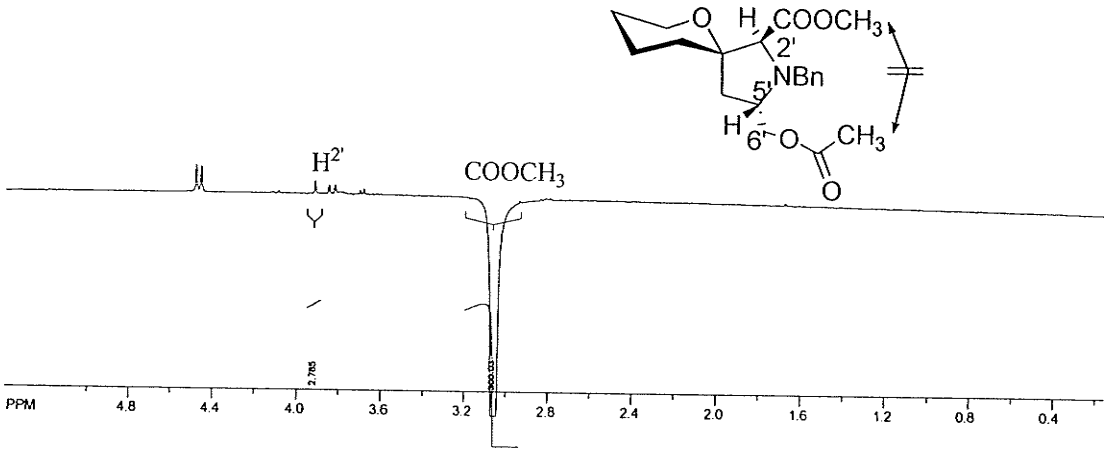

9.2. SI for Chapter 4

9.2.1. Synthetic procedure for compounds 7 and 8

(1*S*)-2,3,4,6-Tetrahydroxy-1′-*N*-acetyl-5′(*S*)-hydroxymethylene-spiro[1,5-anhydro-D-glucitol-1,3′-*L*-proline methylamide] (7). Compound **3** (25 mg, 0.07 mmol) was dissolved in a solution of methylamine in absolute ethanol (4 mL, 33% wt), which is purchased from Aldrich, and stirred for 18 hours at room temperature. The mixture was concentrated and purified by the flash column chromatography (dichloromethane/ methanol: 2/1) to get compound **7** as a colorless oil (23 mg, 95%)

(1*S*)-2,3,4,6-Tetrahydroxy-1′-*N*-acetyl-5′(*R*)-hydroxymethylene-spiro[1,5-anhydro-D-glucitol-1,3′-*L*-proline methylamide] (**8**). Compound **4** (30 mg, 0.09 mmol) was dissolved in a solution of methylamine in absolute ethanol (4.5 mL, 33% wt) and stirred for 18 hours at room temperature. The mixture was concentrated and purified by the flash column chromatography (dichloromethane/ methanol: 2/1) to get compound **8** as a colorless oil (28 mg, 93%)

9.2.2 ^{1}H and ^{13}C NMR spectra for compound 3-8 in D_2O

Compound **3**

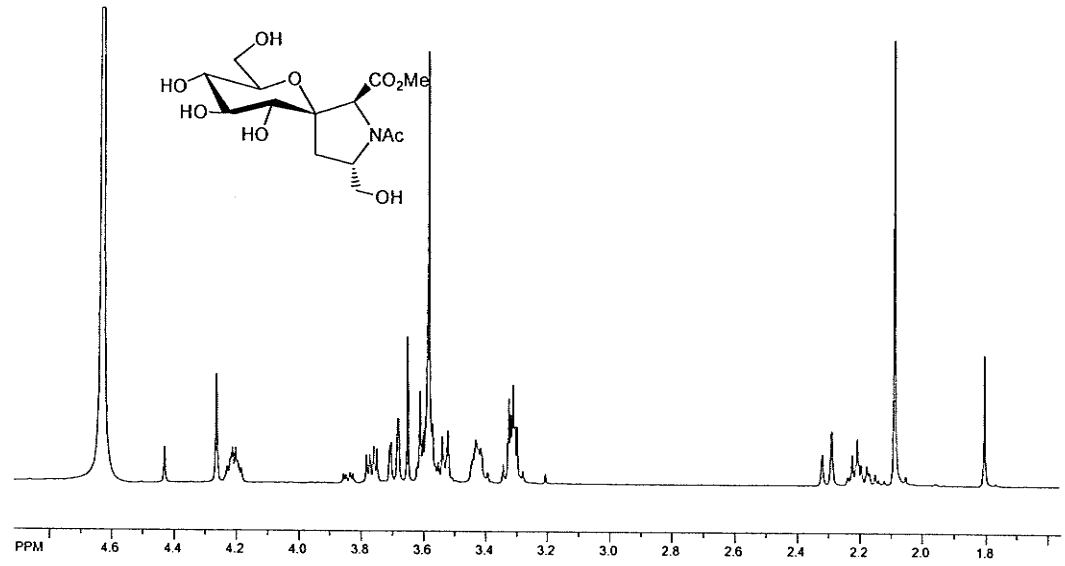

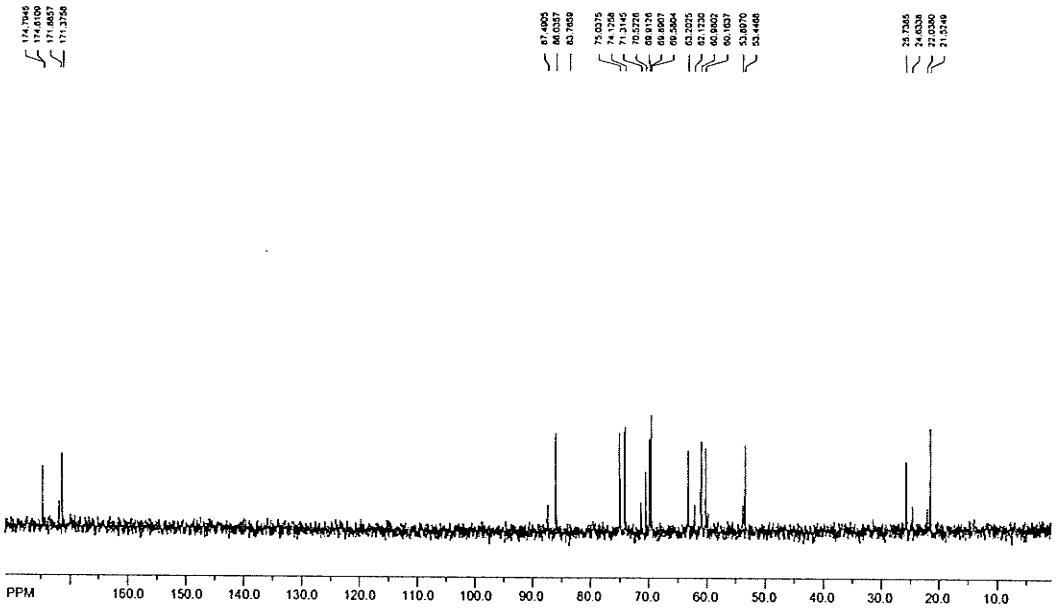

Compound **4**

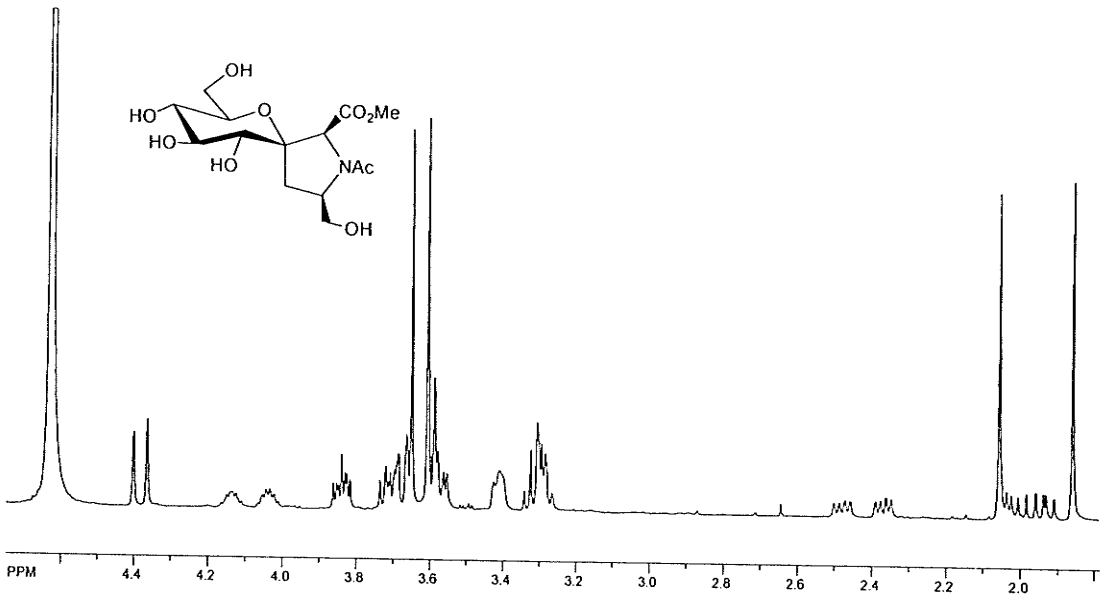
OH
HO
HO
HO
O
CO2Me
NAc
OH
PPM
4.4
4.2
4.0
3.8
3.6
3.4
3.2
3.0
2.8
2.6
2.4
2.2
2.0

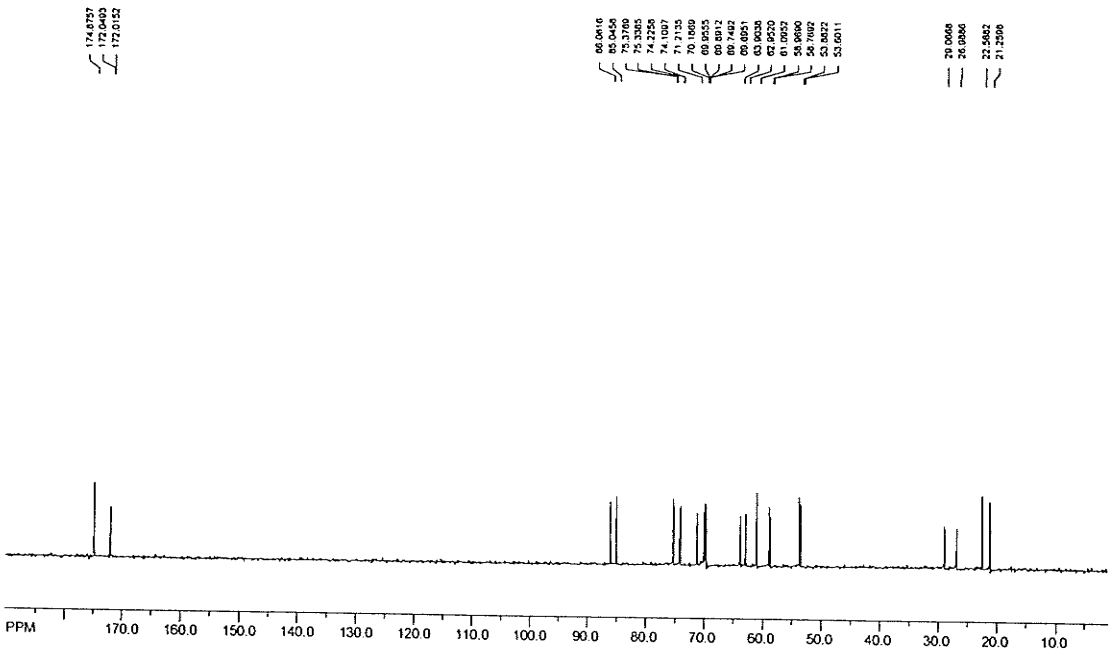
174.8757
172.5493
172.0152
66.0616
65.0456
75.3760
75.3385
74.2256
74.1097
71.2135
70.1869
69.9555
69.8912
69.7424
69.6051
63.9035
62.9520
61.0052
58.9690
58.7692
53.8822
53.6011
29.0068
26.9886
22.5882
21.2596
PPM
170.0
160.0
150.0
140.0
130.0
120.0
110.0
100.0
90.0
80.0
70.0
60.0
50.0
40.0
30.0
20.0
10.0

Compound **5**

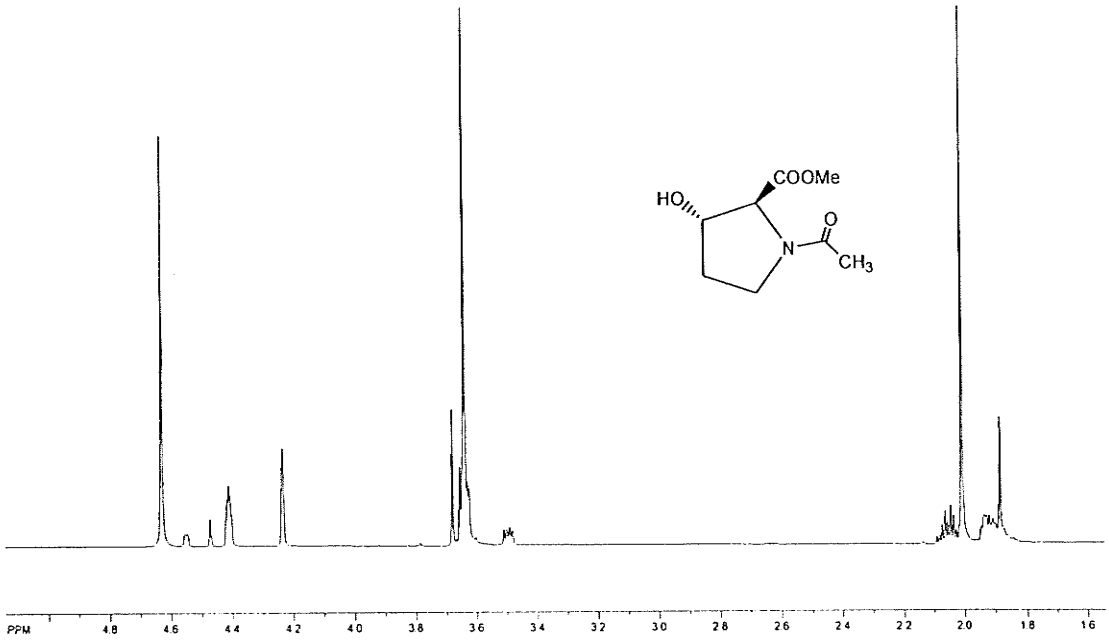
COOMe
HO
O
N
CH3
PPM
4.8
4.6
4.4
4.2
4.0
3.8
3.6
3.4
3.2
3.0
2.8
2.6
2.4
2.2
2.0
1.8
1.6

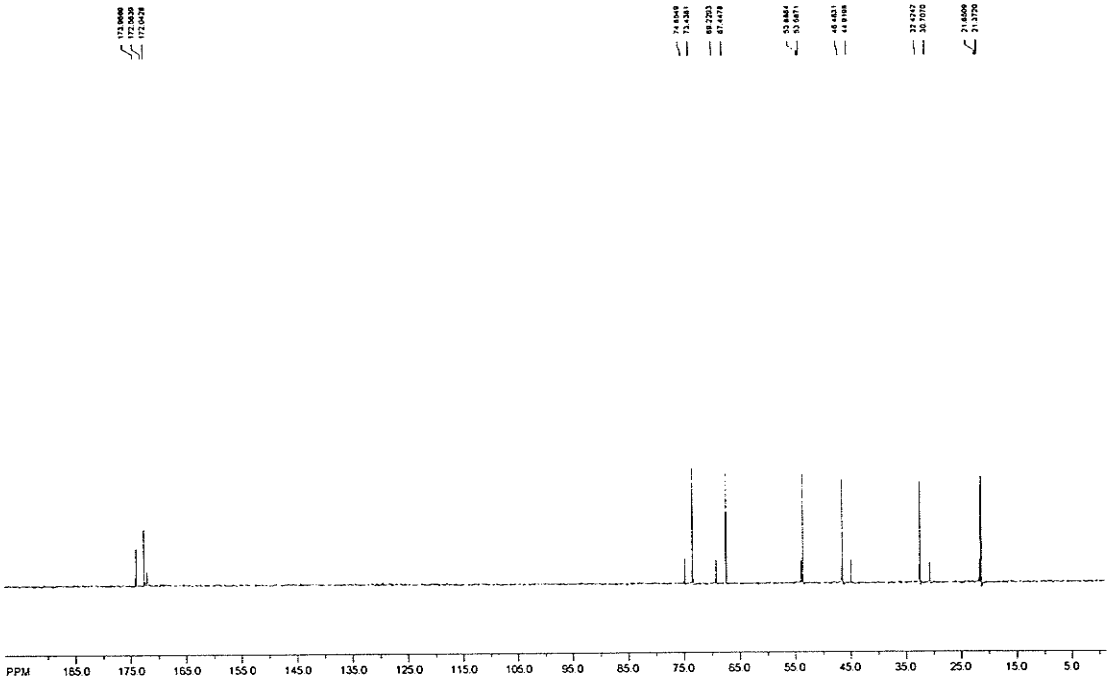
PPM
185.0
175.0
165.0
155.0
145.0
135.0
125.0
115.0
105.0
95.0
85.0
75.0
65.0
55.0
45.0
35.0
25.0
15.0
5.0

Compound **6**

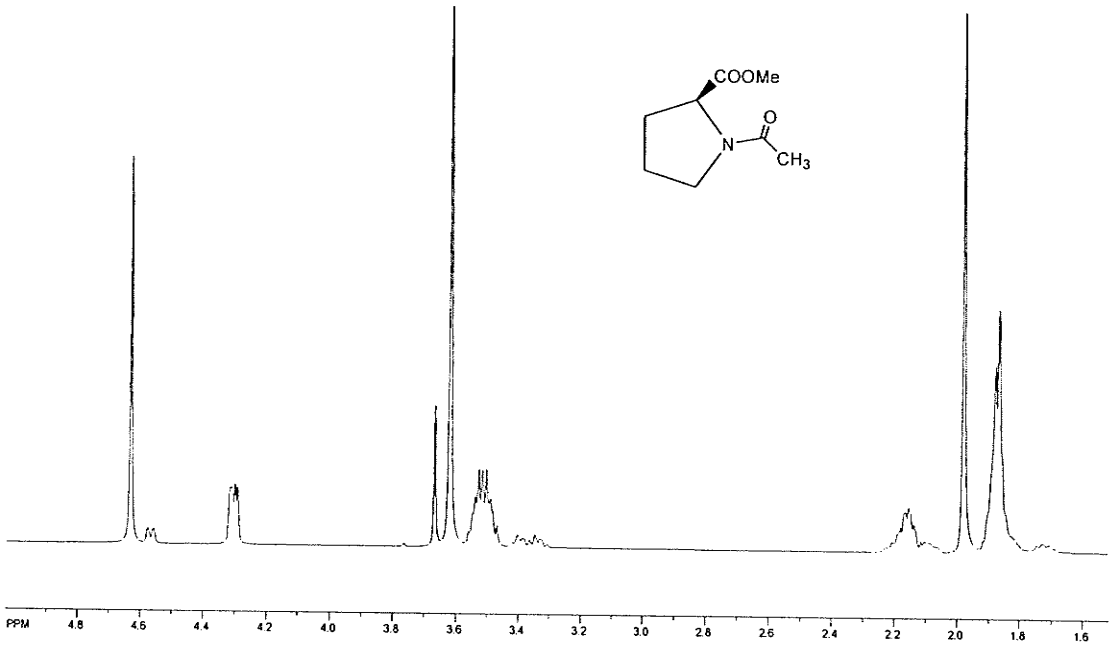
COOMe
O
N
CH3
PPM
4.8
4.6
4.4
4.2
4.0
3.8
3.6
3.4
3.2
3.0
2.8
2.6
2.4
2.2
2.0
1.8
1.6

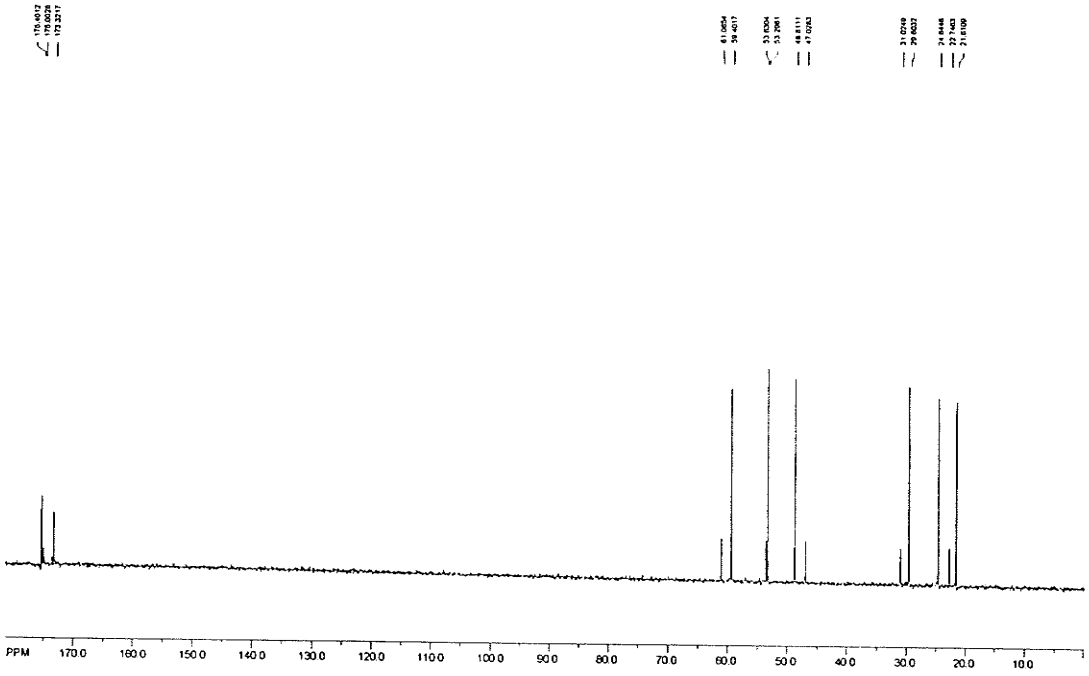
PPM
170.0
160.0
150.0
140.0
130.0
120.0
110.0
100.0
90.0
80.0
70.0
60.0
50.0
40.0
30.0
20.0
10.0

Compound 7

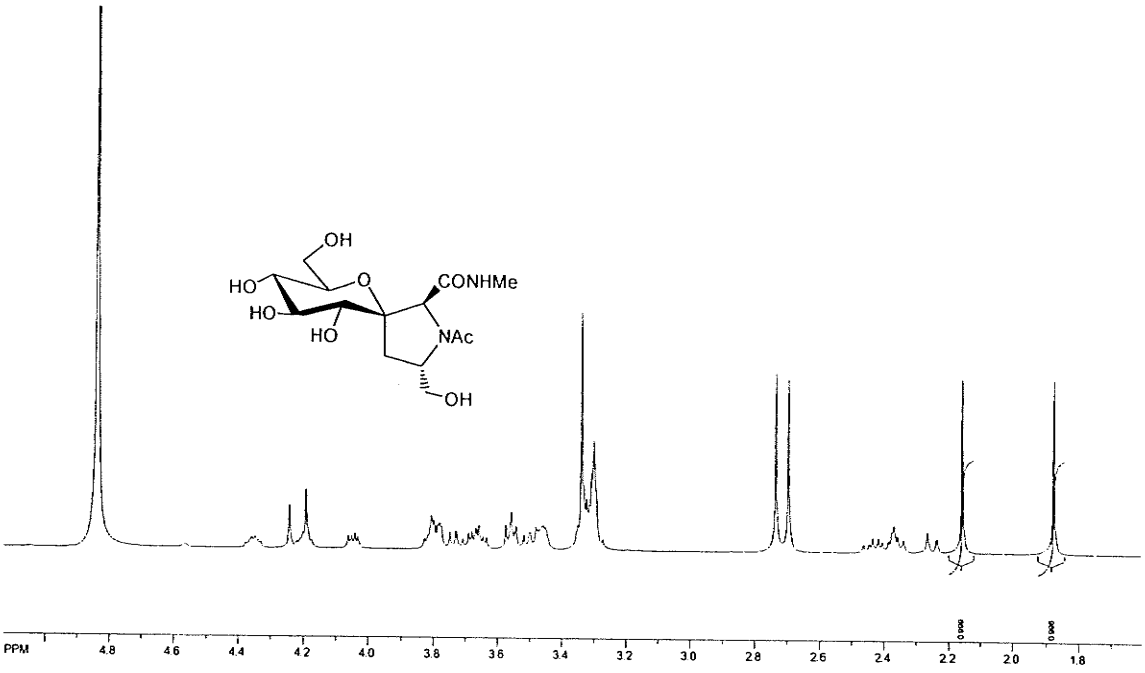
OH
HO
O
CONHMe
HO
NAc
HO
OH
PPM
4.8
4.6
4.4
4.2
4.0
3.8
3.6
3.4
3.2
3.0
2.8
2.6
2.4
2.2
2.0
1.8

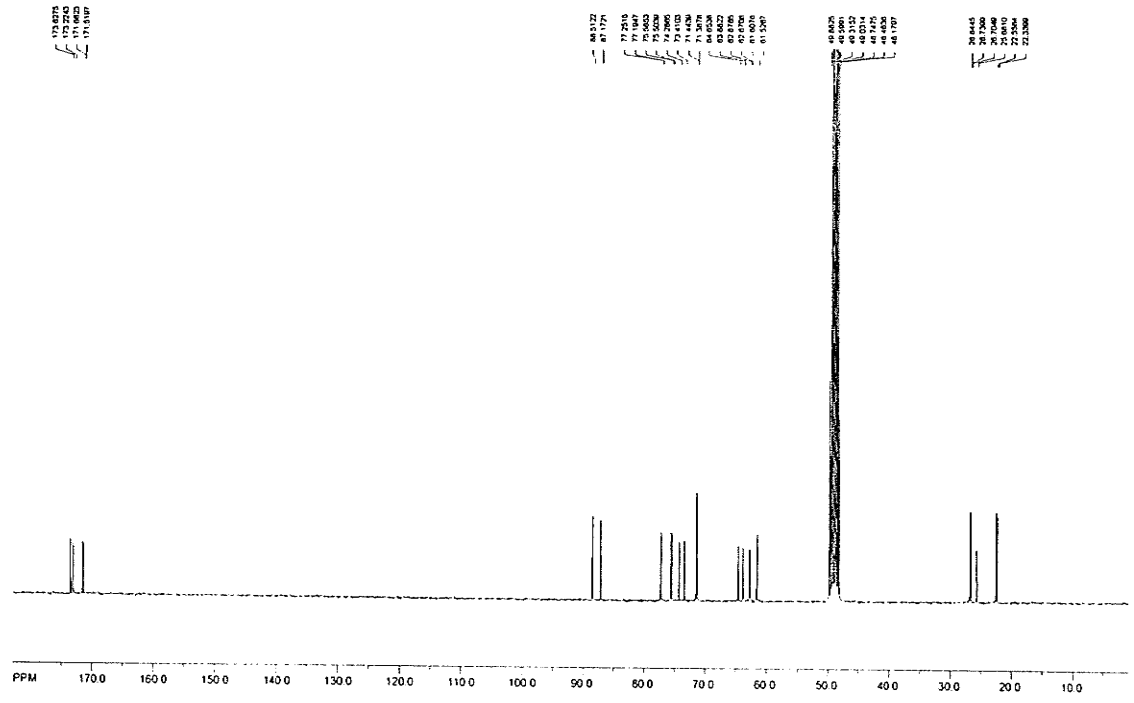
PPM
170.0
160.0
150.0
140.0
130.0
120.0
110.0
100.0
90.0
80.0
70.0
60.0
50.0
40.0
30.0
20.0
10.0

Compound **8**

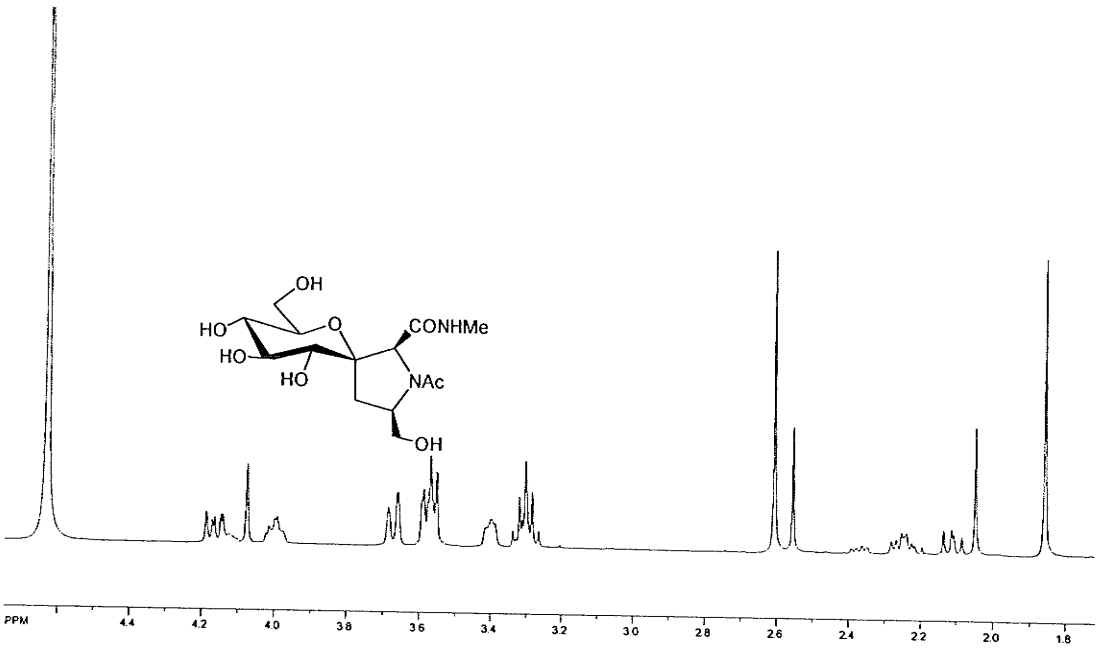
OH
HO
O
CONHMe
HO
NAc
HO
OH
PPM
4.4
4.2
4.0
3.8
3.6
3.4
3.2
3.0
2.8
2.6
2.4
2.2
2.0
1.8

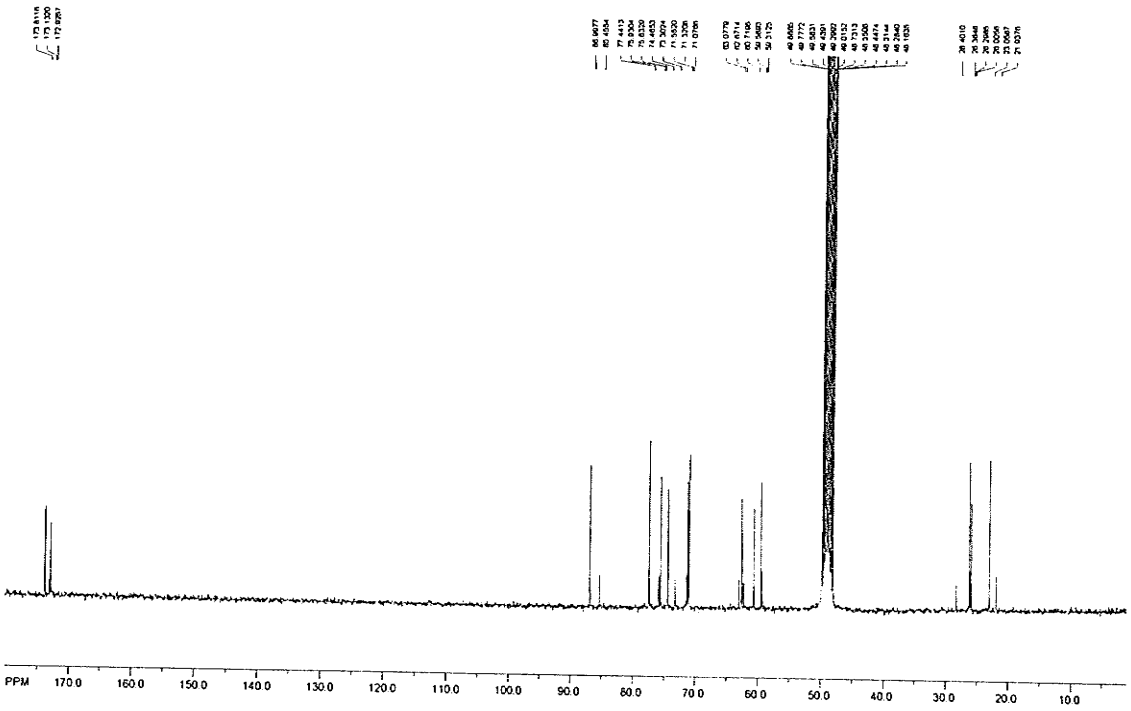
PPM
170.0
160.0
150.0
140.0
130.0
120.0
110.0
100.0
90.0
80.0
70.0
60.0
50.0
40.0
30.0
20.0
10.0

9.2.3. Assignment of *cis* and *trans* rotamers of compounds 3, 4, 7 and 8 through 1D nOe experiments

Compound **3** in CD_3OD

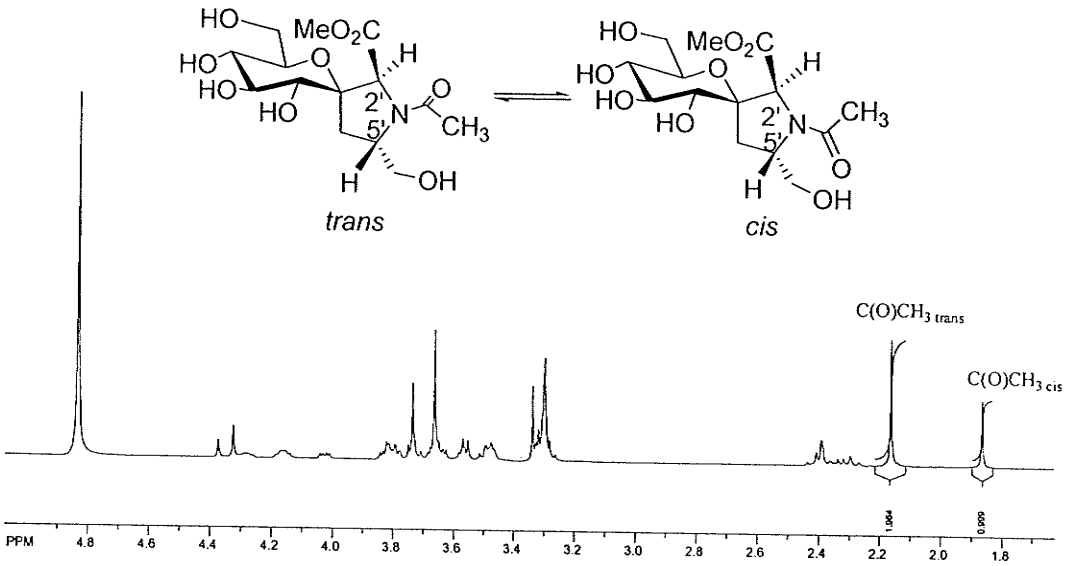

1D nOe spectrum

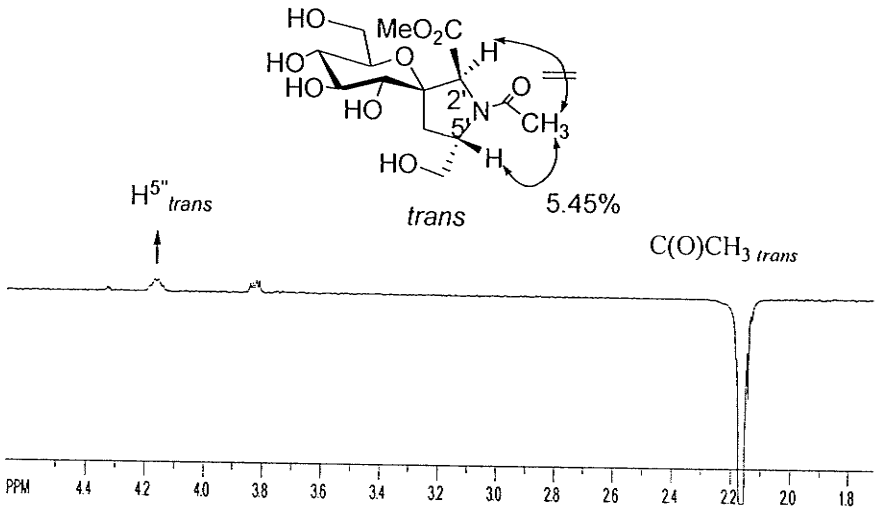

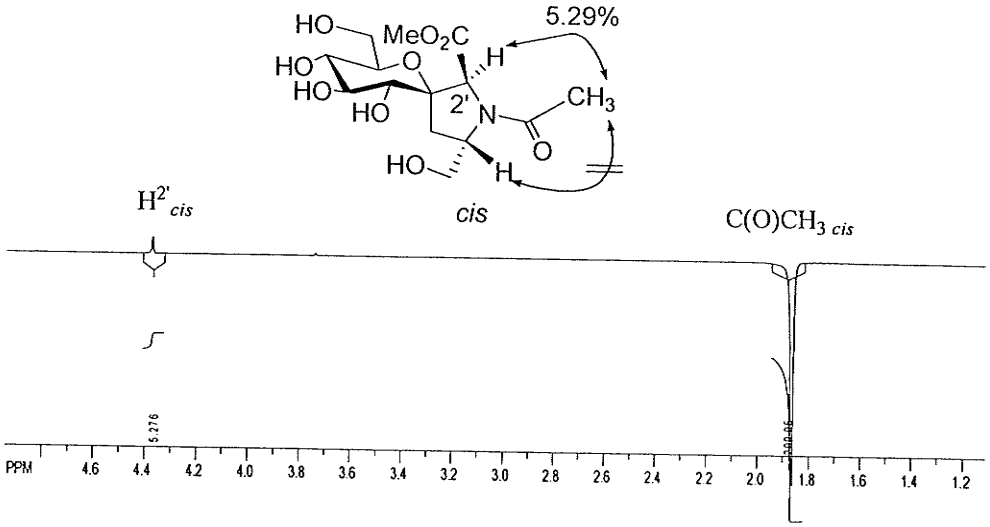

Different Chemical shift of C-2′ (α-carbon) for *cis* and *trans* rotamers of compound 3 in CD_3OD (HSQC)

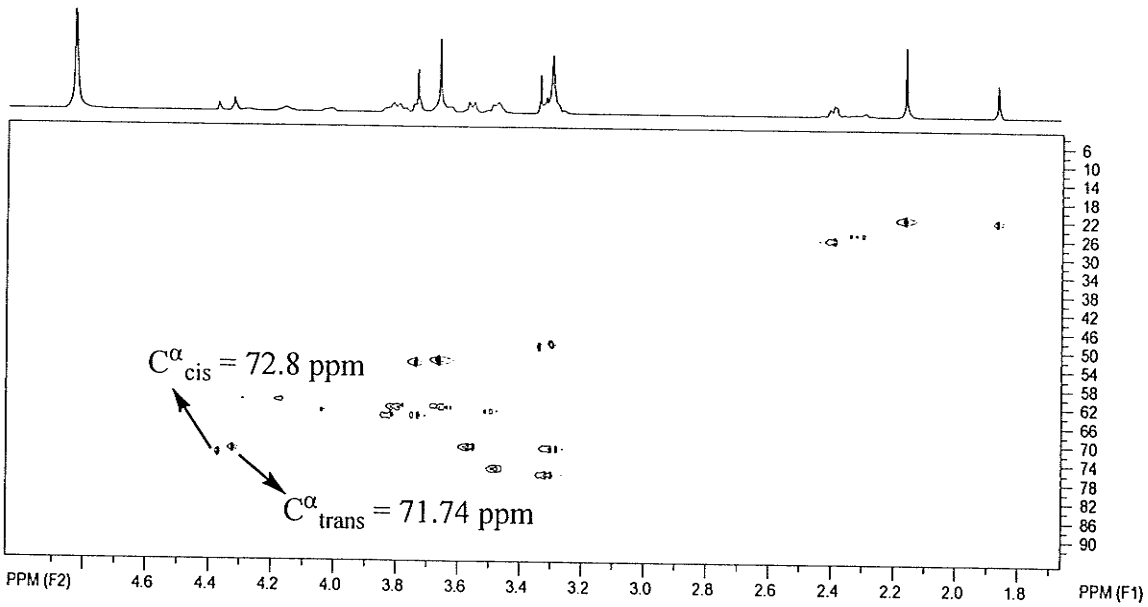

Compound **3** in D_2O

1D nOe spectrum

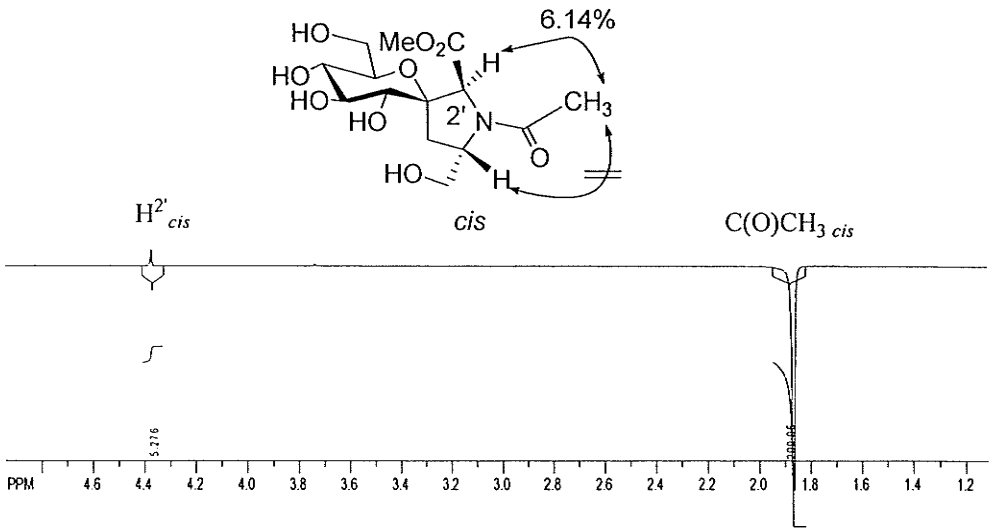

Different chemical shift of C-2′ (α-carbon) for *cis* and *trans* rotamers of compound 3 in D_2O (HSQC)

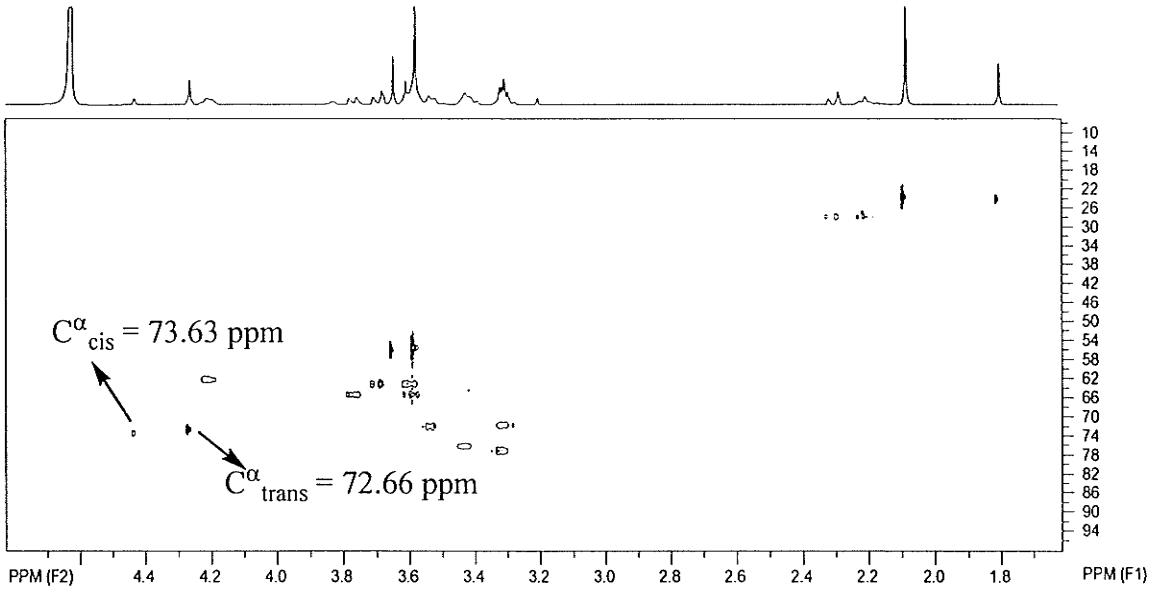

Compound **4** in CD_3OD

^1H NMR spectrum

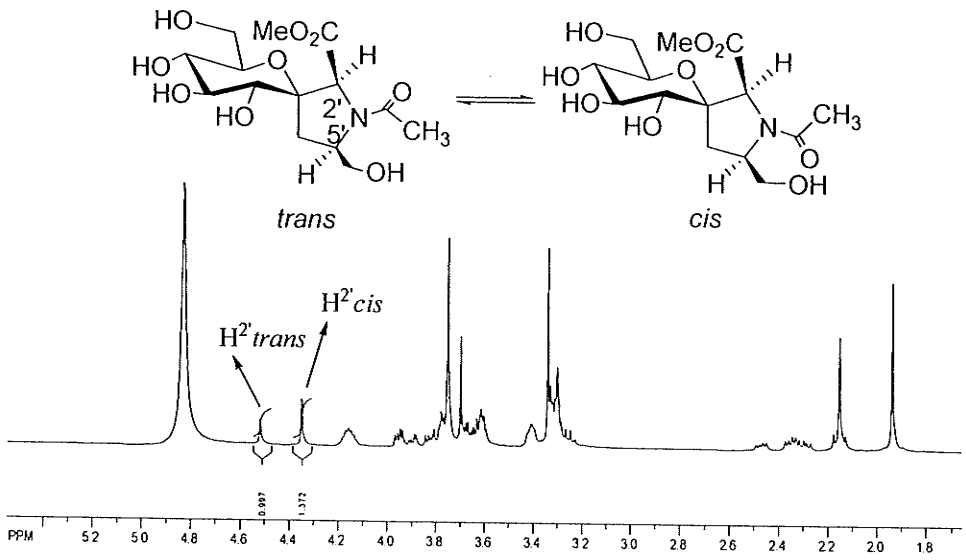

1D nOe spectrum

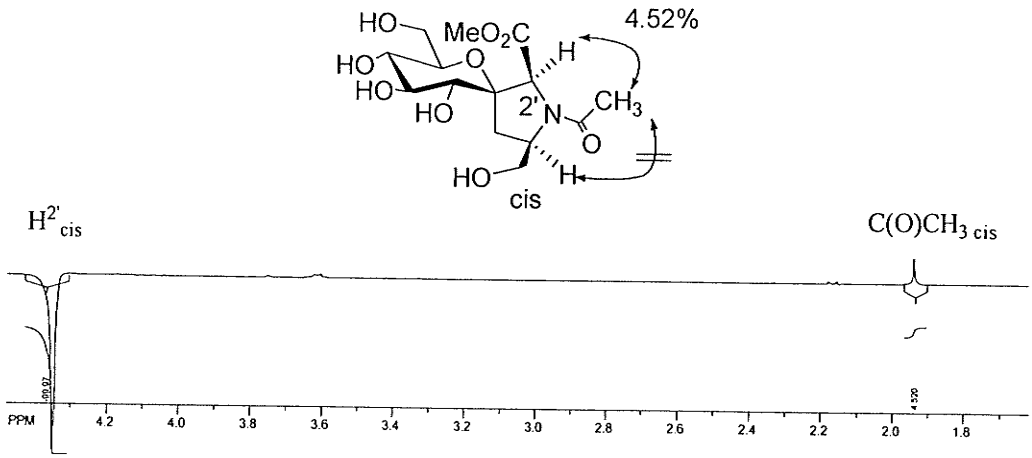

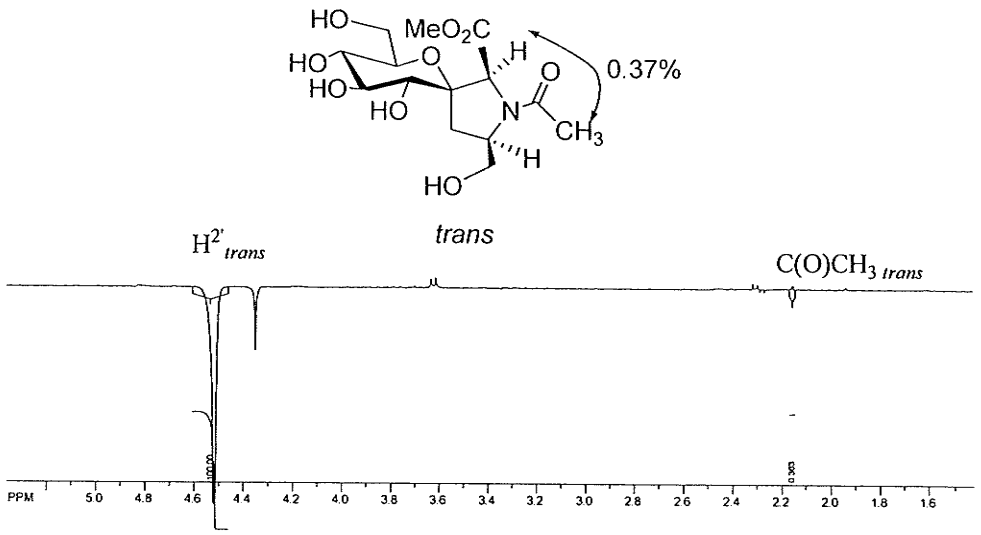

Different chemical shift of C-2′ (α-carbon) for *cis* and *trans* rotamers of compound **4** in CD_3OD (HSQC)

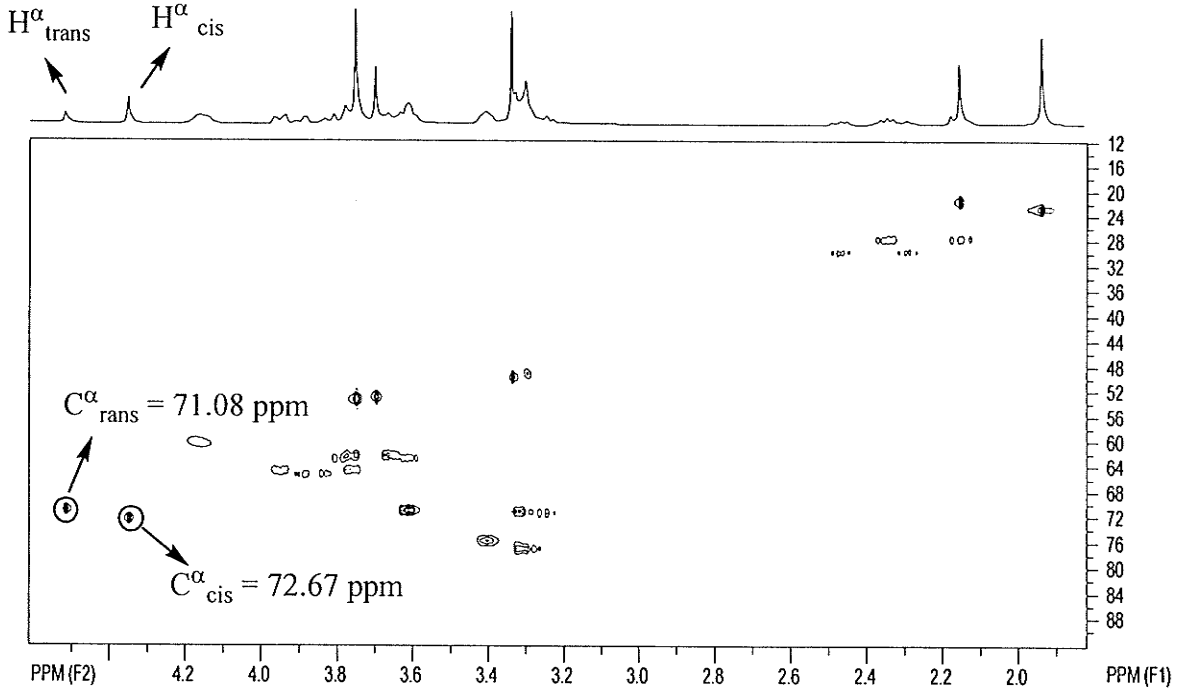

Compound **4** in D_2O

1D nOe spectrum

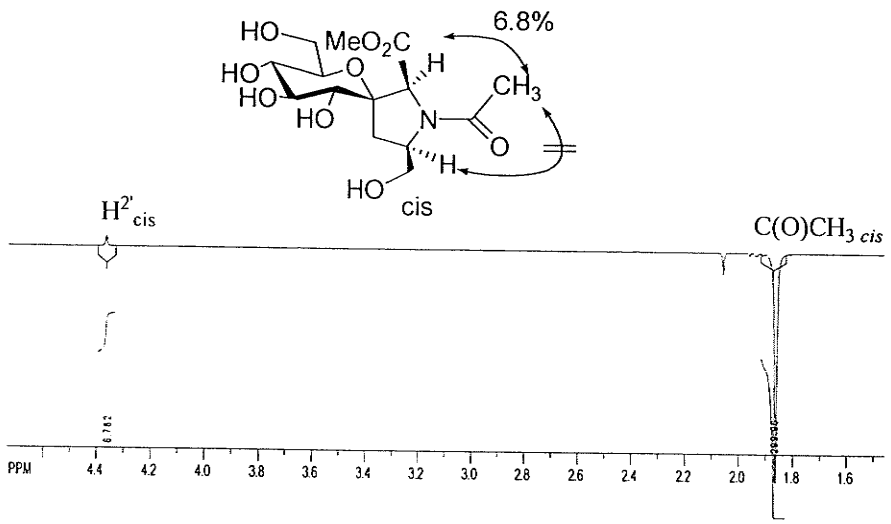

Different chemical shift of C-2′ (α-carbon) for *cis* and *trans* rotamers of compound **4** in D_2O (HSQC)

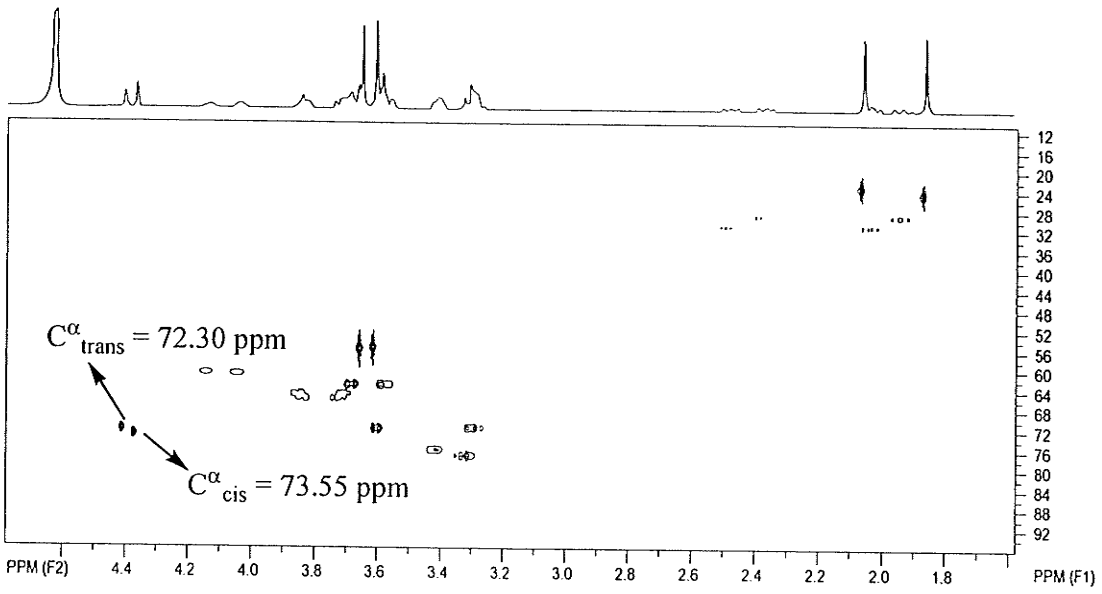

Different chemical shift of α-carbon for *cis* and *trans* rotamers of compound **5** in D_2O (HSQC)

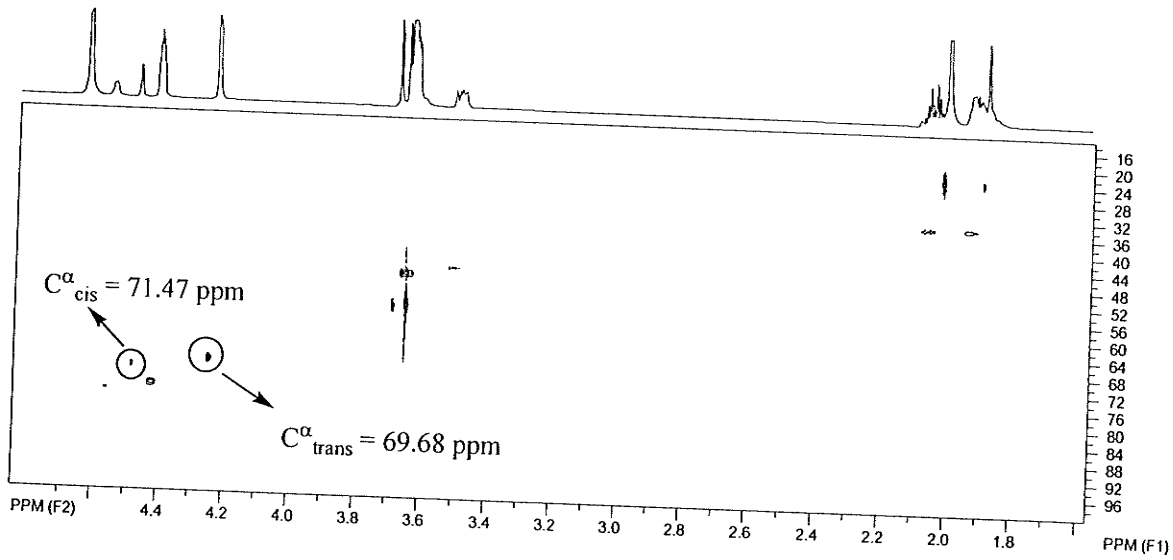

Different chemical shift of α-carbon for *cis* and *trans* rotamers of compound 6 in D_2O (HSQC)

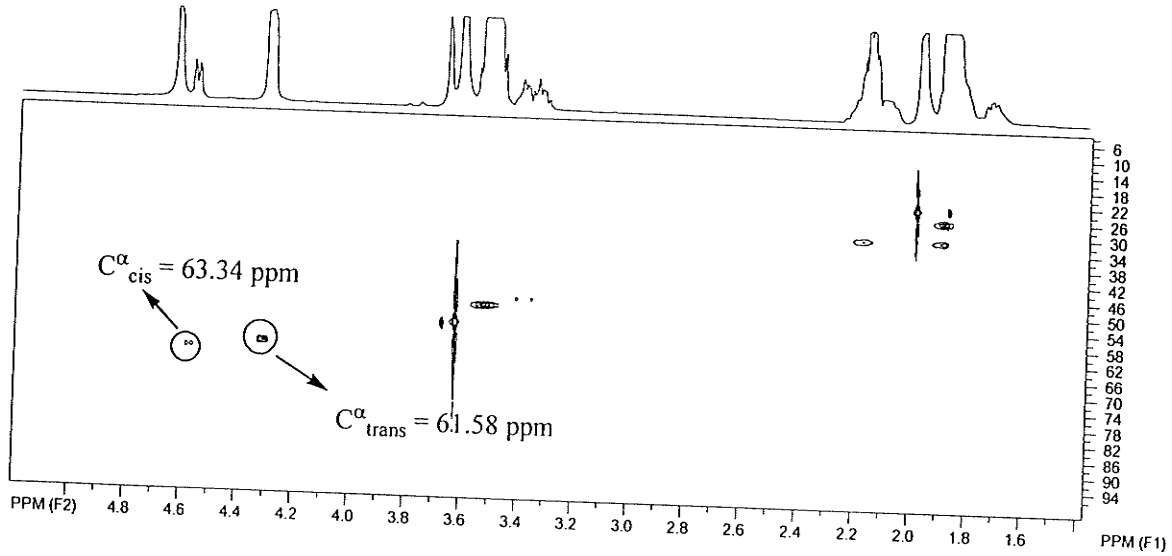

Compound 7 in D_2O

1D nOe spectrum

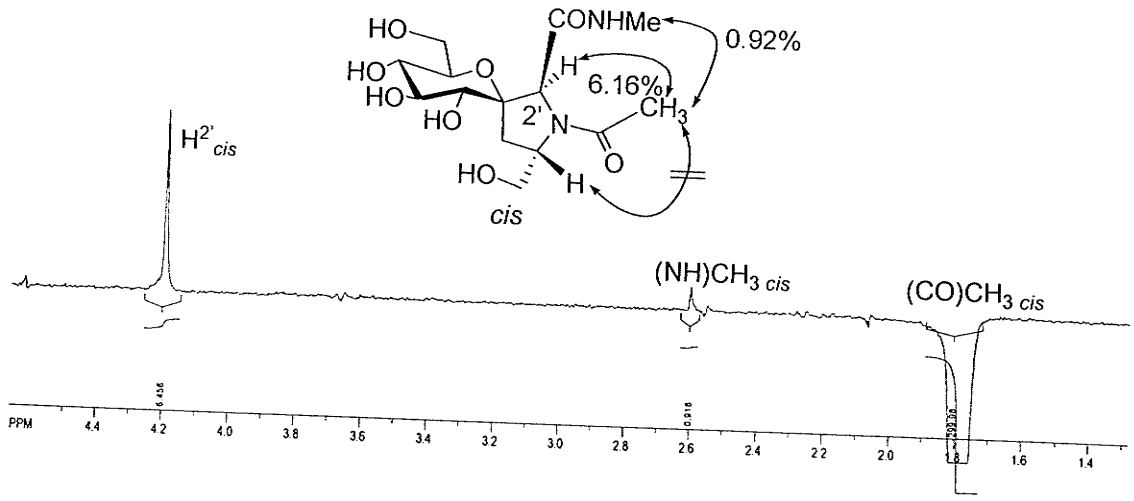

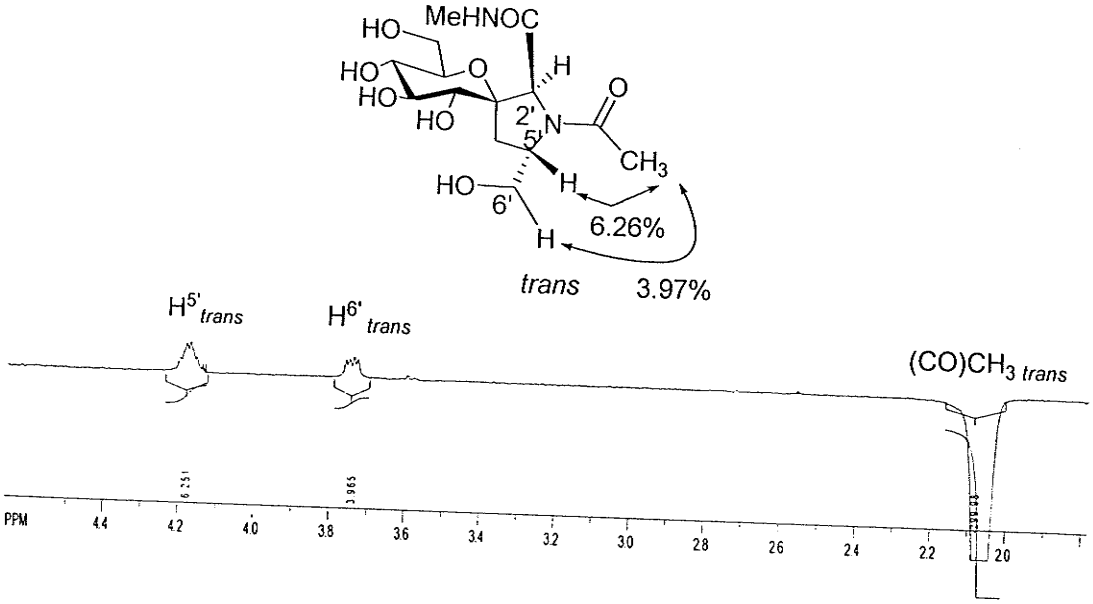

Compound **7** in CD_3OD

1D nOe spectrum

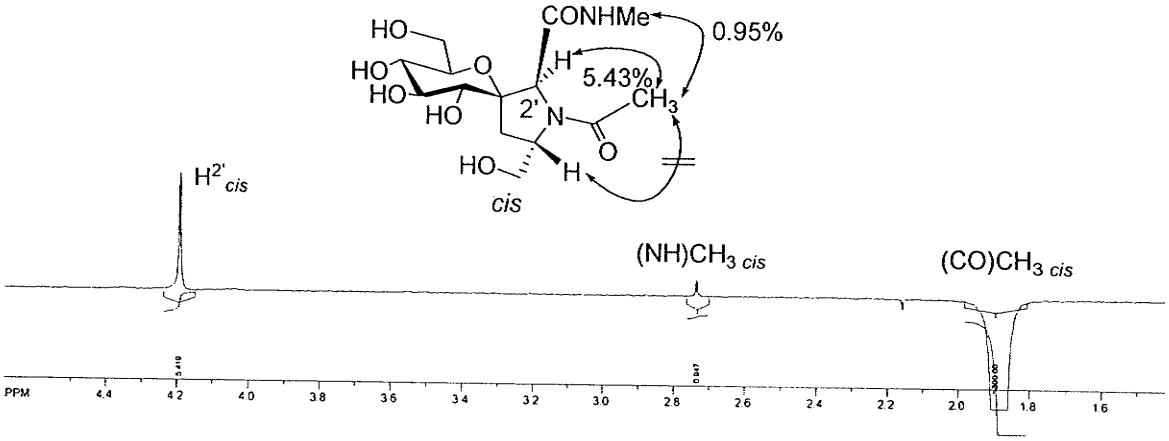

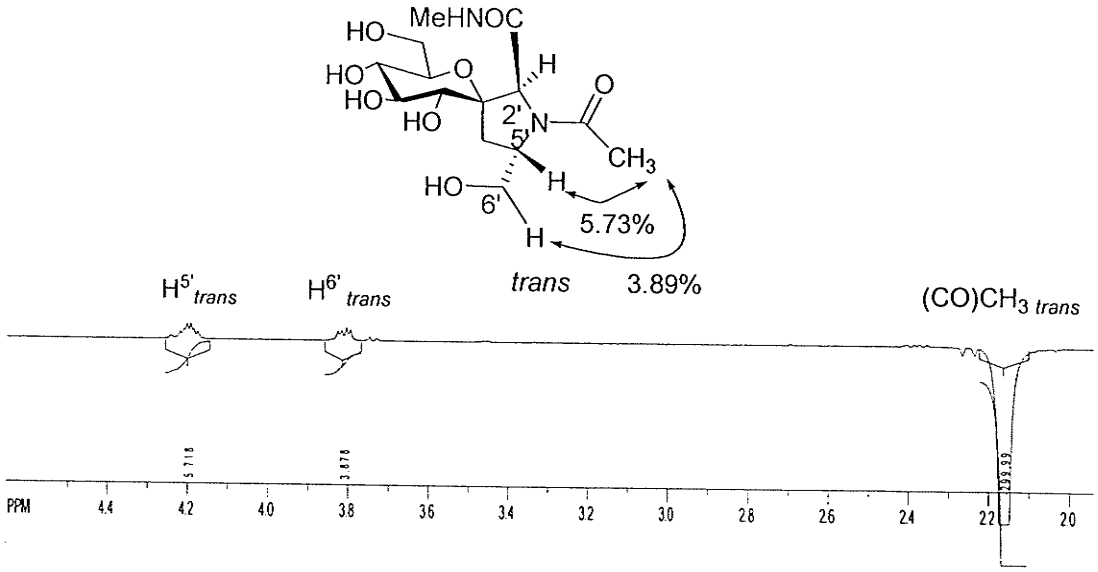

Compound **8** in D_2O

1D nOe spectrum

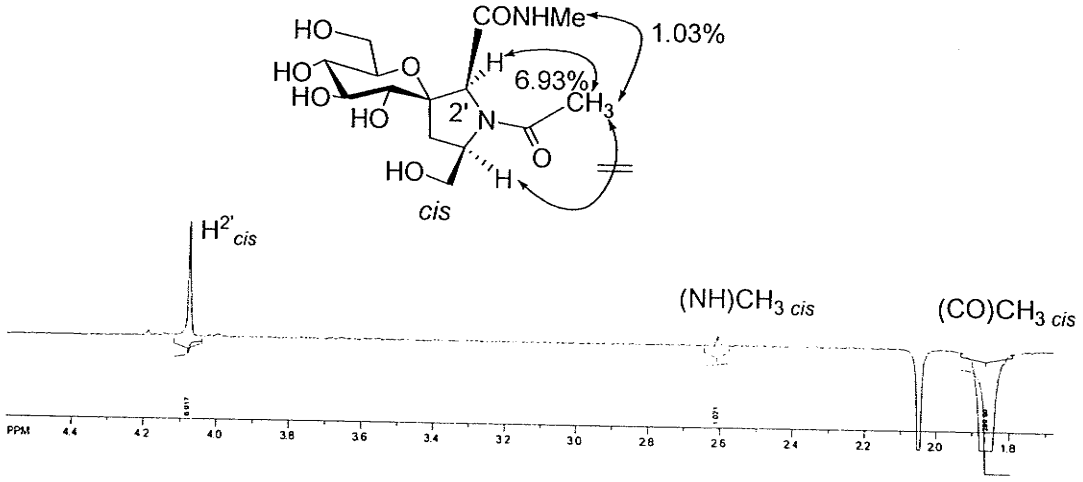

Compound **8** in CD_3OD

1D nOe spectrum

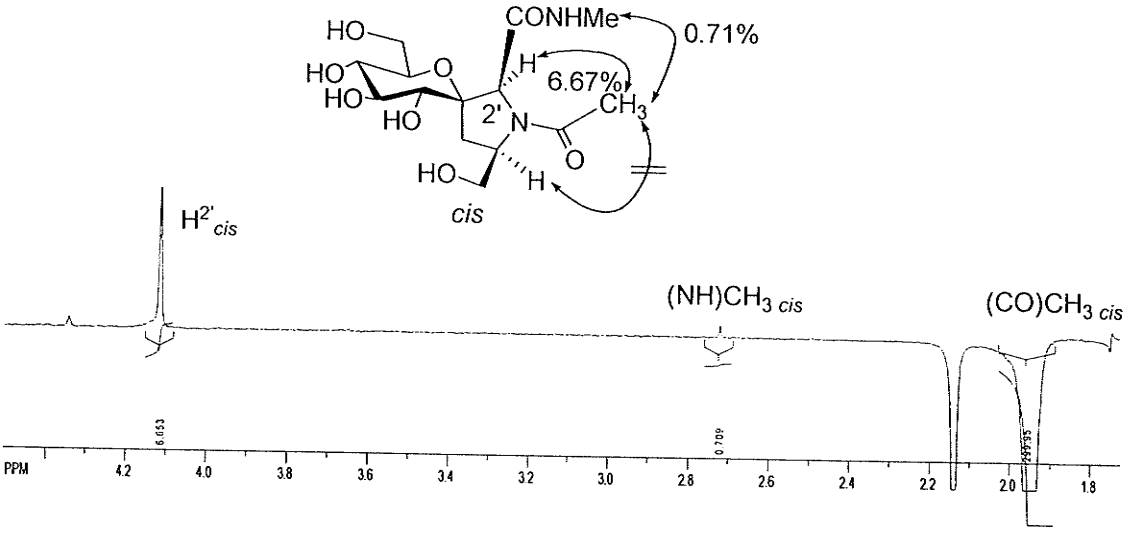

9.2.4. Magnetization transfer NMR experiments were performed on Bruker AMX500 spectrometer, equipped with selective excitation units and a triple resonance (^{1}H, ^{13}C, ^{15}N) gradient inverse probehead. Experiments were performed over several temperatures between 318 and 364 K. Temperature settings of spectrometer were calibrated using an ethylene glycol standard. Selective inversion of proton *trans*- and *cis*-isomer signals were done with Gaussian pulses centered on resonance ±12.5 Hz. Relaxation time was 15 s (**3**), 12 s (**4**), 35 s (**5**) and 40 s (**6**). The inversion-recovery delay of between 1 ms and relaxation time was used. Data for each inversion recovery point were averaged over 32 points. Samples of **3-6** were prepared at concentration of 0.01 M in D_2O. Here, selective inversion of the protons for each compound was different due to their different well-resolved ^{1}H peaks. i.e. The methyl group of prolyl amide (*trans*) for compound **3**, the axil H^{γ} (*cis*) for compound **4**, α-proton for compound **5** and **6** were selectively inversed. ^{1}H NMR spectroscopy was used in preference to ^{13}C NMR since over the course of an experiment, the signal/noise ratio is much higher for ^{1}H than ^{13}C, and heating effects caused by decoupling for ^{13}C causes uncertainty in the temperature of the sample.

The time-dependent magnetization transfers of the *cis* ($M_c(t)$) and *trans* ($M_t(t)$) NMR signals as a function of the inversion transfer time (t) were simultaneously fit to equations 1 and 2 (Alger and Prestegard, 1977; Mariappan and Rabenstein, 1992) below for compounds **3-6** using *Mathematica* (v. 5.0). In the following pulse sequence, the ^{1}H one isomer resonance such as *trans* is selectively inverted using a shaped pulse. Its recovery during t is determined by its intrinsic T_{1t}, magnetization transfer to and from the *cis*

resonance, and the T_{1c} of the *cis* resonance:

π(x)sel----------t----------π/2(x,y.-x.-y)---acquire

The resonances of the *trans* and *cis* isomers show the following time dependences:

$M_t(t) = (c_1)(\tau_t)(\lambda_1+1/\tau_{1c})\exp(\lambda_1*t) + (c_2)(\tau_2)(\lambda_2+1/\tau_{1c})\exp(\lambda_2*t) + M_{c\infty}$---------- 1

$M_t(t) = (c_1)\exp(\lambda_1*t) + (c_2)\exp(\lambda_2*t) + M_{t\infty}$---------- 2

T_{1c} and T_{1t} are the longitudinal relaxation times of the resonances in the absence of exchange.

τ_c and τ_t are the lifetimes of the *cis* and *trans* conformers and k_{ct} and k_{tc} are the corresponding rate constants.

τ_{1c} and τ_{1t} are the effective relaxation times of the *cis* and *trans* resonances when relaxation and exchange are both occurring and are defined below in terms of T_{1c} and τ_c, T_{1t} and τ_t.

λ_1 and λ_2 are related to the time constants τ_c, τ_t, τ_{1c}, and τ_{1t}, and are defined below.

c_1 and c_2 are defined below.

$M_{c\infty}$ and $M_{t\infty}$ are determined experimentally from the magnetization measured after 5 T_1 periods for the *cis* and *trans* resonances, respectively.

Mathematica then calculates τ_t from τ_c, $M_{c\infty}$, and $M_{t\infty}$ as: $\tau_t = \tau_c * Mt_\infty/Mc_\infty$

Thus, $k_{ct} = 1/\tau_c$, $k_{tc} = 1/\tau_t$, $K_{eq} = M_{t\infty}/M_{c\infty}$,$\tau_{1c} = (T_{1c} * \tau_c)/(\tau_c + T_{1c})$, $\tau_{1t} = (T_{1t} * \tau_t)/(\tau_t + T_{1t})$

λ_1=(0.5)*(-((1/τ_{1c})+(1/τ_{1t}))+(((((1/τ_{1c})+(1/τ_{1t}))1/2)-(4)*(((1/τ_{1c})*(1/τ_{1t}))-((1/τc)*(1/τt)))))1/2)

λ_2=(0.5)*(-((1/τ_{1c})+(1/τ_{1t}))-(((((1/τ_{1c})+(1/τ_{1t}))2)-(4)*((((1/τ_{1c}))*((1/τ_{1t})))-

((1/τc)*(1/τ_t)))))1/2)

$c_2 = ((1/(\tau_t))*(\lambda_1-\lambda_2))*((\tau_t*(\lambda_1+(1/\tau_{1c}))*((M_{0c}-M_{c\infty})+(M_{t\infty}-M_{0t}))$

$c_1 = M_{0c}-M_{c\infty}-c_2$

All experimental data for each compound at different temperature were fit by using Mathematica 5.0 to give the following inversed and inversion-recovery fitting curves:

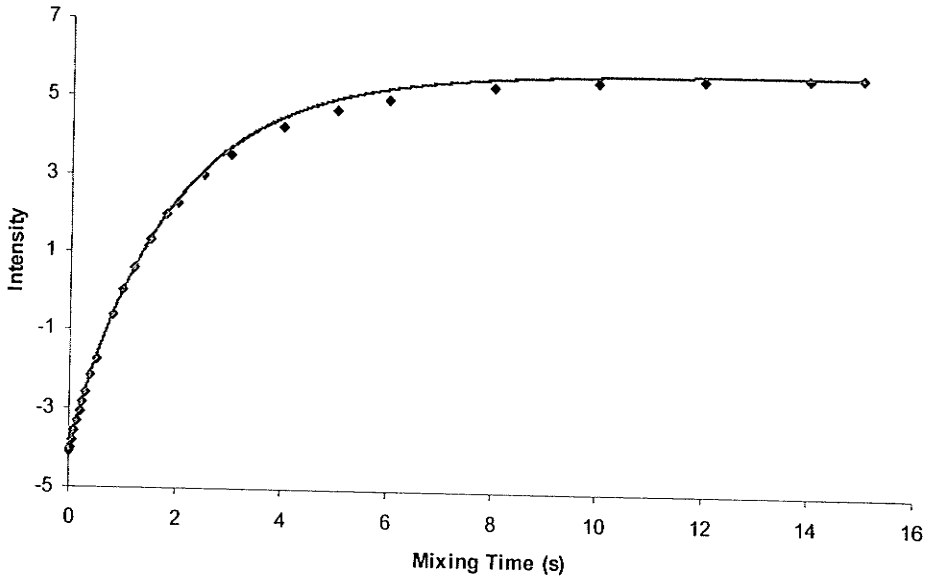

Figure 1. Inversed *N*-amide methyl group (*trans*) for compound **3** at 83°C in D_2O

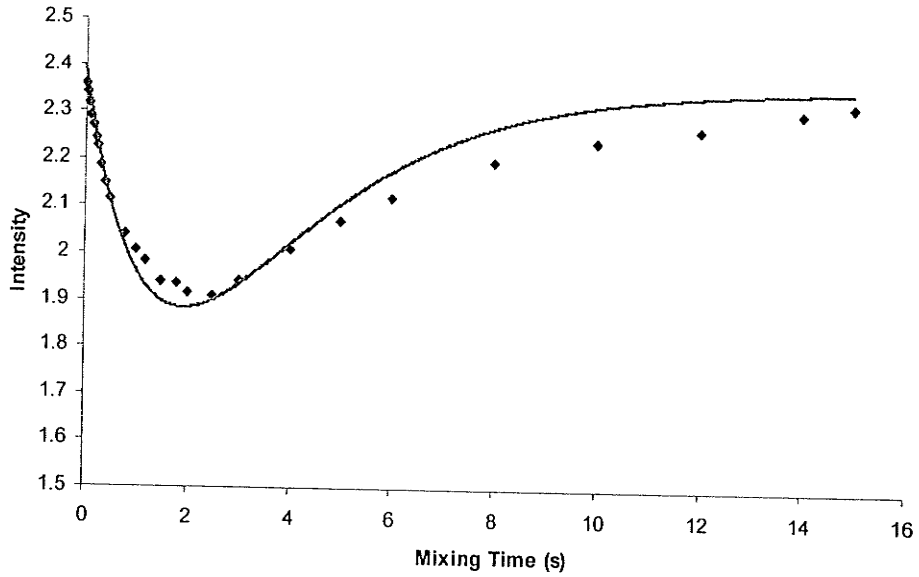

Figure 2. Inversion-recovery of *N*-amide methyl group (*cis*) for compound **3** at 83°C in D_2O

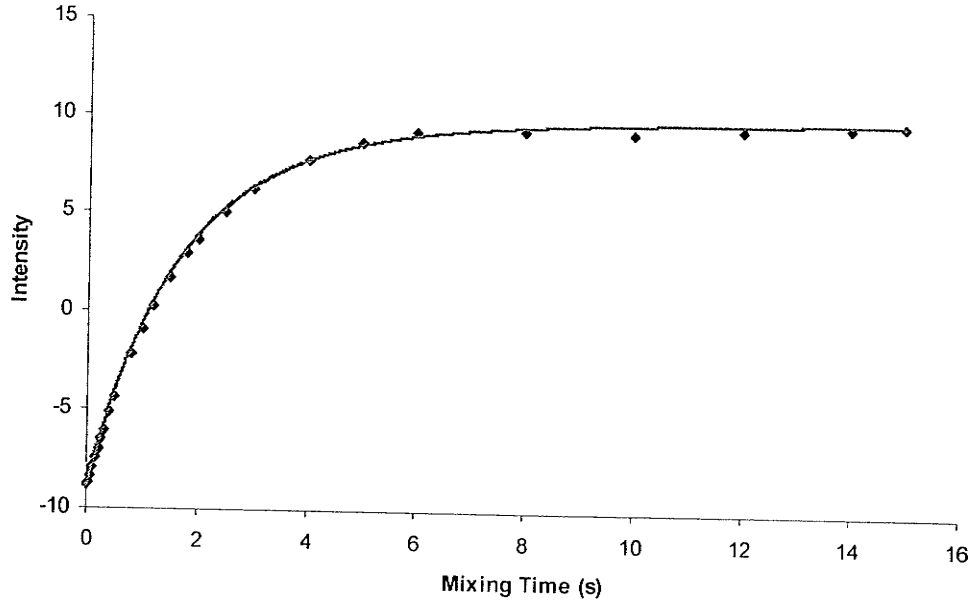

Figure 3. Inversed *N*-amide methyl group (*trans*) for compound **3** at 86°C in D_2O

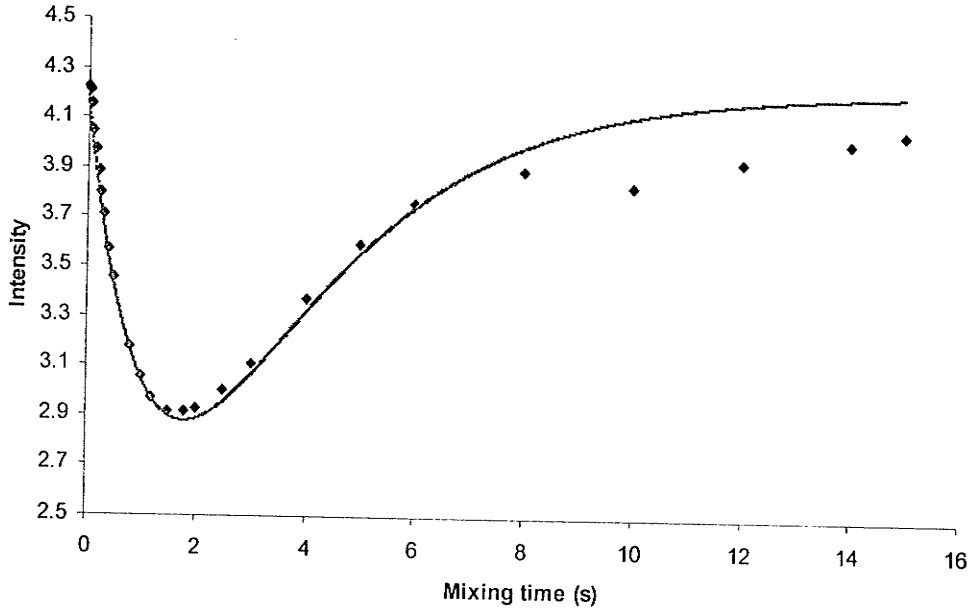

Figure 4. Inversion-recovery of *N*-amide methyl group (*cis*) for compound **3** at 86°C in D_2O

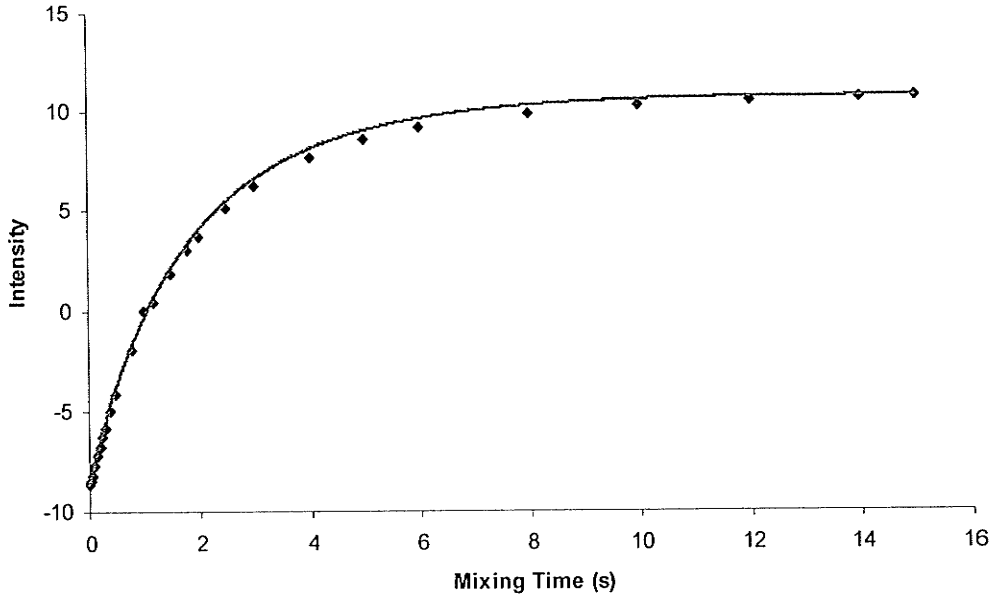

Figure 5. Inversed *N*-amide methyl group (*trans*) for compound **3** at 89°C in D_2O

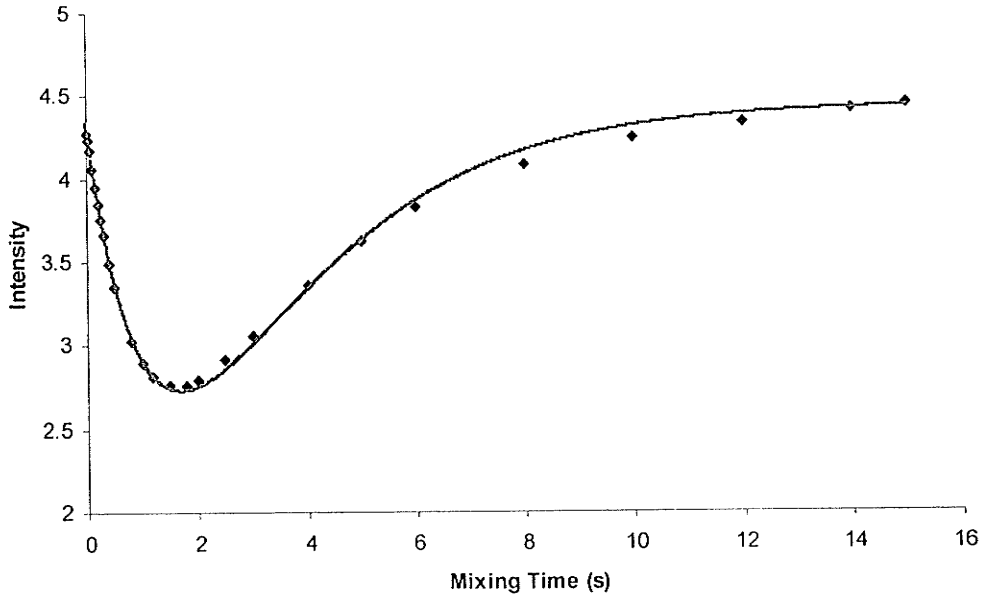

Figure 6. Inversion-recovery of *N*-amide methyl group (*cis*) for compound **3** at 89°C in D_2O

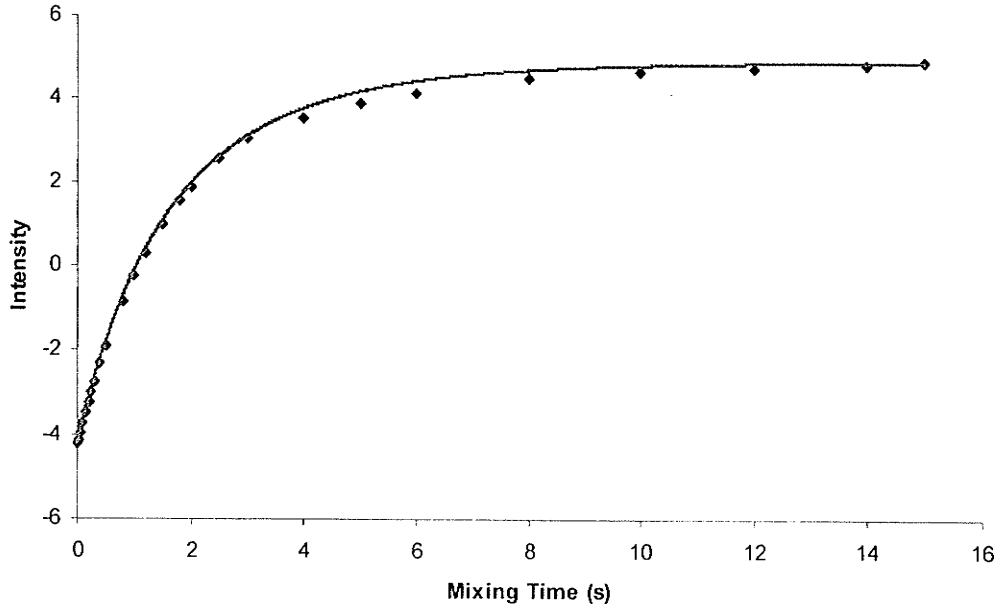

Figure 7. Inversed *N*-amide methyl group (*trans*) for compound **3** at 91°C in D_2O

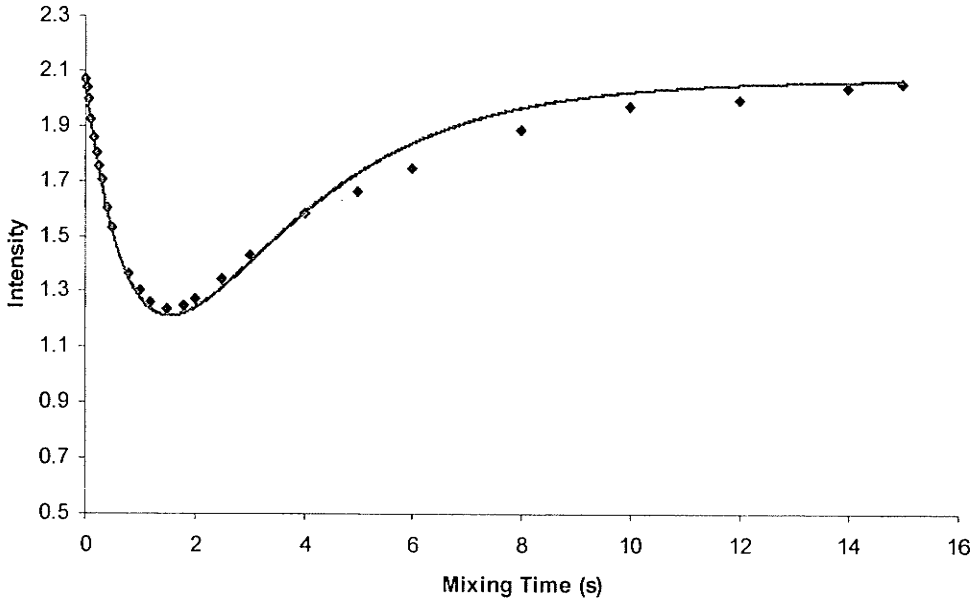

Figure 8. Inversion-recovery of *N*-amide methyl group (*cis*) for compound **3** at 91°C in D_2O

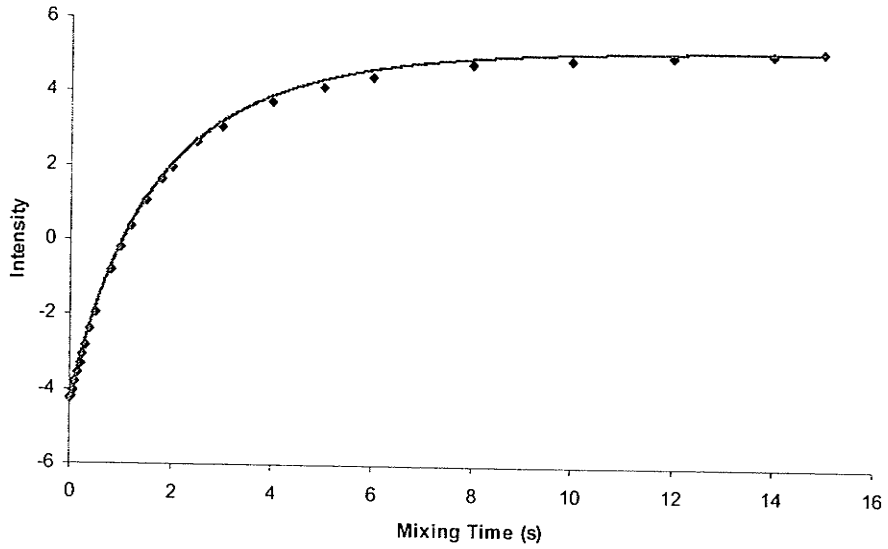

Figure 9. Inversed *N*-amide methyl group (*trans*) for compound **3** at 93°C in D_2O

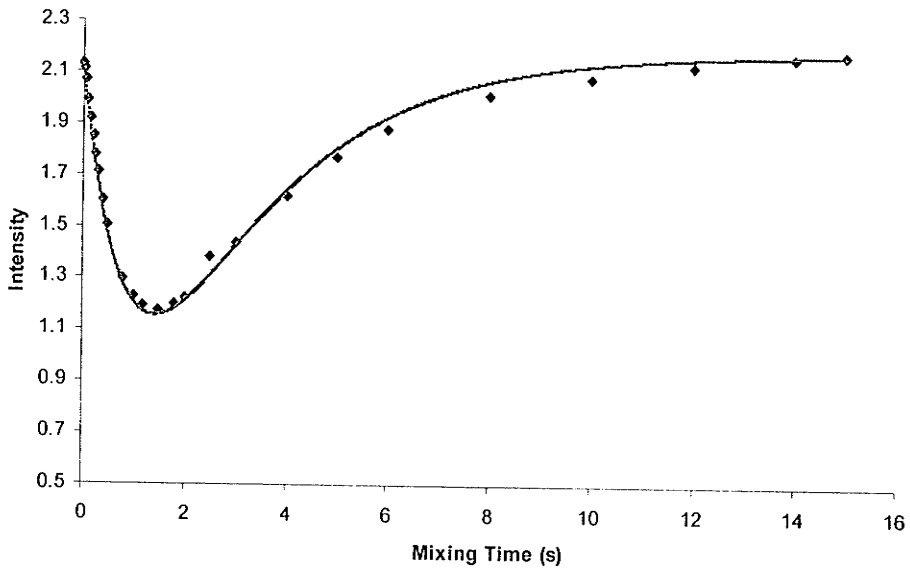

Figure 10. Inversion-recovery of *N*-amide methyl group (*cis*) for compound **3** at 93°C in D_2O

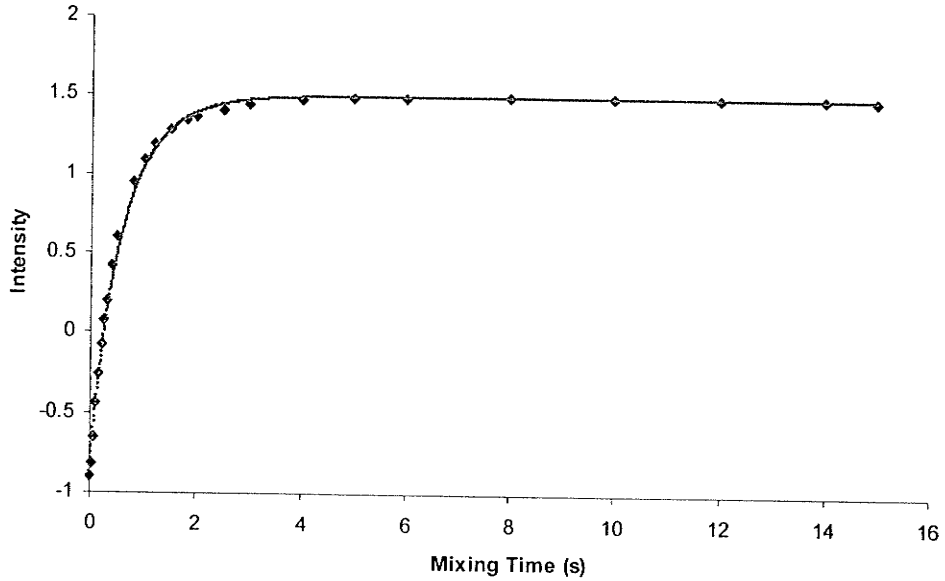

Figure 11. Inversed δ-position axial proton (*cis*) for compound **4** at 46°C in D_2O

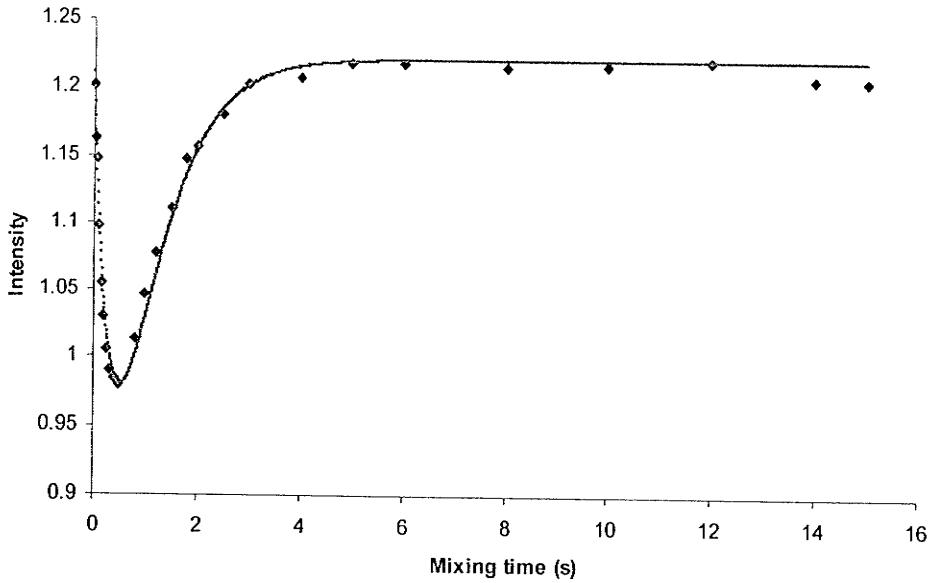

Figure 12. Inversion-recovery of non-inversed δ-position axial proton (*trans*) for compound **4** at 46°C in D_2O

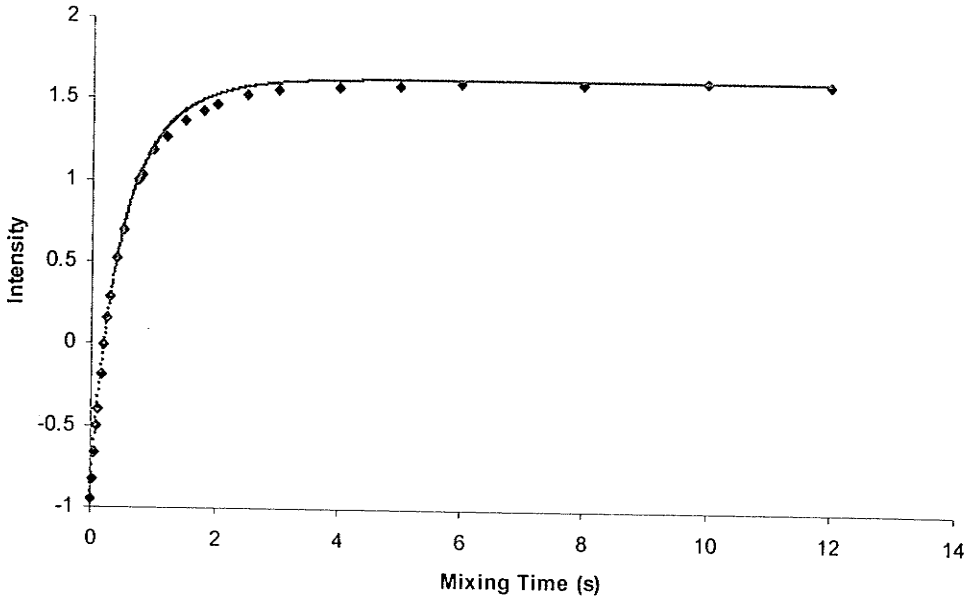

Figure 13. Inversed δ-position axial proton (*cis*) for compound **4** at 52°C in D_2O

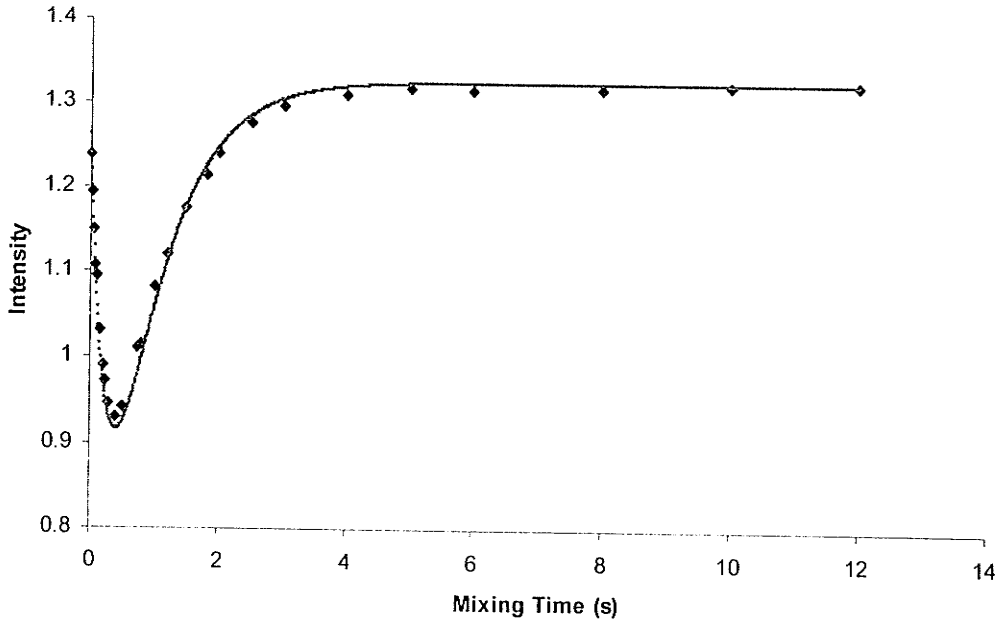

Figure 14. Inversion-recovery of non-inversed δ-position axial proton (*trans*) for compound **4** at 52°C in D_2O

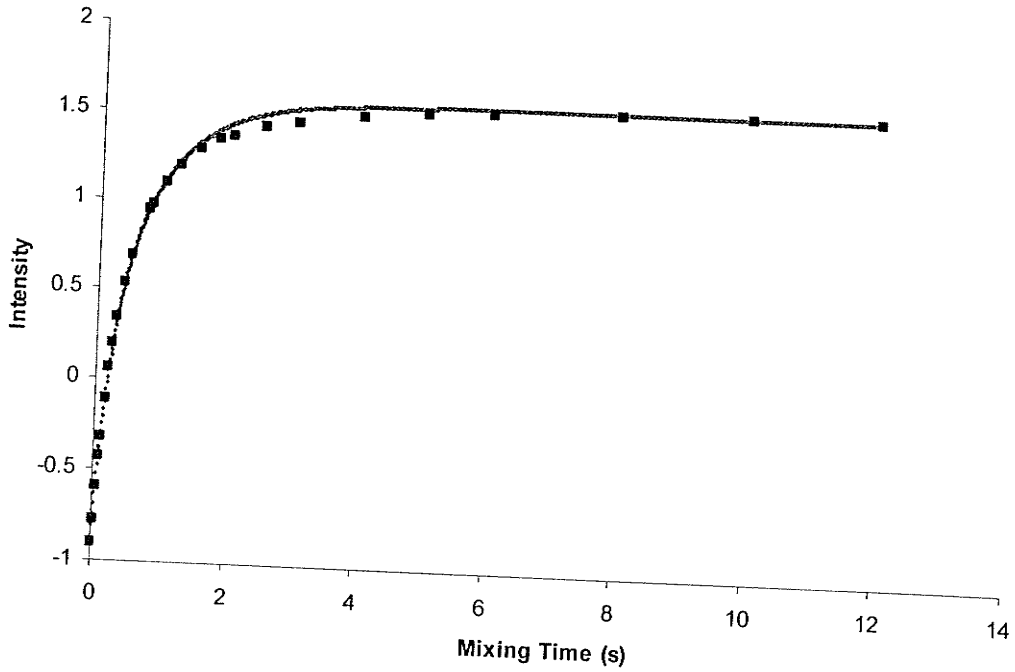

Figure 15. Inversed δ-position axial proton (*cis*) for compound **4** at 57°C in D_2O

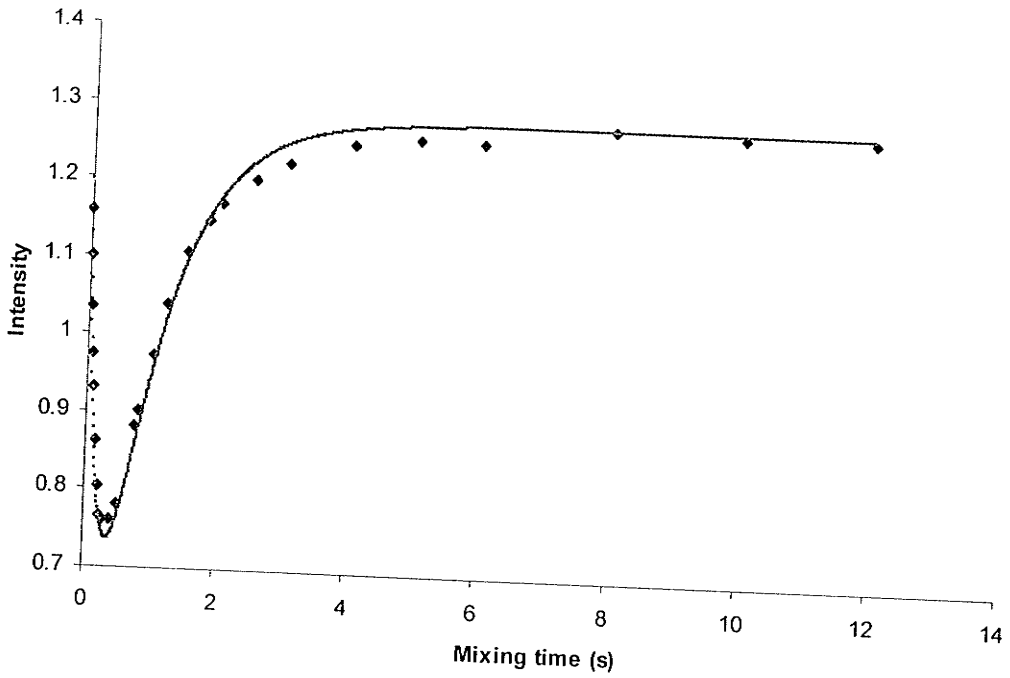

Figure 16. Inversion-recovery of non-inversed δ-position axial proton (*trans*) for compound **4** at 57°C in D_2O

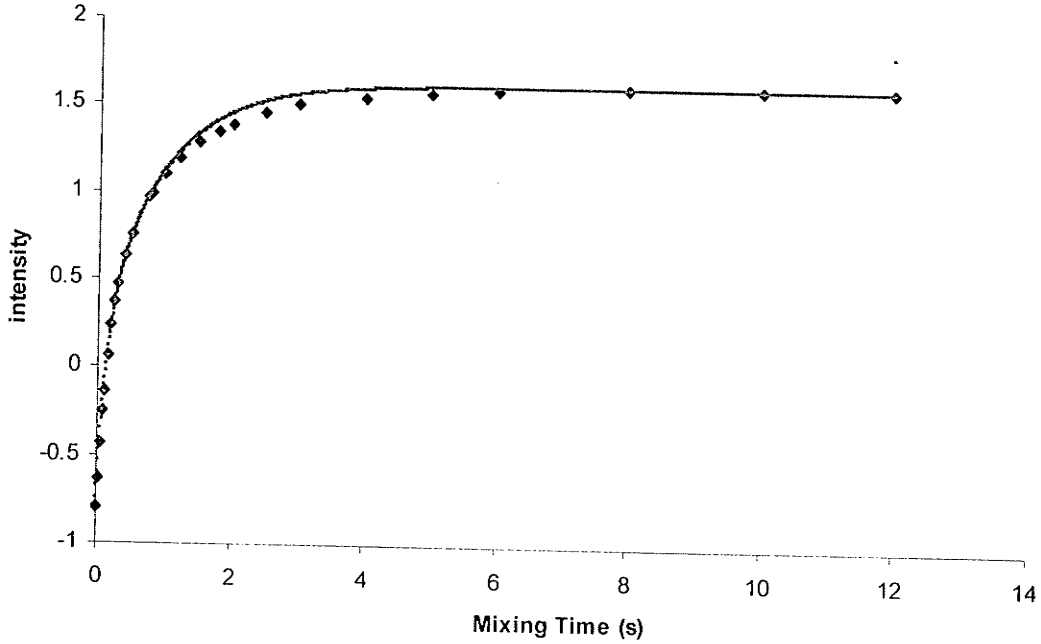

Figure 17. Inversed δ-position axial proton (*cis*) for compound **4** at 62°C in D_2O

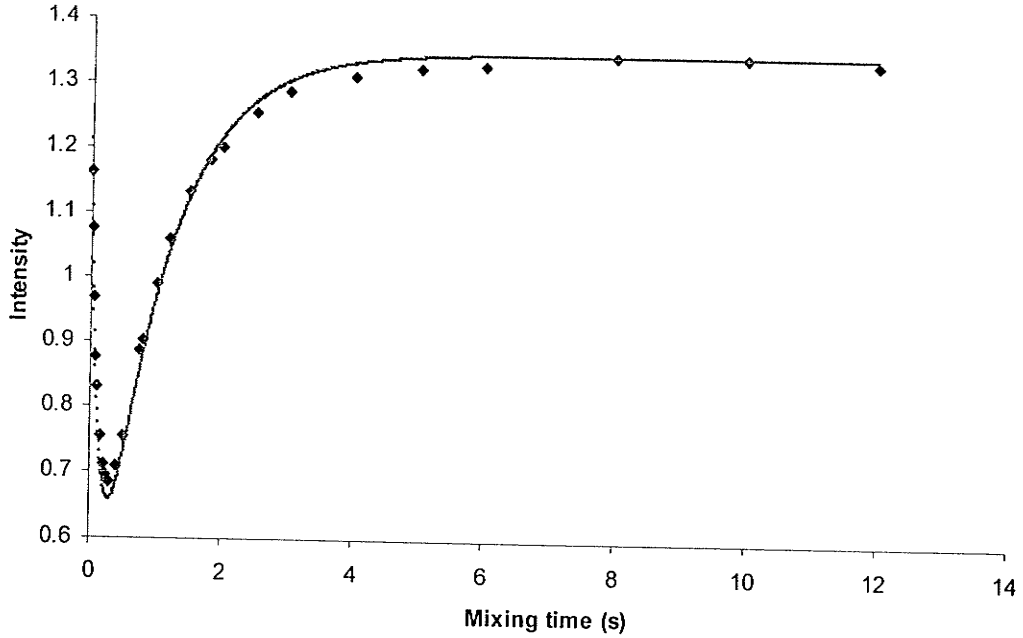

Figure 18. Inversion-recovery of non-inversed δ-position axial proton (*trans*) for compound **4** at 62°C in D_2O

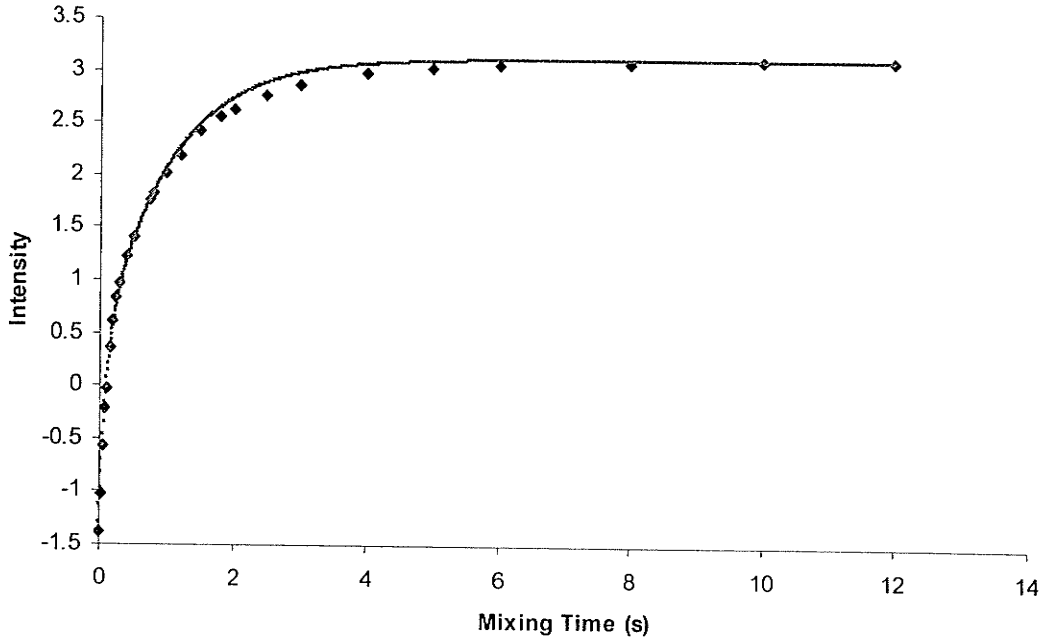

Figure 19. Inversed δ-position axial proton (*cis*) for compound **4** at 67°C in D_2O

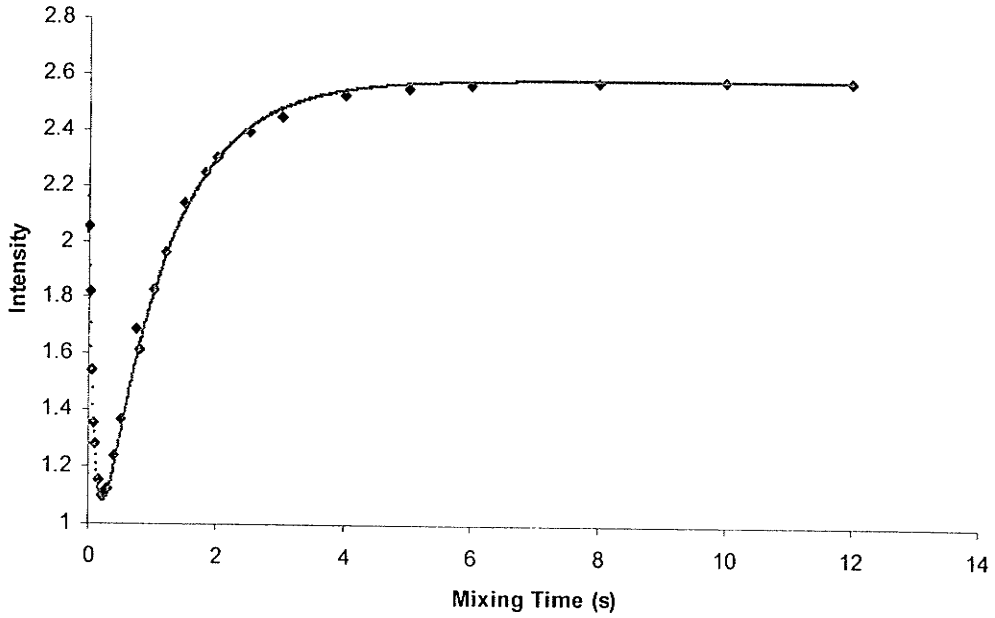

Figure 20. Inversion-recovery of non-inversed δ-position axial proton (*trans*) for compound **4** at 67°C in D_2O

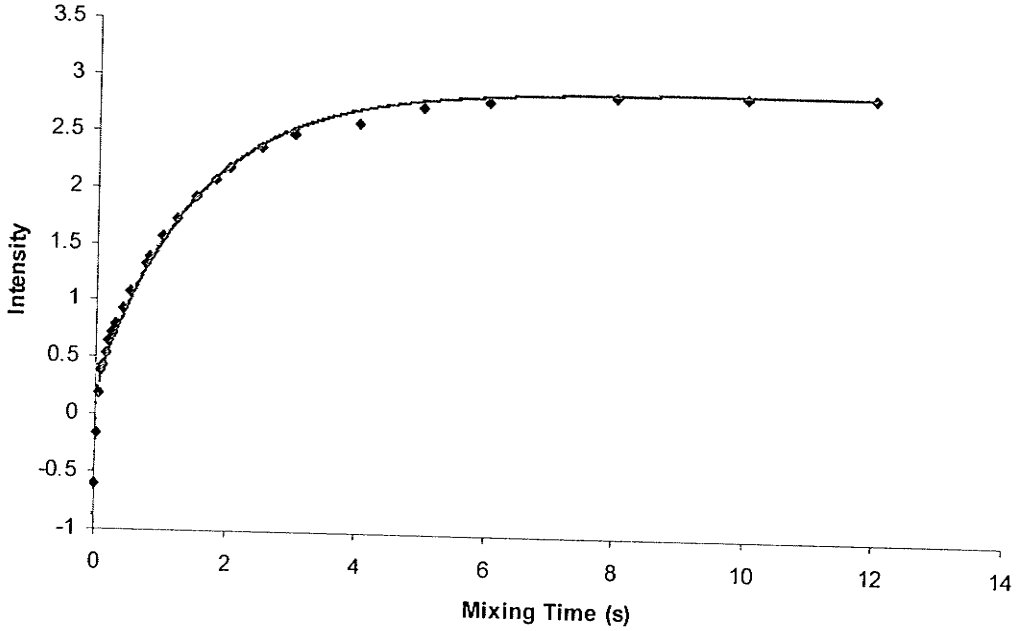

Figure 21. Inversed δ-position axial proton (*cis*) for compound **4** at 83°C in D_2O

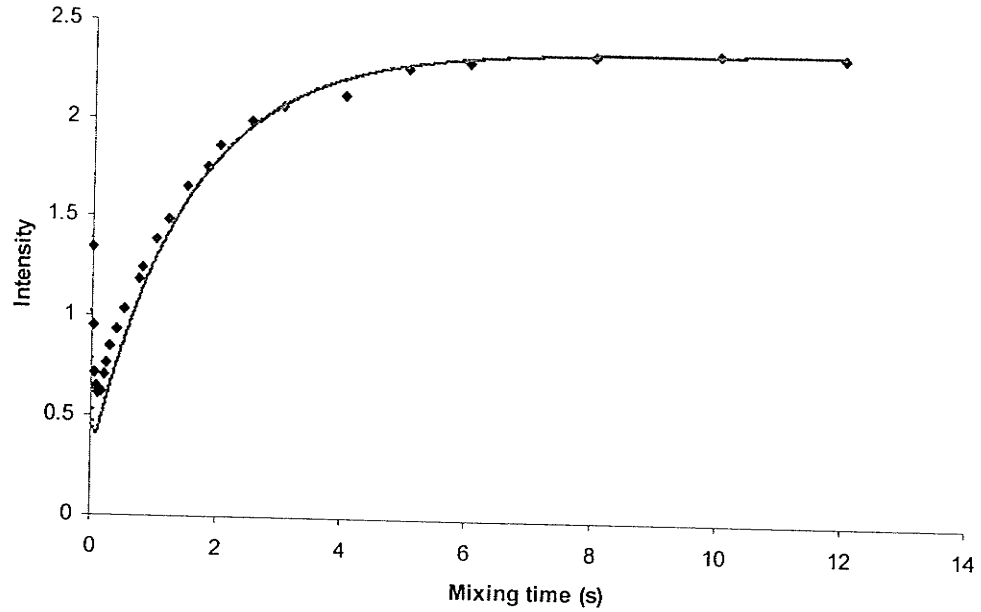

Figure 22. Inversion-recovery of non-inversed δ-position axial proton (*trans*) for compound **4** at 83°C in D_2O

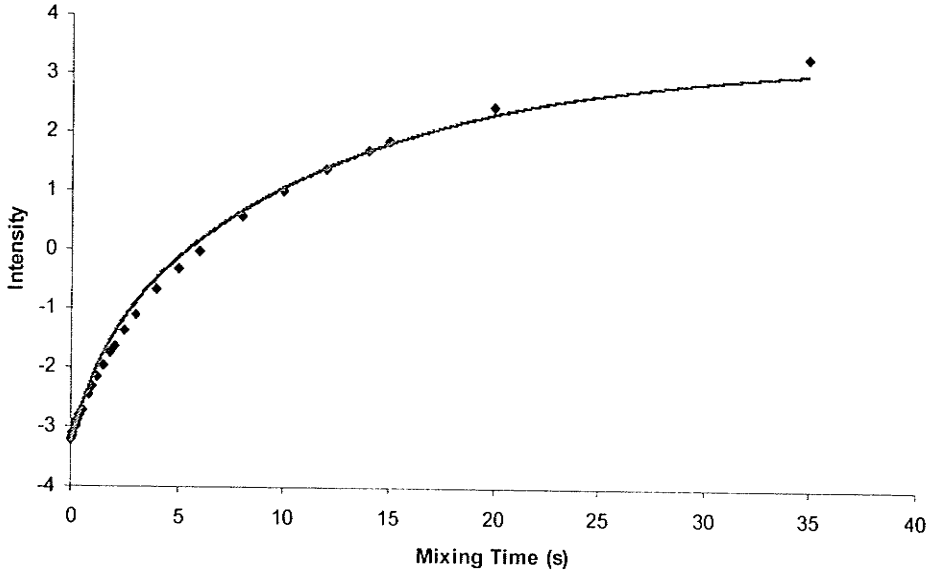

Figure 23. Inversed α-proton (*trans*) for compound **5** at 62°C in D_2O

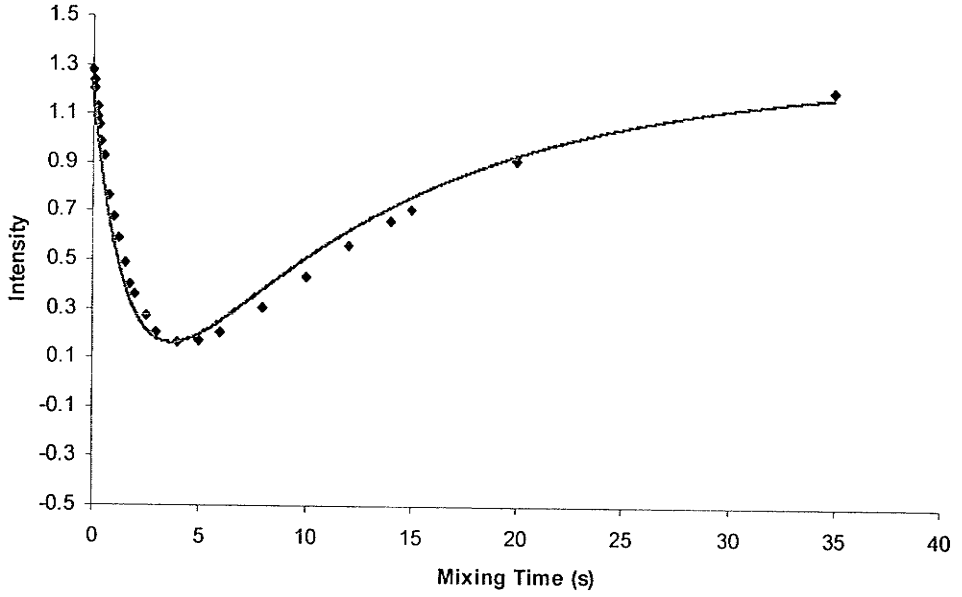

Figure 24. Inversion-recovery of α-proton (*cis*) for compound **5** at 62°C in D_2O

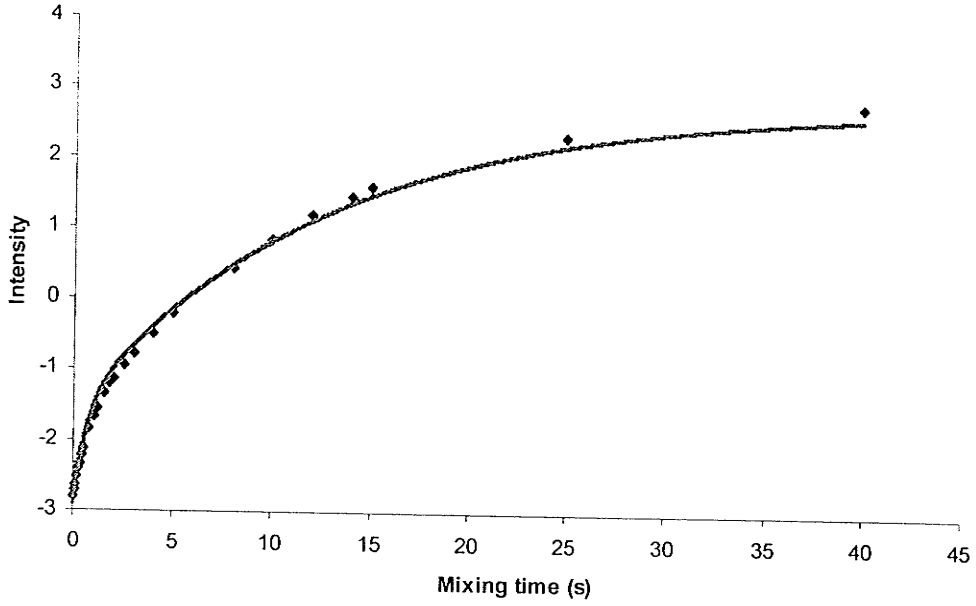

Figure 25. Inversed α-proton (*trans*) for compound **5** at 73°C in D_2O

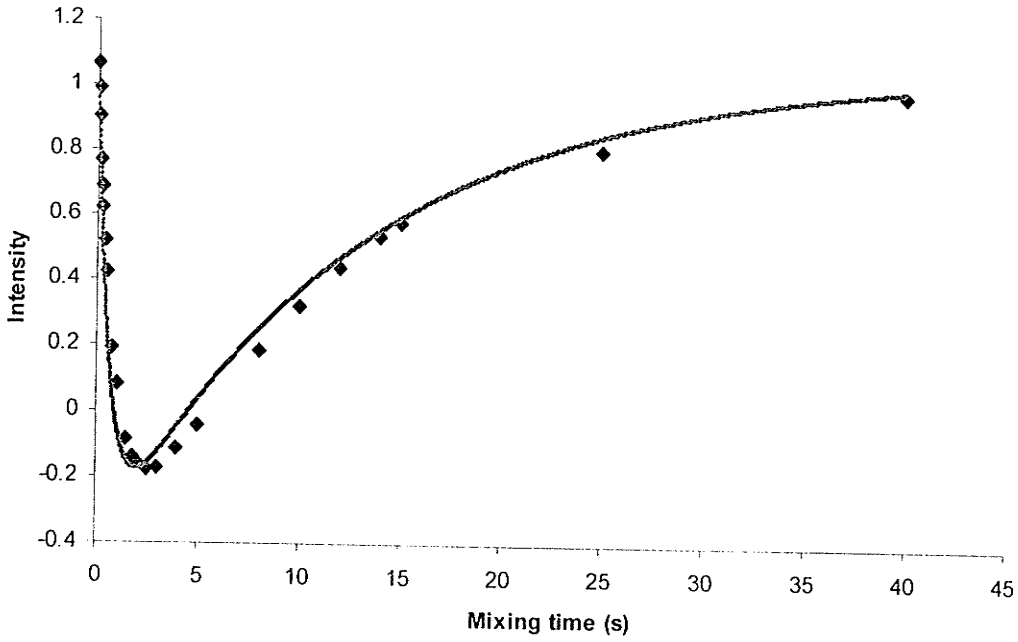

Figure 26. Inversed α-proton (*cis*) for compound **5** at 73°C in D_2O

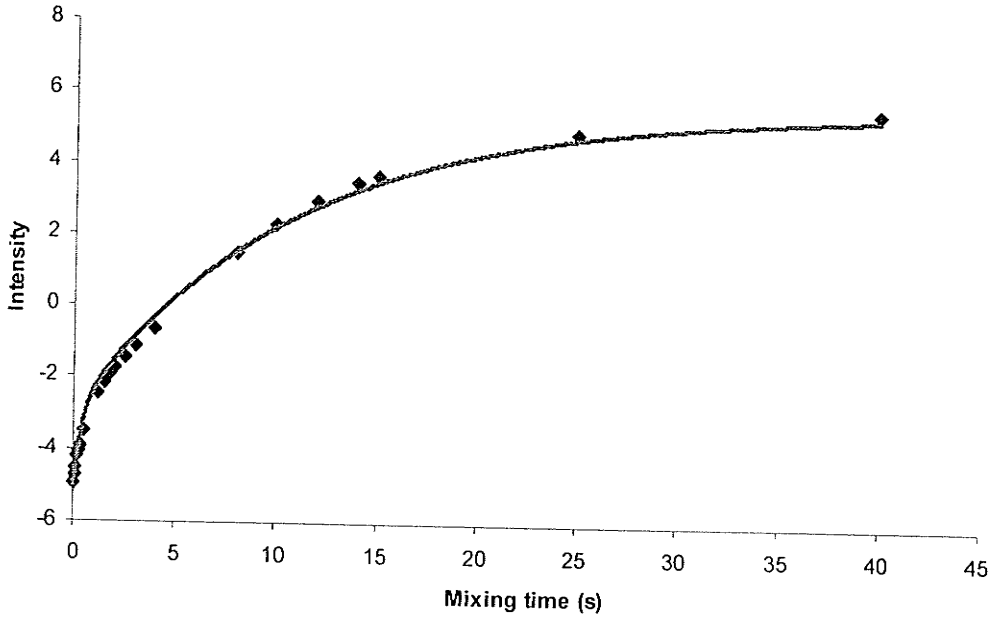

Figure 27. Inversed α-proton (*trans*) for compound **5** at 78°C in D_2O

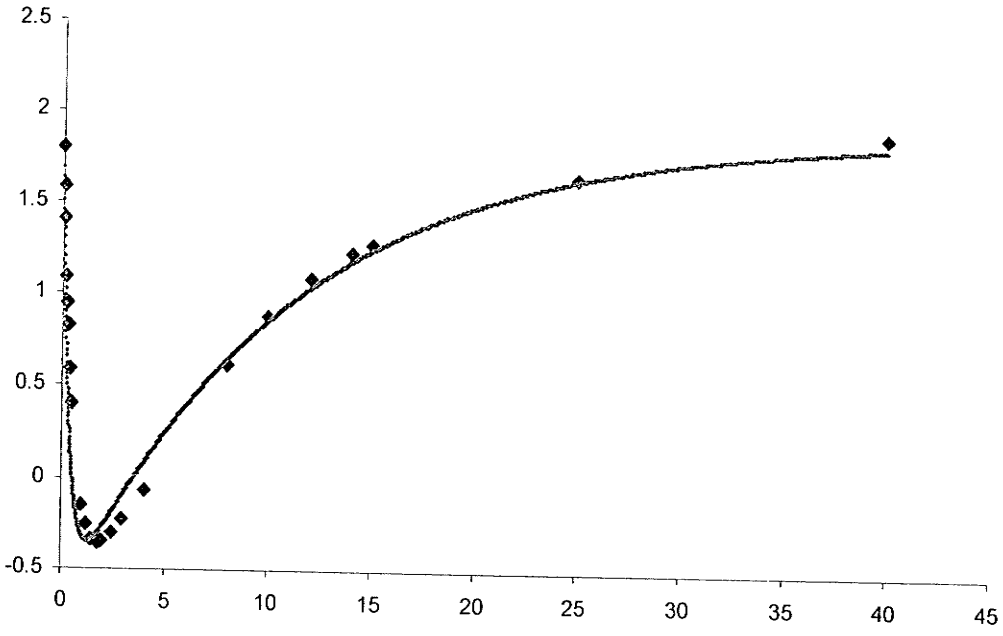

Figure 28. Inversed α-proton (*cis*) for compound **5** at 78°C in D_2O

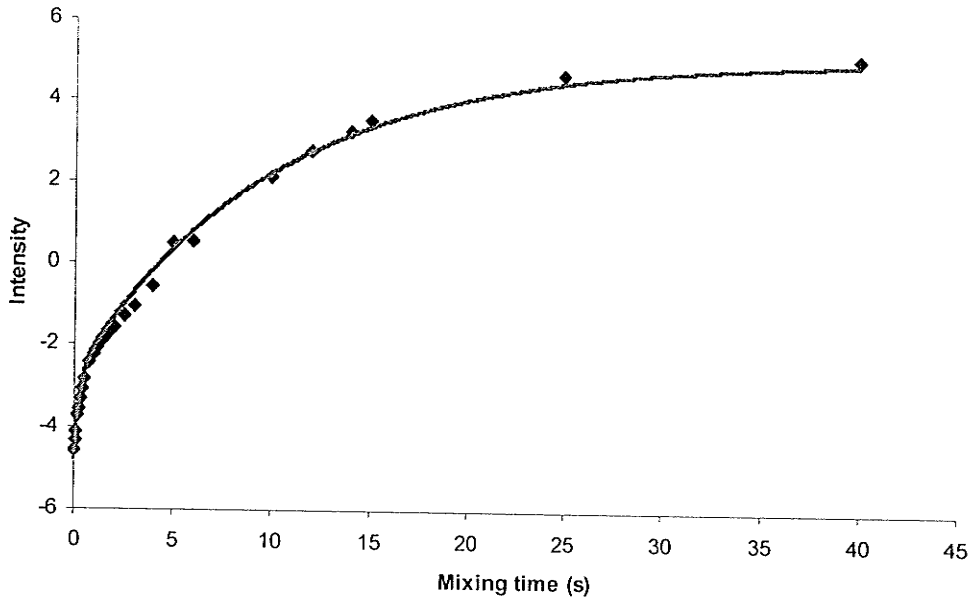

Figure 29. Inversed α-proton (*trans*) for compound **5** at 83°C in D_2O

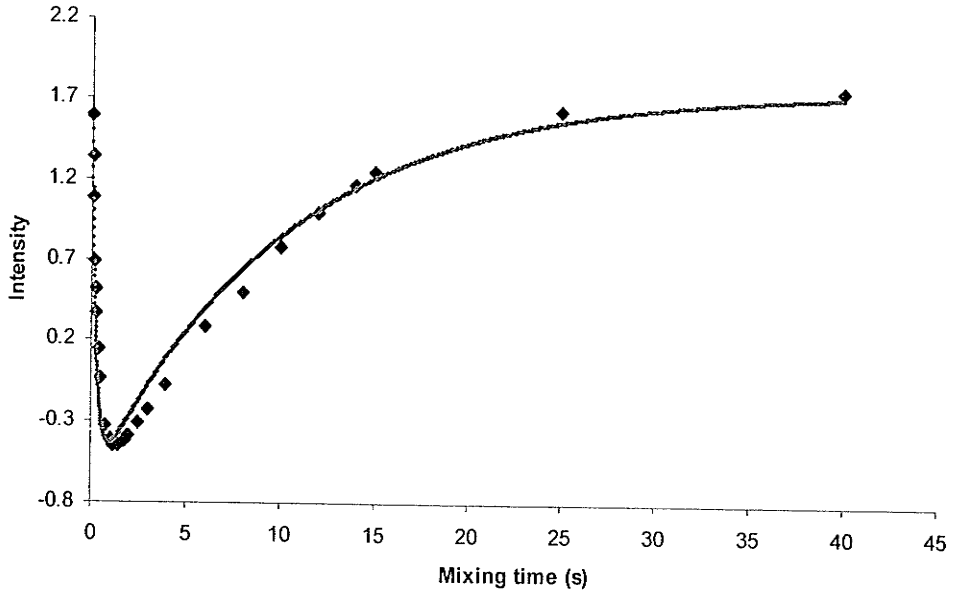

Figure 30. Inversed α-proton (*trans*) for compound **5** at 83°C in D_2O

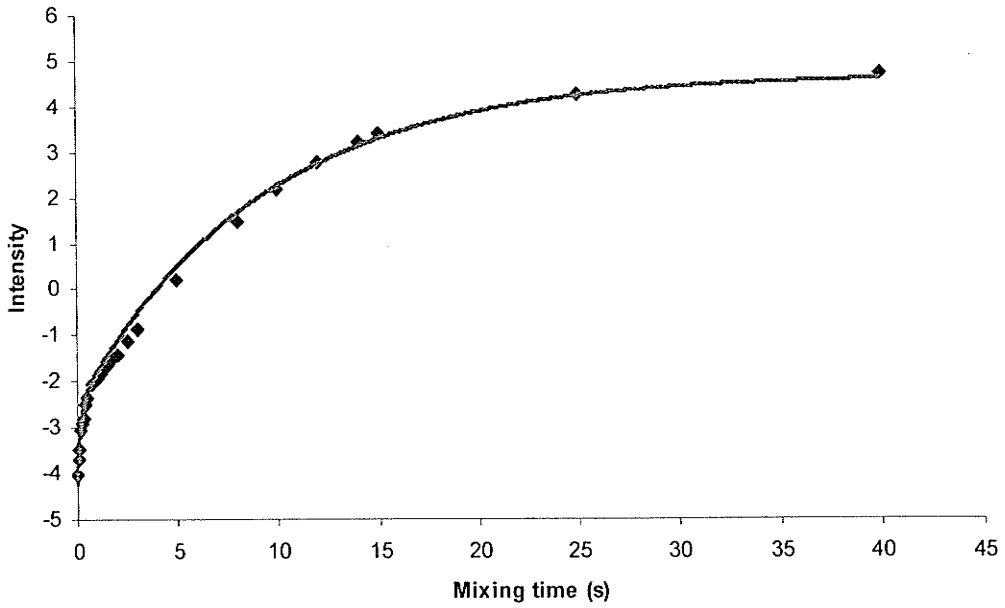

Figure 31. Inversed α-proton (*cis*) for compound **5** at 89°C in D_2O

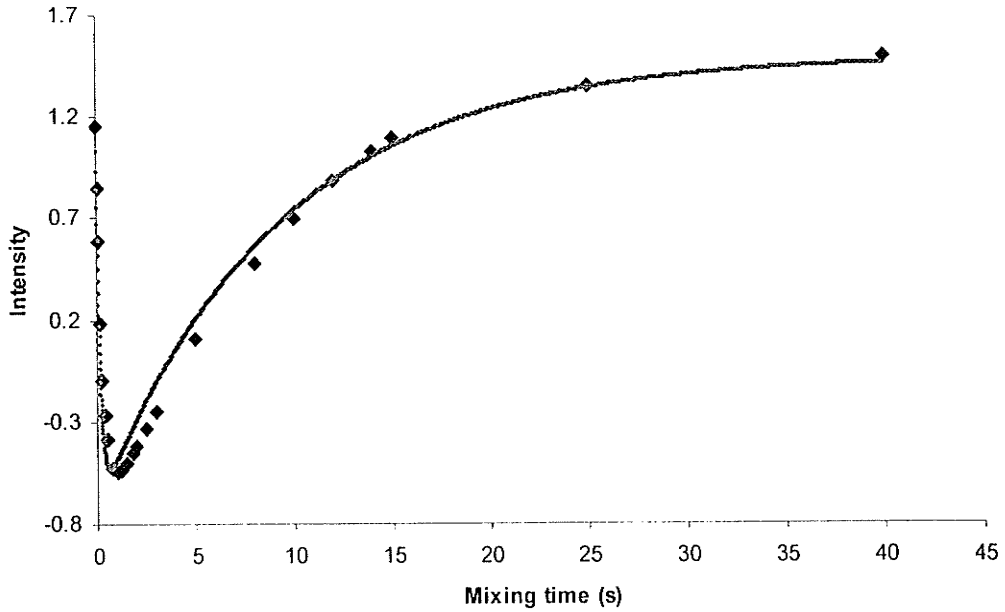

Figure 32. Inversed α-proton (*trans*) for compound **5** at 89°C in D_2O

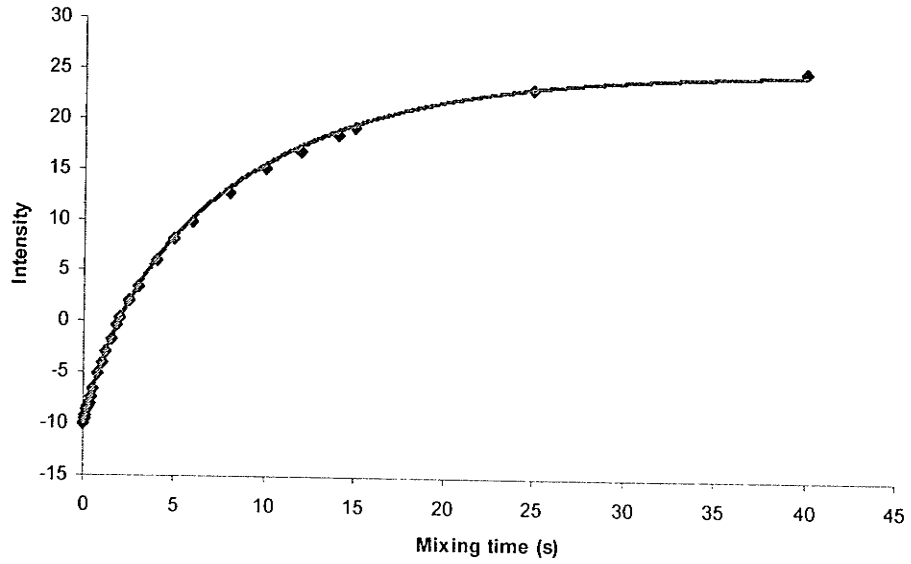

Figure 33. Inversed α-proton (*trans*) for compound **6** at 62°C in D_2O

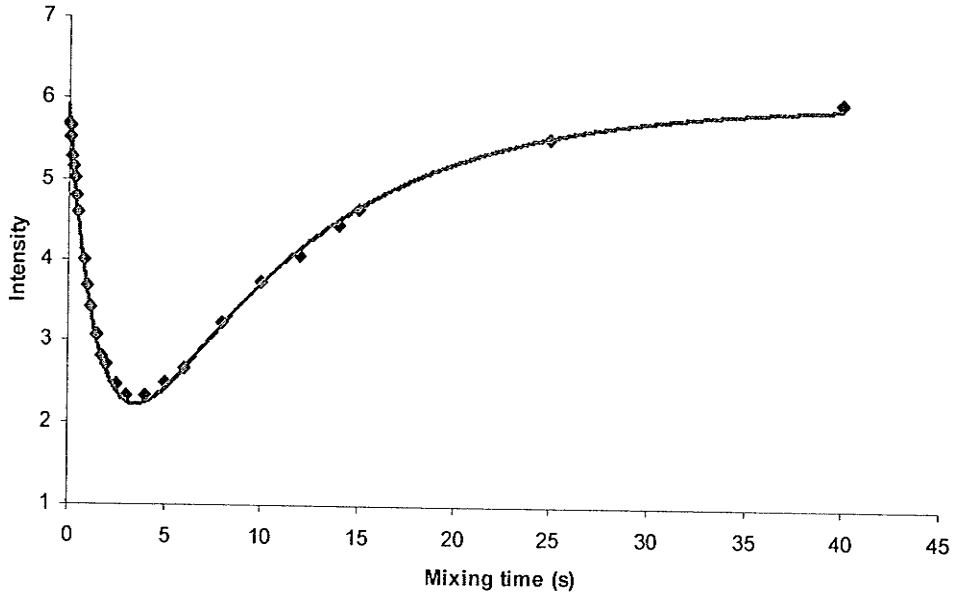

Figure 34. Inversed α-proton (*cis*) for compound **6** at 62°C in D_2O

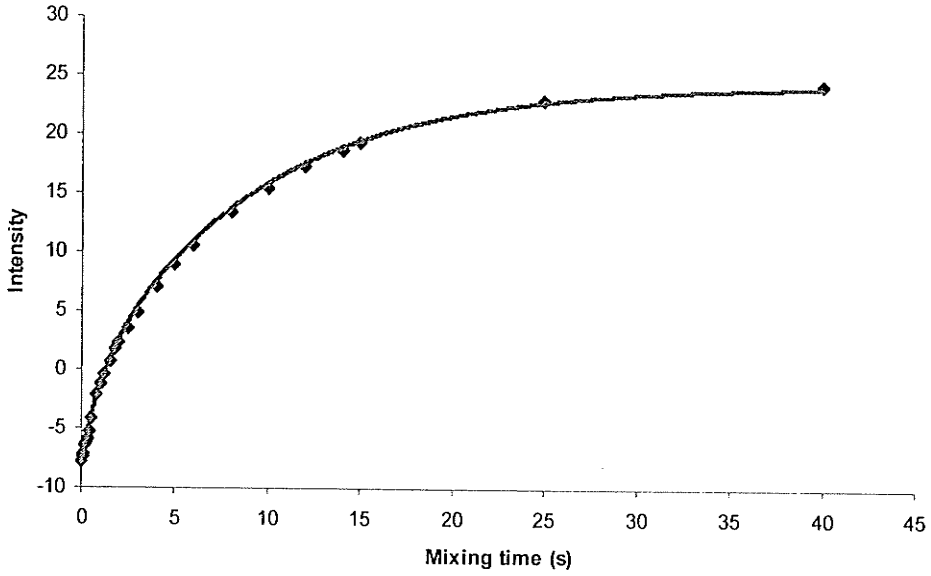

Figure 35. Inversed α-proton (*trans*) for compound **6** at 67°C in D_2O

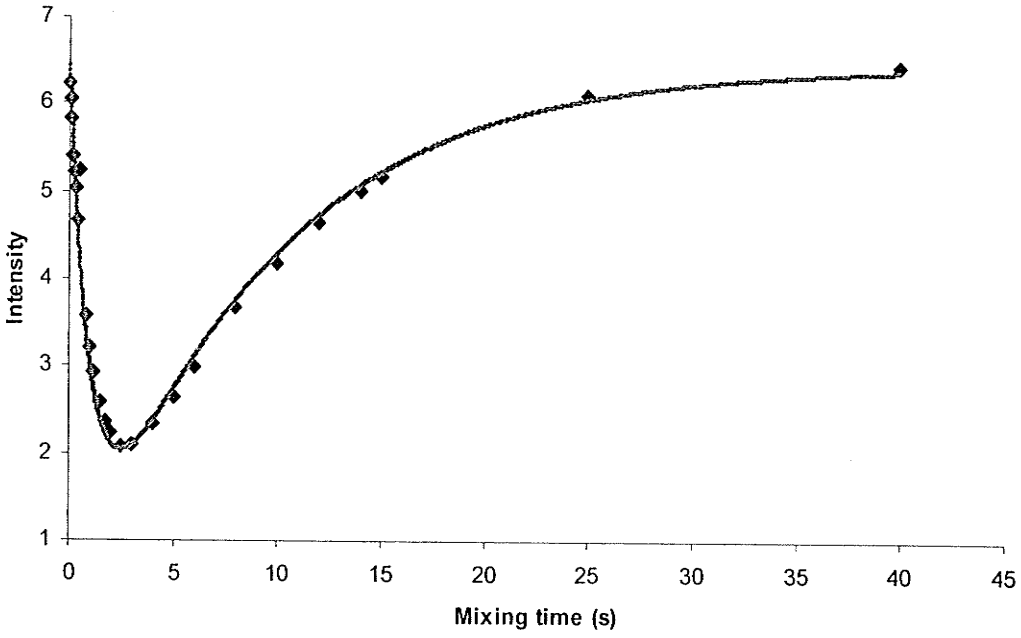

Figure 36. Inversed α-proton (*cis*) for compound **6** at 67°C in D_2O

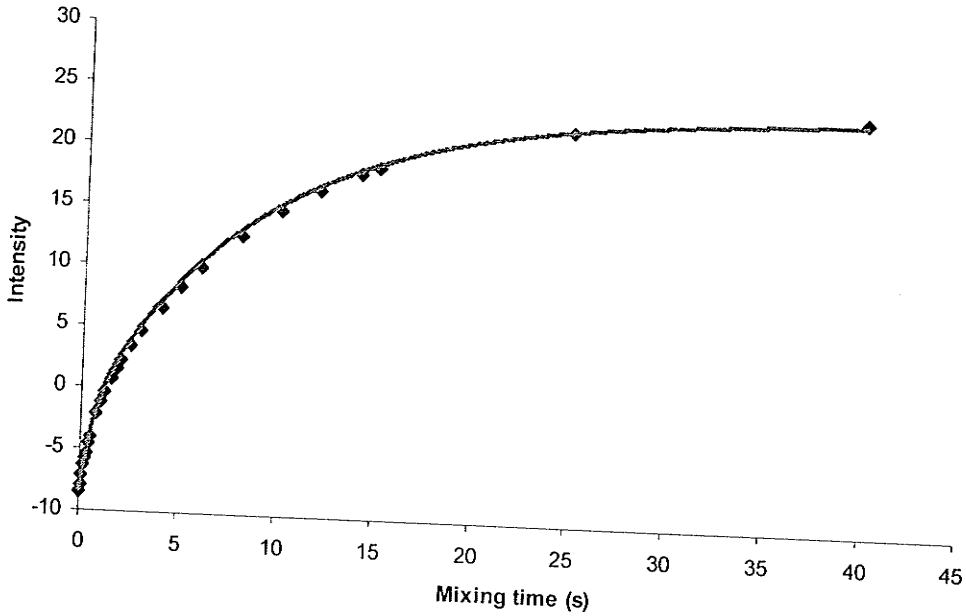

Figure 37. Inversed α-proton (*trans*) for compound **6** at 73°C in D_2O

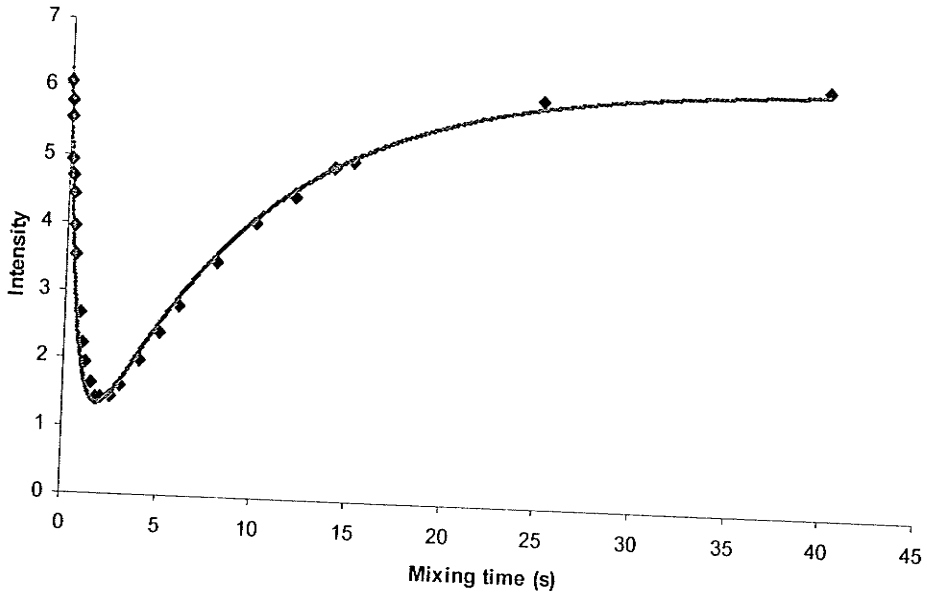

Figure 38. Inversed α-proton (*cis*) for compound **6** at 73°C in D_2O

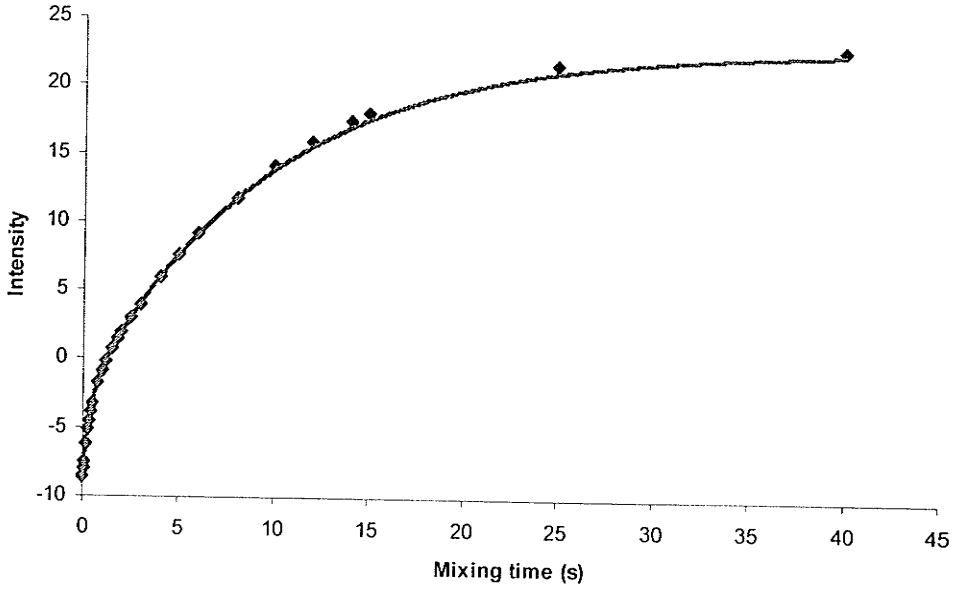

Figure 39. Inversed α-proton (*trans*) for compound **6** at 78°C in D_2O

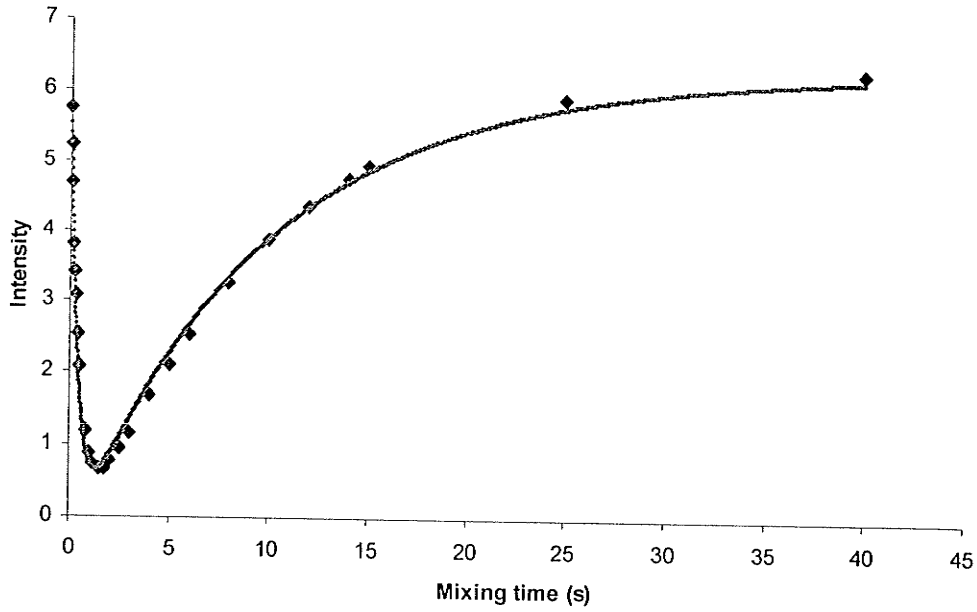

Figure 40. Inversed α-proton (*cis*) for compound **6** at 78°C in D_2O

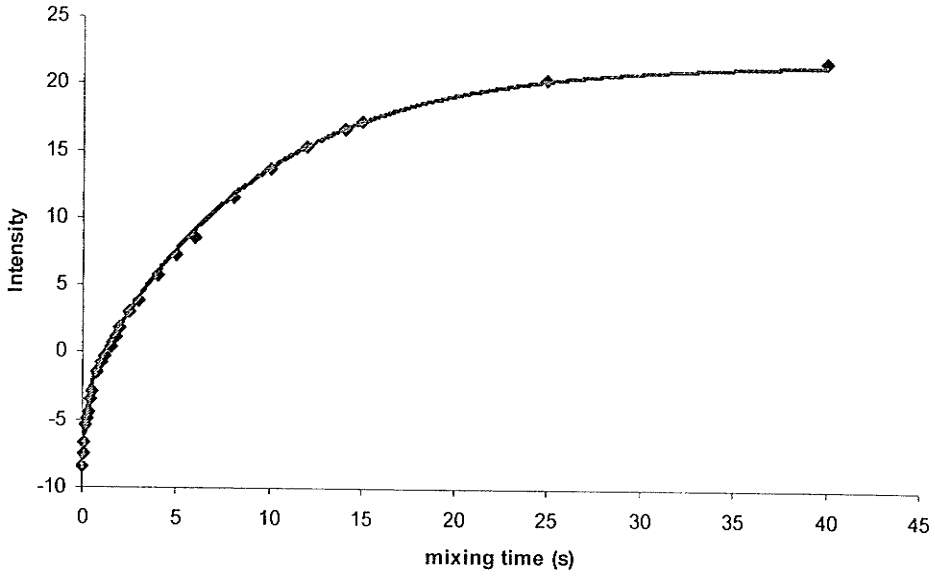

Figure 41. Inversed α-proton (*trans*) for compound **6** at 83°C in D_2O

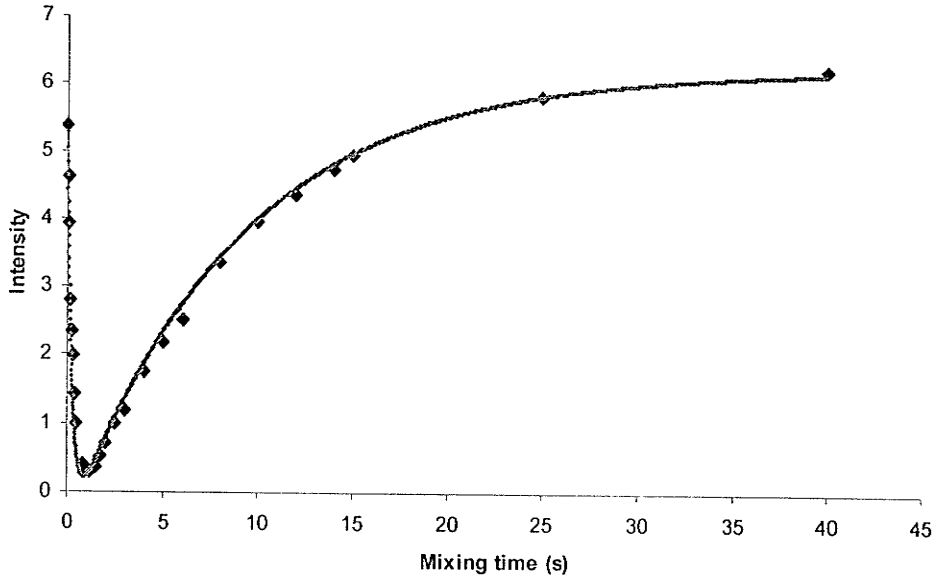

Figure 42. Inversed α-proton (*cis*) for compound **6** at 83°C in D_2O

Table 1. Data for inversion-magnetization transfer experiments

Temp. (°C)		93	91	89	86	83	81	78	73	67	62	57	52	46
Temp. (K)		366	364	362	359	356	354	351	346	340	335	330	325	319
3	k_{ct}	0.494	0.400	0.324	0.255	0.182	-	-	-	-	-	-	-	-
	k_{tc}	0.208	0.169	0.135	0.107	0.076	-	-	-	-	-	-	-	-
4	k_{ct}	-	-	-	-	16.186	-	-	-	4.240	2.984	1.592	0.966	0.554
	k_{tc}	-	-	-	-	19.820	-	-	-	5.118	3.125	1.949	1.184	0.679
5	k_{ct}	-	-	4.347	-	2.634	-	1.669	1.053	-	0.363	-	-	-
	k_{tc}	-	-	1.632	-	1.022	-	0.610	0.390	-	0.139	-	-	-
6	k_{ct}	-	-	-	-	2.947	-	1.812	1.111	0.666	0.386	-	-	-
	k_{tc}	-	-	-	-	0.818	-	0.497	0.295	0.177	0.102	-	-	-

Table 2. Equations for *Eyring* plots

$\Delta H^{\neq}$, $\Delta S^{\neq}$, $\Delta G^{\neq}$ were calculated by the following equations:

Compd	Equation	Slope ± SE	Intercept ± SE
3	*Cis-trans* y = -13.15 x + 29.34	-13.15 ± 0.08	29.33 ± 0.22
	Trans-cis y = -13.30 x + 28.88	-13.30 ± 0.08	28.88 ± 0.22
4	*Cis-trans* y = -9.96 x + 24.86	-9.96 ± 0.06	24.86 ± 0.18
	Trans-cis y = -9.85 x + 24.73	-9.85 ± 0.08	24.73 ± 0.26
5	*Cis-trans* y = -10.86 x + 25.58	-10.86 ± 0.12	25.58 ± 0.35
	Trans-cis y = -10.83 x + 24.54	-10.83 ± 0.13	24.54 ± 0.38
6	*Cis-trans* y = -11.04 x + 26.18	-11.04 ± 0.04	26.18 ± 0.13
	Trans-cis y = -11.33 x + 25.71	-11.33 ± 0.05	25.71 ± 0.15

$\Delta H^{\neq}$, $\Delta S^{\neq}$, $\Delta G^{\neq}$ were calculated by the following equations:

$\Delta H^{\neq}$ = Slope x R x 1000, $\Delta(\Delta H^{\neq})$ = (ΔSlope) x R (3)

$\Delta S^{\neq}$ = (Intercept – $Ln(k_B/h)$) x R, $\Delta(\Delta S^{\neq})$ = (ΔIntercept) x R (4)

$\Delta G^{\neq} = \Delta H^{\neq} - T\Delta S^{\neq}$ $\Delta(\Delta G^{\neq}) = \Delta(\Delta H^{\neq}) + T\Delta(\Delta S^{\neq})$ (5)

R = 8.3145. $k_B = 1.381 \cdot 10^{-23}$ J·K^{-1}, $h = 6.626 \cdot 10^{-34}$ J·s

8.2.5. Thermodynamics. The equilibrium constants for the interconversion of the *cis* and *trans* isomers of **2-5** were determined by measuring the peak area of the 1H resonance for the two isomers. Peak areas were measured with the program Spinworks 2.5. Experiments were conducted at 298-360 K. Equilibrium constants ($K_{t/c}$ = *trans*/*cis* ratios)

Table 3. Data for various temperature NMR experiments

$LnK_{(t/c)}$ values for compounds **3-6** at various temperatures

Temperature (°C)	93	91	89	86	83	81	78	73	67	62	51	41	30	25
Temperature (K)	366	364	362	359	356	354	351	346	340	335	324	314	303	298
1/T X 10^3	2.732	2.747	2.762	2.786	2.809	2.825	2.849	2.890	2.941	2.985	3.086	3.185	3.300	3.356
3	0.788	-	0.859	-	0.900	-	-	0.952	-	-	1.105	1.211	-	1.335
4	-	-0.136	-	-0.144	-	-0.172	-	-0.203	-	-0.246	-0.236	-0.248	-0.288	-0.294
5	-	-	1.258	-	1.286	-	1.316	1.348	-	1.401	1.442	1.562	-	1.586
6	-	-	-		1.330	-	1.361	1.394	1.428	1.463	1.526	1.581	1.639	1.664

*Ln*K(t/c) values for , Ac-3(*S*)-GlcPro-OMe(**3**),Ac-3(*R*)-GlcPro-OMe(**4**) Ac-3(*S*)-OH-Pro-OMe (**5**) and Ac-Pro-OMe (**6**)

were calculated directly from the peak areas.

Table 4. *Van't Hoff* plots for $K_{t/c}$

Compd	Equation	Slope ± SE	Intercept ± SE
3	y = 0.838 x - 1.475	0.838 ± 0.033	-1.475 ± 0.010
4	y = -0.247 x + 0.527	-0.247 ± 0.028	0.527 ± 0.085
5	y = 0.546 x – 0.242	0.546 ± 0.014	-0.242 ± 0.042
6	y = 0.607 x – 0.361	0.607 ± 0.019	-0.361 ± 0.060

ΔH^o, ΔS^o, ΔG^o were calculayed by the following equations:

ΔH^o = slope x R x 1000, $\Delta(\Delta H^o)$ =Δslope x R (R = 8.3145) (6)

ΔS^o = intercept x R, $\Delta(\Delta S^o)$ =Δintercept x R (7)

$\Delta G^o = \Delta H^o - T\Delta S^o$ $\Delta(\Delta G^o) = \Delta(\Delta H^o) + T\Delta(\Delta S^o)$ (8)

8.2.6. FT-IR spectroscopy. Samples of **3-6** were prepared at concentration of 0.10 M in D_2O. FTIR spectra were recorded on a Nicolet 5PC spectrometer. Experiments were performed at 25 °C using CaF_2 in a Spectra Tech circle cell. The frequency of amide I vibrational modes was determined to within 2 cm^{-1}

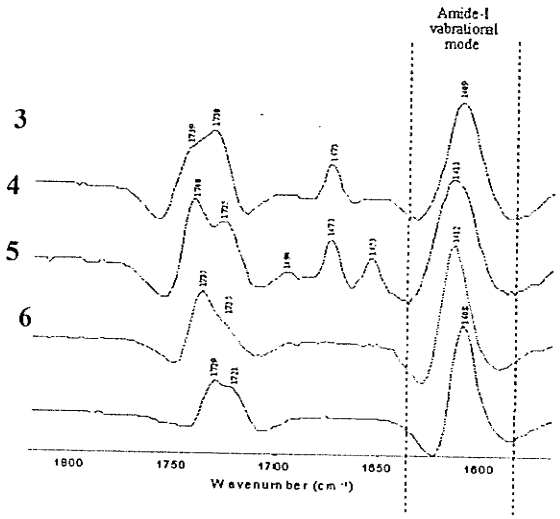

Figure 43. FT-IR spectra of amide-I (C=O) vibrational mode for **compounds 3-6.**

8.2.7. Temperature coefficient (Δδ/ΔT) experiment: 1 D ^{1}H-NMR spectroscopy of 17mM solutions of **3** and **4** in 100.0% Me_2SO-d_6 were recorded on Bruker AMX500 at 20 °C, and from 20 to 45 °C with increments of 5 °C, using routine techniques. Chemical shift (δ) are expressed in ppm and calibrated with respect to the residual DMSO signal (^{1}H: 2.49 ppm).

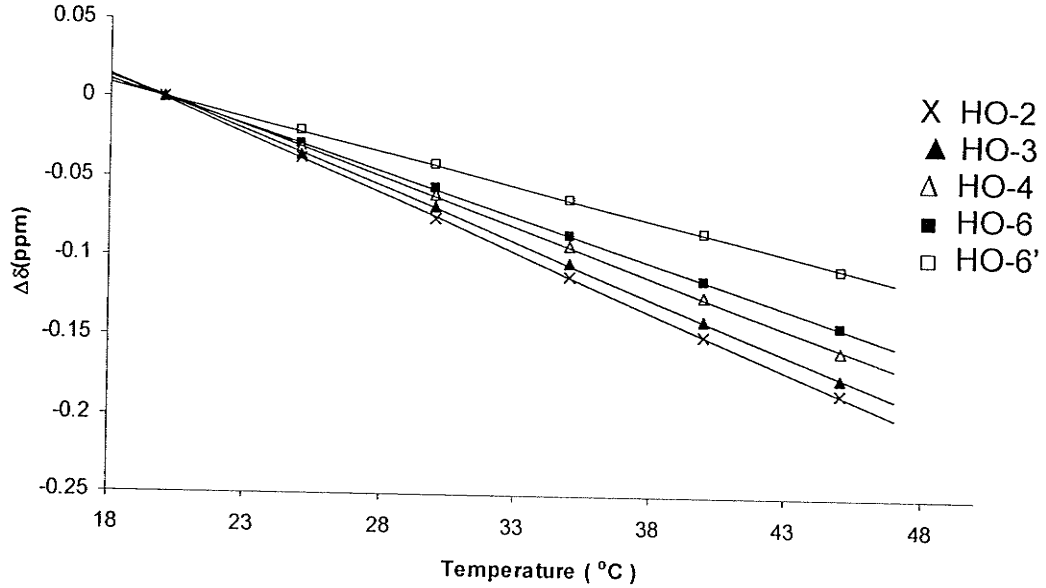

Figure 44. Temperature dependence of hydroxyl proton resonances of the *cis* isomer of Ac-3'(*R*)-GlcPro-OMe (**3**) in DMSO-d_6.

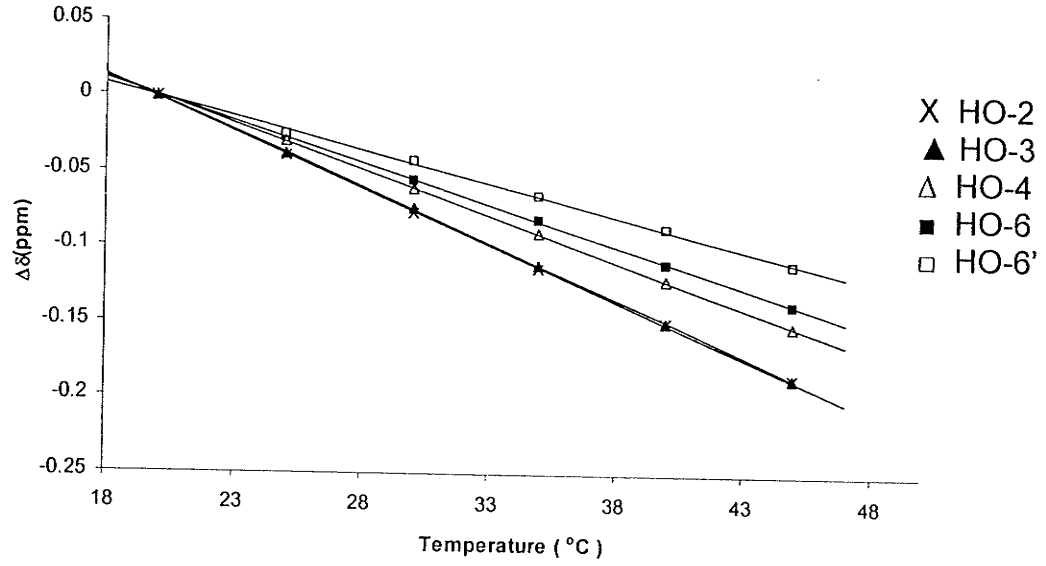

Figure 45. Temperature dependence of hydroxyl proton resonances of the *trans* isomer of

Ac-3'(*R*)-GlcPro-OMe (**3**) in DMSO-d_6.

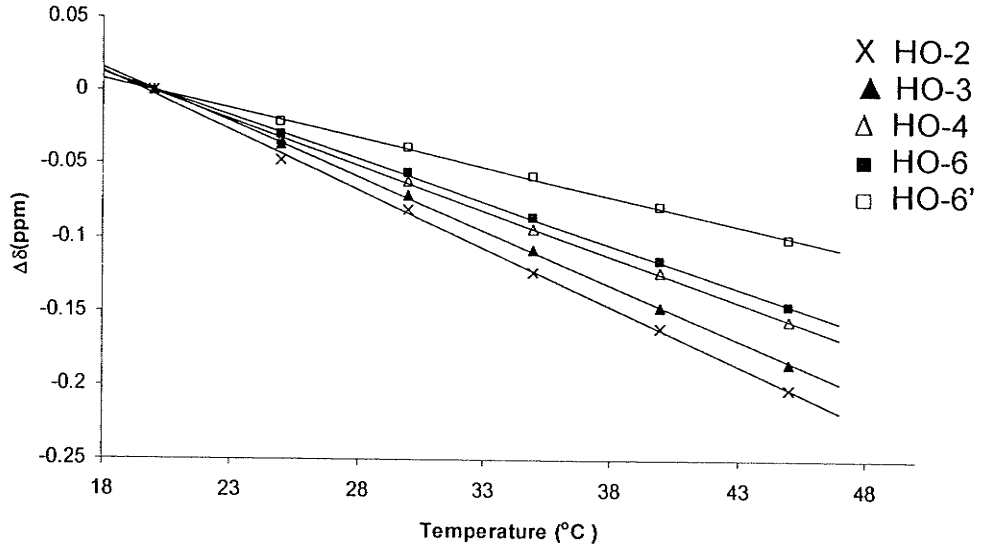

Figure 46. Temperature dependence of hydroxyl proton resonances of the *cis* isomer of Ac-3'(*R*)-GlcPro-OMe (**4**) in DMSO-d_6.

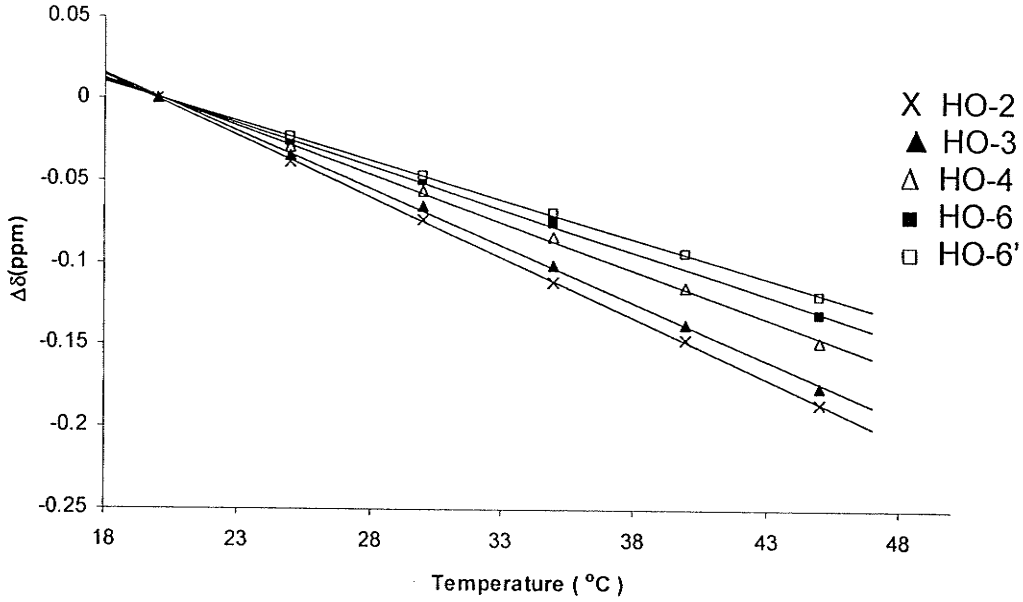

Figure 47. Temperature dependence of hydroxyl proton resonances of the *trans* isomer of Ac-3'(*R*)-GlcPro-OMe (**4**) in DMSO-d_6.

9.2.8. Computational methods (The data were provided by Dr. Schreckenbach's group)

A computational approach was used for detailed structural assignments and determination of the conformational distributions of compounds **3** and **4** in water. Due to the complexity of the potential energy surface of these compounds, a systematic conformational search routine was employed. First, the MMFF94 force field implemented in the SPARTAN '02 program was used to generate an initial set of trial structures or conformers. Specifically, a Monte-Carlo or random conformational search was performed starting from an initial energy minimized guess structure drawn in SPARTAN. Although Monte-Carlo was designed to fairly sample all regions of the conformational space, one cannot guarantee that all lowest energy conformers are located. As a result of this limitation in the random sampling technique, some very important conformers might be missed during the search. To avoid this inherent problem, we adopted a strategy of searching the conformational space by re-starting the search with different initial conformations and checking for the completeness of the analysis. Once a redundant outcome was observed, we assumed that the conformational space was fully covered and the conformations were gathered. This 'build and search' approach identified a set of 2700 structures for each compound (**3** and **4**). However, when these structures were superimposed, a set of 443 unique conformers for compound **3** and 457 for compound **4** were isolated.

Once the unique local minima were identified using MMFF94, the remaining conformers were used as guess structures (input structures) for gas phase B3LYP/6-31+G(d, p) optimizations as implemented in the GAUSSIAN 03 program package[1]. Full B3LYP/6-31+G(d, p) optimizations lead to 443 and 453 unique conformers for

compounds **3** and **4**, respectively. All B3LYP structures were real local minima as characterized by the absence of imaginary frequencies.

Subsequently, solvent effects were taken into account through re-optimization of the gas-phase B3LYP/6-31+G(d, p) minima in water at the same level of theory using Tomasi's Polarized Continuum Model (PCM). This led to only 355 and 258 real local minima for compounds **3** and **4**, respectively. The remaining structures either had large imaginary frequencies, which were very difficult to avoid, or the structures were difficult to converge. When the SCF convergence behavior for structures with convergence problems was checked by analyzing the energy change for each iterative step, it was found that there is no dramatic change in their energy from one step to the next. Moreover, these structures are at a higher energy level compared to the collected conformers, which suggests that they are relatively unimportant for our total analysis. Thus, such structures were discarded after repeated attempts to reach convergence had failed.

Using the B3LYP optimized geometries in water, the total free energies of each conformer were calculated. The total free energies were subsequently used to determine the *cis/trans* ratio of the local minima according to a Boltzmann distribution (Boltzmann statistics) calculated at 25°C. In Tables 5 and 6, we report data for the most stable conformers**3** and **4**. Only those conformers have been listed in the tables that have a statistical weight of at least 0.5%, according to the Boltzmann distribution. For each conformer, we provide the total energy, statistical weight, as well as various torsion angles (key geometry parameters.) The calculated dipole moment has been included for future reference since it has a strong influence on the free energy of solvation.

TABLE 5. Backbone torsion angles, endocyclic torsion angles, and conformational distribution of cis-trans isomers of compound **3**, which are optimized at the B3LYP/6-31+G(d) level of theory in the water.

Conformers	B3LYP/6-31+G(d)		Dipole moment [b]	Backbone Torsion Angles and Endocyclic Torsion Angles [a]								
	H_2O (a.u.) Total Free Energy	Conformer Distribution	In H_2O	ω'	ϕ	ψ	ω	χ^1	χ^2	χ^3	χ^4	χ^0
Conformer1	-1279.15805900	4.70017076	5.1329	175.253	-64.198	153.736	177.502	28.915	-34.773	26.879	-8.378	-13.164
Conformer2	-1279.15797400	4.29548658	5.6868	174.849	-63.973	153.458	177.498	29.437	-34.414	25.781	-6.852	-14.482
Conformer3	-1279.15786500	3.82710817	7.6872	175.55	-61.41	-28.681	-179.498	27.616	-33.469	26.027	-8.356	-12.356
Conformer4	-1279.15761700	2.94297812	8.8327	175.706	-61.659	-28.731	-179.405	28.154	-34.144	26.603	-8.633	-12.497
Conformer5	-1279.15749700	2.59170305	9.6162	175.751	-61.884	-28.605	-179.79	28.405	-34.608	27.1	-8.983	-12.439
Conformer6	-1279.15748700	2.56439600	5.7266	175.486	-61.371	-28.421	-178.709	27.881	-33.682	26.107	-8.272	-12.569
Conformer7	-1279.15748500	2.55896921	6.6757	174.313	-64.422	153.418	177.149	30.688	-34.505	24.71	-4.861	-16.547
Conformer8	-1279.15744600	2.45541259	6.9431	174.809	-63.748	153.48	177.554	29.199	-34.614	26.354	-7.622	-13.835
Conformer9	-1279.15733500	2.18304566	7.5057	176.059	-61.619	-29.02	-179.011	27.947	-34.48	27.349	-9.547	-11.775
Conformer10	-1279.15718900	1.87025420	12.0112	177.627	-67.256	154.625	176.597	27.487	-33.487	26.314	-8.613	-12.088
Conformer11	-1279.15718800	1.86827423	10.7905	-10.903	-63.708	154.37	177.909	31.884	-34.728	23.936	-3.193	-18.36
Conformer12	-1279.15716100	1.81560020	7.8150	174.055	-64.29	153.729	177.029	30.79	-34.36	24.383	-4.444	-16.879
Conformer13	-1279.15711000	1.72012283	7.2059	175.399	-61.183	-29.02	-179.311	28.093	-33.767	26.084	-8.126	-12.779
Conformer14	-1279.15705000	1.61420453	7.5512	-10.713	-64.058	153.755	177.811	31.792	-34.917	24.354	-3.726	-17.943
Conformer15	-1279.15704400	1.60397824	7.5835	-10.972	-63.957	154.078	177.621	31.89	-35.01	24.411	-3.721	-18.01
Conformer16	-1279.15700800	1.54396672	11.3666	177.548	-66.781	154.711	177.005	27.948	-33.772	26.306	-8.315	-12.573
Conformer17	-1279.15696000	1.46742941	8.3907	-10.68	-62.642	-27.379	-177.946	30.963	-34.117	23.815	-3.727	-17.428
Conformer18	-1279.15685100	1.30742140	5.3364	-10.749	-63.601	153.891	177.725	31.447	-34.857	24.607	-4.229	-17.401
Conformer19	-1279.15682900	1.27730691	7.4783	175.365	-61.205	-29.374	-178.796	28.155	-33.865	26.186	-8.187	-12.779
Conformer20	-1279.15674100	1.16362742	8.7979	175.163	-61.389	-28.169	-179.668	28.332	-34.102	26.377	-8.261	-12.856
Conformer21	-1279.15672900	1.14893052	6.7307	-9.63	-62.972	-27.043	-177.84	30.548	-34.302	24.547	-4.794	-16.464

Conformer22	-1279.15669700	1.11063994	10.8316	-1.733	-70.669	153.388	177.641	33.395	-35.71	23.807	-2.004	-20.045
Conformer23	-1279.15669000	1.10243549	9.4318	178.559	-64.409	-27.738	-179.68	26.06	-33.108	27.07	-10.435	-9.993
Conformer24	-1279.15668300	1.09429164	3.8631	-9.77	-62.77	-27.496	-177.25	30.428	-34.185	24.488	-4.807	-16.378
Conformer25	-1279.15666800	1.07704254	10.8443	-1.876	-71.231	153.371	177.594	33.611	-35.857	23.82	-1.878	-20.26
Conformer26	-1279.15665800	1.06569446	5.4082	-9.889	-62.33	-27.827	-177.096	30.101	-33.876	24.28	-4.792	-16.197
Conformer27	-1279.15664700	1.05334962	10.8863	170.248	-56.04	-29.592	-178.56	26.461	-35.759	30.851	-14.224	-7.808
Conformer28	-1279.15663300	1.03784461	8.3676	169.778	-59.198	153.487	176.826	28.366	-36.2	29.719	-11.737	-10.635
Conformer29	-1279.15661600	1.01932360	4.5373	175.556	-60.875	-29.808	-178.657	27.684	-33.658	26.29	-8.615	-12.196
Conformer30	-1279.15660500	1.00751591	10.1026	177.233	-66.961	154.345	176.976	27.794	-33.45	25.946	-8.031	-12.662
Conformer31	-1279.15658100	0.98222629	5.4440	174.626	-64.115	151.95	175.367	30.419	-34.763	25.404	-5.81	-15.773
Conformer32	-1279.15656400	0.96469783	14.3113	-3.291	-70.535	153.12	177.54	33.483	-34.36	21.596	0.389	-21.651
Conformer33	-1279.15655600	0.95655772	10.1262	169.712	-55.97	-29.472	-178.615	26.193	-34.771	29.505	-12.975	-8.458
Conformer34	-1279.15654500	0.94547711	8.5896	165.447	-53.435	-29.854	-178.172	25.884	-34.453	29.298	-12.975	-8.285
Conformer35	-1279.15654300	0.94347629	10.1153	175.362	-61.039	-28.822	-178.998	27.718	-33.497	26	-8.297	-12.419
Conformer36	-1279.15649400	0.89575709	9.3623	166.129	-53.334	-30.287	-178.387	25.099	-34.786	30.63	-14.909	-6.521
Conformer37	-1279.15644400	0.84955111	10.4472	178.633	-63.984	-28.88	-178.987	25.955	-33.168	27.273	-10.711	-9.749
Conformer38	-1279.15643900	0.84506368	8.4195	-9.329	-62.914	-27.107	-178.164	30.355	-34.682	25.333	-5.75	-15.738
Conformer39	- 1279.15642200	0.82998297	9.1869	164.495	-56.344	152.993	176.97	28.09	-36.156	29.88	-12.072	-10.264
Conformer40	-1279.15642100	0.82910430	10.1977	171.153	-56.406	-29.716	-177.731	25.545	-35.246	30.974	-14.96	-6.759
Conformer41	-1279.15638400	0.79723914	9.6697	165.788	-53.402	-30.686	-177.616	25.705	-34.994	30.4	-14.258	-7.327
Conformer42	-1279.15636600	0.78218295	9.7219	175.849	-61.72	-28.977	-179.497	28.244	-34.288	26.771	-8.747	-12.481
Conformer43	-1279.15636400	0.78052769	8.4203	-9.462	-62.976	-27.188	-177.981	30.484	-34.706	25.239	-5.549	-15.954
Conformer44	-1279.15632300	0.74735630	9.7530	165.884	-53.481	-30.46	-177.374	25.903	-35.11	30.379	-14.095	-7.55
Conformer45	-1279.15628600	0.71863299	11.2931	170.369	-56.445	-29.143	-178.101	25.724	-34.231	29.135	-12.9	-8.21
Conformer46	-1279.15628300	0.71635303	13.8887	-3.24	-70.809	153.498	177.347	33.778	-34.389	21.342	0.857	-22.13
Conformer47	-1279.15627900	0.71332434	7.9777	171.237	-56.629	-29.889	-177.841	25.746	-35.368	30.976	-14.84	-6.959
Conformer48	-1279.15625400	0.69468300	13.8661	-3.404	-71.046	153.163	177.505	33.693	-34.427	21.477	0.671	-21.966
Conformer49	-1279.15624900	0.69101360	7.1810	-11.075	-63.19	-28.213	-177.649	31.159	-33.869	23.237	-2.969	-18.044

Conformer50	-1279.15624600	0.68882127	9.3977	163.635	-56.031	153.751	176.631	28.087	-35.191	28.346	-10.447	-11.319
Conformer51	-1279.15621300	0.66515990	4.8429	-9.645	-62.458	-27.128	-177.416	30.071	-33.976	24.521	-5.094	-15.955
Conformer52	-1279.15621000	0.66304959	8.3825	176.054	-61.66	-28.593	-179.731	27.959	-34.37	27.172	-9.35	-11.914
Conformer53	-1279.15619500	0.65259808	11.2403	-3.017	-71.674	153.034	177.422	34.082	-34.889	21.823	0.551	-22.121
Conformer54	-1279.15617400	0.63824214	6.6183	165.996	-53.495	-30.433	-177.748	25.711	-35.112	30.56	-14.43	-7.214
Conformer55	-1279.15069300	0.63756646	2.8566	176.006	-41.743	132.539	178.252	-5.605	-14.717	29.215	-34.55	-25.528
Conformer56	-1279.15614100	0.61631819	7.9141	178.168	-63.316	-28.592	-178.828	25.386	-32.416	26.629	-10.42	-9.571
Conformer57	-1279.15614000	0.61566571	8.3052	-11.703	-64.354	153.877	177.66	32.655	-34.571	22.943	-1.625	-19.854
Conformer58	-1279.15610900	0.59577806	9.0827	165.159	-53.272	-30.275	-177.498	25.87	-34.411	29.246	-12.924	-8.307
Conformer59	-1279.15607500	0.57470371	10.3456	165.331	-53.511	-29.889	-177.981	25.949	-34.447	29.227	-12.867	-8.384
Conformer60	-1279.15606900	0.57106285	7.5206	-10.037	-62.966	-27.543	-177.851	30.931	-34.588	24.616	-4.611	-16.84
Conformer61	-1279.15605800	0.56444775	11.9053	165.703	-53.206	-29.521	-177.935	25.342	-34.881	30.585	-14.715	-6.792
Conformer62	-1279.15604300	0.55555047	11.3924	165.649	-53.595	-29.54	-178.976	25.893	-35.017	30.236	-13.973	-7.642
Conformer63	-1279.15599500	0.52801080	8.9909	170.236	-56.546	-29.551	-177.579	25.492	-34.176	29.308	-13.26	-7.839
Conformer64	-1279.15598100	0.52023862	6.9900	-1.77	-70.445	-28.226	-177.256	32.8	-35.235	23.58	-2.187	-19.525
Others*		< 0.5										

Total Population Distribution

	Calc.(%)	Exp. (%)
Total Cis Isomers	**29.15**	**23**
Total Trans Isomers	**70.85**	77

[a] angles are in degrees, [b] units in Debye (D). The relative electronic energies and the relative free energies are in Hartrees. The population distributions were calculated using the Boltzmann statistical weights at 25 °C, including all conformers. In the property table, only those conformers are included that contribute 0.5% or more.

Conformer50	-1279.15624600	0.68882127	9.3977	163.635	-56.031	153.751	176.631	28.087	-35.191	28.346	-10.447	-11.319
Conformer51	-1279.15621300	0.66515990	4.8429	-9.645	-62.458	-27.128	-177.416	30.071	-33.976	24.521	-5.094	-15.955
Conformer52	-1279.15621000	0.66304959	8.3825	176.054	-61.66	-28.593	-179.731	27.959	-34.37	27.172	-9.35	-11.914
Conformer53	-1279.15619500	0.65259808	11.2403	-3.017	-71.674	153.034	177.422	34.082	-34.889	21.823	0.551	-22.121
Conformer54	-1279.15617400	0.63824214	6.6183	165.996	-53.495	-30.433	-177.748	25.711	-35.112	30.56	-14.43	-7.214
Conformer55	-1279.15069300	0.63756646	2.8566	176.006	-41.743	132.539	178.252	-5.605	-14.717	29.215	-34.55	-25.528
Conformer56	-1279.15614100	0.61631819	7.9141	178.168	-63.316	-28.592	-178.828	25.386	-32.416	26.629	-10.42	-9.571
Conformer57	-1279.15614000	0.61566571	8.3052	-11.703	-64.354	153.877	177.66	32.655	-34.571	22.943	-1.625	-19.854
Conformer58	-1279.15610900	0.59577806	9.0827	165.159	-53.272	-30.275	-177.498	25.87	-34.411	29.246	-12.924	-8.307
Conformer59	-1279.15607500	0.57470371	10.3456	165.331	-53.511	-29.889	-177.981	25.949	-34.447	29.227	-12.867	-8.384
Conformer60	-1279.15606900	0.57106285	7.5206	-10.037	-62.966	-27.543	-177.851	30.931	-34.588	24.616	-4.611	-16.84
Conformer61	-1279.15605800	0.56444775	11.9053	165.703	-53.206	-29.521	-177.935	25.342	-34.881	30.585	-14.715	-6.792
Conformer62	-1279.15604300	0.55555047	11.3924	165.649	-53.595	-29.54	-178.976	25.893	-35.017	30.236	-13.973	-7.642
Conformer63	-1279.15599500	0.52801080	8.9909	170.236	-56.546	-29.551	-177.579	25.492	-34.176	29.308	-13.26	-7.839
Conformer64	-1279.15598100	0.52023862	6.9900	-1.77	-70.445	-28.226	-177.256	32.8	-35.235	23.58	-2.187	-19.525
Others*		< 0.5										

Total Population Distribution

	Calc.(%)	Exp. (%)
Total Cis Isomers	**29.15**	**23**
Total Trans Isomers	**70.85**	77

[a] angles are in degrees, [b] units in Debye (D). The relative electronic energies and the relative free energies are in Hartrees. The population distributions were calculated using the Boltzmann statistical weights at 25 °C, including all conformers. In the property table, only those conformers are included that contribute 0.5% or more.

TABLE 6: Backbone torsion angles, endocyclic torsion angles, and conformational distribution of cis-trans isomers of compound **4**, which is optimized at the B3LYP/6-31+G(d) level of theory in the water

Conformers	B3LYP/6-31+G(d)		Dipole moment [b]	Backbone Torsion Angles and Endocyclic Torsion Angles [a]								
	H2O (a.u.) Total Free Energy	Conformer Distribution	In H2O	ω'	ϕ	ψ	ω	χ^1	χ^2	χ^3	χ^4	χ^0
Conformer1	-1279.15838500	4.15042264	10.9153	4.031	-81.347	154.516	176.927	32.683	-37.378	27.191	-6.035	-16.964
Conformer2	-1279.15837300	4.09800180	11.0304	4.297	-80.845	154.838	177.406	32.539	-37.457	27.452	-6.399	-16.641
Conformer3	-1279.15835700	4.02913580	4.9618	-170.077	-85.486	154.199	177.889	32.851	-33.196	20.473	1.061	-21.596
Conformer4	-1279.15822100	3.48858953	10.13710	3.902	-82.254	154.02	177.165	32.835	-37.137	26.661	-5.391	-17.464
Conformer5	-1279.15808700	3.02696829	6.5048	-172.554	-82.246	154.897	178.008	59.846	-30.292	18.116	2.039	-20.834
Conformer6	-1279.15801200	2.79580419	10.9310	3.878	-79.31	154.78	177.459	31.566	-36.457	26.859	-6.415	-16.019
Conformer7	-1279.15800500	2.77515118	10.9293	3.926	-78.782	153.309	177.545	31.75	-36.739	27.139	-6.59	-16.015
Conformer8	-1279.15796200	2.65158775	12.5069	4.344	-81.073	154.429	176.76	32.373	-37.373	27.468	-6.529	-16.447
Conformer9	-1279.15795800	2.64037702	6.5169	-172.448	-82.232	154.292	179.353	30.499	-30.342	18.261	1.836	-20.648
Conformer10	-1279.15791500	2.52281441	7.8114	-172.917	-81.541	154.684	178.19	30.176	-29.97	18.004	1.879	-20.468
Conformer11	-1279.15781500	2.26925765	5.1614	-170.53	-86.917	153.504	177.346	33.723	-33.628	20.387	1.719	-22.572
Conformer12	-1279.15772300	2.05855481	13.7801	4.2	-79.496	154.916	176.881	31.871	-37.151	27.642	-7.035	-15.814
Conformer13	-1279.15770400	2.01753998	8.3455	3.512	-81.193	-28.105	-177.812	32.361	-36.72	26.421	-5.464	-17.112
Conformer14	-1279.15767700	1.96065755	5.1522	-170.208	-86.394	153.91	177.6	33.493	-33.659	20.655	1.279	-22.147
Conformer15	-1279.15756000	1.73212807	9.7505	12.897	-91.14	154.666	177.338	32.641	-33.236	20.844	0.606	-21.173
Conformer16	-1279.15752900	1.67617568	9.7577	12.757	-90.437	154.79	177.186	32.551	-33.191	20.854	0.538	-21.074
Conformer17	-1279.15742100	1.49498874	7.5951	4.217	-79.003	-27.526	-177.594	31.29	-36.44	27.064	-6.843	-15.553
Conformer18	-1279.15738000	1.43145372	8.4981	4.245	-80.608	-28.347	-177.15	31.629	-36.286	26.438	-5.955	-16.341
Conformer19	-1279.15737900	1.42993829	8.7994	4.529	-82.05	152.858	175.989	32.954	-37.887	27.75	-6.464	-16.866
Conformer20	-1279.15736500	1.40889000	7.2791	-170.052	-84.046	-27.779	-179.098	32.501	-32.811	20.21	1.031	-21.333
Conformer21	-1279.15734600	1.38081915	8.5042	3.915	-80.778	-28.379	-177.398	31.934	-36.576	26.596	-5.929	-16.544

Conformer22	-1279.15732300	1.34758590	5.9159	4.935	-78.149	-27.92	-177.228	31.189	-37.028	28.108	-8.014	-14.737
Conformer23	-1279.15721800	1.20574339	6.8370	12.555	-90.425	154.631	177.253	32.497	-32.985	20.554	0.81	-21.207
Conformer24	-1279.15721400	1.20064559	7.6057	4.62	-80.305	-28.143	-177.458	32.019	-37.135	27.458	-6.787	-16.038
Conformer25	-1279.15720500	1.18925420	5.9903	3.744	-80.935	-28.491	-177.344	32.074	-36.59	26.508	-5.756	-16.736
Conformer26	-1279.15714100	1.18925420	9.3605	4.276	-77.968	-27.479	-177.297	31.037	-36.672	27.67	-7.642	-14.882
Conformer27	-1279.15713400	1.10309683	8.0443	12.314	-90.783	153.222	177.425	33.237	-34.026	21.54	0.256	-21.331
Conformer28	-1279.15712300	1.09031872	6.3277	-171.984	-81.833	154.82	178.388	30.76	-31.456	19.83	0.343	-19.863
Conformer29	-1279.15711100	1.07654773	7.4730	-170.08	-83.735	-28.796	-178.569	32.442	-33.185	20.865	0.318	-20.84
Conformer30	-1279.15708100	1.04287641	11.0267	12.45	-90.565	154.9	177.356	32.588	-33.336	21.051	0.357	-20.977
Conformer31	-1279.15706700	1.02752556	5.6968	-171.645	-79.531	-26.81	-179.607	30.626	-31.461	19.901	0.15	-19.636
Conformer32	-1279.15701000	0.96732360	9.6433	-170.626	-84.75	154.602	177.906	32.227	-32.33	19.761	1.395	-21.428
Conformer33	-1279.15700700	0.96425464	9.6433	4.865	-79.122	-28.789	-176.825	31.377	-36.812	27.568	-7.32	-15.299
Conformer34	-1279.15695900	0.91645474	9.2865	-169.534	-84.422	-27.317	-179.049	32.379	-33.319	21.169	-0.052	-20.571
Conformer35	-1279.15695800	0.91548452	6.7779	-171.356	-82.268	153.853	179.034	31.428	-32.728	21.177	-0.623	-19.657
Conformer36	-1279.15689600	0.85729458	8.6034	-170.132	-85.569	153.411	-179.818	32.805	-33.005	20.231	1.281	-21.716
Conformer37	-1279.15688700	0.84916081	12.0283	3.931	-82.023	153.88	177.72	33.075	-37.619	27.186	-5.76	-17.401
Conformer38	-1279.15686200	0.82696965	5.6947	-171.096	-82.727	154.418	177.761	31.508	-33.04	21.605	-1.014	-19.463
Conformer39	-1279.15684500	0.81221184	9.3748	11.487	-91.737	154.783	177.15	32.743	-32.909	20.221	1.309	-21.674
Conformer40	-1279.15679100	0.76705854	7.3595	-170.138	-85.506	154.067	178.014	33.061	-33.416	20.64	1.023	-21.699
Conformer41	-1279.15678100	0.75897656	5.8700	-171.742	-82.677	154.286	177.643	31.176	-31.666	19.763	0.694	-20.348
Conformer42	-1279.15670000	0.69657383	7.6156	-169.538	-83.9	-28.409	-178.713	32.12	-33.097	21.07	-0.119	-20.361
Conformer43	-1279.15668100	0.69657383	8.3135	-171.35	-80.052	-26.936	-179.325	30.15	-31.243	20.044	-0.33	-19.024
Conformer44	-1279.15667000	0.67478699	9.6358	4.091	-81.838	154.139	177.361	32.967	-37.581	27.244	-5.904	-17.226
Conformer45	-1279.15666100	0.66838481	12.3637	11.538	-90.866	155.267	177.139	32.629	-32.982	20.448	0.998	-21.406
Conformer46	-1279.15659900	0.62590100	9.0037	-169.576	-83.957	-27.802	-179.535	32.477	-33.131	20.735	0.47	-20.97
Conformer47	-1279.15655300	0.59613546	13.8152	3.956	-81.412	153.965	177.561	32.564	-37.37	27.294	-6.205	-16.792
Conformer48	-1279.15653600	0.58549704	12.9746	3.907	-82.207	154.239	177.143	32.742	-37.114	26.736	-5.529	-17.326
Conformer49	-1279.15653200	0.58302160	10.3246	-171.452	-84.225	154.551	178.295	31.992	-32.045	19.589	1.414	-21.303

Conformer50	-1279.15650500	0.56658391	9.3459	-170.544	-84.891	154.554	177.422	32.29	-32.307	19.654	1.548	-21.559
Conformer51	-1279.15649400	0.56002069	10.4355	3.759	-82.204	-27.891	-178.006	32.7	-36.942	26.448	-5.26	-17.46
Conformer52	-1279.15645600	0.53792720	12.3176	11.31	-91.845	154.642	176.438	32.758	-32.898	20.179	1.352	-21.704
Conformer53	-1279.15645200	0.53565288	10.2786	-171.622	-83.652	154.359	178.253	31.855	-31.854	19.37	1.568	-21.317
Conformer54	-1279.15643200	0.52442471	5.4632	12.852	-89.47	-28.305	-178.455	32.443	-33.58	21.54	-0.319	-20.44
Conformer55	-1279.15641700	0.51615831	15.1406	4.236	-81.741	153.895	177.438	32.835	-37.567	27.355	-6.103	-17.018
Others*		< 0.5										

Total Population Distribution

	H_2O (%)	**Exp. H_20 (%)**
Total *Cis* Isomers	57.75	53
Total *Trans* Isomers	42.25	47

[a] angles are in degrees, [b] units in Debye (D). The relative electronic energies and the relative free energies are in Hartrees. The population distributions were calculated using the Boltzmann statistical weights at 25 °C, including all conformers. In the property table, only those conformers are included that contribute 0.5% or more.

Hydrogen Bonds: The most stable conformers were studied for internal hydrogen bonding. For the hydrogen bonding characterization, we used a ≤ 2.5Å bond length cutoff to ensure that only strong hydrogen bonds were selected.[2] We increased the bond distance cutoff from ≤ 2.1Å to ≤ 2.5Å to check the sensitivity of the cutoff. However, the results found from both cutoffs remains the same. Based on this criterion we found two types of hydrogen bonds in those conformers of compounds **3** and **4** that contribute to a population distribution greater > 0.5% (Table 1-2). For compound **3**, the first major hydrogen bond exists between OH-6′ and OH-6 (6′-OH-------OH-6). The average hydrogen bond distance is ≈ 1.9Å. This hydrogen bond was found in prolyl amide *trans* conformers **10, 16, 23, 30, 37** and **56** (Table 5). The second type of hydrogen bond in compound **3**, exists between OH-6′ and *N*-terminal carbonyl (6′-OH-------O=C-N) and is found in the *cis* conformers only. Conformers **22, 25, 32, 46, 48, 53**, and **64** possess this hydrogen bond (Table 5). The bond distance of this hydrogen bond is ≈ 1.8Å. In addition, a third type of hydrogen bond is found between OH-2 and the *C*-terminal carbonyl (2-OH---O=C′-C^{α}) with a bond distance of 1.9Å. This hydrogen bond was found in only one out of 43 *trans* conformers.

For Compound **4**, the first major hydrogen bonding exists between 6′-OH and the *N*-terminal carbonyl (6′-OH---O=C′-N) and the bond distance is ≈ 1.8 Å. These conformers with this kind of hydrogen bond are conformers **1, 2, 4, 6, 7, 8, 12, 13, 17, 18, 19, 21, 22, 25, 33, 37, 44, 47, 48, 51,** and **55** (Table 6). All these above-mentioned twenty-one conformers favor a *cis* prolyl amide structure. The second hydrogen bond exists between 6′-OH and the *C*-terminal carbonyl (C^{δ}-CH_2-OH---O=C′- C^{α}) and is found in both *cis* and *trans* conformations. The conformers with this kind of hydrogen bond that favor the *cis*

prolyl amide structure are conformers **15, 16, 23, 30, 39,** and **52** and the conformers that favor the *trans* structure are also conformers **3, 5, 10, 32, 36, 40, 49, 50,** and **53** (Table 6). The bond distance of this hydrogen bonding is ≈ 1.9 Å.

Figure **47** shows the most stable *cis/trans* prolyl amide conformer for compound **3** while the most stable *cis/trans* prolyl amide conformer for compound **4** is shown in Figure **48**.

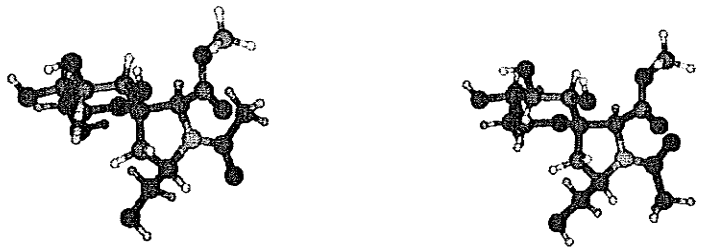

Figure 47. The most stable conformers of compound **3**: the most stable *cis* conformer is shown on the left while the most stable *trans* conformer is shown on the right. In these two conformers no intramolecular hydrogen bond was identified

Figure 48. The most stable conformers of compound **4**: the most stable *cis* conformer is shown on the left while the most stable *trans* conformer is on the right. The intramolecular hydrogen bonds between 6′-OH ···· O=C-N (*cis* isomer) and 6′-OH ···· O=C-C^{α} are indicated

9.2.9. References:

1. Frisch, M. J.; Trucks, G. W.; Schlegel, H. B.; Scuseria, G. E.; Robb, M. A.; Cheeseman, J. R.; Montgomery, J. A.; Vreven, T.; Kudin, K. N.; Burant, J. C.; Millam, J. M.; Iyengar, S. S.; Tomasi, J.; Barone, V.; Mennucci, B.; Cossi, M.; Scalmani, G.; Rega, N.; Petersson, G. A.; Nakatsuji, H.; Hada, M.; Ehara, M.; Toyota, K.; Fukuda, R.; Hasegawa, J.; Ishida, M.; Nakajima, T.; Honda, Y.; Kitao, O.; Nakai, H.; Klene, M.; Li, X.; Knox, J. E.; Hratchian, H. P.; Cross, J. B.; Bakken, V.; Adamo, C.; Jaramillo, J.; Gomperts, R.; Stratmann, R. E.; Yazyev, O.; Austin, A. J.; Cammi, R.; Pomelli, C.; Ochterski, J. W.; Ayala, P. Y.; Morokuma, K.; Voth, G. A.; Salvador, P.; Dannenberg, J. J.; Zakrzewski, V. G.; Dapprich, S.; Daniels, A. D.; Strain, M. C.; Farkas, O.; Malick, D. K.; Rabuck, A. D.; Raghavachari, K.; Foresman, J. B.; Ortiz, J. V.; Cui, Q.; Baboul, A. G.; Clifford, S.; Cioslowski, J.; Stefanov, B. B.; Liu, G.; Liashenko, A.; Piskorz, P.; Komaromi, I.; Martin, R. L.; Fox, D. J.; Keith, T.; Al-Laham, M. A.; Peng, C. Y.; Nanayakkara, A.; Challacombe, M.; Gill, P. M. W.; Johnson, B.; Chen, W.; Wong, M. W.; Gonzalez, C.; Pople, J. A. Gaussian 03, revision D.02; Gaussian, Inc.: Wallingford CT, 2004.

2. Morozov, A.; Kortemme, T.; Tsemekhman, K.; Baker, D. *Proc. Natl. Acad. Sci. U S A* **2004**. *101*, 6946.

9.3. SI for Chapter 5.

9.3.1. Synthetic procedure for 4, 6, 8, 10, 12

(1*S*)-2,3,4,6-Tetra-*O*-methoxymethyl-1′-*N*-benzyloxycarbonyl-5′(*S*)-methyl methoxymethyl ether-spiro[1,5-anhydro-D-glucitol-1,3′-*L*-proline methyl ester] (4) To a mixture of compound **2** (90 mg, 0.29 mmol) and benzyl chloroformate (0.21 mL, 1.45 mmol) in water (2 mL) was added sodium carbomate (93 mg, 0.88 mmol). The reaction was stirred for 12 hours at room temperature and extracted with ethyl acetate (5 × 10 mL). The organic layers were collected, concentrated and purified by the flash column chromatography (ethyl acetate/ methanol: 4/1) to get Cbz-propected intermediate (106 mg, 83%). Which was treated with 3 mL dichloromethane and cooled in an ice bath under nitrogen atmosphere, diisopropylethylamine (1 mL) was added dropwise, followed by a careful addition of chloromethyl methyl ether (0.71 mL, 9.36 mmol). A significant amount of white smoke formed in the reaction vessel. The reaction mixture was stirred in the dark for 48 hours during which the solution gradually turned red. After cooling to 0 °C, saturated aqueous ammonium chloride (5 mL) was added. The contents diluted with water and extracted with dichloromethane (3 × 10 mL). The combined organic layers were dried ($NaSO_4$), filtered, and concentrated. The crude product was chromatographed on silical gel (from ethyl acetate /hexanes (1:1) to ethyl acetate) to afford the product **4** (125 mg, 72%).

(1*S*)-2,3,4,6-Tetra-*O*-methoxymethyl-1′-*N*-benzyloxycarbonyl-5′(*S*)-methyl methoxymethyl ether-spiro[1,5-anhydro-D-glucitol-1,3′-*L*-proline] (6)

To a solution of compound **4** (100 mg, 0.15 mmol) in dioxane (3 mL) was added 2M lithium hydroxide aqueous solution (0.76 mL, 1.5 mmol). The reaction mixture was stirred at 60 °C for 48 hours. Afterwards the solution was cooled to room temperature and neutralized with Amberlite IRC-50S H^+ ion-exchange resin. The mixture was filtered and concentrated to afford the crude product, which was purified by flash charomatography (ethyl acetate/ methanol: 20/ 1) to get pure product **6** (51 mg, 53%).

Dipeptide H-5′(*S*)-(MOM)GlcTSPro-Val-NMe_2 (8) The amino acid TFA·NH_2-Val-NMe_2 (44 mg, 0.16 mmol) was dissolved in DMF (1 mL) and then added to a solution of acid **6** (35 mg, 0.05 mmol) and *N, N*-diisopropylethylamine (70 μL, 0.32 mmol) in DMF (3 mL). The reaction mixture was stirred for 10 minutes at room temperature followed by the addition of TBTU (41 mg, 0.11 mmol) and stirred for another 8 hours. After that the reaction is quenched with water (8 mL) and extracted with ethyl acetate (4 × 10 mL). The combined organic layer was dried with sodium sulfate and concentrated. The residue was purified by flash chromatography (ethyl acetate/methanol: 30/1) to afford the Cbz-protected intermediate, which was dissolved in ethyl acetate (5 mL) and treated with $Pd(OH)_2$ (20 mg, 20% wt on charcoal) under hydrogenation condition (H_2, 10 psi). The mixture was stirred for one and half hours at room temperature and filtered, concentrated. The resulted crude product was purified by flash chromatography (ethyl acetate/

methanol: 20/ 1) to afford the dipeptide 206 (28 mg, 85%).

Tripeptide H-D-Phe-5′(*S*)-(MOM)GlcTSPro-Val-NMe$_2$ (10) To a solution of dipeptide **8** (50 mg, 0.08 mmol) and *N, N*-diisopropylethylamine (72 μL, 0.38 mmol) in DMF (3 mL) was added the D- Fmoc-Phe-OH (93 mg, 0.23 mmol) and PyBOP (122 mg, 0.23 mmol). The mixture was stirred for 18 hours at room temperature before addition of sodium bicarbonate (27 mg, 0.30 mmol). The resulted mixture was dilutated with water (5 mL) and extracted with ethyl acetate (5 × 10 mL). The combined organic layers were dried (Na_2SO_4) and concentrated. The crude product was purified by flash chromatography (ethyl acetate/methanol: 20/1) to provide the Fmoc-protected intermediate, which was dissolved in a mixture of piperidine and DMF (0.2 mL + 0.8 mL) and stirred for 1 hour at room temperature. The solution was concentrated and purified by flash chromatography (ethyl acetate/methanol: 10/1 to 6/1; TLC was charred with the iodine) to get tripeptide **10** (28 mg, 46%).

Tetrapeptide Ac-Leu-D-Phe-5′(*S*)-(MOM)GlcTSPro-Val-NMe$_2$ (12) To a solution of tripeptide **10** (30 mg, 0.04 mmol) and *N, N*-diisopropylethylamine (35 μL, 0.19 mmol) in DMF (3 mL) was added the Fmoc-Leu-OH (41 mg, 0.12 mmol) and TBTU (37 mg, 0.12 mmol). The mixture was stirred for 18 hours at room temperature before addition of sodium bicarbonate (13 mg, 0.16 mmol). The resulted mixture was dilutated with water (5 mL) and extracted with ethyl acetate (5 × 10 mL). The combined organic layers were

dried (Na_2SO_4) and concentrated. The crude product was purified by flash chromatography (dichloromethane/methanol: 20/1) to provide the Fmoc-protected intermediate, which was dissolved in a mixture of piperidine and DMF (0.2 mL + 0.8 mL) and stirred for 1 hour at room temperature. The solution was concentrated in vacuum. The resulted mixture was dissolved in methanol (2 mL) followed by the addition of pyridine (16 μL, 0.19 mmol) and acetic anhydride (11 μL, 0.12 mmol). The mixture was stirred for 2 hours at room temperature. The solution was concentrated and purified by flash chromatography (methylene chloride/methanol: 25/ 1 to 15/ 1; TLC was charred with the iodine) to get tetrapeptide **12** (29 mg, 90%).

9.3.2. ^{1}H and ^{13}C NMR spectrum

Compound **3**

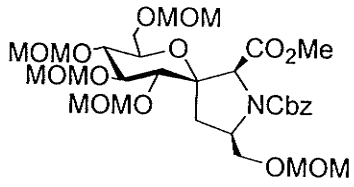

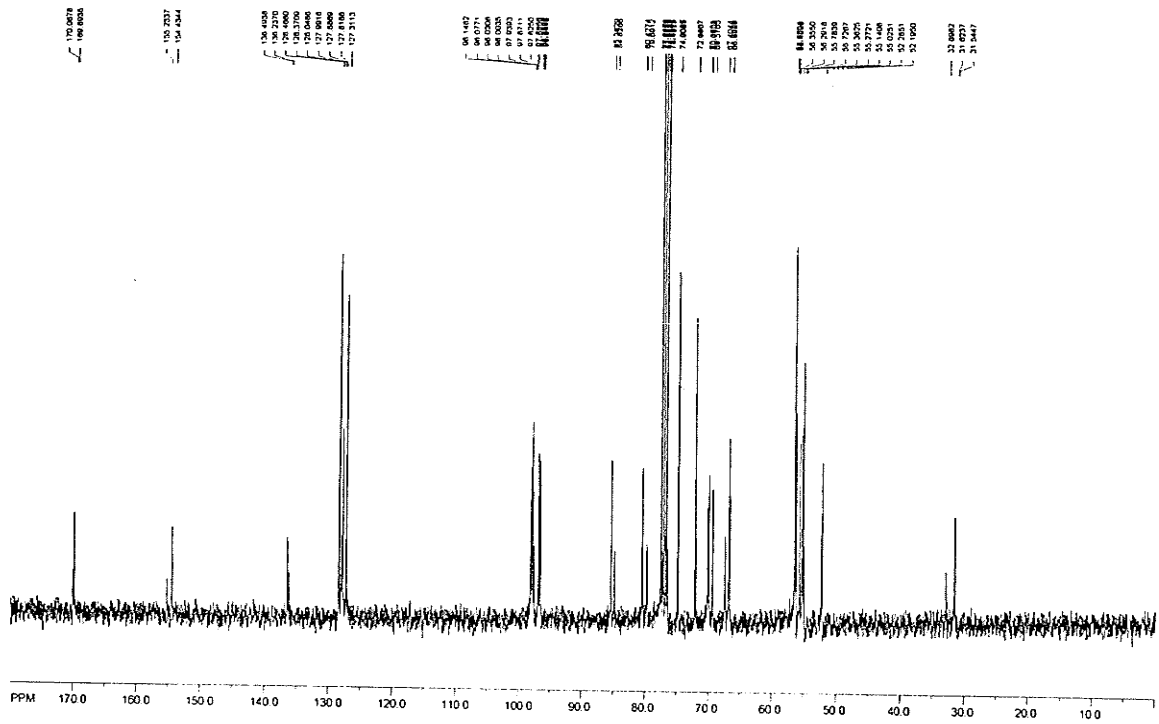

Compound **4**

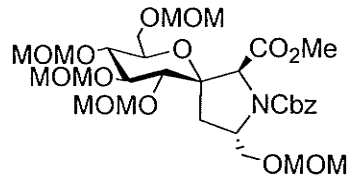
OMOM
MOMO
MOMO
MOMO
O
CO2Me
NCbz
OMOM

PPM
7.2
6.8
6.4
6.0
5.6
5.2
4.8
4.4
4.0
3.6
3.2
2.8
2.4

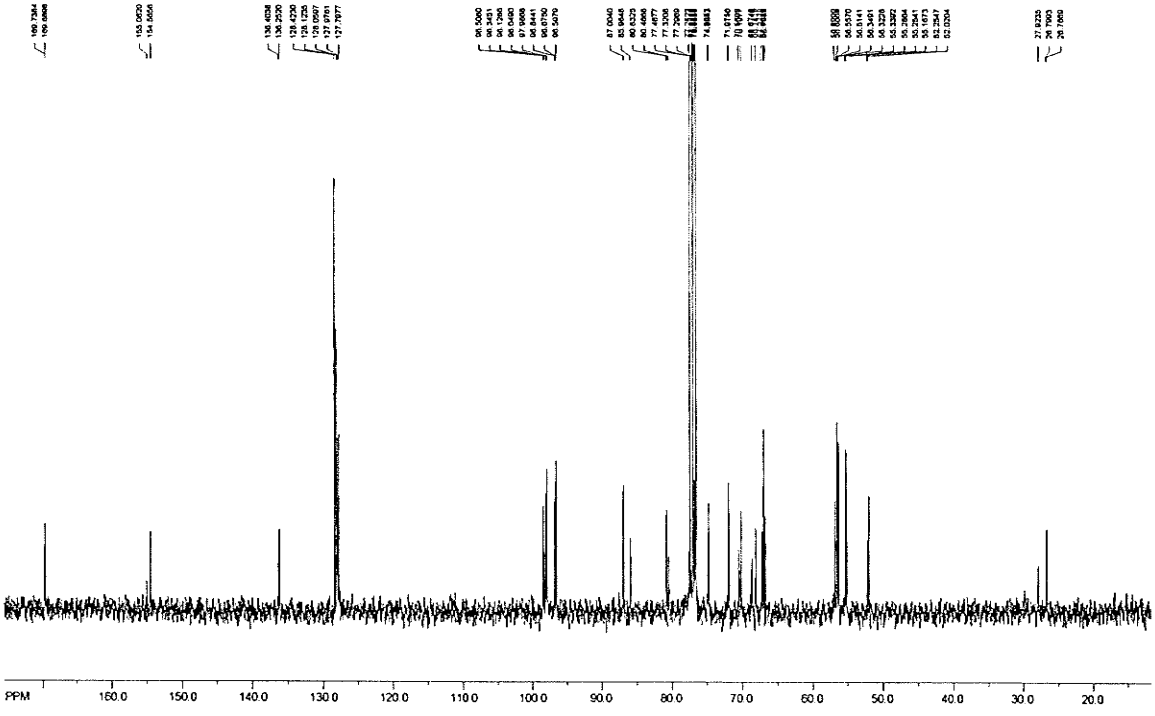
PPM
160.0
150.0
140.0
130.0
120.0
110.0
100.0
90.0
80.0
70.0
60.0
50.0
40.0
30.0
20.0

Compound 5

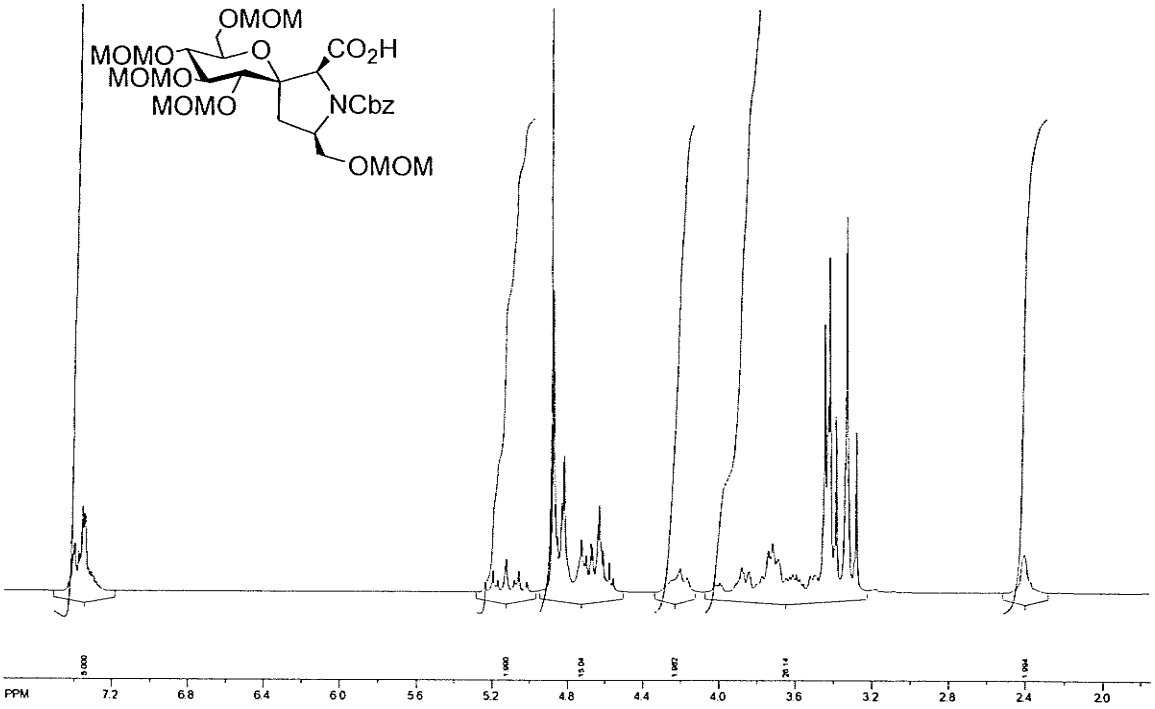
OMOM
MOMO
MOMO
MOMO
O
CO2H
NCbz
OMOM
PPM
7.2
6.8
6.4
6.0
5.6
5.2
4.8
4.4
4.0
3.6
3.2
2.8
2.4
2.0

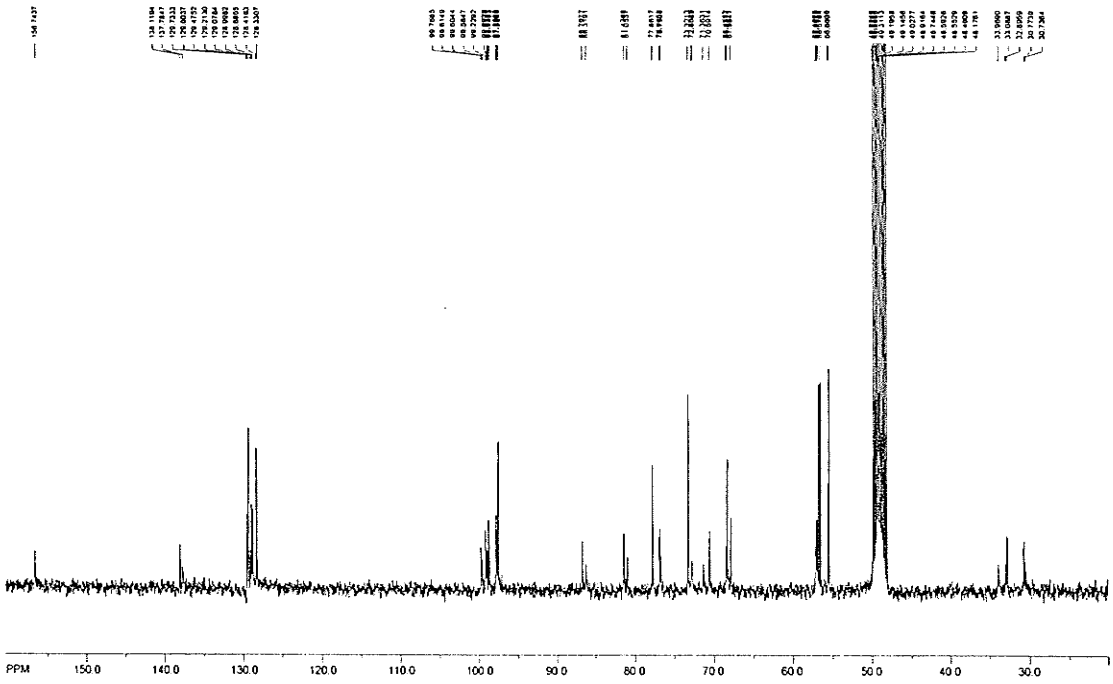
PPM
150.0
140.0
130.0
120.0
110.0
100.0
90.0
80.0
70.0
60.0
50.0
40.0
30.0

Compound **6**

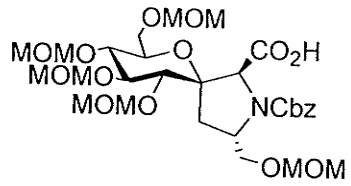
OMOM
MOMO
MOMO
MOMO
O
CO2H
NCbz
OMOM

PPM
7.2
6.8
6.4
6.0
5.6
5.2
4.8
4.4
4.0
3.6
3.2
2.8
2.4

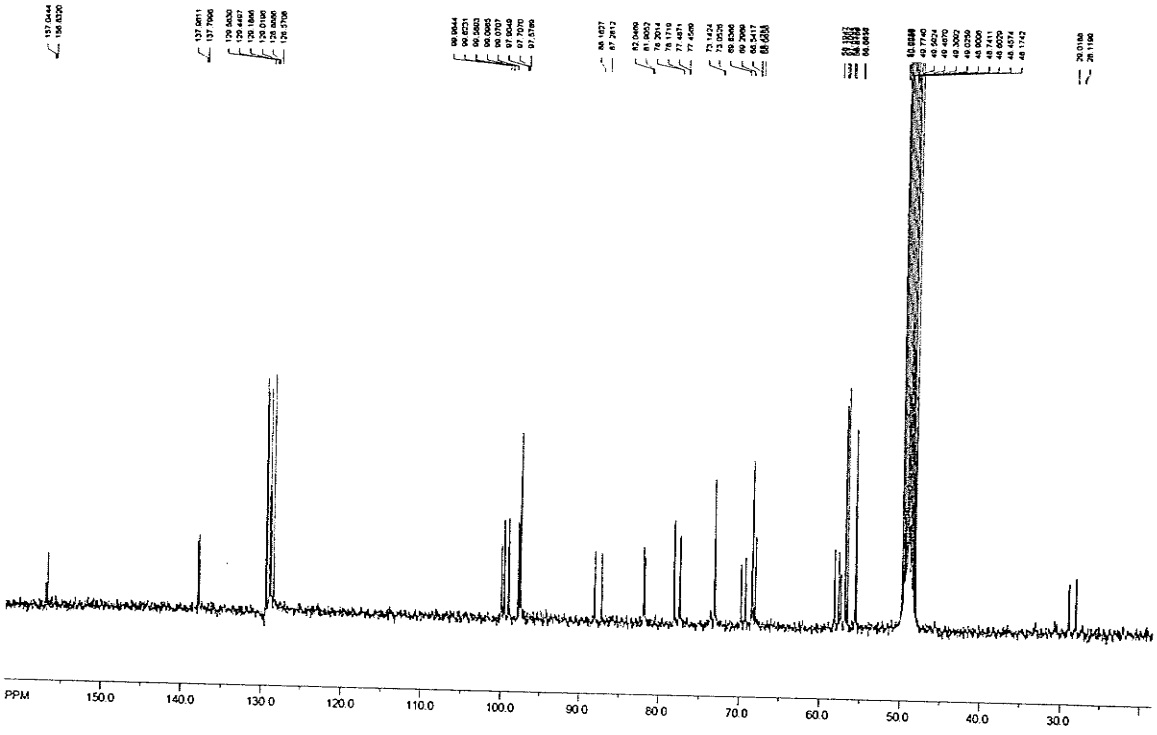
PPM
150.0
140.0
130.0
120.0
110.0
100.0
90.0
80.0
70.0
60.0
50.0
40.0
30.0

Compound **7**

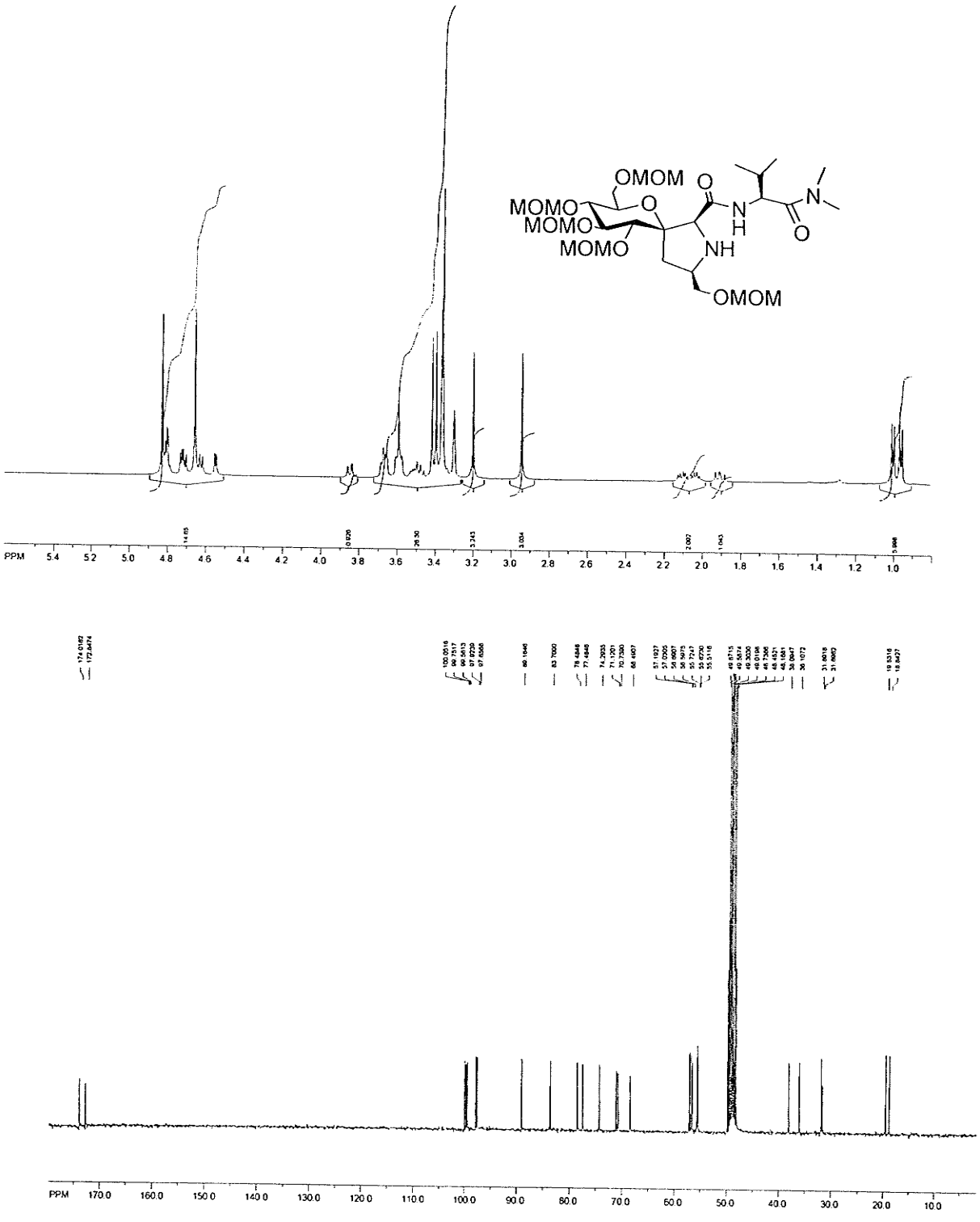

Compound **8**

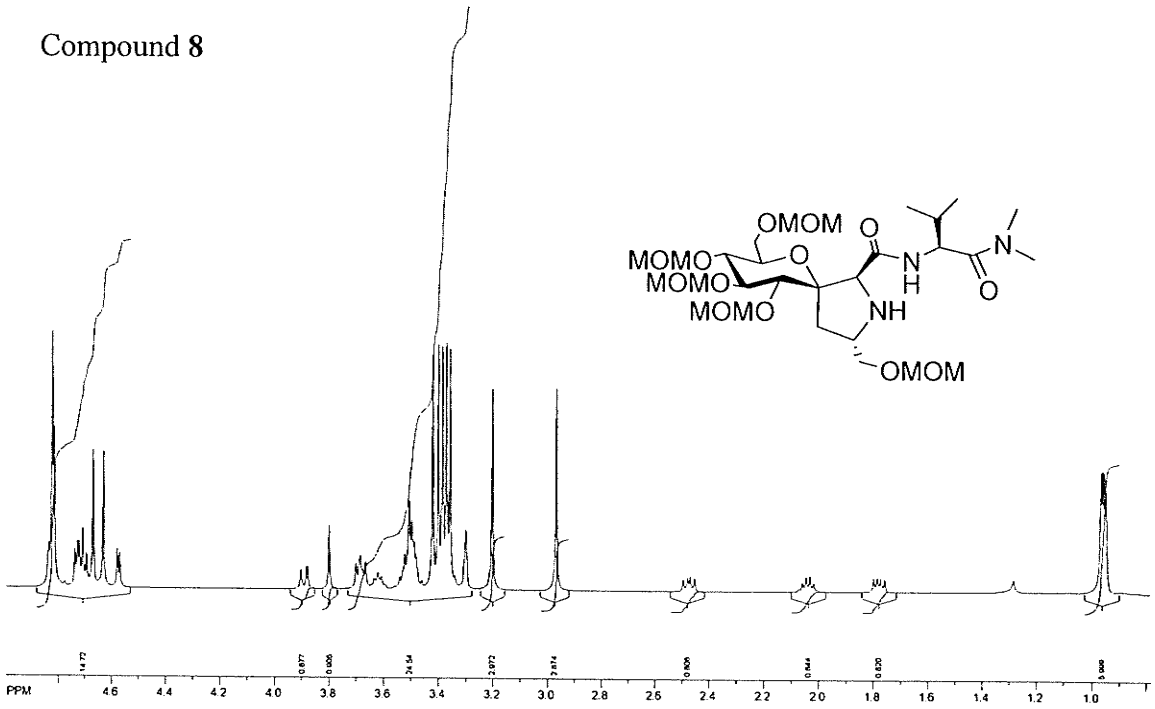
OMOM
MOMO
MOMO
MOMO
O
N
H
NH
N
O
OMOM
PPM
4.6
4.4
4.2
4.0
3.8
3.6
3.4
3.2
3.0
2.8
2.6
2.4
2.2
2.0
1.8
1.6
1.4
1.2
1.0

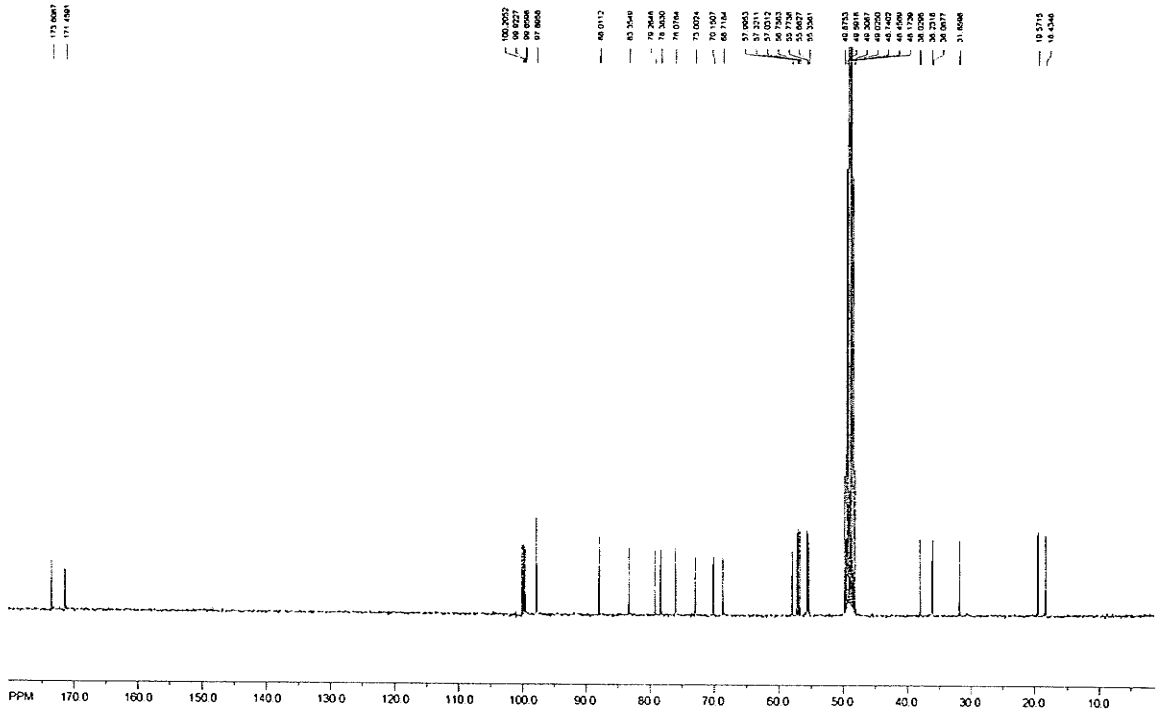
PPM
170.0
160.0
150.0
140.0
130.0
120.0
110.0
100.0
90.0
80.0
70.0
60.0
50.0
40.0
30.0
20.0
10.0

Compound **9**

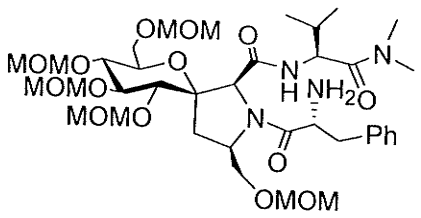
OMOM
O
MOMO
O
MOMO
MOMO
N
H
NH2
O
N
Ph
O
OMOM

PPM
7.2
6.8
6.4
6.0
5.6
5.2
4.8
4.4
4.0
3.6
3.2
2.8
2.4
2.0
1.6
1.2

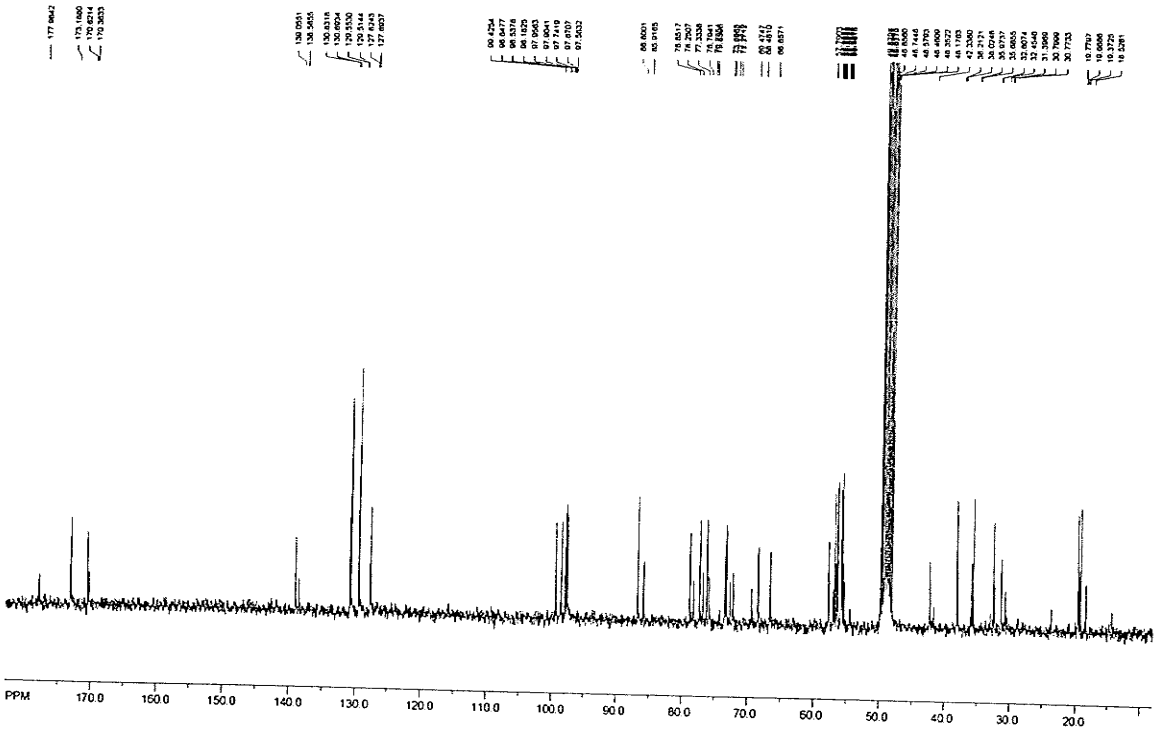
PPM
170.0
160.0
150.0
140.0
130.0
120.0
110.0
100.0
90.0
80.0
70.0
60.0
50.0
40.0
30.0
20.0

Compound **10**

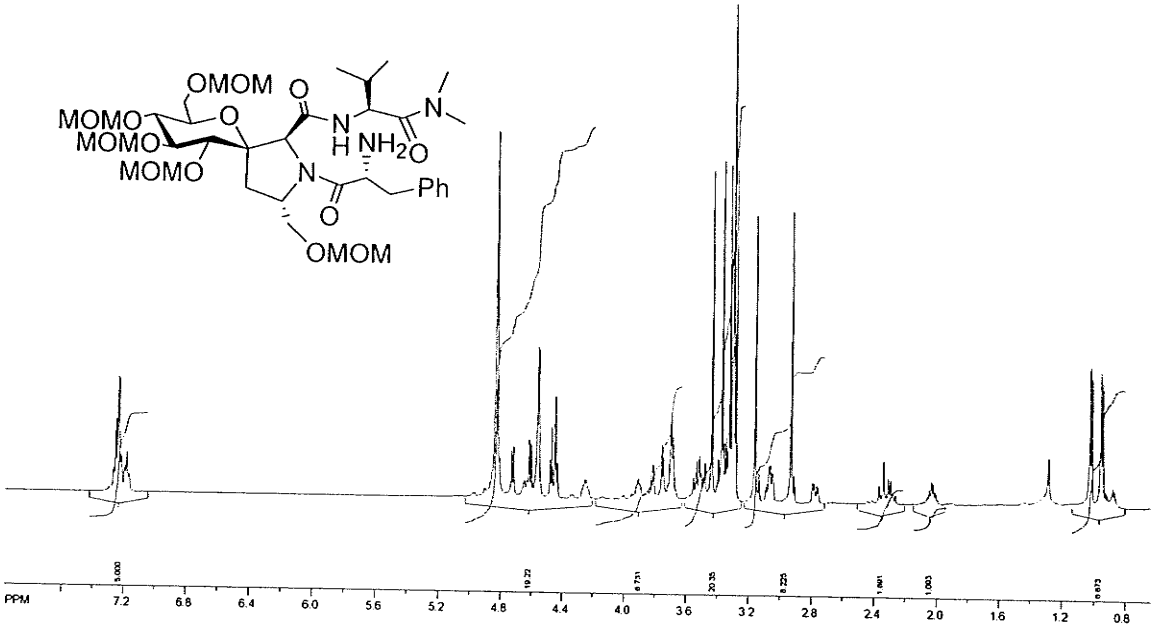
OMOM
MOMO
MOMO
MOMO
O
N
H
NH2
O
N
Ph
O
OMOM
PPM
7.2
6.8
6.4
6.0
5.6
5.2
4.8
4.4
4.0
3.6
3.2
2.8
2.4
2.0
1.6
1.2
0.8

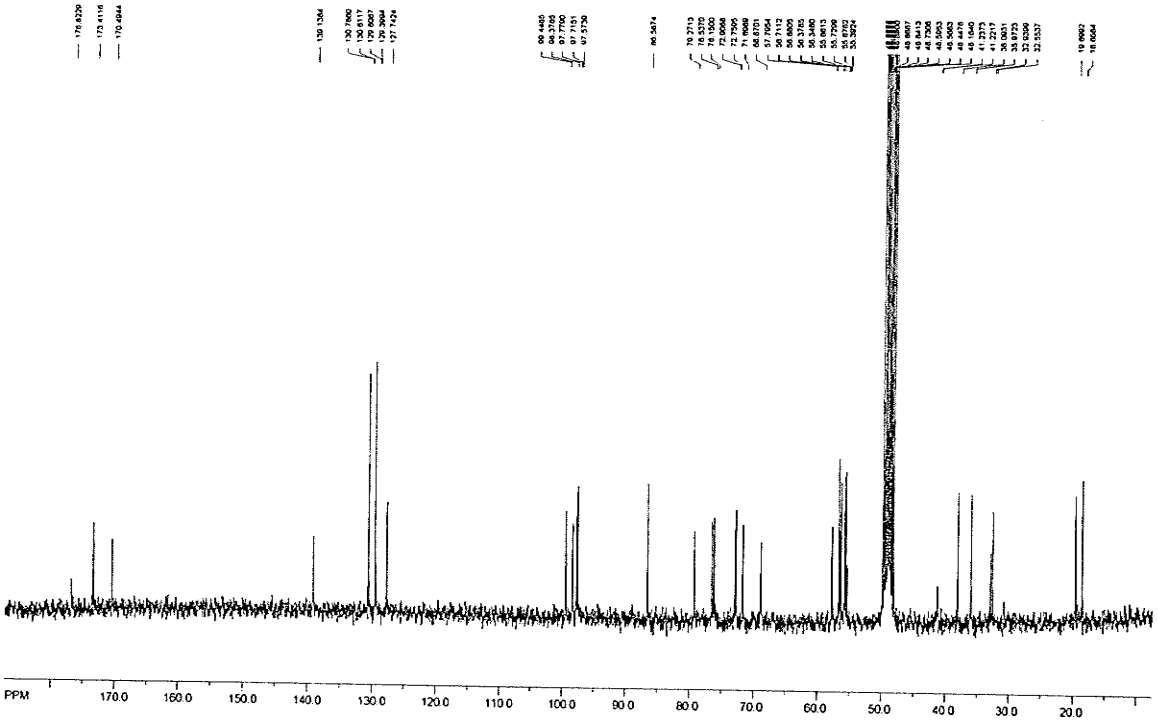
PPM
170.0
160.0
150.0
140.0
130.0
120.0
110.0
100.0
90.0
80.0
70.0
60.0
50.0
40.0
30.0
20.0

Compound **11**

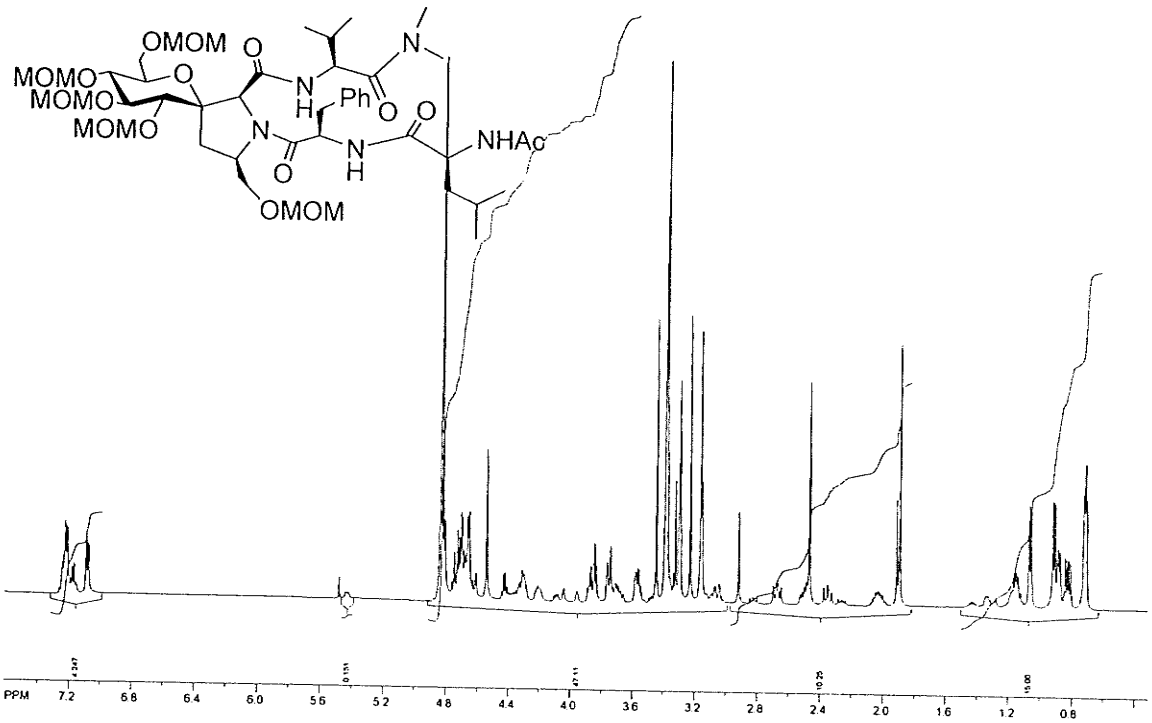
OMOM
MOMO
MOMO
MOMO
O
N
H
Ph
O
O
N
O
N
H
NHAc
OMOM
PPM
7.2
6.8
6.4
6.0
5.6
5.2
4.8
4.4
4.0
3.6
3.2
2.8
2.4
2.0
1.6
1.2
0.8

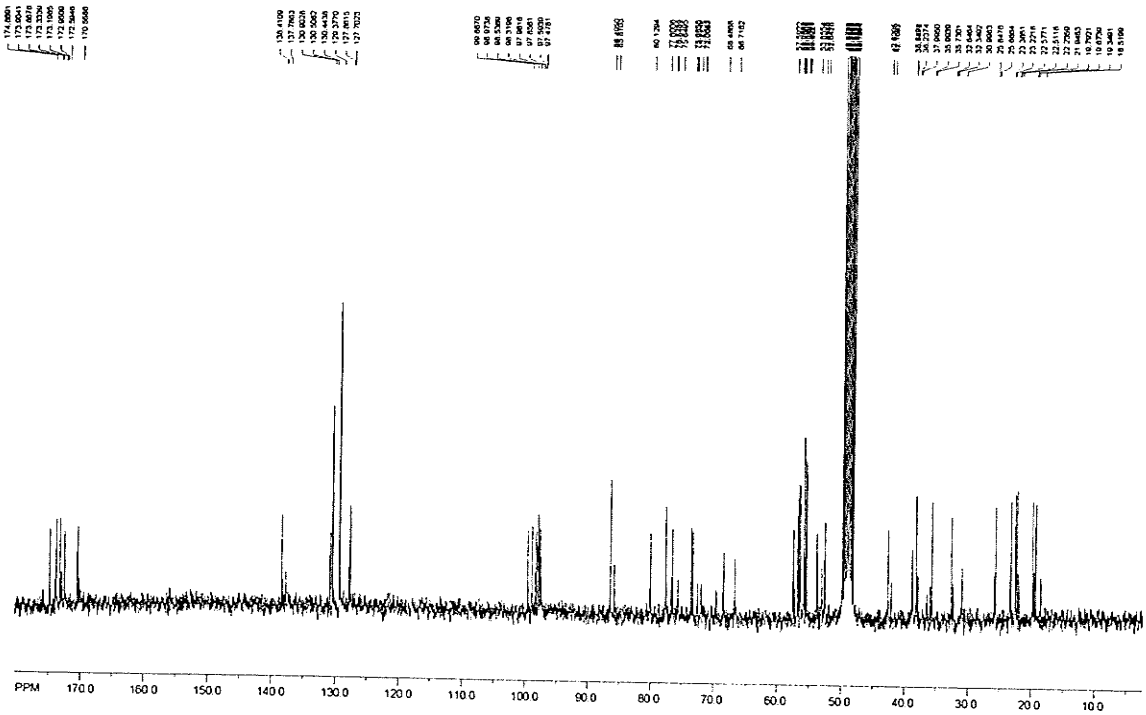
PPM
170.0
160.0
150.0
140.0
130.0
120.0
110.0
100.0
90.0
80.0
70.0
60.0
50.0
40.0
30.0
20.0
10.0

Compound **11**

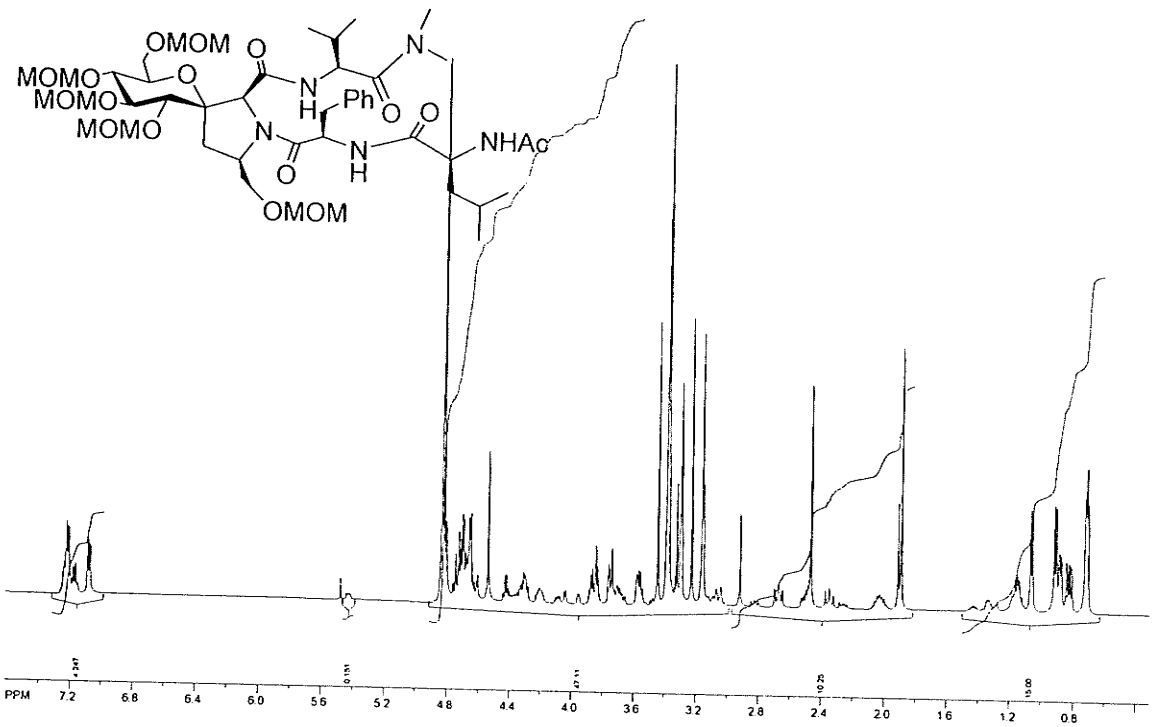
OMOM
MOMO
MOMO
MOMO
O
N
H
Ph
O
O
N
O
N
H
NHAc
OMOM
PPM
7.2
6.8
6.4
6.0
5.6
5.2
4.8
4.4
4.0
3.6
3.2
2.8
2.4
2.0
1.6
1.2
0.8

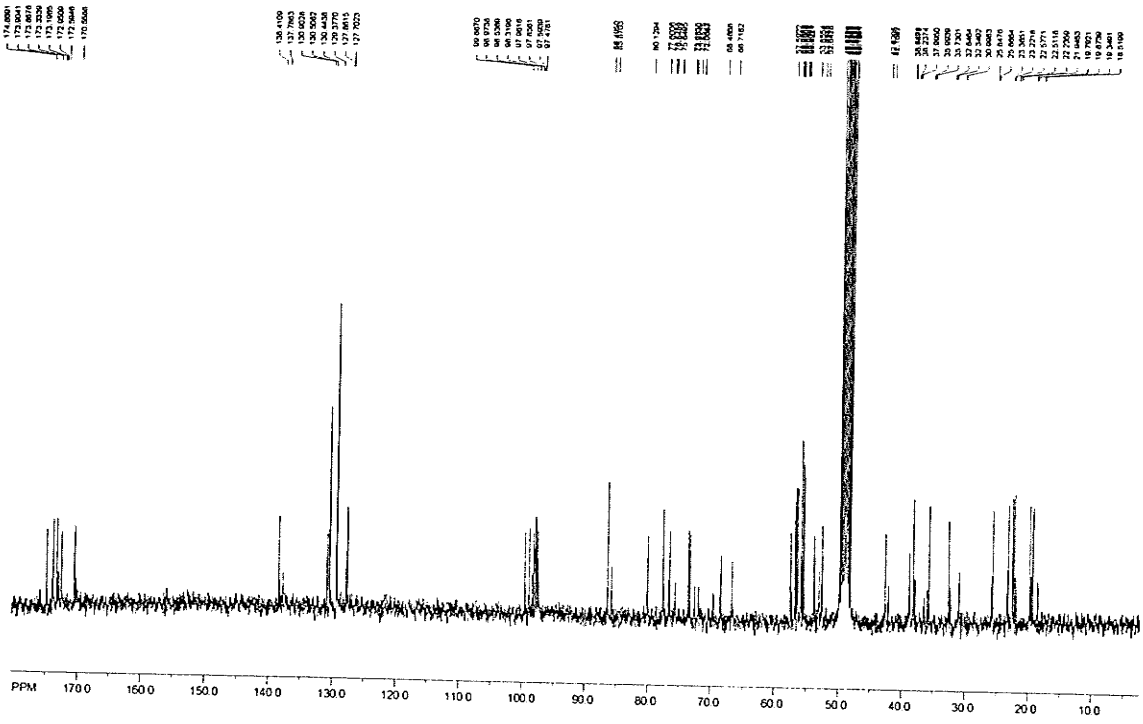
PPM
170.0
160.0
150.0
140.0
130.0
120.0
110.0
100.0
90.0
80.0
70.0
60.0
50.0
40.0
30.0
20.0
10.0

Compound **12**

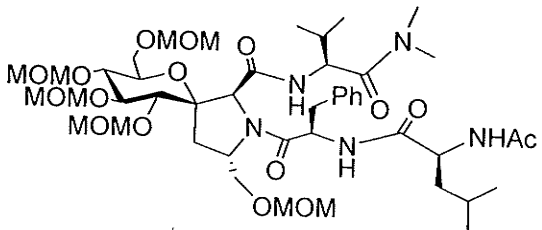
OMOM
MOMO
MOMO
MOMO
O
N
H
Ph
O
N
O
O
N
H
NHAc
O
OMOM

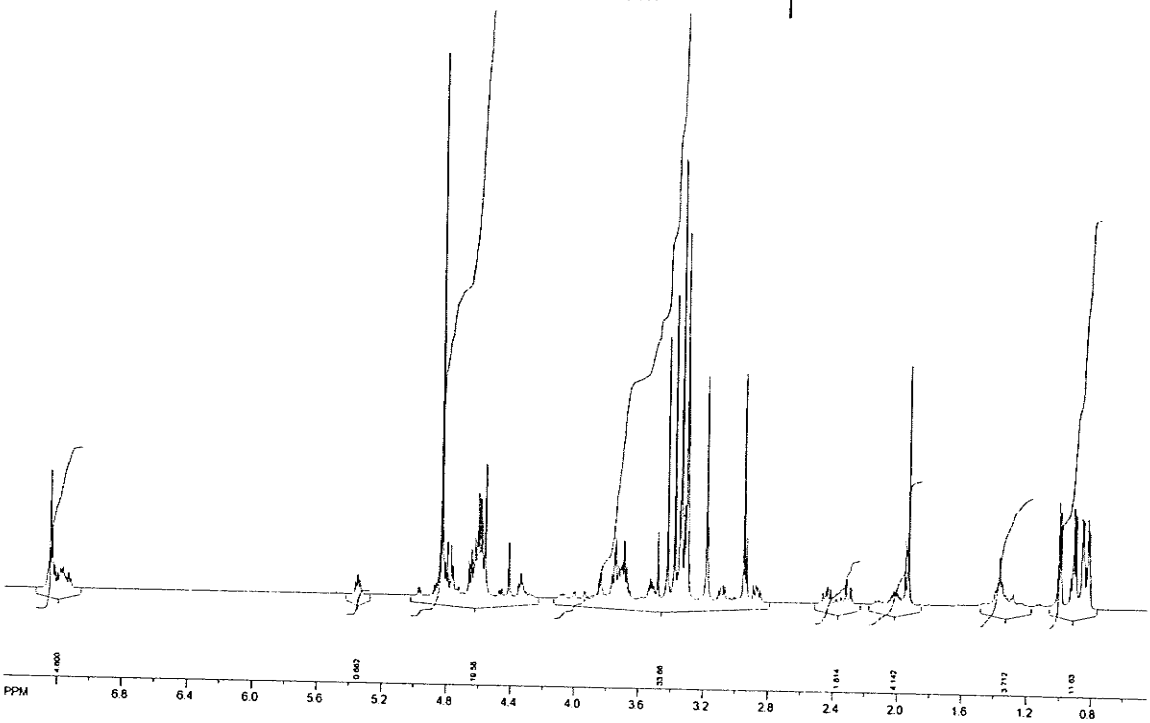
PPM
6.8
6.4
6.0
5.6
5.2
4.8
4.4
4.0
3.6
3.2
2.8
2.4
2.0
1.6
1.2
0.8

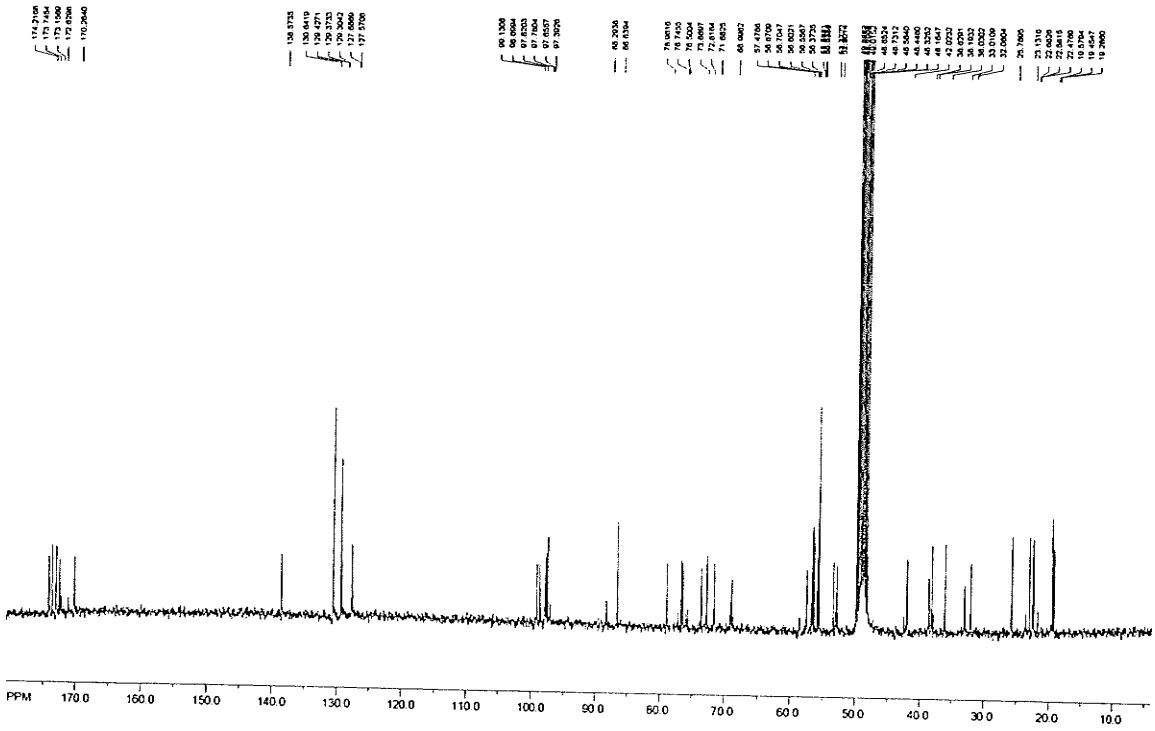
PPM
170.0
160.0
150.0
140.0
130.0
120.0
110.0
100.0
90.0
80.0
70.0
60.0
50.0
40.0
30.0
20.0
10.0

Compound **13**

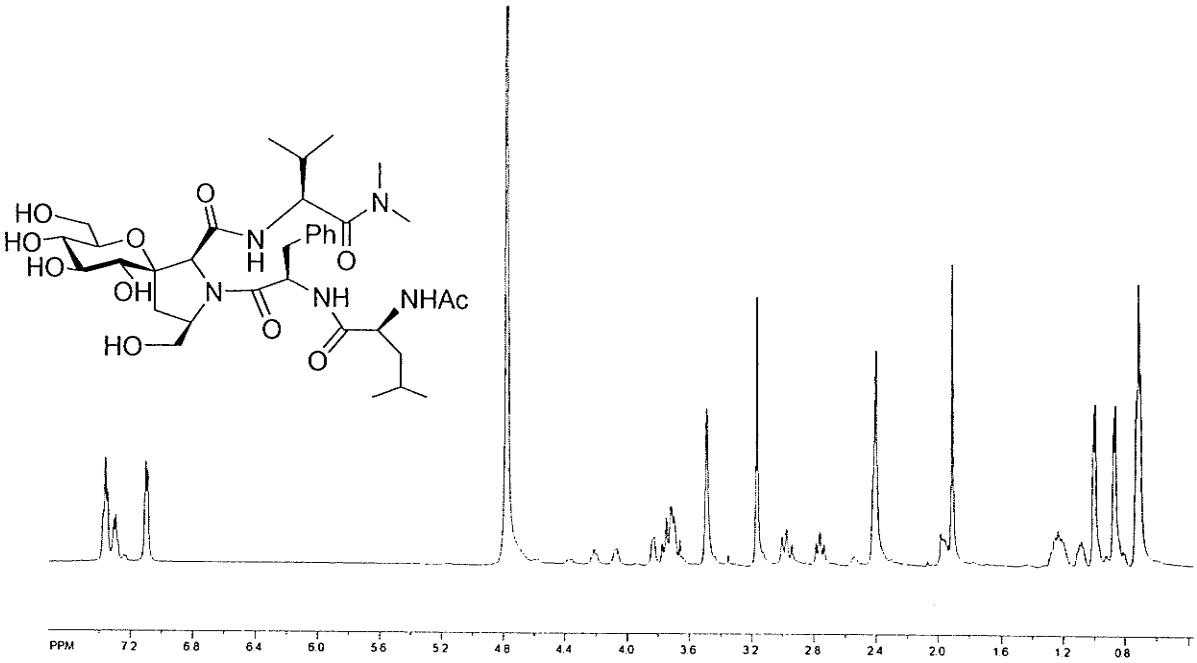
HO
HO
HO
O
OH
HO
N
O
N
H
Ph
O
N
O
NH
NHAc
O
PPM
7.2
6.8
6.4
6.0
5.6
5.2
4.8
4.4
4.0
3.6
3.2
2.8
2.4
2.0
1.6
1.2
0.8

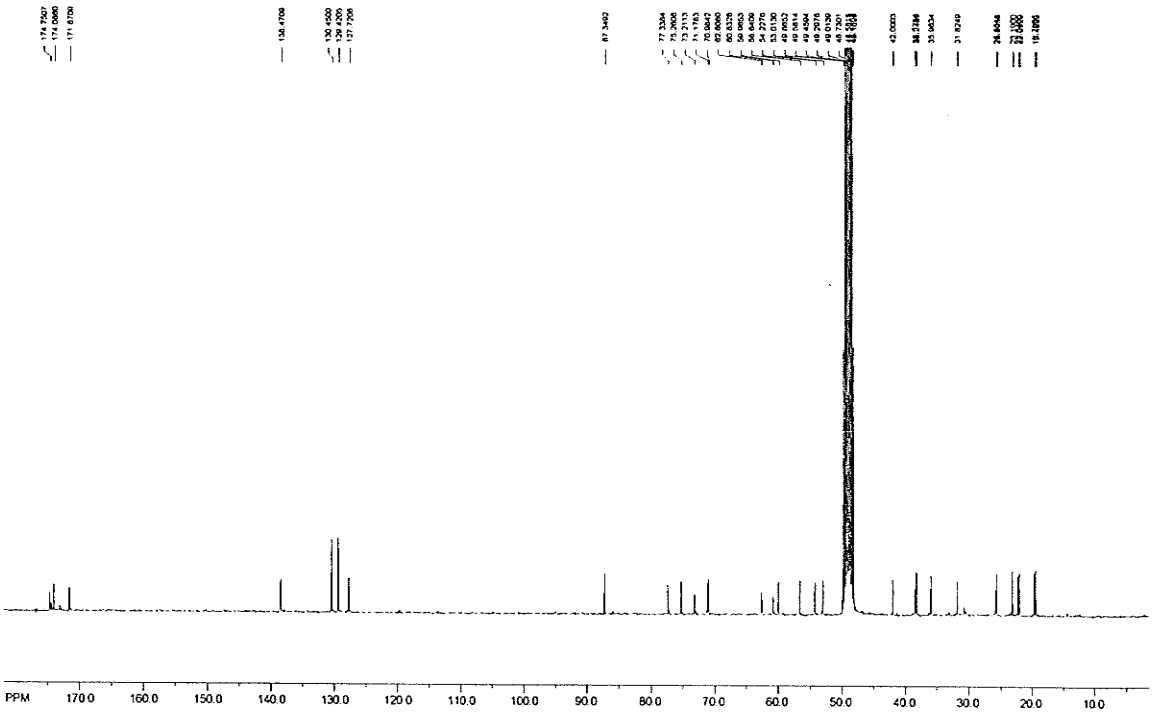
PPM
170.0
160.0
150.0
140.0
130.0
120.0
110.0
100.0
90.0
80.0
70.0
60.0
50.0
40.0
30.0
20.0
10.0

9.3.3. ROESY spectrum for tetrapeptides 11-13 and 16

2D ROESY Spectrum for **11**

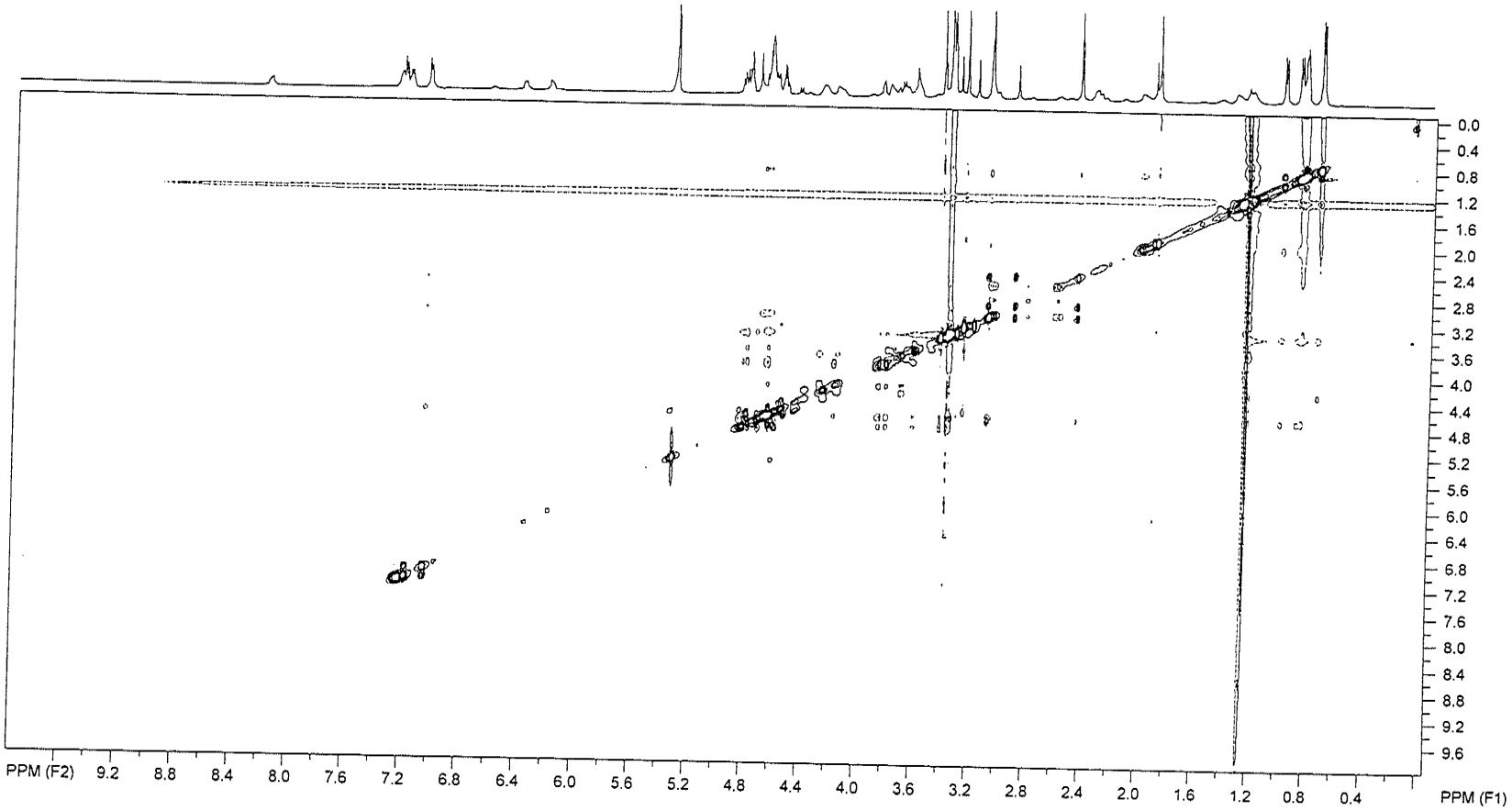

2D ROESY Spectrum for **12**

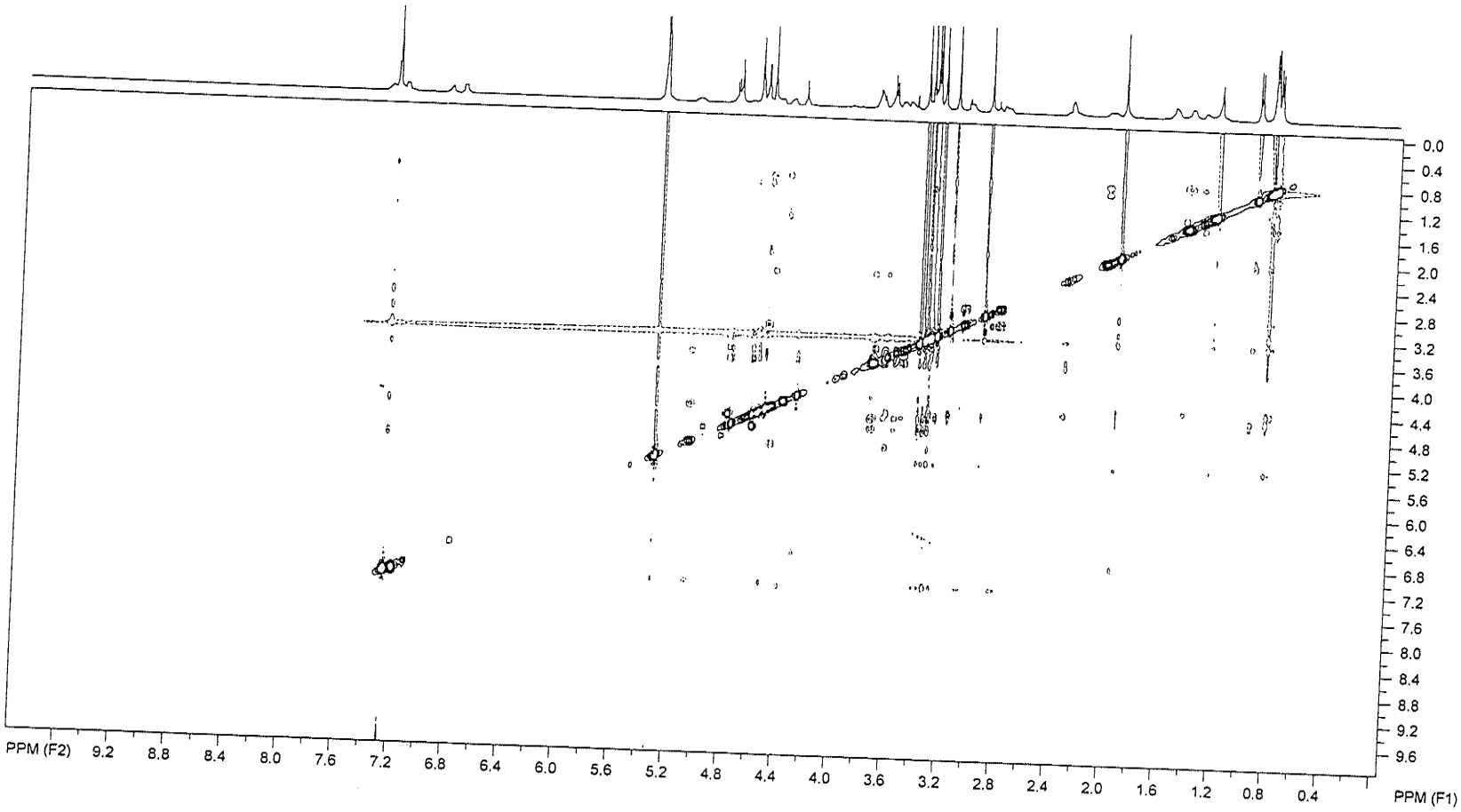

2D ROESY Spectrum for **13**

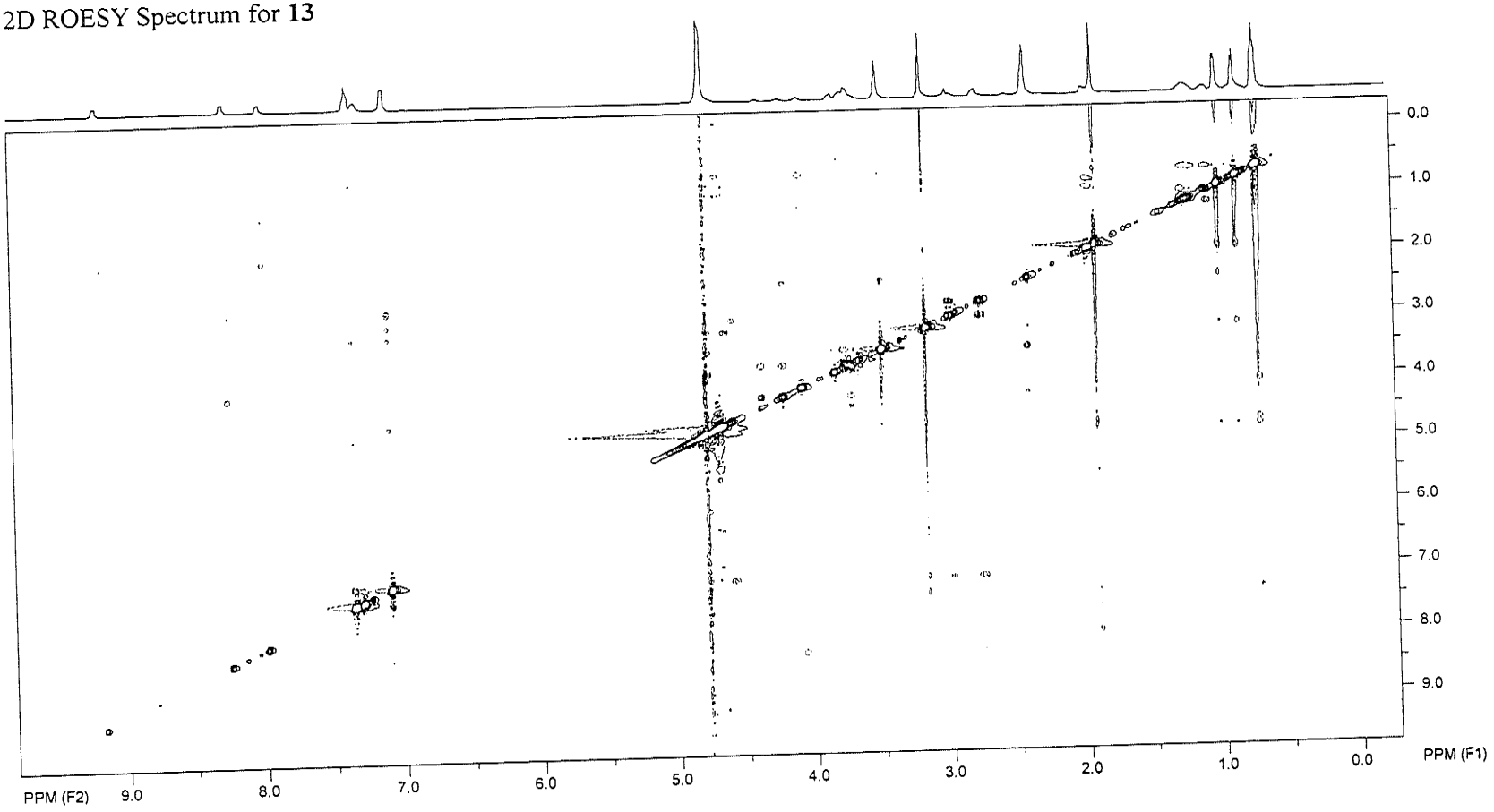

2D ROESY Spectrum for **16**

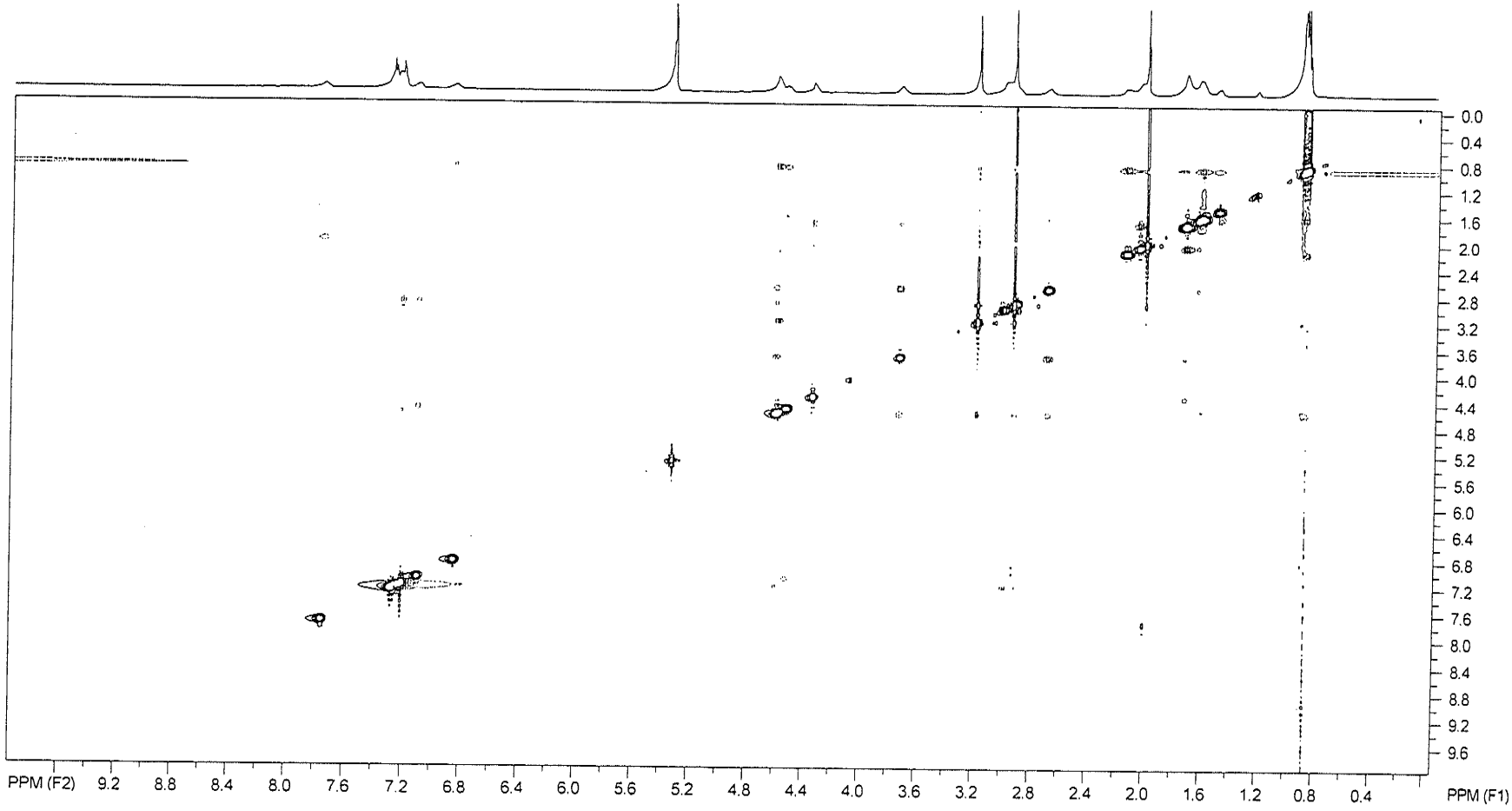

9.4. SI for Chapter 6

9.4.1. ^{1}H and ^{13}C NMR

Compound **5**

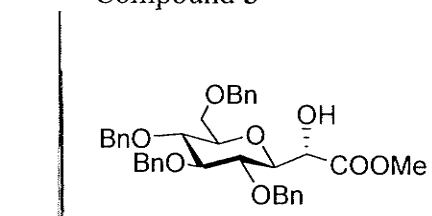

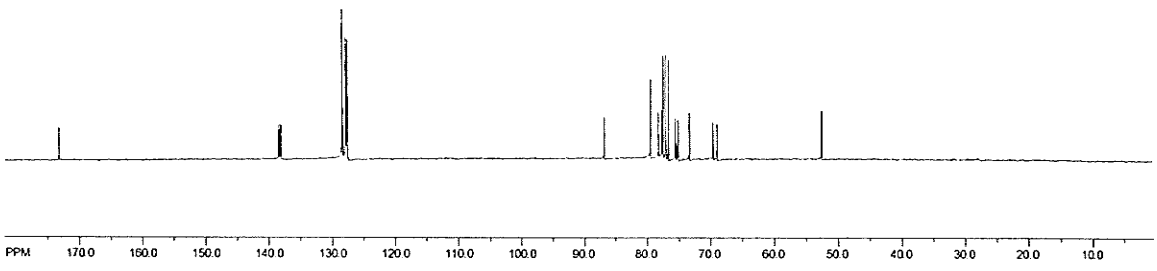

Compound **6**

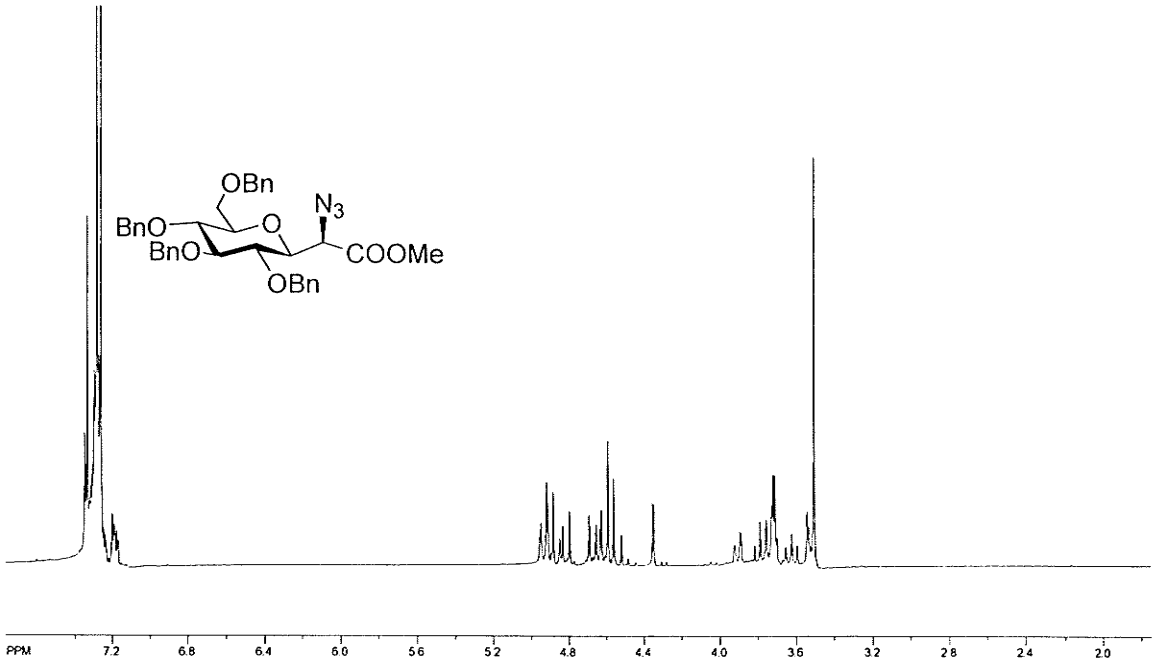
OBn
BnO
BnO
O
N3
COOMe
OBn
PPM
7.2
6.8
6.4
6.0
5.6
5.2
4.8
4.4
4.0
3.6
3.2
2.8
2.4
2.0

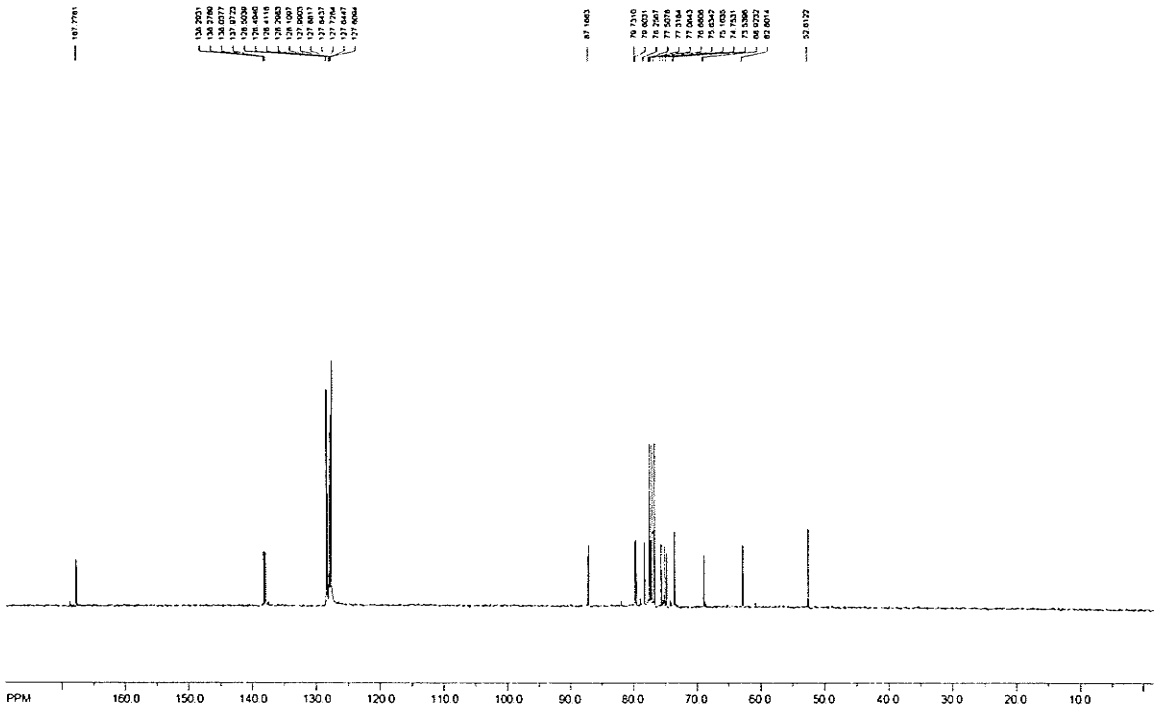
PPM
160.0
150.0
140.0
130.0
120.0
110.0
100.0
90.0
80.0
70.0
60.0
50.0
40.0
30.0
20.0
10.0

Compound **7**

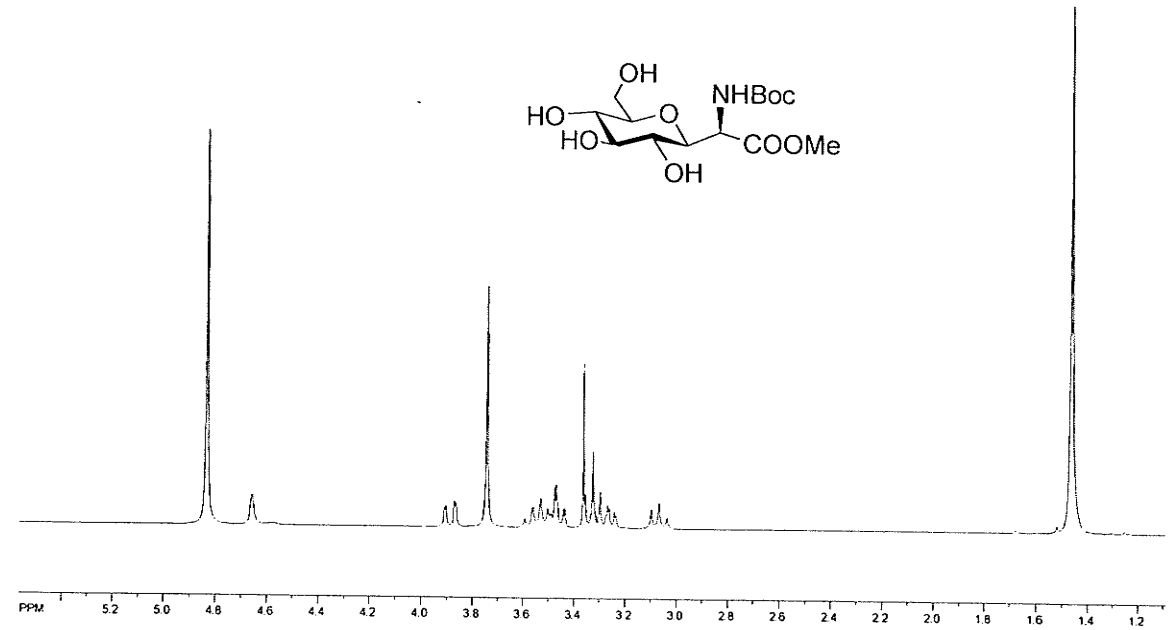
OH
NHBoc
HO
O
HO
COOMe
OH
PPM
5.2
5.0
4.8
4.6
4.4
4.2
4.0
3.8
3.6
3.4
3.2
3.0
2.8
2.6
2.4
2.2
2.0
1.8
1.6
1.4
1.2

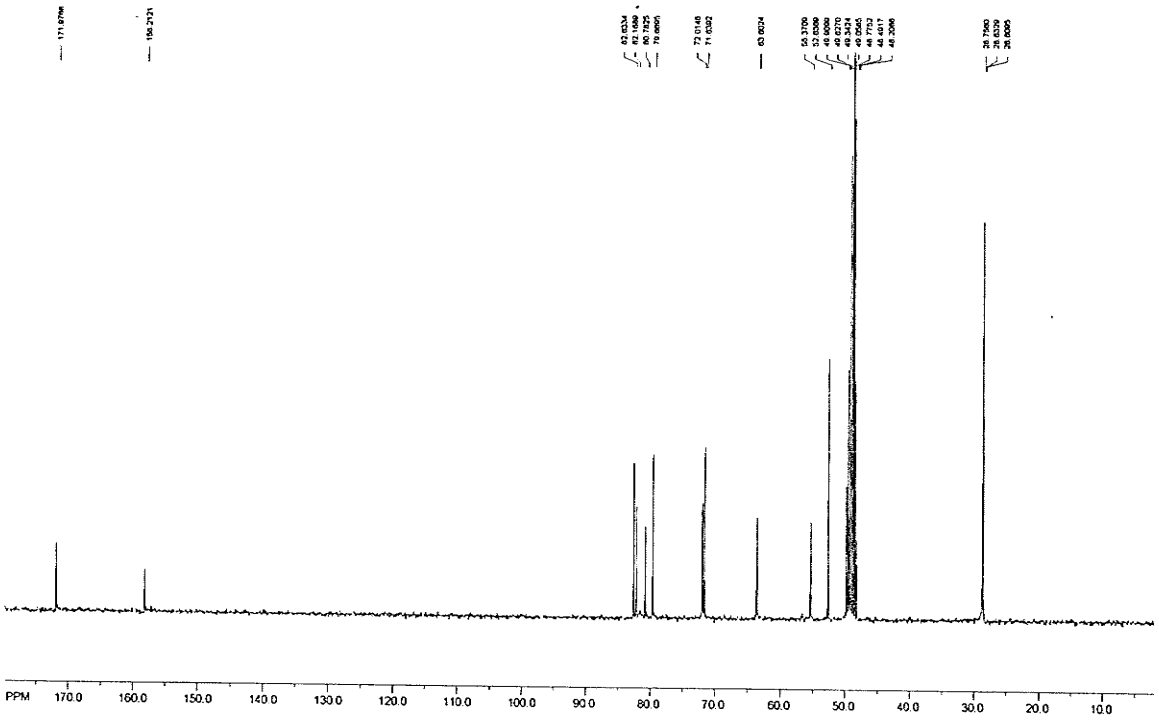
PPM
170.0
160.0
150.0
140.0
130.0
120.0
110.0
100.0
90.0
80.0
70.0
60.0
50.0
40.0
30.0
20.0
10.0

Compound **8**

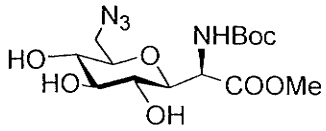
N3
NHBoc
HO
O
HO
COOMe
OH

PPM
5.4
5.2
5.0
4.8
4.6
4.4
4.2
4.0
3.8
3.6
3.4
3.2
3.0
2.8
2.6
2.4
2.2
2.0
1.8
1.6

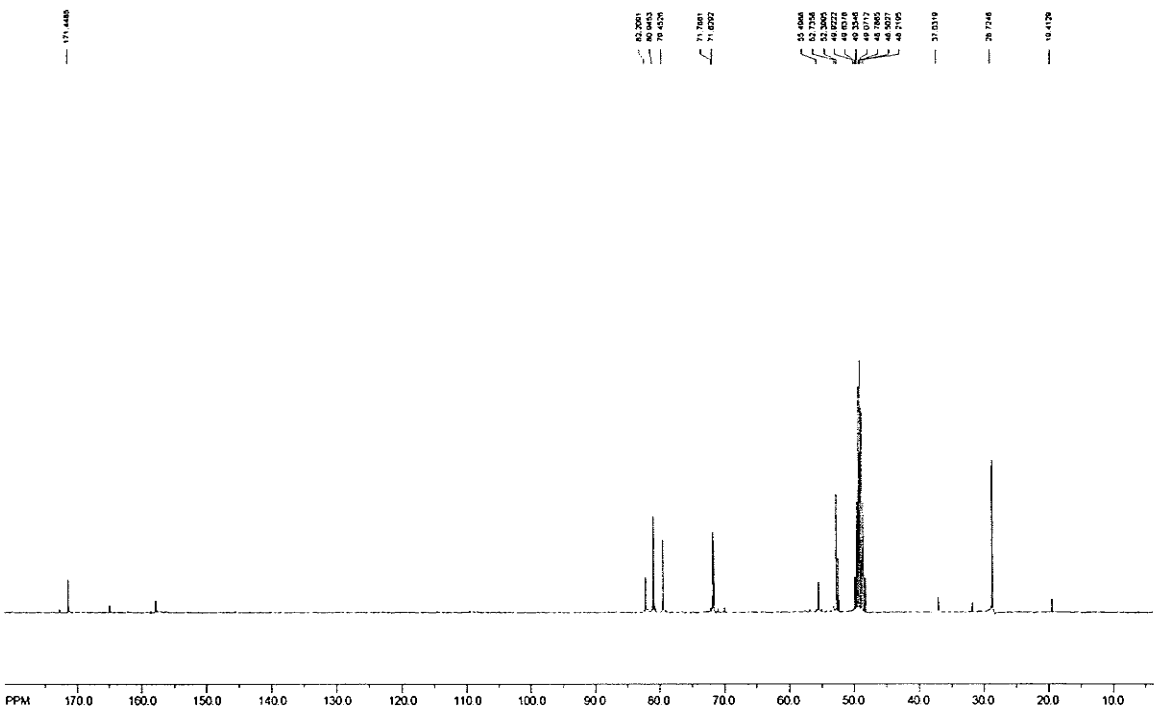
PPM
170.0
160.0
150.0
140.0
130.0
120.0
110.0
100.0
90.0
80.0
70.0
60.0
50.0
40.0
30.0
20.0
10.0

Compound **9**

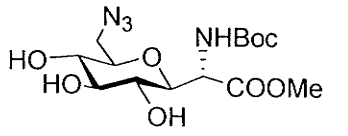
N3
NHBoc
HO
O
HO
COOMe
OH

PPM
5.4
5.2
5.0
4.8
4.6
4.4
4.2
4.0
3.8
3.6
3.4
3.2
3.0
2.8
2.6
2.4
2.2
2.0
1.8
1.6
1.4

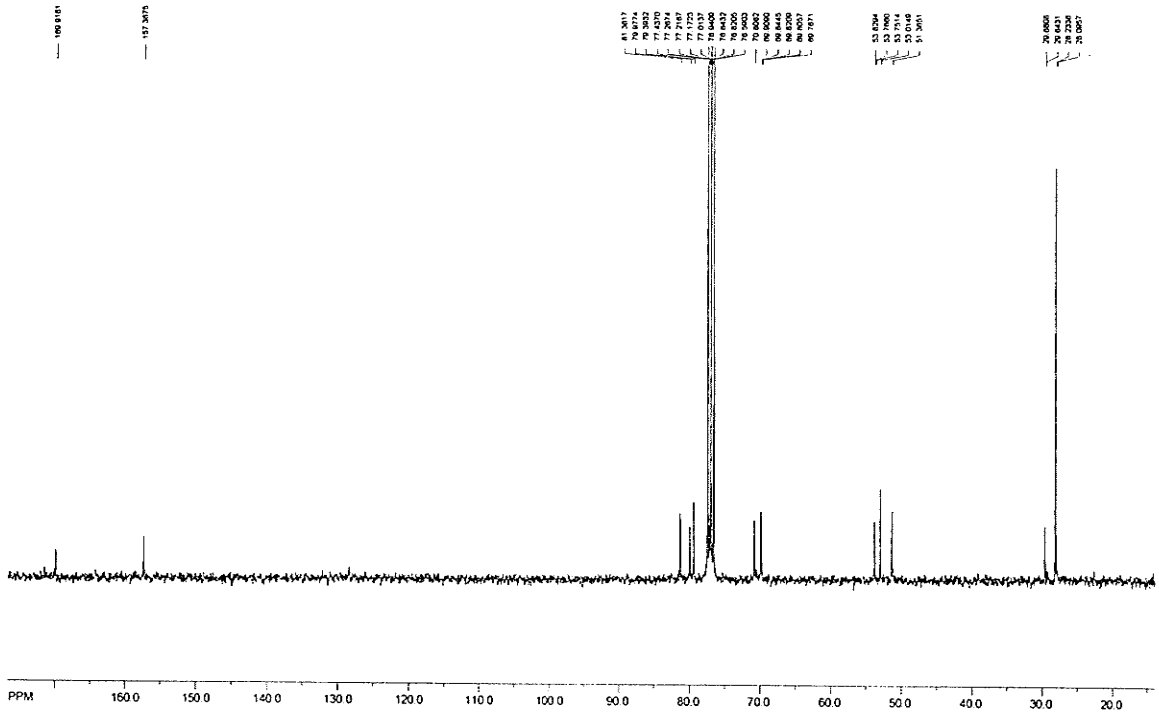
PPM
160.0
150.0
140.0
130.0
120.0
110.0
100.0
90.0
80.0
70.0
60.0
50.0
40.0
30.0
20.0

Compound **10**

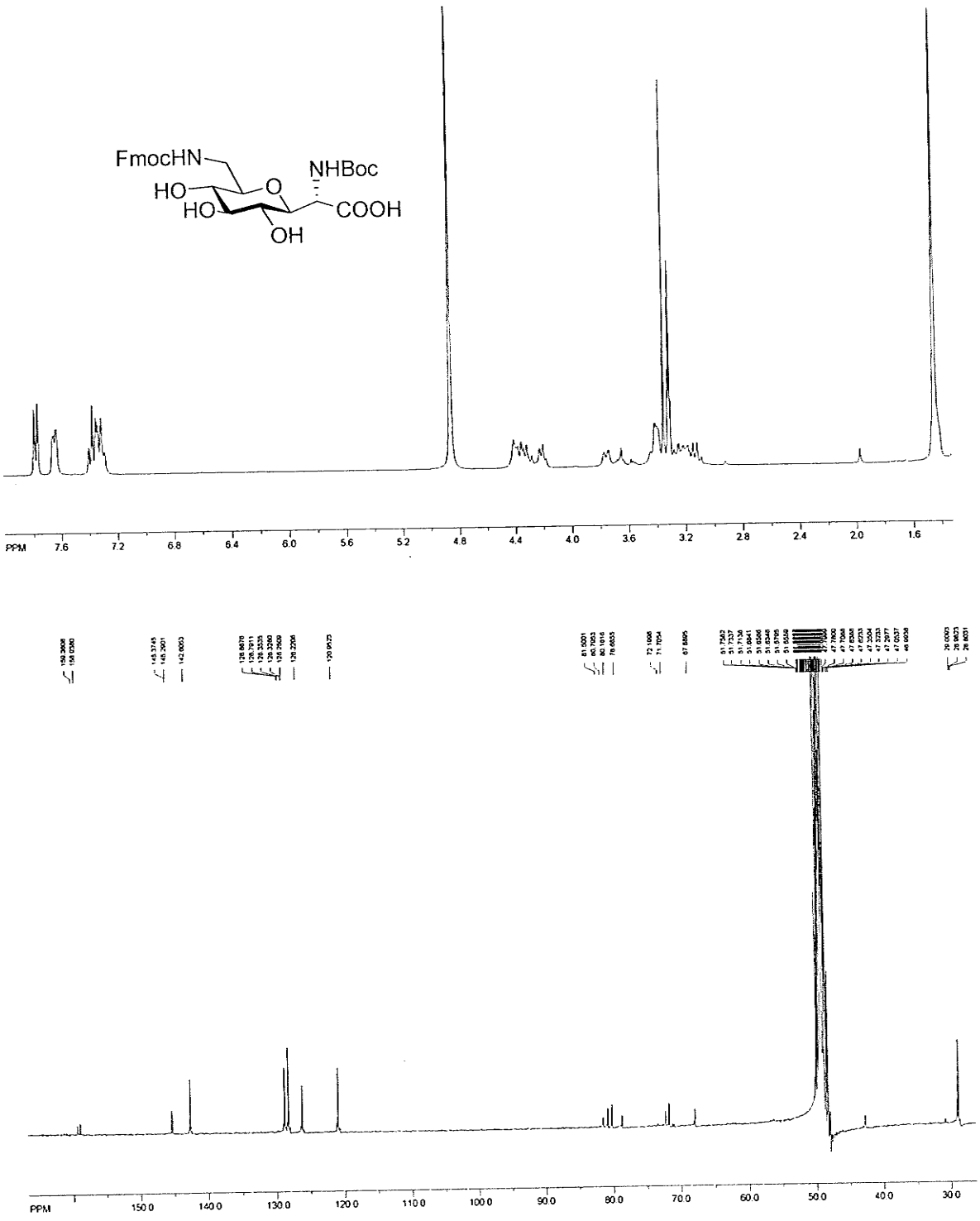
FmocHN
NHBoc
HO
O
HO
COOH
OH
PPM
7.6
7.2
6.8
6.4
6.0
5.6
5.2
4.8
4.4
4.0
3.6
3.2
2.8
2.4
2.0
1.6
PPM
150.0
140.0
130.0
120.0
110.0
100.0
90.0
80.0
70.0
60.0
50.0
40.0
30.0

Compound **11**

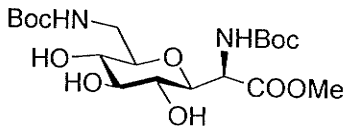
BocHN
HO
HO
O
OH
NHBoc
COOMe

PPM
4.8
4.6
4.4
4.2
4.0
3.8
3.6
3.4
3.2
3.0
2.8
2.6
2.4
2.2
2.0
1.8
1.6
1.4

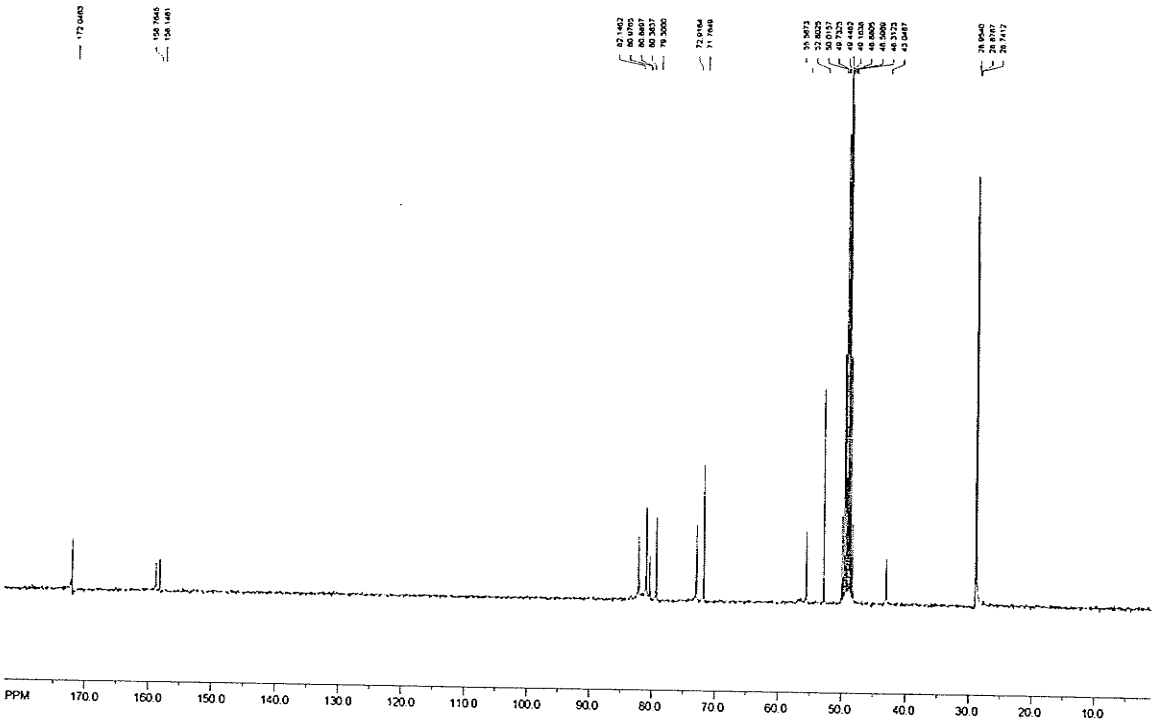
PPM
170.0
160.0
150.0
140.0
130.0
120.0
110.0
100.0
90.0
80.0
70.0
60.0
50.0
40.0
30.0
20.0
10.0

Compound **13**

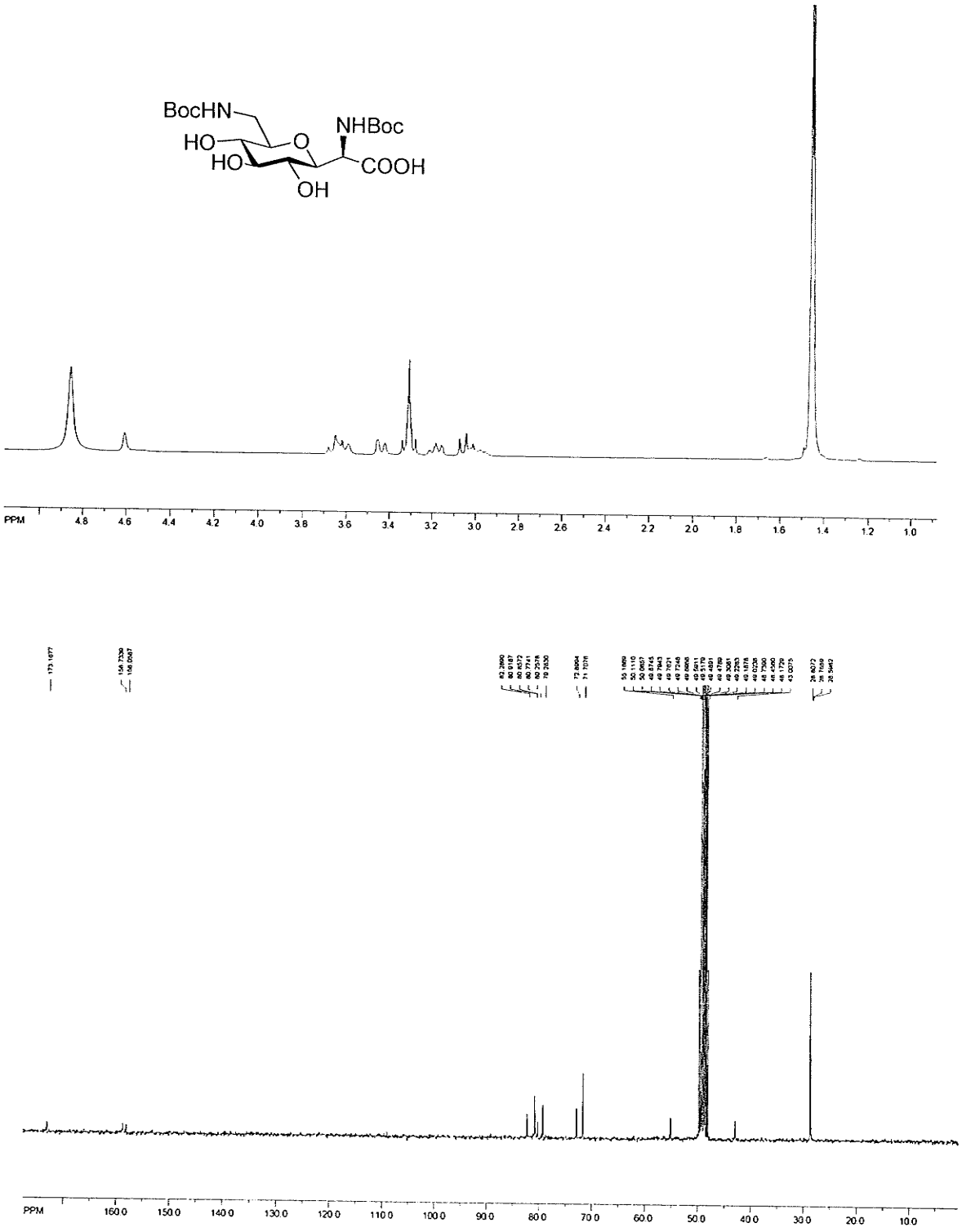
BocHN
NHBoc
HO
O
HO
COOH
OH
PPM
4.8
4.6
4.4
4.2
4.0
3.8
3.6
3.4
3.2
3.0
2.8
2.6
2.4
2.2
2.0
1.8
1.6
1.4
1.2
1.0
PPM
160.0
150.0
140.0
130.0
120.0
110.0
100.0
90.0
80.0
70.0
60.0
50.0
40.0
30.0
20.0
10.0

Compound **16**

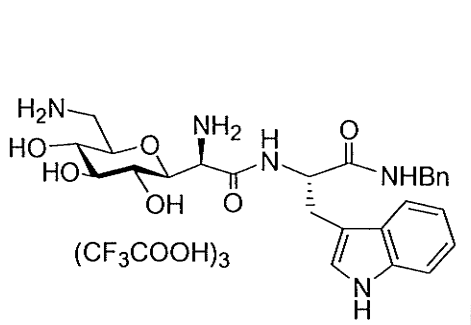
H2N
HO
HO
O
NH2
H
N
O
NHBn
OH
O
(CF3COOH)3
N
H

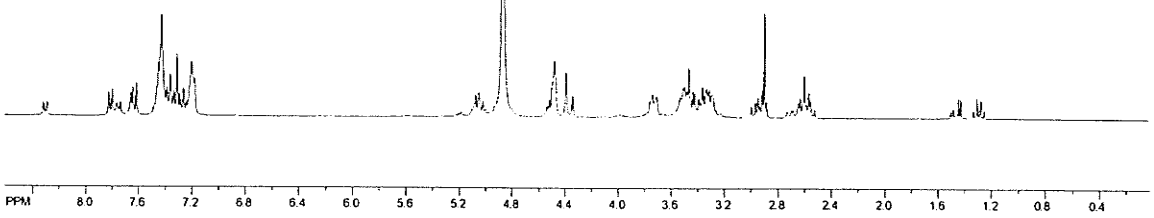
PPM
8.0
7.6
7.2
6.8
6.4
6.0
5.6
5.2
4.8
4.4
4.0
3.6
3.2
2.8
2.4
2.0
1.6
1.2
0.8
0.4

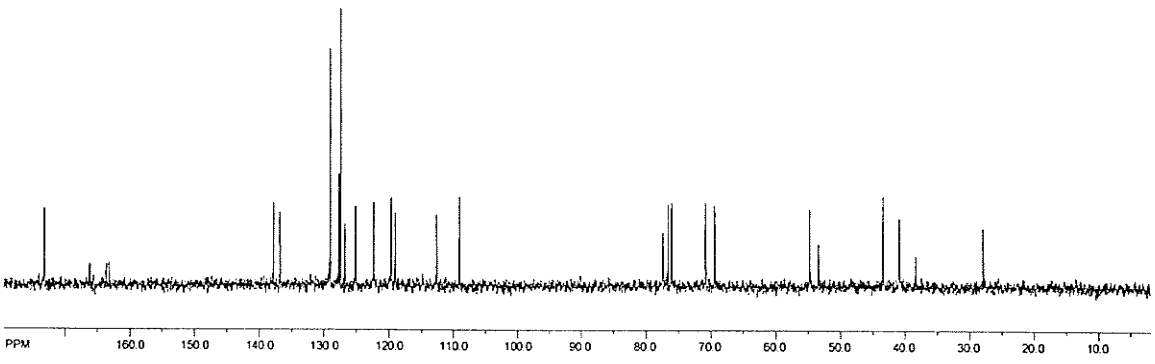
PPM
160.0
150.0
140.0
130.0
120.0
110.0
100.0
90.0
80.0
70.0
60.0
50.0
40.0
30.0
20.0
10.0

Compound **17**

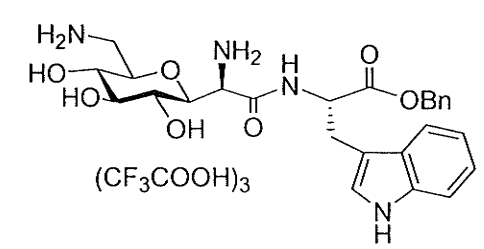
H2N
NH2
HO
O
H
N
O
OBn
HO
OH
O
(CF3COOH)3
N
H

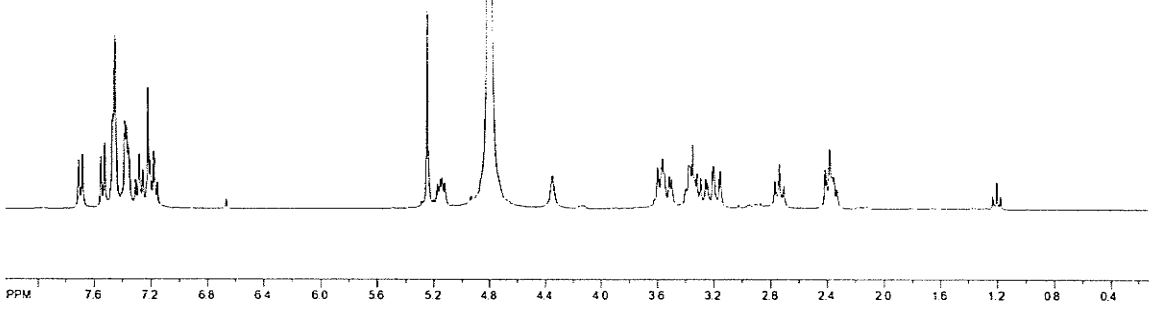
PPM
7.6
7.2
6.8
6.4
6.0
5.6
5.2
4.8
4.4
4.0
3.6
3.2
2.8
2.4
2.0
1.6
1.2
0.8
0.4

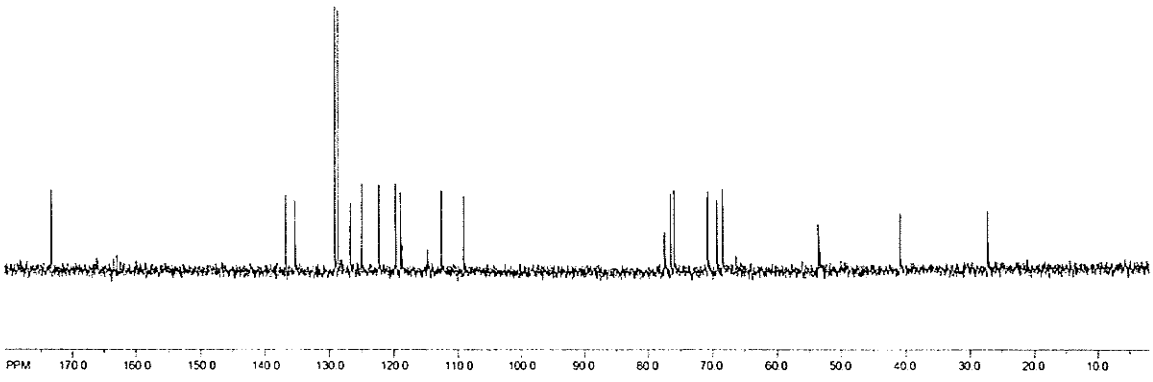
PPM
170.0
160.0
150.0
140.0
130.0
120.0
110.0
100.0
90.0
80.0
70.0
60.0
50.0
40.0
30.0
20.0
10.0

9.5. SI for Chapter 7

9.5.1. Synthetic procedure for compounds 4, 6, 8, 10, 12

(1*S*)-1′-*N*-*tert*-butoxycarbonyl-5′(*S*)-methylenehydroxy acetate-spiro[1,5-anhydro -D-glucitol -1,3′-*L*-proline methyl ester] (4) To a mixture of **2** (100 mg, 0.13 mmol) and $Pd(OH)_2$ (40mg, 20 % wt on charcoal) in methanol (10 mL) was added the solution of hydrochloride (250 μL of 1M HCl solution, 0.25 mmol) and stirred under H_2 (15 psi) for 8 hours at room temperature. The catalyst was removed by the regular filtration and the solvent was removed under the vacuum. The unprotected product was treated with triethylamine (53 μL, 0.38 mmol) and di-tert-butyl dicarbonate (56 mg, 0.25 mmol) in methanol (2 mL) for 1 hour at room temperature. The solvent was removed under the vacuum. The crude product was purified by flash column chromatography (CH_2Cl_2 / MeOH: 7/ 1) to get **4** (35 mg, 62%)

(1*S*)-6-Azido-6-deoxy-1′-*N*-*tert*-butoxycarbonyl-5′(*S*)-methylenehydroxy acetate -spiro[1,5 -anhydro-D-glucitol-1,3′-*L*-proline methyl ester] (6) To a solution of compound **4** (40 mg, 0.09 mmol) in pyridine (1 mL) was added *p*-tolunesulfonyl chloride (42 mg, 0.22 mmol) and stirred for 12 hours at room temperature. The mixture was concentrated and purified by flash column chromatography (CH_2Cl_2 / MeOH: 10/ 1) to provide tosyl ester, which was treated with sodium azide (116 mg, 1.8 mmol) in DMF (1.5 mL) and stirred at 80 °C for 12 hours. The mixture was filtered, concentrated and purified by flash column chromatography (CH_2Cl_2 / MeOH: 15/ 1) to get **6** (39 mg, 94%).

(1*S*)-6-Azido-6-deoxy-1′-*N*-acetyl-5′(*S*)-hydroxymethylene–spiro[1,5-anhydro-D-glucitol-1,3′-*L*-proline methyl ester] (8) The compound **6** (30 mg, 0.06 mmol) was dissolved in a mixture of dichloromethane and trifluoroacetic acid (1.5 mL / 0.5 mL) and stirred for 1 hour at room temperature. The solution was concentrated at vacuum and then treated with a mixture of pyridine and acetic acid (1 mL / 1 mL) and stirred for 12 hours at room temperature and then concentrated at vacuum. After that, it was dissolved in a solution of sodium methoxide in methanol (0.1 M, 2 mL) and stirred for 4 hours at room temperature followed by the neutralization with Amberlite IRC-50S ion-exchange resin (H^+). The mixture was filtered and filtrate was concentrated and purified by the flash column chromatography (ethyl acetate / methanol: 6 / 1) to get compound **8** (18 mg, 80%).

(1*S*)-6-Amino-6-deoxy-1′-*N*-acetyl-5′(*S*)-hydroxymethylene–spiro[1,5-anhydro-D-glucitol-1,3′-*L*-proline methyl ester] HCl salt (10) To a solution of **8** (20 mg, 0.05 mmol) and $Pd(OH)_2$ (20 mg, 20 % wt on charcoal) in methanol (5 mL) was added the solution of hydrochloride (800 μL of 1M HCl solution, 0.08 mmol) and stirred under H_2 (15 psi) for 20 minutes at room temperature. The catalyst was removed by the regular filtration and the solvent was removed under the vacuum to afford pure product **10** (20 mg, quant.).

(1*S*)-6-Amino-6-deoxy-1′-*N*-acetyl-5′(*S*)-hydroxymethylene–spiro[1,5-anhydro-D-glucitol-1,3′-*L*-proline methyl amide] HCl salt (12) To a solution of methylamine in ethanol (37% wt, 1 mL) was added compound **8** (15 mg, 0.04 mmol) and stirred for 18

hours at room temperature. The mixture was concentrated and purified by the flash column chromatography (dichloromethane/methanol: 2/1) to quantitatively afford *C*-terminal methyl amide intermediate, which was dissolved in a solution of $Pd(OH)_2$ (15 mg, 20 % wt on charcoal) and 1 M hydrochloride acid solution (80 μL, 0.08 mmol). The mixture was stirred under H_2 (15 psi) for 20 minutes at room temperature The catalyst was removed by the regular filtration and the solvent was removed under the vacuum to afford pure product **12** (15 mg, 95%).

9.5.2. ^{1}H NMR and ^{13}C NMR spectrum

Compound **3**

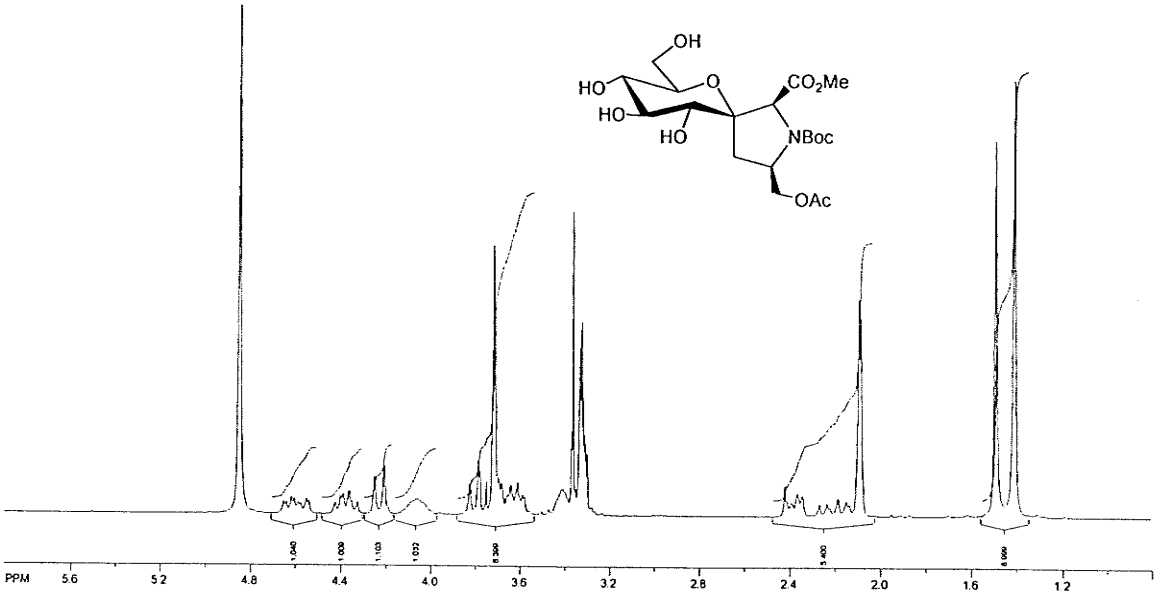

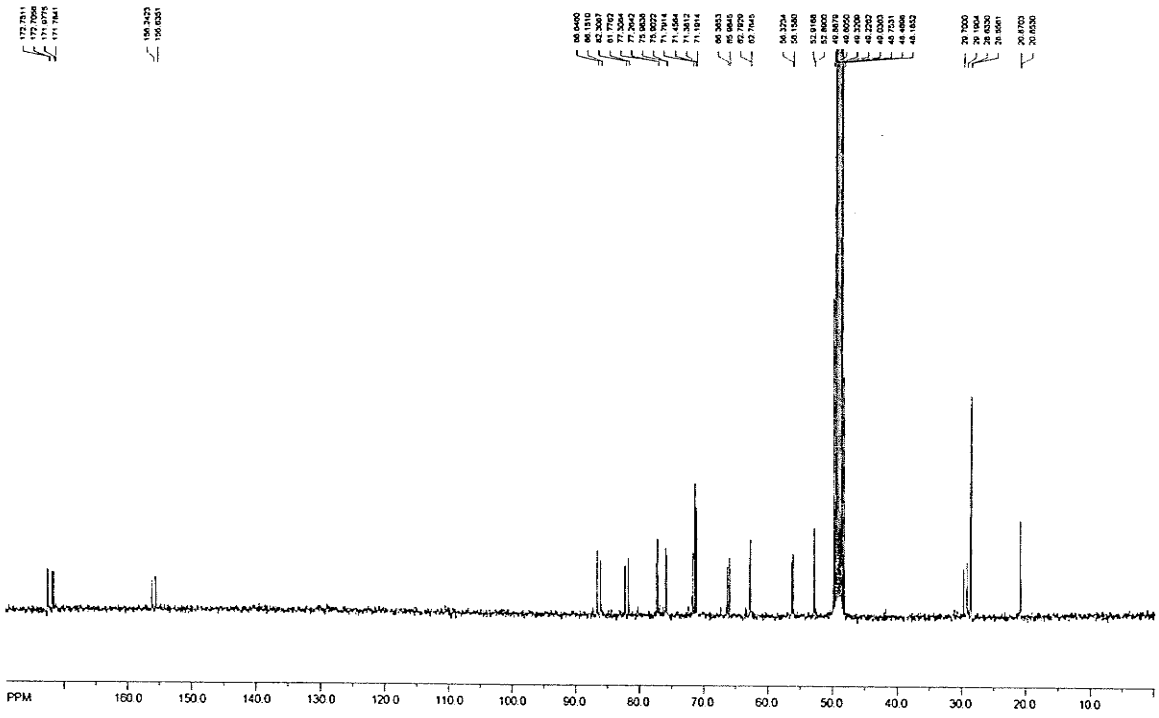

Compound **4**

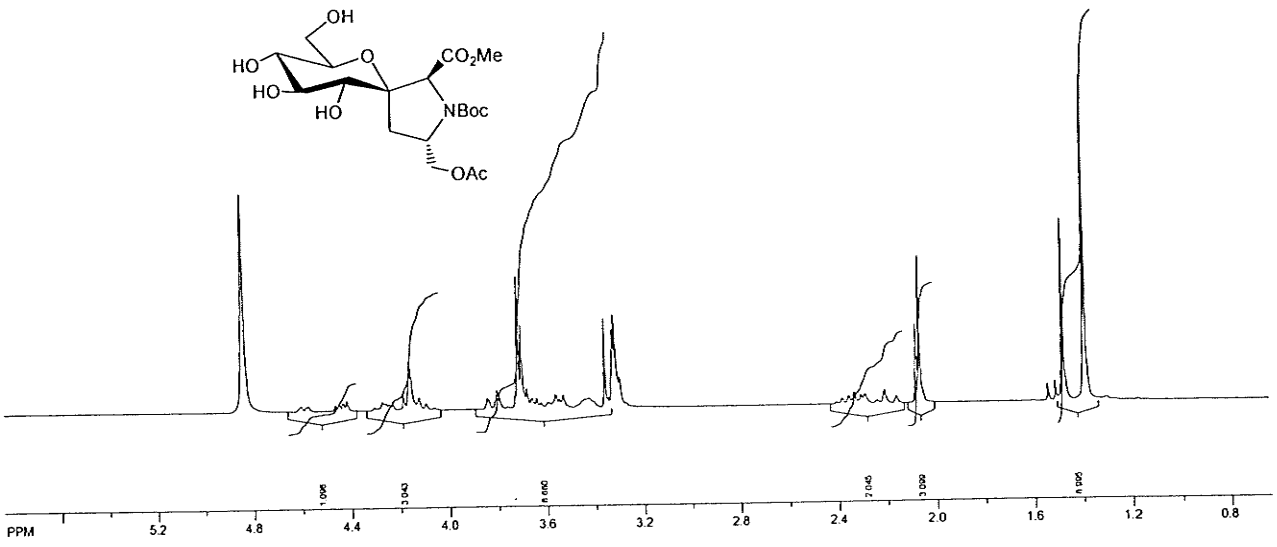
OH
HO
HO
HO
O
CO2Me
NBoc
OAc
PPM
5.2
4.8
4.4
4.0
3.6
3.2
2.8
2.4
2.0
1.6
1.2
0.8

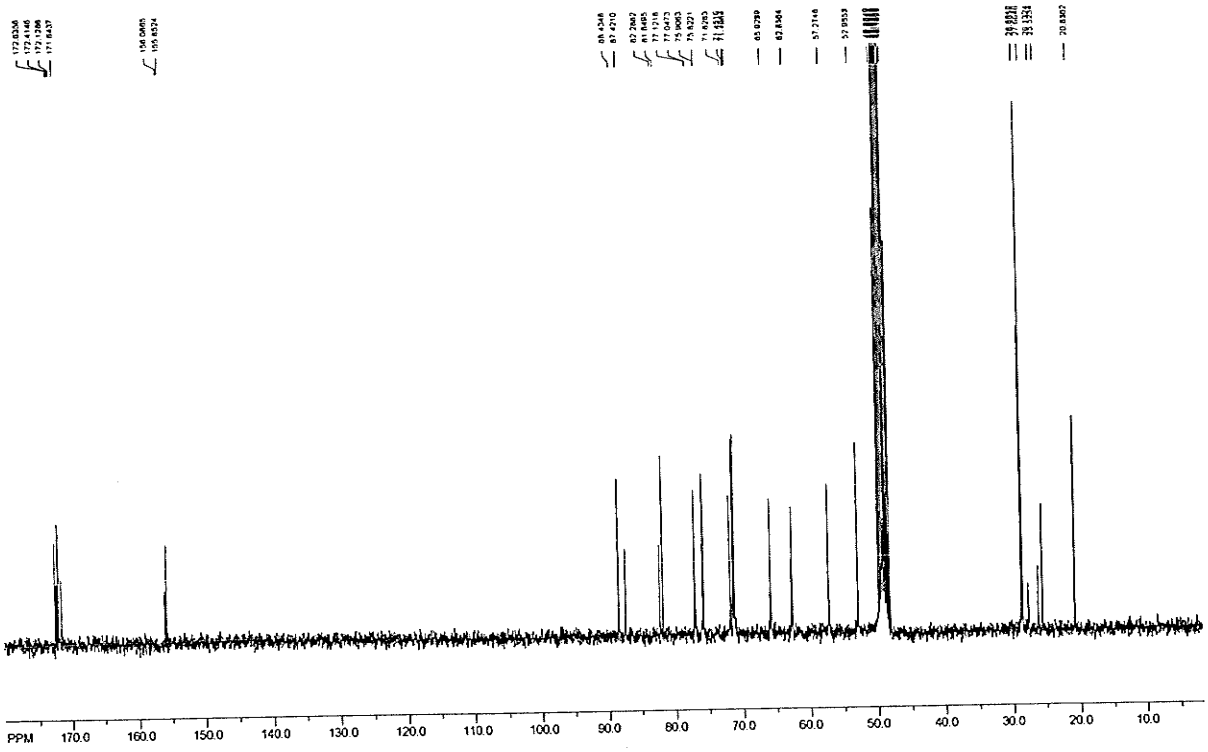
PPM
170.0
160.0
150.0
140.0
130.0
120.0
110.0
100.0
90.0
80.0
70.0
60.0
50.0
40.0
30.0
20.0
10.0

Compound **5**

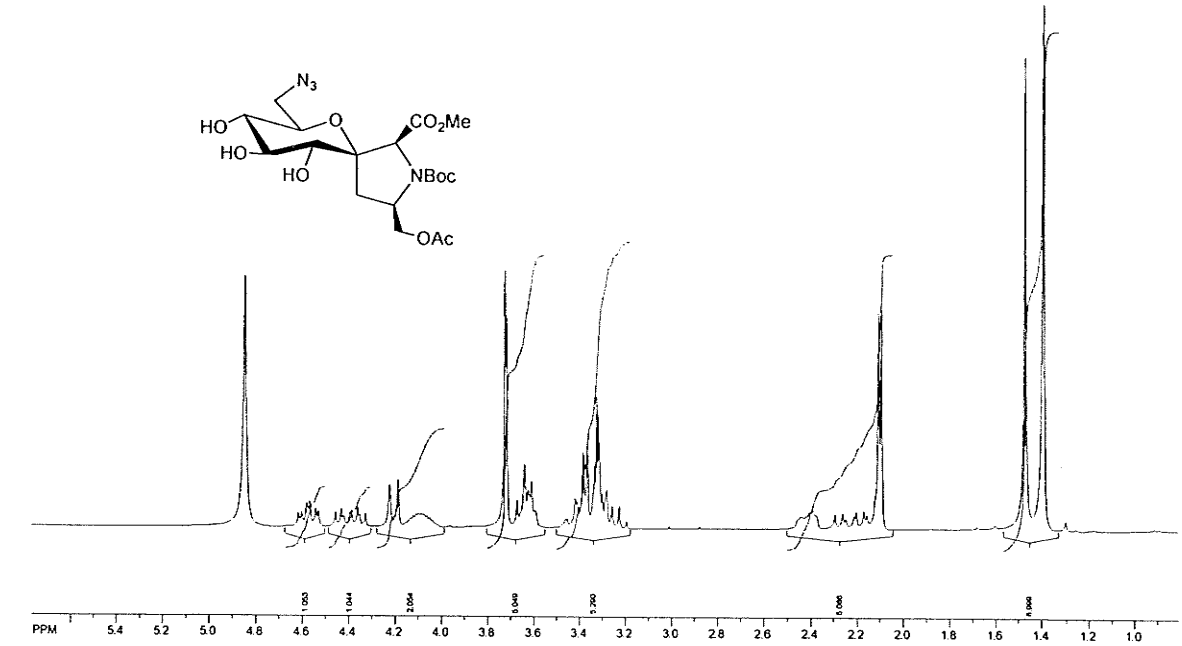

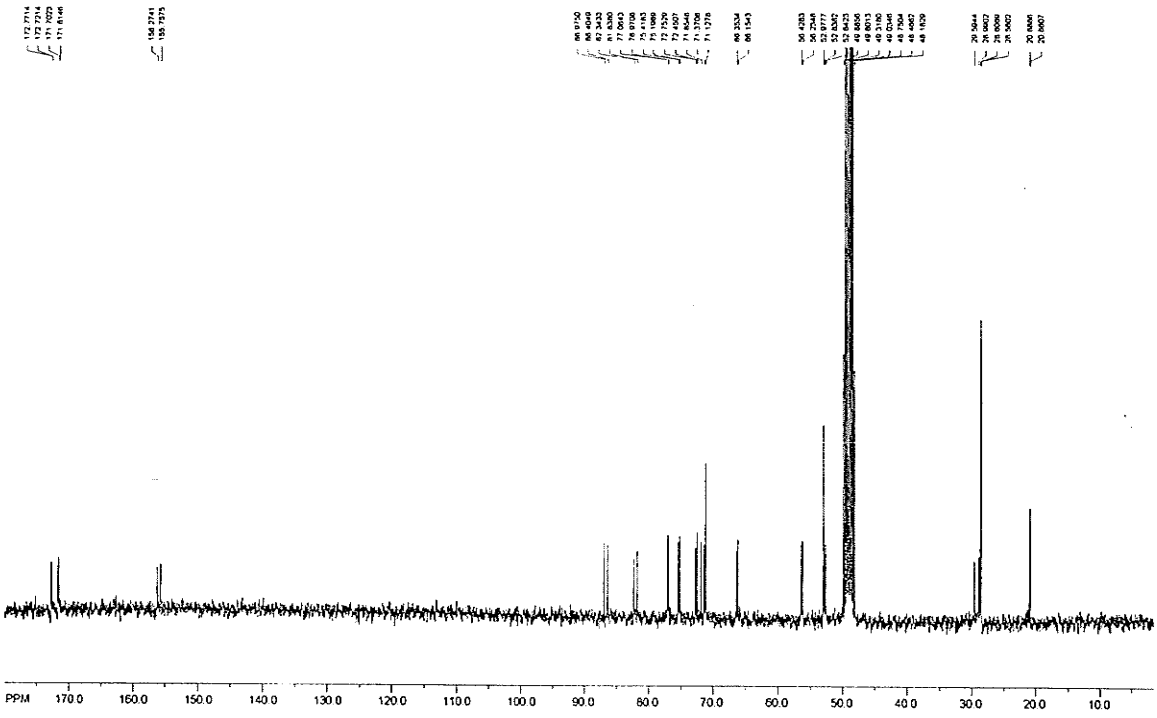

Compound **6**

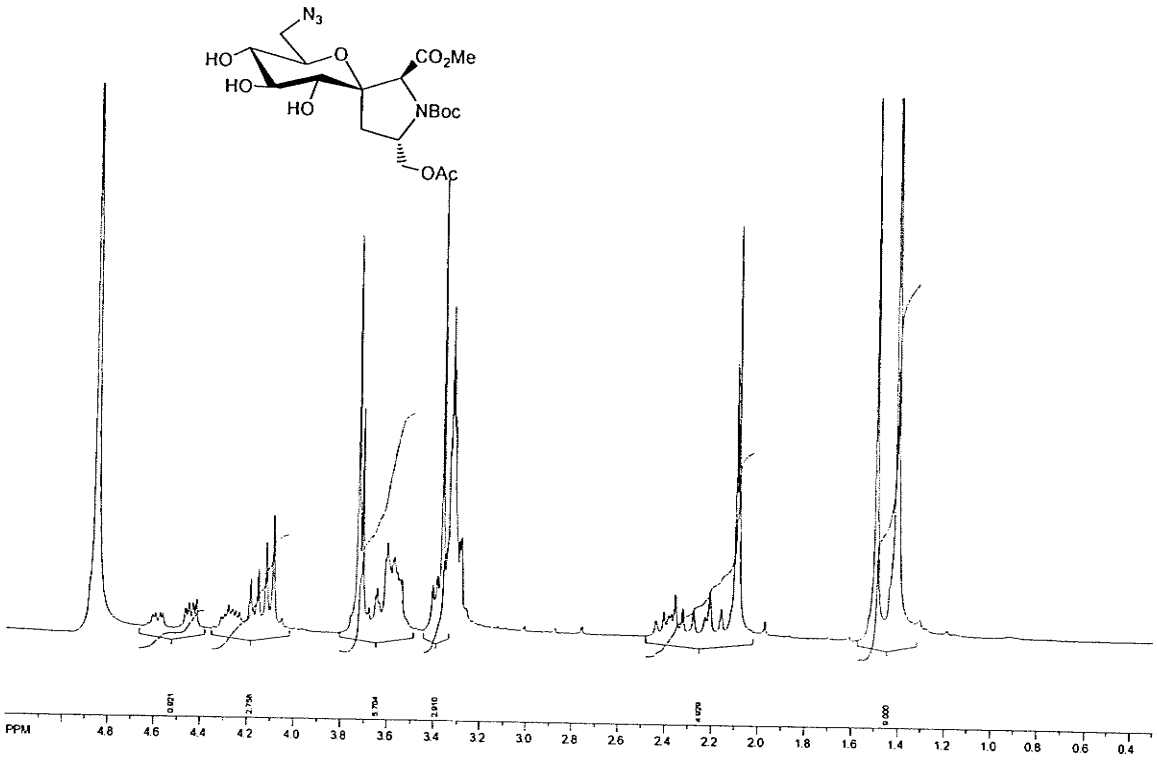
N3
HO
O
CO2Me
HO
HO
NBoc
OAc
PPM
4.8
4.6
4.4
4.2
4.0
3.8
3.6
3.4
3.2
3.0
2.8
2.6
2.4
2.2
2.0
1.8
1.6
1.4
1.2
1.0
0.8
0.6
0.4

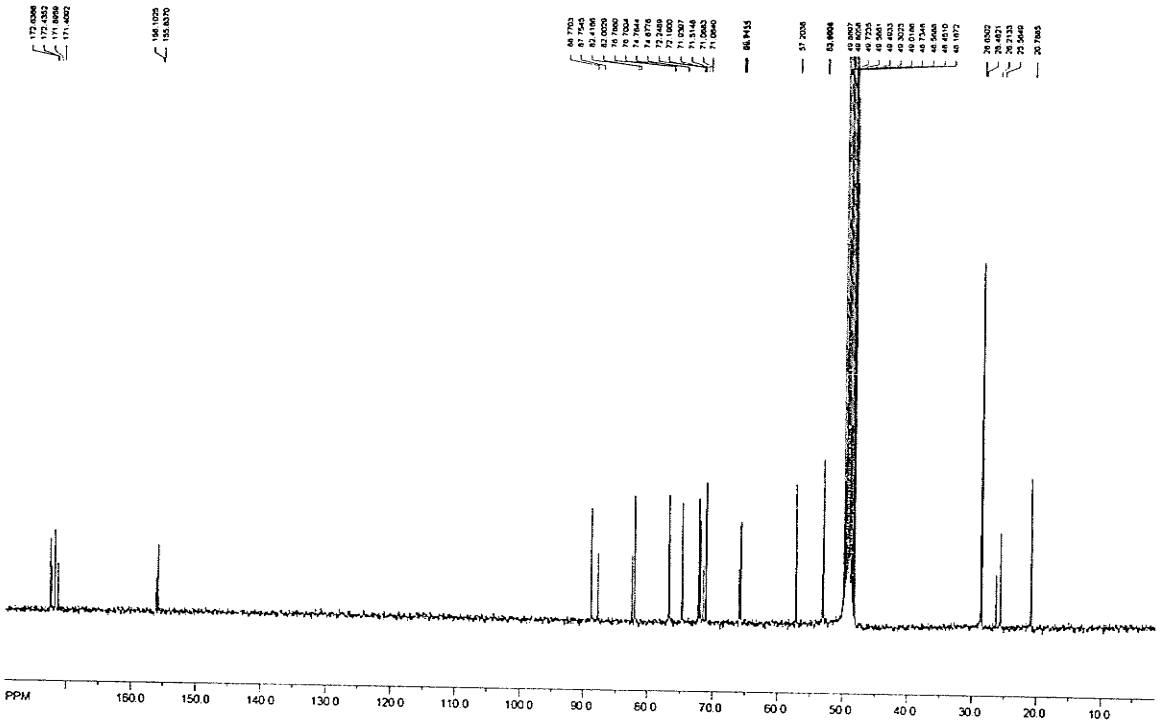
PPM
150.0
140.0
130.0
120.0
110.0
100.0
90.0
80.0
70.0
60.0
50.0
40.0
30.0
20.0
10.0

Compound 7

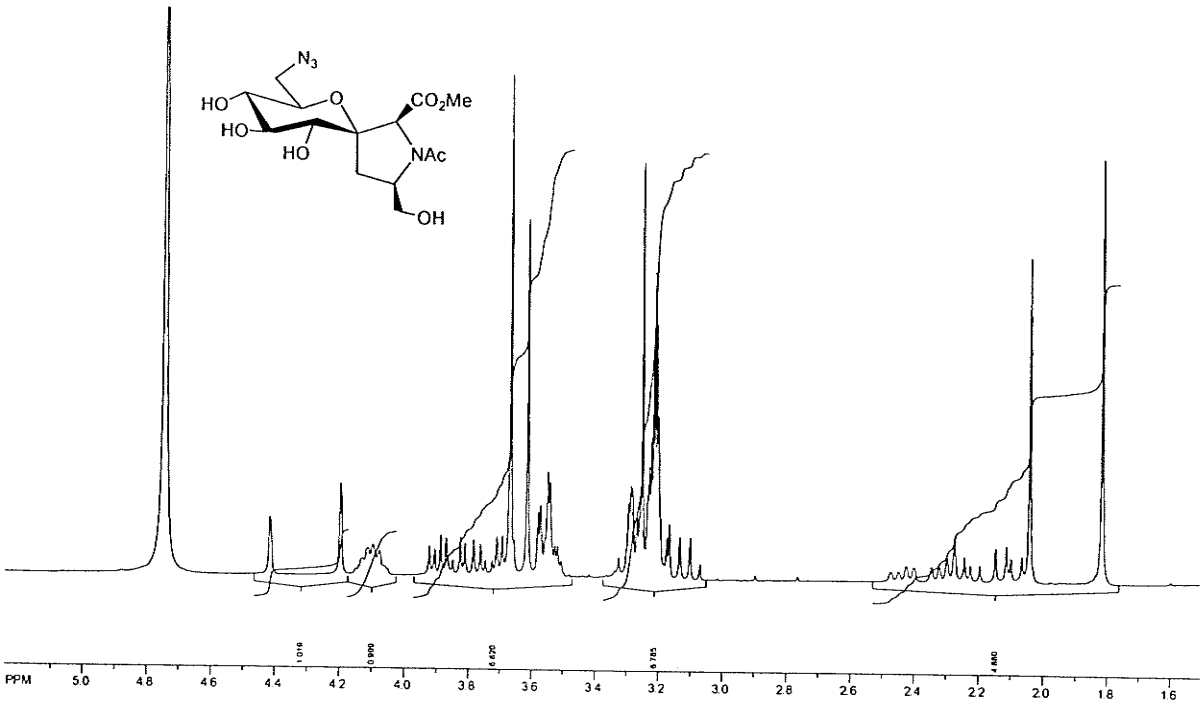
N3
HO
O
CO2Me
HO
HO
NAc
OH
PPM
5.0
4.8
4.6
4.4
4.2
4.0
3.8
3.6
3.4
3.2
3.0
2.8
2.6
2.4
2.2
2.0
1.8
1.6

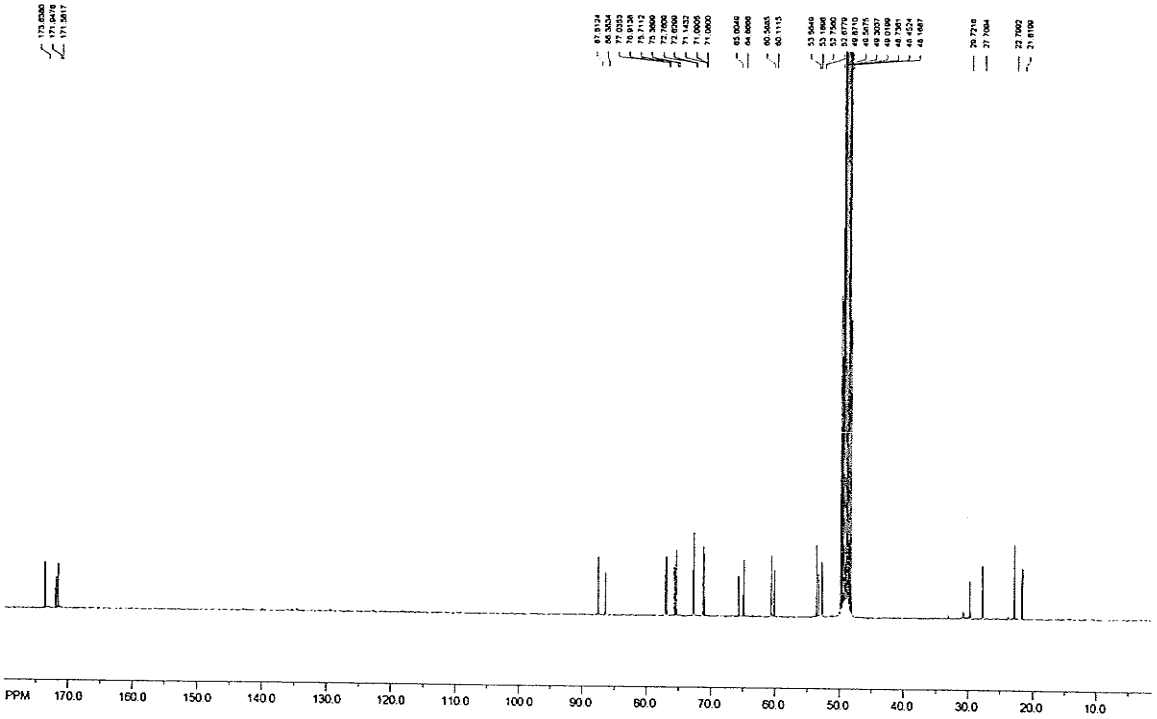
PPM
170.0
160.0
150.0
140.0
130.0
120.0
110.0
100.0
90.0
80.0
70.0
60.0
50.0
40.0
30.0
20.0
10.0

Compound **8**

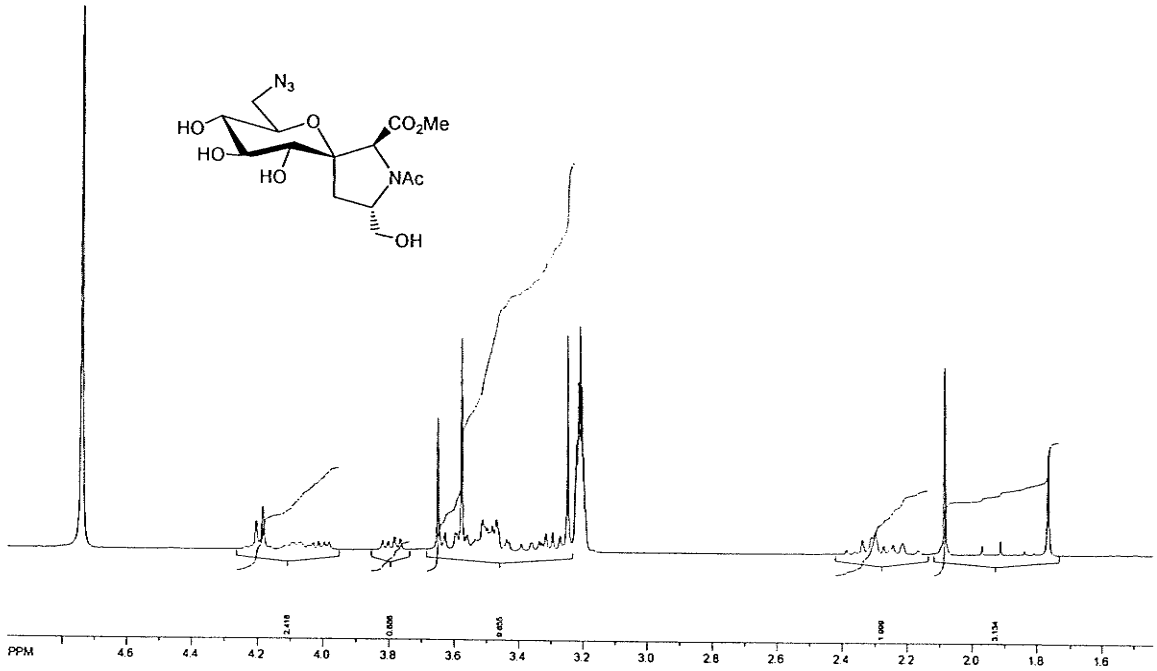
N3
HO
HO
HO
O
CO2Me
NAc
OH
PPM
4.6
4.4
4.2
4.0
3.8
3.6
3.4
3.2
3.0
2.8
2.6
2.4
2.2
2.0
1.8
1.6

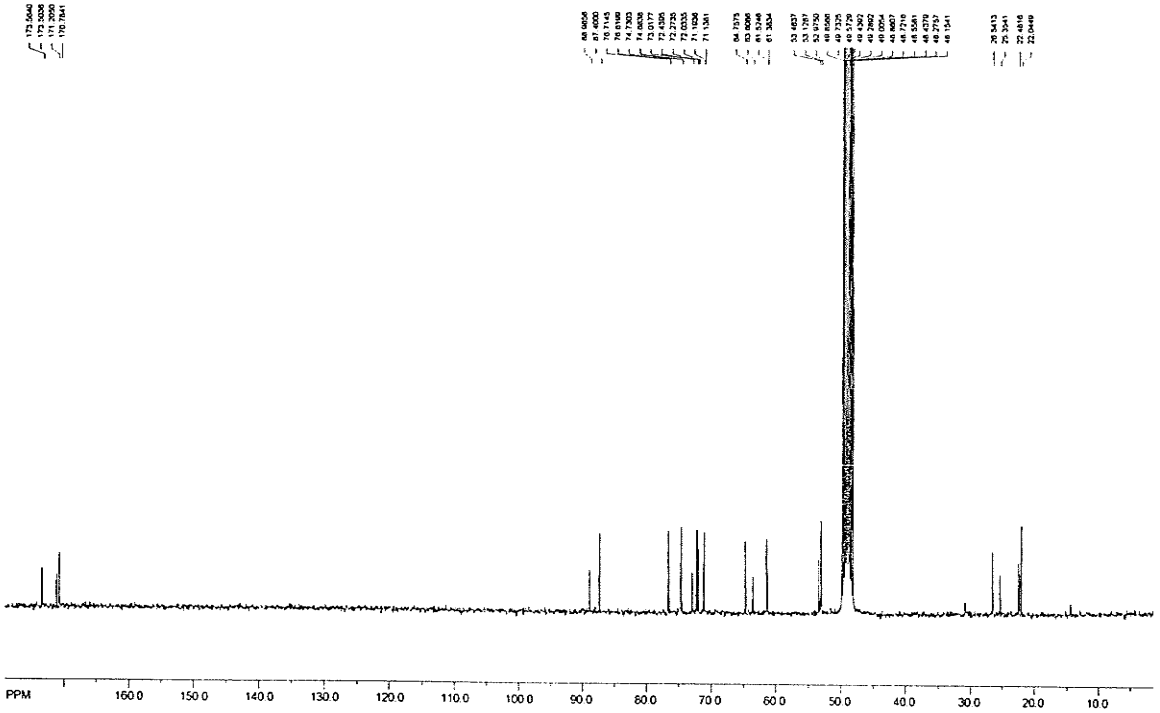
PPM
160.0
150.0
140.0
130.0
120.0
110.0
100.0
90.0
80.0
70.0
60.0
50.0
40.0
30.0
20.0
10.0

Compound **9**

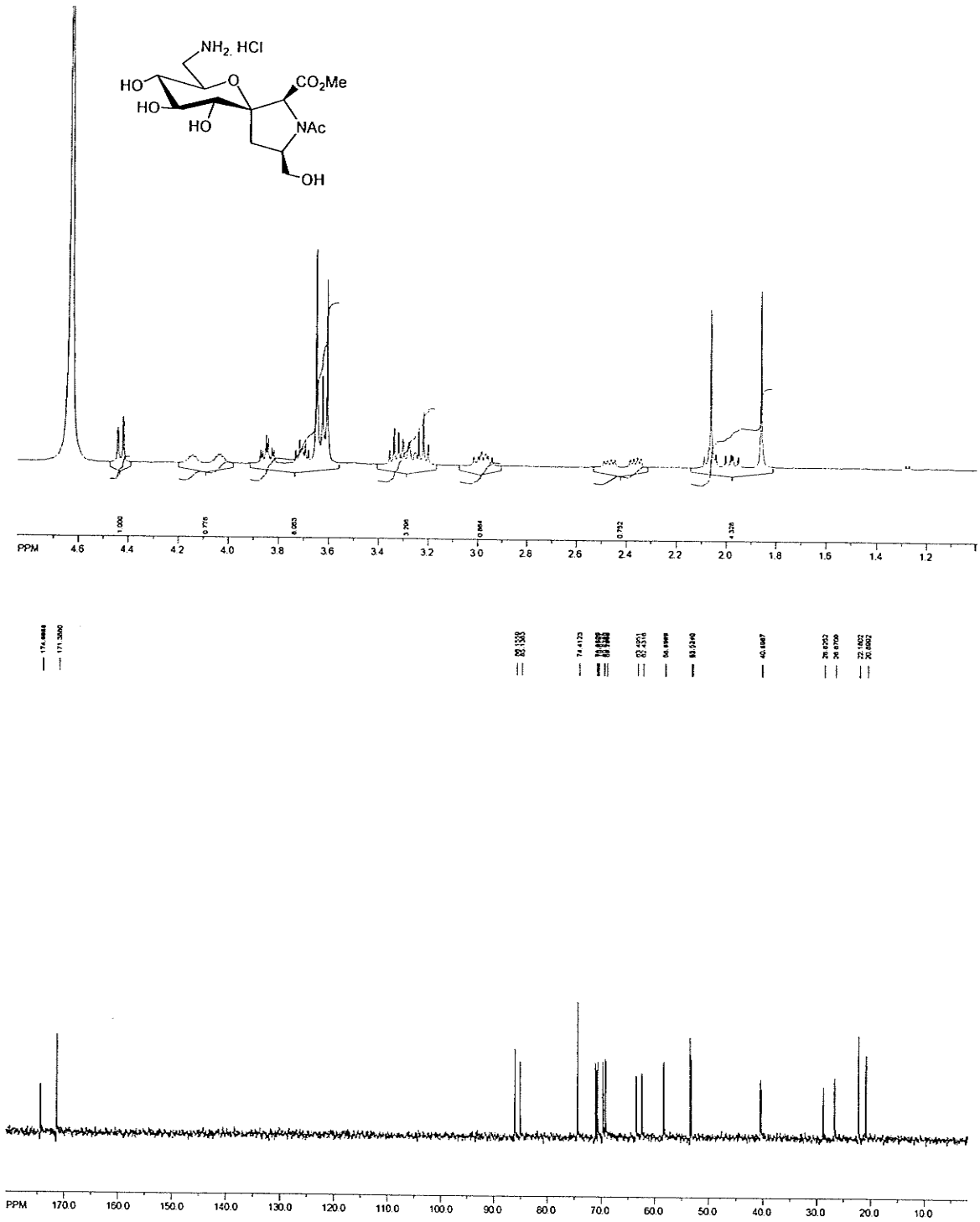
NH2. HCl
HO
HO
HO
O
CO2Me
NAc
OH
PPM
4.6
4.4
4.2
4.0
3.8
3.6
3.4
3.2
3.0
2.8
2.6
2.4
2.2
2.0
1.8
1.6
1.4
1.2
PPM
170.0
160.0
150.0
140.0
130.0
120.0
110.0
100.0
90.0
80.0
70.0
60.0
50.0
40.0
30.0
20.0
10.0

Compound **10**

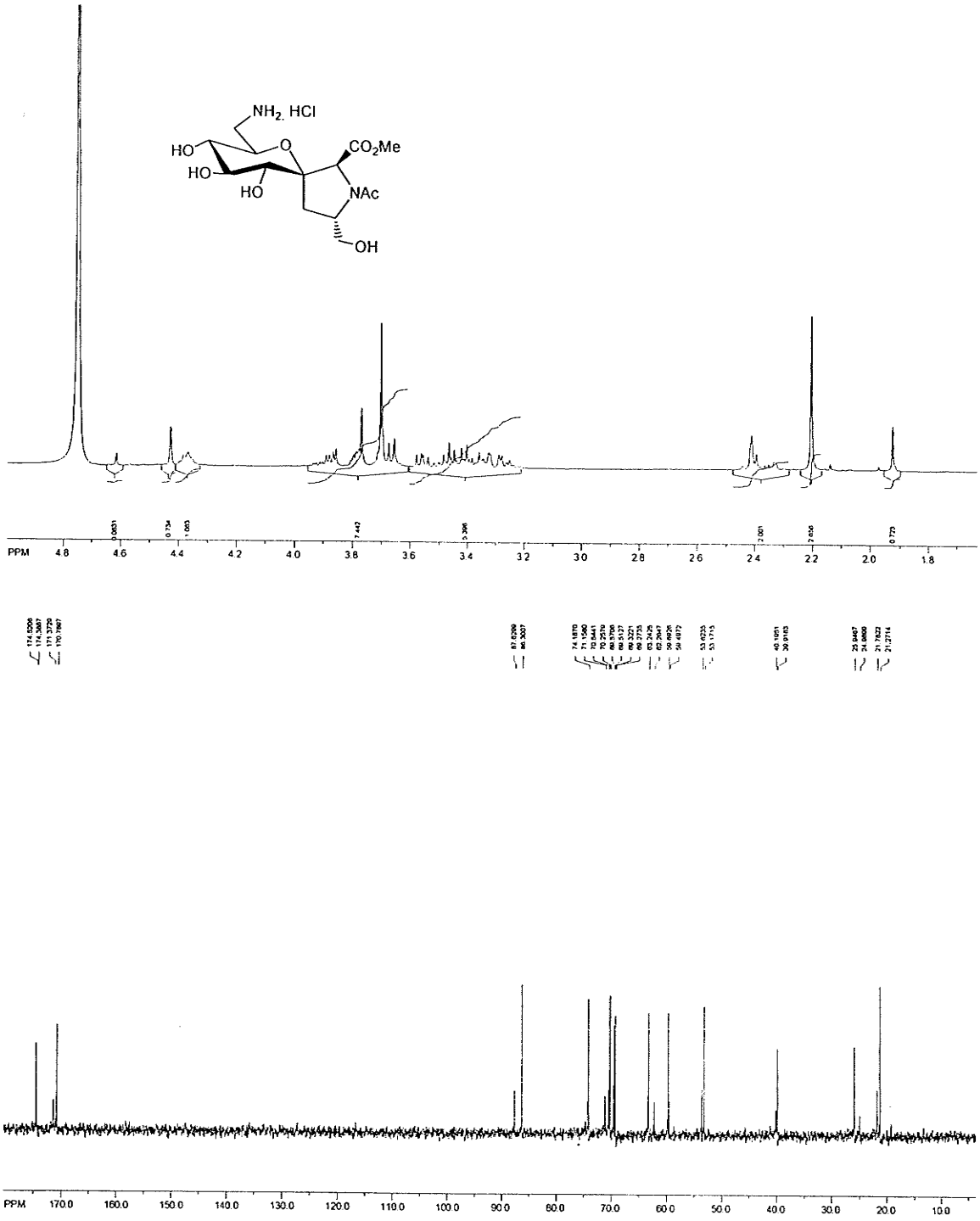
NH2. HCl
HO
HO
HO
O
CO2Me
NAc
OH
PPM
4.8
4.6
4.4
4.2
4.0
3.8
3.6
3.4
3.2
3.0
2.8
2.6
2.4
2.2
2.0
1.8
PPM
170.0
160.0
150.0
140.0
130.0
120.0
110.0
100.0
90.0
80.0
70.0
60.0
50.0
40.0
30.0
20.0
10.0

Compound **11**

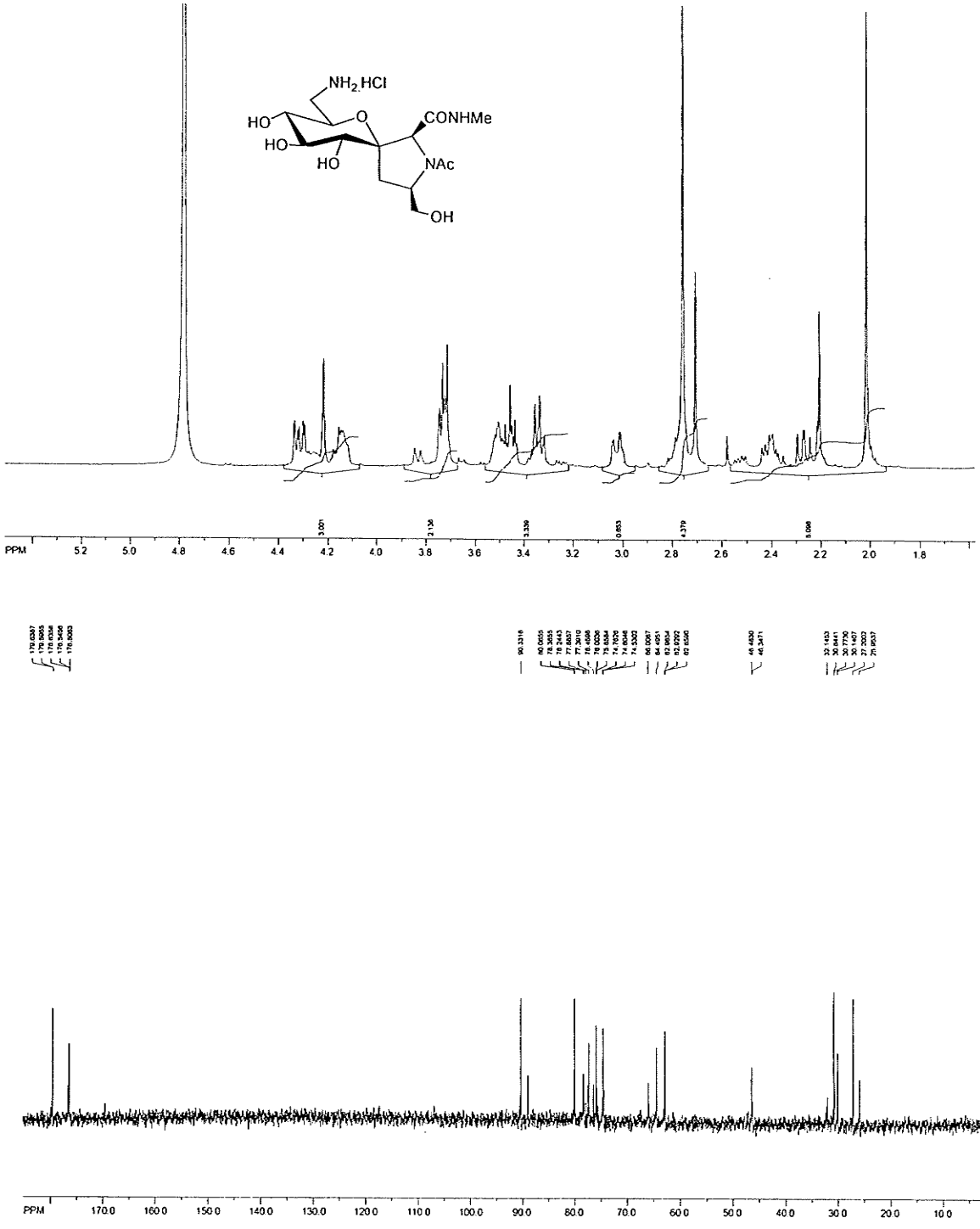
NH2.HCl
HO
HO
HO
O
CONHMe
NAc
OH
PPM
5.2
5.0
4.8
4.6
4.4
4.2
4.0
3.8
3.6
3.4
3.2
3.0
2.8
2.6
2.4
2.2
2.0
1.8
PPM
170.0
160.0
150.0
140.0
130.0
120.0
110.0
100.0
90.0
80.0
70.0
60.0
50.0
40.0
30.0
20.0
10.0

Compound **12**

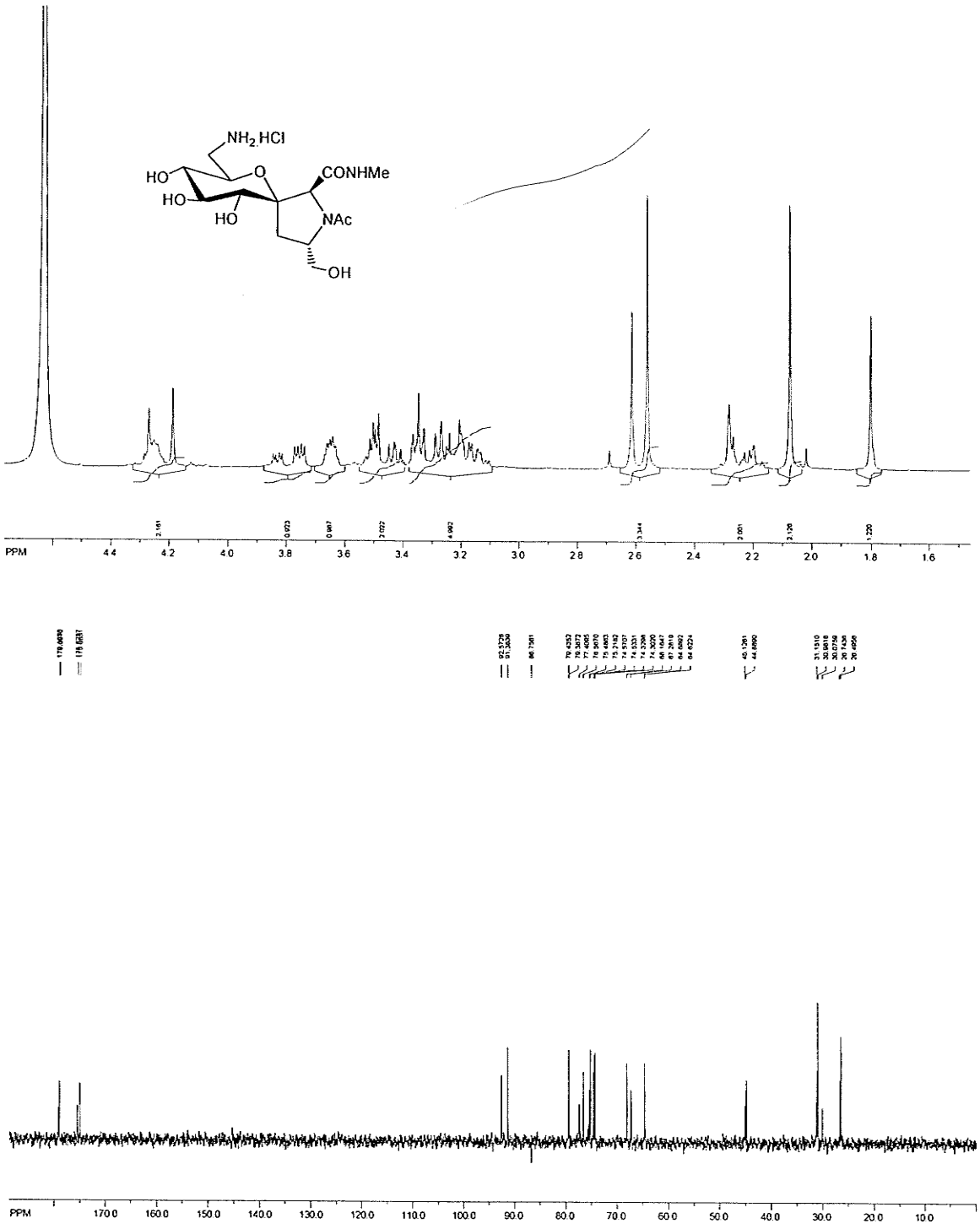
NH2.HCl
HO
HO
HO
O
CONHMe
NAc
OH
PPM
4.4
4.2
4.0
3.8
3.6
3.4
3.2
3.0
2.8
2.6
2.4
2.2
2.0
1.8
1.6
PPM
170.0
160.0
150.0
140.0
130.0
120.0
110.0
100.0
90.0
80.0
70.0
60.0
50.0
40.0
30.0
20.0
10.0

9.5.3. Assignment of *N*-terminal Geometry of Compounds 9-12 in Water through 1D nOe.

Compound **9**

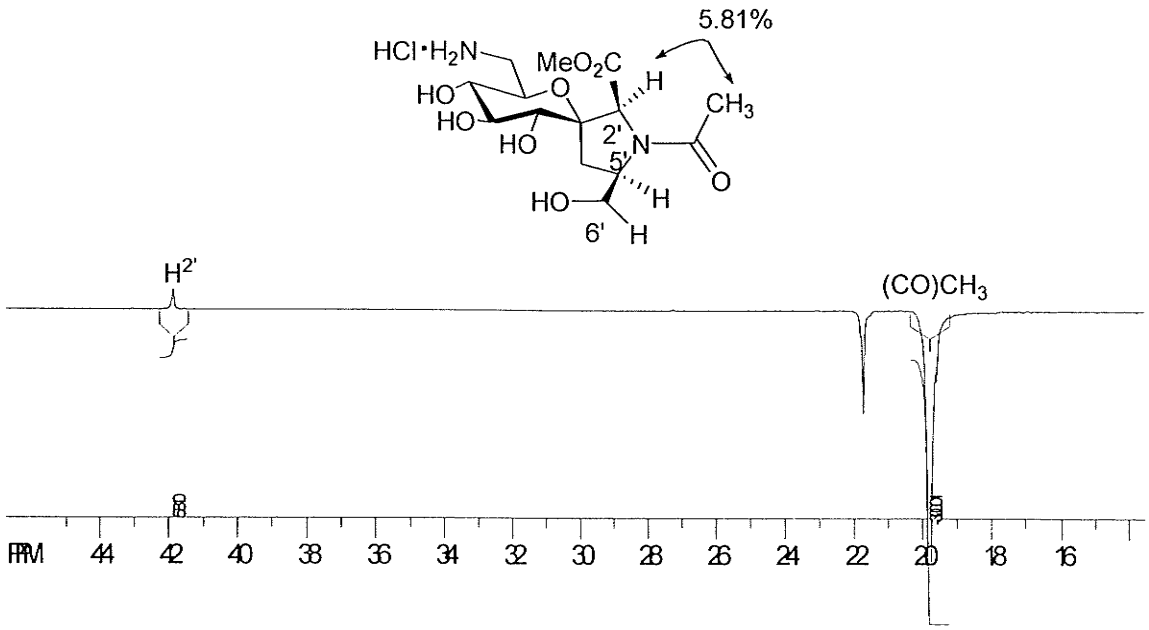

Compound **10**

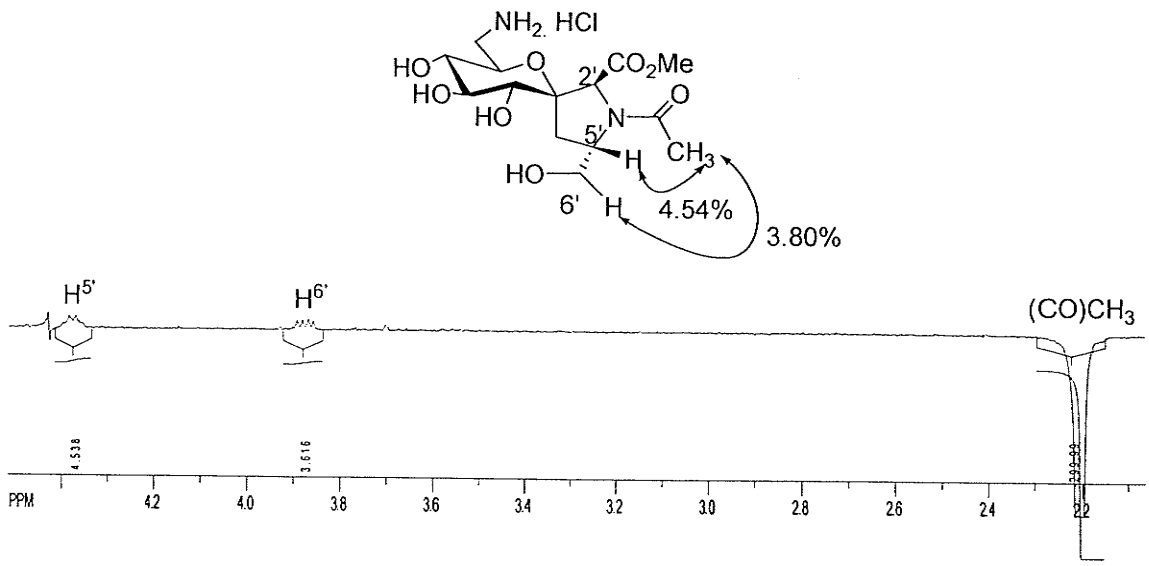
NH2. HCl
HO
HO
HO
O
2'
CO2Me
O
N
5'
H
CH3
HO
6'
H
4.54%
3.80%
H5'
H6'
(CO)CH3
PPM
4.2
4.0
3.8
3.6
3.4
3.2
3.0
2.8
2.6
2.4
2.2

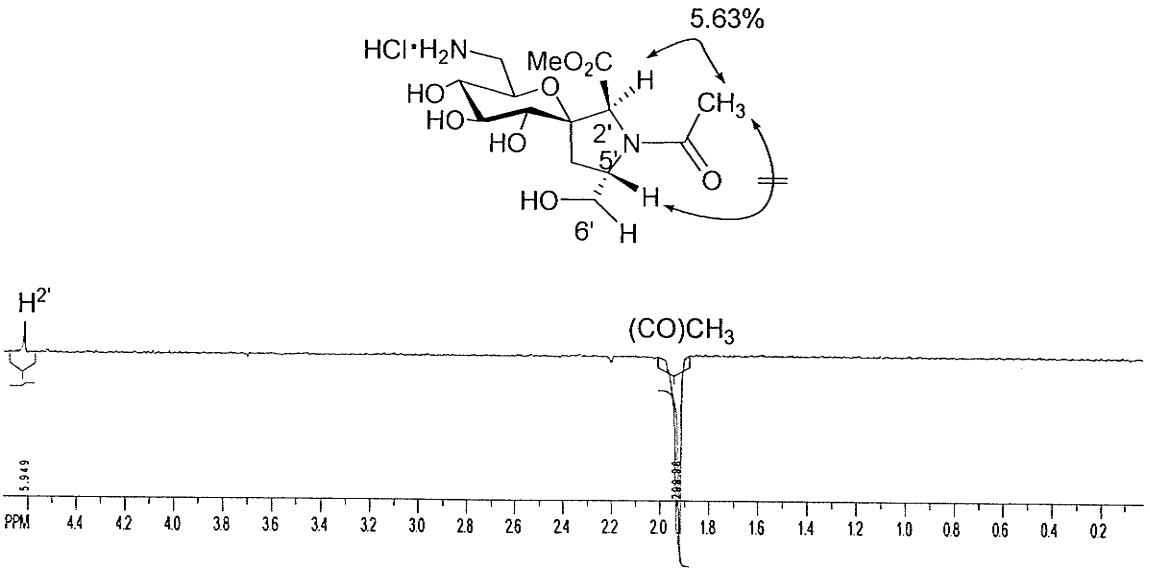
5.63%
HCl·H2N
MeO2C
H
HO
HO
HO
O
2'
N
5'
CH3
O
HO
6'
H
H
H2'
(CO)CH3
PPM
4.4
4.2
4.0
3.8
3.6
3.4
3.2
3.0
2.8
2.6
2.4
2.2
2.0
1.8
1.6
1.4
1.2
1.0
0.8
0.6
0.4
0.2

Compound **11**

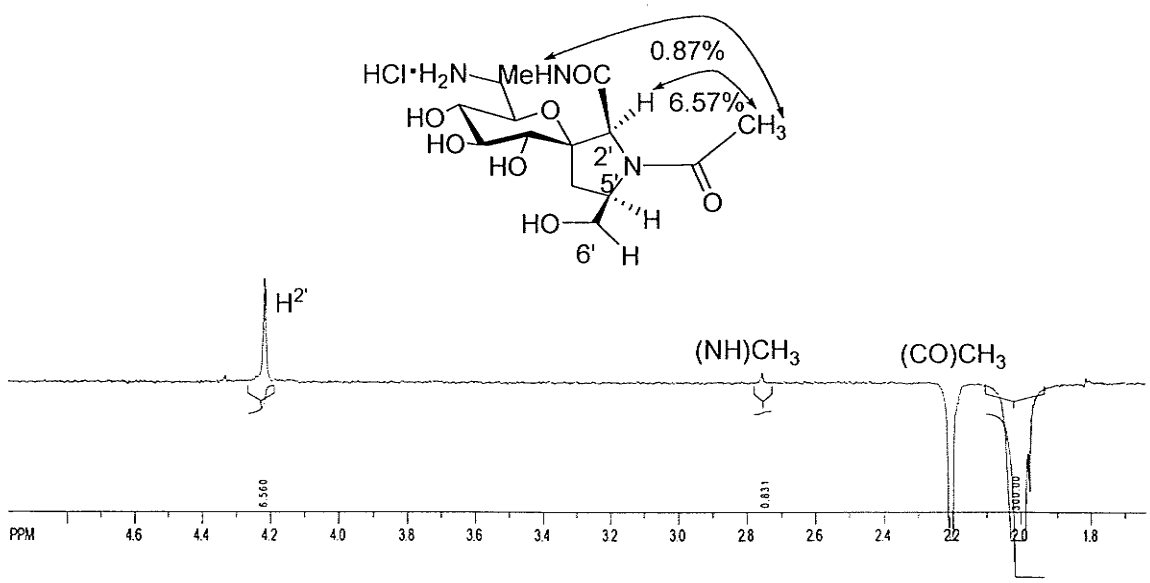

Compound **12**

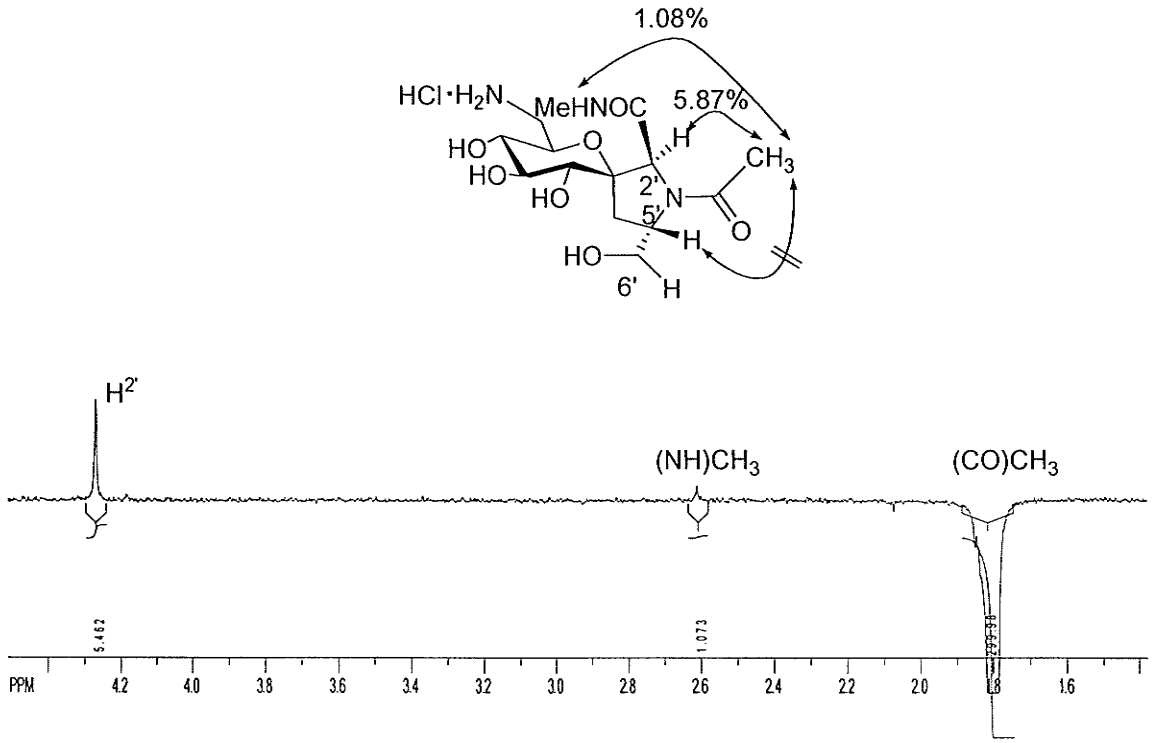

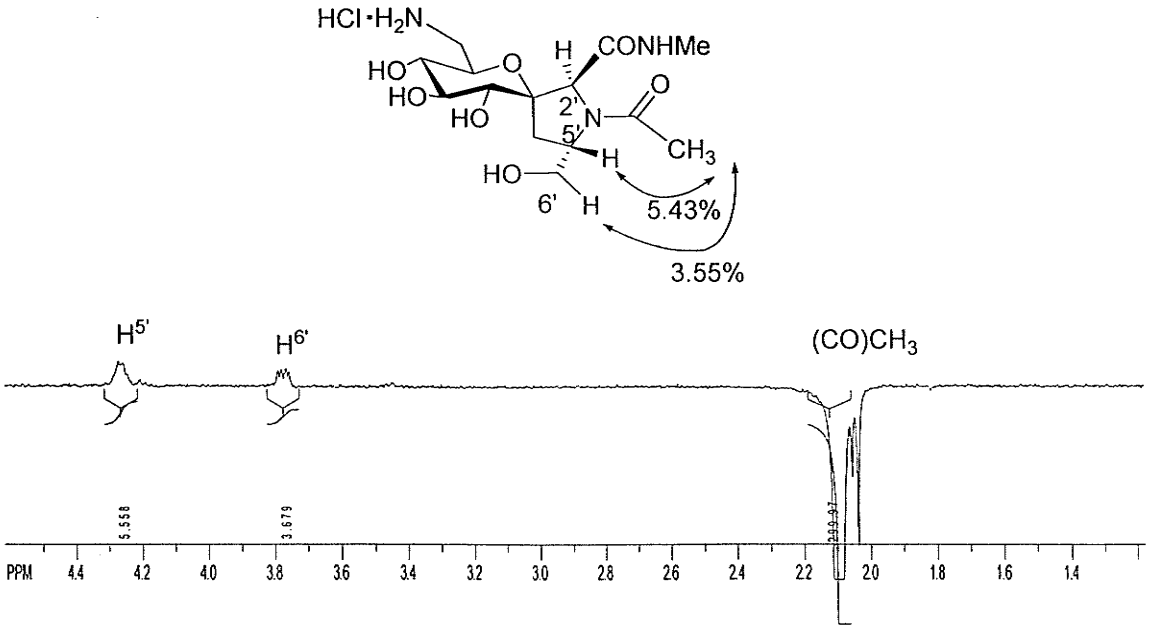

9.5.4. Preparation of buffer solution:

Table 1. Preparation of buffer solution

	pD = 2.6	pD = 7.4	pD =12.4
D_2O	1.2 mL	1.2 mL	1.2 mL
$Na_2HPO_4 \cdot 12H_2O$	-	32.6 mg	14 mg
1.0 M HCl	32 uL	29 uL	-
1.0 M NaOH	-	-	42 uL
KCl	15.5 mg	-	-

List of Publications and Patents Related to Thesis Work

Publications

1. **Influence of Glucose-Templated Proline Hybrids on the β-turn Conformation at the peptide Ac-Leu-D-Phe-Pro-Val-NMe_2 of Gramicidine S.** Kaidong Zhang and Frank Schweizer (manuscript in preparation).

2. **Design and Synthesis of Glucose-templated Proline-Lysine Chimera: Polyfunctional Amino Acid Chimera with High Prolyl *Cis* Amide Rotamer Population** Kaidong Zhang and Frank Schweizer (submitted).

3. **Intramolecular Hydrogen Bond-controlled Prolyl Amide Isomerization in Glucosyl 3(*S*)-hydroxyproline Hybrids – The Influence of a C^{δ}-hydroxymethyl Substituent on the Thermodynamics and Kinetics of Prolyl amide *Cis/Trans* Isomerization** Kaidong Zhang, Robel B. Teklebrhan, Hans G. Schreckenbach, Stacey Wetmore and Frank Schweizer (submitted).

4. **Synthesis of Glucose-templated Lysine Analogs and Incorporation into the Antimicrobial Dipeptide Sequence kW-OBn** Zhang, Kaidong; Mondal, Dhananjoy; Zhanel, George G.; Schweizer, Frank *Carbohydrate Research.* **2008**, *343*, 1644-1652.

5. **Synthesis of Sugar-Lysine Chimera with Integrated *Gluco*-Configured 1,3-Hydroxyamine Motif.** Kaidong Zhang, Jialiang Wang, Zhizhi Sun, Dung-Huang Nguyen and Frank Schweizer *Synlett.* **2007**, *02*, 239-242.

6. **Synthesis of Spirocyclic Glucose-Proline Hybrids (GlcProHs).** Kaidong Zhang and Frank Schweizer *Synlett.* **2005**, *20*, 3111-3115.

Patents

1. **Synthesis of Carbohydrate-Templated Amino Acids, Particularly Glucose-Lysine Chimeras, and Their Use as Coupling Components in the Preparation of Antimicrobial Peptides.** Schweizer, Frank; Zhang, Kaidong; Owens, Neil; Zhanel, George. PCT Int. Appl. 2008, 55pp. CODEN: P1XXD2 A2 20080327.

2. **Synthesis of Spirocyclic Glucose-Proline Hybrids.** Schweizer, Frank; Zhang, Kaidong. Can. Pat. Appl. 2008, 24pp. CODEN: CPXXEB CA 2568954 A1 20080527.